Development and Applications of the Modular Automotive Technology Testbed (MATT) to Evaluate Hybrid Electric Powertrain Components and Energy Management Strategies

Henning Lohse-Busch

Dissertation submitted to the faculty of the Virginia Polytechnic Institute and State University in partial fulfillment of the requirements for the degree of

Doctor of Philosophy

In

Mechanical Engineering

Nelson, Douglas J., Committee Chair

De La Ree, Jaime Committee Member

Ellis, Michael W. Committee Member

Kornhauser, Alan A. Committee Member

von Spakovsky, Michael R. Committee Member

Ball, Kenneth Steven Department Head

September 11th, 2009

Blacksburg, VA

Keywords: Modular Automotive Technology Testbed, Hybrid electric vehicle, Plug-in hybrid electric vehicle, Component testing, Hydrogen internal combustion engine

Development and Applications of the Modular Automotive Technology Testbed (MATT) to Evaluate Hybrid Electric Powertrain Components and Energy Management Strategies

Henning Lohse-Busch

ABSTRACT

This work describes the design, development and research applications of a Modular Automotive Technology Testbed (MATT). MATT is built to evaluate technology components in a hybrid vehicle system environment. MATT can also be utilized to evaluate energy management and torque split control strategies and to produce physical measured component losses and emissions to monitor emissions behavior.

In the automotive world, new technology components are first developed on a test bench and then they are integrated into a prototype vehicle for transient evaluation from the vehicle system perspective. This process is expensive and the prototype vehicles are typically inflexible in hardware and software configuration. MATT provides flexibility in component testing through its component module approach. The flexible combination of modules provides a vehicle environment to test and evaluate new technology components. MATT also has an open control system where any energy management and torque split strategy can be implemented. Therefore, the control's impact on energy consumption and emissions can be measured. MATT can also emulate different types and sizes of vehicles. MATT is a novel, unique, flexible and powerful automotive research tool that provides hardware-based data for specific research topics.

Currently, several powertrain modules are available for use on MATT: a gasoline engine module, a hydrogen engine module, a virtual scalable energy storage and virtual scalable motor module, a manual transmission module and an automatic transmission module. The virtual battery and motor module uses some component Hardware-In-the-Loop (HIL) principles by utilizing a physical motor powered from the electric grid in conjunction with a real time simulation of a battery and a motor model. This module enables MATT to emulate a wide variety of vehicles, ranging from a conventional vehicle to a full performance electric vehicle with a battery pack that has virtually unlimited capacity.

A select set of PHEV research studies are described in this dissertation. One of these studies had an outcome that influenced the PHEV standard test protocol development by SAE. Another study investigated the impact of the control strategy on emissions of PHEVs. Emissions mitigation routines were integrated in the control strategies, reducing the measured emissions to SULEV limits on a full charge test.

A special component evaluation study featured in this dissertation is the transient performance characterization of a supercharged hydrogen internal combustion engine on MATT. Four constant air-fuel ratio combustions are evaluated in a conventional vehicle operation on standard drive cycles. Then, a variable air fuel ratio combustion strategy is developed and the test results show a significant fuel economy gain compared to other combustion strategies, while NOx emissions levels are kept low.

Dedication

To Emily, my loving wife, who encouraged and supported me on the long and difficult road that led to this dissertation.

To Professor Nelson and the Hybrid Electric Vehicle Team, thanks to whom I discovered my passion for advanced powertrains and alternative fuels.

To all of the victims of the tragic events that struck our Virginia Tech family on April 16th 2007.

AKNOWLEDGEMENT

Table of Contents

Table of Figures

Table of Tables

List of Abbreviations

Abbreviations

AC	Alternating current
AER	All electric range
ANL	Argonne National Laboratory
ANL	Argonne National Laboratory
APRF	Advanced Powertrain Research Facility
APRF	Advanced Powertrain Research Facility
Blended PHEV	PHEV which has to use the engine since the motor can not provide enough power to provide vehicle performance
CAFÉ	Corporate Average Fuel Economy
CD	Charge Depleting (or charge depletion)
CH4	Methane
CO	Carbon Monoxide
CO2	Carbon Dioxide
CS	Charge Sustaining
CVT	Continously Variable Transmission
DOE	Department of Energy
DOHC	Dual Over Head Camshafts
EC	Electric consumption
ECU	Engine Control Unit
ECVT	Electrically Continously Variale Transmission
EPA	Environmental Protection Agency
EV	Electric Vehicle
EV capable PHEV	PHEV which uses the electric traction motor only to provide full performance
FC	Fuel consumption
FE	Fuel Economy
FTP	Fedearl Test Procedure
H2	hydrogen
H2ICE	Hydrogen Internal Combustion Engine
HC	Hydrocarbon(s)
HEV	Hybrid Electric Vehicle
HIL	Hardware-In-the-Loop
HV	High Voltage
HWFET	Highway Fuel Economy Test
IPCC	Intergovernmental Panel on Climate Change
MATT	Modular Automotive Technology Testbed
NEDC	New European Drive Cycle
NIPCC	Nongovernmental International Panel of Climate Change
NMOG	Non-Methane Organic Gases
NOx	Nitrogen Oxides
O2	Oxygen
OCV	Open Circuit Voltage
OEM	Original Equipment Manufacturer
PHEV	Plug-In Hybrid Electric Vehicle
PSAT	Powertrain Systems Analysis Toolkit
SOC	State of Charge

SULEV	Super Ultra Low Emissions Vehicle
THC	Total Hydrocarbons
Trace	Drive cycle trace
UDDS	Urban Dynamometer Driving Schedule
ULEV	Ultra Low Emissions Vehicle
WTW	Well to wheel
ZEV	Zero Emissions Vehicle

Units

A	ampere(s)
Ah	ampere × hour(s)
deg C	degree Celsius
g/mi	grams per mile
g/s	gram(s) per second
J	joule(s)
kg	kilogram(s)
km	kilometer(s)
kW	kilowatt(s)
kW*hr	kilowatt × hour(s)
L	liter(s)
m	meter(s)
mg	milligram(s)
mg/s	milligram(s) per second
MJ	megajoule(s)
mph	mile(s) per hour
ms	millisecond(s)
N.m	newton meter(s)
rpm	revolution(s) per minute
s	second(s)
V	volt(s)
VDC	volt(s) direct current
W*hr	watt × hour(s)
mpg	miles per gallon
mpgge	miles per gallon gasoline equivalent
gal	gallon
mi	mile
mph/s	mile per hour per second (acceleration rate)

1. Introduction

1.1. Modular Automotive Technology Testbed

The unique and novel tool at the center of this work is a Modular Automotive Technology Testbed (MATT). The tools' purposes are to test new powertrain technology components or serve to generate hardware-based data for specific automotive research topics. The novel concept is in the component module approach which involves clamping component modules to an automotive frame and testing different configurations in the vehicle system environment. Using the modular concept, a hybrid vehicle is available and the controller that executes energy management strategy is open, which means that any control strategy can be implemented. This flexibility is the key to making MATT a good instrument for a variety of specific studies. Figure 1-1 illustrates the concept of MATT.
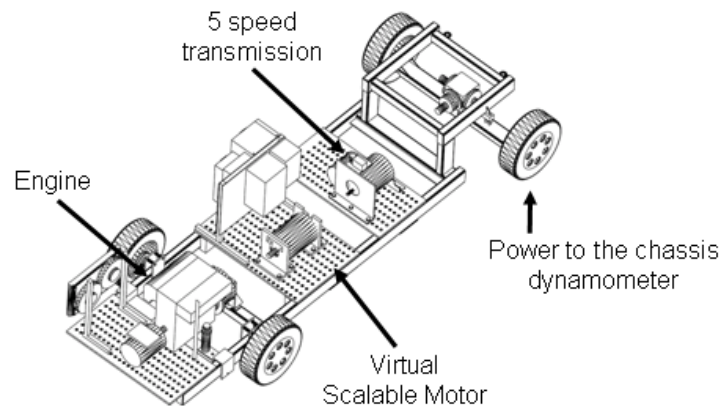
Figure 1-1: Illustration of the Modular Automotive Technology Testbed

With the concept of this tool in mind, the next few pages will build the context of the work from the high level challenges that global transportation faces to the modest contribution that this tool can provide in evaluating solutions.

1.2. Today's Transportation Challenges Motivate this Work

At the start of the 21st century, the United States of America is facing some major challenges with its transportation system, particularly in the automotive sector. The first issue is dependence on foreign oil. The US consumes vast amounts of fuel every day and thus the US imports more oil from politically unstable and 'unfriendly' parts of the world. The second concern is the impact of the 210 million cars [Ref. 1] producing tailpipe emissions, which are harmful to humans and have been a large factor in the climate change observed in the last few decades. The final hurdle is that both of the aforementioned problems need to be addressed while meeting or exceeding the consumer expectations for performance, cost and reliability.

1.2.1.   Petroleum dependence

Figure 1-2 shows the history of American petroleum usage over the last 50 years. Not only has consumption almost tripled since 1950, but the domestic production of oil is in decline and currently over half of the US's petroleum is imported. There are many other compelling graphs and statistics, but this graph depicts the addiction to petroleum as well as the supply issues faced.
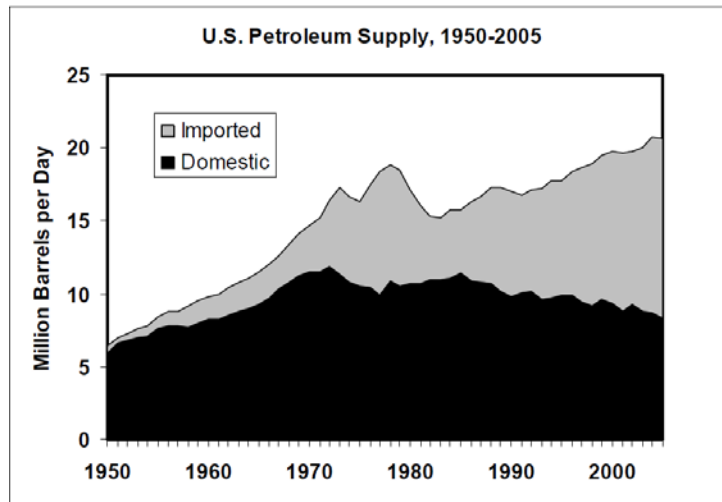
[Ref. 2]

Figure 1-2: Split between imported and domestic portions of US petroleum supply

In addition to the national security problems associated with energy dependence, limited fossil fuel resources are a global concern and cannot be denied. Experts debate over the capacity of the crude oil reserves across the world. Some suggest that we are already running out [Ref. 3, Ref. 4, Ref. 5, Ref. 6, Ref. 7 and Ref. 8] while others project our reserves will last for decades to come [Ref. 9, Ref. 10, Ref. 11, Ref. 12]. Neither side denies that easy and affordable crude oil is a finite resource, and the supply will eventually run out. Therefore, now is the time to find solutions that displace and eventfully eliminate our global dependence on petroleum. In the transportation sector, short term solutions for replacing petroleum include using advanced vehicle technologies such as hybrid electric vehicles (HEV) and plug-in hybrid electric vehicles (PHEV). In the long term, renewable and sustainable alternative fuels or energy carriers are necessary to eliminate our dependence on petroleum. These new alternatives must also address the environmental impact of the transportation sector, and include options such as biofuels, 'green' electricity and hydrogen.

1.2.2.   Pollution

The emissions from the transportation sector are a major contributor to air pollution [Ref. 13 and Ref. 14]. In 1970 the Environmental Protection Agency was created to enforce the Clean Air Act and to regulate the pollution across a wide spectrum of industries, including the transportation sector. The EPA estimates that 'Today, motor vehicles are responsible for nearly one half of smog-forming volatile organic compounds (VOCs), more than half of the nitrogen oxide (NOx) emissions, and about half of the toxic air pollutant emissions in the United States'. [Ref. 15]. Currently, the EPA's Tier II standards are almost phased in. In order to achieve today's stringent emissions standards, a mandate to reduce sulfur content in fuel was enacted. The regulated tailpipe emissions of vehicles are hydrocarbons (HC), carbon monoxide (CO), nitrogen oxides (NOx) and particulate matter (PM). Most of these elements are bad for human health. Again advanced hybrid electric and alternative fuel powertrains offer new opportunities to minimize these tailpipe emissions.

Global climate change is another issue that is typically linked to CO2 emissions. Two sides emerge in this debate. The intergovernmental panel on climate change (IPCC) claims that augmented fossil fuel use increases the atmospheric concentration of CO2 which leads to an amplified greenhouse effect, causing global warming and the drastic predicted climate change. [Ref. 16, Ref. 17] For the IPCC, immediate regulations on greenhouse gases (GHG) are required to save the world. The nongovernmental international panel of climate change (NIPCC) claims that the modern warming is driven by nature and is not anthropogenic. NIPCC believes the arguments of the IPCC are not presented with scientific rigor, and therefore no new emissions regulations should be mandated on GHG emissions. Regardless, the CO2 production from a petroleum based fuel vehicle is directly proportional to the vehicle's fuel consumption. This leads back to the issue of crude oil dependence. Limiting CO2 production has global benefits.

Today the approach to finding new transportation fuels is a lot more comprehensive, and considers the full life cycle impact on energy and emissions. The typical focus used to be on the vehicle fuel consumption and tailpipe emissions (also called the tank-to-wheel portion of fuel life cycle). Now, the energy and the pollution generated in the harvesting of the raw material, processing and distribution of the fuel are also taken into account. To evaluate this energy and emissions impact, tools such as the Greenhouse Gases, Regulated Emissions, and Energy Use in Transportation (GREET) model can be used, GREET considers not only the fuel life but also the life cycle of advanced technology vehicles. [Ref. 18]

1.2.3.   Performance

The performance tradeoff must be considered when maximizing fuel economy and minimizing emissions. Figure 1-3 shows the fuel economy trends in the US fleet as well as the performance trends. It is remarkable that the fuel economy averages stayed relatively constant in the last decades and the performance of vehicles improved dramatically. New technologies such as hybrid electric powertrains can also improve vehicle performance, as demonstrated by Honda's 2005 Accord hybrid whose 0 to 60

mph time was 6.7 seconds and EPA sticker fuel economy numbers were city/highway 30/37 mpg as compared to the standard four cylinder Accord that obtained 7.5 seconds and 26/34 respectively [Ref. 19, Ref. 20].
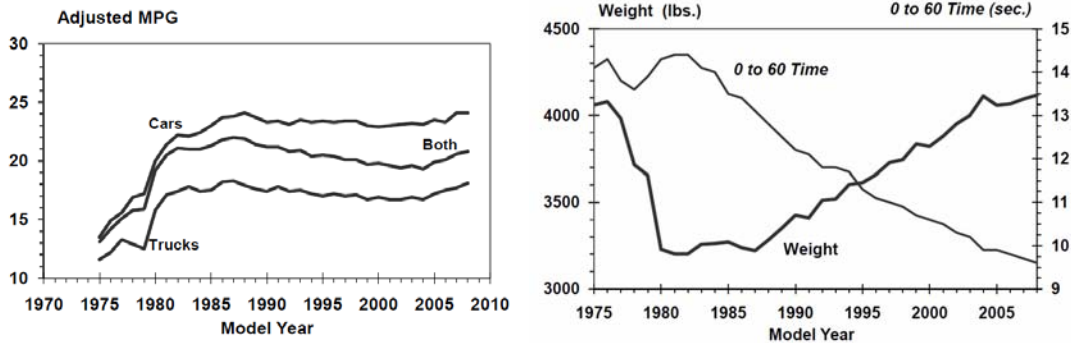
[Ref. 21]

Figure 1-3: (a) EPA fleet adjusted fuel economy and (b) weight and performance data from 1975 to 2008

On a side note, the weight increase that is noted above is due to safety requirements and "creature of comfort creep" required by the customer. This weight increase has a negative impact on fuel economy. Also interesting to note is the fuel economy increase starting in 2005, which is due to the introduction of new technologies in the market such as variable valve timing, cylinder deactivation and gasoline direct injection [Ref. 21].

1.2.4.   Technology driver

A number of solutions exist to address the energy and emission challenges. Hybrid electric vehicles and alternative fuels are the technical answer. Before expanding on theses technical options, one should realize that the market for future vehicle development is ultimately driven by the consumer demand for such changes. The consumer, in turn, is ultimately concerned with the bottom line, including purchase price and operation costs such as gas prices. Currently the price of gasoline is relatively low in the US market compared to other developed countries such as Europe. If the price jumps close to $5, the consumer changes his/her behavior, trading in their larger vehicles for smaller, more fuel-efficient vehicles as demonstrated by the gas price peaks in 2008, where hybrid vehicles were in higher demand. During those times the demand for cheaper alternative fuels also dominates the news cycle. Therefore, one option for reducing petroleum dependence is to instate a fuel tax to set the fuel price to a given value in order to provide gas price stability and drive the technology innovations. The money from the tax should be reinvested in the research and infrastructure development required for the future. This dissertation is focused on the technical solutions, but the author felt compelled to acknowledge the driving force for the technology development.

1.2.5. Testing new technology

Component testing process

The development cycle of a new technology in a vehicle starts with an idea for a small improvement or a radically new technology component. That idea is then translated into hardware in a laboratory setting. Typically, a smaller scale version of the technology is first built and evaluated. From that data, a simulation is performed to estimate the potential for the new technology in a vehicle. Then, a full scale version of the component is constructed and tested in the laboratory on a specific set of tests. For an engine, that testing occurs on an engine dynamometer at steady state speed with limited open loop transients. If all those steps are successfully completed, the component is evaluated in the final environment on a test mule. At this stage the final operating conditions are exerted on the component.

There is a new intermediate step between the laboratory setting and the vehicle testing. This step is Component Hardware-In-the-Loop (HIL). The component is tested in an emulated vehicle environment. The physical component is connected mechanically and/or electrically to pieces that emulate the vehicle environment that the component will ultimately experience. Figure 1-4 shows an example of the process for the development and testing of a new plug-in lithium-ion battery pack.
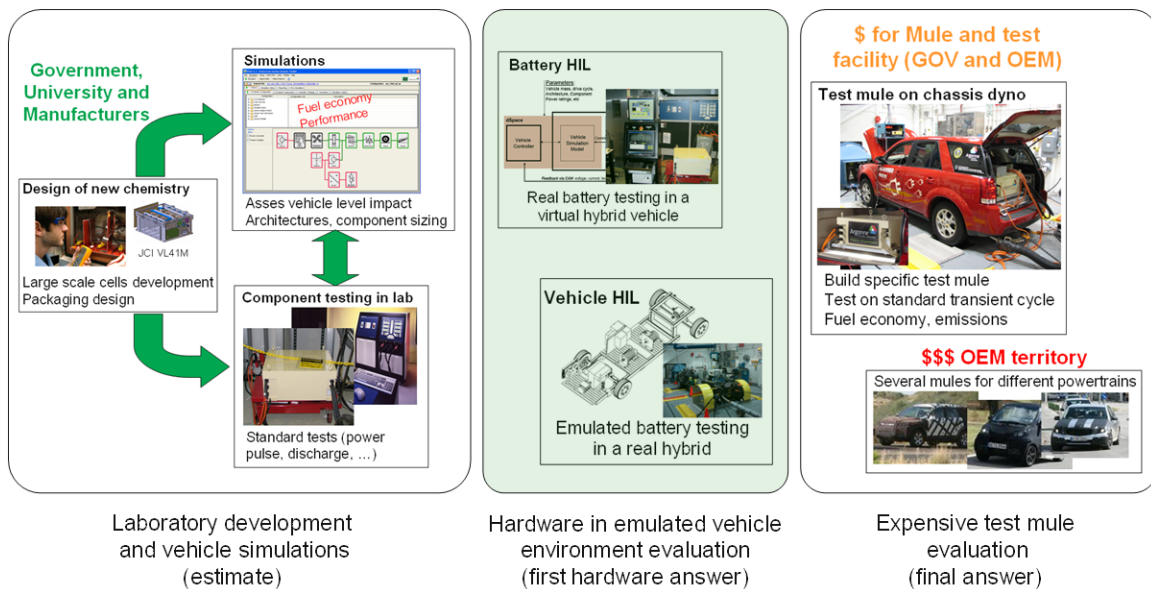
Figure 1-4: Sample development and testing process of a new automotive component such as a plug-in battery pack (based on Argonne example)

The process in Figure 1-4 is the actual process that Argonne National Laboratory followed in the development and testing of a new Lithium-ion battery pack. Highlighted in green is the HIL process that was introduced at Argonne. All the steps of the testing process have advantages and disadvantages, as shown in Table 1-1. Each step in the

process is crucial. The HIL testing adds a new, cheaper intermediate step, which enables the evaluation of the component closer to the vehicle testing. This enables the engineer to gain some insight into the transient operation and modes without building an expensive mule. As the engineer progresses through the testing process, the accuracy of the measurements increases.

Table 1-1: Evaluation of different testing processes for a new component

	Lab tests	Simulation	Component HIL	Vehicle HIL	Test mule
Pros	Required start	Cheap, can be fast, flexible, explore design space, anything can be simulated	Component performance in vehicle system, cost, vehicle flexibility	Modular, flexibility on emulated component, reusable	All physical hardware
Cons		Model limitations, Thermal related losses, emissions, everything is possible	Rest of vehicle only as accurate as models	Component model limitation, requires test facility	Expensive
Cost	/	Low	Medium	High (reusable)	Extreme
Fuel-Electric consumption	Steady state efficiency map	+	+	+++	+++
		+	+++	++	+++
Emissions	Steady state emissions map	--- May be good enough for trends		+++	
Performance	Maximum performance envelop	+	+	++	+++

Figure 1-4 as well as Table 1-1 are based on a specific example of a new lithium battery development, but other new technology components would follow the same process and the qualifiers would be changed only slightly.

Vehicle testing for new technology components

The current test method to quantify fuel consumption and emissions are well proven for conventional petroleum fueled vehicles. The future technologies may not fall into the current test standards. Alternative fuels may generate pollutants that are not yet regulated. For example, urea injection during the selective catalytic reduction process in diesel after treatment systems can generate and release ammonia into the air. This is an irritant, but is not yet regulated. New hybrids, such as plug-in hybrids, use two sources of energy (gasoline and electricity), which poses the question of energy consumption representation for the consumer [Ref. 22]. The car can get 100 mpg or even infinite mpg, but it consumes electricity, which has a cost just like a fossil fuel. Furthermore the PHEVs may not turn on their engines during the first test cycle, but PHEVs will eventually use their engines in subsequent cycles, thus triggering the question of emissions accountability. Thus, new standard test procedures need to be established as these alternatives reach viability in the market.

The tool at the center of this work is designed to test these new technology alternatives and measure the fuel economy, emissions and performance. The two major

technical solutions to petroleum dependence can be divided into two categories. First, the fuel used to move the cars and second, the powertrain configurations.

1.3. *Alternative Fuels*

1.3.1. Renewable in contrast to sustainable fuels

The petroleum dependence and the emissions are fundamentally linked to the fuel used in vehicles today. In order to make a vehicle run without using our limited fossil based petroleum, one can use a bio-fuel such a corn-based ethanol or cellulosic ethanol. This approach can solve the petroleum dependence by using a renewable fuel. In order to be both a renewable and sustainable fuel, which fuel needs to be able to be produced at a fast enough pace to supply the transportation sector. Cellulosic ethanol, for example, is a renewable fuel but not a sustainable alternative fuel today since it can not be produced at a sustainable rate to continuously feed the transportation sector. These alternative fuels sometimes also face ethical barriers, such as the questions raised by the use of corn ethanol. If corn ethanol is used in transportation, the food supply and transportation energy supply are in direct competition.

1.3.2. Environmental impact of alternative fuels

In the search for a renewable and sustainable fuel, a major consideration is the environmental impact of these alternative fuels, both from the production perspective as well as the possible tailpipe emissions at the vehicle level. In the example of electricity, which is sometimes considered an alternative fuel for transportation (although technically is a new energy carrier), the up stream production emissions can be very large. In the United States, the majority of the electricity in the grid is produced by coal fired power plants. This electricity can be referred to as 'black electricity'. In contrast, France produces most of its electricity in nuclear power plants, which are much cleaner. This electricity can be referred to as 'green electricity' similar to solar or hydro-electric power plant electricity. It should be noted that an alternative fuel that has zero vehicle level emissions but upstream emissions has a significant advantage in that the pollution is from a single source at the power plant. It is much easier to clean a single source such as a power plant than it is clean emissions for millions of individual vehicles.

1.3.3. Upstream energy requirements for alternative fuels

Another aspect by which alternative fuels can be evaluated is the upstream energy required to produce and distribute the fuel. For bio-fuels, that would include the solar energy absorbed by the biomass, the farming of the land (if required), the harvesting process, the distilling and refining processes and the final distribution to the fueling stations. The ideal alternative fuel would have the lowest losses in the upstream energy requirements.

7

Argonne National Laboratory's GREET model provides the energy and emissions data for the well-to-wheel processes for different alternative fuels.

1.3.4. Further factors defining alternative fuels

The safety hazards defined by the chemical properties of the fuel can be a major barrier to the success of a fuel. Due to its function, fuels contain large amounts of energy on a per volume and mass basis. Energy always has the potential for safety risks. Different fuels present different risk factors due to properties such as ignition energy levels, volatility and flammability range.

The range of distance that can be driven on a fill of an alternative fuel may be reduced as compared to that of petroleum fuels, and the fill time may be increased. For hydrogen, a fill can take up to 20 minutes due to thermal compression limits and the best ranges demonstrated are up to 300 miles. An electric charge can take over 8 hours and with a range resulting less then 150 miles.

Some alternatives, such as hydrogen, would require a complete overhaul and reconstruction of the transportation fueling infrastructure. Rebuilding the entire infrastructure is an enormous financial commitment and would require a long, slow phase-in process by diverting the annual investment of the conventional fuel infrastructure to building the alternative fuel infrastructure.

Finally, consumers' preconceived notions about certain alternative fuels may present major obstacles. These include safety-related fears in regard to hydrogen and ethical judgments such as corn-ethanol competition with food supplies.

1.3.5. The hydrogen engine application as a center piece of this dissertation

In the near term there is not a clear alternative fuel winner and experts anticipate that the alternative fuel mix will vary from region to region based on local resources. In the long term no clear winner has emerged either, but the fuel needs to be renewable, sustainable, clean (at source and destination), safe and practical. Currently, electricity and hydrogen appear to be good candidates, but both require a technological breakthrough in on-board storage (infrastructure, fill speed, and total energy capacity on-board).

The tool at the center of this dissertation is used to evaluate an alternative fuel technology component. A hydrogen internal combustion engine is evaluated in a transient way in a vehicle system environment.

1.4. Hybrid electric powertrains

1.4.1. Understanding power requirements in a vehicle

No alternative fuel is currently used on a large scale. An alternative path is to change the powertrain to reduce fuel consumption, thus reducing the fuel dependence.

Hybrid electric powertrains and the electrification of vehicles are enablers for fuel savings.

To understand the benefits of hybridization, the basic power requirements of conventional vehicles need to be understood. The power to move a vehicle falls into two physical components: power to overcome the vehicle inertia (acceleration) and the power to overcome the road load (aerodynamic drag and spin losses). Figure 1-5 defines these terms.

$$F_{roadload} = A + B \times V + C \times V^2$$

Inertia force: overcome change in momentum

Road load force: caused by wind resistance and other vehicle level losses

$$Power_{propulsion} = \left(\left(m \times \frac{\partial (V)}{\partial t} \right) + F_{roadload} \right) \times V$$
(At the wheel)

where

m is the vehicle test mass
A, B and C are the vehicle loss coefficients
V is the vehicle speed

Figure 1-5: Formulas defining propulsion power at the wheel.

In a conventional vehicle that power comes from the internal combustion engine at all times. The engine speed is constrained by the vehicle speed and the gear ratios in the transmission. This leaves the engine operating in low efficiency areas. During braking, the kinetic energy stored in the vehicle is dissipated by the mechanical friction system. With the addition of a hybrid system in a vehicle, a second power source shares the load of the engine. Typically, the second power source is bidirectional which means that it can provide energy for traction as well as store energy on-board the vehicle.

1.4.2.   Benefits of hybridization

Hybrid systems enable a number of functionalities:

- *Engine idle stop (or engine start stop)*: Using an electric motor the hybrid system is the enabler for the engine start and stop feature while the vehicle is at rest. This eliminates the fuel used by an engine during the idle phase.

- *Engine load control*: In a hybrid vehicle the engine does not have to be coupled with the road load and vehicle speed. In a mild hybrid an electric motor can assist or load the engine in order to optimize the engine operating regimes. In a full hybrid the engine can be completely decoupled from the road load and vehicle speed. The engine can be run on an optimal engine torque speed curve to always reach the highest engine brake thermal efficiency.

- *Regenerative braking*: Hybrid vehicles can slow down by applying a braking (negative) torque with the electric motor, thus recapturing and storing the recovered energy in the battery pack. The amount of kinetic energy recovered varies depending on the size and capacity of the hybrid systems as well as the driving aggressiveness and vehicle drag characteristics.

- *Downsizing engine:* During driving, a major portion of the power goes to accelerating the vehicle. If the hybrid system provides the extra power to accelerate, the engine only has to overcome the road load at grade, thus enabling the use of a smaller engine in a hybrid compared to the engine size required in a conventional vehicle of the same size. A smaller engine has to work at higher loads thus operating at higher efficiencies on average. But in recent years, it appears that the engine downsizing is not practical with consumer demands and does not provide the predicted savings.

- *Electric launch:* In a conventional vehicle the launch is quite inefficient because of the clutch engagement or automatic torque converter losses and engine revving.

Figure 1-6 demonstrates some of the classic hybrid features described above.
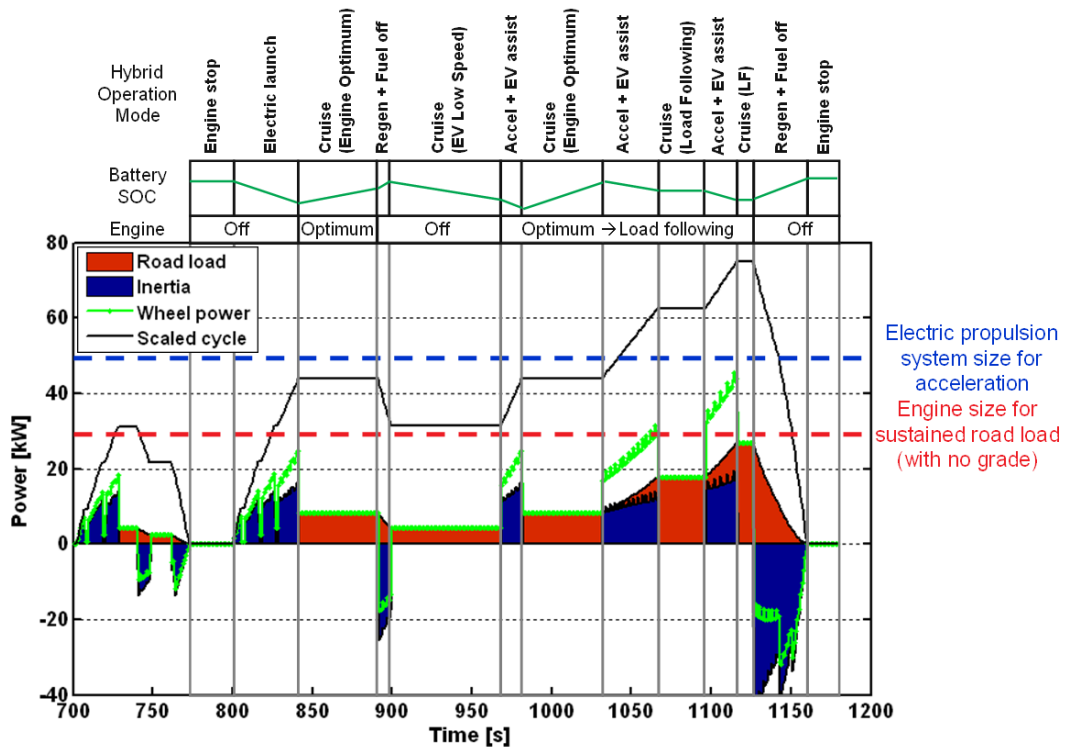
Figure 1-6: Inertia and road load power proportion on 2nd mode of UDDS cycle for mid size sedan with hybrid feature annotation

There are a few secondary features that hybrid systems enable:

- *Electrification of vehicle accessories:* Most mechanical accessories that were once driven by the engine are now becoming electric components. The alternators, air conditioning compressor, power steering, cooling fans, and even the engine coolant pump are electric components. The electrical counterparts to the mechanical components are more efficient (example: a DC/DC which charges the 12V battery with high efficiency ~95% compared to an alternator ~30%) or can be operated in more efficient regimes (Air conditioning compressor) or enable better component control (electric coolant pump enables faster engine warm up).

- *Special engine operation:*

    o *Emissions mitigation:* Using the hybrid system, the engine and the exhaust after-treatment system can be warmed up in a more controlled and load leveled mode which reduces the cold start emissions.

    o *Flexible thermal management:* The hybrid system enables active thermal management of the engine as well as some of the hybrid components such as active cooling with the AC or active warming algorithms in freezing environments of the battery pack.

    o *Cylinder deactivation:* In vehicles with cylinder deactivation, the hybrid system can actively smooth the transitions between the engine modes and also actively compensate for engine roughness while operating on a limited number of cylinders.

- *Petroleum displacement through electricity:* The latest breed of hybrids is the plug-in hybrid, which operates its energy storage system in a charge depletion mode. If the hybrid uses electricity, it represents fuel that does not need to be burned. The energy storage system needs to be recharged while the vehicle is not operating.

1.4.3.   Handicaps to hybridization

The hybrid vehicle also presents some downsides. The major obstacle is the cost of the hybrid system, which can add several thousands dollars to a vehicles price. As Figure 1-5 shows, mass is a contributor to the power required to move a vehicle, so each additional component in a hybrid system increases the mass of the vehicle and thus the energy required to move the vehicle. Another negative aspect of hybrid system is the added complexity on the hardware integration as well as the control level. Each component added has inherent losses. The battery system is especially expensive, heavy, and large. The battery system causes some recycling challenges. So for a hybrid system to become beneficial, it needs to overcome the aforementioned intrinsic drawbacks.

1.4.4. Plug-in hybrid applications as a centerpiece of this dissertation

The purpose of the tool at the center of this dissertation is to evaluate individual hybrid powertrain components in a vehicle system environment as well as the energy management strategies and special benefits of these components. One of the major studies was to evaluate the potential of reducing emissions for plug-in hybrid vehicles.

1.5. Means to evaluate new technologies

Currently, in order to test new technologies, the automotive industry builds dedicated prototype vehicles, each specifically designed to test one technology. These new technologies range from alternative fuel engines or dual clutch transmissions in conventional vehicles to advanced energy storage systems and electric motors in more complex hybrid vehicles. The different hybrid powertrain architectures can use several torque split and energy management strategies to achieve a balance between fuel economy, emissions and performance. All of these hardware and software variations require vast amounts of resources to characterize the potential viability of new technologies.

Due to resource constraints, it is not practical in an academic or government research setting to build a large number of vehicles to evaluate the potential of each new technology or energy management strategy. Also, the goal of both academia and government is to research the potential for new automotive technologies, not to spend excessive time and funds building multiple vehicles. Therefore, simulation tools with today's fast computing power are a sensible alternative, and enable researchers to evaluate the benefits or limitations of new ideas in a virtual automobile. Simulations run extremely fast, enabling a researcher to test a wide range of powertrains or energy management strategies at the click of button. Simulations are also very flexible in terms of powertrain and component performance, allowing a researcher to estimate advantages of future technologies in vehicles. Simulations do also come with some limitations. Simulation results are only as accurate as the component models and physics on which they are based. For example, it is very difficult to accurately simulate the complex exhaust emissions behavior of internal combustion engines for transient behavior. Another difficult task is accounting for thermal effects on component efficiencies in simulation.

A modular component powertain testbed is an alternative solution for testing different technologies in a hybrid vehicle environment while keeping the cost and required resources relatively low. MATT is composed of physical hardware component modules including an internal combustion engine and a transmission as well as emulated component modules such an energy storage system. MATT is the tool at the center of this dissertation.

1.6. *Goals and objectives of the dissertation*

1.6.1. The goal

The goal of this Ph.D. work is to design, build and demonstrate a modular powertrain test bench that can evaluate technology components in a hybrid vehicle system environment. This test bench will also be used to evaluate torque split and energy management control strategies with hardware data on emissions behavior.

In order to evaluate new technologies being developed by the National Laboratory system, the United States Department of Energy (DOE) needs a tool. It would be possible to build test mules but that would require a new financial investment for each mule before the component can be tested in the vehicle system environment. Each new technology is tested in a stand alone system during the development phase. In the example of an engine, it is generally tested on an engine dynamometer at steady state operating conditions or limited transients. The final test occurs in a vehicle system environment where the component is operating in the intended system with transients and warm up constraints. To reduce the cost to DOE, it is proposed to build the MATT tool to eliminate the need to build prototype vehicles.

1.6.2. The objectives

The primary objective of the dissertation work is to develop the Modular Automotive Technology Testbed (MATT) hardware and control software.

The second objective is to test the conventional vehicle architecture, starting with the engine performance and efficiency characterization. The specific component control for the engine, the clutch, the transmission and the friction brakes are developed. To complete a test cycle the controller needs to 'drive' MATT, thus, an automated driver is implemented. The conventional vehicle testing results include fuel economy and emissions results with the focus on the urban and the highway cycles. On the urban cycle, an energy balance for the different components will show the efficiencies over a transient drive cycle. Summary fuel economy results are also reported for other classic drive cycles and steady state speeds. To demonstrate the vehicle size emulation, MATT completes the UDDS as three different size vehicles.

The next objective of the dissertation is to detail and test the electric vehicle architecture. On the component level, physical hardware is built to emulate the energy storage model and the electric motor. In an electric vehicle, the regenerative braking and the mechanical brakes share the deceleration load and therefore pose a challenge for developing interacting hardware. As an example of electric vehicle operation, cold start efficiencies of the driveline are determined.

The next objective is to operate MATT as hybrid vehicle. Different algorithms are developed to control and protect the engine while it is in hybrid mode. Then diverse simple torque split approaches are tested, ranging from simple engine start/stop to full hybrid control mode tests. The controller flexibility and ability to control torque split and energy management ease these developments. A specific example of MATT's flexibility

is a Pulse and Glide operation performed in conventional vehicle operation and then in hybrid operation.

The subsequent objective is to demonstrate plug-in hybrid (PHEV) applications. First, simple torque split and energy management code is used to develop different hybrid modes. Then, MATT is applied to investigate the cold start correction on highway cycles for the Society of Automotive Engineers (SAE) and California Air Resource Board (CARB) PHEV test procedures. A final application is the development and calibration of a more complex code to evaluate the impact of the energy management control and torque split approach on fuel economy and emissions.

The final objective is to demonstrate the evaluation of a new technology component. DOE supported the development of a hydrogen engine with different ECU calibrations. The development work is performed on an engine dynamometer and the evaluation of transient operation in a vehicle is required.

1.7.   Outline

The dissertation will first present the concept behind MATT as well as the design and development. Next, the basic vehicle operations including conventional vehicle, electric vehicle and hybrid electric vehicle modes are detailed.

The applications are presented in the second phase of the work. First, the plug-in hybrid studies are presented, which include some investigations and evaluation of very specific proposed test procedures as well as a major investigation into engine emission reduction for PHEVs. The final application is the hydrogen engine calibration development on the dynamometer and in-vehicle evaluation with MATT to show a combustion strategy optimized for transient fuel economy improvement while maintaining low emissions.

In the final part of the dissertation, some of the tool's limitations are discussed and future work suggestions are summarized.

2.   Literature review

Due to the wide scope of the work, the literature review covers a number of areas. Since MATT and its software tools are built on Hardware-In-the-Loop (HIL) principles, that area is investigated first. The review focuses on projects similar to MATT. These comparative works define MATT's appropriate use in the context of today's research activities.

The subsequent sections of the literature review will focus on exploring the research fields in which MATT is used. First, a summary of the hybrid and especially pre-transmission parallel hybrid energy management strategies is established, since that is the configuration MATT is used in for the purposes of this dissertation work. The first application studies are performed using plug-in hybrid electric vehicles, thus a section is dedicated to this new breed of vehicle, including both its advantages and challenges. The final application for MATT focuses on the evaluation of hydrogen internal combustion engines. Supporting literature is reviewed in the final part of this section.

2.1.   Hardware-In-the-Loop Concept

One of the best, and earliest, definitions of HIL is one from Hanselmann in 1993 (Ref. 1): "A single component or even a whole vehicle can be replaced by mathematical models simulated in a real time on small and cost effective hardware systems, while other components which need testing or are just part of the test setup, are connected to the simulation in a closed loop configuration." Thus an engine running against an engine dynamometer which is controlled by a real time simulation to represent the vehicle operating on a transient drive cycles is an example of HIL. By the same definition, a physical hybrid vehicle controller connected with a full vehicle wiring harness to a computer which runs simulations of all powertrain components also fits into the realm of HIL. In addition, a real vehicle with a virtual component such as a battery pack emulated by a large power supply is also contained in Hanselmann's definition of HIL. The three examples are referred to as Engine (Component) HIL, Hybrid (Controller) HIL, and Vehicle HIL, respectively. Figure 2-1 illustrates the different types of HIL. Vehicle HIL can also be referred to as rapid control prototyping (RCP).
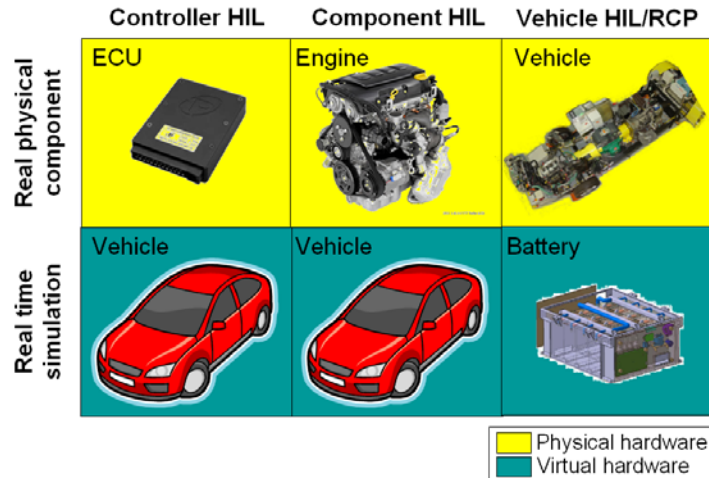
Figure 2-1: Illustration of different types of HIL

The first uses of computer simulation in the automotive world occurred in the 1970s, when the focus was on vehicle dynamics (Ref. 24). In the same decade, the progress in the computer processor power was such that real time simulation was achievable at an acceptable cost (Ref. 25). In 1977, something quite remarkable happened; real time computer simulation was linked to hardware (Ref. 26). The simulation provided adjustable vehicle and road characteristics to evaluate wheel lock-up for trucks. This evolved in a more refined process in 1987, when anti-lock brake systems (ABS) were developed (Ref. 27). In fact, the real time simulations of the braking process allowed researchers to test varying vehicles, environmental conditions and control system parameters independently in the safety of the laboratory while testing on the physical hardware. So researchers can recreate the same test conditions in a very repeatable manner and adjust the design and control. The process reduces the amount of upfront in-vehicle testing required which decreases development cost. In 1993, Hanselmann formalized the HIL definitions and referred to his experience using a vehicle dynamics model linked to ABS in hardware (Ref. 28). Hanselmann started to focus on controller HIL. During a test of a controller, simple or complex sequence of faults can be programmed on a plant computer which emulates the powertrain hardware. These faults might be difficult to induce on-road in a repeatable manner and the on-road test may become excessively dangerous. Hanselmann started dSapce GmbH, a company that focuses on building hardware to emulate entire vehicle powertrain plants in real-time simulations. Today dSpace is the recognized leader in automotive controller HIL systems as well as rapid control prototyping (RCP).

In 1987, Von Thun presented the world with the first Engine HIL (Ref. 29), which was then called a dynamic engine test stand with real-time simulation of the vehicle drive line. The engine dynamometer was capable of fast transient behavior and was able to apply loads during transients representative of those encountered by the engine in an actual vehicle. The benefit is that this substantially reduced the need for prototypes and on-road testing. In these early versions of engine HIL, the scope of testing was limited to conventional vehicle operation.

The 1990s saw a rapid proliferation of mechatronic systems in the automotive area. Car manufacturers started to integrate active vehicle dynamics algorithms (traction control, ABS), active safety systems (air bags), electronic fuel injection, on-board diagnostics, emissions control, and even some of the early hybrid drivelines. All of these new complexities increased the possibility for errors, thus longer and more detailed testing of these new systems was required. The HIL systems enable this systematic way of testing and inserting simulated software and hardware faults into the vehicle controllers for debugging purposes. HIL setups also shine in wiring and network verifications such as testing the CAN bandwidth and overload conditions.

Ford Motor Company invested in a dedicated laboratory for HIL testing, which included a chassis dynamometer, some transient engine dynamometers, motor dynamometers and a software development center for real time simulation (Ref. 30). The comprehensive approach gave the researchers the ability to test hardware components for hybrid powertrains as well as the software algorithms in the controllers. Thus, Ford applied both facets of HIL: controller and component HIL.

In the last decade, the controller HIL became the major HIL application to a point that now 'HIL' implies 'controller HIL'. This is mainly due to the proliferation of electronics, thus vehicle control complexity and the need to debug it. In fact, a majority of all recent papers contain controller-oriented HIL research results and entire HIL sessions at conferences such as SAE World Congress are dedicated to controller HIL. All of the major car manufacturers use this technique to prototype their hybrid vehicle networks and to test their control logic, including energy management strategies and active safety responses. By simulating the driveline components, fault insertions to the controllers are easy. This is essential for evaluating the system response to the faults (Ref. 31). A key aspect of the HIL system is the accurate repeatability of fault events, meaning that a situation can be recreated once a fix is determined (Ref. 32, Ref. 33).

MATT resides at the opposite end of the controller side of the HIL spectrum, as compared to the work described above. Now that controller HIL is understood, the next section can focus on the component HIL.

2.2.   Component Hardware-In-the-Loop projects

The MATT platform is most closely related to the component HIL. This HIL is intended to aid a powertrain engineer who is considering testing a piece of hardware in a vehicle system environment, but does not have the resources to build a full prototype vehicle. In order to be considered component HIL, there needs to be a closed loop interaction between the physical component and the real time vehicle environment simulation in the form of effort and flow. For example, some engine dynamometer tests apply an open loop speed load trace to an engine, which is not considered HIL because there is no dynamic interaction.

Any powertrain component can potentially be tested in an HIL environment. In the single component HIL, the biggest advantage is that the rest of the vehicle and powertrain architecture can be simulated to be anything and therefore offer an infinite number of testable environments. The major limitation is that the test results will only be

as good as the accuracy of the real time models and the dynamic response equipment simulating the rest of the vehicle (Ref. 35).

Since component HIL is a lesser-known area of research, it is more difficult to find quality publications concerning the findings. There are a number of single component HIL setups such as engine HIL, motor HIL, battery HIL, and transmission HIL. The literature provides examples of each.

2.2.1. General Engine HIL

As was mentioned earlier, engine HIL started in 1987, but at that time it was limited to conventional vehicle operation. After 2000, with the start of hybridization, the engine HIL took on new significance in testing the engine in an emulated hybrid vehicle environment. In the ideal engine HIL setup, the engine can be tested in any hybrid vehicle architecture under an unlimited number of control strategies. Although the internal combustion engine has been around for over a century, it is still the hardest component to simulate accurately in a vehicle. The emissions from transient behavior and the thermal effects on efficiency and emissions are extremely complex to simulate (Ref. 34). It is not possible to run them more accurately in real time. Therefore, engine HIL provides the best compromise between the flexibility of accurate real time vehicle models and measured emissions and thermal data from a physical engine.

2.2.2. University of Michigan: Engine-In-the-Loop (EIL) testing

A collection of papers (Ref. 35, Ref. 36, Ref. 37, Ref. 38) present the Engine-In-the-Loop (EIL) research at the University of Michigan lead by Professor Fillipi Zoran. This work is the most complete and detailed engine HIL included in this literature review.

The EIL is quite different from MATT. This application is moving a HMMWV and MATT is more centered around light duty vehicles. In the University of Michigan setup, a medium duty diesel engine is coupled with a fast transient dynamometer that simulates the vehicle environment. First, a baseline is established using a test where the engine moves a virtual conventional vehicle on an urban drive cycle. The baseline data is used to understand and explain the engine transient emissions behavior. In a second phase, the engine is used in a parallel hybrid HMMWV. Using the emission knowledge again in the conventional testing, two hybrid control strategies are developed; a rule based control strategy and a stochastic dynamic control strategy. The motivating factors for the setup are the limitations involved with predicting the emissions behavior of the engine. The secondary factor for the setup is the dynamic behavior and response time, which is also difficult to simulate accurately.

The two pillars of the EIL are the simulation models and the highly dynamic dynamometer setup. An in-house Matlab simulink-based vehicle simulation software program called VESIM simulates the virtual vehicle. Although software limitations were a driving factor in the build up of the EIL, that same simulation made it possible with

accurate and dynamic models of the vehicle and the hybrid powertrain. This software integrates with the dynamometer controller, which commands the engine torque and the dynamometer speed to apply the powertrain loads to the engine. The software then uses the actual sensor feedback from the engine (such as engine torque readings) to close the loop on the simulation. The large dynamometer is designed to operate with fast dynamic power (250 Hz) to simulate engine transients occurring in vehicles. The test cell has state-of-the-art diesel emissions equipment including a state-of-the-art particulate sizer that measures the particulate emissions continuously. The engine is a medium duty 6-liter V8 diesel, which is appropriate considering that the vehicle application is a military HMMWV.

The University of Michigan also mentioned the three major integration challenges encountered with HIL. First, they refer to the interaction between the engine torque and the dynamometer emulating the torque of the powertrain. The engine performs in torque control and the dynamometer is speed controlled based on the simulation calculation using the torque. This does not apply to MATT, because MATT is a full powertrain which is tested on the chassis dynamometer and the dynamometer performs the vehicle road load and inertia emulation. Second, they refer to the signal noise and communication delays, which are both certainly relevant for MATT. The solutions to the noise problem are found in hardware and software signal conditioning. The noise issue is not a problem in the idealistic simulation word where the control strategies are developed. Thus, one must anticipate the noise problems and their impact on the vehicle control. Finally, the University of Michigan study states that the virtual driver was a problem, which was eventually solved by using a PID loop with anti wind-up and an additional look-ahead. The software driver used on MATT was also a challenge. The basic driver logic uses the same approach as presented by the university of Michigan.

The results of the research are a comparison between the baseline vehicle operation and several hybrid control strategies based on fuel economy and emissions. The results show that hybridization provides an improvement of fuel economy and NOx emissions at the expense of particulate emissions. The stochastic control further improves the fuel economy, but the frequent engine starts caused even higher particulate emissions. The energy management strategies were developed based on steady state engine maps and thus illustrate the fact that simulation cannot accurately predict these emissions.

This project is similar to MATT in that it uses a physical engine in an emulated vehicle in order to collect fuel economy data and emissions data, but the vehicle size and the fuel type differentiate the work. MATT has also more physical components.

2.2.3. Southwest Research Institute: Engine-and transmission HIL testing

Southwest Research Institute invested several years in developing an engine and transmission HIL (Ref. 39). The major motivation for this work was to develop a transient test bench to map and calibrate an engine and transmission combination in a controlled and repeatable environment. This setup also enables the tuning of the same engine and transmission combination for different vehicle types. The same setup can be

used as a single component HIL for the engine. In that case, the real time simulation also emulates the transmission, which can be a manual, an automatic or a continuously variable transmission.

The system configuration is composed of the powertrain and vehicle simulation models, the interface software between the simulation and the real hardware, the test article (engine and/or transmission), an inertia simulation, low inertia dynamometer, and the real time software/hardware. A portion of the paper focuses on engine instability at constant throttle below the maximum torque speed curve, but this issue is specific to the powertrain emulation with a engine dynamometer. The inertia simulation discussion provides the inertia equations to emulate the reflected inertias of the vehicle at the engine shaft. Three basic methods are mentioned to achieve inertia simulation with the dynamometer: speed control, torque control and acceleration control. The hardest event is shifting gears with the inertia reflection due to the fast nature of the transient. Finally, a specific engine and transmission HIL example is provided. A good correlation from test data collected in a physical vehicle is demonstrated for the HIL emulation.

Southwest Research believes that HIL is now ready to enable transient engine calibration with sufficient fidelity, although continuous verification and validation within the vehicle is required. This work focuses on the process of component HIL and does not provide much insight into the possible applications. The intent of the engine and transmission HIL is to calibrate, not to investigate the engine behavior in hybrid powertrain vehicles although engines intended for hybrid application require a different calibration, especially for the impact of the frequent engine starts on emissions.

2.2.4. General Motors: Battery (Electrochemical cells) HIL

HRL Laboratories collaborated with General Motors to develop a battery HIL setup (Ref. 40). In this case the group used an individual cell and capacitor setup instead of using a full size hybrid battery pack. By scaling the real time model input and output to the smaller energy storage system it is possible to use the single battery cell and extrapolate the results for a large pack. This approach enables the evaluation of small-scale experimental energy storage systems from the vehicle systems perspective. The paper describes the hardware setup, which includes a thermal chamber that houses the energy storage system, a power cycler that emulates the vehicle with real time simulation. A special state of charge algorithm is developed for the cell and capacitor combination. In the last section, a test sample shows the full hybrid vehicle completing a US06 drive cycle, a very aggressive test for the hybrid system.

2.2.5. Arsenal Research: Electric motor HIL

The focus of this HIL setup at Arsenal Research (Ref. 41) is on testing electric motors in an emulated vehicle environment (such as electric vehicles and hybrid electric vehicles). The setup uses a low inertia fast transient dynamometer to apply the load to the test subject motor. The paper presents the physical setup in detail. The factors for

successful component HIL are similar to the other HIL setups, such as the software and models used as well as the hardware that interfaces with the test subject. A test performed on a smaller electric scooter motor is provided as an example.

2.2.6.   Argonne National Laboratory: Battery HIL

Argonne has been working on the component HIL for about a decade. Their most recent HIL setup is a Battery HIL (BHIL) system (Ref. 42). The purpose of the setup is to test plug-in hybrid electric battery packs and more advanced energy storage systems such as a combination of electro-chemical batteries and ultra capacitors. The interface used for the battery pack is a fast transient power processing system which cycles the battery based on a real time vehicle simulation. Figure 2-2 illustrates the setup. Currently, Argonne is on the second hardware iteration for this BHIL setup which uses an AeroViroment ABC-170 by-directional power supply. The ABC 170 provides the full transient capability needed to replicate the fast electric power transfers in a vehicle. A thermal chamber is part of the setup so that the battery systems can be tested at extreme temperatures both hot and cold. This is important since battery performance varies widely with temperature changes.
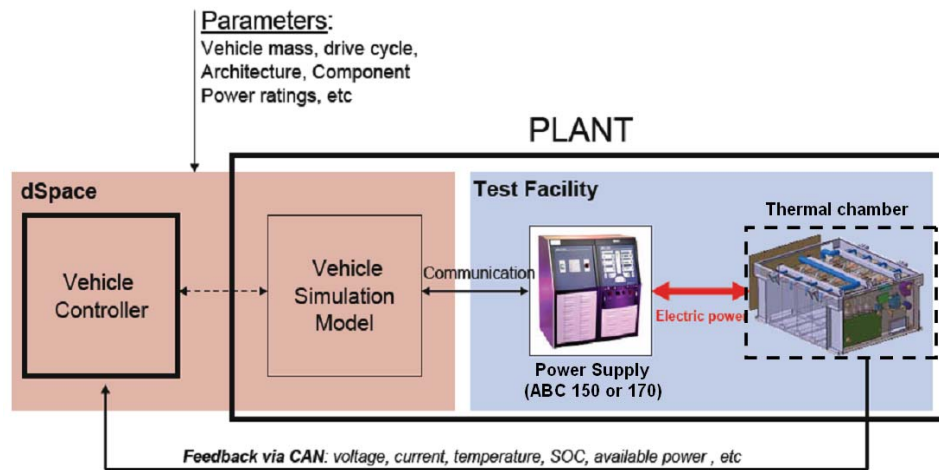
Figure 2-2: Schematic of Argonne's Battery HIL setup.

Argonne uses their in-house simulation software: Powertrain Systems Analysis Toolkit (PSAT Ref. 44) for the modeling section. A real time version called PSAT-Pro (Powertrain Systems Analysis Toolkit Prototyping) was developed, and enables the real time simulations as well as the interface to the power processing unit and the battery pack. A version of PSAT-Pro is used to control MATT.

The battery system is the enabler for the operation of plug-in hybrid electric vehicles. Therefore, testing physical batteries is necessary in order to evaluate their performance both in the charge depleting operation and the charge sustaining operation of the plug-in hybrid vehicle. The battery management systems integrated into the battery

pack provide maximum charge and discharge power levels, which are a function of battery state of charge and temperature. These are pieces of information that are not easily and accurately available in simulation.

Some of the studies performed are related to the revision of the hybrid standard test protocol (Ref. 45) and thus include all electric range tests, charge sustaining and charge depleting tests and full charge tests. For all of these tests, battery round trip efficiency is also calculated.

A further study investigates cold temperature performance of a PHEV battery pack (Ref. 43). It was found that the electric range is decreased by 13% at a temperature of -7 degrees Celsius, which is the temperature of the cold FTP test required by the new EPA 5 cycle test. This testing was performed in a controlled thermal chamber and the comparison between the hot and cold test was easy to make, since the vehicle, the control strategy and the driver operated in a very repeatable manner.

2.2.7. Brief summary of component HIL

The purpose of component HIL is to evaluate a component's behavior and performance in a vehicle environment context that is very controlled and repeatable. In some cases HIL is used to calibrate and tune transients on certain components. In all cases HIL is used because it is more cost effective than building a prototype vehicle and it provides a more controlled environment for testing. The ingredients for the setup include a fast transient means to apply loads to the test component and real time accurate vehicle and driveline models.

2.3. Vehicle/Powertrain Hardware-In-the-Loop projects

Vehicle level HIL implies that almost the entire powertrain is composed of real components. These setups are still typically connected to an engine dynamometer and do not involve full prototype vehicles.

2.3.1. Argonne's Diesel hybrid HIL

Argonne has worked and led research in this area since early 2000 (Ref. 46, Ref. 47, Ref. 48, Ref. 49). The most prominent project was the evaluation of a compression ignition direct injection diesel engine pre-transmission parallel hybrid drivetrain with a continuously variable transmission (CVT). The goals of the setup were: 1) to better understand the component/subsystem performance and control requirements in a simulated vehicle environment and 2) to test the effect of the control strategy on emissions and efficiency.

A diesel engine with a belted traction motor was connected to a CVT. The output of the CVT was coupled to an engine dynamometer. Friction brakes were mounted between the CVT and the dynamometer to simulate mechanical brakes in a vehicle. The motor was connected to an ABC 150 power processing unit, which would emulate

different battery packs. The engine can be uncoupled via a dry clutch from the system. Figure 2-3 illustrates the physical setup of the system. The CVT, which was modified to work for this application, was the crucial powertrain component to control via the ratio command, since it would dictate the engine operating point.
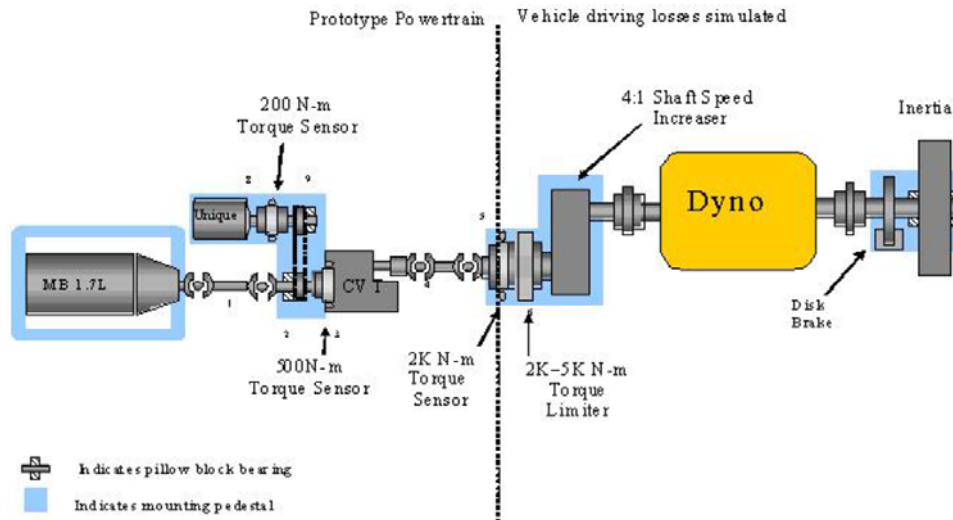
Figure 2-3: Argonne diesel engine parallel CVT hybrid powertrain HIL

The aforementioned PSAT-Pro software was used to control all of the hardware components in the powertrain as well as the vehicle emulation though the dynamometer. PSAT (Ref. 50, Ref. 51, Ref. 52) is a forward-looking model that is based on the bond graph effort and flow principle for each individual component in the simulation. Both of these elements simplify the HIL integration. The forward-looking method enables the command and feedback sequence operation. The component-oriented simulation setup makes it simple to replace a component model using the interface to the physical component.

The setup was first operated as a conventional vehicle with two CVT operation modes. First, discrete ratios were commanded in order to simulate a conventional discrete ratio transmission. In a second test set the CVT was used in the continuously variable mode to maintain the engine in an efficient operating range. On a UDDS cycle, a 10% improvement in fuel economy was measured (including transmission and CVT losses) while all emissions species were reduced significantly.

The hybrid operation used a control strategy intended to minimize fuel usage. The fuel economy improvements in hybrid operation were well above 50% as compared to the baseline case (conventional with the discrete gear ratios). The fuel economy improvement came from engine start/stop operation and pushing the engine operation to higher efficiency operation areas. In this case the NOx emissions were about 40% higher as compared to the baseline case. In response, a new control strategy was devised to minimize the engine operation in the high NOx areas while maintaining operation in

higher efficiency areas. The final fuel economy improvement was 40% compared to the baseline with a measured NOx reduction of 50% as compared to the baseline case.

The setup showed the interaction between the different powertrain components and illustrated the impact of the control strategy and the need to approach the powertrain development and control from a vehicle systems perspective. This particular test setup was the precursor to MATT. One of the lessons learned from this setup was the hindrance caused by lack of modularity. At the end of the project an entirely new powertrain setup would have to be built from a blank page design. Thus, the modular approach idea was generated.

2.3.2. ITAQ's Modular powertrain prototype vehicles

ITAQ (Advanced Transportation Institute of Quebec) recently unveiled their new transportation laboratory (Ref. 53). Along with some state-of-the-art test facilities, a new 'Generic Test Vehicle' (GTV) was unveiled. Unfortunately, no technical information or research is yet published in the open literature and a request for further information was unsuccessful. Some information is available from news releases and the ITAQ online brochure (Ref. 54). The GTV is a vehicle that enables the powertrain to integrate into the front or rear ends of the vehicle. Each end (under hood or trunk) may contain a powertrain module which attaches to the center of the vehicle. Each module is equipped with wheels, brakes and suspension. Three distinct sizes of module units are available to implement different powertrain elements.

It appears that the GTV can be front wheel drive, rear wheel drive and all wheel drive, a feature that makes it a degree of complexity above MATT. In addition, all of the module units are required to hold on the powertrain elements in an integrated unit, whereas different driveline components are individual modules on MATT. The GTV is a self-contained vehicle with no emulated hardware or HIL element. It is truly a more cost effective prototyping approach than a full test mule.

2.3.3. TNO's flexible prototype vehicles

TNO (Toegepast Natuurwetenschappelijk Onderzoek) is the Organization for Applied Scientific Research in the Netherlands. TNO developed the 'Ecofront demonstrator' (Ref. 55). It is a vehicle shell in which a diesel series hybrid powertrain is implemented. The entire powertrain is composed of the actual physical components and no HIL elements were used. The goal was to determine the best fuel economy and emissions trade-offs through system control. The major findings were that the exhaust after-treatment was rather complex because of the engine start/stop behavior. This emissions control issue is not discernable in simulation.

Similar to the GTV, the TNO vehicle uses a fully integrated powertrain and no HIL element. The strength of MATT is the modular powertrain approach and the ability to use HIL elements such a virtual battery pack to increase the flexibility of the powertrain test bench.

2.3.4. Vehicle HIL summary

Argonne's diesel engine powertrain HIL setup preceded MATT, and provided some valuable insight into the larger scale HIL systems, integrating a full physical powertrain along with some emulated elements such as the battery pack. The systems approach to powertrain operation enabled fuel economy improvements and a reduction in emissions. The HIL methodology, process and software are described. Due to the lack of flexibility in integrating or changing to new components or building different architectures, a more modular and vehicle-like HIL setup was built; MATT.

Two modular test vehicles exist, but both are full prototype vehicles with completely integrated powertrain modules. No HIL component is used in these vehicles, thus limiting the breadth of tests that can be performed.

2.3.5. MATT's contribution to HIL

From a hardware perspective, several elements make MATT new and unique. The modular powertrain approach is a novel idea. No other powertrain testbed is built to integrate different powertrain component modules by design. The HIL component on MATT is the virtual scalable energy storage system and traction motor module. With this module, an infinite number of degrees of hybridization can be emulated and tested without any hardware changes. Many of the positive features of other HIL setups are present on MATT, including open source control code, parallel of real time model to full vehicle simulation software, easy instrumentation and physical and measurable means of collecting emissions and fuel economy data.

2.4. HEV and PHEV literature review

2.4.1. Hybrid electric vehicle classification

A discussion of the basic concepts of hybrid electric vehicles along with the benefits and challenges associated with the technology has already been shown in section 1.4.

Modern hybrid vehicle work started to emerge in the mid 1990s. Hybrid vehicles can use more than one power source to move a vehicle. This review will only address electric hybrid vehicles. The hydraulic hybrid system that works well for heavy duty vehicles undergoing frequent stops and starts (such as buses or waste management trucks) and the mechanical hybrids such as the flywheel hybrids (which are found in Formula 1 racing cars) are not considered here. Hybrid electric vehicles are defined by their powertrain architecture, their degree of hybridization and their grid connectivity (Ref. 58).

The major hybrid architectures are parallel, series and powersplit. The parallel hybrid can use either the engine or the traction motor to move the wheels directly. The series hybrid can only use the traction motor to move the wheels while the engine-

generator set can only provide electricity to the electric power bus. A series hybrid could be described as a continuously variable electric transmission. The powersplit hybrid can use a series path to power the wheels via a generator coupled to the engine and the electric traction motor or it can use a direct mechanical path from the engine to the wheels. Powersplit hybrids, such as Toyota and Ford hybrid systems, use planetary gear sets. A parallel hybrid with a generator coupled to the engine can also operate as a powersplit hybrid.

The degree of hybridization refers to the electric power available compared to the engine power available. Typically, a mild hybrid has a low degree of hybridization and uses an engine-dominant powertrain. Mild hybrids are usually limited to engine idle off operation and engine assist as well as limited regenerative braking. Full hybrids have a high degree of hybridization and are capable of extended electric-only propulsion. Some full hybrids, such as series hybrids, have full electric performance. In other words the vehicle achieves its maximum performance without using the engine.

Grid connectivity refers to plug-in hybrids versus non-plug in hybrids. For the last decade manufacturers have fought the perception that hybrid vehicles need to be charged overnight. In fact, all OEM hybrid vehicles currently available for purchase in the market are charge-sustaining hybrids. Recently, when America declared the goal to reduce petroleum dependence by 20% by 2017, the plug-in hybrid spark was reignited, due to its potential for petroleum displacement.

A key component in a hybrid vehicle is the transmission. In fact, most electric motors for hybrid vehicles are directly integrated into the transmission housings. The transmission type, such as CVT or 6-speed automatic, will also dictate the energy management strategy.

Using its virtual scalable energy storage system and scalable motor module, MATT can emulate a large range of hybrid vehicles, from a full hybrid with full electric performance to a mild hybrid to a conventional vehicle. The current hybrid configuration is a pre-transmission parallel hybrid electric vehicle and this is the only configuration considered in this dissertation.

2.4.2.   Hybrid electric vehicle benefits

Comprehensive studies were completed by EPRI (Ref. 56) and Argonne National Laboratory (Ref. 57, Ref. 59) in 2001. The resulting report compared hybrid electric vehicles and conventional vehicles based on fuel economy benefits, emissions, and performance, cost and consumer preferences. It also addressed the commercialization aspect and barriers of the technology. Some of the major findings from 2001 were:

- Hybrids provide the largest fuel economy gain in slow driving
- Parallel hybrids are likely more efficient than series hybrids
- Hybrids also increase the vehicle performance as compared to conventional vehicles
- Hybrid life cycle costs are extremely sensitive to assumptions

- Grid connectivity (or plug-in hybrids) can achieve large reductions in oil use
- The incremental costs for hybrids vary from 12% to 32%.

These reports were published as the first two hybrid electric vehicles came to the US market: the Toyota Prius and the Honda Insight. At the moment the third generations of the Toyota power split hybrids and the Honda parallel hybrids are for sale. Today, all large car manufacturers have their version of charge sustaining hybrid electric vehicles, ranging from mild hybrids to full hybrids.

MATT can use hardware to quantify the fuel economy and emissions benefits. In fact, MATT is built to enable the in-depth analysis of the powertrain performance. The cost, consumer preferences and reliability factors cannot be addressed with MATT.

2.4.3. Hybrid electric vehicle challenges

The hybrid systems add complexity to a vehicle. With complexity comes a cost increase as compared to the conventional vehicle as well as reliability and durability questions. On the emissions front, the vehicle warranties are up to 100,000 miles and 10 years (Ref. 60). This is especially challenging for the battery packs, which are also the main contributor in cost and added weight.

A little known challenge for hybrid vehicles is tailpipe emissions. The hybrid mode enables the frequent engine start-stop operation. Completing an engine start without emissions slip is a difficult task. The engine stop is a crucial part of a clean engine start. Testing performed on charge-sustaining hybrids at Argonne shows that emissions slip can occur (Ref. 61), and when it occurs, SULEV is not attained any more as shown in Figure 2-4.
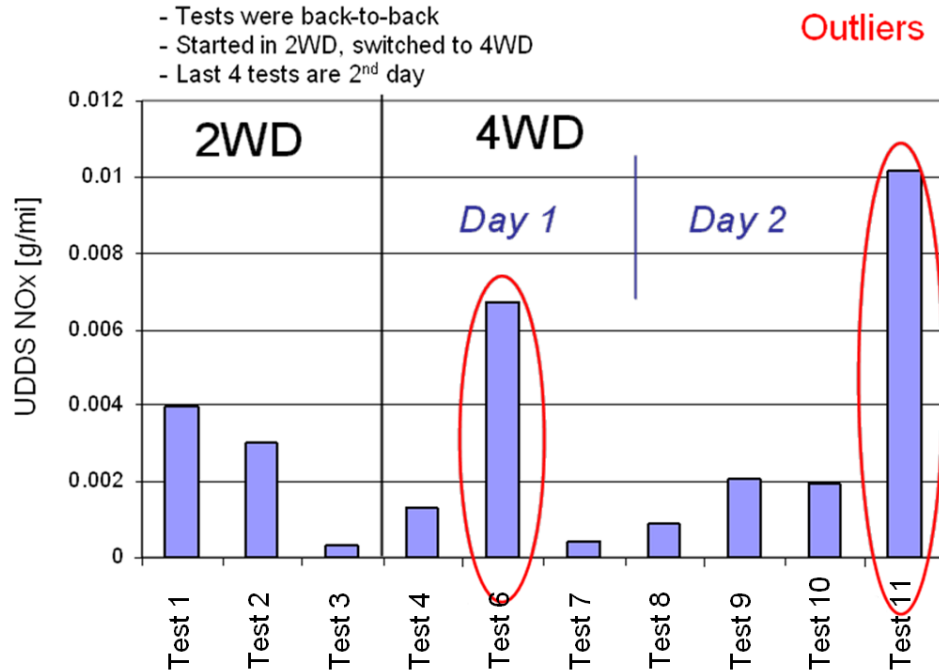
Figure 2-4: UDDS emissions results for a full hybrid tested at the APRF

The hybrid electric vehicle is able to move via two sources. This opens a new dimension in the powertrain control. This new degree of freedom creates energy management and torque split strategy challenges for the powertrain. The control strategy problem involves how to use the engine and electric motor on a transient cycle to minimize the energy consumed and minimize the emissions produced by the powertrain while operating within the constraints of the energy storage system. This work is often developed using simulation, which does not address the emissions accurately. Due to a lack of emissions simulation accuracy, the energy consumption reduction is the first goal of most papers. Other issues that the simulations do not address include drivability concerns and realistic hardware operation limitations. For example, repeated engine on off cycles, where the engine turns on and off within seconds, were used in early simulation models and had a negative effect on all of the aforementioned items. There has been extensive research and countless papers have been written on the topic of energy management and torque split strategies. Some of these are discussed in the next section.

2.4.4.   Hybrid control strategy philosophies

Before embarking on the different control philosophies, one should understand the factors that influence the control strategy development. The following is a brief summary of these factors:

- Vehicle architecture, vehicle size, component sizes and vehicle intent (passenger car versus delivery vehicle)
- Driver inputs such as accelerator and brake pedal. For testing or simulation purposes these are defined by the drive cycle.

- Engine, battery and motor performance and limitation
- State-of-charge (SOC) of the energy storage system
- Engine, motor and transmission efficiency maps as well as battery usage losses
- Shift strategy. This is particularly important for hybrids, which uses a transmission with discreet ratios. The ratio control is also important for CVT and E-CVT hybrids.

These factors are fairly independent of the vehicle architecture and are identical in most papers (Ref. 62, Ref. 63, Ref. 64).

The next information that is important to understand is the vehicle operating mode. Based on the literature, Table 2-1 was compiled (Ref. 65, Ref. 66). A '0' means that no power is transferred in or out of the component. A '+' or a '-' indicates the power flow through the component in that particular mode.

Table 2-1: General modes of operation of a full hybrid vehicle

	Engine	Motor	Battery	Wheels
Idle engine off	OFF	0	0	0
Idle battery charge engine on	ON	-	charge	0
Electric operation only	OFF	+	discharge	+
Electric operation with engine assist	ON	+	discharge	+
Electric operation with engine charging (series mode)	ON	+	Charge or discharge	+
Engine operation only	ON	0	0	+
Engine operation with electric assist	ON	+	discharge	+
Engine operation with battery charging	ON	-	charge	+
Regenerative braking	OFF		charge	-

Table 2-1 is a generalization of hybrid modes based on a power split or a parallel-series hybrid. Some of these modes may not be possible depending on the hybrid architecture.

The final step to address is the power loss, or efficiencies of the different operating modes (Ref. 67, Ref. 68). Boyd has done a very detailed work in this area (Ref. 65, Ref. 69). Since the engine typically is the most inefficient component in the powertrain, the main focus is on pushing the engine operation to higher efficiency areas at higher loads. Using the hybrid system to store and use electric energy also presents inefficiencies which may prove significant. It is important to understand the cost or penalty of the energy used in the different modes.

The energy management and torque split strategy types are numerous. The simplest is the quite effective rule-based control strategy. In the rule-based strategy, the engine is typically turned on based on a combination of driver pedal request and battery state of charge. Once the engine is used, it will operate between an engine optimum efficiency torque speed line and a load following mode where the engine provides the

propulsion power to move the vehicle at higher speeds. Usually, once the engine is used it stays on for a minimum amount of time (Ref. 70, Ref. 35). The vehicle operation is thus often divided into operating modes, or states, as described in Table 2-1 (Ref. 71, Ref. 72, Ref. 73).

Most rule based control strategies can be optimized by varying the mode selection thresholds, such as the engine turn on power demand and the minimum engine torque. As with all optimizations, the results are specific to the given conditions, which are the drive cycles. The issue is that the certification drive cycles do not represent real world driving. In a fuel economy robustness study, Argonne demonstrated that the fuel economy of hybrid vehicle varies more than the fuel economy of comparable conventional vehicles when the drive cycle aggressiveness is changed (Ref. 74). Hybrid vehicles still achieve a better fuel economy than conventional vehicles on the more aggressive cycles, though.

In energy management strategies, the methods for splitting the torque between the engine and the motor are key to higher powertrain efficiencies. Most control strategies assign a cost to using electric energy from the battery pack and relate that cost to using fuel (Ref. 75, Ref. 76, Ref. 77). The costs of the different paths are then calculated and the lowest cost path is used. The National Renewable Energy Laboratory took a similar approach but added an additional emissions cost based on steady state emissions maps for the engine used (Ref. 78).

At this point, the rest of the optimization process uses special techniques such as stochastic dynamic programming (Ref. 35, Ref. 79), fuzzy logic (Ref. 80, Ref. 81, Ref. 82) and global optimization (Ref. 83, Ref. 84, Ref. 85). All of these methods are extremely interesting but do not have relevance to this dissertation beyond proving that there is an incredibly large body of work in the area of control optimization, but that most of these resulting strategies cannot or have not been tested in a vehicle. It should be noted that global optimization techniques only work in simulation and serve as a reference to improve the rules of control strategies.

In summary MATT can serve as an open controller platform to investigate some of these different control strategies with real hardware and provide a full picture with emission data, hardware limitations and a small degree of drivability feedback.

2.4.5.   Plug-in Hybrid Electric vehicles

As mentioned earlier, HEVs were initially divided into two categories based on grid connectivity (Ref. 56, Ref. 58). Plug-in hybrids were envisioned to be the natural follower of the electric vehicle (EV). Hybrid research started just as the electric vehicle period was ending in bitter disappointment with the termination of the only dedicated OEM production electric vehicle, which was designed from a blank page: the GM EV1. There are many theories about the 'death' of the electric vehicle, but the technical explanation from GM is that the majority of the consumers could not live with the electric vehicle range anxiety (Ref. 86). The EV1 could travel between 55 and 95 miles on a single full charge under ideal conditions (Ref. 87). The short range and the variability of the range caused anxiety about getting stranded on the side of the road. In other words, the battery technology was the weak point of the early EVs. These batteries

were good enough as small energy buffers on HEVs, though. One way of classifying plug-in hybrids is as EVs with an engine that serves as a range extender. GM would use the E-REV label, which stands for Electric Range Extended Vehicle.

In recent years, a breakthrough revived the idea of driving using electricity. The lithium ion battery technology made tremendous progress thanks to the consumer electronics market and items such as laptops and cell phones. The lithium ion battery technology is the enabler for today's PHEV (Ref. 88). An ideal PHEV operates as an electric vehicle, and once the battery state-of-charge is low, the internal combustion engine provides the motive power and therefore the range anxiety is eliminated. The progress in lithium ion technology has also prompted a small resurgence of electric vehicles, which now have an acceptable range. One example is the Tesla roadster with an advertised range of over 200 miles (Ref. 89).

In April 2007, President's Bush administration set forth the target of a 20% reduction of fossil fuel consumption in 10 years. In the State of the Union address, plug-in hybrid vehicles were mentioned as a major technology for achieving that goal (Ref. 90). A PHEV with 40 miles of all-electric range is often mentioned as a target on the vehicle technology. A range of 40 miles is used as the benchmark because, based on driving statistics in the United States (Ref. 91), 63% of all people drive less than 40 miles in a day. Therefore, if all vehicles were PHEV with an electric range of 40 miles, 63% of all petroleum could be displaced by electricity (Ref. 92). Plug-in hybrids have significant potential for displacing petroleum and thus enabling the US to rid themselves of the petroleum addiction. The Department of Energy created the Plug-In Hybrid Electric Research and Development Plan in response to the President's initiative (Ref. 93).

The challenges faced by Plug-in hybrids are amplified versions of the challenges faced by the hybrid electric vehicles. The cost of the plug-in battery system is much higher than the cost of the small hybrid battery systems. The ultimate plug-in hybrids are supposed to have full electric performance, which implies much larger and more expensive electric motors and power electronics as well as much added weight to the vehicles. The battery system needs to hold its capacity under warranty. On the emissions front, automotive warranties are up to 100,000 miles and 10 years (Ref. 60). Meeting the emissions standards with plug-ins get more challenging because of the reduced engine operating time, which makes it hard for the exhaust after treatment to maintain effective conversion temperatures. Figure 2-5 shows that all PHEV conversion have increased emissions compared to the stock HEV using data collected at the APRF. That data shows that there is still a far amount of work to be done in the field of PHEVs and tailpipe emissions.
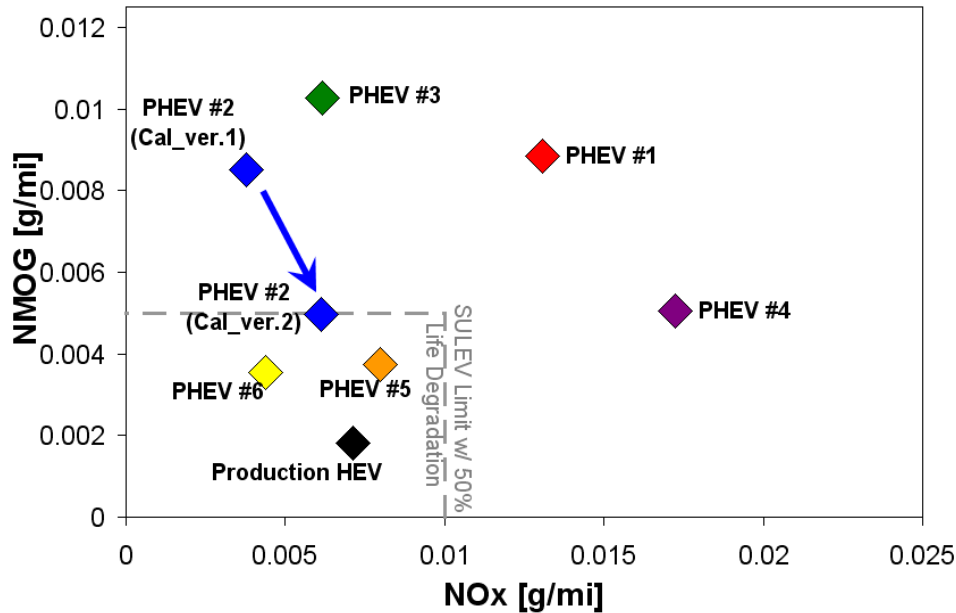
Figure 2-5: FTP Emissions of six PHEV conversions compared to the stock HEV

The electricity used to drive the vehicle has some upstream emissions (Ref. 94). As mentioned in the introduction, a large portion of the electricity in the U.S. comes from the grid, which is generated by coal fire-power plants. These are not as clean as the nuclear power plants which produce the majority of electricity in France. Thus, the total environmental impact of PHEVs depends on the origin of the electricity (Ref. 95). The charging infrastructure is also a challenge to address with plug-in hybrids.

2.4.6.   Test procedures for PHEVs

Since PHEVs use fuel and electricity, the testing and evaluation needs to reflect the consumption of the two energy types. SAE establishes the standard test protocols to test hybrid electric vehicles and plug-in hybrid electric vehicles. The standard, which is referenced as SAE J1171, was first ratified in 1999 and is about to expire in 2009 (Ref. 96). The first version of the standard does not explicitly address the testing of PHEVs but focused on the HEVs which were becoming a reality in 1999. The renewal focuses on the addition of PHEV testing. As plug-in hybrids move from the conversions (Ref. 97, Ref. 98) and early prototypes vehicles to small OEM test fleets in costumer hands (Ref. 99), these test procedures are reviewed. J1711 is a 'Recommended Practice' and the EPA and California can reference or adopt parts of J1711.

Two important types of PHEVs exist (Ref. 100, Ref. 101): the Blended Type and the All-Electric Range (AER). The blended PHEV powertrain (Ref. 102) does not have enough electric traction power to move the vehicle without the engine. Most of the current PHEV conversions based on Toyota's Prius are blended type plug in hybrids. The AER PHEVs are capable of full performance in electric mode only. A series hybrid (Ref. 103) is a good example of an AER PHEV. The Chevrolet Volt is an AER PHEV. The

AER PHEVs are more expensive and more beneficial in terms of petroleum displacement. PHEVs will typically have two operation modes: charge depleting (CD) and charge sustaining (CS). During the charge depleting stage, electric energy is used to propel or help propel the vehicle, thus depleting the battery pack. Once the state of charge of the battery pack is low the vehicle will operate in a charge-sustaining mode where the net electric energy used from the battery is zero. The standard proposed test for PHEVs is a Full Charge Test (FCT) where the vehicle is fully charged overnight and then tested on consecutive certification cycles until an entire charge sustaining cycle is completed. The full charge test provides the picture for all of the vehicle behaviors as shown in Figure 2-6.
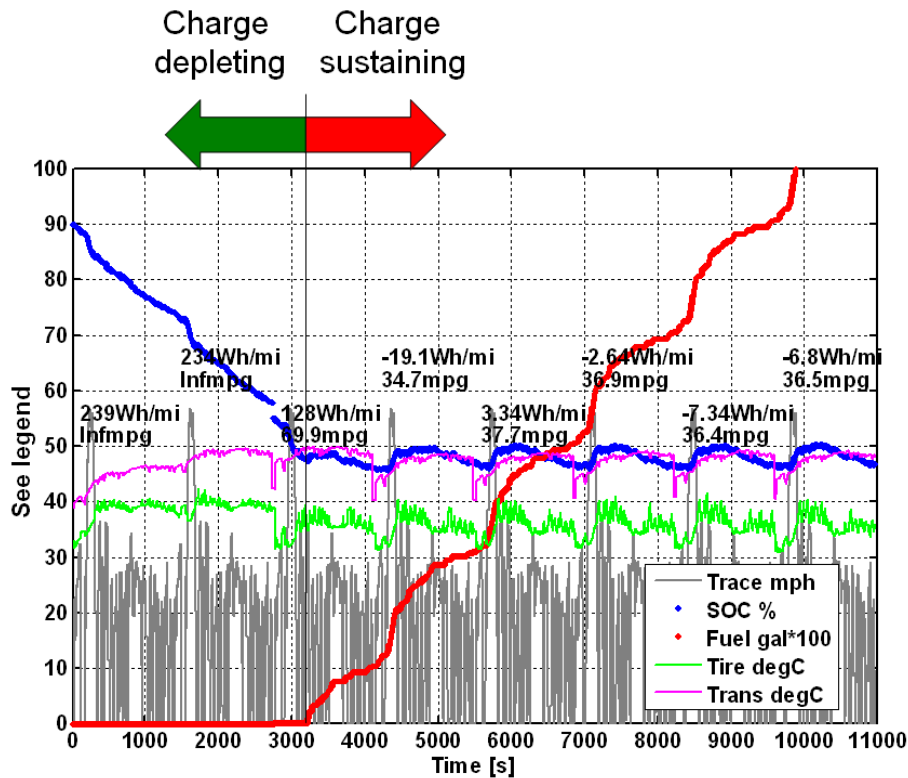
Figure 2-6: Sample Full Charge Test for an AER PHEV

The example here is an AER PHEV based on MATT data. In the first cycle, the engine was never used and therefore the fuel economy is infinite. In the transitional cycle (third UDDS) some of the energy to move the vehicle still comes from the battery, thus, the fuel economy is still high. In the last cycles, the fuel economy is the charge-sustaining fuel economy. Depending on the distance driven with the vehicle between charges, the fuel economy may vary from the CS fuel economy to an infinite number of miles per gallon. Based on current US driving statistics, the proposed representation is to use a weighted fuel economy between CD and CS.

The PHEV applications in this dissertation are mainly special tests that support the development and verification of the proposed SAE J1711 renewal of the testing. With

the virtual scalable energy storage system and scalable motor module, MATT can behave as a blended PHEV and as an AER. With the open control, many special PHEV behaviors can be forced to generate fuel economy, electric consumption and emissions data for the proposed test procedure. The SAE hybrid committee is in the final phases of revising J1711, but an intermediate paper (Ref. 104) provides some insights into the final version.

2.4.7.   Energy management strategies for PHEVs

In terms of the energy management strategy, the major difference between PHEV and HEV is how they handle the charge depleting phase. In the charge-sustaining phase, a PHEV should operate as an HEV. As seen earlier, this leaves many options for the control strategy approach. If the PHEV is an AER, then the CD phase is performed in an electric vehicle only mode. The challenge occurs for blended PHEVs where the energy split between the fuel and electricity used during the CD phase can vary. As more electricity is used to propel the vehicle, the engine load is minimized and the overall engine efficiency is lower. An ideal scenario for a given trip is for the battery to be fully depleted as the driver pulls back into the garage at home at the end of the day. In that case, the electricity used maximized petroleum displacement and the engine operated at the best efficiencies. Again, many different types of optimization studies were performed, but no vehicle can predict what the driver will do next (Ref. 105, Ref. 106, Ref. 107, Ref. 108). Some studies did look at using the in-vehicle GPS information to adapt the control strategy based on the trip length and the topography ahead (Ref. 109). Some other learning algorithms were suggested based on time. For example, every Monday morning, the driver will probably commute to the same work location and come back the same way in the evening.

2.4.8.   MATT's contribution to HEV and PHEV

Again, since MATT has an open controller, any energy management strategy can be implemented and tested with measured fuel economy, electricity consumption and emission data. MATT can provide hardware-based reality check points to support simulation activities. In fact, the DOE PHEV R&D plan specifically points to MATT as the tool of choice for that task. The engine cold start tailpipe emissions did not get much consideration in the control strategy papers review. This is due to the fact that most energy management strategy studies are based on simulations and not hardware. One of the applications demonstrated with MATT in the PHEV area is the mitigation of cold start emissions in PHEVs.

2.5.   *Hydrogen*

2.5.1.   Motivation and scope of this review

The main component evaluation application featured in this dissertation is the calibration and evaluation of a hydrogen engine using MATT. The intent of this section is to provide the background information on the state of hydrogen internal combustion engine research for the application. For those reasons, hydrogen fuel cells, the on-board storage systems and hydrogen direct injection internal combustion engines are mentioned only briefly in this review. The candidate has extensive experience working with integrating hydrogen fuel cells and hydrogen engines in hybrid electric vehicles for the FutureTruck competition (Ref. 110, Ref. 111, Ref. 112) as well as benchmarking a fuel cell hybrid electric vehicle in the APRF (Ref. 113). The ultimate goal of the hydrogen economy is fuel cell powered vehicles because of the high conversion efficiency of the stacks (Ref. 114). Currently, the hydrogen internal combustion engine is considered the bridging technology to the fuel cells (Ref. 115). The internal combustion engines are fairly inexpensive, benefit from a century of development and can burn more than one fuel (Ref. 116). In fact, the multi-fuel capability enables the internal combustion engine to be the bridging technology while the hydrogen infrastructure develops. The consumer can refuel at the local hydrogen station if one exists near his or her home, and while on a trip where no hydrogen station is available, gasoline can be used in the engine as well.

The DOE goals for hydrogen internal combustion engine are a peak brake thermal efficiency of 45% and NOx emissions lower than 0.02 g/mile on the FTP (Ref. 117).

2.5.2.   Benefits and challenges of hydrogen as an automotive fuel

Hydrogen is a renewable and sustainable energy carrier with no carbon content, which makes hydrogen attractive as a 'transportation fuel'. Hydrogen is an energy carrier that can be produced in many ways through electrolysis from different electricity sources, steam-methane reformation, thermochemical processes, biological processes (algae) and photoelectric processes (Ref. 118). Most of the hydrogen today is produced as a chemical feedstock by steam methane reformation, but the potential for clean hydrogen produced through electrolysis using a renewable energy source such as solar power, wind power or hydro-electric power is extremely appealing. In that case, the upstream emissions Well to Wheel (WTW) could be environmentally friendly and cost effective on a large scale. The emissions at the vehicle level are also dramatically reduced since hydrogen does not contain any carbon to produce greenhouse gases (Ref. 120). With a fuel cell stack, the electricity production is truly zero emissions since the electrochemical reaction only produces water vapor. In an internal combustion engine, NOx may be produced with the high temperatures and pressures of the combustion chamber, but with appropriate combustion strategies, the NOx production can be less then 10% of the SULEV limit (Ref. 119). Overall, if used as a transportation fuel, hydrogen from solar and wind could noticeably reduce the greenhouse gases emissions and criteria emissions on a well-to-wheel basis as compared to other alternative fuels.

Hydrogen also presents some significant challenges as a transportation fuel. Although hydrogen has a higher specific energy than most fuels, the challenge is to store enough mass of hydrogen on board a vehicle. Compressed gas storage is the most common method, but it uses a large amount of space in a vehicle (Ref. 112, Ref. 121). Liquid cryogenic storage (Ref. 122) minimizes some of the space usage, but cryogenic storage has some safety concerns as well as 'boil off issues'. Metal hydride storage (Ref. 123) has been demonstrated in some prototype vehicles but the weight of the storage system is too significant to be practical. With all of these systems, the fill up time and the range are major issues. The hydrogen production, distribution and fueling infrastructure is the next major obstacle. Rebuilding a new national and global fuel infrastructure would be prohibitively expensive (Ref. 124). Finally, hydrogen suffers a bit from consumers' preconceived notions and fears. The perceived safety issues still have to be overcome.

2.5.3.   Hydrogen engine configurations

Naturally aspirated port-inject hydrogen engines can suffer a power output loss of half compared to a gasoline engine. This is due to two factors. First, the hydrogen displaces air from the combustion chamber. The liquid fuel only takes up a small volume in the combustion chamber due to its high density. In other words, the low mixture calorific value for hydrogen with stoichiometric combustion alone results in a disadvantage of approximately 30% in the indicated mean effective pressure with external mixture formation (Ref. 125). The second factor involves combustion anomalies at stoichiometric operation with port injected engines. Therefore, most port injected hydrogen engines are operated with excess air (very lean) to prevent preignition, backfires, and knocking (Ref. 126). To overcome the power loss, boosting methods such as supercharging or turbocharging are typically employed (Ref. 127). The combustion abnormalities cannot be avoided in the external mixture formation concepts. Hydrogen direct injection can address these combustion anomalies as well as the low mixture calorific values of port injected hydrogen engines.

The hydrogen engine evaluated on MATT is port injected. To overcome the power loss a belted supercharger boosts the engine. A liquid-to-air intercooler is used to cool the compressed air in the intake manifold. The engine was acquired through Ford Motor Company and built to their standard specifications (Ref. 128). Ford has published their hydrogen engine work in a series of excellent papers (Ref. 129, Ref. 130, Ref. 131). Ultimately, Argonne was able to acquire a hydrogen internal combustion engine, but the cost of a fuel cell system was prohibitively expensive.

2.5.4.   Air/fuel ratio influence

Hydrogen has some properties which are desirable for combustion, such as low flammability limits and fast flame speeds, which allow very lean engine operation. Leaner operation typically results in higher brake thermal efficiency due to reduced pumping losses and heat wall losses so at the same engine speed and load point, the leaner combustion is more efficient. Other beneficial effects of leaner combustion are the lowered combustion temperature and reduced in-cylinder pressures, which reduces the

NOx formation. NOx is the only major emissions criteria produced by hydrogen engines. The formation of NOx from air (21% O2 and 79% N2) is favored by high temperature and pressure. The NOx formation trend as a function of air/fuel ratio is shown in Figure 2-7 (Ref. 132). Around an air/fuel of 2, the NOx production increase exponentially, thus operation at an air/fuel ratio above 2 keeps the NOx production low and keeps the combustion anomalies to a minimum.
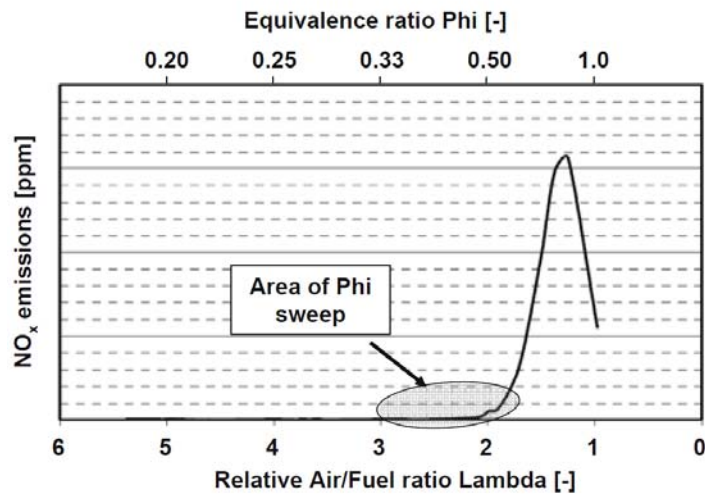
Figure 2-7: NOx production from a hydrogen engine as a function of air/fuel ratio

The lean combustion strategy has a major drawback: the inherent lack of torque due to the minimal amount of fuel that is injected. The reduced power output of port-injected hydrogen engines is in part due to the leaner operating strategies. Typically, the engine combustion strategies are only tested on steady state engine dynamometers where the reduction of power output is just measured and reported. In the vehicle, maximum power output determines performance, a critical feature for the consumer.

2.5.5. Concept study of Phi sweep on a hydrogen powered vehicle

At Argonne National Laboratory, during the course of his day job as research engineer, this PhD candidate performed a study in 2006 that involved testing different constant air/fuel ratio combustions on a hydrogen internal combustion engine pickup truck (Ref. 132). The major conclusion was that the leaner combustion reduced the emissions significantly below the SULEV limit without emissions after treatment while doubling the time required to accelerate from a stop to 60 miles per hour. Those results were as expected. The fuel economy results were surprising in that the leanest combustion achieved the lowest fuel economy. The engine had to operate at much higher average engine speeds because of the reduced engine torque output, thus the average engine loads were lower and the average engine efficiency was lower. Unfortunately, the vehicle was not instrumented with an engine crankshaft torque sensor and therefore the

reasoning is only theoretical. Table 2-2 shows a summary of the expected engine behavior based on air/fuel ratio.

Table 2-2: Qualitative impact of air/fuel ratio on hydrogen engine combustion

	Air/fuel ratio (Lambda)	Efficiency (BTE)	Emissions (NOx)	Performance (Power Output)
Extremely lean	Greater then 2	Higher	Lower	Lower
Lean	Equal to 2	Base	Base	Base
Less lean	Lower then 2	Lower	Higher	Higher

2.5.6. The dissertation's contribution to hydrogen internal combustion engine work

MATT is used to evaluate several constant air/fuel ratios around the 'Area of Phi sweep' labeled in Figure 2-7. In addition to the engine work performed on the engine dynamometer (after which many studies stop), the engine was tested on MATT in the transient environment of standard drive cycles. Therefore, the measured engine fuel economy and emissions related to the vehicle goals set by DOE.

2.6. Literature review summary

MATT is a large-scale powertrain HIL system, or vehicle HIL. MATT provides measured component data that is difficult to model, including emissions and temperature related fuel consumption data. The modular powertrain component approach enables higher flexibility to test different technologies compared to building a more expensive and dedicated prototype mule or component HIL test cell. MATT's virtual HIL component is the virtual scalable energy storage system and scalable motor module which enables it to emulate a wide range of vehicles, from a conventional vehicle to a full EV capable PHEV with a battery pack of virtual infinite capacity. Several modular test vehicles exist but they lack the flexibility of HIL and the ease of instrumentation of MATT. From a hardware perspective, these elements make MATT new and unique.

After brief review of the state of HEVs and PHEVs, it is determined that MATT's open controller enables the evaluation of any energy management strategy with measured fuel economy, electricity consumption and emission data. The engine cold start tailpipe emissions did not get much consideration in the control strategy papers review. This is due to the fact that most energy management strategy studies are based on simulations and not hardware. One of the applications featured in this dissertation demonstrates the reduction of cold start emissions on PHEVs. The tailpipe emissions from the early PHEVs are an issue that requires further investigation. In this application, MATT's open

controller and HIL flexibility is used to develop and mitigate cold start emissions control strategies for PHEVs.

The final phase of the literature review focused on the state of hydrogen internal combustion engines. The second major application featured in this dissertation is an evaluation of constant air/fuel ratios on a hydrogen internal combustion engine. Then, a new and unique variable air/fuel ratio combustion strategy is demonstrated on MATT to combine the best fuel economy and lowest emissions. In this application, MATT's unique modular powertrain approach is used to evaluate a new technology in a vehicle environment.

Based on the review of the literature, it can be stated that MATT is a unique and novel tool to evaluate components and energy management strategies in vehicle environment using the HIL flexibility. In summary, the features that make MATT unique are the powertrain component module approach, the open controller with simulation tool linkage, the virtual HIL scalable energy storage system and scalable motor module and the ease of instrumentation. The two major applications that use MATT in the PHEV area and the hydrogen engine area will contribute to the body of knowledge in both specific areas.

3. MATT: the Modular Automotive Technology Testbed

3.1. Concept: The automotive component bread board bench

3.1.1. The idea described

A modular component powertrain testbed is an alternative solution for testing different technologies in a hybrid vehicle environment while keeping the cost and required resources relatively minimal. MATT is composed of physical hardware component modules including an internal combustion engine and a transmission as well as emulated component modules such an energy storage system. Figure 3-1 shows the modular concept of MATT.
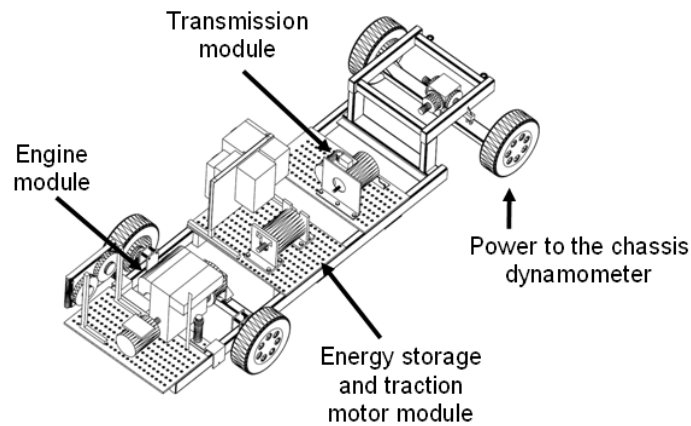
Figure 3-1: Illustration of the Modular Automotive Technology Testbed

MATT can be compared to an automotive "Erector set". The base is a frame with four wheels. Different component modules are bolted to the frame and connected with shafts to compose the hybrid powertrain. The modules are built on ¾ inch thick steel plates with bolt-hole patterns for mounting. Each module is composed of the main component as well as all of the support systems required for its operation. For example, the engine powertrain module has an engine with its ECU (Engine Control Unit), wiring, cooling system, clutch actuation system and extensive instrumentation.

These modules can be 'real' physical components such as an engine or they can emulate a hardware component such as a battery pack and electric motor combination. The real components capture those effects that a simulation may not accurately represent, such as variable losses in components based on temperatures and/or emissions from the engine. The emulated components are defined by models running in a real-time simulation based on physical inputs from sensors. These emulated components then use physical hardware to add or subtract torque from the driveline based on the real-time simulation and the energy management strategy. For example, a single electric motor is

used to emulate a multitude of energy storage systems of varying capacities as well as an electric traction motor model.

3.1.2. Instrumentation benefits

The components and subsystems on the modules are easy to instrument since all parts are open and not constrained by packaging limitations or sheet metal. The instrumentation is individual to each specific module and can be put in place before implementing a module on MATT. The minimum instrumentation should capture all power flows on a module in order to characterize the components and establish drive cycle energy balances. The mandatory sensors for each module are torque and speed sensors. In order to capture tailpipe emissions, MATT is tested on a chassis dynamometer with emissions equipment at Argonne's Advanced Powertrain Research Facility (APRF). A complete description of the APRF is in Appendix 1.

3.1.3. Open controller vehicle platform

The high level controller interfacing with all of the modules and their subsystems commands the components according to an energy management strategy. The controller has three functions:

- *Lower level component control*: The purpose of the lower level component control is to interface with the actuators of the different modules to assure their proper operation. An example of lower level component control is the dry clutch actuator to enable the launch in a conventional vehicle.
- *Energy management and torque split strategy:* The energy management strategy can also be referred to as the hybrid control strategy. This part of the controller decides how to split the torque request from the driver between the engine and hybrid system.
- *Component Emulation:* In some modules the controller also computes a real time simulation using models for energy storage systems and electric machines. These simulations use sensor inputs and generate outputs that are added to the driveline using physical hardware.

3.1.4. Different size vehicle emulation

MATT has been tested to emulate different sized vehicles using a modern chassis dynamometer. Specific vehicle characteristics such as the vehicle test weight and the vehicle road load losses enable chassis dynamometers to apply appropriate force at the wheels to emulate the vehicle. The physical forces are summarized in Figure 1-5. The vehicle characteristics are determined using coast down techniques on a level test track to derive the vehicle loss coefficients. On the dynamometer, the coast down test is repeated and the dynamometer controller adjusts in terms of internal vehicle on dynamometer loss to accurately represent the vehicle as tested on the track.

3.1.5. Synapses of concept

To summarize, the modular approach makes it possible to test different technologies and combinations without having to rebuild the entire vehicle. The physical components provide the advantage of being able to measure component losses (which vary due to thermal conditions) and engine emissions, both of which are difficult to capture accurately in computer simulations. All of the components can be highly instrumented since the modules are open on the testbed and the packaging is not limited by a vehicle body shell. The high level controller is open and can be programmed with any hybrid energy management strategy. On the dynamometer, MATT can even be tested as different sized vehicles.

3.2. *Goals and enabling features of MATT*

MATT is a flexible and unique automotive powertrain tool that enables:

- *the study of physical components* in a conventional and hybrid vehicle system environment on transient drive cycles.
- *the validation or supplementation of some simulation work* (emissions and losses)
- *the evaluation of torque split and energy management* including emissions and thermal related losses of components.
- *the generation of hardware-based data* for a wide range of very specific studies.

The key features that make MATT a flexible tool and help it accomplish its aforementioned goals are:

- *Modular hardware approach.* It enables the system-based testing of different powertrain components in a flexible hybrid vehicle environment.
- *The virtual scalable energy storage system and motor module.* This special hardware module can emulate different battery types and capacities as well as different traction motors. Additional benefits for this module include the ability to recharge the energy storage system instantaneously to a specific and repeatable state of charge.
- *Open controller for energy management and torque split strategy.* Any energy management strategy can be tested on the hardware, including a conventional vehicle operation, an electric vehicle operation and a large number of hybrid control strategies. Special investigations require some specific hybrid behaviors that may not be optimal, and as MATT is an open controller tool it can be especially useful in those situations.
- *Flexible driver options.* MATT has a software robotic driver which provides good test-to-test repeatability in all operating modes. A physical pedal set is also available for an operator to drive MATT as a vehicle.
- *Test facility.* The APRF dynamometer enables the vehicle size emulation capability and provides data acquisition and emissions measurements.

3.3.   *Chronology of the MATT development*

The design and initial construction started in 2004. The frame's basic construction and further elements were laid out. The initial powertrain components were acquired and integrated on the platform. Once the hardware integration was completed the lower level component control development started. During that process several iterations on major hardware components as well as support system components were upgraded or improved to insure better functionality of the vehicle as a whole. Figure 3-2 shows early pictures of the hardware build phase.
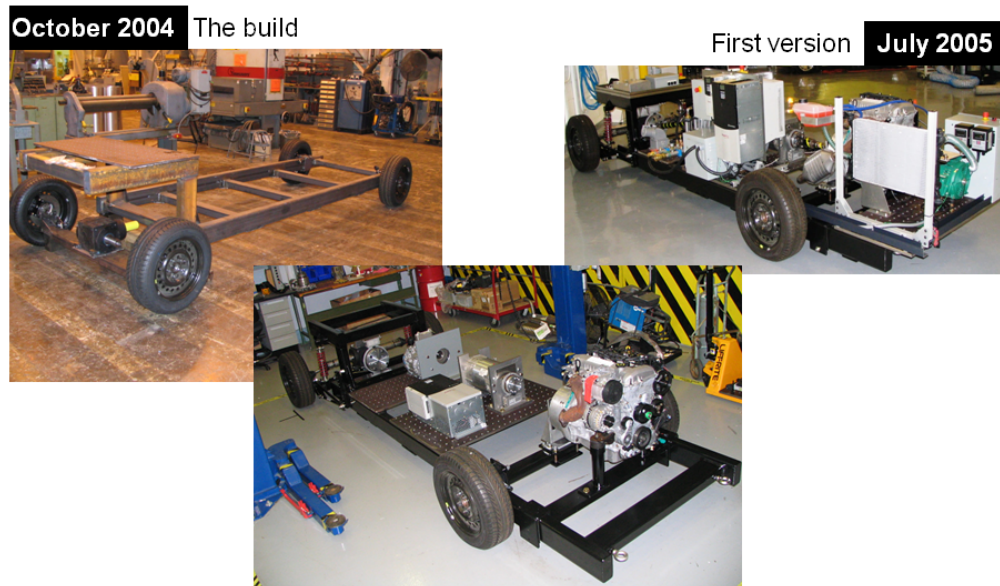
Figure 3-2: Pictures of the initial hardware build up phase

The original transmission was a 6 speed dual clutch transmission from Borg Warner. Despite the fact that after several months of reverse engineering, that transmission was operational, it was deemed unsafe to utilize that transmission since it was possible to engage two gears simultaneously, leading to possible hardware damage and safety hazards. In the summer of 2005 a manual transmission module was implemented.

The original motor was an automotive production AC induction motor. After considerable tuning and calibrating, the motor only provided a fraction of its rated power. A standard industrial NEMA motor was matched to the existing power electronics. Once the new motor was proven operational to peak power, it was modified to operate as a double-ended shaft motor for the MATT platform.

With these major mechanical changes completed, MATT was tested on Argonne's Clayton chassis dynamometer for basic operation. During that phase multiple iterations on the engine coolant system were necessary to emulate a normal vehicle

operation. The instrumentation installed on MATT helped to determine the required engineering changes. During the conventional vehicle operation it became clear that the clutch actuator also required a hardware upgrade. Further clutch system requirements were determined for precision position control for vehicle launch as well as speed control for shifting. The pictures in Figure 3-3 show the early phases of solving the hardware issues.
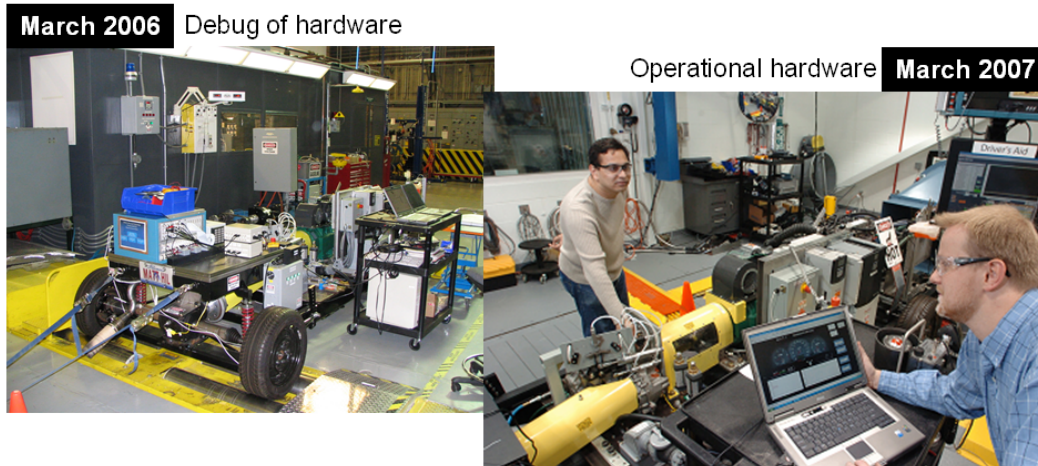
Figure 3-3: Hardware debugging on the Clayton chassis dynamometer as well as the Advanced Powertrain Research Facilities chassis dynamometer

The final hardware breakthrough necessary for MATT to be fully functional was the Engine Control Unit software (ECU) for the gasoline engine. The original engine ECU was not a standalone unit, thus an outside vendor provided a standalone dynamometer unit with stock vehicle combustion strategies. Once the new ECU and wiring harness were implemented, the conventional vehicle operation was successfully achieved with SULEV emissions levels.

In 2007 the first hybrid operations were successfully completed. Throughout 2007, small hardware issues became present and were overcome. The first studies for PHEVs were completed and hardware limitations were discovered in 2007 as well. In 2008, an automatic transmission module was developed to supplement the manual transmission module and the major study on plug-in hybrid control strategy impact on emissions was performed.

The hydrogen engine combustion strategies were investigated on an engine dynamometer starting 2006. Once the combustion research was completed, a novel variable air/fuel ratio combustion strategy was developed based on the findings. In 2008 the hydrogen engine module was constructed and tested on MATT on the standard vehicle drive cycles. Figure 3-4 shows MATT in its latest hardware configuration.
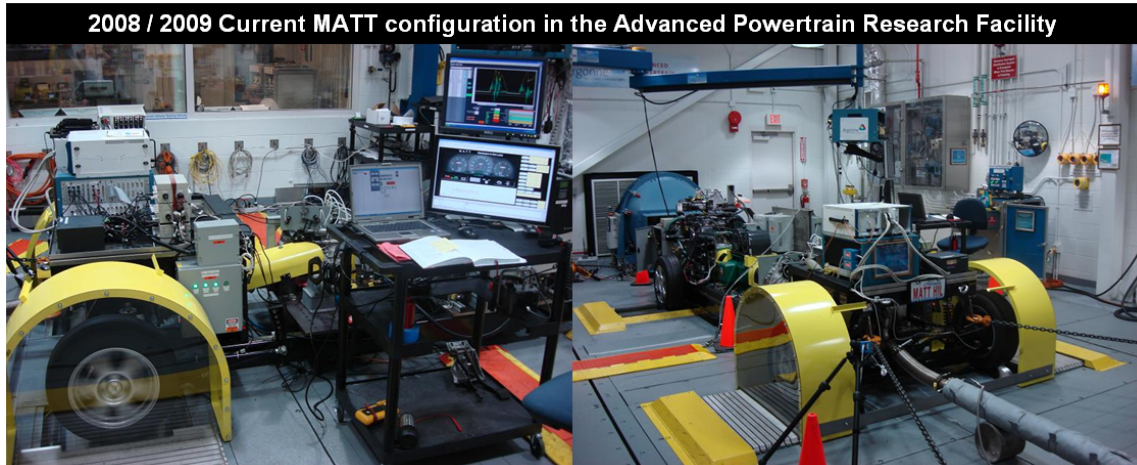
Figure 3-4: MATT shown in the APRF in its current configuration

The timeline described above is summarized in Table 3-1.

Table 3-1: Timeline of the MATT development and studies

	2004	2005	2006	2007	2008	2009 (Today)
MATT design and build phase	■	■				
First wheel spin (Clayton dynamometer)		■				
Conventional vehicle (APRF)			■			
Electric vehicle		■	■			
MALHE Engine calibration breakthrough			■			
Hardware upgrade (doing it right)				■		
Hybrid electric vehicle				■		
Plug-in hybrid electric vehicle				■		
PHEV cold start correction factor study					■	
Automatic transmission module					■	
Conventional vehicle baseline incl. SULEV					■	
PHEV simulation code transfer to MATT (debug)					■	
Phase 1 baseline					■	
Model validation					■	
Phase 2 emissions iteration						■
Hydrogen engine test cell and calibration		■			■	
Hydrogen engine in-vehicle evaluation on MATT					■	

3.4. The final baseline configuration

The current configuration of MATT is as a pre-transmission parallel hybrid electric vehicle. The current setup is composed of a conventional gasoline powered 2.3 liter gasoline engine, an emulated electric propulsion system and a 5 speed automatic transmission. Figure 3-5 illustrates the powertrain architecture of MATT used of all the

work in this dissertation. Figure 3-6 shows an overlay of a powertrain schematic overlaid with a picture of MATT.
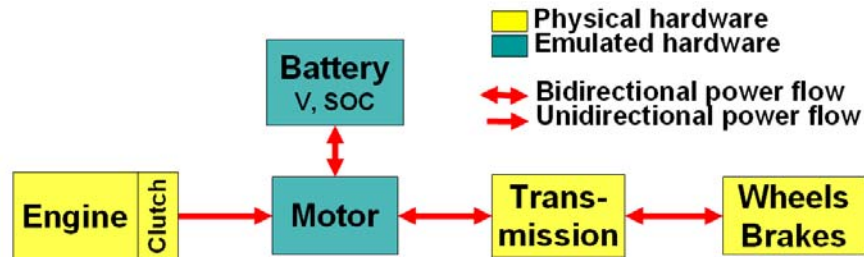
Figure 3-5: The powertrain architecture used for MATT in this work
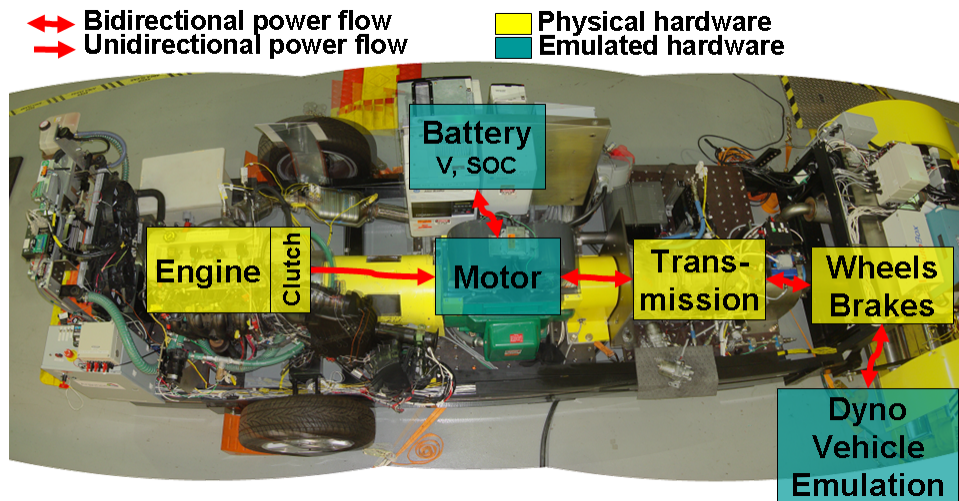
Figure 3-6: Top view of MATT with component schematic overlay

The engine has a conventional dry clutch and thus can be disengaged from the rest of the driveline. The physical electric motor is only used to provide torque based on the real time simulation of an energy storage and traction motor model. The automatic transmission has been modified to transfer reverse torque for regenerative braking and to allow electric launch with the motor only. Together, these components enable different vehicle operating modes.

MATT's operating modes are:

- *The conventional vehicle.* By using the engine, the conventional clutch and the transmission and by bypassing the motor, MATT operates as a conventional gasoline vehicle. The conventional vehicle sets the baseline for fuel economy and emission data as comparison for the hybrid operation.
- *The electric vehicle.* By disengaging the engine with the clutch, MATT operates as a pure electric vehicle. Using models of the hardware, MATT is

able to emulate small and large motors as well as different battery technologies with various capacities and power levels.

- *The hybrid electric vehicle.* By using the virtual scalable motor emulation, different types of hybrids can be tested, ranging from a mild assist hybrid with engine start-stop to a full EV capable hybrid. Plug-in hybrids are also possible since MATT can easily emulate the large battery pack required.

3.5.   *Major powertrain modules available*

3.5.1.   Gasoline engine module

The gasoline engine module is composed of a gasoline engine, the ECU, an exhaust after treatment, a coolant system, a clutch actuator, a 12V starter and instrumentation. The engine module layout is presented in Figure 3-7. Table 3-2 shows the engine specification. This engine size is used in small sedans and small crossover SUVs.
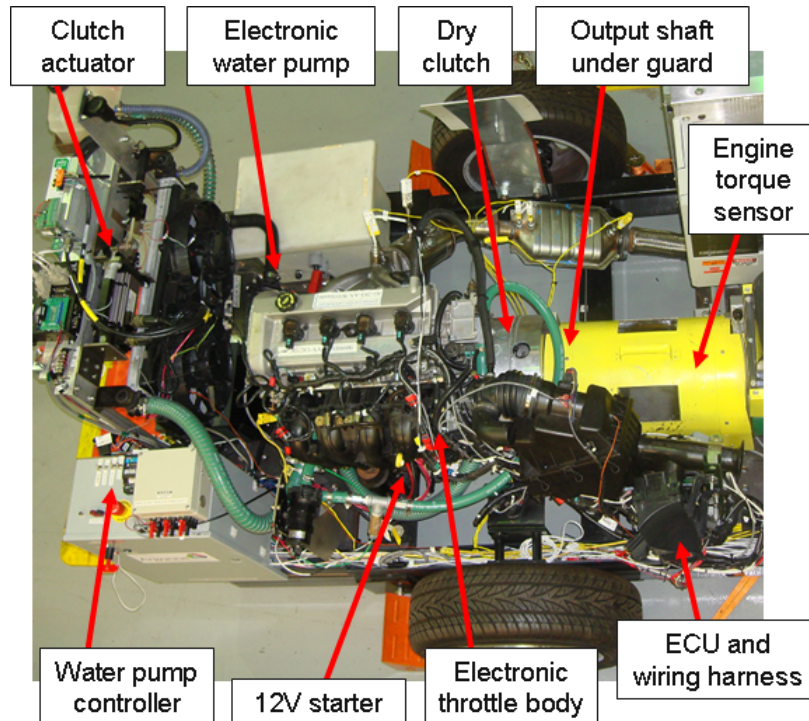
Figure 3-7: Top view of the gasoline engine module

47

Table 3-2: Gasoline engine specifications

Displacement	2.3 liter
Engine type	Inline 4 cylinder 16 valve DOHC (no variable valve timing) Naturally aspirated
Family	DURATEC
Fuel	Gasoline (certification fuel) Port injected
Calibration	Stock calibration
Throttle control	Electronic throttle control
Exhaust	Two stock catalysts
Max torque	180 N.m @ 4000 rpm
Max power	100 kW @ 5000 rpm

The engine is a production engine with its stock ECU. The electronic throttle is controlled by the ECU based on the acceleration pedal position and engine feedback. MATT's high level controller commands engine torque by sending a virtual pedal position signal to the ECU.

The engine uses a standard automotive 12V starter for cranking. That starter is wired to be computer controlled. The crank time is limited in the software to prevent hardware damage. The controller switches the ignition to the ECU for engine start and stop. In hybrid mode the engine can also be bump started by engaging the clutch while the electric motor is already spinning since a conventional 12V starter would not be used for hybrid start/stop operation.

The engine exhaust system is built with all of the components used in a production vehicle. From the exhaust headers the gases runs through two catalytic converters, then through the exhaust pipe under the vehicle, and finally through a silencer and muffler before coming out at the end of the testbed. The catalytic converters are instrumented with thermocouples as well as a wide band oxygen sensor. The exhaust setup is presented in Figure 3-8.
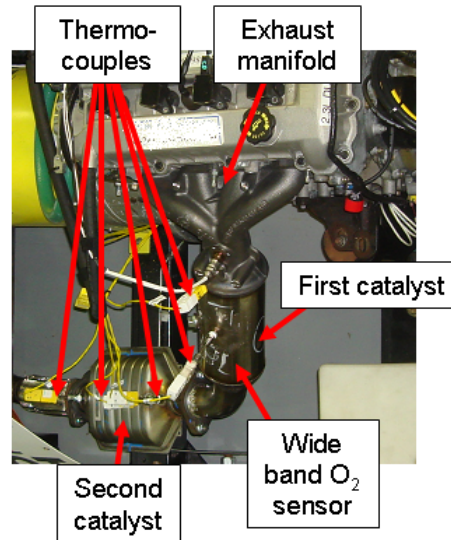
Figure 3-8: The engine exhaust setup and instrumentation

During the tests, the exhaust gases are collected and analyzed in a Pierburg AMA 4000 5 gas analyzer bench (HC, CH4, CO2, CO, NOx). Exhaust sample bags are filled with diluted exhaust gases. At the end of the test, the bags are analyzed to provide the total emissions information and the fuel economy based on the carbon balance. The exhaust gases are also continuously analyzed, providing modal information that gives insight into the transient engine emissions behavior. This becomes increasingly important for hybrid operation, especially of the plug-in hybrid operation. Plug-in hybrid use more electricity as a charge sustaining hybrid, thus the engine typically remains OFF more frequently and for longer periods of time, which causes the engine temperature and catalytic converter temperature to be lower compared to a conventional vehicle. Typically the engine start emissions can be responsible for 90% of the total emissions on a drive cycle.

Fuel is provided by a stock vehicle fuel pump to ensure proper delivery pressure. A positive displacement fuel scale measures the volume of gasoline delivered to the engine. The instantaneous fuel flow compliments the modal information from the calculated fuel flow by the emissions bench. The flow measurement captures transients and dynamics of the fuel flow more accurately. Along with the engine torque and speed sensor mounted on the output shaft of the engine, the quasi-instantaneous engine efficiency can be measured. Figure 3-9 shows an example of calculated instantaneous brake thermal engine efficiency.
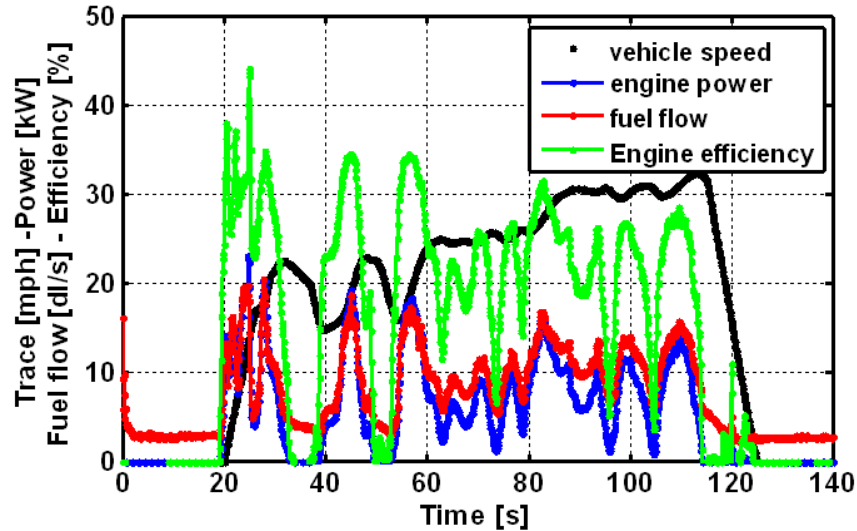
Figure 3-9: Engine data from the first mode of the UDDS in conventional vehicle operation

The data in Figure 3-9 was collected while MATT was running a UDDS as a conventional vehicle. The launch used the dry clutch and MATT shifted with the 5-speed automatic transmission. During gear shifts the inertia of spinning elements becomes significant and causes torque spikes. The spikes during shifts are reflected in the calculated engine power data, thus causing spikes of calculated brake thermal efficiencies higher than 35%. The spikes that are greater than 35% are not a true efficiency number. Post processing of measured data with estimates of rotating inertias can be used to correct the engine efficiency estimates and provide an overall energy balance.

Additional instrumentation includes in-cylinder pressure sensors installed in cylinders 1 and 3. The crank position is resolved with an encoder. A high speed data acquisition system records the pressure traces for individual combustion cycles in both cylinders. With this system, indicated mean effective pressure, also known as indicated torque, is calculated and the mechanical engine losses are inferred. Engine catalyst warm up behavior is also observed using the pressure traces. During the warm up phase the peak pressures are lower and the combustion duration reach into the exhaust valve opening.

Table 3-3 summarizes the instrumentation on the engine module.

Table 3-3: Summary of engine module instrumentation

	Element measured	Sensor
Power input	▪ Fuel flow ▪ Fuel use from carbon balance	▪ Positive displacement fuel scale ▪ Emissions bench
Power output	▪ Engine brake torque and output speed	▪ High accuracy torque and speed sensor
Module specific	▪ Indicated mean effective pressure	▪ In-cylinder pressure sensor with indicating system
	▪ Engine emissions	▪ Emissions bench
	Other elements to understand operation	Thermo-couples, pressure sensors, wide band O2 sensor, flow sensor. ECU provided data among others

The coolant system is set up to work with different engines with and without an internal water pump. In the coolant system a variable flow pump pushes the water/glycol mixture through the system. The pump controller uses a temperature probe to vary the flow to achieve a target temperature. During a cold start, when the engine needs to warm up fast, the flow is slowly pulsed. A cold start refers to an engine which it at ambient standard temperature. Conversely, the pump will operate at a high flow if the engine is already hot and under high power to reject more heat. To ensure that the temperature probe for the controller measures an appropriate temperature, an auxiliary pump flows coolant though the engine block. This is important during a cold start because otherwise the coolant flow may be so slow that the probe might only register the hot coolant after the coolant in the block has overheated. In the test cell a vehicle wind simulator fan provides air flow across the radiator. If more heat rejection is required, two automotive pull fans on the radiator are triggered by a thermal switch at the radiator inlet. Figure 3-10 illustrates the coolant system setup. The gasoline engine used on MATT does not have an internal mechanical belt driven water pump. The target temperature of the variable flow coolant pump is set to 90 deg C. The fans are set to turn on at 95 deg C.
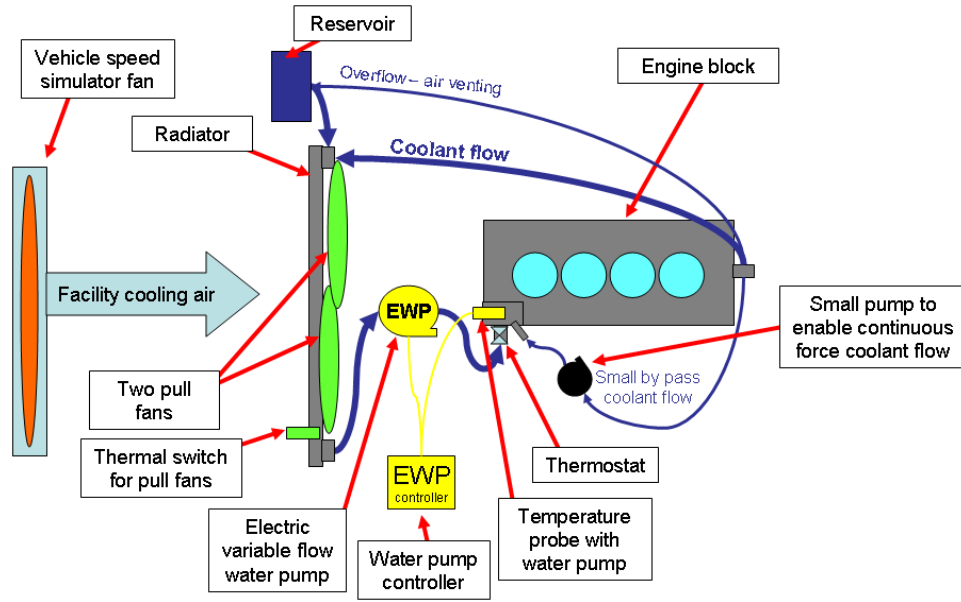
Figure 3-10: Schematic of coolant system for the engine

Another major subsystem on the engine module is the clutch actuation mechanism. The engine is equipped with a standard automotive dry clutch. That clutch has two functions; 1. as the launch device for the vehicle in conventional operating mode and 2. to disconnect the engine from the rest of the driveline during shifting or in hybrid operation. The first function requires the clutch actuator to perform a position control problem to find the clutch engagement point and then slowly engage the clutch to transfer engine torque without stalling the engine to launch the vehicle forward. The second function requires the actuator to perform a fast disengagement and reengagement of the clutch so that the shift time is as short as possible. The actuator pushes directly on the master cylinder, thus eliminating the mechanical advantage of the clutch pedal. Therefore, the actuator needs to be a position control device that can push 400 lbs of force over 1 inch in less than a half of a second. The third and final iteration of the clutch actuator, which fulfills the above requirements, is shown in Figure 3-11.
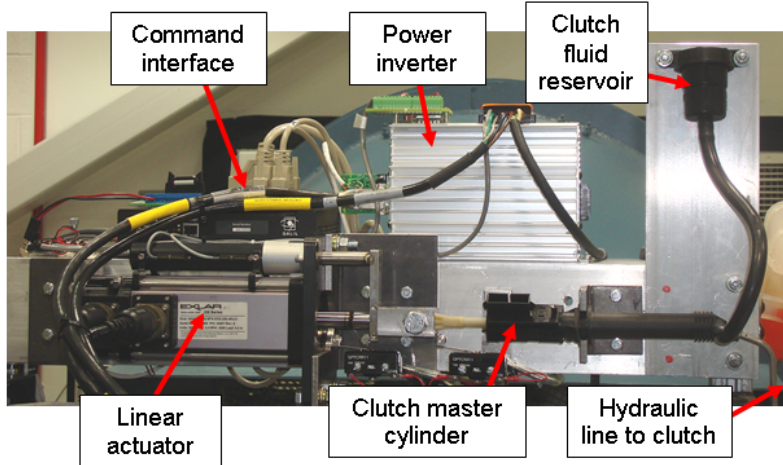
Figure 3-11: Position control actuator system for the hydraulic clutch

3.5.2. Hydrogen engine module

The hydrogen engine module is similar to the gasoline engine module. It is composed of a supercharged hydrogen engine, an aftermarket ECU with in-house calibrations and extra safety systems. The hydrogen engine module layout is presented in Figure 3-12. Table 3-4shows the engine specifications. For comparison, this engine is the same base engine used in the gasoline module.
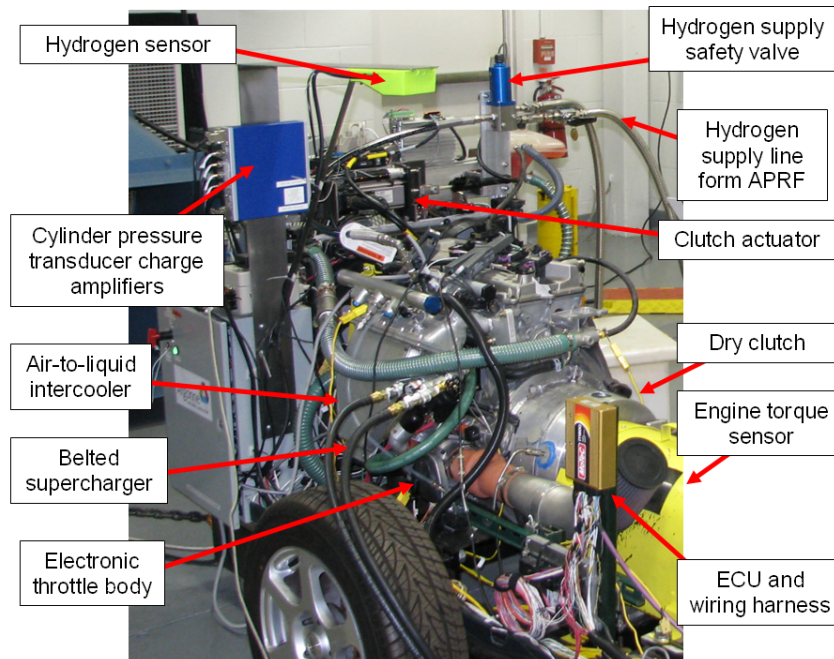
Figure 3-12: The hydrogen engine module mounted on MATT

Table 3-4: Hydrogen engine specifications

Displacement	2.3 liter
Engine type	Inline 4 cylinder 16 valve DOHC (no variable valve timing) Belted supercharger
Family	DURATEC
Fuel	Hydrogen (99.999% pure) Port Injected
Calibration	Calibrated by researcher
Throttle control	Electronic throttle control
Exhaust	No exhaust after-treatment
Max torque	180 N.m @ 3000 rpm (calibrated to 3000 rpm for combustion stability)
Max power	56.5 kW @ 3000 rpm

The hydrogen engine was obtained in a collaborative effort with Ford Motor Company but it was not provided with any ECU or calibration information. Thus the engine had to be calibrated on an engine dynamometer in Argonne's hydrogen engine test cell. The engine was fully instrumented including in cylinder pressure transducers in each cylinder. Several calibration strategies were developed including a novel variable air fuel ratio combustion strategy. Further details about the hydrogen work are presented in Section 9.

The exhaust system does not have any after-treatment devices. Since hydrogen is a carbon free fuel, the combustion of hydrogen only produces NOx as a tailpipe emission. The tailpipe emissions sampled are raw engine-out exhaust. The AMA 4000 is still used to sample all 5 gases, but the NOx analyzer results provide the only relevant emissions. In addition to the emissions bench, a hydrogen exhaust content sensor and a water analyzer were used during the hydrogen engine testing to further qualify the engine performance.

The APRF, a fully hydrogen rated vehicle test facility, supplied the hydrogen for MATT. The APRF has an integrated hydrogen supply and metering system. The hydrogen is stored outside in bundles of 12 cylinder packs. In the test cell the hydrogen distribution system integrates all of the safety systems, the final vehicle pressure regulation and the hydrogen mass flow meters.

Additional instrumentation includes in-cylinder pressure sensors installed in all four cylinders. The crank position is resolved with an encoder. A high speed data acquisition system records the pressure traces for individual combustion cycles in both cylinders. With this system, indicated mean effective pressure, also known as indicated torque, is calculated and the mechanical engine losses are inferred.

Table 3-5 summarizes the instrumentation on the hydrogen engine module.

Table 3-5: Summary of hydrogen engine module instrumentation

	Element measured	Sensor
Power input	▪ Hydrogen mass flow	▪ Mass flow sensor
Power output	▪ Engine brake torque and output speed	▪ High accuracy torque and speed sensor
Module specific	▪ Indicated mean effective pressure	▪ In-cylinder pressure sensor with indicating system
	▪ Engine emissions ▪ Hydrogen content in exhaust	▪ Emissions bench ▪ Exhaust hydrogen content sensor
	Other elements to understand operation	Thermo-couples, pressure sensors, wide band O2 sensor, flow sensor. ECU provided data among others

The coolant system and the clutch system are exactly as the same in the hydrogen and gasoline engine modules.

3.5.3.   Virtual scalable energy storage and scalable motor module

A key feature of MATT is the virtual scalable energy storage and scalable motor module. A physical motor on the module provides positive or negative torque to the driveline just as it would in a hybrid powertrain. The physical motor drives get their power from the electric power grid in the test facility instead of from a battery pack, which is the power source in most hybrids. The motor is an AC induction machine selected for its fast transient response. The motor was modified to have a double end shaft in order to couple to the engine and the transmission. Figure 3-13 shows a picture of the motor module's physical hardware.
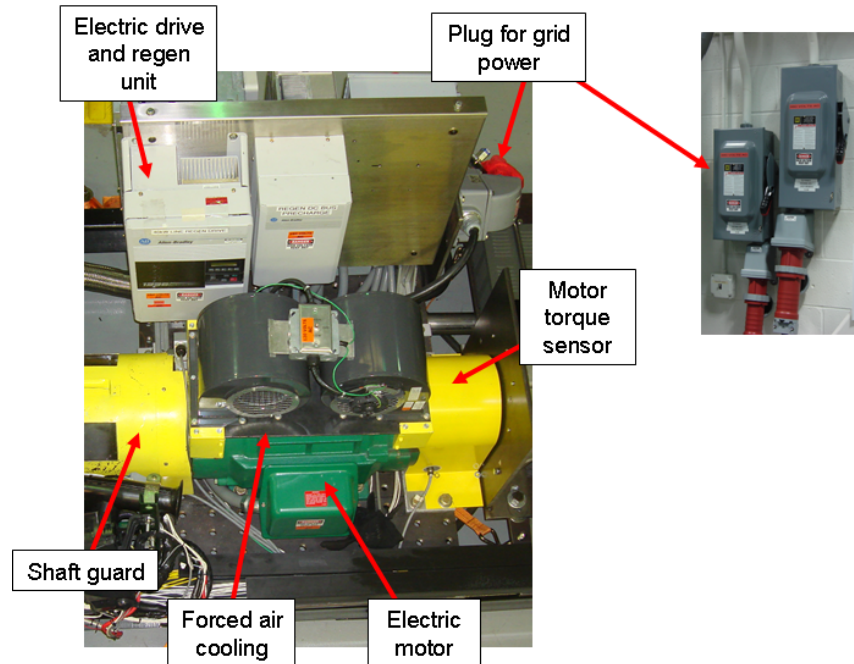
Figure 3-13: Top view of virtual scalable energy storage and scalable motor

The virtual scalable energy storage system and the virtual scalable motor are defined in a real time simulation in the hybrid vehicle controller. The principles of component hardware-in-the-loop (HIL) are used here. The hardware interacts in parallel with a real time simulation of component models and the physical hardware feedback from MATT. Figure 3-14 illustrates this interaction. When the energy management system requests a given torque from the motor, the controller first verifies that the virtual motor and the virtual battery pack can provide the requested current and the torque. The controller then sends the torque command or the maximum available torque command to the physical motor. Next, the virtual current is derived from the commanded torque based on the motor model. That current is applied to the virtual battery pack model where the simulation tracks voltage and state-of-charge. Battery temperature is not included in the model.
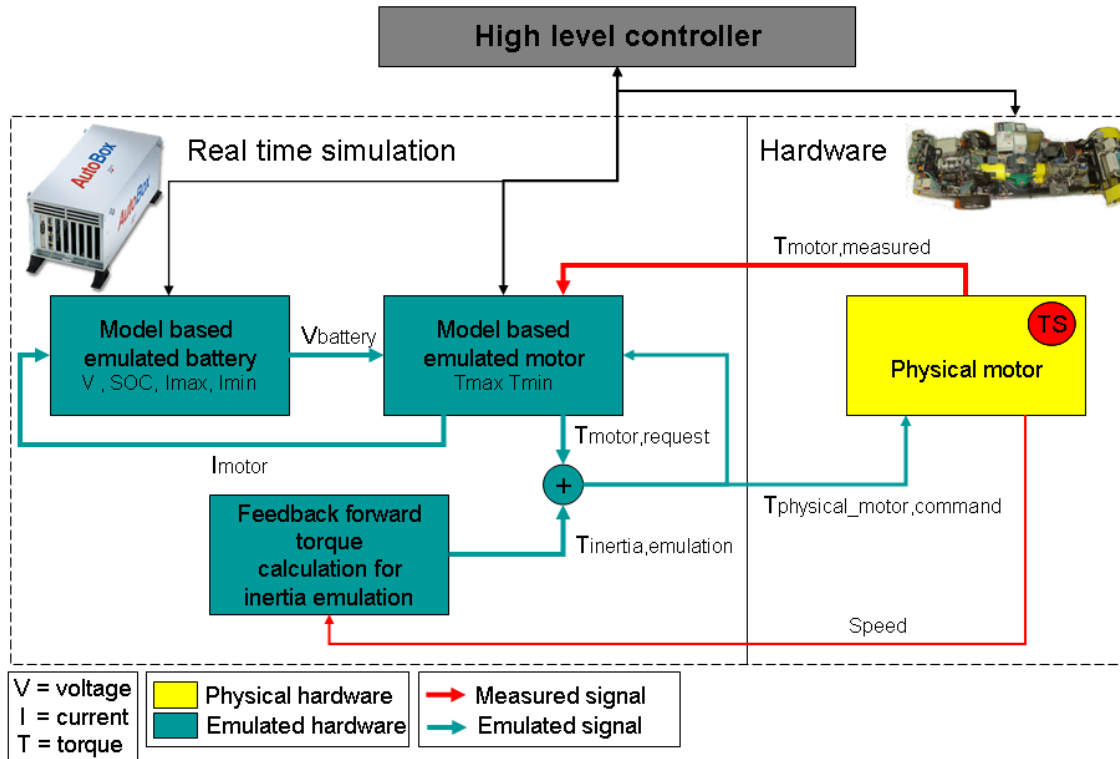
Note: Only the electric traction load is shown and the ancillary loads are omitted for simplicity's sake.

Figure 3-14: Component hardware in the loop logic for the virtual scalable motor module

Another notable aspect of the virtual scalable energy storage and scalable motor module is the motor inertia emulation mode. The controller measures motor speed and speed change to calculate the torque required to cancel the physical motor's inertia as well as the reaction torque that inertia of the virtual motor would add to the driveline. The inertia emulation brings the virtual scalable motor module a step closer to reality. During extremely fast transients such as gear shifts, both the physical and emulated inertia torques are too high for the physical motor to accurately execute the emulation reliably, but these events are short and represent a insignificant amount of energy on a drive cycle.

The main limitation of the virtual scalable energy storage system and motor module is the true capability of the physical motor. The physical motor is an AC induction limited to a maximum torque of 200 N.m and a base speed to 2880 rpm. The maximum electric power from the test facility is 48 kW. To return power to the grid a regenerative unit is used, which is limited to 36 kW. Using these constraints, the operating regions of the physical motor are defined in Figure 3-15. Also shown are motor torque-speed data points from an actual test of MATT emulating a full electric vehicle version of a 3750 lb small crossover SUV with a single gear on an UDDS (Urban Dynamometer Driving Schedule).
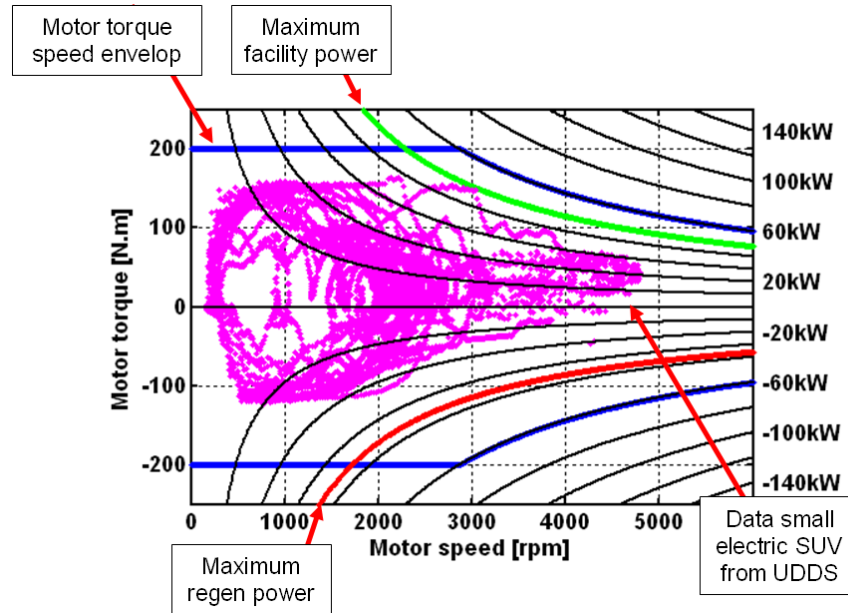
Figure 3-15: Limits of the physical motor overlaid with the motor torque speed requirements for a small SUV on a UDDS

The current hardware is sized to emulate an electric vehicle up to a small SUV on the UDDS. The propulsion system cannot quite supply enough power for an SUV during the US06, which is the most aggressive cycle in the standard selection. The power levels are high enough for a mid size sedan to meet the US06 trace demands.

Although the motor is not rated to run continuously at 60 kW, the propulsion system is adequate since the drive cycles are transient in nature. In other words, higher power demands only occur during high-speed accelerations. For the example given in Figure 3-15, the peak power is close to 50 kW, which occurred during the high-speed acceleration of the 2nd mode on the UDDS. Conversely, the average positive propulsion power on the cycles is 10 kW for the small SUV, a number that is well within the continuous rating of the physical electric machine.

The virtual scalable energy storage system and motor module can actually emulate a motor that is larger than the physical motor as long as the torque speed profile is within the operating envelope of the physical machine. That torque speed envelope is determined by the vehicle's characteristics and the drive cycle.

An essential element of the emulation is based on the simulation and the fidelity of the component models. The real time simulation occurs in the controller that manages the higher level energy management and torque split strategy as well as the lower level component control. The code is based on Argonne's Powertrain System Analysis Toolkit (PSAT), which is a forward-looking vehicle simulation tool. Currently, the electric motor is based on a UQM 75 motor and the energy storage system model emulates a 41Ah lithium ion battery pack intended for plug-in hybrid applications. Both models have been validated against physical hardware data. The models include efficiency maps as well as constraints that limit the component operation to the limits of the physical hardware. The

entire electric vehicle emulation has been correlated to hardware in Argonne's APRF as shown in section 6.4.

The key feature of this virtual inertia scalable motor module is the flexibility to emulate different battery technologies and electric motors. The energy storage system can be changed to facilitate different technologies and capacities in software without having to change any hardware. The motor emulation capability ranges from no motor or a small hybrid assist motor to a full EV capable electric machine. This module is extremely useful for Plug-in Hybrid Electric Vehicle (PHEV) studies.

Some other benefits beyond sizing flexibility are as follows:

- *'Instant recharge'*. The virtual battery system is recharged from any SOC at the click of a button. For most Plug-in hybrid vehicles the charge time ranges from a few hours to a full night depending on the battery capacity and the charger used. This significantly shortens the time in the test cell between tests.

- *'Start SOC repeatability'*. The charging is not only instantaneous but repeatable. The battery can be charged to the exact same SOC for several tests in a row. This is practical for studies where minimum variability from test to test is crucial. An example is given in section 8.2.

- *No battery degradation.* The virtual battery does not experience degradation over time. It cannot be damaged even if extremely deep discharge cycles are put on the battery.

- *Low cost.* Compare to a full battery pack especially plug-in hybrid battery packs this module was cheap to build.

- *Safety.* Some battery technologies, such as Lithium Ion batteries, exhibit some sensitivity to higher temperature which can cause some safety concerns. The virtual battery has no hardware safety concern.

The instrumentation on this electric propulsion module is composed of an input torque speed sensor shared with the engine and an output torque speed sensor. The rest of the power and energy flow information are collected from the real time simulation. Table 3-6 summarizes the instrumentation on the virtual scalable energy storage system and motor module.

Table 3-6: Summary of motor module instrumentation and saved signals

	Element measured	Sensor
Power input	▪ Input torque ▪ Input speed	▪ High accuracy torque and speed sensor
Power output	▪ Output torque ▪ Output speed	▪ High accuracy torque and speed sensor
Module specific	▪ Battery	NOTE: The following signal are generated in the real time simulation: ▪ Voltage ▪ Current ▪ SOC ▪ Maximum discharge current ▪ Maximum charged current
	▪ Motor	▪ Torque command ▪ Maximum propulsion torque ▪ Maximum regenerative braking torque

3.5.4. Manual transmission module

The first transmission module is a manual transmission module. It is a 5-speed manual transmission that was modified to be computer shifted. Due to the mechanical integration complexity, a clutch is not yet used in this transmission. Therefore, the electric motor is directly coupled to the transmission input shaft. The transmission is designed for a transverse application, but used in a longitudinal application, thus the differential is welded up and only one output is connected to the rear end. Note that for this transmission, the rear end is a high efficiency bevel gear box with a 1-to-1 ratio. Automotive half shafts connect the bevel gear box to the wheel hubs and wheels. A 5000 N.m torque speed sensor is installed between the transmission output and the bevel gear box input. The hardware is shown in Figure 3-16 and defined in Table 3-7.
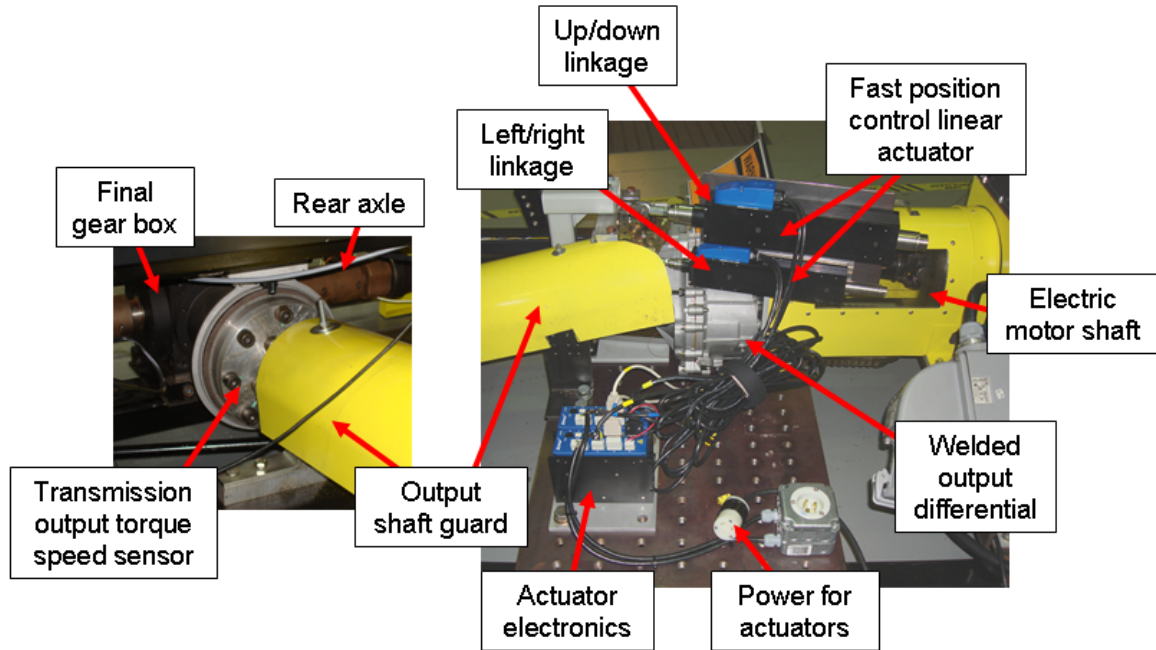
Figure 3-16: Manual transmission hardware

Table 3-7: Manual transmission characteristics

Transmission type	5 speed manual	
Family	Ford MTX	
Architecture	Transverse	
Automation	Computer shifted via linear actuators acting on the shift linkage (version 2)	
Mechanical modification	Welded internal differential and single output used	
Gear #	Ratio	Vehicle speed at 1000 rpm
1st	13.11	5.2 mph
2nd	8.21	8.1 mph
3rd	5.56	12.1 mph
4th	3.95	17.3 mph
5th	2.95	23.5 mph
Final drive ratio	1	

The shift is performed by position control actuators which act directly on the shift linkage on the manual transmission. Since there is no clutch between the transmission and the electric motor, the shifting is a bit more complicated. On a shift request, the transmission is shifted to neutral once the torque input and output are zeroed. Then, the electric motor is active, speeding up or down to the transmission input speed required in the next geared, based on wheel speed. Once a speed match occurs between the

transmission input shaft and the motor shaft, the next gear is engaged by the actuators in the linkage. Unfortunately, this increases the shift time significantly compared to an automatic transmission shift time. The exact details of the shift algorithm are detailed in section 5.3.2.

The instrumentation on the manual transmission module includes an input torque speed sensor shared with the electric motor and an output torque speed sensor. Further instrumentation includes a thermocouple in the transmission oil pan and one in the transmission case. Table 3-8 summarizes the instrumentation on the manual transmission module.

Table 3-8: Summary of the manual transmission module instrumentation

	Element measured	Sensor
Power input	▪ Input torque ▪ Input speed	▪ High accuracy torque and speed sensor
Power output	▪ Output torque ▪ Output speed	▪ High accuracy torque and speed sensor
Module specific	▪ Oil temperature ▪ Case temperature	▪ Thermocouples ▪ Engaged gear ▪ Engine clutch position

The manual transmission module was intended as a starter transmission module since it is easiest to implement and can be used to debug the other hardware. After the initial manual transmission module was finished, an automatic transmission module was started. The manual transmission module is currently being upgraded with a dry clutch at the transmission input to overcome the shift time shortcomings.

3.5.5.   Automatic transmission module

This module uses a 5-speed automatic transmission. For the electric vehicle and hybrid application on MATT, the automatic transmission is modified to accommodate two additional functions:

- *Electric vehicle launch.* An automatic transmission launches the vehicle using the torque converter with the engine idling. In the electric launch mode it would be very inefficient to run the motor at 1000 rpm and launch using the torque converter. The converter was therefore removed. An auxiliary pump now provides the pressure required to close the clutches and hold the gear until the input shaft spins and thus the internal pump spins fast enough to provide the transmission line pressure.

- *Reverse torque capability.* For regenerative braking negative or reverse torque is transmitted through the transmission. To allow reverse torque transfer all the way to zero vehicle speed in 3rd, 4th and 5th gear some mechanical modifications

were implemented, thus enabling regenerative braking. Further detail is provided in section 6.3.1.

A solid axle rear end holds the differential that is paired with the automatic transmission module. The final drive ratio in the differential can be changed to accommodate different overall gearing. A 5000 N.m torque speed sensor is installed between the transmission output and differential input. Figure 3-17 shows the hardware implementation of the automatic transmission module. The transmission specifications are detailed in Table 3-9.
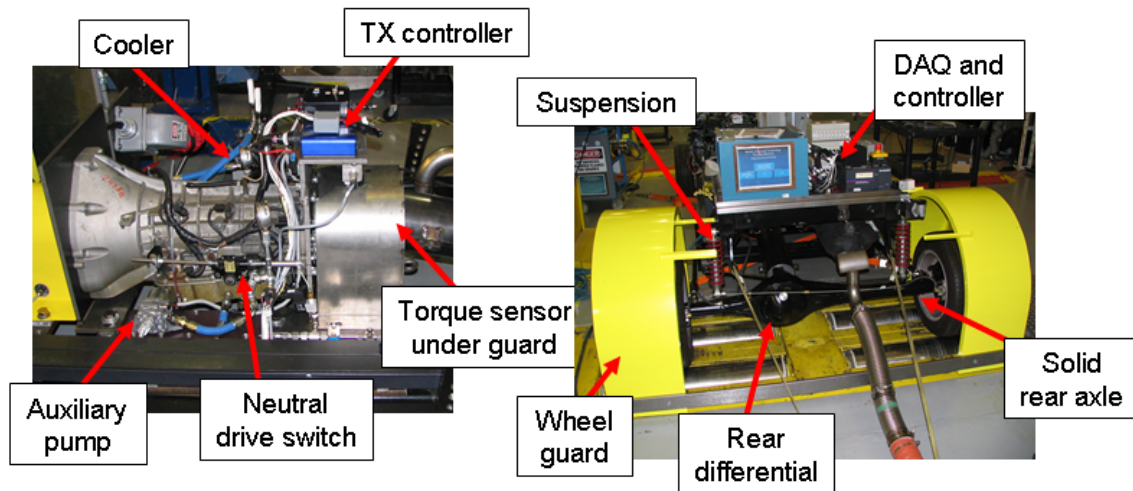
Figure 3-17: Automatic transmission module and rear end hardware

Table 3-9: Automatic transmission characteristics

Transmission type	5 speed automatic	
Family	Ford 5R55	
Architecture	Longitudinal	
Automation	Aftermarket controller with calibration tables	
Mechanical modification	No torque converter for EV launch Auxiliary pump to pressurize the fluid for launch Mechanical modification for reverse torque	
Gear #	Ratio	Vehicle speed at 1000 rpm
1st	3.22	6.2 mph
2nd	2.41	8.8 mph
3rd	1.55	12.5 mph
4th	1	19.1 mph
5th	.75	25.8 mph
Final drive ratio	3.55	

The after-market transmission controller has digital inputs for the up-shift and down-shift commands, making the lower level control of the transmission much easier and faster. During shifts, the control reduces the torque from the motor or the engine by 15% of the driver request in order to facilitate the shift. When the engine is engaged, the clutch is partially disengaged so the engine is pulled to the transmission input speed, but since the clutch slips, the inertia forces are softened. Shift times with the automatic transmission are about 400 ms with continuous lower torque transfer.

As a safety feature, the transmission's mechanical gear select switch needs to be actively shifted to drive using a small air solenoid. In case of an emergency stop or power loss the transmission will automatically return to neutral.

The transmission controller requires a torque input signal to adjust the clamping pressure on the appropriate clutches to hold the torque transferred across the transmission. Since MATT has two power sources; the engine and the motor, the signal sent to the transmission controller is the sum of the torque requests. During braking, the signal is the regenerative torque requested from the motor. In some cases of extreme regenerative braking at lower input speeds, the transmission fluid pressure is not high enough to maintain the required clamping force on the clutches. This was resolved by increasing the turn-on threshold of the auxiliary pump and, if needed, applying mechanical braking to reduce the regenerative braking. This is only necessary on aggressive cycles such as the US06.

Table 3-10 summarizes the instrumentation on the automatic transmission module.

Table 3-10: Summary of the automatic transmission module instrumentation

	Element measured	Sensor
Power input	▪ Input torque ▪ Input speed	▪ High accuracy torque and speed sensor
Power output	▪ Output torque ▪ Output speed	▪ High accuracy torque and speed sensor
Module specific	▪ Oil temperature ▪ Case temperature ▪ Line pressure	▪ Thermocouples ▪ Pressure sensor ▪ Engaged gear

3.5.6. Mechanical brake system

The mechanical brake system on MATT is a traditional automotive brake system. Since MATT is a single axle vehicle, the brake system is oversized to stop the entire vehicle inertia on one axle. Brake pads are pushed onto the brake rotors by single piston calipers. The hydraulic line is pressurized by a standard master brake cylinder, which is actuated by a pneumatic air solenoid. The pressure on the air solenoid is dictated by a variable pressure regulator which is computer controlled. Therefore, the computer controls the braking force. The computer can use an infrared temperature sensor to adjust the brake pressure based on the rotor temperature. The computer translates a wheel brake torque into a hydraulic pressure based on an empirical relationship. Figure 3-18 shows the hardware that composes the mechanical braking system.
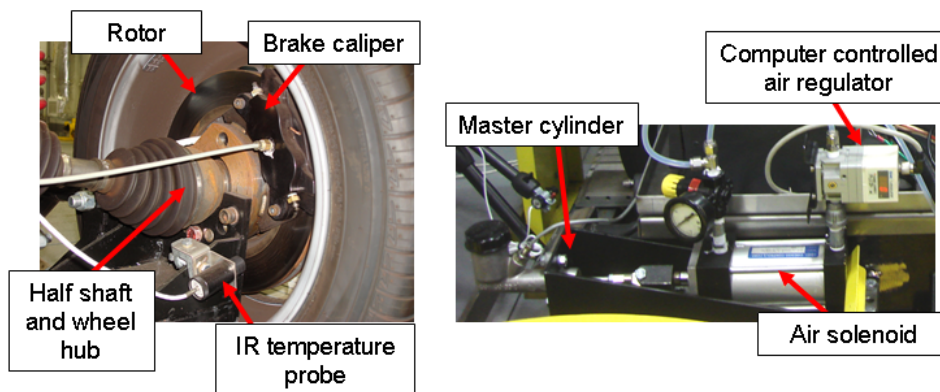
Figure 3-18: Mechanical brake hardware

The automatic transmission module and the manual transmission module do not share the same rear axle and thus the brake hardware is not identical. However, it is composed of similar components, the exact same layout and the same operating strategy.

To establish a relationship between computer command and brake torque, a number of special tests were performed. MATT was set in cruise control mode and operated at varying steady state speeds. At each steady state speed the brakes were ramped in and out at different rates. The wheel torque sensor records the torque between the brakes and the motor applying torque to maintain the steady state vehicle speed. Figure 3-19 shows the results of such a test. A linear relationship with an offset is derived as the default brake command to wheel brake torque conversion. The offset is explained by the minimum pressure to move and apply the pads to the rotor. The data was taken starting in 3rd gear, then 4th, and finally in 5th gear at different speeds for each gear. The brake fading is apparent in the data set for 5th gear, where the wheel brake torque is weaker for a given break command.
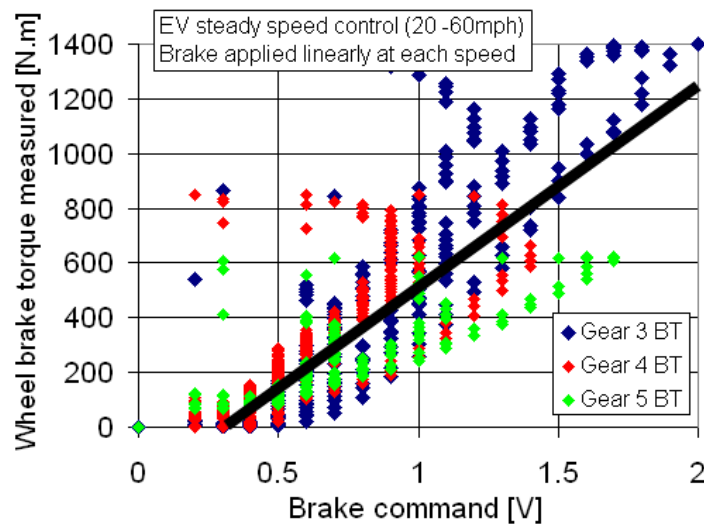
Figure 3-19: Wheel brake torque data for steady state speed data

For the conventional vehicle, the mechanical brakes work well and the control is relatively simple. In hybrid operation the braking is shared between the electric propulsion system and the mechanical brakes. On MATT, both the motor and the mechanical brakes can be commanded independently which provides flexibility to test different strategies and calibrations. Whenever possible, regenerative braking is used to maximize the capture of the kinetic energy into electric energy. In some cases, such as aggressive decelerations or fully charged energy storage systems, the mechanical brakes supplement the regenerative braking when the electric motor cannot provide enough braking torque or the battery cannot accept the electric power. At lower vehicle speeds, at mph, the regenerative braking is faded out and the mechanical brakes are used to come to a standstill.

3.6.   *Instrumentation for component and vehicle control evaluation*

Most of the instrumentation has been covered in the module-specific sections. The data collection from a single test comes from the instrumentation on MATT, data saved in the high level controller (control data and emulated component data), the dynamometer data, the test cell data and the emissions bench and optional systems (such as the engine pressure trace indicating system). Both the facility's data acquisition system and MATT's are designed to be very flexible in adding sensors and signals. Another great advantage is the open component module approach which makes the instrumentation and sensors easily accessible. Most of the data is recorded by the APRF main host computer and some information is merged in post-processing after the test.

The sensors on MATT are wired into signal conditioning boxes. These boxes condition the incoming signal to a standard isolated 0 to 5V signal. Each signal has two output connectors in order to share the signal between the high level controller and the data acquisition system. The high level controller uses the signal for component control and energy management strategies. The data acquisition system is dedicated to recording the data.

Beyond individual component investigations, the major goal is to understand the performance and the efficiency of the components in a hybrid vehicle system environment and to track their effect on the system. The instrumentation must be able to track transient power and energy in the driveline throughout the duration of the test cycles. Figure 3-20 summarizes the instrumentation that enables this analysis. The data is also used to debug, understand and recalibrate the component control and the overall energy management strategy.
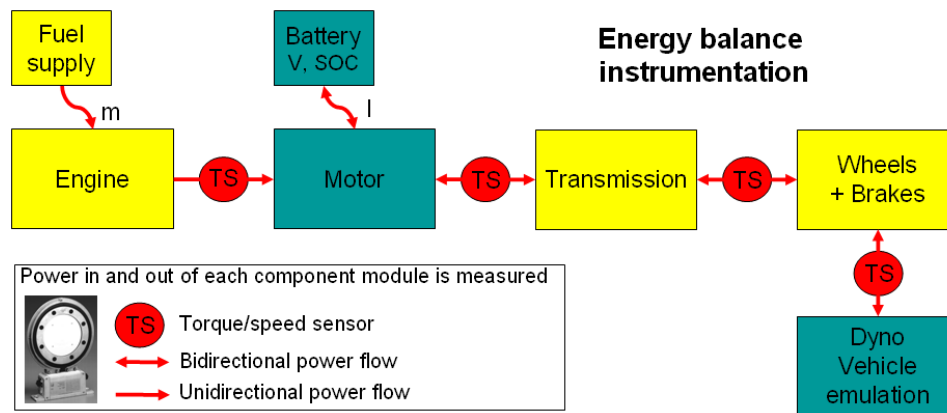
Figure 3-20: Instrumentation summary with respect to power and energy flows between the module

3.7. Open controller software for energy management strategy evaluation

3.7.1. Main MATT controller

The high level controller is an Autobox from dSpace with an analog output board, a digital output board, an analog input board and a CAN communications card. That controller runs the lower level component control and the higher level energy management strategy as well as the real time simulations which emulate the virtual components such as the energy storage.

PSAT-Pro is the software used in the controller. It has been developed by Argonne as a companion to PSAT, Argonne's automotive simulation tool. The software is used in Argonne's HIL experiments including a diesel CVT hybrid powertrain and Battery HIL setup. The software uses the simulation code structure with supplemental layers of code for safety purposes and hardware interfaces. The software enables energy management development in simulation before transferring the strategy to the hardware for testing. The hardware results can then be used to improve the model fidelity and gain additional insights, such as the impact of engine operation on emissions.

Since the code in the controller is based on simulation software, it uses physical component signals to feed the real time simulation and translates the simulation commands to physical component commands. For example, in the powertrain section of the code, the engine model is bypassed with a throttle command output to the hardware and an engine speed and torque signal from the hardware.

3.7.2. Energy management and torque split shell

The energy management and torque split strategy is in state-flow diagram form. The input is the driver torque request (positive or negative) as well as any vehicle information available. The output can be represented by the following:

- *Engine on or off:* The lower level code enables the ECU ignition and starts the engine with the 12V starter at a stop. It can also use the clutch to bump start the engine if the drivetrain is already spinning.

- *Engine torque command:* The engine torque command can only be positive. In conventional mode the engine torque command would be a function of the driver torque request at the pedal and the gear engaged in the transmission. In hybrid mode the engine torque command and the motor command need to equal the total driver torque request as a function of the gear engaged.

- *Motor torque command:* In electric-only mode, the motor torque command would be a function of the driver torque request at the wheels and the gear engaged in the transmission. The motor torque would be positive in propulsion and negative during regenerative braking. In hybrid mode, the motor torque and the engine torque need to relate to the driver torque request.

- *Wheel brake torque command:* In conventional mode, the wheel brake torque is equal to the negative driver torque demand. In hybrid mode, the brakes are

typically used to provide additional stopping torque when the motor or battery is limited in regenerative braking power. The mechanical brakes are also used at lower vehicle speeds to bring MATT to a stop.

The state flow code is a shell to test different energy management codes easily. One of MATT's key features is this open control approach that enables the user to test any energy management strategy ranging from very simple to complex. Figure 3-21 illustrates the standard code shell.
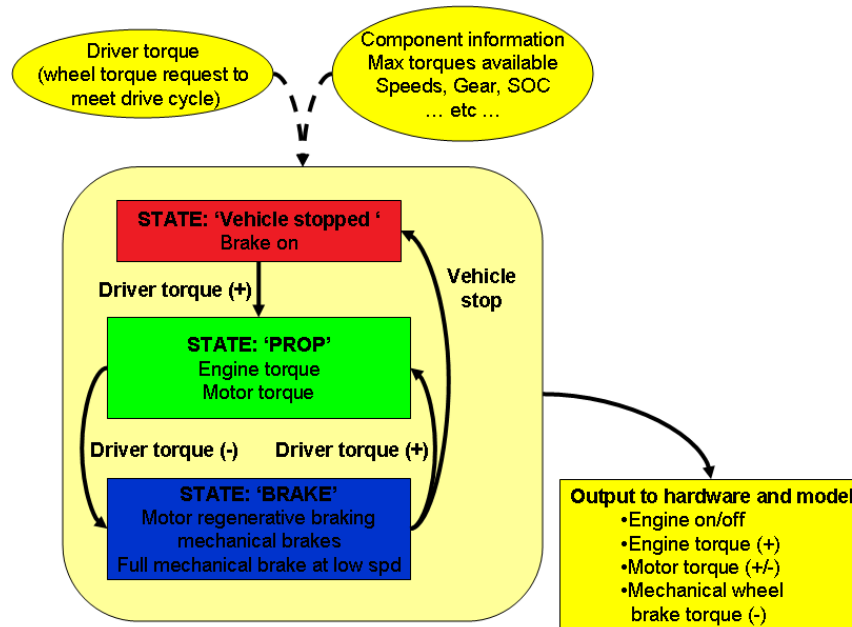
Figure 3-21: Illustration of the energy management strategy shell

The lower level control code translates the commands from the energy management strategy at the component level while protecting the hardware. For example, the conventional vehicle launch using the clutch and throttle are taken into account for the lower level control for the component.

3.7.3. User interface

The user interface is based on dSpace's control desk, the standard software in which user interfaces to the Autobox are developed. During testing the user has access to the visual feedback and calibration possibilities in a graphical user interface. Any control parameter can be calibrated in real time as MATT is running a test. Two distinct interface modes were developed. First is the actual test mode, where a virtual key is turned to start the automated drive cycle test with the current energy management strategy. Second is manual override mode, where the operator can command all of the actuators on MATT independently of the energy management strategy or drive cycle in order to test

individual operation of actuators for debugging purposes. Figure 3-22 shows the testing user interface.
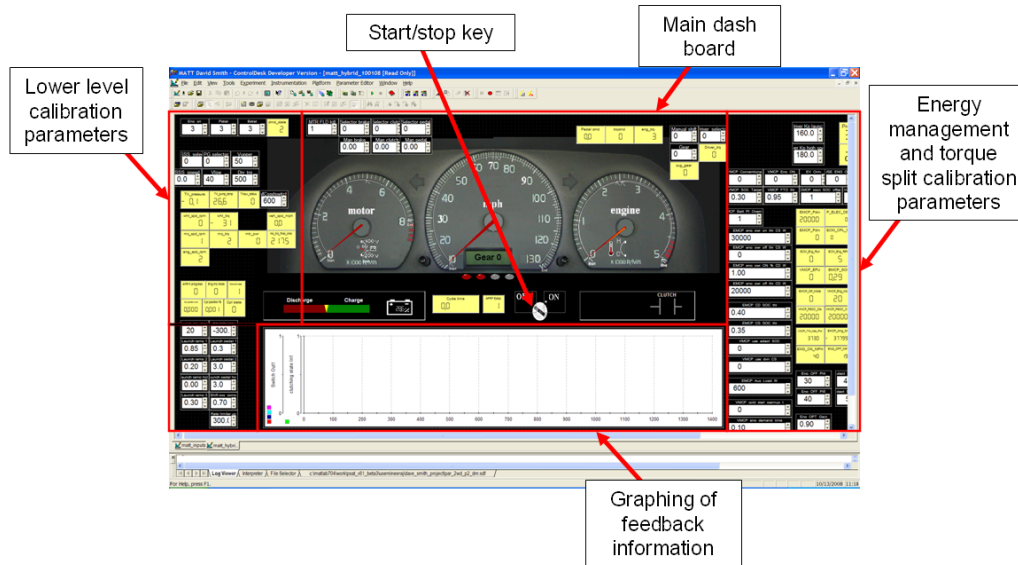
Figure 3-22: Screen shot of MATT's test mode interface in control desk

3.7.4. Computer driver

A PID loop is used to emulate a driver. A pre-programmed drive cycle starts once the virtual key is turned. Once started, the PID loop adjusts the driver torque request to minimize the speed difference between the wheel speed and the drive trace. The gains for the PID loops have different calibrations for low and high vehicle speed. The PID loop looks ahead on the trace by 1 second. Only the driver PID loop looks ahead, and it is not used to influence the energy management strategy. In real vehicle testing on a dynamometer, a driver also looks ahead and can anticipate required changes in accelerator or brake pedal position on the trace ahead. The PSAT-Pro 'driver' has extra features which include cruise control from any target speed as well as a 'pulse and glide' mode. The pulse and glide mode was developed to emulate and investigate hypermiler driving techniques.

Another useful input option is a pedal set that can replace the software robotic driver. An operator can use an accelerator pedal and a brake pedal to drive MATT. This capability is very useful during initial troubleshooting phases when a new hardware module is put into place. It is also useful to compare a human driver input to the PSAT-Pro PID driver to ensure that the computer driver is realistic.

The driver, be it the virtual driver or a human driver, ultimately closes the loop on powertrain torque control to meet the desired vehicle speed dictated by the drive cycle.

3.8. *Integrated safety system*

The MATT platform is an experimental test bench for hardware components and therefore, hardware failures may not be uncommon. Control strategy software mistakes are also part of the debugging phase of a new experiment. These facts drove the integrated safety system design. Four major protection systems are built in, and are explained below.

3.8.1. First safety guard: Trained operators

While MATT is being tested, an operator is always stationed at the interface computer next to the running platform in the test cell. That user can follow the feedback of the hardware on the screen as well as hear, smell and feel the hardware running next to him. If any abnormal and/or emergency situations occur, the operator is trained to click the software disable button on the user interface. If that fails, an emergency stop push button is within reach of the operator. MATT's operators are fully trained on the hardware as well as on the software interface. The operators are the first line of defense for safety.

3.8.2. Hardware wired emergency stop on MATT and Facility

A hardwired emergency stop (Estop) system is a 12V signal that can be interrupted by different triggers such as physical push buttons and computer monitored sensors. The 12V signal is used to enable and disable all the power flow components on the test bed as well as the APRF system. When MATT is used in the APRF, both Estop systems are combined in a series such that a trigger from MATT or the APRF will lead both systems to respond.

MATT has three red push emergency stop buttons spread across the different powertrain modules. The control computer also has to ability to trigger the hardwired emergency stop system. The APRF has a red emergency stop push by the operator console in the control room and two more in the test cell. The APRF uses diverse sensors such as toxic gas sensors, hydrogen sensors, and others to trigger an Estop. Several of these sensors are linked to the Argonne Fire Department as well.

Once an Estop is triggered the following will occur on MATT: The power to the fuel injectors, the power to keep the electric drive system running and the power to the transmission drive switch are all physically interrupted, thus isolating any power source in the driveline. The APRF will response by disabling the active dynamometer control, letting the vehicle coast to a stop and then engaging the dynamometer brakes. In a hydrogen related Estop trigger, a smoke related Estop trigger or a toxic gas related trigger, the Fire warning system is enables, the building is evacuated according to the emergency plan and the Fire Department is contacted to respond to the emergency.

The diverse safety systems are tested on a periodic basis. The emergency stop loop on MATT is tested as part of the start-up procedures. The emergency stop system

has been used especially when new control strategies were tested and the hardware engaged in unexpected behavior.

3.8.3. Software safety features in the controller

The control software primarily uses the PSAT simulation code, but in order to operate with hardware some safety layers are added, as shown in Figure 3-23. To protect the hardware, safety functions are built into the code and thus can trigger an emergency stop. All input sensors are monitored continuously and can trigger a shutdown if any reading is outside of the expected operating range. All the control signals are saturated to individual set levels before being sent to the components. The shut down occurs in the emergency block. For example, if the engine speed exceeds 6000 rpm, the controller will stop the experiment, zero the throttle command, open the clutch, zero the motor torque, shift to neutral and let the wheels coast to a stop.
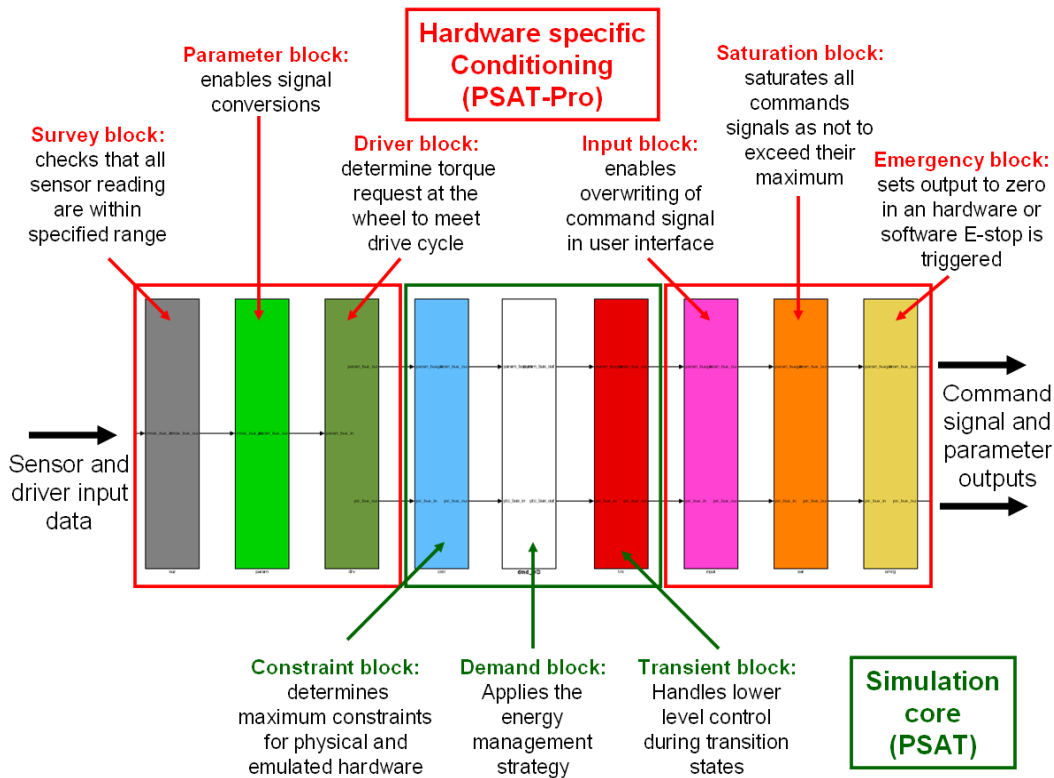
Figure 3-23: Powertrain controller data flow and safety conditioning

3.8.4. Guarding rotating elements

All rotating parts such as shafts and belts are covered by guards. These guards serve two purposes. First, they prevent anything or anyone from getting caught in rotating parts. All of the guards are designed to be 'finger proof' so that no one can inadvertently touch rotating parts with their fingers. The guards second purpose is to protect operators

and other hardware from flying parts and debris when a shaft or another component fails. A selection of safety guards on MATT is shown in Figure 3-24.
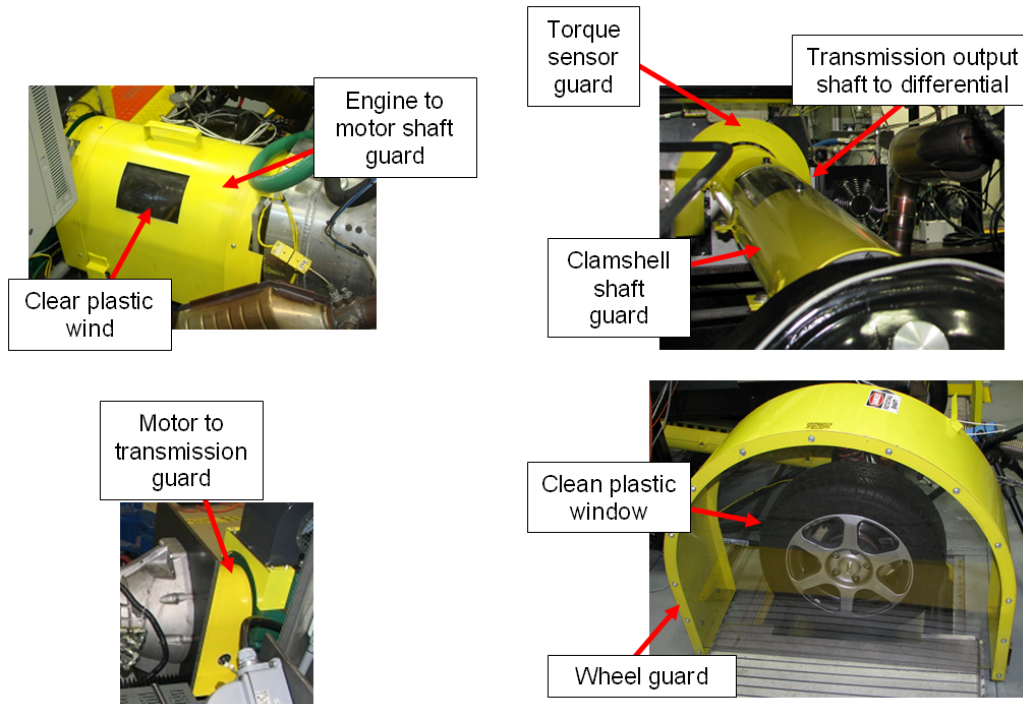
Figure 3-24: A selection of safety guards on MATT

3.9. Hardware summary

A modular component powertain testbed is an alternative solution to building prototype vehicles for testing different technologies in a hybrid vehicle environment while keeping the cost and required resources relatively low. MATT is composed of real powertrain component modules including an internal combustion engine and a transmission as well as emulated powertrain component modules such as energy storage systems. The modular approach makes it possible to test a multitude of different technologies and vehicle architecture combinations without having to rebuild the entire vehicle.

The hardware was developed in an iterative process over several years. Currently, several powertrain modules are available: a gasoline engine module, a hydrogen engine module, a virtual scalable energy storage and scalable motor module, a manual transmission module and an automatic transmission module.

A key feature of MATT is the virtual scalable energy storage and scalable motor module. MATT's physical motor provides positive or negative torque to the driveline, but the motor drives get their power from the electric power grid in the test facility instead of from a battery pack. The energy storage system is defined in a real-time simulation in the hybrid vehicle controller. Thus the energy storage system can accommodate different technologies and different capacities in software without having to modify any hardware. This technology is extremely useful for Plug-in Hybrid Electric Vehicle (PHEV) studies.

All of the components are instrumented to enable a full energy balance of the powertrain on drive cycles as well as to establish component loss maps for steady state conditions. Further special instrumentation is easy to implement due to the open space modular approach and the flexible data acquisition setup.

The high-level controller is open and can be programmed with any hybrid energy management strategy. The physical powertrain components provide the advantage of being able to test emissions and thermal effects, which are lacking in computer simulations. All of the components can be instrumented to a high level since the modules are open on the test bed and the packaging is not limited by a vehicle body shell.

MATT was built with integrated safety systems since it is an experimental test bench for new technologies. MATT is only operated by trained operators with access to software feedback and disabling commands. A comprehensive and tested emergency stop system that links to the test cell facility disables all power flows if triggered. The software continuously monitors sensors and can trigger a control shut down or an emergency stop if needed. Guarding is also in place around all rotating parts for safety reasons.

In conclusion, the Modular Automotive Technology Testbed is fully operational from the hardware perspective. Several powertrain modules are available for experimental purposes. The control software is an open controller which enables MATT to evaluate any energy management strategy.

4. Overview of the applications and studies performed with MATT

MATT is a unique and flexible tool used to investigate specific studies. The tool is an enabler for many types of research. The second part of this dissertation is dedicated to showcasing the major studies executed using MATT. First, the conventional gasoline operation is demonstrated. Then the electric vehicle operation is investigated. Finally, the major specific studies are discussed. These studies fall into two categories; the plug-in hybrid electric vehicle investigations and the evaluation of several combustion strategies of a hydrogen engine.

As a first application, the conventional gasoline vehicle operation was emulated. The purpose was to obtain fuel economy and emission data to form a baseline case for the conventional vehicle. The conventional vehicle operation provides some insight into the component characteristics, such as performance and efficiency. The engine and the transmission module are fully defined. In addition to the component characterization, the lower level component control is debugged. The conventional vehicle operation is the hardest vehicle mode since it includes launching the vehicle using the clutch as well as additional shifting. Results for different drive cycles are presented.

The second baseline study is the opposite of the conventional gasoline vehicle study, the electric vehicle study. The electric vehicle baseline testing provides electric energy consumption for different drive cycles. The electric vehicle study allows the emulated battery and virtual electric traction motor to be validated against some actual hardware available and tested at Argonne. Argonne has two physical prototypes of the 41 Ah Lithium Ion battery pack emulated on MATT. One battery is used in a HIL battery setup and the other battery is used in a prototype vehicle which also uses the emulated electric motor. Thus, the hybrid system on MATT can be validated.

Once the baseline vehicle modes are described and the first results are established, hybrid modes are investigated. Some basic hybrid vehicle modes are evaluated. Since MATT is an open controller system, any hybrid mode, from micro hybrid to full hybrid mode is evaluated. Next, Plug-in hybrid operations are demonstrated.

The major PHEV studies are then presented. Four major topics were researched. The first was a very specific investigation for PHEV standard test protocol developments. The cold start correction of highway cycles investigation was performed with MATT since no other PHEV was available at Argonne. This study supported and influenced the test procedure development. Further test procedure studies determined the impact of time between the different tests on energy consumption and the impact of drive cycle intensity on the charge depleting phase. The final and major PHEV study researched the impact of the energy management strategy on emissions for PHEVs.

The final application presented is a component evaluation. A hydrogen engine with 5 different combustion strategies was tuned and calibrated at Argonne on an engine dynamometer. The different combustion strategies are then evaluated in transient operation on the standard drive cycles in MATT. In addition, the optimum variable air fuel ratio combustion strategy is confirmed.

These applications and their ensuing research the final purpose and this are more important than the tool itself.

5. Gasoline conventional baseline vehicle

5.1. Baseline vehicle setup

For the remainder of the tests conducted in this dissertation, MATT was run using a Ford Focus as the conventional reference vehicle. The gasoline engine used on MATT comes as an option in a Ford Focus. The Focus was chosen because Argonne uses a 2004 Ford Focus as the correlation vehicle and standard measure with the APRF. Twice a year and after any dynamometer and emissions bench upgrade, the Focus is tested to verify that the test results are consistent before and after. The Focus is also used because of the hydrogen engine evaluation. Ford performed all their work on the 2 liter ZETEC and 2.3 liter DURATEC engine and published results that provide a reference for the hydrogen engine work established in this dissertation. The vehicle size will stay the same throughout the dissertation.

MATT has evolved over the years. The conventional vehicle was the first operating mode in development on MATT. At the start, MATT used the gasoline engine with the original Ford ECU and the manual transmission with automated shifting. In the later stages, MATT used the same engine with an upgraded standalone ECU, an automatic transmission and dramatically improved cooling. It is important that the reader keep this in mind as the different setups resulted in different fuel economy and emissions results. Generally, the hardware control development (launch and shift) were performed with the early ECU and manual transmission, and the detailed results that appear later in this dissertation are based on an updated ECU and an automatic transmission.

The gasoline conventional vehicle data is the baseline for comparison between different hybrid electric operations, plug-in hybrid electric hybrid operations and new component evaluations including the hydrogen engine evaluation. The different hardware modules are described in further detail in section 3.5. MATT configuration for the conventional vehicle is shown in Figure 5-1.
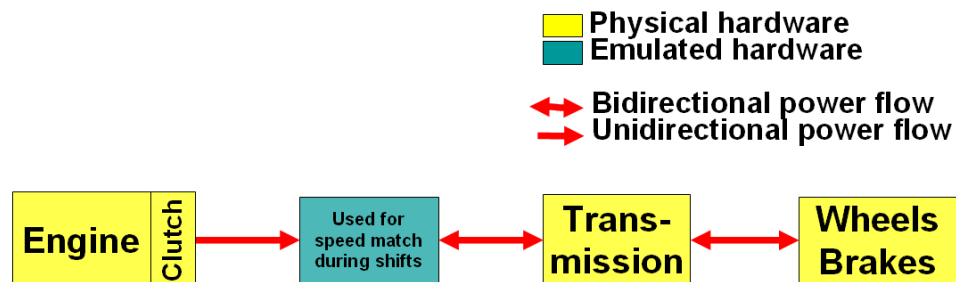
Figure 5-1: Configuration of the conventional vehicle.

5.2. Vehicle operating strategy

The energy management strategy is relatively simple. Once the vehicle is launched the positive driver wheel torque request is translated into the engine torque

request by dividing it by the ratio of the current gear. The negative torque request is turned into a brake command for the mechanical wheel brakes. During a stop, the engine idles and the mechanical brakes are engaged. The shift schedule is predetermined as it would be for a manual transmission vehicle.

5.3.   *Conventional vehicle challenges*

The conventional vehicle operation is actually the most complicated from the component control level perspective. Conventional mode requires the vehicle to launch using clutch and throttle as well as good shift time in order to obtain reasonable fuel economy and emissions. This was one of the more challenging portions of the control and hardware development.

5.3.1.   Launching

The physical hardware on the engine is a clutch system from a pickup truck application that uses the matching 2.3 liter engine. The vehicle clutch system includes the clutch assembly (which bolts to the flywheel), the hydraulic slave cylinder with an integrated throw out bearing and a master cylinder matched to the slave cylinder. The hardware gets abused during the development and tuning phase and therefore the final clutch system was selected from the heavy duty pickup truck application. Figure 5-2 shows the clutch system hardware on the vehicle side.
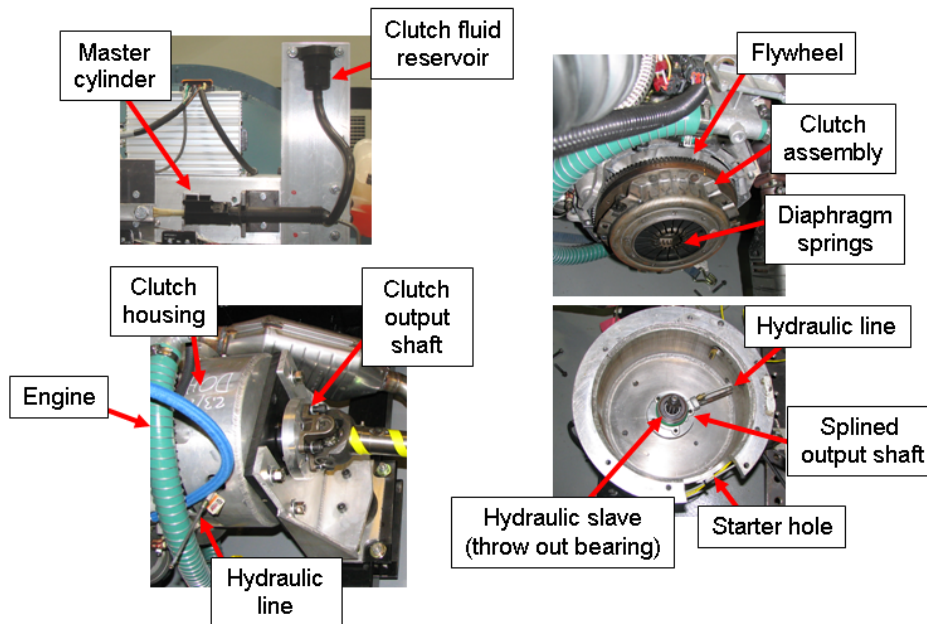
Figure 5-2: Hardware of the engine clutch system employed on MATT

On the first iteration, the master and slave cylinder did not match perfectly. This prevented full travel on the slave cylinder and rendered the performance inconsistent.

Another important factor for consistency is to fully bleed the hydraulic line between the master cylinder and the slave cylinder. The systems in a vehicle are designed to bleed air out at the slave. On MATT, the hydraulic line has a local maximum and thus the bleeding procedure is more complicated compared to a production vehicle. Even the smallest air bubbles will impact the response of the slave cylinder, making the tuning process appear inconsistent. These are some of the hardware problems that had to be overcome.

After the first iteration, the system requirements could be better understood. The clutch actuator is directly linked to the master cylinder, which would typically be connected to a clutch pedal in a vehicle. The clutch pedal provides mechanical advantage by increasing the travel and reducing the force that the driver needs to apply to the pedal. After extensive testing on the first iteration actuator system, the actual travel and force in motion on the master cylinder were determined to be 1 inch and 350-400 lb of force, respectively. From the control and actuator perspective, the launch using the clutch presents a precision position control problem. It is not a force problem, despite the fact that a high force has to be overcome by the actuator. The actuator has to be able to resolve small motion around the clutch engagement point. Right at this engagement point, the actuator position translates into the torque transfer. The speed of motion is the final dimension needed to determine the actuator requirements. For shifts, which are discussed in detail in the next section, the fastest engagement and disengagements are the most beneficial. A one second time frame was set as a requirement to complete a 1 inch travel distance. For the engagement and disengagement, the full 1 inch travel distance is not used and thus the shift event is still completed quickly. Figure 5-3 illustrates the initial and the final clutch actuator systems. The size of the system should be an indicator of the power upgrade between the generations.
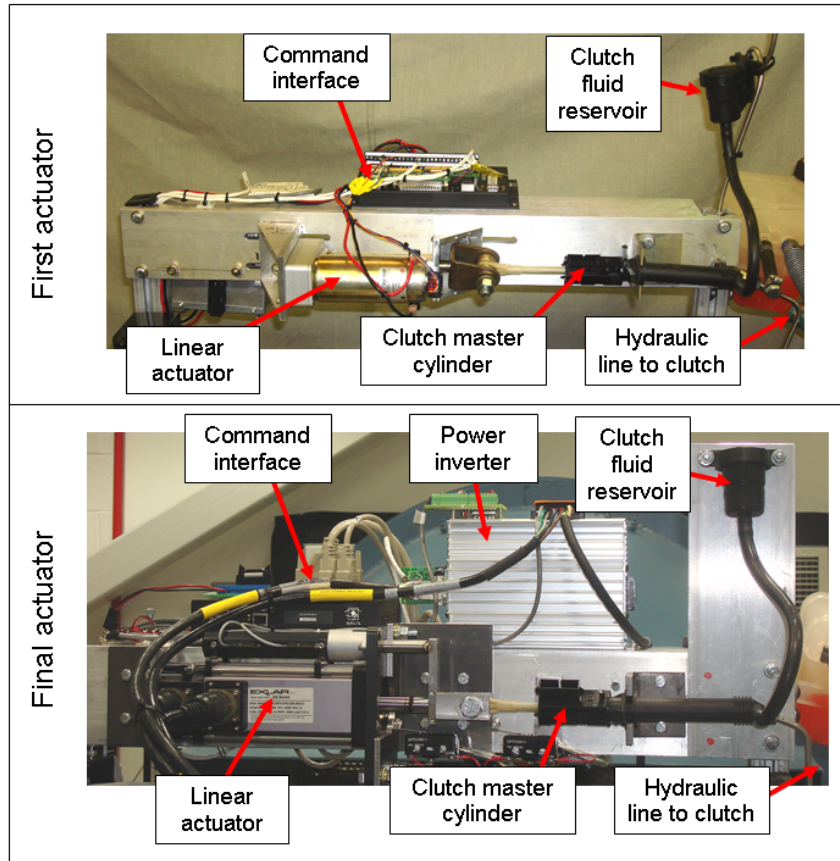
Figure 5-3: First and final iteration of the clutch actuator on the engine for MATT

Further testing of the clutch characteristics was performed to understand the torque transfer during the engagement phase. The details are shown in Appendix 2. A clear correlation exists between clutch actuator position and torque transfer while the wheels are not spinning. Figure 5-4 illustrates that correlation. The clutch engagement point is reached once the torque is between 5 and 10 N.m, based on the data. That will be used by the computer to determine the clutch engagement point.
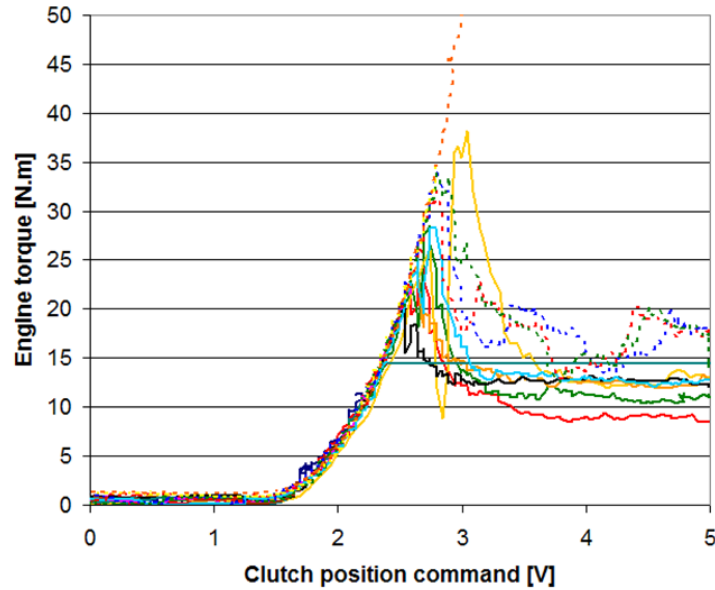
Figure 5-4: Correlation between torque transfer and clutch position from different conditions

The clutch and throttle control algorithm for launch

The lower level control code actuates the clutch during the conventional vehicle launch. The process is composed of three phases. First, a minimum throttle command is set to increase the engine speed to slightly above idle. At the same time the clutch is closed at a medium speed until the clutch engagement point is determined. The torque engagement point is determined when the 5-10 N.m threshold is exceeded on the engine torque sensor. The second phase is the critical launch phase. The clutch is further engaged at a slow speed while the engine based throttle command is increased and an additional throttle is set, based on driver torque request. If the engine speed is pulled below idle speed, it enters a recovery state where the clutch engagement is stopped or slowly reopened while more throttle is applied until the engine speed is above idle. Once the clutch engagement calibration is optimized, the recovery state is very rarely used. The final phase starts when the engine speed and transmission input speed match and the clutch is engaged past a certain point. In the final phase the clutch is fully engaged as fast as possible and the throttle command is directly linked to the request from the energy management strategy. Figure 5-5 illustrates the conventional vehicle launch logic. If, during a launch, the vehicle speeds up faster than the drive cycles, the launch is aborted and restarted and MATT stays within the drive cycle boundaries.
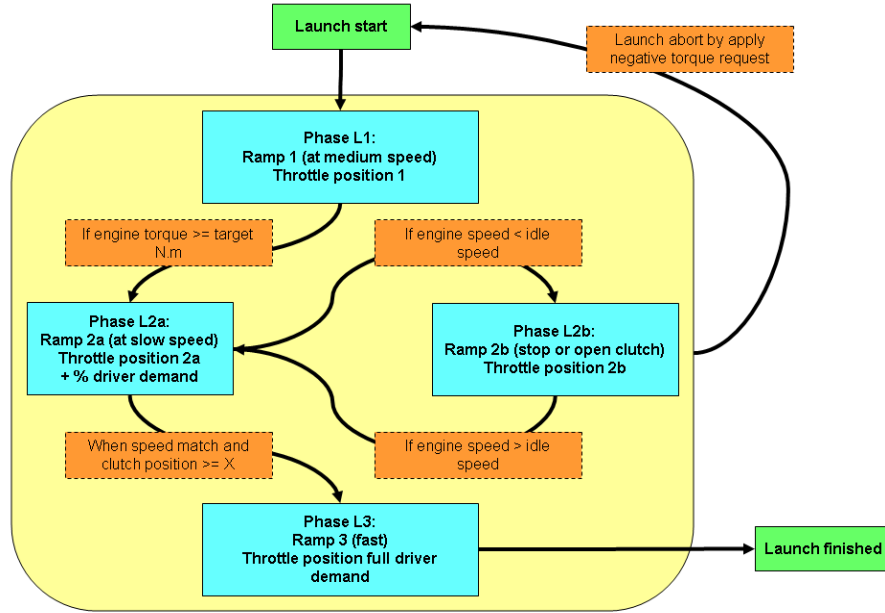
Figure 5-5: Conventional vehicle launch logic

The ramp rates for the clutch engagement and the throttle positions for each phase are calibrated by utilizing the user interface described earlier. Once the parameters are tuned appropriately, the launch is reliable and fast. Figure 5-6 illustrates the launch process with data from one of the early launch calibrations.
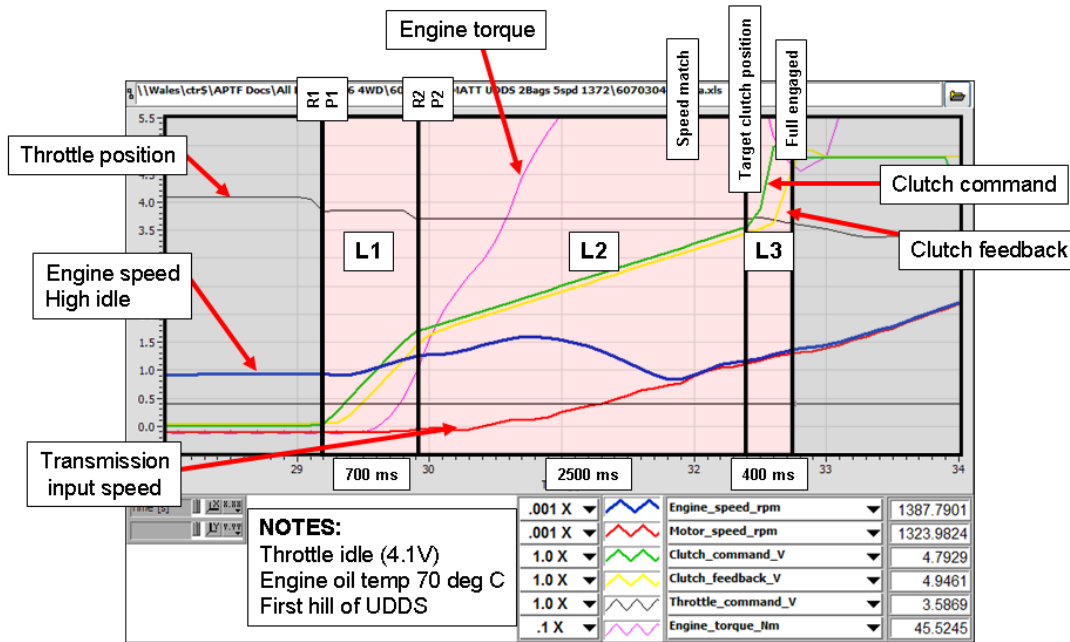
Figure 5-6: Data from a launch in conventional mode with MATT

The missed launch has an impact on fuel consumption as well as engine emissions. The engine can stalled on t be close to stalling or the engine can spin to a high rpm without load before the clutch closes enough to pull the engine down. The tuning and calibration required to get the launch 'just right' requires a strong understanding of the engine and of the vehicle's dynamics.

Limitations of launch

The algorithm is close to that of an open loop. The clutch engagement rates are set by calibration and do not vary. The throttle command is slightly increased depending on the driver torque demand. If the driver torque demand is low a minimum throttle will be applied and if the driver torque demand is high, as it would be on an aggressive acceleration, extra throttle is applied, keeping the engine speed up during the launch. The initial acceleration rates for all vehicle launches on certification cycles are relatively similar and certainly limited in aggressiveness. Therefore, the open loop calibration works quite well for most launches on most cycles.

There are a few exceptions, such as the section between 1250 seconds and 1257 seconds on the UDDS cycle, which is a steady state speed portion held constant at about 1 mile per hour. The speed is slower than the vehicle speed with the engine idling in first gear. In order for MATT to meet the driver trace on that section, a smarter code with clutch slip is required. Currently, the vehicle launches at the normal rate, which causes the robotic driver to request a negative torque and thus aborts the launch as shown in Figure 5-5. Once the launch is aborted, the vehicle coasts close to the trace. This technique works well enough to maintain the vehicle within the mandatory 2 mile per hour band around the trace. Therefore, MATT still completes valid drive cycles.

Ideal launch algorithm

One of the next steps for the conventional vehicle launch would be a new algorithm for the vehicle launch. The engine would enter an engine speed regulation mode and the clutch position would be controlled based on the driver demand. Figure 5-7 shows this ideal clutch launch control.
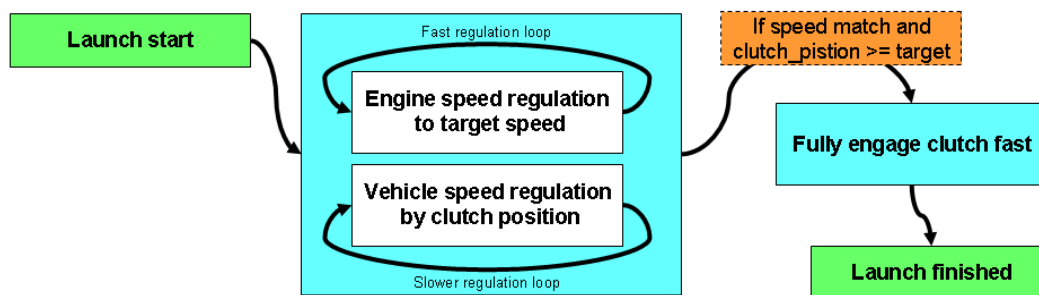
Figure 5-7: Ideal vehicle launch algorithm

The engine speed regulation challenge prevents the implementation of this logic. An engine is most sensitive to throttle inputs at idle with no load applied. Any little throttle changes will induce large speed changes, thus making the engine speed regulation extremely complicated for the launch.

Launch control summary

The current launch control is robust, repeatable and works quite well from a fuel consumption as well as an emissions standpoint, despite the open loop control. Full drive cycles are completed without excursions outside of the prescribed drive cycle boundaries. One should also keep in mind that the most interesting work is with hybrid control strategies is not the conventional launch, which it just needed to establish a baseline for comparison. For these purposes the conventional vehicle launch was deemed sufficient.

All of the data shown for the launch is based on the manual transmission. The same algorithm is used for the automatic transmission with a slightly altered launch calibration.

5.3.2. Manual transmission shifting

The shifting is extremely dependent on the hardware used. MATT has two transmission modules. The overview of the manual transmission module and the automatic transmission module are in section 3.5.4 and section 3.5.5, respectively. The manual transmission module underwent a major upgrade in the middle of the work cycle.

Manual transmission shifter linkage

To automate the manual transmission, linear actuators are directly mounted to the shift linkages. Figure 5-8 shows the linkage mounted on the transmission and their correlation to a manual shifter H grid.
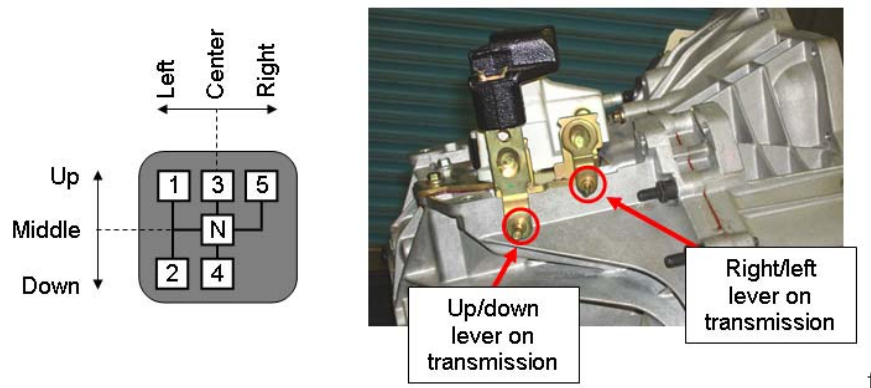
Figure 5-8: Linkage system on the manual transmission with correlation to shift grid

Generic manual transmission shift algorithm

In order to describe the shift logic, one must assume that the actuators can move the linkage to engage any gear, including neutral. In the manual transmission, there is no clutch assembly because the mechanical integration was deemed too challenging and time consuming. The absence of the clutch between the motor shaft and the input shaft to the transmission creates a control challenge. The electric motor is used to actively speed match to the next transmission input speed based on the next gear selected.

The shift algorithm is described as follows. When the shift is requested in the conventional vehicle mode, the engine clutch needs to be disengaged to create a zero torque differential across the transmission. To shorten the torque hole, the throttle command is zeroed once the clutch is partially disengaged (the tractive motor torque is always zero in the conventional mode). As soon as there is no torque transfer across the transmission, the transmission can be forced into neutral (this does not work if there is a torque difference or transfer across the transmission). Then, the electric motor is used in speed control mode to spin the transmission input shaft to the speed required to move to the next gear. Once speed match is detected the linkage is forced to engage the next gear and then the clutch is reengaged. Once the clutch reaches a certain engagement point the throttle is reapplied. The process is summarizes by Figure 5-9.
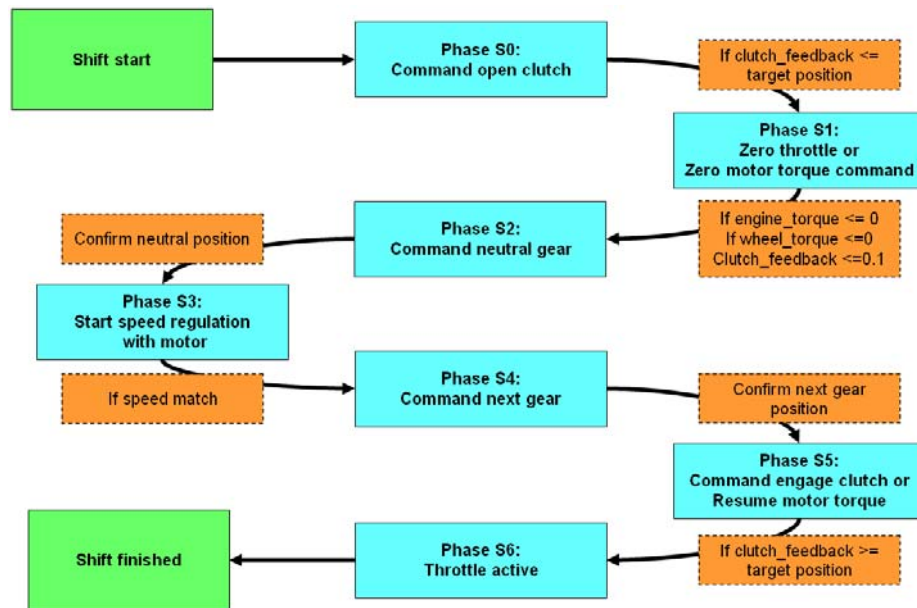
Figure 5-9: Manual transmission lower level shifting algorithm

The process is simplified in electric operation since the throttle or engine clutch operations do not apply. The speed match is performed using a PID control loop that is calibrated for each gear number. Shifting in low gears, such as 1st to 2nd gear, takes the longest since the transmission input speed difference is the greatest in low gears.

Manual transmission pneumatic actuators

The first iteration of hardware in the manual transmission used bidirectional air solenoids to actuate the shift linkages. The difficulty with this system is in the return to neutral. In order to return to neutral the 'up/down' linkage needs to stop in the middle of its run. A special neutral stopper was designed. An air solenoid plunger on a wheel travels on an arched arm. During a motion from a gear to neutral, the plunger solenoid is pressurized, which pushes the wheel on the track and at the neutral point the wheel falls into the neutral hole on the track which stops the 'up/down' linkage in neutral. Once the 'up/down' linkage is in neutral the spring detent of the 'left/right' linkage brings that lever back to a neutral position. The mechanism and its design are shown in Figure 5-10.
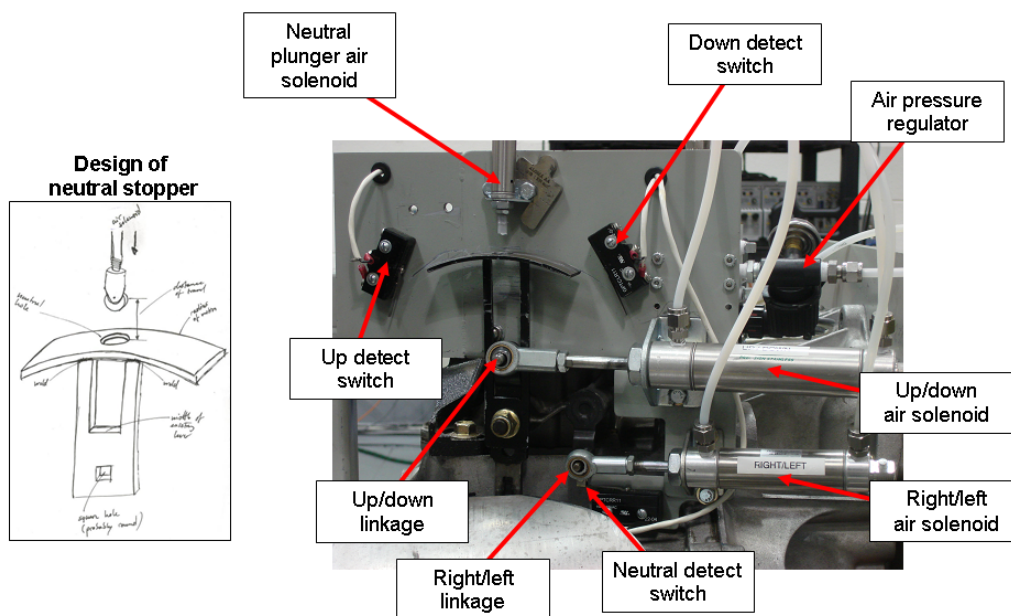
Figure 5-10: Air actuators on manual transmission linkage with neutral stopper system

During the gear engagement, the 'left/right' actuator is moved into the appropriate position. The controller gets the feedback from an electric switch. Then the 'up/down' air actuator is pressurized. Once the gear is engaged, the electric contact switch at the end of the travel is activated which signals the completion of the shift. Figure 5-11 illustrates the logic employed to shift gears from the transmission linkage perspective.
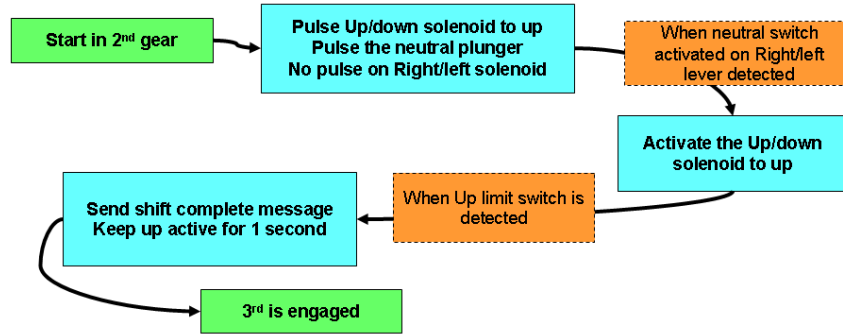
Figure 5-11: Gear shift logic for the air actuator on the linkage

Once tuned and calibrated, the air solenoid system worked quite well. But the time required for shifting, especially to return to neutral, was significant compared to the shift period. The empirical wait time to achieve neutral is 250 ms. Using the sequence detailed in Figure 5-9 and Figure 5-11, a 1st to 2nd gear shift was executed. The data is shown in Figure 5-12.
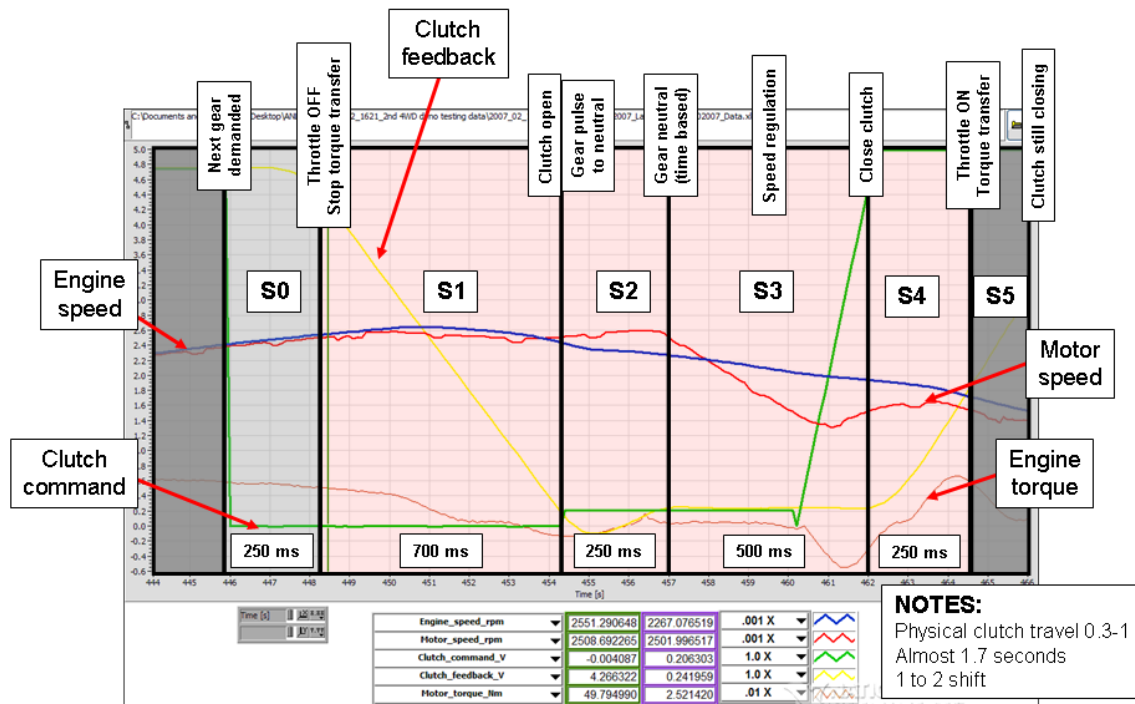
Figure 5-12: 1st to 2nd gear shift data with the manual transmission and the air actuators

This data shows the worst case scenario for shift time. The 1.7 seconds it takes to shift gears causes the vehicle to miss the drive cycle and therefore, once the gear is engaged, the robotic driver is forced to request full torque to catch up with the trace. This has a negative impact on fuel economy and emissions. By carefully optimizing the

actuator speed, keeping engine torque transfer while the clutch starts to disengage before slip occurs, tuning the speed match of the motor, and applying torque as soon as the clutch engagement is sufficient to handle torque transfer, the shift time was reduced from 1.7 seconds to 1.4 seconds, as shown in Figure 5-13.
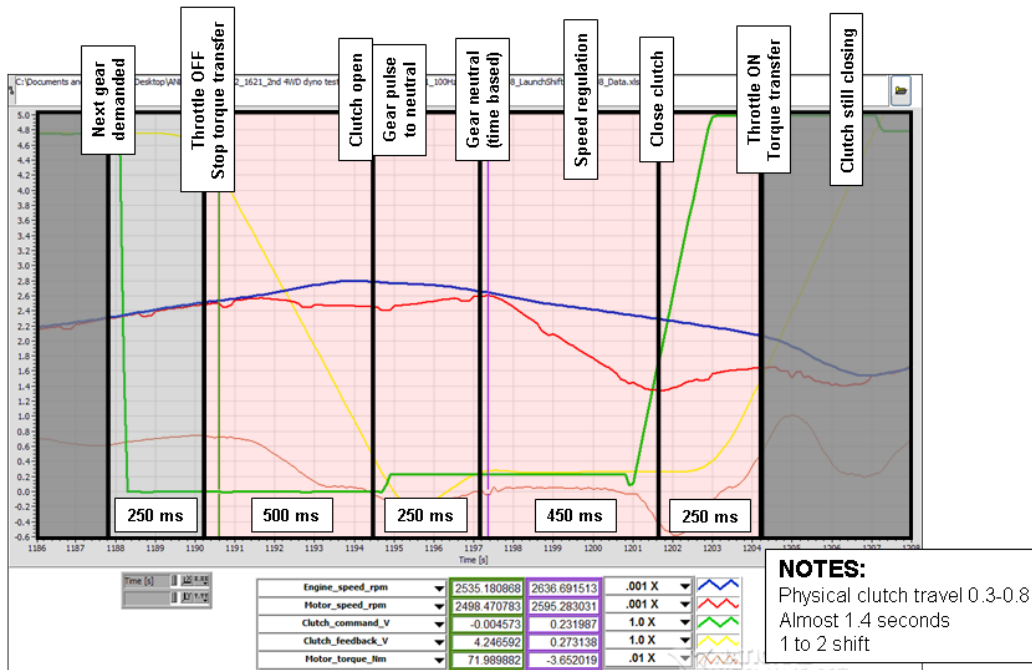
Figure 5-13: Improved shift time with manual transmission and the air actuators

Manual transmission position control actuators

In order to increase the shifting speed further, the actuators were upgraded to fast position control actuators. With this new setup, digital commands are sent to the power electronics units for motion command. Feedback about completed motion and fault messages are sent back via digital signals. The two motion controllers are programmed to operate together to achieve the appropriate path on the linkage system. These new actuators are tuned for smoother continuous engagement of the gear, instead of the choppy and decomposed first left, check, then up, check motion,. This reduces the shift time even further, and reduces the wear and tear on the transmission's hardware.
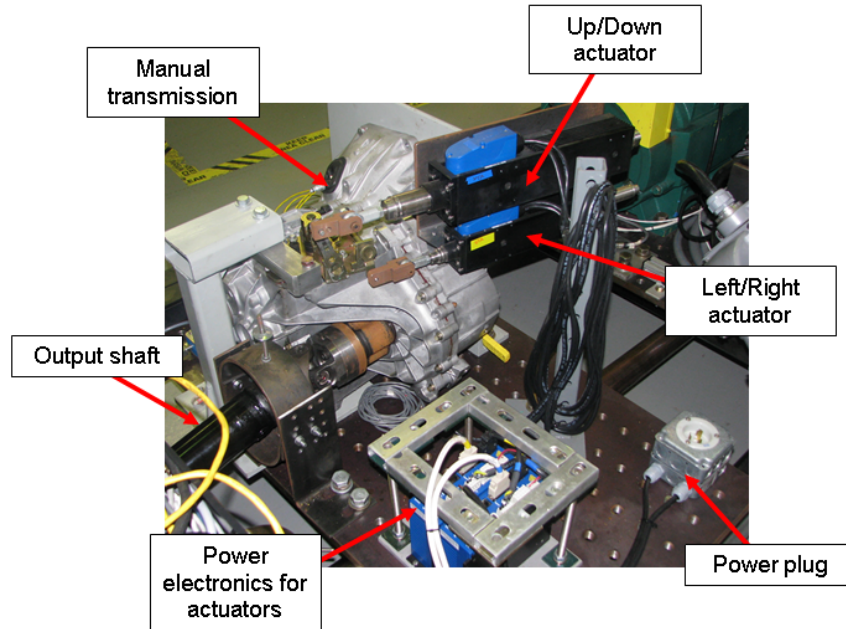
Figure 5-14: Position controlled actuators on the manual transmission

Limitations of the manual transmission module

The main limitation of the manual transmission module is the long shift time due to the lack of integrated clutch in the transmission. The longest shift is the 1 to 2 shift since the input speed difference is the largest in order to match all of the gears. Initially, the shift time of about 2 seconds created a shift torque hole that was so long that the vehicle would not meet the trace within the required boundaries. After optimizing the process and the calibration, the shift time was reduced to 1.2 seconds in conventional operation.

Figure 5-15 shows a comparison of shift times for the manual transmission and the automatic transmission. The data shows MATT operated as a conventional vehicle on the 5th mode of the UDDS, which is one of the more aggressive accelerations from a stop. This data set for the manual transmission is one of the early, slower calibrations, presented to contrast the automatic transmission. During the 1 to 2 shift, the manual transmission vehicle loses the trace since the engine does not transfer any torque, as seen in the torque data. Once the shift is complete, the driver requests high torque to catch up with the trace. The 'close to wide open throttle' events have a negative impact on fuel economy and emissions. In contrast, the automatic transmission data shows that the engine torque is average while the vehicle meets the trace without a problem. The smoother torque request with the automatic transmission has a positive impact on the emissions behavior of the engine. Certifying a manual transmission vehicle is also an issue for OEMs.
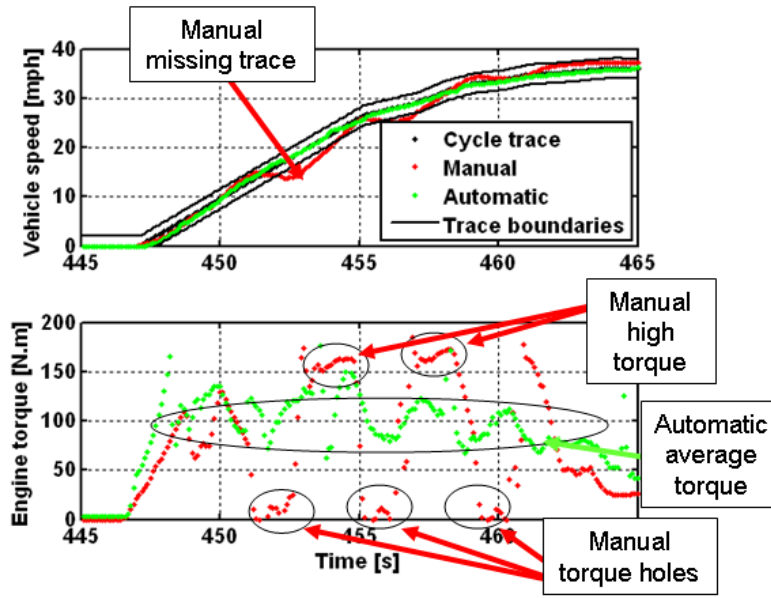
Figure 5-15: Comparison of the manual to the automatic transmission in conventional operation

Concluding manual transmission module comments

The solution to the manual transmission shift time problem is to integrate a clutch in order to eliminate the speed match phase. A clutch is currently being integrated into the manual transmission.

Looking ahead to the hybrid and electric operation, the 1 to 2 gear shift is not an issue since the launch is typically performed in 2nd or even 3rd gear for full hybrid operation. The vehicle is launched in 2nd gear which eliminates the 1 to 2 shift. Regenerative braking and full torque reversal does not present any problems for the manual transmission.

5.3.3. Automatic transmission shifting

Control hardware setup

The automatic transmission is controlled by an aftermarket transmission controller. The controller connects directly to the stock wiring harness for the 5R55 automatic transmission using the three speed sensors as well as all the pressure sensors. The controller commands the line pressures via the integrated hydraulic valves in the transmissions valve body. Although shift pattern tables are available, the controller does not select the gear. The high level controller commands the gear by sensing up shift and down shift signals to the transmission controller. The electric interface to this aftermarket unit is the up shift and down shift signals which simulate the modern transmission steering wheel paddle shifter.

A few mechanical modifications were made to the automatic transmission. First the PRNLD switch in the side of the transmission is shifted from neutral to drive using a small air solenoid. A return spring ensures that the default switch location is neutral. In neutral, a mechanical valve is opened to relieve the automatic fluid pressure so that all of the clutches are open and no torque can be transferred. Thus the 'Neutral' and 'Drive' actuator is part of the safety design. In case of emergency, the air solenoid loses power and the transmission is forced to neutral and will spin to a stop.
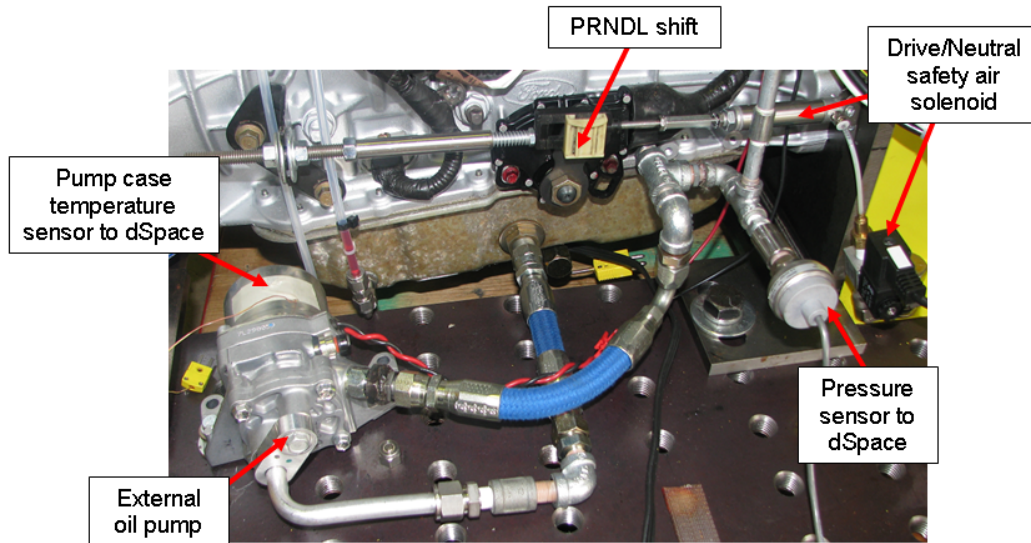
Figure 5-16: Details of the external modifications to the automatic transmission

To make MATT capable for electric launch, the torque converter was removed from the transmission. In hybrid or electric mode, the electric motor is capable of launching the vehicle from zero motor speed at full torque. The challenge in removing the torque converter was to build a replacement input 'device' or shaft. The new shaft has to mate up to the spline transmission input shaft, spin the internal pressure pump with flats, circulate the transmission fluid internally as the torque converter would, seal under pressure, hold in the transmission under back pressure and have a standard flange adaptor at the input to receive the motor shaft. Without a torque converter, a new means of pressurizing the transmission fluid below 700 rpm (engine idle speed) was necessary. Therefore, an external pump was implemented to pressurize the oil galleries for the electric launch. After burning up the first external pump, an elaborate pump control logic was develop to run the pump from 0 to 600 rpm during launch and engage the pump at 800 rpm during a deceleration while continuously monitoring the pump case temperature and pressure output. The special shaft assembly is shown in Figure 5-17.
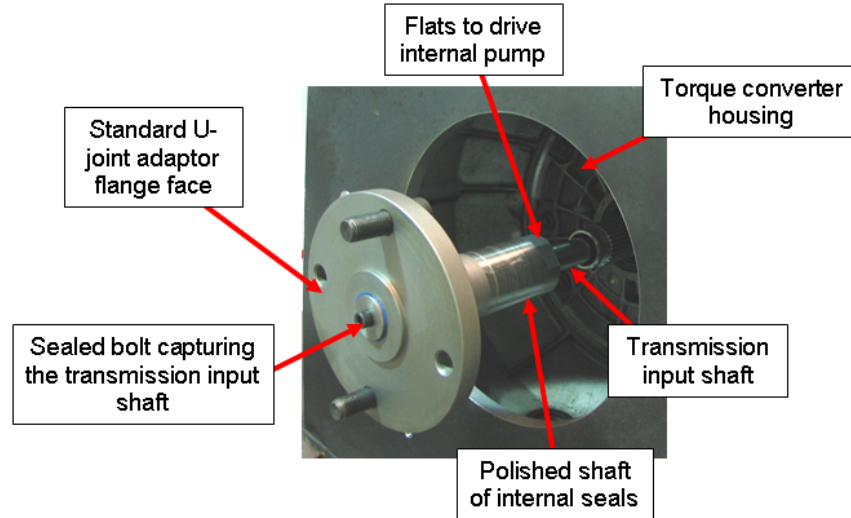
Figure 5-17: Automatic transmission torque converter replacement shaft assembly

One final element is required for the proper operation of the system. A synthesized transmission torque input signal is required for the transmission controller to modulate the line pressure and to maintain the correct pressure on the internal clutches to enable torque transfer. In the higher level hybrid controller, the engine torque is added to the motor to create the transmission torque input signal which is sent as an analog signal to the transmission controller. Like the manual transmission control explanation, it is necessary to look past the conventional vehicle operation here. In hybrid or electric mode, the torque input to the transmission can be negative for regenerative braking events. In that case, the transmission controller needs to increase the line pressure to enable the torque transfer across the transmission. During a regenerative braking event, the high level controller senses the absolute value of the motor torque to the transmission controller and enables that torque transfer. The regenerative braking is discussed further in section 6.3.1.

Shift algorithm for the automatic transmission module

Now that all of the control elements are in place, the focus is on the control algorithm to shift from one gear to the next. Because the automatic transmission can transfer torque during acceleration, since the torque converter is eliminated, the first step is to reduce any torque transfer across the transmission to 20%. This calibrateable parameter was determined empirically. The pulse for an up shift or down shift is simultaneously sent to the transmission controller. In the next state, the high level controller determines the shift completeness by waiting for a speed match between the motor speed and the wheel speed multiplied by the gear ratio of the expected gear. Once the speed match is determined, the shift is complete and the full torque request of the driver is commanded from the drivetrain. If the speed match does not occur within 400 ms, the pulse request is sent out again. This is rarely necessary. Figure 5-18 illustrates the algorithm of a shift with the automatic transmission.
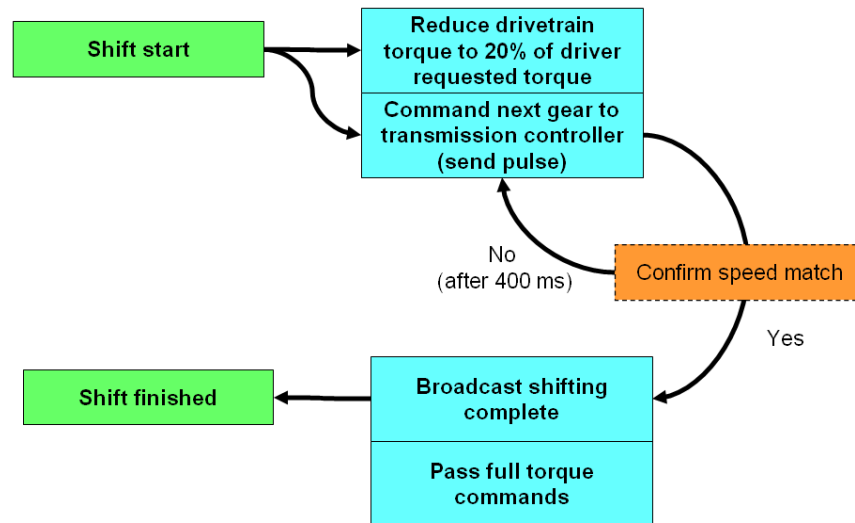
Figure 5-18: Shift algorithm for the automatic transmission module

Transmission controller calibration

Once all of the hardware and logic were in place for launch and shift phases, the calibration of the transmission controller unit was begun. The first phase is to ensure that the transmission can transfer torque. The concept is to maintain the line pressure of the automatic transmission fluid high enough so that the internal clutches do not slip and transfer torque. Therefore, in high torque situations such as vehicle launch or accelerations, the line pressure needs to be elevated to enable the higher torque transfer. It should be noted again here that the torque input level information is sent to the transmission controller from the high level vehicle controller. During cruise situations the line pressure should be reduced in order to reduce the parasitic losses of the internal oil pump which is input shaft driven. Therefore, cruise phases require a balance between having enough pressure to hold the clutches closed and keeping the pressure low enough to increase the transmission efficiency. In fact, in the initial calibration, the pressures were too low and the clutches slipped and caused some premature wear that required repairs. The cruise pressure is set slightly higher than required to prevent hardware damage, but this generates extra transmission losses. The calibration is performed for each gear at all load points.

The second phase is the shifting, which requires control setup and tuning. The process will only be briefly described, as it is rather complex and not a main topic of research for this dissertation. The first step is to understand the internal configuration of an automatic transmission. The lever diagram shown in Figure 5-19 describes this best. In order to shift from 1st gear to second gear, the coast clutch needs to be released and pressure needs to be applied to the OD band as shown in Figure 5-20. The timing and pressure levels matter for these event in order to make a smooth and fast shift. Two elements can happen during a shift: the engine can flair, which means that torque is not fully transferred through the transmission or the transmission can tie up, which means that two clutches are fighting.
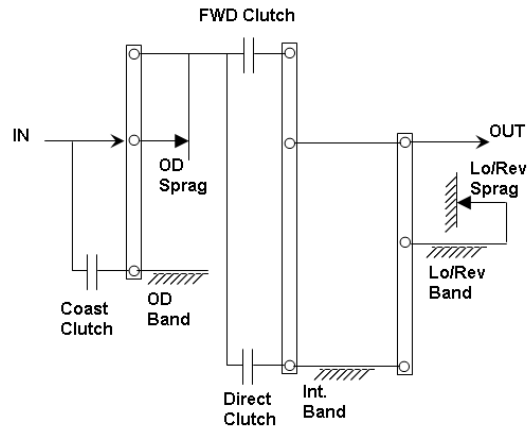
Figure 5-19: 5R55 lever diagram
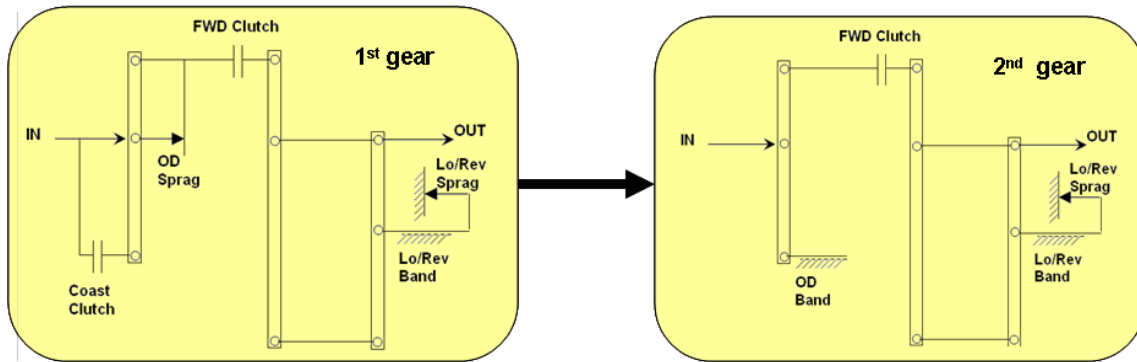
Figure 5-20: Lever diagram illustration of shifting from 1st to 2nd gear

The transmission controller calibration was quite a complex and empirical task with many hours spent on the chassis dynamometer tuning the shift for different conditions, including mild and aggressive driving. Further details on the automatic transmission are available in Appendix 3.

Personal acknowledgment

At this point, the author would like to expresses his deep gratitude to colleague Richard 'Barney' Carlson for his expertise, work, and mentorship during the implementation of this automatic transmission module for MATT. Mr. Carlson took the lead on the hardware and tuning of the automatic transmission module.

General shifting limitations and failures

Regardless of the transmission module used, almost all mechanical hardware failures on MATT occurred at the transmission input or output level. Several reasons may

have contributed to these failures. First, the transmission experiences high torque values (low gears) and high speeds (high gears). The torque in the driveline has natural frequencies in components and shafts and these torque fluctuations can fatigue the transmission. The most probable reason for failure around the transmission is the torque spikes experienced during hard shifting events. In order to reduce the shift time, the transmission needs to process inertia energies from a rotating input and output shaft. These events can be quite traumatic to the hardware. A hard shift can cause the input or output couplers to fail from the impact.

Final thoughts on shifting

Both transmission modules provided good shifting behavior, resulting in realistic powertrain behavior. Currently the manual transmission is being retrofitted with a clutch that is integrated into the transmission bell housing. This should fix the shift time issue and fix the last drawbacks of the manual transmission module.

5.4. Component characterization

5.4.1. Gasoline engine

Engine mapping

MATT is built to evaluate components on transient drive cycles in a vehicle system environment, but the component can also be characterized in steady state operation. As such, the engine efficiency was tested at different torque speed points on MATT. The chassis dynamometer was set to speed mode, thus absorbing all excess energy to maintain the target speed. With the transmission in a locked gear, the chassis dynamometer can be used as a surrogate for a steady state engine dynamometer.

Using the chassis dynamometer, the 2.3 liter gasoline engine was evaluated at different speed and brake torque points. The speed range started at 1000 rpm and was increased in 500 rpm increments to 4000 rpm. On most drive cycles, 3000 rpm is the upper limit experienced by the engine, so mapping the engine to 4000 rpm provides the full speed range used by MATT on most cycles. Another reason to stop at 4000 rpm is to minimize the chance of hardware failure by keeping the maximum steady state power transfer through the components on MATT lower. At each speed, torque levels ranging from 0 to wide open throttle in 25 N.m increments were held. Each torque speed point was held until all elements reached a steady state level. Using the engine speed and torque as well measured fuel flow and the brake thermal efficiency was calculated using Equation 5-1.

$$Efficiency_{engine\_brake\_thermal} = \frac{Power_{out}}{Power_{in}} = \frac{Power_{brake}}{Power_{fuel}} = \frac{Speed_{engine} \times Torque_{crankshaft}}{flow_{fuel} \times HeatingValue_{net}}$$

Equation 5-1: Brake thermal efficiency calculation

The resulting brake thermal efficiency for the gasoline engine is presented in Figure 5-21. The figure shows the actual measured efficiency points at the different torque speed levels. Efficiency isobars are calculated and overlaid to provide a visual aide. The graph also shows the maximum torque speed envelope available with this engine.
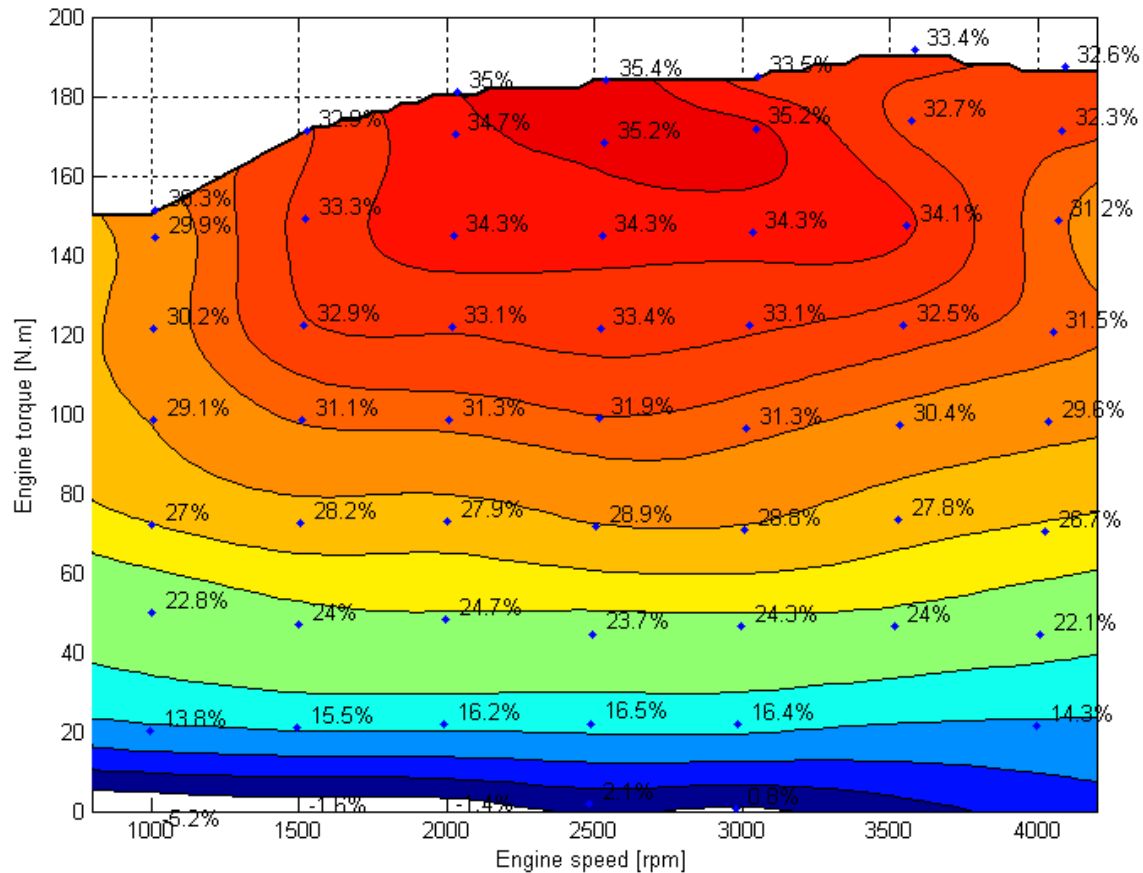
Figure 5-21: Measured engine brake thermal efficiency of the 2.3 liter gasoline engine used on MATT

Note that the peak brake thermal efficiency is 35.4%. All of the engine accessories have been removed. Therefore, this efficiency is at the crankshaft without any accessories. The first general trend is that the brake thermal efficiency increases with engine load. Above 90 N.m, the brake thermal efficiency is above 30%. Further available information was recorded from ECU including spark advance, EGR command and many other elements. Due to the collaboration with Ford, the data is not published in this dissertation. In future sections, some extra engine information is provided when relevant.

The main take-away is that MATT can be used to evaluate components in a steady state sense for mapping purposes and the data collected can be extremely in-depth.

Engine efficiency on drive cycles

The in-cylinder pressure data provides some insight into the engine operation. On the majority of the tests, the indicating system was used to record the pressure trace of the combustion events. From that information, several combustion related factors can be derived, including Indicated Mean Effective Pressure (IMEP) for gas exchange phase and work phase, peak pressure, peak pressure raise, 50% mass fraction burn, injector time and ignition time.
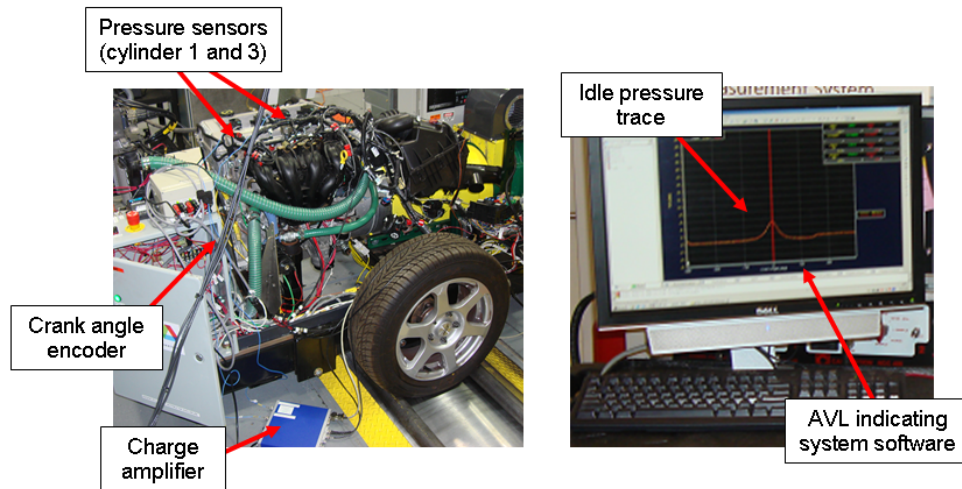
Figure 5-22: In-cylinder pressure recording and computing hardware

The in-cylinder pressure traces provide large amounts of information. Figure 5-23 shows two raw pressure traces as a function of the crank angle position. The four phases of combustion are the air fuel mixture intake, the compression stroke, the expansion and the evacuation of the exhaust. The motored trace shows the engine being spun without fuel or combustion. Therefore, this trace provides information on the amount of work used for the gas exchange (intake and exhaust) as well as the losses between the compression and expansion. The fired trace shows the pressure rise caused by the combustion after the ignition event.

The pressure traces are recorded with respect to the crank angle basis. Using the basic engine geometry, the relationship between crank angle position and sweep volume is established. The pressure profile as a function of volume (also referred to as the PV diagram in the thermo-dynamic world) is derived. The work performed by the piston is defined as the integral of the pressure with respect to the displacement, as shown in Equation 5-2. From the PV diagram, the work performed by the cylinder can be calculated as well as the Indicated Mean Effective Pressure (IMEP). The process is summarized in Figure 5-24.
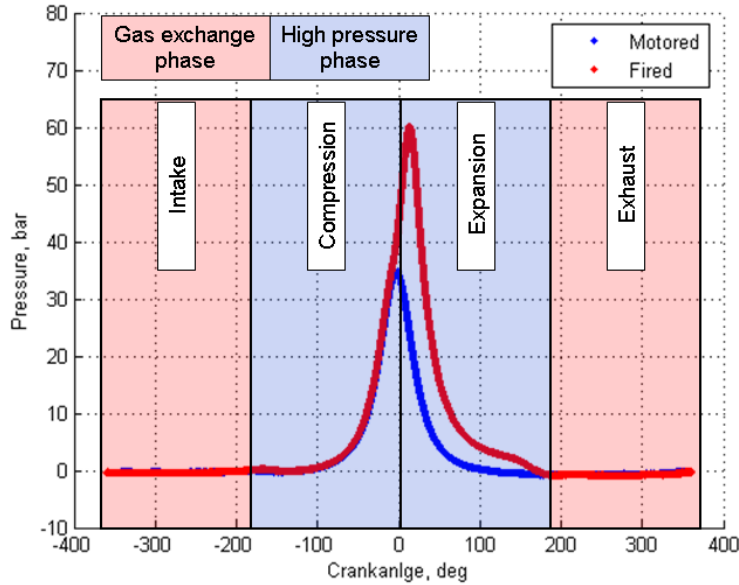
Figure 5-23: Sample pressures trace (motored and fired) as a function of crank angle

$$Work = \int PdV$$

Equation 5-2: Definition of work as a function of pressure and displacement

1. Pressure traces
2. PV diagram
3. Work vs volume
4. Work over crank angle

IMEP = Work / Volume

5. Indicated Mean Effective Pressure
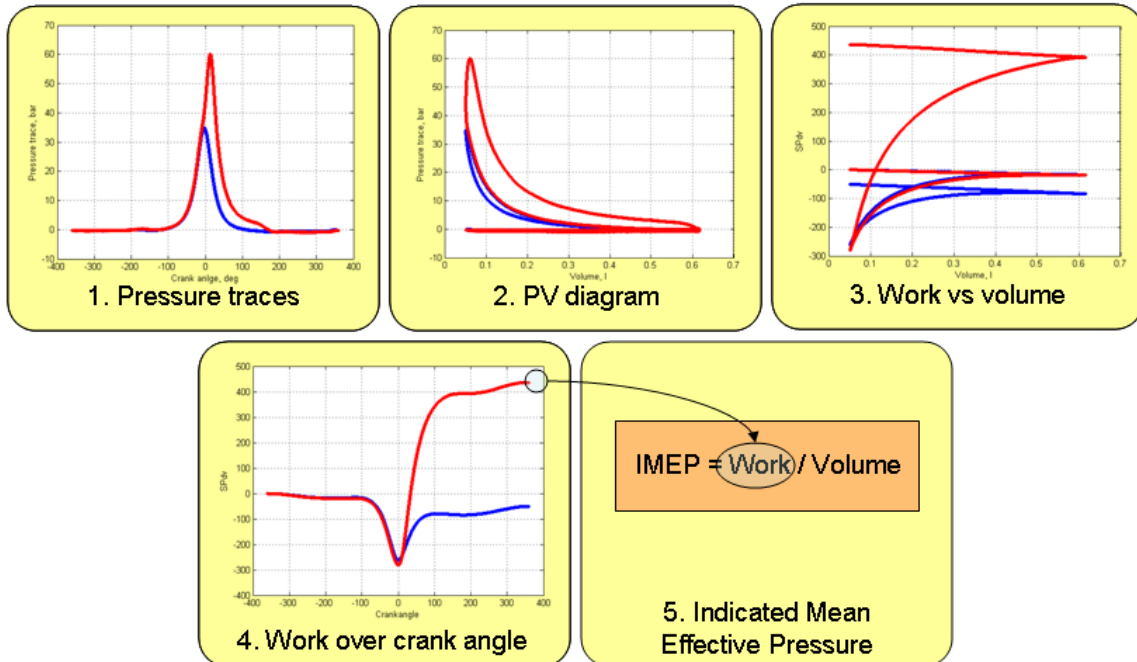
Figure 5-24: Work flow to derive IMEP from the pressure traces

This is part of the instrumentation that makes MATT an in-depth tool to investigate components, including engines. The following is a brief analysis of the information collected using the indicating system along with other instrumentation on MATT.

The several engine efficiencies, such as indicated and brake, can be derived from the data collected during the UDDS. Figure 5-25 shows these efficiencies for a hot start UDDS test. The difference between the indicated efficiency and brake efficiency represents the mechanical losses. These losses are relatively constant with a slight increase through the power ranges. As this data is derived from a test cycle, the higher power is typically higher speed, which explains the slight increase in mechanical losses since frictional losses are higher at higher speeds. The difference between the indicated efficiency with (gas exhaust and high pressure phase) and without (high pressure phase only) pumping losses shows the throttling losses. The data clearly shows the higher pumping losses at lower power levels which are due to throttling losses.
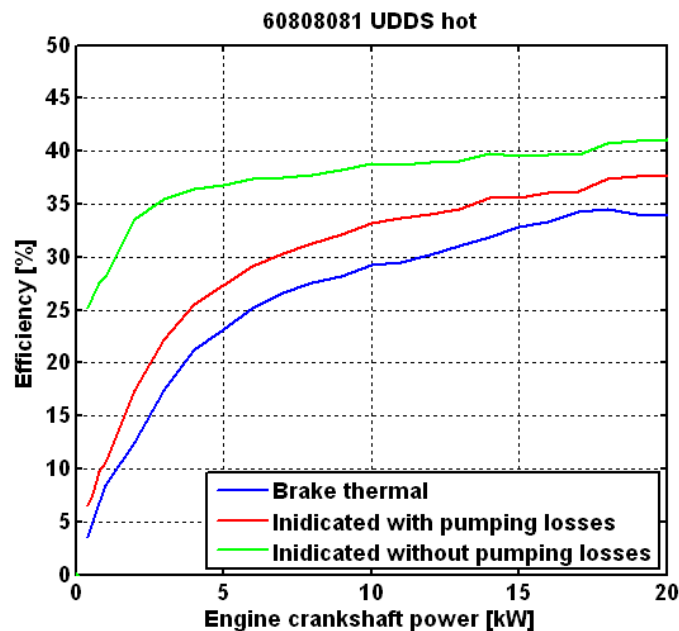
Figure 5-25: Different engine efficiency lines versus engine crankshaft power

Figure 5-25 can also be used to anticipate the engine operation in hybrid mode. If the engine is only used at a power level above 10 kW, the throttle losses are minimal and the brake thermal efficiency is around or above 30%.

Engine information used to improve control

Some information collected from the mapping exercise is used to improve the component control. For example, on the engine, a correlation between the engine speed, the engine torque and the pedal position command is established. The correlation is used for open loop pedal command to achieve a desired torque from the engine. Figure 5-26 shows this correlation used in the high level controller.
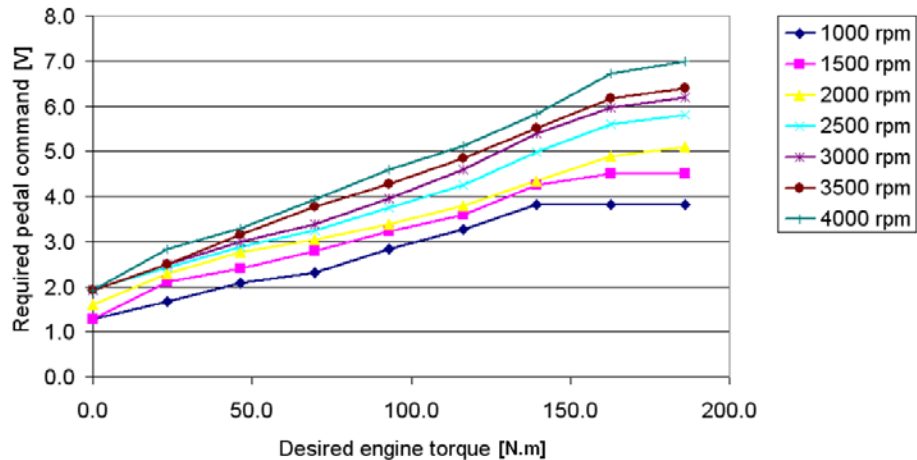
Figure 5-26: Engine pedal position as a function of designed engine speed and torque

5.4.2. Manual transmission

The transmission mapping process is very similar to the engine mapping process. The chassis dynamometer is used in steady state speed mode. The electric motor is then used in torque mode, which enables a precise torque input to the transmission. The torque and speed sensors at the input and output of the transmission are then used to compute the efficiencies.

Figure 5-27 shows the test points for 3rd gear. Note that as the torque input increases the actual input speed increases slightly. The speed difference is tire slip. The chassis dynamometer maintained the exact same speed, but as the torque at the wheel increased, the tire slipped slightly on the steel roll. In the right graph, the torque input points show the motor's maximum torque speed envelope with the constant torque region as well as the constant power region.
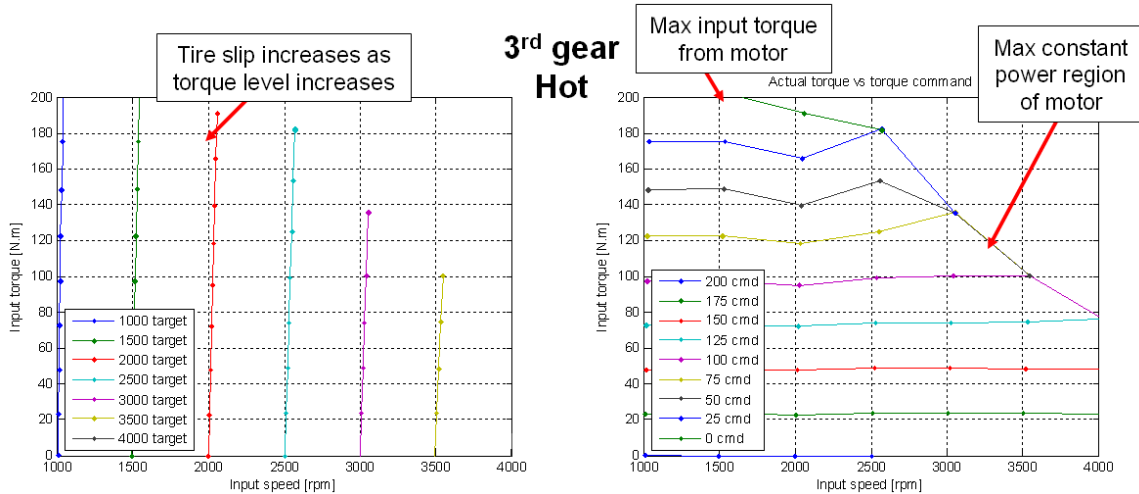
Figure 5-27: Manual transmission test points for 3rd gear

After processing all of the data, including eliminating the transient data to calculating the input and output power for each test point, the efficiencies are calculated. The results are shown in Figure 5-28; The efficiency is fairly constant over the speed range. The efficiency does vary with load. The higher the load, the higher the efficiency. A good average efficiency number is 95-96%.
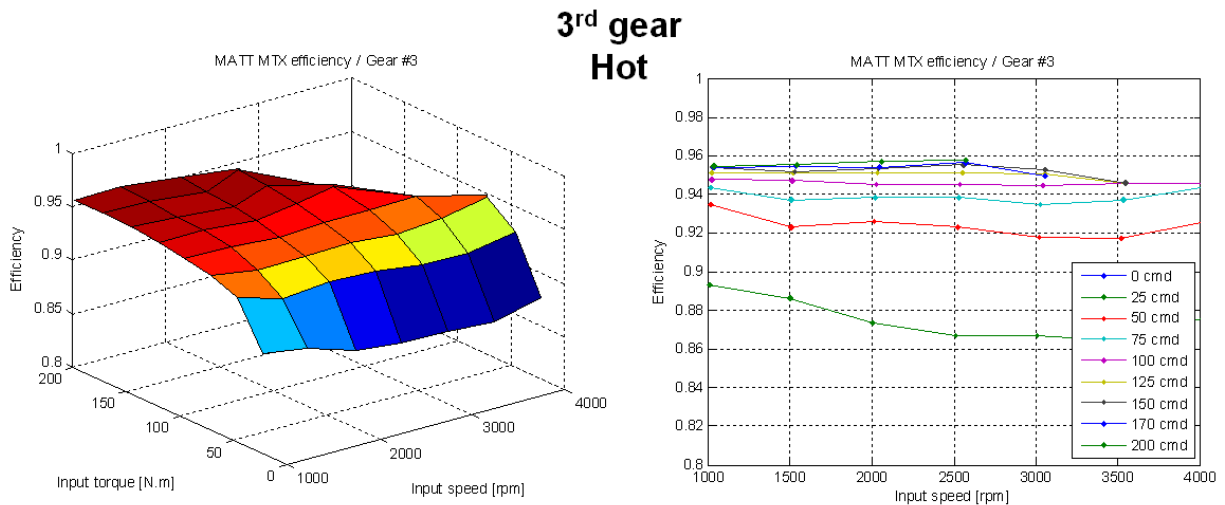
Figure 5-28: Manual transmission efficiencies for 3rd gear with a hot transmission

Note that the results are presented in terms of efficiency. The other important dimension is losses in terms of power. Although the efficiency is lower at low load, the losses in terms of power are low compared to the higher load point where the losses are quite higher despite a higher efficiency. Figure 5-28 shows the efficiency surfaces for 2nd, 3rd, 4th and 5th gears. 4th gear is the most efficient, with a 1 to 1 ratio.
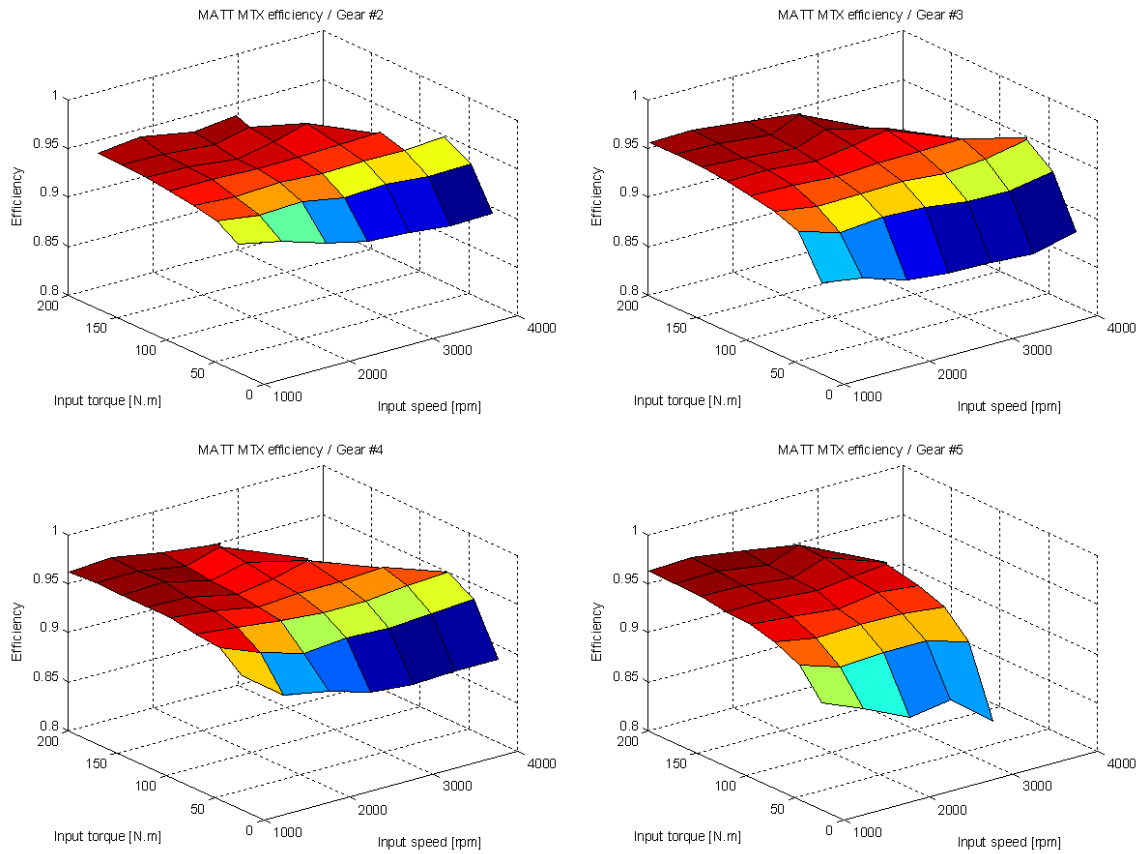
Figure 5-29: Warm manual transmission efficiency for 2nd, 3rd, 4th and 5th gear

In 1st gear at medium to high loads, the tire traction limit was hit. The tires broke loss at 1400 N.m of torque at the wheel at all of the speeds tested as shown in Figure 5-30. The tires 'whine' quite loudly and then become silent once the traction breaks. This data is useful for traction limits in simulation.
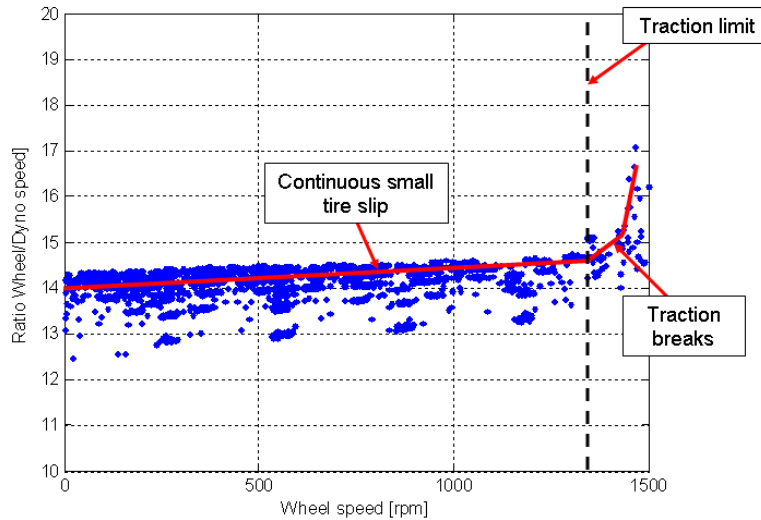
Figure 5-30: Tire traction limit from 1st gear testing at different wheel speeds

The manual transmission is straight-forward in terms of efficiency mapping. Regardless of the speed and power level transferred across the transmission, the efficiency is fairly high, in the mid-90s, percentage-wise. Further results on the manual transmission efficiency mapping are shown in Appendix 4.

5.4.3.   Automatic transmission

The automatic transmission mapping will not be presented since the efficiency is highly dependent on the tuning and calibration. As explained in section 5.3.3, the automatic transmission is managed by an aftermarket controller with calibrations that were developed on the chassis dynamometer in the APRF. These calibrations will not reflect the true efficiencies that could be achieved if the calibrations used were OEM quality and developed by a transmission calibration engineer with experience. The cycle average efficiencies are between 70 and 80 %.

This reveals one of the major limitations of MATT; that the evaluation of the different components tested is only as good as the control and calibration available for the component.

5.4.4.   Summary of the component evaluation

As shown with the conventional vehicle components, MATT can be used to evaluate each powertrain element in a systematic steady state operation with accuracy and precision. The data presented here is only a sample of the component mapping performed. The torque and speed sensors enable a complete efficiency evaluation of these components. The open powertrain modules make is easy to instrument the components and measure data. The component analysis can be quite in depth as shown by the

indicated efficiency data for the engine. The evaluation of the components is only as good as the control available.

5.5.　　　*Test results from the urban drive cycle*

For simplification purposes, the results shown for the conventional vehicle are using the automatic transmission module as well as the updated engine controller and coolant system. The data collected may be shown for comparison but it will be clearly stated. The shift schedule is based on simulation results. The simulation software has a gear shift logic which considers the vehicle characteristics, vehicle speed as well as the driver demand and deducts a gear.

The UDDS (Urban Driving Dynamometer Schedule) is the city certification cycle from the EPA on which the sticker fuel economy numbers are based as well as the emissions certifications and the Corporate Average Fuel Economy (CAFÉ). This drive cycle contains mild accelerations and low speeds to represent city driving as shown in Figure 5-31. The cycle was created over 30 years ago, when cars were slower and driving patterns different. Today the cycle is still used for certification purposes. The driving sections between stops are referred to as modes or hills. For the emissions tests, the most important timeframe is hill 2, which represents the largest acceleration. By 160 seconds, all of the after treatment systems, including the catalytic converter need to be at operating temperature or emissions are not likely to be met.
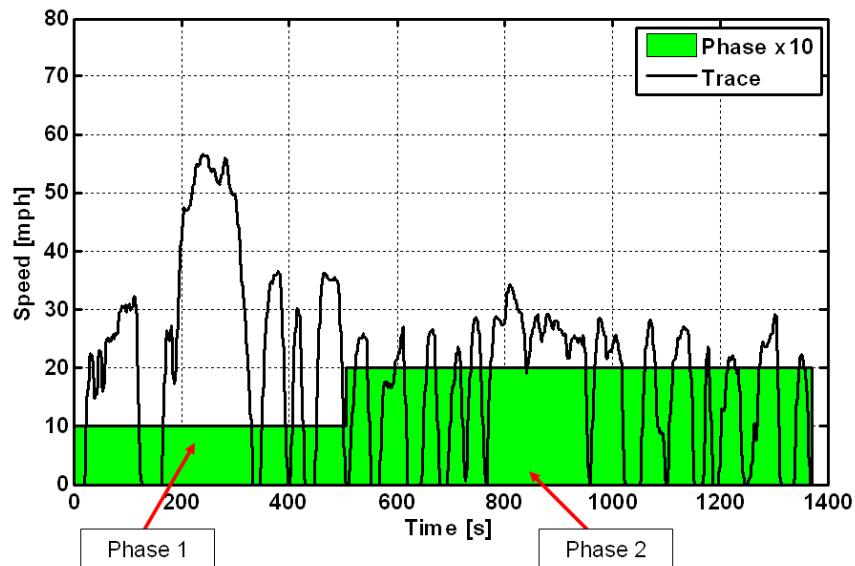
Figure 5-31: UDDS cycle profile

The power and acceleration provide some useful information on the cycle's aggressiveness. Figure 5-32 shows this information for the UDDS for a Ford Focus sized vehicle. This graph was derived using Figure 1-5. It is interesting to note that the

acceleration clipped at 1.48 m/s². In 1975, the chassis dynamometer used was the 8 inch twin-roll Clayton dynamometer, which imposed this acceleration limit for the cycle design. The speed point around 50 mph is Hill 2, and thus, the maximum power of 40 kW is the acceleration on Hill 2. Most power points are positive in order to overcome acceleration and road load. All of the negative power points represent braking on decelerations. In the conventional vehicle, this power is 'burnt' off in the braking system. Electric vehicles and hybrid vehicle can recover some of this power with regenerative braking.
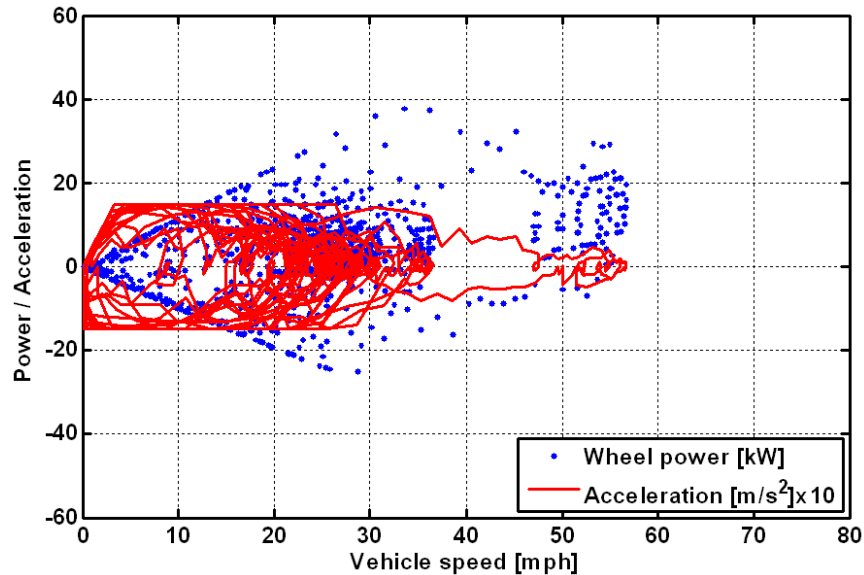
Figure 5-32: UDDS wheel power and acceleration values

Note the for the FTP cycle which starts with a preparation cycle ('prep' cycle), that is the UDDS cycle driven 12 hours before the real test. The intention is for the ECU to adjust the trim maps to the cycle and the fuel as well as to prepare the exhaust after treatment system. The car is then 'soaked' (i.e. exposed) at 25 deg C for at least 12 hours before the FTP cycle is started. The FTP is composed of an UDDS followed by a 10 minute stop with the vehicle keyed off and then the first phase of the UDDS ('505' seconds). This test is used to calculate the fuel economy and emissions. The idea is to provide a composite look of a cold start test and a hot start test. The reason the 2nd UDDS is not driven completely is that the car is considered 'hot' in phase 2 of the 1st UDDS. Thus, to save time, the data from the 2nd phase is used for what would be the 4th phase. The process is shown in Figure 5-33.
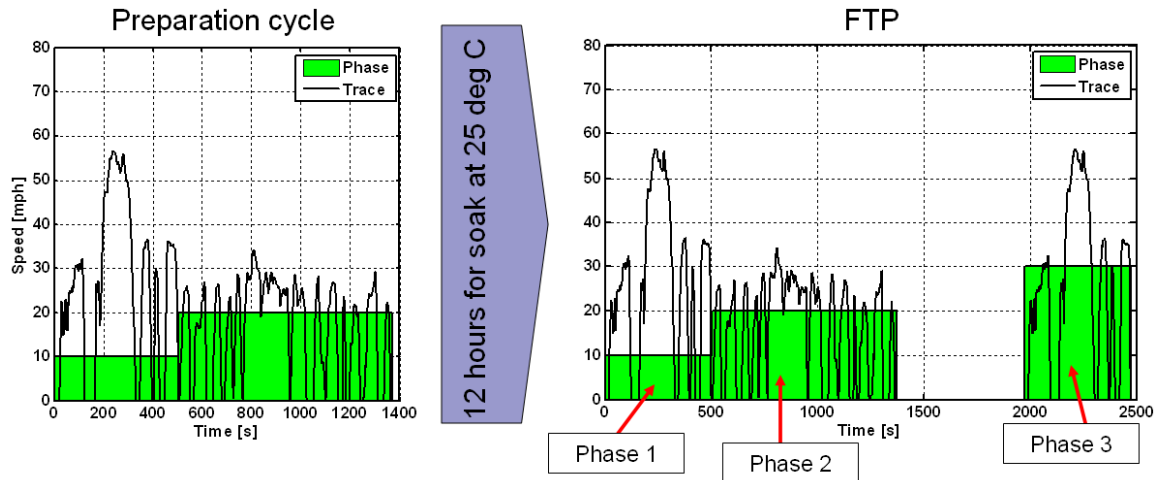
Figure 5-33: Test process for an FTP

5.5.1. Summarized test results for UDDS

For certification purposes, a cold start UDDS test is performed followed by a 10 min soak and then another UDDS. The test results are summarized in Table 5-1. The cold start test is a test where the vehicle has rested in ambient temperature conditions of 25 deg C for at least 12 hours and is started for the first time at the start of the UDDS. MATT, operating as a conventional vehicle, achieves SULEV.

Table 5-1: Conventional vehicle UDDS test results (as mid-size sedan)

	UDDS (cold start)	UDDS (hot start)	Hot-Cold weighted
Fuel economy bag [mpg]	25.5	27.2	26.5
THC [g/mi]	0.010	0.001	0.006
NOx [g/mi]	0.007	0.001	0.005

Argonne's correlation vehicle, which MATT is emulating, achieves 26.6, 27.5 and 27.1 mpg on a cold start UDDS, a hot start UDDS and the hot-cold weighted test, respectively. These fuel economy results are similar, and the variations come from the hardware. The correlation vehicle uses a 2 liter engine and a 5-speed automatic transmission, since the purpose of the correlation vehicle is to verify fuel economy and emissions measurements of the APRF on a regular basis.

5.5.2. Data from UDDS cycle in the time domain

During these drive cycles, the driver stayed within the required boundaries of the trace at all times. Figure 5-34 shows the entire drive trace, the vehicle speed and different

temperature information. All of the temperatures start at 25 deg C, which indicates the cold start conditions. The engine coolant and the catalytic converter reach operating temperatures by the start of mode 2 (Hill 2). The engine oil temperature and transmission temperature steadily increase throughout the test and almost reach a steady state temperature.
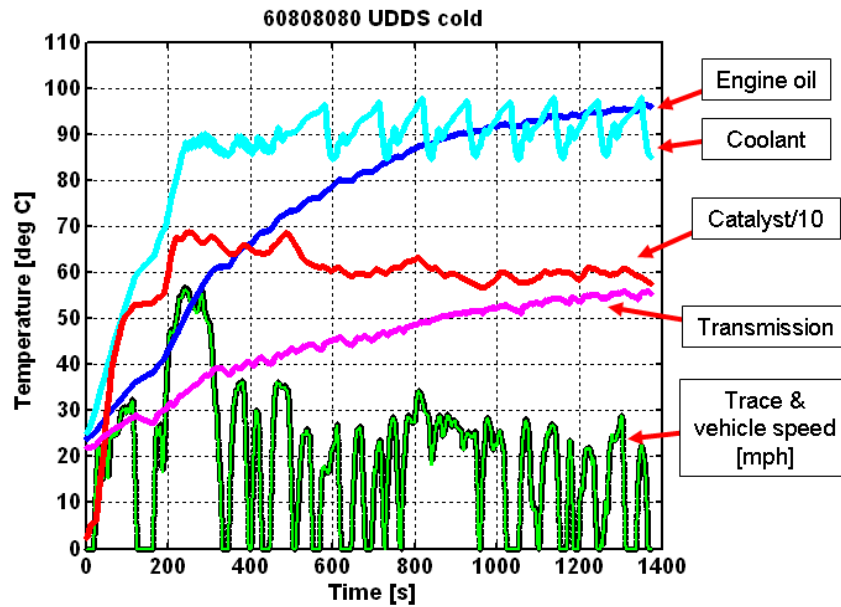
Figure 5-34: Trace and temperature information for the conventional vehicle on cold start UDDS

Using the instrumentation on MATT, the power flow from the fuel input to the wheels is calculated. Figure 5-35 shows the power levels on the first mode of the UDDS to illustrate the details of the transients. The fuel power is calculated using the fuel flow measurement and the net heating value of the certification fuel. The indicated engine power is based on the IMEP data converted to indicated torque and the engine speed. The engine brake power is calculated with the engine torque and speed sensor. In a similar way, the transmission torque speed sensor is used to compute that power. The dynamometer power is calculated based on the reported tractive force and dynamometer speed. All power measured between the components shows the losses of each component. The biggest loss is in the fuel conversion to the engine crankshaft torque and speed. Most other conversion processes are more efficient.
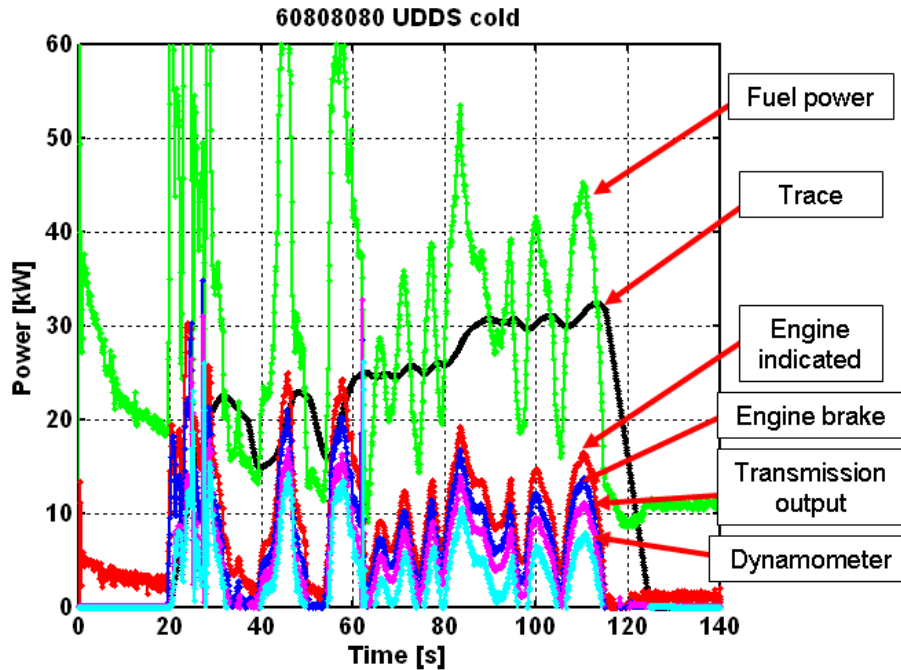
Figure 5-35: Power calculation based on the sensors for the conventional vehicle

Another important piece of information is the modal emissions data. Figure 5-36 shows the cold start emissions of the first engine start while the catalyst is cold. The catalytic converter is far from light-off temperature and, thus, cannot convert the excess hydrocarbons caused by the engine still operating in open loop. It should be noted that over 95% of emissions are generated by the end of the first mode. Figure 5-37 shows the same engine start and mode 1 of the urban cycle after a 10 minute soak following the end of the cold start UDDS. The hot start emissions for the engine are significantly lower since the converter is already at 300 deg C. Thus, the conversion efficiency is already high and the engine is already operating in a closed loop at stoichiometric operation.
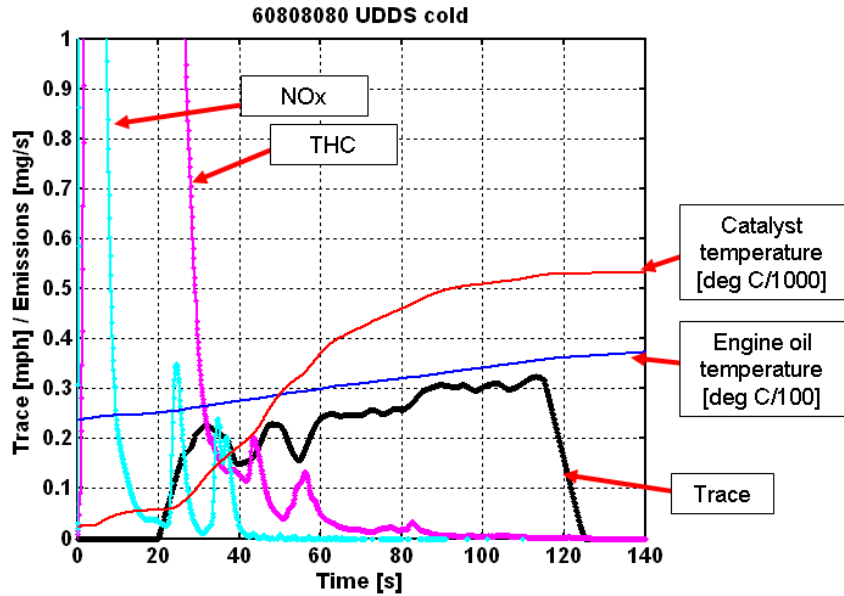
Figure 5-36: Emissions measurement for the conventional vehicle for the cold start
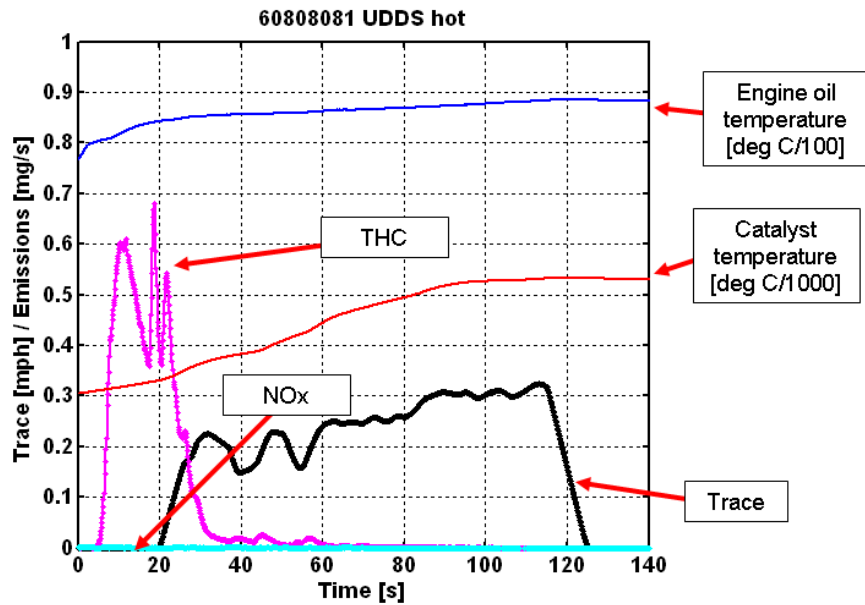
Figure 5-37: Emissions measurement for the conventional vehicle for a hot start

5.5.3. Component performance on cold start and hot start UDDS test cycles

Using the recorded data, the total energies for each component are calculated from the all of the cycles. The dynamometer energy calculations are based on the integration of the positive dynamometer power only. All of the other components only experience positive torque in the conventional mode. Table 5-2 summarizes these results.

Table 5-2: Cold and hot UDDS total positive energy measured for the components (7.45 miles)

Energy [MJ]	UDDS (cold start)	UDDS (hot start)
Fuel	34.50	31.90
Engine indicated	10.26	9.26
Engine crankshaft	8.61	8.09
Transmission	6.52	5.76
Dynamometer	4.50	4.51
Braking (possible regen)	2.22	2.22

8% more fuel is used to complete the UDDS on a cold start compared to the hot start. During the cold start test, more energy went through every component. While the components are operating at room temperature, they are less efficient. In general, friction losses are higher at lower temperatures. Some energy is also used to bring components up to operating temperature. The engine, during its own warm up phase, will typically retard sparks to exhaust more heat, thus lowering the MEP. Therefore, more energy is put into the transmission to meet the drive cycle during the cold start and even more fuel is used by the engine due to increased mechanical losses. The overall powertrain efficiency using the positive power all the wheels and the fuel energy used is 13% and 14% for the cold start and hot start respectively.

Each component's average efficiency for the drive cycle is computed in Table 5-3. Note that the automatic transmission efficiency is a bit lower than expected. This is due to the lack of professional calibration. This demonstrates that the component evaluation is only as good as the control of the component.

Table 5-3: Average UDDS cycle component efficiencies

Average cycle efficiency	UDDS (cold start)	UDDS (hot start)
Engine indicated	29.7 [%]	29.0 [%]
Engine brake	24.9 [%]	25.3 [%]
Transmission	75.8 [%]	78.4 [%]

The average indicated efficiency is higher for a cold start test despite the fact that the brake thermal efficiency is lower. During the cold start, the engine has to produce more energy through the cycle, thus, it operates at a higher average power and yields a higher average indicated efficiency. The brake thermal efficiency includes the mechanical losses that, during the cold start, are so significant that despite the higher indicated efficiency the brake thermal efficiency is lower. Figure 5-38 compares the

average power losses from the fuel input to the engine crankshaft for the first 505 seconds of a UDDS test. The cold start and the hot start results are compared.
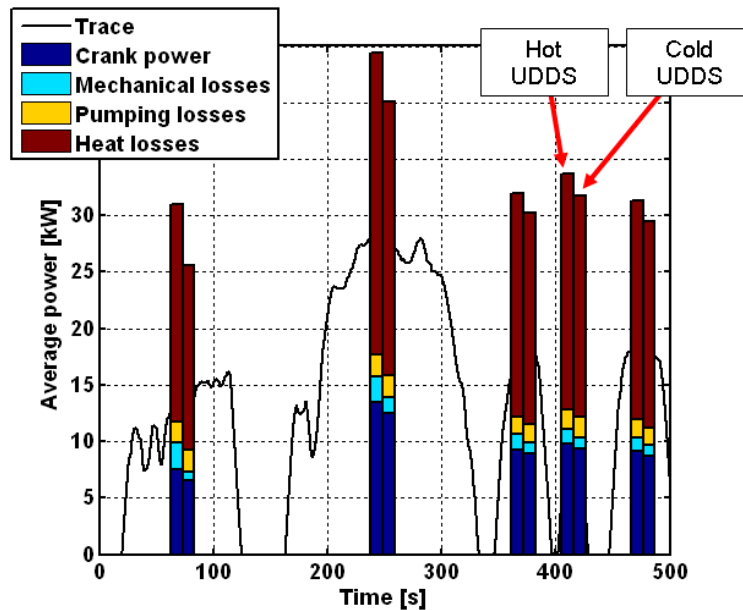
Figure 5-38: Decomposing the average fuel power into the losses to the engine crankshaft

The crank power is higher for the cold start for each hill, but as the components warm up, that difference is diminished. The mechanical losses are four times as high for the cold start on the first hill and only 50% greater on Hill 5 for the cold start, thus demonstrating that frictional losses are proportional to temperature (see Figure 5-34). At the same time, the pumping losses are lower for the cold start because the engine is required to produce more torque at the crank and thus the throttle is, on average, more wide open on cold starts, reducing the pumping losses. The 'heat losses' label mainly represents the heat losses due to the exhaust gases and heat wall losses, but also includes unburnt fuel. These heat losses are also more significant for the cold start.

5.5.4.   Engine operating area on UDDS

Since the conventional vehicle is the baseline, a final interesting plot to consider is an engine torque speed contour plot of the amount of energy used. This is shown in Figure 5-39. In hybrid operation, the engine can be decoupled from the wheel load using the hybrid system. Also notice from Table 5-2 that 2.22 MJ of kinetic energy is dissipated in heat and could be available for regenerative braking in a hybrid.
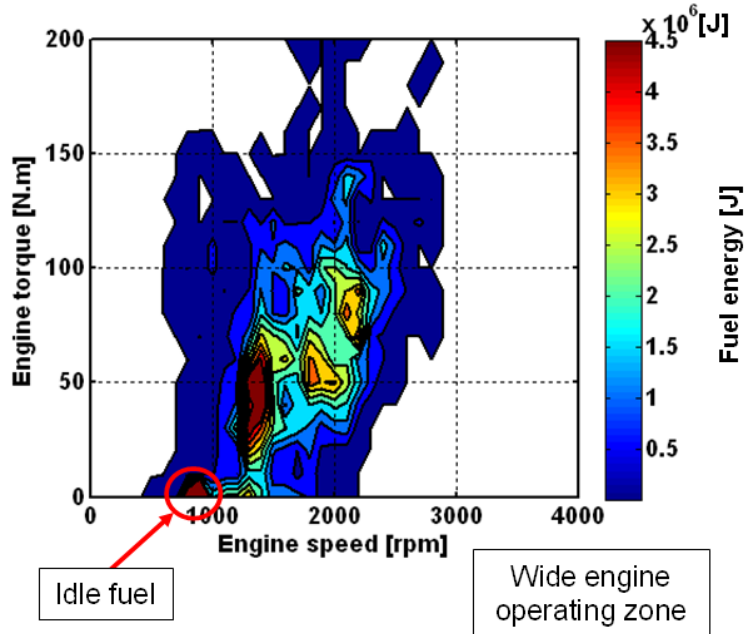
Figure 5-39: Conventional vehicle fuel energy used over engine torque speed ranges on UDDS

5.5.5. Fuel losses of a conventional vehicle

While the vehicle is stopped during the drive cycles, the engine still consumes fuel while idling and the launch operation is fairly inefficient. Figure 5-40 shows both situations.
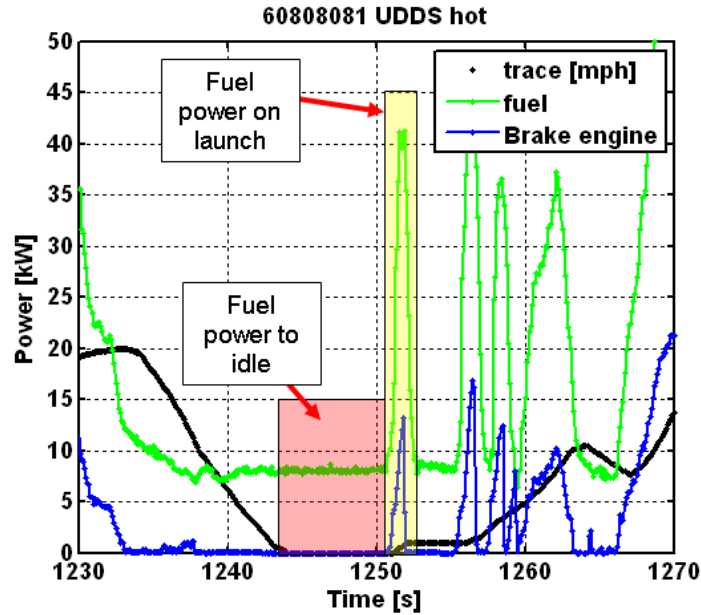
Figure 5-40: Engine idle and launch losses on the UDDS

During a UDDS, the vehicle is stopped over 17% of the time. Using the data from the hot start, this represents 0.019 gallons of fuel out of the total 0.229 gallons used. So 6.9% of the fuel could be saved by preventing idling, which is possible in a hybrid vehicle.

By assuming an average engine and transmission efficiency and using the power at the wheel during launch, a theoretical ideal fuel flow rate can be calculated. Using this approach, the fuel losses due to engine revving and clutch slip can be estimated. About 0.009 gallons of fuel are used during the launches throughout the UDDS, which represents over 3% of the total fuel used.

5.5.6.   Conventional vehicle operation on UDDS

The fuel economy and emissions results of the conventional vehicle operation on the UDDS were presented and analyzed in detail. The UDDS cycle is the most important cycle since it is the benchmark cycle for the fuel economy and emissions measurements. Therefore, this section covered the conventional vehicle behavior in depth on the UDDS. MATT behaves quite similarly to the correlation Ford Focus that is emulated in this work. It was noted that the automatic transmission has a lower than expected cycle efficiency due to the lack of refined calibration. But this transmission is used in most other tests, thus keeping this handicap across the different vehicle modes constant.

5.6.   *Test results from the highway drive cycle*

For simplification purposes, the results shown for the conventional vehicle use the automatic transmission module as well as the updated engine controller and coolant system. The data collected may be shown for comparison, but it will be clearly stated in those cases. The shift schedule is based on simulation results.

The highway cycle goes hand-in-hand with the UDDS, and represents the highway driving for sticker fuel economy and CAFE. Compared to today's driving patterns, this cycle is also mild and low speed. In general, when testing a vehicle on the highway cycle on a chassis dynamometer, two cycles are repeated back to back. The first cycle is the preparation cycle which serves to warm up all the powertrain components and the second cycle is the test cycle where fuel economy is measured. The highway cycle is pictured in Figure 5-41. The average power levels and the vehicle speed are higher compared to those components in the UDDS, as shown in Figure 5-42.
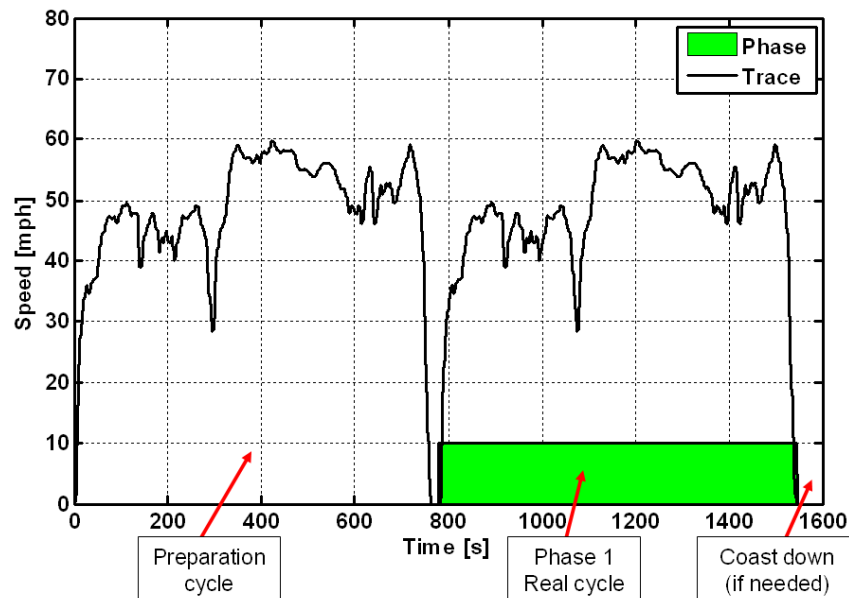
Figure 5-41: Highway cycle profile
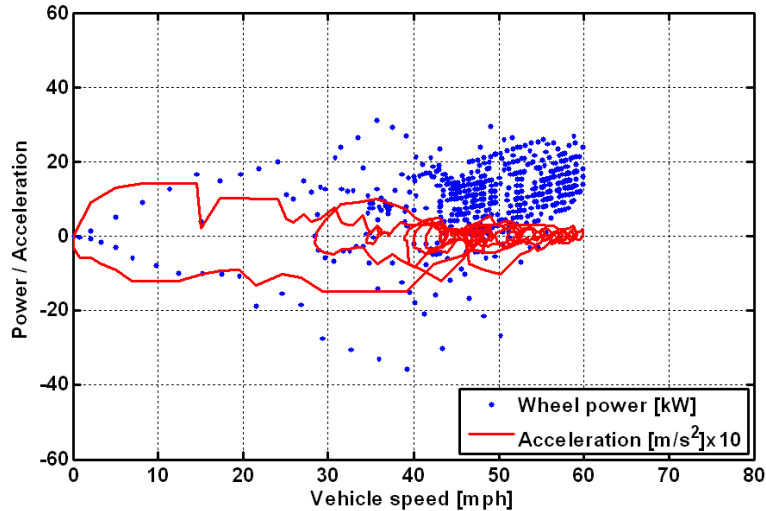
Figure 5-42: Highway cycle power and acceleration values

The fuel economy measured on the 2nd hot highway cycle is 36.7 mpg, which is similar to the Focus correlation vehicle, which achieves 38 mpg. The shift schedule used by MATT on the highway cycle was derived from simulation results. With a modified shift schedule that did not downshift as often, 39.5 mpg was measured with MATT.

The energy summary of the powertrain components is presented in Table 5-4. The efficiency of these components is presented in Table 5-5. The average engine efficiency is higher compared to the engine efficiency for the UDDS. The engine operates with a higher load on average, thus operating the engine in a higher efficiency area. The lower transmission efficiency as compared to that of the UDDS is another side effect of the lack of refinement of the automatic transmission calibration. In fact, the line pressure at higher speeds was increased from the base calibration after some of the internal clutches slipped and overheated the transmission fluid leading to some hardware failure. The 'high speed' portion of the automatic transmission calibration was then tuned toward protecting the hardware. This was achieved to the detriment of operating efficiency.

Table 5-4: Highway total positive energy measured for the components (10.25 miles)

Energy	Highway (hot)
Fuel	33.3 [MJ]
Engine indicated	13.4 [MJ]
Engine crankshaft	11.4 [MJ]
Transmission	10.2 [MJ]
Dynamometer (positive traction)	7.6 [MJ]
Braking (possible regen)	0.6 [MJ]

Table 5-5: Average highway cycle component efficiencies

Average cycle efficiency	HWY (hot)
Engine indicated	34.3 [%]
Engine brake	29.7 [%]
Transmission	75.1 [%]

The engine operation range is shown in Figure 5-43. The graph shows the fuel energy used during the highway cycle in the torque speed range. For the majority of the time, the engine operates in a more restrained area of speed and load range compared to the range for the UDDS cycle. The fuel used during idle is insignificant compared to the city cycle. Thus, the fuel economy is relatively high, since little fuel is wasted on idle, inefficient engine operating range, acceleration and braking. Thus, a hybrid vehicle provides the most gains on the UDDS and only marginal benefits on the highway cycle.
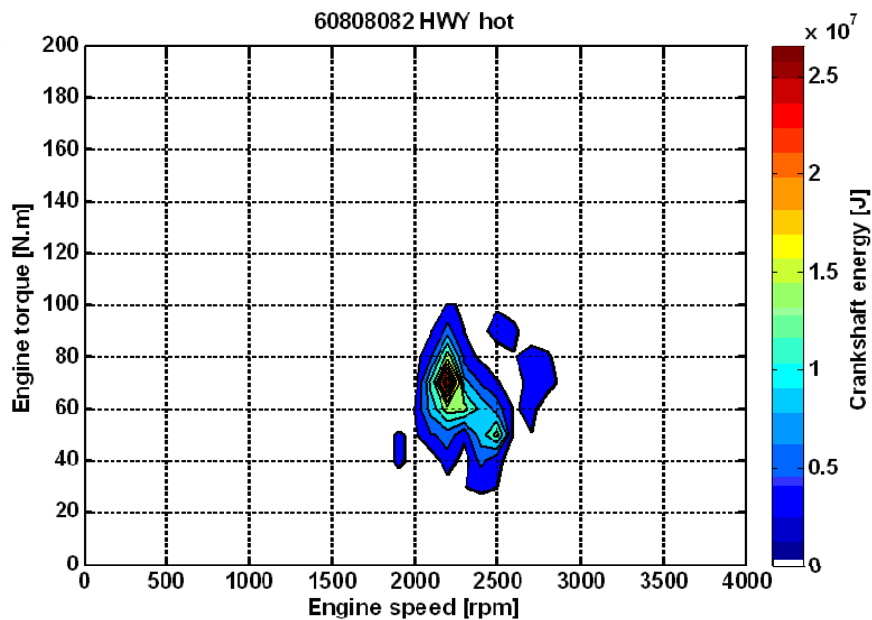
Figure 5-43: Conventional vehicle fuel energy used over engine torque speed ranges on highway cycle

The control of the conventional vehicle is easier on the highway cycle than on the UDDS, due to fewer vehicle launches and shifts. The baseline results correspond to the correlation vehicle.

5.7. *Test results for other drive cycles*

A large number of drive cycles were tested with MATT as a conventional vehicle. The major drive cycles are the UDDS and the HWY, which are analyzed in depth in the previous sections. The next sets of drive cycles can be broken down into linear drive cycles and smooth drive cycles. Figure 5-44 illustrates MATT's progression from a simple linear drive to a smooth complex drive cycle.
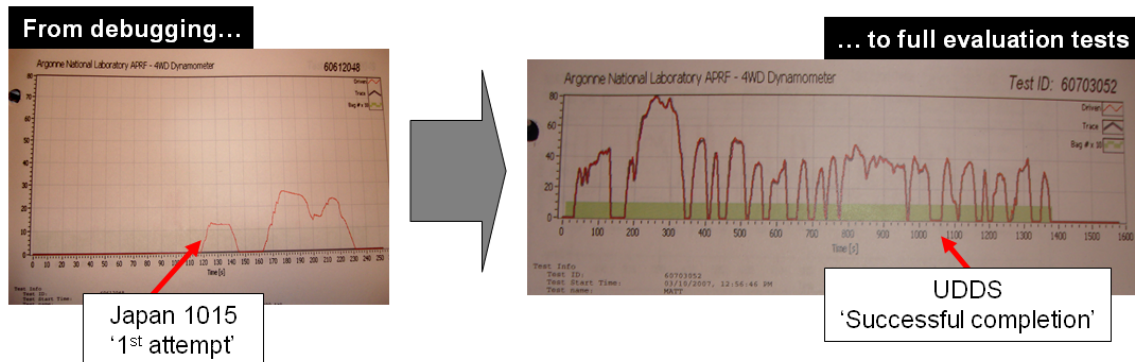
Figure 5-44: From first cycle attempt to successful completion of complex cycles

Appendix 5 presents all of the drive cycles used in this dissertation including vehicle speed, acceleration and power graphs, along with a full statistical analysis of the cycle and MATT cycle specific power numbers. All of the test results on the drive cycles presented here are hot start tests. The list of data collected on each cycle in detailed in Appendix 6.

The NEDC (New European Drive Cycle) and the Japan 1015 are the typical linearized tests. These tests are excellent tests to debug any vehicle operating mode on MATT, or even to debug new hardware components. The simplicity of these cycles allows testing of the basic driving modes; accelerations, steady state speed driving, braking and stop. The test results for the NEDC and Japan 1015 are presented Table 5-6. The full details with graphs are presented in Appendix 7. Note that these tests are also useful to evaluate the basic component performance.

Table 5-6: Measured test data for the simple linear drive cycles

	NEDC	**Jap 1015**
Test number	60807056	60807055
Distance	6.9 [mi]	2.6 [mi]
Fuel economy	**35.01 [mpg]**	**30.69 [mpg]**
Emissions		
THC	0.0017 [g/mi]	0.0028 [g/mi]
CH4	0.0005 [g/mi]	0.0035 [g/mi]
NMHC	0.0016 [g/mi]	0.0016 [g/mi]
NOx	0.0023 [g/mi]	0.0620 [g/mi]
CO	0.0766 [g/mi]	0.0299 [g/mi]
CO2	253.8 [g/mi]	289.7 [g/mi]
Energy summary		
Fuel	27.8 [MJ]	12.45 [MJ]
Engine indicated	10.23 [MJ]	4.00 [MJ]
Engine crankshaft	6.88 [MJ]	2.53 [MJ]
Transmission	5.35 [MJ]	1.84 [MJ]
Dynamometer (positive traction)	3.96 [MJ]	1.42 [MJ]
Braking (possible regen)	1.39 [MJ]	0.82 [MJ]
Average cycle efficiency		
Engine indicated	36.8 [%]	32.1 [%]
Engine brake	24.8 [%]	20.3 [%]
Transmission	74.1 [%]	77.5 [%]

The next set of drive cycles emulates real driving with smooth drive traces at varying speeds, acceleration and deceleration rates. The LA92, ATDS and JC08 represent these cycles. The measured test results are shown in Table 5-7. Again, the full details with graphs are presented in Appendix 7

Table 5-7: Measured test data for more complex drive cycles

	LA92	**ATDS**	**JC08**
Test number	60807061	60807063	60807062
Distance [mi]	9.8 [mi]	15.7 [mi]	6.4 [mi]
Fuel economy	**28.22 [mpg]**	**30.22 [mpg]**	**30.80 [mpg]**
Emissions			
THC	0.0019 [g/mi]	0.0001 [g/mi]	0.0021 [g/mi]
CH4	0.0010 [g/mi]	0.0009 [g/mi]	0.0017 [g/mi]
NMHC	0.0015 [g/mi]	0.0002 [g/mi]	0.0015 [g/mi]
NOx	0.0064 [g/mi]	0.1091 [g/mi]	0.0564 [g/mi]
CO	0.0408 [g/mi]	0.0211 [g/mi]	0.0749 [g/mi]
CO2	315.08 [g/mi]	294.20 [g/mi]	288.55 [g/mi]
Energy summary			
Fuel	47.06 [MJ]	69.00 [MJ]	29.47 [MJ]
Engine indicated	18.99 [MJ]	30.24 [MJ]	10.74 [MJ]
Engine crankshaft	12.42 [MJ]	19.16 [MJ]	6.28 [MJ]
Transmission	9.67 [MJ]	15.17 [MJ]	4.69 [MJ]
Dynamometer (positive traction)r	7.68 [MJ]	12.30 [MJ]	3.66 [MJ]
Braking (possible regen)	3.70 [MJ]	3.80 [MJ]	1.92 [MJ]
Average cycle efficiency			
Engine indicated	40.4 [%]	43.8 [%]	36.4 [%]
Engine brake	26.4 [%]	27.8 [%]	21.3 [%]
Transmission	79.4 [%]	80.1 [%]	78.0 [%]

On all of the tests, the transmission efficiency is a bit lower than expected. As already explained, this is due to a lack of refinement in tuning and calibration on the aftermarket transmission controller.

In summary, MATT completed all of the standard drive cycles in conventional mode while emulating a Focus. For all of these baseline cases, the component efficiency, fuel economy and emissions were measured and reported.

5.8. Special studies

5.8.1. Steady state speeds

Using the integrated software driver, steady state speeds are precisely maintained. The power required to maintain a vehicle's speed is defined by the vehicle's characteristics at that speed. Also, the higher the load is on the engine, the higher the engine efficiency. Thus, at a given speed, the highest possible gear should be selected.

Figure 5-45 confirms that logic with the data. At 30 mph, 3rd, 4th or 5th gear can be used and the fuel economy changes from 32 mpg to 49 mpg to 58 mpg, respectively. From a drivability standpoint, 5th gear does not give the driver as much torque to accelerate quickly, but the fuel economy advantage is almost doubled compared to other gears.
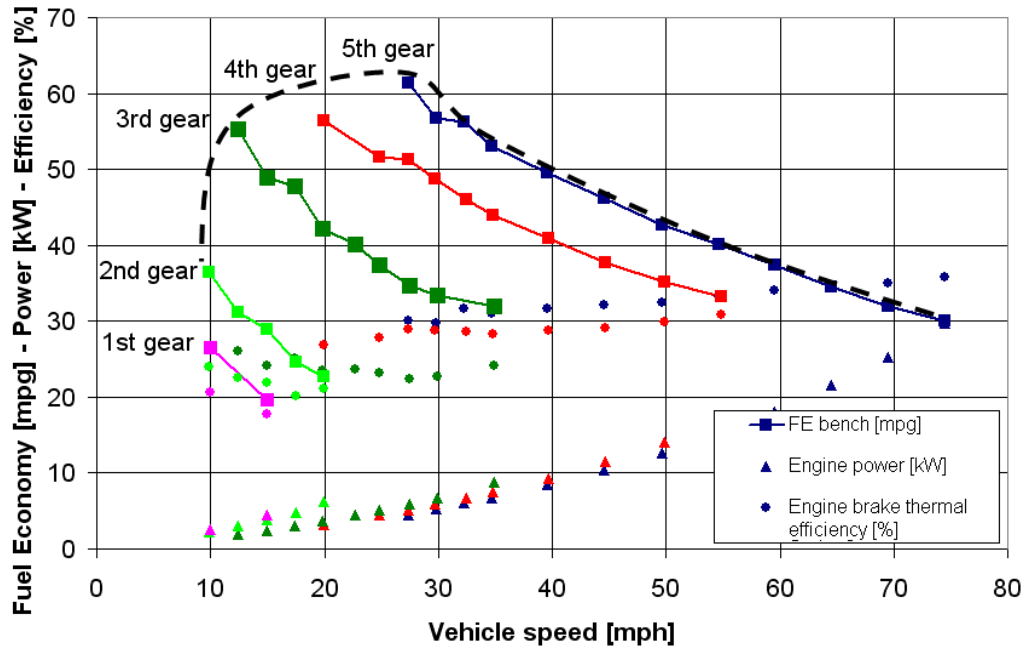
Figure 5-45: Conventional vehicle steady state speed results

Although the engine efficiency is increased at higher speeds, the overall energy required to maintain the speed negates the advantage of the increased engine efficiency. The peak fuel economy is at 27.5 mph in 5th gear, which is the trade off point between lower power required at the wheel and engine efficiency.

5.8.2. Fuel economy sensitivity to drive cycle intensity study

EPA's sticker fuel economy numbers are derived from the UDDS and highway cycles. These cycles are from the 1970s and are not representative of today's driving patterns in the U.S. In recent years, the EPA has addressed the problem, applying a correction factor to the test results. The disparity between sticker fuel economy displayed in the showroom and 'real world driving' fuel economy was a focal point in the media when fuel prices were at record highs. This prompted Argonne to investigate the fuel economy sensitivity to drive cycle intensity, which resulted in a landmark paper (Ref. 74).

To investigate the fuel economy sensitivity, the UDDS cycle is scaled by factors of 0.8, 1.2 and 1.4. First, only the speed trace is scaled. In a second test set the time and

the speed trace are scaled so that the total distance driven is the same 7.45 miles of the UDDS cycle. MATT completed the same test sets, as summarized in the Figure 5-46, Table 5-8, Figure 5-47 and Table 5-9.
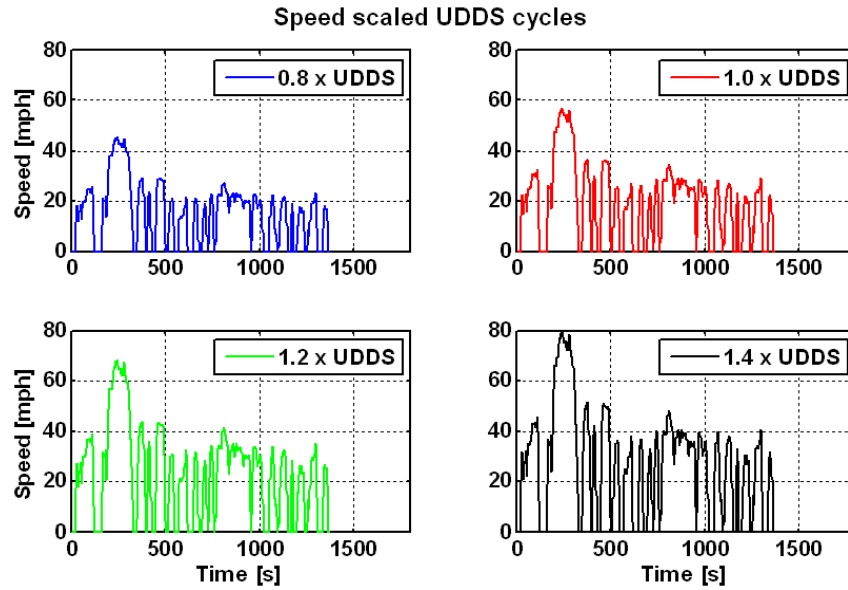
Figure 5-46: Scaled speed UDDS cycles (time constant)

Table 5-8: Measured test data from scaled speed UDDS drive cycles (time unchanged)

	UDDS	**0.8 UDDS**	**1.2 UDDS**	**1.4 UDDS**
Test number	60807041	60807051	60807049	60807050
Distance	7.45 [mi]	5.96 [mi]	8.94 [mi]	10.43 [mi]
Fuel economy	**30.76 [mpg]**	**34.06 [mpg]**	**29.57 [mpg]**	**27.93 [mpg]**
Emissions				
THC	0.0015 [g/mi]	0.0010 [g/mi]	0.0007 [g/mi]	0.0013 [g/mi]
CH4	0.0015 [g/mi]	0.0027 [g/mi]	0.0038 [g/mi]	0.0000 [g/mi]
NMHC	0.0010 [g/mi]	0.0001 [g/mi]	0.0006 [g/mi]	0.0013 [g/mi]
NOx	0.5025 [g/mi]	0.0201 [g/mi]	0.0310 [g/mi]	0.0907 [g/mi]
CO	0.0200 [g/mi]	0.0477 [g/mi]	0.0350 [g/mi]	0.0504 [g/mi]
CO2	289.06 [g/mi]	261.03 [g/mi]	300.68 [g/mi]	318.24 [g/mi]
Energy summary				
Fuel	33.33 [MJ]	25.63 [MJ]	40.50 [MJ]	49.96 [MJ]
Engine indicated	N/A	8.36 [MJ]	14.67 [MJ]	18.99 [MJ]
Engine crankshaft	7.89 [MJ]	5.22 [MJ]	10.29 [MJ]	13.78 [MJ]
Transmission	5.71 [MJ]	3.63 [MJ]	7.84 [MJ]	10.80 [MJ]
Dynamometer (positive traction)	4.27 [MJ]	2.69 [MJ]	6.34 [MJ]	8.85 [MJ]
Braking (possible regen)	2.20 [MJ]	1.43 [MJ]	3.16 [MJ]	4.26 [MJ]
Average cycle efficiency				
Engine indicated	N/A	32.6 [%]	36.2 [%]	38.0 [%]
Engine brake	23.6 [%]	20.4 [%]	25.4 [%]	27.6 [%]
Transmission	74.9 [%]	74.2 [%]	80.8 [%]	81.9 [%]

Time and speed scaled UDDS cycles

Figure 5-47: Scaled time and speed UDDS cycles

Table 5-9: Measured test data from scaled time and speed UDDS drive cycles

	UDDS	0.8 UDDS	1.2 UDDS	1.4 UDDS
Test number	60807041	60807054	60807052	60807053
Distance	7.45 [mi]	7.45 [mi]	7.45 [mi]	7.45 [mi]
Fuel economy	**30.76 [mpg]**	**34.45 [mpg]**	**28.77 [mpg]**	**24.12 [mpg]**
Emissions				
THC	0.0015 [g/mi]	0.0004 [g/mi]	0.0023 [g/mi]	0.0023 [g/mi]
CH4	0.0015 [g/mi]	0.0003 [g/mi]	0.0015 [g/mi]	0.0007 [g/mi]
NMHC	0.0010 [g/mi]	0.0005 [g/mi]	0.0018 [g/mi]	0.0021 [g/mi]
NOx	0.5025 [g/mi]	0.0114 [g/mi]	0.0832 [g/mi]	0.6823 [g/mi]
CO	0.0200 [g/mi]	0.0273 [g/mi]	0.0263 [g/mi]	0.0452 [g/mi]
CO2	289.06 [g/mi]	250.80 [g/mi]	309.08 [g/mi]	368.63 [g/mi]
Energy summary				
Fuel	33.33 [MJ]	30.77 [MJ]	35.17 [MJ]	41.134 [MJ]
Engine indicated	N/A	9.95 [MJ]	13.47 [MJ]	16.13 [MJ]
Engine crankshaft	7.89 [MJ]	6.02 [MJ]	9.42 [MJ]	11.82 [MJ]
Transmission	5.71 [MJ]	4.17 [MJ]	7.27 [MJ]	9.31 [MJ]
Dynamometer (positive traction)	4.27 [MJ]	2.94 [MJ]	5.90 [MJ]	7.73 [MJ]
Braking (possible regen)	2.20 [MJ]	1.40 [MJ]	3.19 [MJ]	4.34 [MJ]
Average cycle efficiency				
Engine indicated	N/A	32.4 [%]	38.3 [%]	39.2 [%]
Engine brake	23.6 [%]	19.6 [%]	26.8 [%]	28.7 [%]
Transmission	74.9 [%]	70.5 [%]	81.2 [%]	83.0 [%]

As the drive cycle scaling factor is increased, the drive cycle appears more aggressive (has a higher intensity). On the slowest and least aggressive cycle, the engine cycle efficiency is 19.6%, due to the low average loading. In comparison, the engine cycle efficiency for the most aggressive cycle is 28.7%. Despite the higher component efficiencies on the most aggressive drive cycles, the average power (or total energy over the cycles) at the wheel is so high that the fuel economy is the lowest. Figure 5-48 summaries the fuel economy results with respect to the drive cycle intensity.
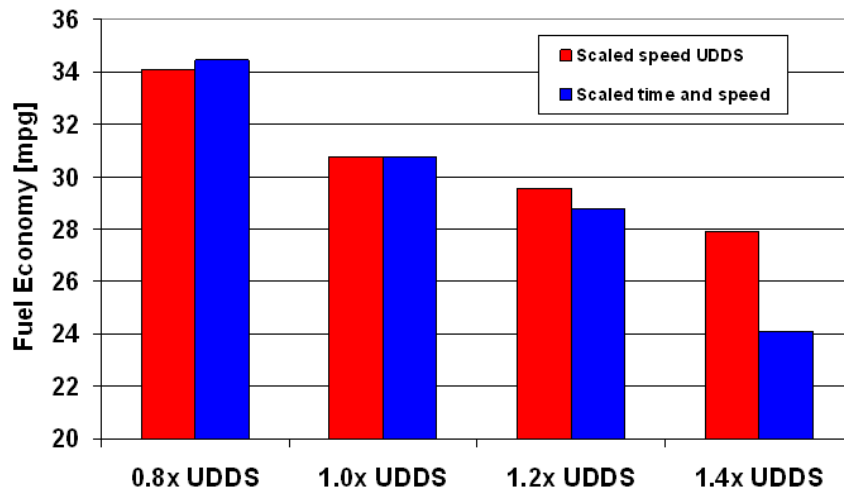
Figure 5-48: Fuel economy results as a function of drive cycle intensity

The fuel economy variation is larger with both the speed and the time scaled. If the speed trace is scaled up, the accelerations are more aggressive. If the time to achieve these higher speeds is reduced by scaling the time, these accelerations are even more severe. As the drive cycles get more aggressive, a larger portion of the energy required to complete the cycle is attributed to the inertia energy for accelerations and a much smaller portion goes to the road load.

This variation in fuel economy depending on drive cycle intensity is more pronounced in hybrid operation, as shown later.

5.8.3.   Impact of the shift differences on FE

A further topic that needs to be mentioned is the shift schedule or shift algorithm used on MATT. Both the manual transmission module and the automatic transmission module must be shifted by the high level controller. Thus, shift algorithms or shift schedules are used for specific drive cycles. A shift algorithm is a logic that determines which gear to use based on vehicle speed and engine load. A shift schedule, which is typically used with manual transmission vehicles, is a table that defines the time when the dynamometer driver needs to shift to each gear during a specific cycle.

At this stage, a shift schedule is used on MATT. Several shift schedules were developed over time for the specific transmission modules as well as the vehicle operation such as conventional, electric or hybrid vehicle operation. These shift schedules have a significant impact on the fuel economy, especially for the conventional vehicle. Two major shift schedules are used in this work.

The first one is a shift schedule developed on the hardware. It is based on the engine load capabilities, thus it tries to maintain the engine speed low and load high while ensuring enough torque reserve for accelerations. This shift schedule was then tuned and calibrated on the hardware in the test cell based upon general hardware feedback.

The second shift schedule is based on the PSAT simulation shift logic. This schedule was slightly modified to accommodate some hardware limitations. This shift schedule is used most often. The simulation based shift schedules ensure consistency across different drive cycles such as the scaled UDDSs.

The impact of these shift schedules can affect the fuel economy results by 10%, as shown in Figure 5-49. This demonstrates the need for consistency in the shifting.
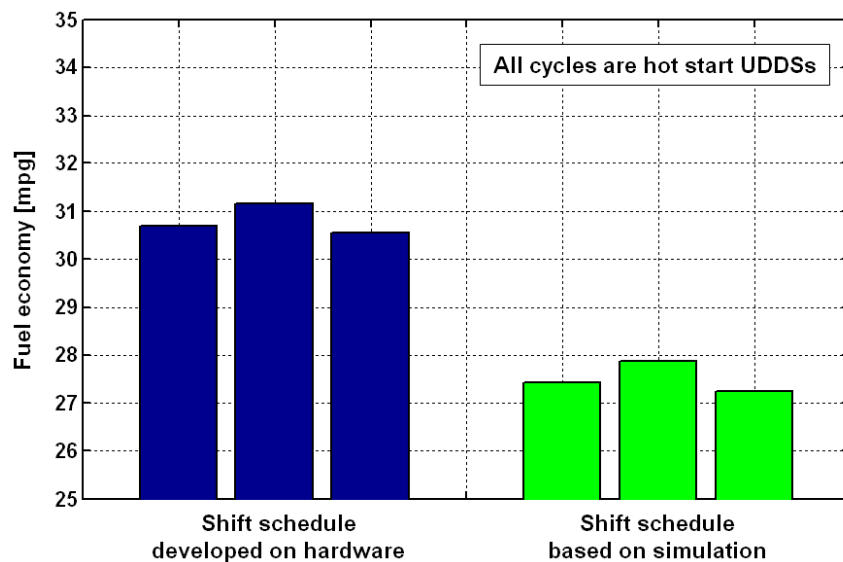
Figure 5-49: Fuel economy results for two different shift schedules

Figure 5-50 explains the reason for the fuel economy change. With a more aggressive shift schedule, the engine load is higher at lower speeds, which results in high cycle average efficiency. The hardware based shift schedule shows much tighter operating areas around 1400 rpm at higher loads. In the simulation based schedule, the engine speed range is higher and more spread out, with a secondary operation island at 2000 rpm and lower load. The simulation shift logic considers drivability and thus keeps the engine at higher speeds to increase the reserve torque that is available.

125
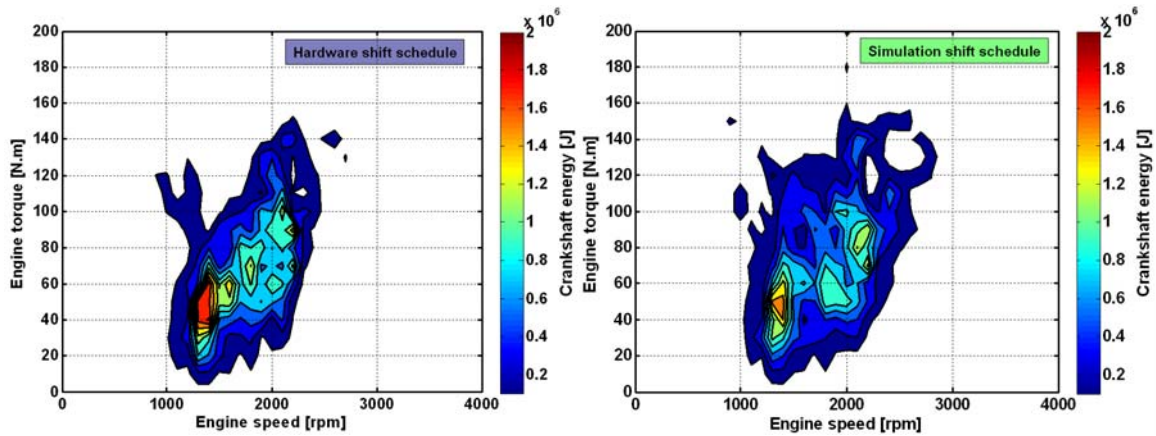
Figure 5-50: Engine operating range for different shift schedules

The brake thermal efficiency for the hardware based shift schedule is 24.8% whereas the simulation shift schedule resulted in 24.0% brake thermal efficiency. As mentioned before, since the shift schedule impact is significant, most studies use the simulation shift schedule, which is based on a shift algorithm and provides consistency across different cycles.

5.8.4. Emulating a small to a large conventional vehicle

This study was performed with the manual transmission. Furthermore, the shifting timing was done manually through the user interface. The purpose of this experiment was to evaluate the ability of MATT to emulate different sized vehicles.

The purpose of emulating different sized vehicle is to demonstrate the hardware's flexibility. The Ford Focus emulation served as the baseline vehicle. A Honda Insight was emulated as a smaller sized vehicle, which is not only light but also has low road load losses. The large vehicle is a Ford Escape, which is classified in the cross over SUV category. The 2.3 liter DURATEC engine used on MATT was also available in the Escape. All of these vehicles were tested at Argonne in the past as shown in Figure 5-51. Table 5-10 describes the main characteristics of the different emulated vehicles.

2004 Ford Escape   2004 Ford Focus   2000 Honda Insight

Figure 5-51: Vehicles of different sizes emulated with MATT

Table 5-10: Characteristics of the different size vehicles

	Honda Insight	Ford Focus	Ford Escape
Vehicle type	Small efficient two seater	Mid size sedan	Crossover SUV
Test mass [lbm]	2125	3125	3750
A [lbf]	18.00	30.85	40.19
B [lbf/mph]	0.0520	0.5080	0.3891
C [lbf/mph^2]	0.0137	0.0165	0.02994

For each vehicle emulation, MATT complete a double highway set with coast downs to ensure that the dynamometer emulated the vehicle load correctly. After the coast down determination, a hot start UDDS cycle and a hot start highway cycle were completed. The hardware completed all of the emulations without any hardware failure or problems. For the Insight, the engine was never stressed, but for the Escape emulation the engine sounded quite loaded but successful completed both the UDDS and the highway cycle. The fuel economy results are shown in Table 5-11.

Table 5-11: MATT's fuel economy results for the emulated vehicles

	Honda Insight	Ford Focus	Ford Escape
UDDS	30.0 [mpg]	25.7 [mpg]	23.5 [mpg]
Highway	45.0 [mpg]	39.8 [mpg]	36.0 [mpg]

These fuel economy numbers from MATT emulating different vehicles cannot be compared to the actual vehicle results since the Escape had a 6 cylinder engine with a 4 speed automatic and the Insight had a 3 cylinder engine with a hybrid system. The main goal was achieved by demonstrating that MATT can and has successfully emulated smaller and larger sized vehicles with the same hardware.

5.8.5.   Pulse and glide

A final conventional study presented in this dissertation is a series of pulse and glide driving technique investigations performed with MATT. The pulse and glide driving is intend to increase fuel economy by replacing steady state speed driving with an acceleration (pulse) followed by a coasting period (glide) around a given speed. The intent is to increase the engine efficiency by loading it higher for a shorter period of time. An in-depth investigation of the topic has been performed by a colleague, Jeongwoo Lee (REFXX), who is also a PhD candidate under Professor Nelson. For this investigation, a set of vehicles was tested on the chassis dynamometer. It was difficult for a driver to accurately repeat the pulse event at the same tip in rate and engine loading.

The software robotic driver for MATT can easily perform this repetitive task accurately. A pulse and drive algorithm for the robotic driver was developed for MATT. During the pulse phase, a tunable engine torque is applied. This torque can be changed in the user interface during the test. Once the calibratable upper speed limit is achieved, the engine torque is zeroed until the lower speed limit is reached. Then the engine torque is applied again, as shown in Figure 5-52. This is accomplished in a fixed gear. Even the glide occurs in the fixed gear not neutral.
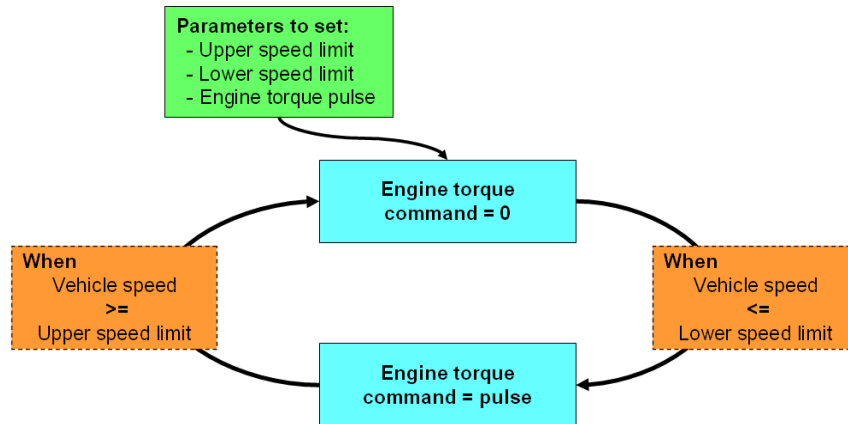
Figure 5-52: Pulse and glide driver algorithm

With this algorithm, different speed brackets and different engine loads were investigated. A typical pulse and glide result is illustrated in Figure 5-53. For this case the lower speed limit is 40 mph and the upper speed limit is 50 mph. The engine torque on the pulse is 110 N.m.
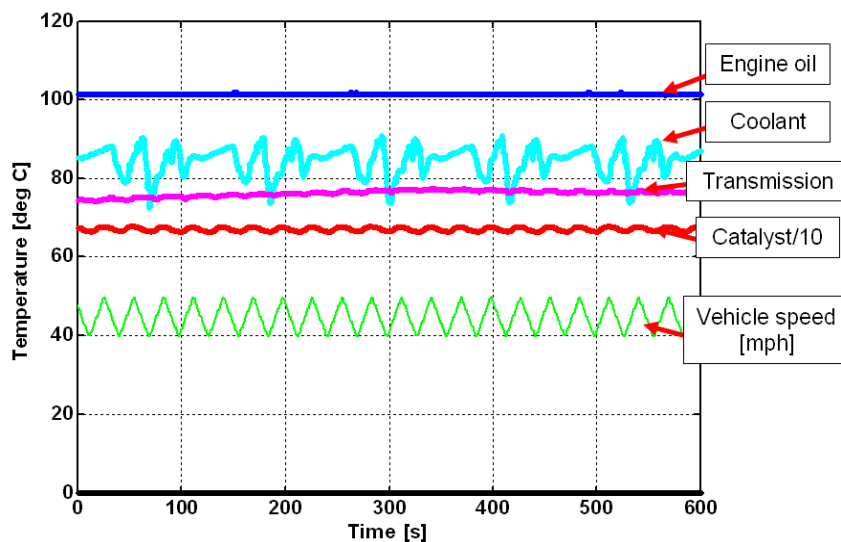
Figure 5-53: Pulse and glide test data

The repeatability of the engine torque level for the pulse is shown in Figure 5-54. All of the test points for the 10 minute section are overlaid on the same graph. A human driver cannot achieve this repeatability.
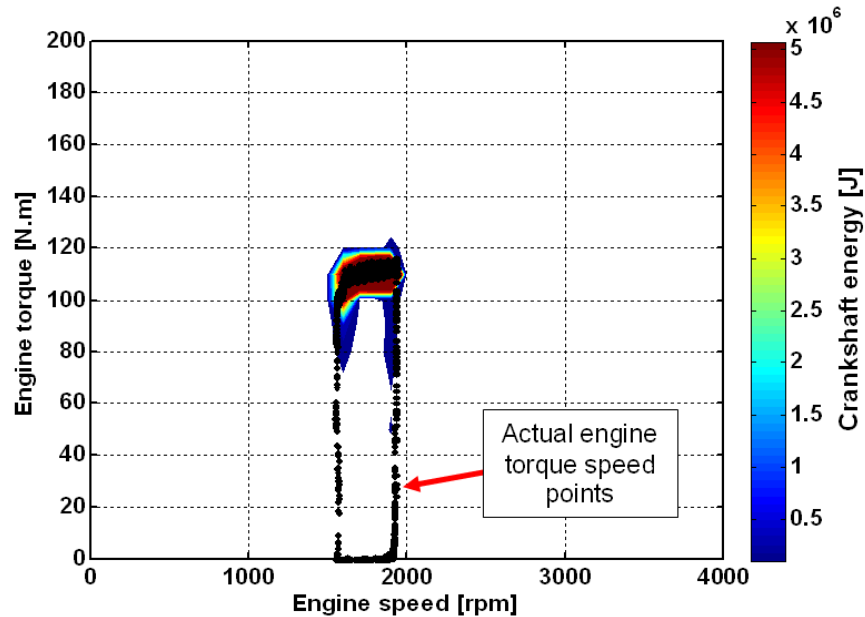
Figure 5-54: Pulse and glide engine operation

In this particular case, 40.9 mpg was achieved with the pulse and glide technique while the steady state speed fuel economy was 45 mpg. At higher speeds, the transmissions are geared is such a way that the engine speeds are low and the engine loads are higher, thus increasing the fuel economy. Pulse and glide works best at lower speeds. If the engine has the fuel cut off during deceleration (which is common on newer direct injected gasoline engines), pulse and glide can even improve the fuel economy at higher speeds. If the fuel during the glide phase is disregarded, the fuel economy on this test would be 50.9 mpg. In effect, pulse and glide is a way of altering the engine operating range without a hybrid system.

Due to MATT's open control system, the software robotic driver was easily modified to perform accurate and repeatable pulse and glide investigations.

5.9.   Limitations

The major limitations for MATT are linked to the transmission modules. The automatic transmission has low cycle average efficiencies since the calibration is not completely refined. The manual transmission module does not shift fast enough since it has no integrated clutch and thus requires time consuming speed matching with the

electric motor. The manual transmission problem can be solved by integrating a clutch into the module. This integration is currently being implemented.

The shift schedules are restrictive and laborious to implement on MATT. The shift schedules also have a significant impact on fuel economy, thus a better, more consistent method should be used. In the future, a shift algorithm that can accommodate different vehicle operations such as conventional or hybrid modes should be developed. Some good ideas have been suggested, but there has not been sufficient time as of yet to implement and test.

The conventional vehicle launch could be improved, but the time and effort required to do this would be too great to justify any minimal improvements. The baseline conventional launch works sufficiently in over 95% of all cases.

Furthermore, the original tests were performed with a hardware setup that has been improved over time. Currently, the engine calibration is a stock engine calibration with a realistic engine coolant system. Significant work was required to achieve this operating state. Another limiting factor was the hardware reliability. Over time, several shafts failed under the loads, but with hardware improvements along with control improvements in the component control, the failure rate was dramatically reduced.

5.10.   *Synopsis of conventional vehicle operation*

The conventional vehicle mode on MATT represents the baseline vehicle to which fuel economy and emission numbers can be compared. The baseline data is presented for the UDDS and highway cycles as well as a multitude of other standard tests.

The engine and transmission component evaluations are characterized in-depth. The components are evaluated from a steady state perspective as well as a drive cycle performance perspective. Special attention is paid to the operation of the different components.

Finally, a few special studies are presented, such as the steady state speed fuel economy numbers, the fuel economy sensitivity to drive cycle intensity, the emulation of different sized vehicles as well as some drive cycle investigations.

MATT is a flexible tool that can perform a wide selection of studies while providing comprehensive and in-depth data for the components.

6.   Electric vehicle operation

6.1.   *Basic vehicle setup*

In this study, the Ford Focus is again the baseline vehicle. The virtual scalable energy storage system and virtual scalable electric motor module emulate the JCS VL41M lithium ion battery pack and the UQM 75 electric traction motor. The functionality for this module was explained in section 3.5.3.

The majority of the results presented in this section are based on the manual transmission module since the development was performed with this module.

6.2.   *Vehicle operating strategy*

In the electric vehicle operation the energy management strategy is relatively simple. Positive torque requests from the software robotic driver are translated to a torque command for the electric traction motor. The torque command is limited to the maximum available torque from the virtual battery pack and motor. In general, the braking is performed by the electric motor through regenerative braking. The motor is limited by the maximum regenerative brake torque it can apply based on its physical torque limits and the maximum charge current the battery system can accept. Therefore, the regenerative braking is supplemented by the mechanical brakes when the maximum regenerative brake torque is reached. As the vehicle approaches a stop, the brake effort is blended from the regenerative braking to the mechanical brakes. The regenerative braking is affected by the transmission capability to transfer reverse torque, which is an issue with the automatic transmission module.

6.3.   *Electric vehicle challenges*

6.3.1.   Regenerative braking and mechanical braking blending

The blending of the regenerative braking and the mechanical braking occurs in the high level controller and thus varies depending on the different energy management strategies. From a hardware perspective, the blending can be accomplished in a smooth fashion at high speeds or low speeds. Figure 6-1 shows two examples of mechanical and regenerative braking combinations. The first graph shows the start of the full charge test (FCT) with the battery pack at a high state of charge (90%). During the decelerations of the first hill of the UDDS, the battery can not accept the electric energy at the high rate. The limited brake torque from the electric motor is clearly visible at about negative 50 N.m and thus the mechanical brakes are commanded to provide the rest of the deceleration torque required to meet the trace. For comparison, the right graph below shows the same hill but this time it is the start of the 4th cycle, thus, the battery pack is already low in charge. Here the charge acceptance is large enough to slow the vehicle to meet the trace. Also note that when the vehicle comes to a stop the mechanical brakes are

fully blended while the motor torque is zeroed. During the stop the mechanical brakes maintain minimum braking pressure.
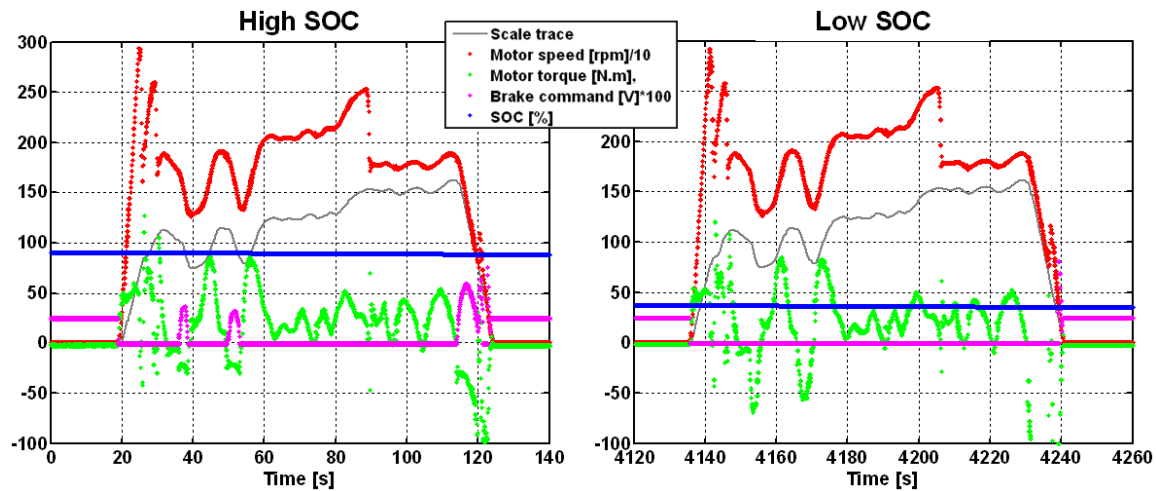
Figure 6-1: Regenerative braking limit at high state of charge compared to low state of charge of the battery pack

One of MATT's interesting components is that both the regenerative braking and the mechanical brake can be commanded independently to enable more flexibility.

6.3.2. Reverse torque through transmissions

Manual transmission module

The regenerative braking torque is not an issue with the manual transmission. Once a gear is engaged, the torque transfer is continuous. The downshifting during braking requires the mechanical brakes to be quickly blended in to fill the torque hole during the shift. In hybrid mode and electric vehicle mode, the vehicle is stopped in 3rd gear and bypasses most of the downshifting on the UDDS. MATT is then launched in 2nd or 3rd gear, which can be done because of the available torque of the traction motor. Launching in a higher gear helps with the long shift delays since the longest shifts (1-2 and 2-3) are not performed.

Automatic transmission module

Regenerative braking is more complex with the automatic transmission. In the final calibration, which is focused on shift speed and hardware protection, it is not possible to transfer reverse torque in 1st or 2nd gear. Therefore regenerative braking with the automatic transmission is only possible in 3rd, 4th and 5th gear. Again, the vehicle is stopped in 3rd gear to maximize the benefits of regenerative braking.

On some decelerations while using regenerative braking, the line pressure of the transmission fluid may drop to a point where some of the internal clutches slip and the transmission cannot transfer any torque. This pressure drop may occur below 700 rpm where the auxiliary transmission fluid pump provides the line pressure, as detailed in section 3.5.5. The mechanical brakes need to be blended earlier to prevent the motor from spinning backwards during the regenerative braking event. Overall, when MATT runs as an electric vehicle or hybrid with an automatic transmission, it can only recapture a portion of the regenerative braking recovered with the manual transmission module.

6.4. *Emulated component validation*

6.4.1. Using Argonne's TTR hybrid

Researchers at Argonne built a PHEV hybrid test mule that is a Through The Road (TTR) parallel hybrid electric vehicle. The base for the mule is a Saturn Vue Belted Alternator Starter (BAS) hybrid. The UQM 75 traction motor with a gear reduction and the JCS VL41M battery pack is integrated on the rear axle as shown in Figure 6-2. With this configuration, the vehicle can operate as the standard charge sustaining hybrid vehicle with the front powertrain. With the rear powertrain, the vehicle can operate as an electric vehicle. Combining both powertrains allows the mule to run as a Through the Road parallel plug-in hybrid electric vehicle. The vehicle is intended to test large plug-in battery packs. It is an excellent complement to MATT, which emulates the battery and motor.
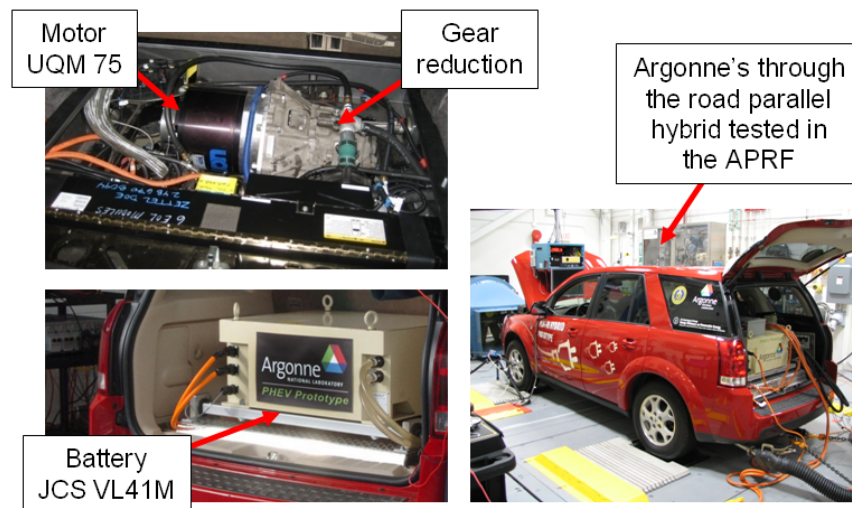
Figure 6-2: Illustrations of Argonne Through The Road parallel plug-in hybrid vehicle

Using the chassis dynamometer, the road load and inertia loads of a Ford Focus are applied to the TTR parallel hybrid. The TTR parallel hybrid can be operated as an electric vehicle using on the battery pack and the traction motor. This is the exact

133

configuration that MATT is emulating as an electric vehicle except for the transmission modules. The electric vehicle full-charge test results for the TTR parallel hybrid with the physical hardware and MATT with the emulated hardware are shown in Table 6-1. The MATT results are measured with the manual transmission module. The energy consumption results are within 3% and 9%. The difference is acceptable since the energy consumption can vary more than that based on the aggressiveness of capturing regenerative braking. This is discussed later.

Table 6-1: Comparison of electric energy consumption results for a Ford Focus sized vehicle

	UDDS 1	UDDS 2	UDDS 3
TTR (real motor and battery)	279 [Wh/mi]	262 [Wh/mi]	248 [Wh/mi]
MATT with manual (emulation)	256 [Wh/mi]	249 [Wh/mi]	241 [Wh/mi]

The hardware emulation of the traction motor and battery pack correlates well with the measured performance of the physical components, based on the chassis dynamometer test data.

6.4.2.　　　Real time Battery HIL run

Another tool in Argonne's plug-in hybrid research portfolio is the Battery Hardware-In-the-Loop (BHIL) setup mentioned in section 2.2.6. The setup tests the physical battery pack using a power supply to charge and discharge it based on a real time hybrid vehicle simulation as shown in Figure 6-3. The JCS VL41M was tested on the BHIL.
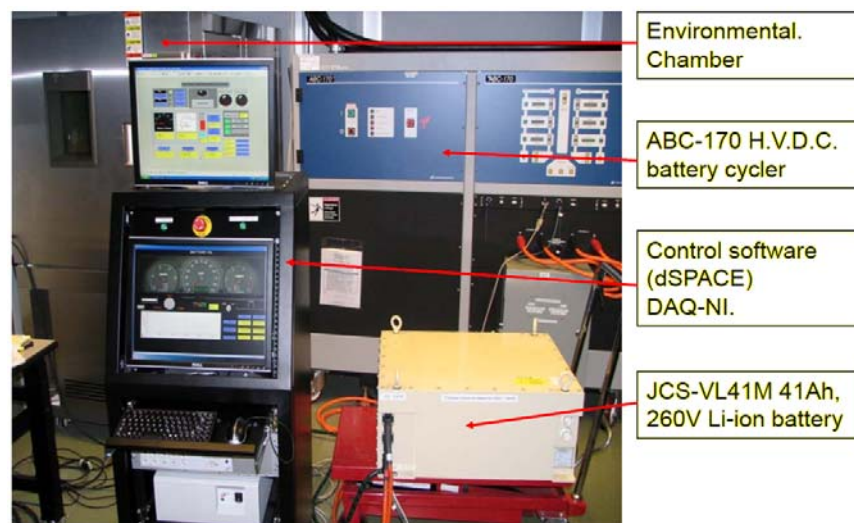
Figure 6-3: Argonne's Battery Hardware-In-the-Loop setup

The setup was used to test the JCS VL41M in an electric vehicle environment emulating a Ford Focus sized vehicle, but a more conclusive test allows a researcher to make a better correlation between the physical and emulated battery. MATT and BHIL were both run in real time while communicating via a CAN. MATT was operating as a PHEV on the chassis dynamometer using information from the physical battery from the BHIL such as the charge and discharge limits. The BHIL applied the electric load to the battery pack as dictated by MATT, which was operating as an electric vehicle on the chassis dynamometer.

A full charge test for a blended PHEV was performed. The test results are shown in Table 6-2. In this test set, the engine was used in every single test, thus, the electric consumption changed from test to test. The difference between the measured energy consumption from BHIL and the simulation energy consumption from MATT is less than 3% in all cases. Another interesting metric to compare is the state of charge at the end of each test. The physical battery pack's battery management system only reports integers, as shown in the table. The SOC results from the simulation on MATT correlated to the record SOC from the physical battery.

Table 6-2: Comparison of test results from MATT and BHIL for a PHEV emulation

	UDDS 1	UDDS 2	UDDS 3	UDDS 4	UDDS 5
	Electric energy consumption				
BHIL	245 [Wh/mi]	217 [Wh/mi]	166 [Wh/mi]	156 [Wh/mi]	49 [Wh/mi]
MATT with automatic	239 [Wh/mi]	212 [Wh/mi]	163 [Wh/mi]	153 [Wh/mi]	47 [Wh/mi]
	State of charge at end of test				
BHIL	73 [%]	58 [%]	46 [%]	35 [%]	29 [%]
MATT	72.6 [%]	58.2 [%]	45.3 [%]	34.8 [%]	29.5 [%]

Unfortunately, it is impossible to show the graphical correlation for maximum charge and discharge limits since both the battery model and most of the measured information from the battery pack are proprietary. Regardless, the reported charge and discharge limits (which vary over time based on SOC, among other elements) match very well.

The hardware emulation of the battery pack correlates well with the measured performance of the physical battery back based on the measured data from the parallel testing of MATT and BHIL.

6.5. *Test results form the urban drive cycle*

6.5.1. Manual transmission module

The manual transmission module results are shown in Figure 6-4 and Table 6-3. The first cycle has a high energy consumption compared to the subsequent cycles due to the charge acceptance limit at high state of charge as shown in Figure 6-1. The tire and transmission also had to warm up, causing some extra losses. The energy consumption at the wheels is 160 Wh/mi, as shown in Appendix 5. Therefore, the power train efficiency is between 62% and 66 % percent on the UDDS cycle. The improvement is significant with respect to the conventional vehicle, which yielded 13% and 14% powertrain efficiency. The transmission efficiency was around 93%
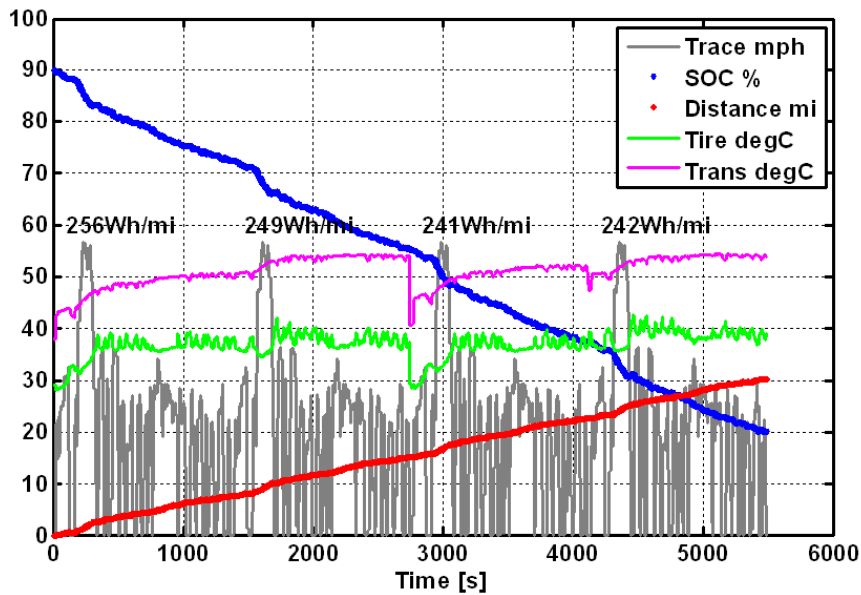
Figure 6-4: All electric operation and range on the UDDS with the manual transmission

Table 6-3: Electric consumption summary on the UDDS with the manual transmission

	UDDS 1	UDDS 2	UDDS 3	UDDS 4
Test #	60706083	60706083	60706084	60706086
Electric consumption	256 [Wh/mi]	249 [Wh/mi]	241 [Wh/mi]	242 [Wh/mi]
Cycle battery energy	1.93 [kWh]	1.88 [kWh]	1.82 [kWh]	1.83 [kWh]

With the manual transmission module, the electric range is 25.7 miles using the battery charge from 90% to 30%. In this control, the braking energy recovery was quite aggressive.

6.5.2. Automatic transmission module

The results for the electric vehicle operation using the automatic transmission module are shown in Figure 6-5. The energy consumption is about 25% higher than the consumption with the manual transmission module. This is due to two factors. First, the transmission efficiency of the automatic is about 75% to 80% compared to the 93% of the manual transmissions. The rest of the energy consumption increase is due to the lack of energy recovery through regenerative braking. As explained earlier, the automatic transmission is limited to 3rd, 4th and 5th gear for reverse torque and can only transfer this reverse torque to motor speed above 700-800 rpm. Therefore, this hardware limitation has a serious impact on the electric energy consumption. For these reasons, the powertrain efficiency drops to between 45% and 48% in electric vehicle operation with the automatic transmission.
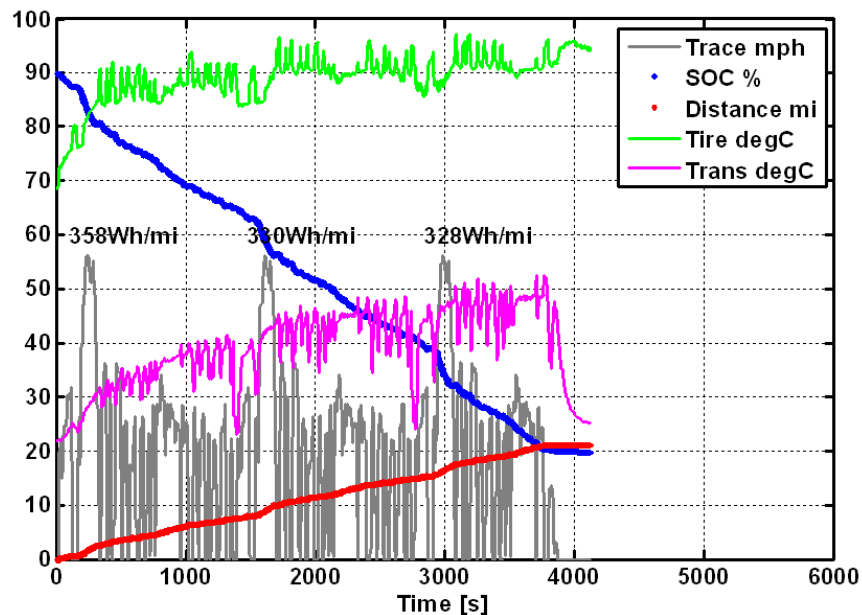
Figure 6-5: All electric operation and range on the UDDS with the automatic transmission

With the automatic transmission, the all-electric range is 18 miles, using the battery from between 30% and 90% of the absolute capacity.

This example truly shows the downfalls of the automatic transmission's low efficiency. Therefore, the current transmission module for MATT presents the trade-off between realistic shift times (important for conventional operation) and realistic efficiencies (more apparent in electric mode).

6.6.   Test results on highway drive cycle

The highway cycle results for the electric vehicle operation are shown in Figure 6-6. The manual transmission module was used for this test. Generally, even with a fully charge battery pack, the charge limits are not a problem since the first significant deceleration occurs after 6 minutes when enough energy has already been taken from the battery pack. Moreover, the braking energy is minimal on the highway cycle as compared to the tractive energy required to complete the cycle, as shown in Appendix XX.
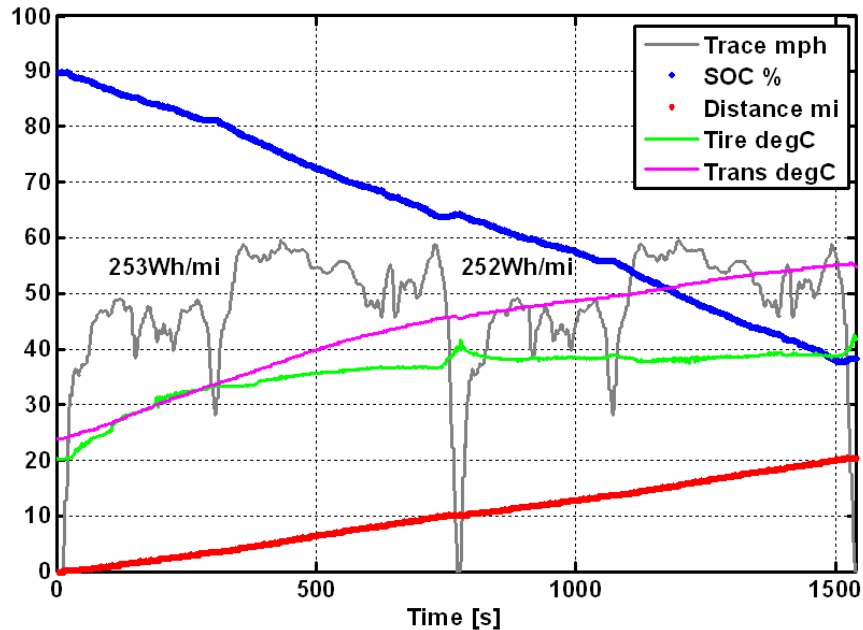
Figure 6-6: Electric vehicle operation on the highway with the manual transmission

Note that the transmission is still warming up, even after two full highway cycles. The powertrain efficiency for this cycle on MATT with the manual transmission is 87%. With few regenerative braking events, the battery charge discharge losses are low. The manual transmission efficiency is 94%. The electric vehicle operation is very efficient on cycles such as the highway cycle.

6.7.   Special studies

6.7.1.   Hot vs. cold energy consumption

The losses in a cold driveline are higher due to higher mechanical friction. In order to investigate this phenomenon for the electric vehicle operation with the manual transmission, a special set of tests were completed. First, a cold start set of two UDDS cycles was tested. The cold start means that MATT was soaked at 25 deg C in the test cell for over 12 hours, ensuring that all of the components start the test at room temperature. The 2nd UDDS cycle of the cold start set was started immediately after the

end of the first one without any pause in between. The second set of the two UDDS cycles was tested right after a warm up period at high speeds and accelerations to ensure that all of the components were above their normal operating temperatures.

The initial state of charge was set at 70% for both sets of tests. The ability to set exactly the same initial conditions is an advantage of the virtual battery pack. The 70% initial SOC was chosen so that charge acceptance limits for regenerative braking would not be an issue. All of the tests were performed in 3rd gear only, so that shifting differences would not affect the results.

The results of the tests are shown in Figure 7-24. The electric energy consumption is calculated and displayed for each hill of the UDDS. The colors represent the coldest test in deep blue to the hottest test in red. Considering only hill 1, the energy consumption is lower for the 2nd cold start UDDS than for the 1st cold start UDDS, but the lowest energy consumption was seen in the hot transmission test. The gap between the energy consumption decreases from the first to the second cold start UDDS as the temperature rises.
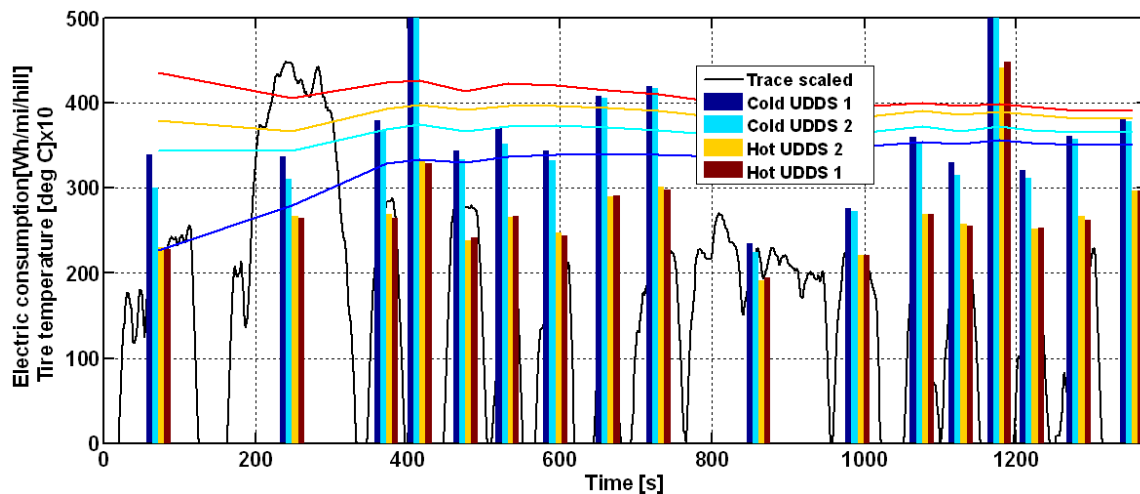
Figure 6-7: Electric vehicle cold start UDDS followed by a second UDDS

The first cold start urban cycle used 289 Wh/mi of electric energy and the second cold start urban cycle, performed immediately after the first test, used 256 Wh/mi. The electric consumption impact is over 10% for a cold start electric vehicle test over a UDDS. The details of the energy consumption are shown in Figure 6-8.
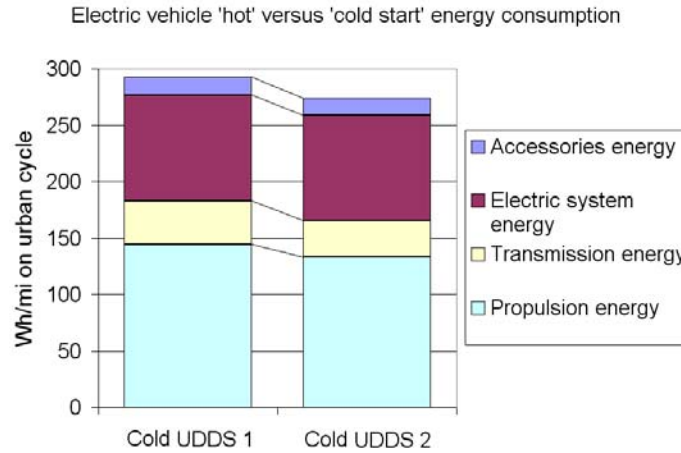
Figure 6-8: Cold start versus hot start component energy consumption

A few limitations need to be noted. The emulated battery and the emulated motor losses are not temperature dependant since the models are based on component data at standard operating temperatures. Thus, this impact is only due to the transmission, driveline and tire losses. In the manual transmission setup, it is possible to recover more regenerative braking energy since full reverse torque is possible through the transmission. The manual transmission is also 96% efficient in hot operation

6.7.2.   Emulating a small to a large electric vehicle

This is the continuation of work presented in section 5.8.4, where a small, Honda Insight sized vehicle as well as a large Ford Escape sized vehicle, are emulated to test the hardware. The manual transmission module was used in this testing. The results are presented in Table 6-4.

Table 6-4: MATT's electric energy consumption results for the emulated vehicles

	Honda Insight	**Ford Focus**	**Ford Escape**
UDDS	210 [Wh/mi]	286 [Wh/mi]	375 [Wh/mi]

The electric energy consumption is slightly different from the number presented before. This is largely due to calibration changes in regenerative braking. The regenerative braking was detuned (especially at low speeds) after a transmission output drive shaft failed due to a large regenerative braking torque spike.

Due to these continuous software and some hardware changes, comparison tests need to be performed back to back with the same hardware and software versions, as was done for the vehicle size emulation tests.

The electric vehicle operation at different vehicle sizes did not present any problems for the hardware.

6.8.   Limitations

The main limitation of the hardware again resides in the transmission modules. The manual transmission module transfers torque at high efficiency, including reverse torque, but the shift times are too long. The automatic transmission, which shifts fast, presents some high losses that become quite significant in electric vehicle operation since the rest of the powertrain operates at such high efficiencies. The automatic transmission imposes a powertrain efficiency penalty of 25% compared to the manual transmission.

Another limitation of MATT is that the flexibility of the control results in calibrations that improve, and thus change, frequently. Comparison tests need to be performed back to back to ensure hardware and software consistency. Extreme care needs to be taken to reload the same energy management strategy or calibration between different tests if it is important for the comparison that it be consistent.

6.9.   Synopsis of electric vehicle operation

The electric vehicle operation on MATT is fairly simple except for the regenerative braking strategy, which is coupled to hardware limitations. The battery and motor emulated with the virtual scalable energy storage system and virtual scalable motor module correlate well with a test mule vehicle using the battery and motor as well as the Battery HIL setup, which tests the physical battery.

The electric energy consumption of the UDDS is greatly affected by the transmission module used. The manual transmission module enables an all-electric range of 25.7 miles compared to only 18 miles for the automatic transmission module. The automatic transmission module is handicapped by a lack of refinement in the calibration as well as the hardware limitations of transferring reverse torque at low speeds.

Two final studies are shown. First, it was determined that a 10% penalty is associated with a cold start in the electric vehicle operation using the manual transmission. The hardware has proven itself capable of emulating both a small and a large vehicle

Again, even in electric vehicle operation, MATT is a flexible tool that can perform a wide selection of studies while providing comprehensive and in-depth data for the components.

7.   Hybrid and Plug-in Hybrid Electric Vehicle Operation

7.1.   Basic vehicle

The Ford Focus sized vehicle is still emulated in this test. The JCS VL41M and the UQM 75 are used as the battery pack and traction motor, which are both emulated as the hybrid system. In this chapter, the conventional vehicle operation and the electric vehicle operation are combined and developed further into the hybrid operation. In the first section, simple algorithms are presented to enable basic hybrid operation modes. These basic building algorithms are then turned into complete plug-in hybrid electric energy management strategies. The manual transmission module was used for the hybrid development from section 7.2 to section 7.7. The final control strategy is a more complex and refined hybrid control strategy. This refined control strategy, the automatic transmission module, was used in section 7.8.

The goal of this chapter is to provide a brief overview of the different operating strategies, which were part of the first hybrid development steps for MATT. All of the control strategies, from simple to complex, run the exact same hardware, which is enabled by the open controller approach on MATT.

7.2.   Vehicle operating strategy

7.2.1.   Energy management setup

The early development of the energy management is based on the control strategy shell present in chapter 3.7.2. The structure of the energy management and torque split strategy shell is essential to this chapter and thus Figure 7-1 shows the concept again. The inputs for the control strategy shell are the driver command and all of the component information such as component speeds, available torques, SOC and selected transmission gear. The outputs of this control strategy shell are the engine on/of commands, an engine torque request, a traction motor torque request and a mechanical brake command. The 'PROP' state is short for propulsion state. This state is active during accelerations. The 'BRAKE' state is the braking state, which is active during decelerations.
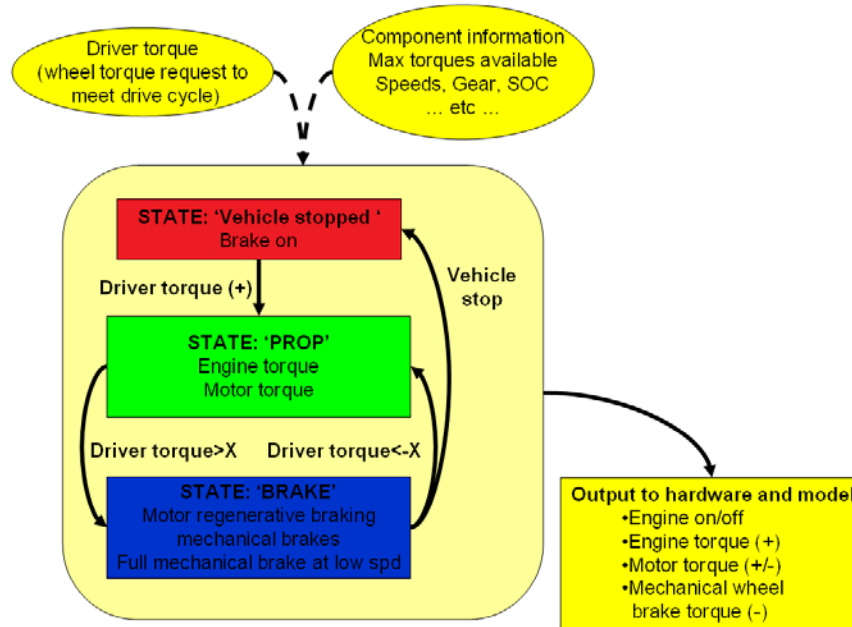
Figure 7-1: Illustration of the energy management strategy shell

The code inside the shell is written in state flow in Matlab®'s simulink®. In the following section, simplified quasi state flow schematics will illustrate the different control approaches. Significant work went into the lower level component control algorithms to enable the simple output of 4 major commands from the energy management strategy shell while maintaining smooth, safe and harmonious operation of the powertrain components to move the vehicle.

The transient event required special attention. The engine can be started with a 12 V start or it can be bump started by closing the clutch with the motor already spinning at higher speeds. The mode changes, such as the start of the engine operation request a tip in rate for torque production after another routine confirms that the engine is firing. The shifting transient algorithm changes with and without engine operation. These are just a few examples of the lower level control code that was developed. The simple hybrid modes presented in this section were mainly developed with the goal of debugging these lower level control routines.

7.2.2. Progress in hybrid development

The development of the hybrid operations is approached in two ways. First, the conventional vehicle operation is hybridized with engine stop during vehicle stops. In a next phase, electric motor assist is added. This approach builds the steps for a mild hybrid electric vehicle. The second approach is to hybridize the electic vehicle. This can be as simple as employing electric launch and regenerative braking. The engine can be started based on wheel power threshold and kept on for a given time. In the next phase, the engine is run on a maximum engine efficiency operating curve. The final step is to implement variable engine-on power at the wheel threshold based on the state of charge

of the battery system. The approach is illustrated in Figure 7-2. The blue path represents the engine dominant hybrid and the orange path represents the electric dominant hybrid operations. Figure 7-3 illustrates how the initial development progressed in the state flow code. The three major states ('Vehicle stopped', 'PROP' and 'BRAKE') are outlined with the same color code used throughout the different sections. In these major states, the different strategies are outlined with the same labels as used in Figure 7-2.
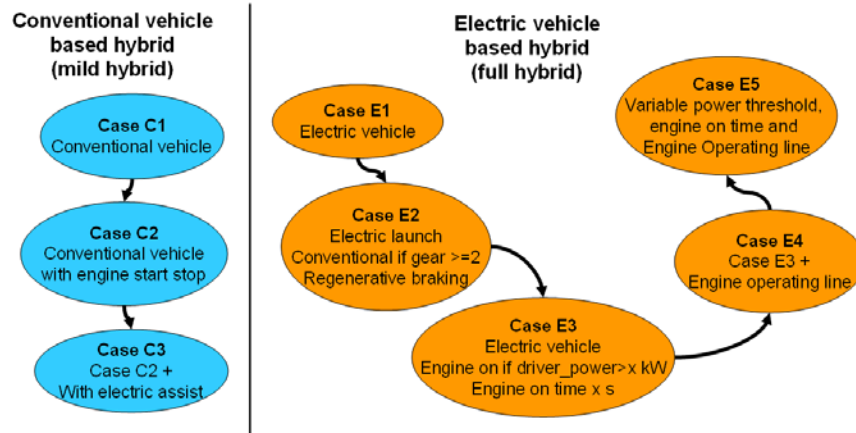
Figure 7-2: Hybrid mode development flow
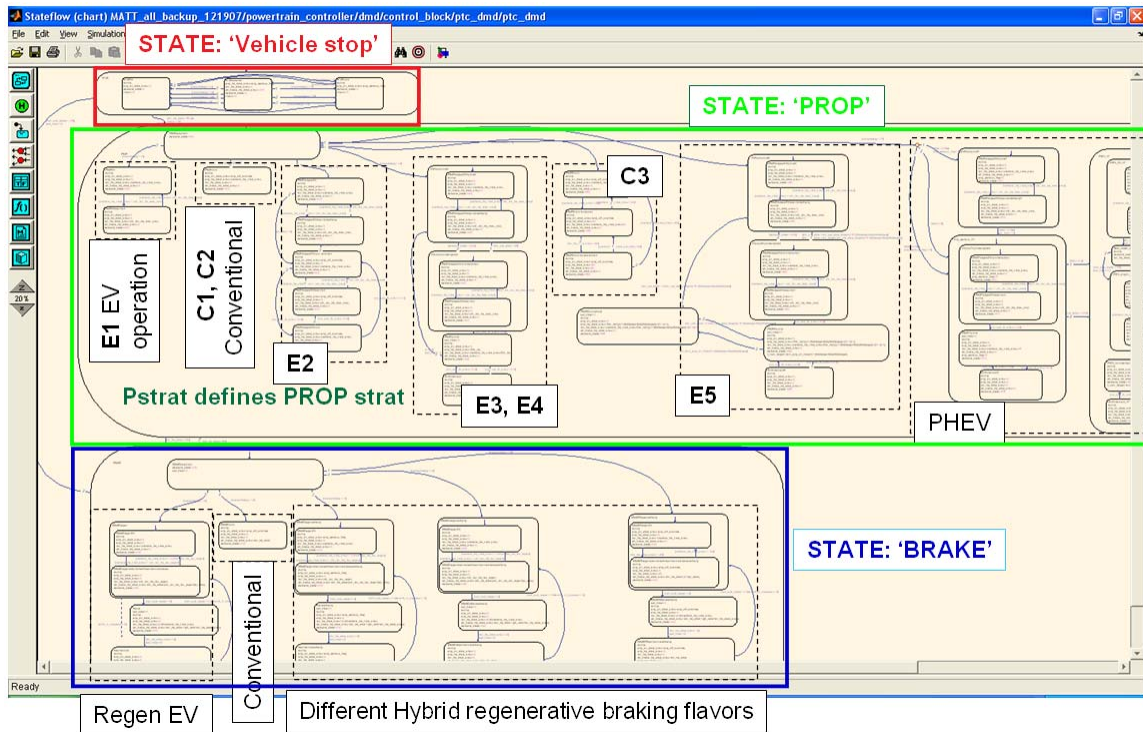
Figure 7-3: Screen shot of the original energy management development with annotations

The following section details each hybrid mode described above and provides some of the data from the testing in the APRF.

7.3. Engine dominant: Micro Hybrid to Mild Hybrid

7.3.1. Engine idle stop hybrid (C2)

An illustration of the control algorithm for this case is presented in Figure 7-4. The flow diagram shows the three main states from the energy management shell presented earlier. The nomenclature used in the diagram is explained in Table 7-1. To change from the 'vehicle stopped' state to the 'PROP' state, driver torque request at the wheel needs to be larger than 50 N.m. Once in the 'PROP' state, the driver torque request at the wheel needs to be lower than negative 50 N.m at the wheel. The (+/-) 50 N.m at the wheel values allow for some hysteresis, which prevents signal noise triggering erratic jumping between states. Even a mild acceleration event will require a wheel driver torque request much higher than 50 N.m. To transition into the 'Vehicle stopped' state the wheel speed need to be lower then 0.25 rad/s, which corresponds to 25 rpm at the wheel. These numbers were empirically determined and stay the same throughout most of this hybrid vehicle development.
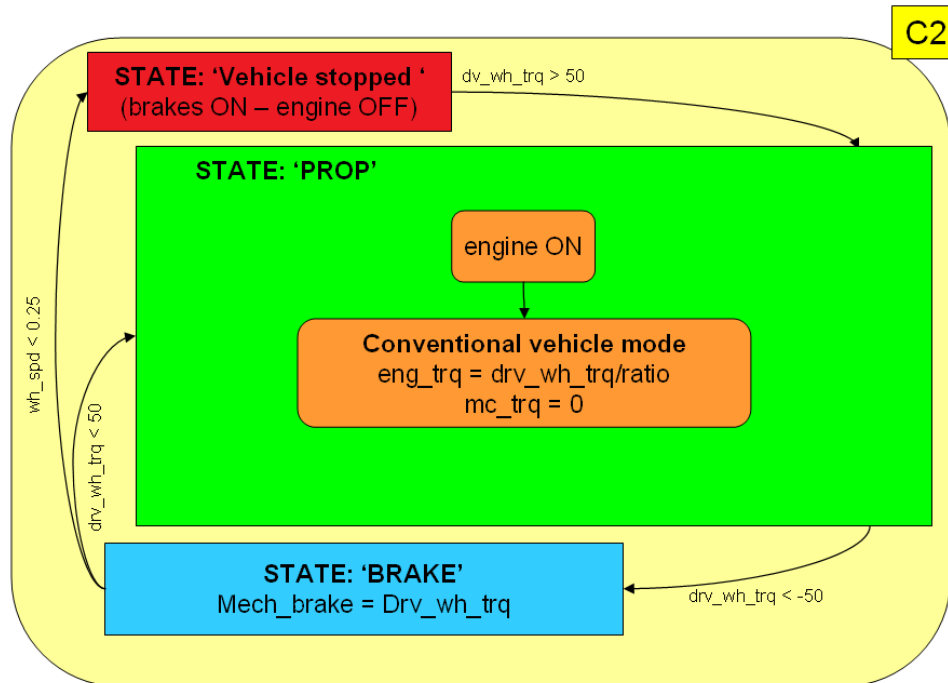
Figure 7-4: Engine idle stop torque split strategy

Table 7-1: The nomenclature guide to the torque split illustrations

Nomenclature	Description
drv_wh_trq	Driver torque request translate to a wheel torque
wh_spd	Measured wheel speed
eng_trq	Engine torque command
mc_trq	Motor controller torque command
mech_brake	Mechanical brake command
ratio	Ratio of the gear engaged

In this engine start stop hybrid mode, the engine is turned OFF while the vehicle is stopped. In the 'PROP' and 'BRAKE' state the engine is ON and the vehicle behaves like the conventional vehicle. Therefore, the full driver torque request is passed to the engine or the mechanical brakes. The driver torque request is referenced to torque at the wheels. In absolute terms, the units on the driver request are irrelevant since the driver will adjust with 'more' or 'less' torque request to meet the drive trace imposed by the drive cycle. For convenience, the driver torque request is linked to torque at the wheels so that the request can be linked to the engine torque and motor torque. In this parallel pre-transmission hybrid vehicle, the torques of the different components are linked as shown in Equation 7-1. Thus, the engine torque in Figure 7-4 is defined as the driver wheel torque request divided by the ratio of the gear selected. This ratio will occur again in the hybrid mode that follows.

Equation 7-1: Torque relationship equation for pre-transmission parallel powertrain (no losses)

$$Wheel\_torque = \frac{Engine\_torque + Motor\_torque}{ratio}$$

The software robotic driver has a one second look-ahead, which provide some extra time for the engine to start and launch the vehicle. The engine is started with the 12V starter in these early developments.

A conventional vehicle test was performed before starting the hybrid vehicle development, which is the baseline to compare the hybrid modes to. The power flows of the components are plotted only on the start of the UDDS cycle in order to effectively show the impact of the hybrid operating modes. Figure 7-5 shows the power flow graph for the conventional vehicle. Note that the UDDS is shown in black as a reference for vehicle speed. The fuel flow power is in green. Idle requires about 10 kW of fuel flow. The engine power in blue provides all of the power to the transmission input in purple. The motor power in red is zero for this data set. The baseline conventional fuel economy for this hot start UDDS was 24.7 mpg. The graphs for all cases will use the same color code.
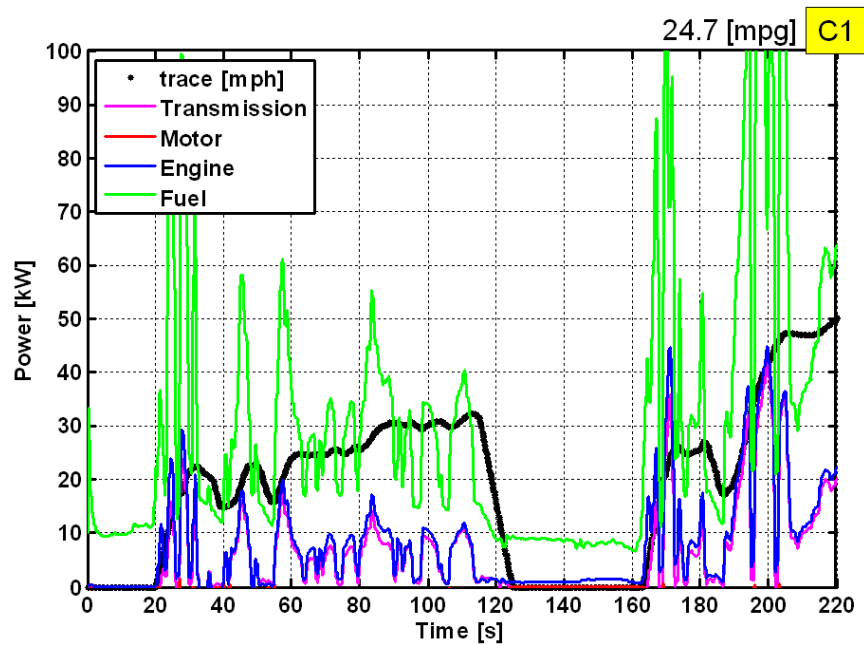
Figure 7-5: Conventional vehicle baseline data on start of UDDS

The engine idle stop test data is presented in Figure 7-6. The fuel flow while the vehicle is stopped is now zero. This is due to the fact that the engine is stopped. During the driving phases, the power flows are similar to the conventional vehicle data. 25.4 mpg was the measured fuel economy on the UDDS for the engine start stop hybrid. Only fuel economy results are provided for the conventional vehicle case and this case since the electric energy used is low enough that the fuel economy numbers are still charge balanced.

25.4 [mpg] C2
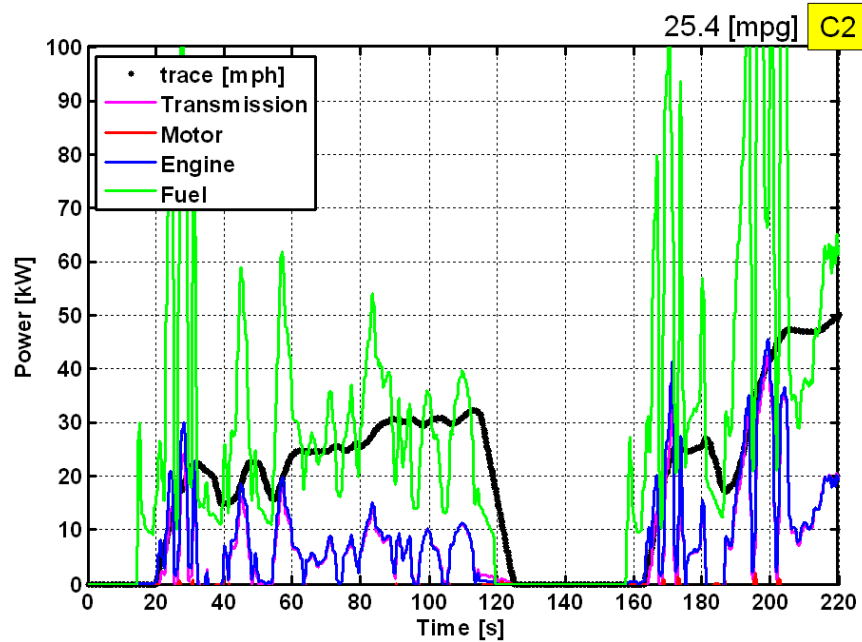
Figure 7-6: Engine idle stop data on start of UDDS

The conventional vehicle used 0.3068 gallons of certification gasoline. Zeroing the fuel flow data (in the 10 Hz data file) while the vehicle is stopped on the conventional baseline test, the fuel usage is calculated to be 0.2806 gallons. Therefore, the maximum fuel saving gain with engine idle stop is 8.5 %. Starting the engine causes a small fuel flow spike as shown in Figure 7-6, thus the measured fuel used on the engine start stop test is only0.2958 gallons. This equates to 6.2 % fuel savings. The individual fuel penalty per start up event is 0.0015 gallons.

7.3.2.   Engine assist hybrid with start stop (C3)

The next engine dominant hybrid case is a conventional vehicle operation with electric assist and heavy acceleration. Figure 7-7 illustrates this control strategy logic. Once in the driver torque demand results in an engine torque command exceeding a target value (calibrated to 80N.m in this example), the engine torque command is fixed to that target value and the electric motor assists the engine by providing the additional torque required. The maximum motor available is limited, thus this logic can result in a vehicle with limited performance. But the primary intent of these hybrid modes was to test the lower level hardware components and to understand the component interactions.
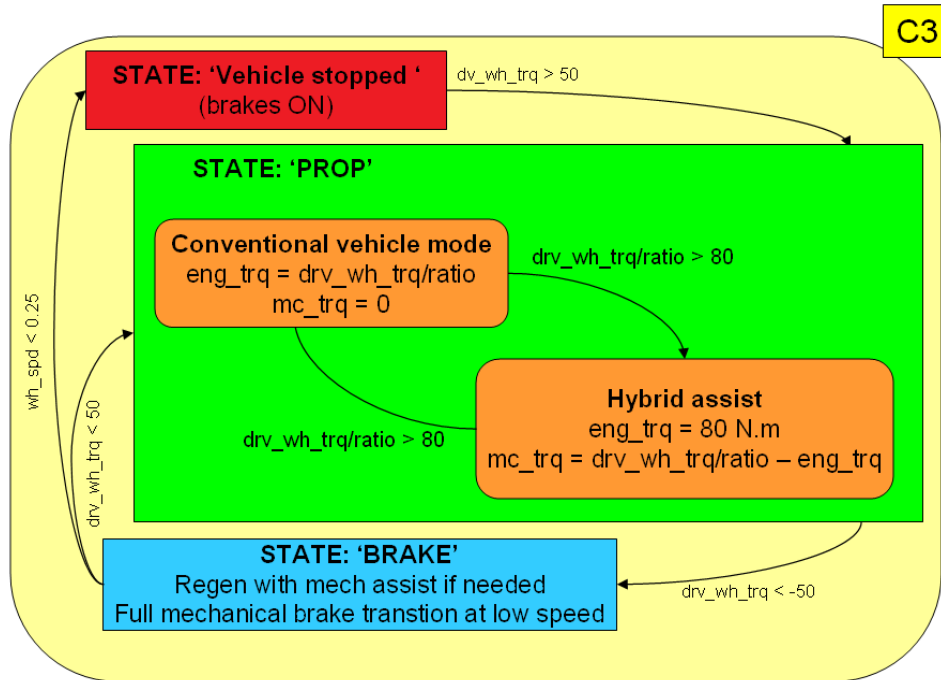
Figure 7-7: Engine with electric assist torque split strategy

The test data for this case is shown in Figure 7-8. In this particular test, the engine idle stop feature was not active, but using the engine idle stop in this logic is trivial. Now the power flows start to show the electric motor power in red during some of the accelerations. The largest assist occurs during the hard acceleration of the UDDS on hill 2. Note that the engine power added to the motor power is equal to the transmission input power. The operation was extremely smooth on the hardware, as the motor provided extra torque while the engine was already running.
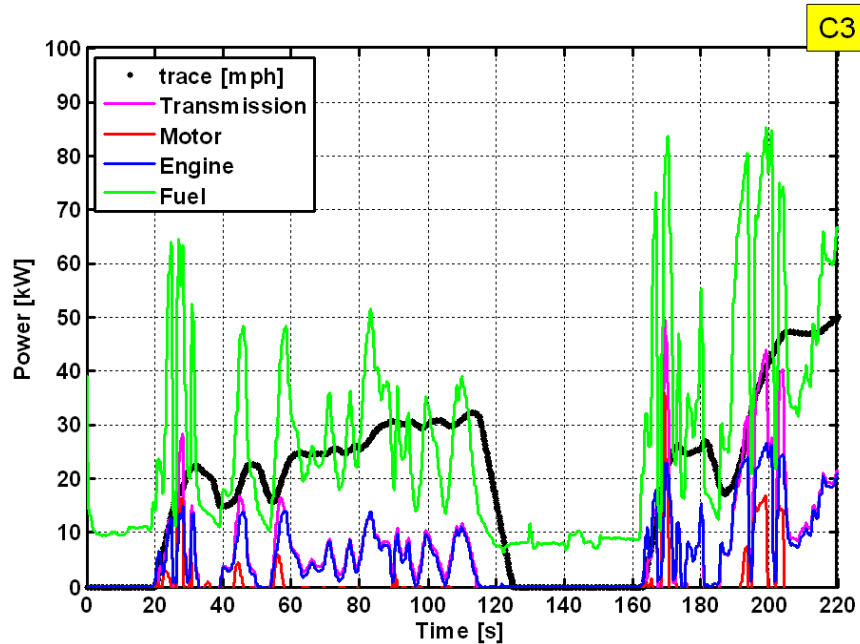
Figure 7-8: Engine with electric assist data on start of UDDS

The test was not charge balanced; therefore the fuel economy will not be presented.

7.4. *Full hybrid: electric dominant*

7.4.1. Electric launch hybrid based on gear selection with regenerative braking (E2)

This case is a hybrid between electric vehicle operation and conventional vehicle operation. The launch is performed as an electric vehicle. Once the gear is shifted to 2nd gear, the engine is started and MATT operates as a conventional vehicle. The braking energy is recovered with the hybrid system. The control logic is illustrated in Figure 7-9 and the test data results are shown in Figure 7-10. While the vehicle is stopped, no fuel is used. During the initial acceleration, the motor power in red accelerates the vehicle, once the 2nd gear is engaged. the engine provides the full power to the transmission. While the engine is started, the motor still provides the full tractive power. The small motor power blips on the graph occur during the shifting since the motor is used to speed match the driveline to the next transmission input speed. The shifting algorithm is described in detail in section 5.3.2 and the graph shows only the shift power flow interruptions, which are most apparent on hill 2.
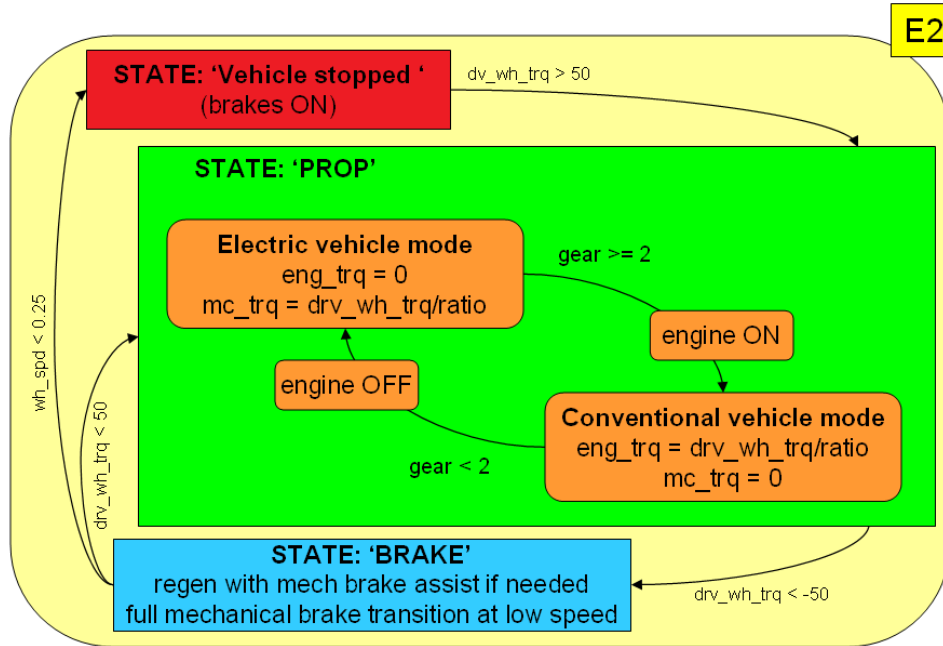
Figure 7-9: Electric launch hybrid torque split strategy
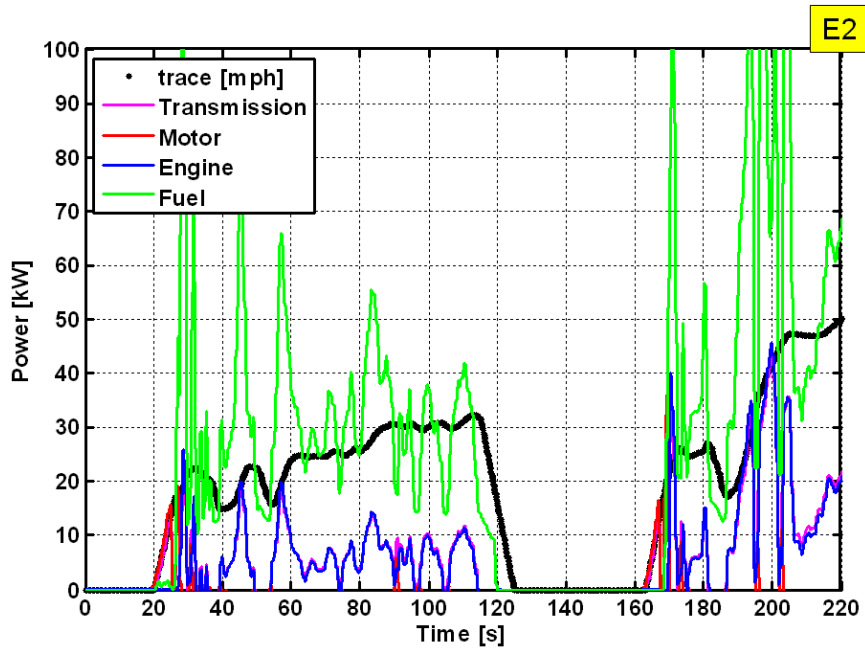
Figure 7-10: Electric launch hybrid data on start of UDDS

The test was not charge balanced; therefore the fuel economy will not be presented.

7.4.2. Electric dominant hybrid with engine turn ON based on power threshold (E3)

The next hybrid mode is an evolution of the previous mode (E2). Instead of triggering the engine start based on the gear change, a calibratable power threshold is used. In summary, if the driver power demand, which is just the product of driver torque request multiplied by the wheel speed, is greater than this threshold, the torque split strategy switches from the electric vehicle operating mode to hybrid state and turns the engine ON. In the hybrid mode, the engine torque request is set at a fixed value. The motor provides the transient power request to meet the driver request using Equation 7-1. Once the engine is turn ON it has to stay ON for a minimum period of time, which is also tunable. This is to prevent the engine from spinning up only to be stropped right away. During decelerations, regenerative braking is used. If the braking required is larger than the available torque from the hybrid system, the mechanical brakes provide the extra stopping torque. At low speeds, the mechanical brakes are fully blended in and the regenerative braking is blended out. The algorithm of this torque split strategy is illustrated in the Figure 7-11.
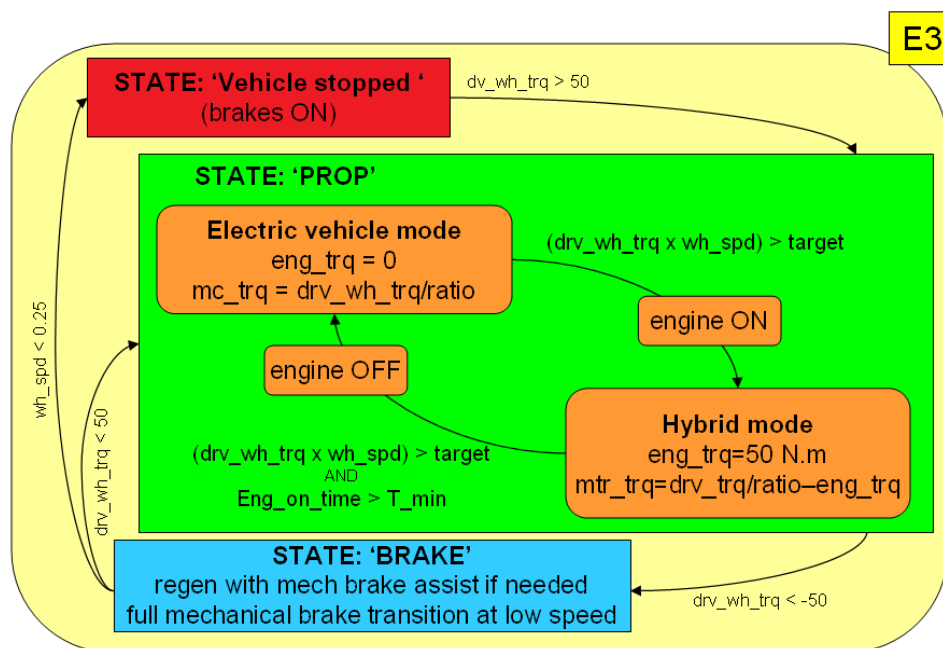
Figure 7-11: Electric dominant hybrid with target power threshold torque split strategy

The test results are shown in Figure 7-12. The first hill of the UDDS is completed in electric vehicle mode. The negative motor power during the deceleration represents regenerative braking and charging of the battery pack. During the large acceleration of hill 2, the driver power demand exceeds the power threshold and the engine is turned ON. The engine provides a fairly constant power output, thus during the acceleration the motor provides extra tractive power, but in the short cruise period the motor power is negative. This means that the battery pack is charged during that period of time.
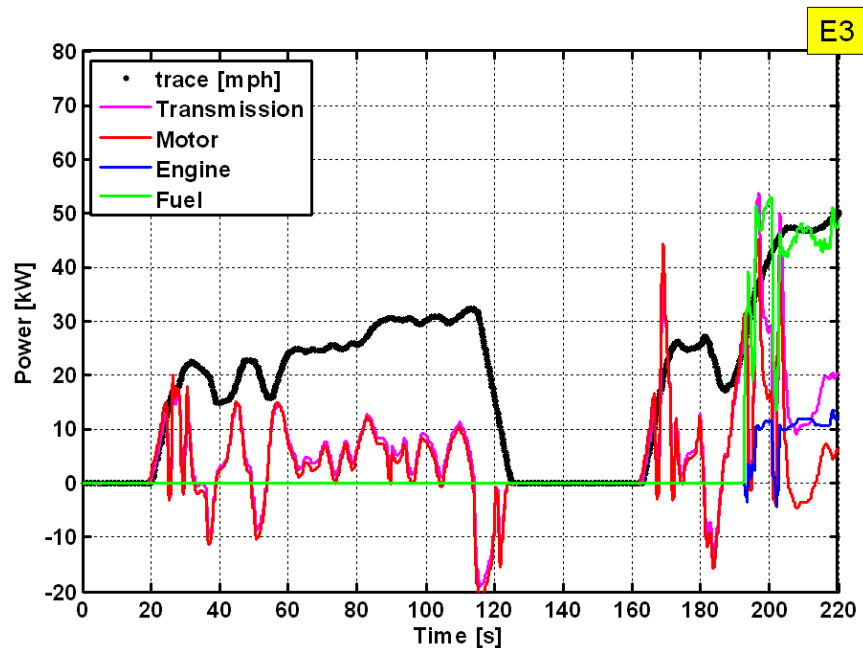
Figure 7-12: Electric dominant hybrid with target power threshold data on start of UDDS

The test was not charge balanced; therefore the fuel economy will not be presented.

This control is fairly hard on the hardware with the engine start and the immediate load request from the engine. The driveline experiences some torque swings in the driveline which can be seen in the power flow graph on hill 2.

7.4.3.   Engine optimum electric capable hybrid (E4)

This hybrid mode is another evolution. The basic states and the path between these states are the same as they are in E3. The new element is the engine operation which is now based on an 'Engine Operating Line' (EOL). The engine operating line defines the engine torque command based on the measured engine speed. In this case, the engine load is completely uncoupled from the road load and operated at high loads to increase the average engine efficiency. The details of the control strategy for this case are illustrated in Figure 7-13. The resulting test data is shown in Figure 7-14. The engine power is proportional to engine speed. The engine speed can be inferred by vehicle speed on hill 2 since 5th gear is engaged continuously.
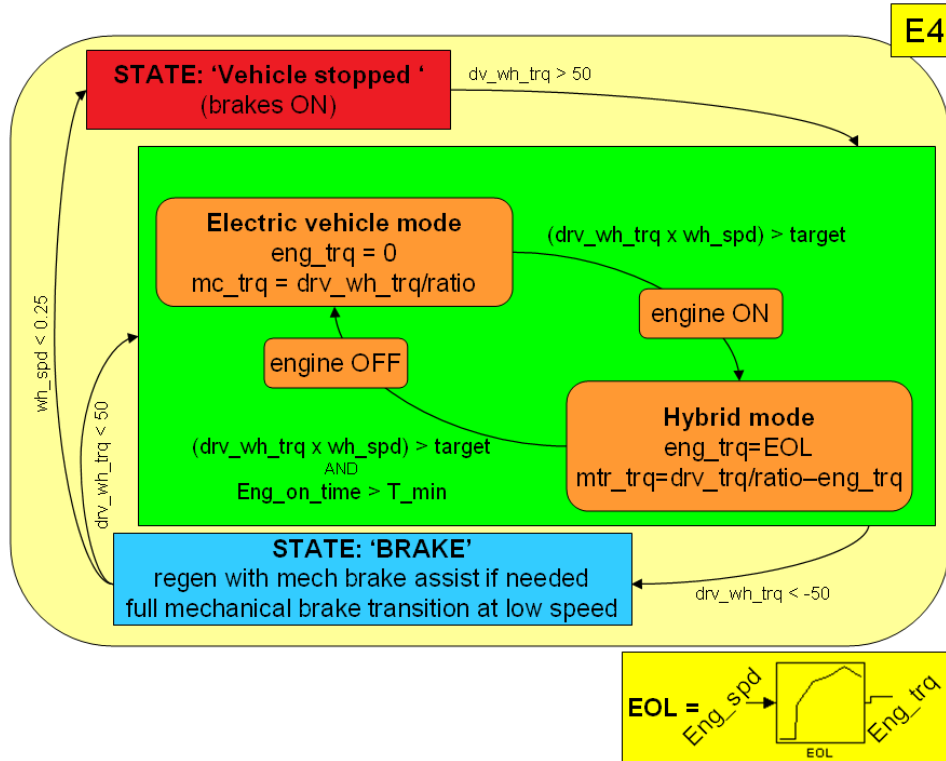
Figure 7-13: Engine operating line hybrid torque split strategy
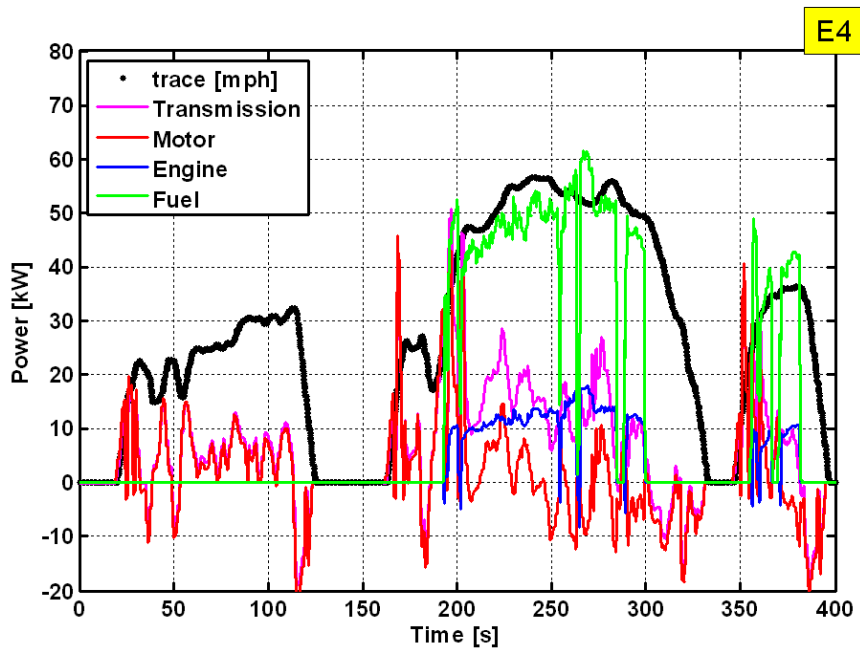
Figure 7-14: Engine operating line hybrid data on start of the UDDS

The test was not charge balanced; therefore the fuel economy will not be presented.

154

Almost all of the building blocks are in place for Plug-in hybrid and hybrid vehicle operation.

7.4.4.   Full hybrid electric with variable engine ON power threshold (E5)

In order to add energy management to the torque split strategy, the threshold variable that enables the different operating states needs to a function of battery energy or state of charge. The three calibratable variables that dictate which state is active are the power threshold of the engine turn ON point, the minimum engine ON time and the EOL. The most important factor is the power threshold, which triggers the engine turn ON point (referred to as 'Power_engon' in the illustrations). The control algorithm is illustrated in Figure 7-15.
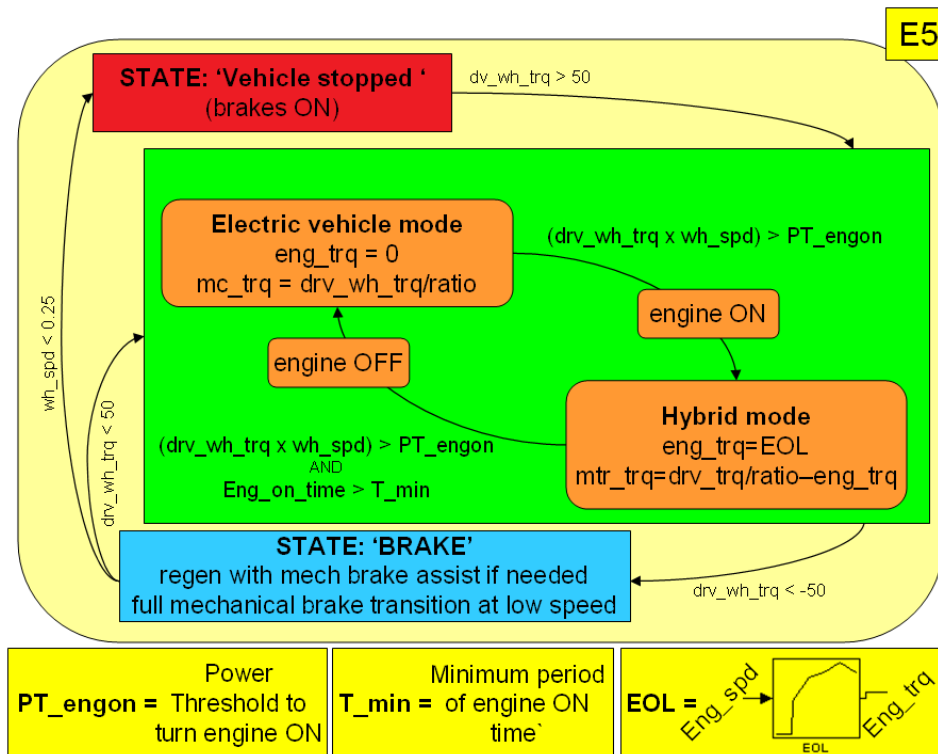
Figure 7-15: Full hybrid with energy management control strategy algorithm

Several ways exist to link the three parameters to state of charge. Two different approaches are presented here. The first one uses continuous function, as explained in section 7.5. The second way is using discontinuous functions, as explained in section 7.6. Each section also presents some test results.

7.5.   Plug-in hybrid with continuously variable charge depleting rate

This example uses the full hybrid algorithm presented in Figure 7-15 along with a set of continuous functions defining the engine turn on power threshold, the engine torque EOL and the minimum engine ON time. The equations are shown in Equation 7-2. Note the ratio of the SOC and SOC_{target} decreases the power threshold and increases the engine load and engine ON time when the actual SOC is lower than the target SOC. If the actual SOC is higher than the target SOC, the engine load and ON time is lowered and the power threshold to trigger the engine is higher. This set of equations will force the SOC to settle on repetitive UDDS cycles. The EOL used for this example is given in Table 7-2: Engine operating line definition.

Equation 7-2: Continuous equation set defining the energy management strategy

$$PT\_engon = \frac{15kW}{2.5 + \dfrac{SOC_{target} - SOC}{SOC_{target}}}$$

$$eng\_trq = EOL\left(1 + \left(\frac{SOC - SOC_{target}}{SOC_{target}}\right) \times 0.1\right)$$

$$T\_min = 5 seconds \times \left(3 + \frac{SOC_{target} - SOC}{SOC_{target}}\right)$$

Table 7-2: Engine operating line definition

Engine speed [rpm]	0	900	1000	2000	3000	4000	5000
Engine torque [N.m]	0	0	70	120	130	150	70

The full charge test was started with the battery pack state of charge set to 90%. At the end of every test the final SOC was used to reprogram the initial SOC of the next test. Figure 7-16 shows the test results. It took over twelve consecutive UDDS cycles for the individual test to become charge balanced. The SOC progression through the drive cycles is a smooth curve that approached the final SOC value asymptotically. The first UDDS cycles were heavily charge depleting with the engine being on for less than 10% of the cycle. The fuel economy for the first cycles is about one third of the charge sustaining cycles but the electric consumption is high. In this test, MATT was a blended PHEV. This approach is an academic exercise since the charge depleting phase for PHEV will be distinctive from the charge sustaining mode. In short, it is sensible to use the electric traction system to its full potential and then charge sustain when the battery pack reaches a low target state of charge. This shows the flexibility of MATT's open control. Generating data for this continuous transition for the PHEV test procedure, from charge

depleting to charge sustaining, was only possible by using MATT. The test procedure needs to address the point at which the charge sustaining mode is achieved.
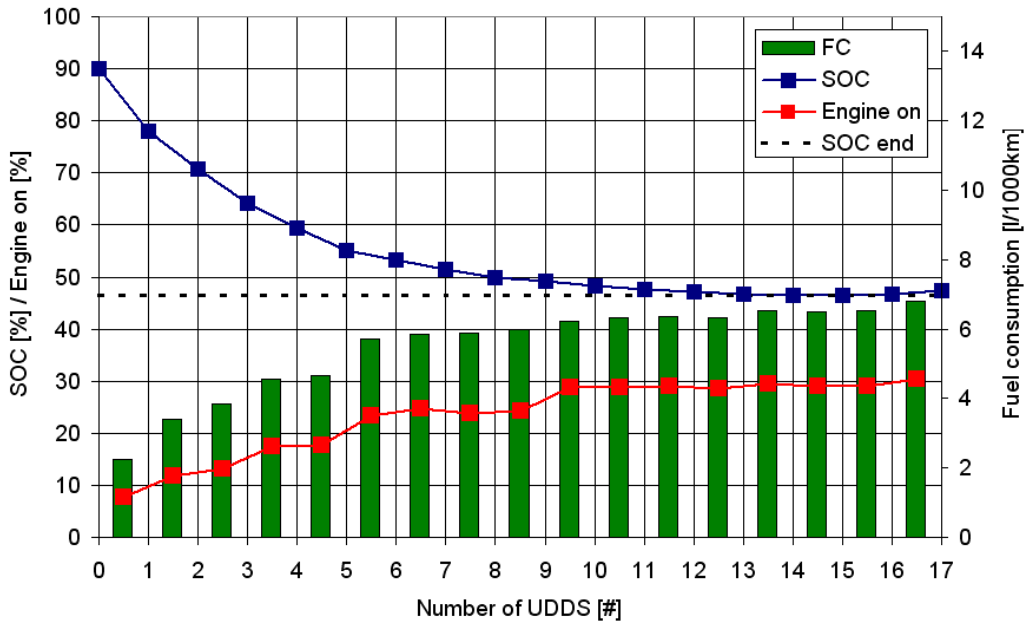
Figure 7-16: Continuous CD to CS PHEV test results

7.6. *Plug-in hybrid with constant charge depletion and charge sustaining phase*

This example again used the code described in Figure 7-15, but in this case, the parameters are calibrated such that there is a distinct charge depleting mode and charge sustaining mode. To do so, the power level required to compete the UDDS needs to be understood. Figure 7-17 exhibits these power levels.
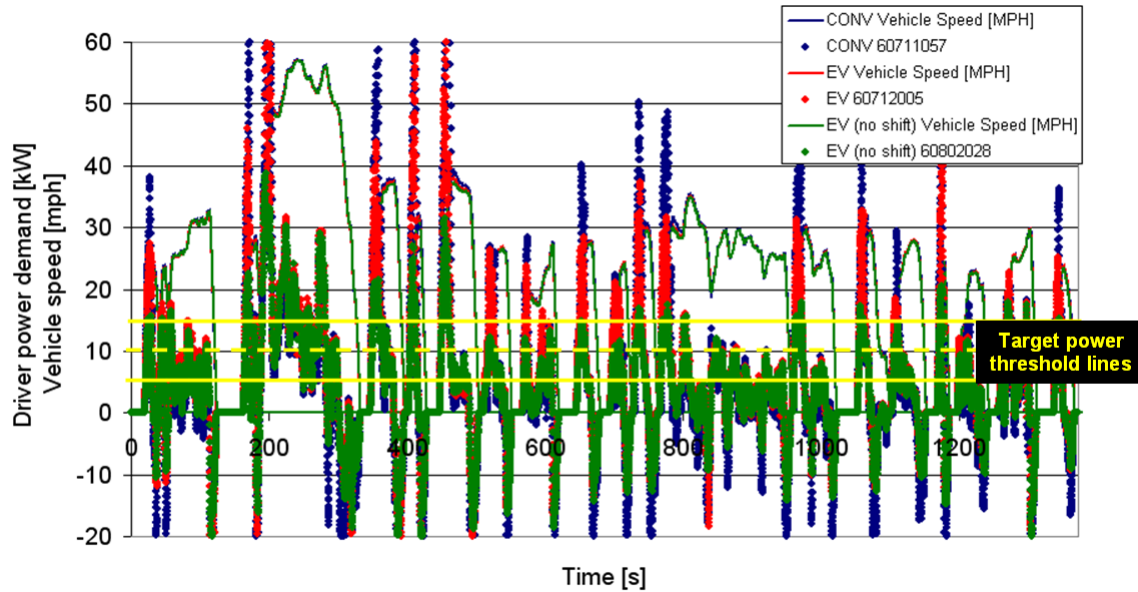
Figure 7-17: Power profile of MATT emulating a Focus size vehicle on the UDDS

The graph shows the driver's power demand at the wheel for the conventional vehicle operation as well as for the electric vehicle operation with and without shifting. The power demand for the shifted cycles (conventional and electric) show power peaks during accelerations. These peaks are due to the torque hole in the acceleration caused by the slow shift time of the manual transmission module. The control strategy is thus modified slightly by introducing a new logic that ensures that the power threshold is exceeded for a minimal amount of time and not during a shift event.

The electric vehicle (with no shifting) power levels are used as the baseline to determine a power threshold target to turn the engine ON. Most of the peak power levels are right above 15 kW. Then the rest of the power is between 5 and 15kW. The peak power level is below 40kW. In order to force electric vehicle operation, the engine ON power threshold needs to be set higher then 40 kW. To force electric vehicle operation for the charge depleting phase, the power threshold to turn the engine ON is set to 100 kW from 100% state of charge to 45% state of charge. Once 46% state of charge is reached, the power threshold is set to 15 kW, which will cause the engine to turn on occasionally. If the target state of charge of the charge sustaining operation is 30%, then a steep slope for the power threshold needs to happen close to that target. Thus, from 35% to 30% SOC, the power threshold varies from 15 to 5kW. This ensures that if the SOC is below the target state of charge, the engine will turn on frequently to charge the battery pack. This strategy is summarized in Figure 7-18.
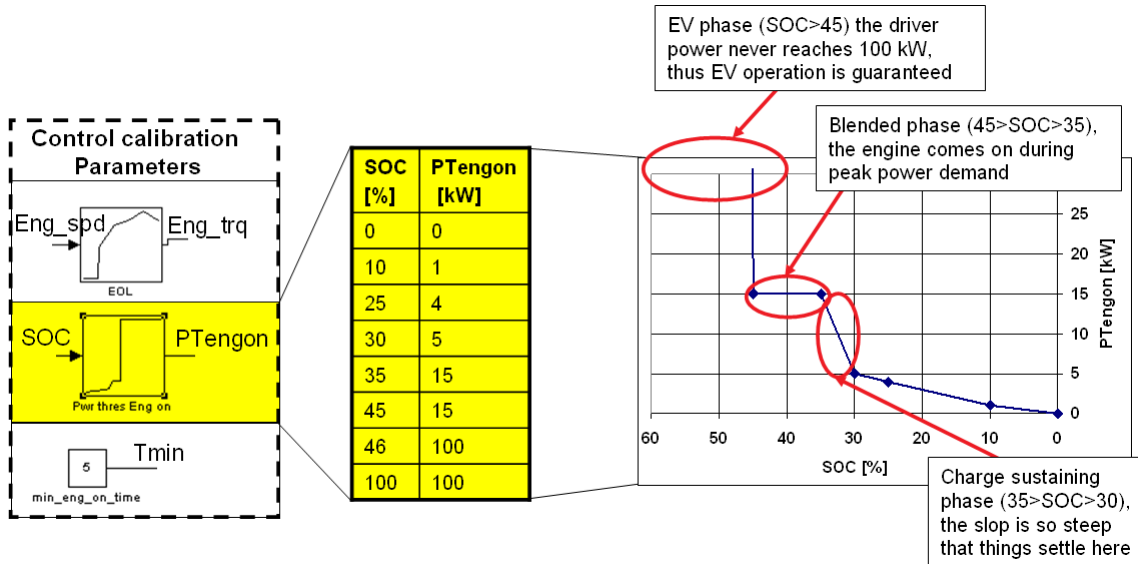
Figure 7-18: Engine ON power threshold strategy

The minimum engine ON time is set to 5 seconds and the engine operating line is the same as in Table 7-2. The test results are presented in Figure 7-19. The first 2 UDDS cycles are completed without the engine. The 3rd UDDS cycle is the transition cycle, which is still charge depleting, but the engine was used for the first time. The follow up cycles are all charge sustaining. This energy management strategy shows a clear brake between the charge depleting phase and the charge sustaining phase.
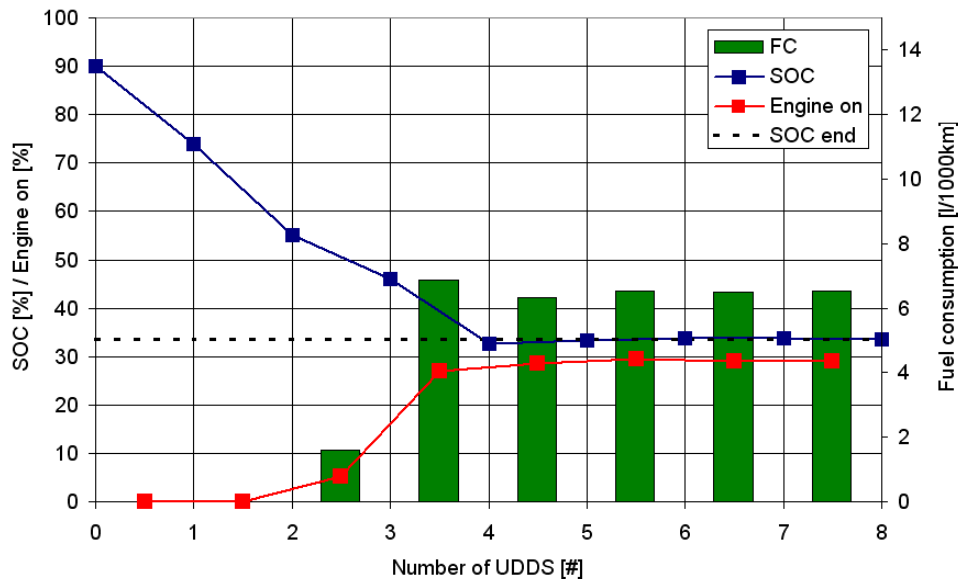
Figure 7-19: Electric vehicle charge depleting to charge sustaining data

When MATT used the exact same hardware, it produced a completely different set of PHEV data by just changing the energy management strategy. The lower level control of the powertrain components is fully debugged and the hardware is robust enough to reliably complete these drive cycles under different energy management and torque split strategies. Again, this shows MATT's flexibility.

7.7.   Plug in hybrid with engine warm up routine

This is the final phase of the plug-in hybrid development based on the energy management strategy presented thus far. In this phase, an engine warm up routine is added. The purpose of the routine is to warm up the engine and especially the exhaust after treatment in a controlled and smooth manner. Catalytic converters eliminate most of the tailpipe emission in a vehicle, but to operate at high conversion efficiency, light off temperature must first be reached, as shown in section 5.5.2. The engine retards sparking during its warm up phase to increase the exhaust temperatures and prepare the catalytic converter. To prevent large emissions spikes, the engine should be operated at low constant loads. Therefore, the warm up routine loads the engine to a constant and light load while the motor is still the primary mover. The routine is entered when the battery state of charge approaches the target state of charge within a certain margin. The routine is completed when the catalytic converter reaches its light off temperature. The energy management algorithm, including the warm up routine, is shown in Figure 7-20.
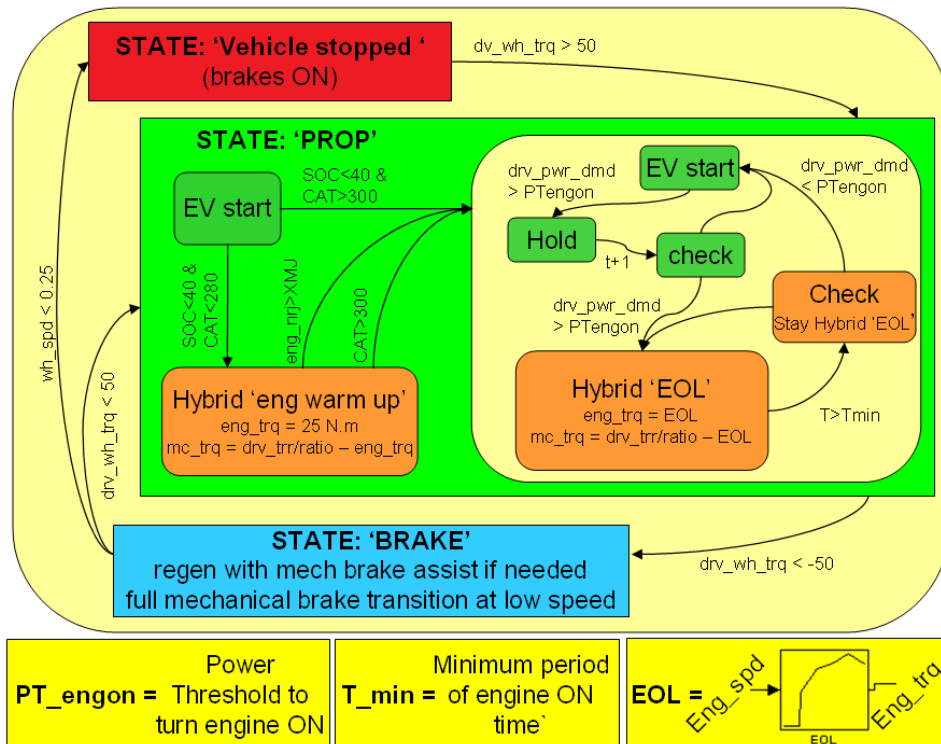
Figure 7-20: PHEV control strategy with engine warm up routine to minimize emissions

On MATT, the catalytic converter brick is instrumented as shown in Figure 3-8. That temperature reading is used by the high level controller. In production vehicles, the engine controllers use a simple but effective catalytic converter temperature model, as shown in Figure 7-21. The engine model shows faster temperature rise, but that can be explained by the fact that the thermocouples in the catalytic converters are place at the end of the brick and thus while the core of the brick may be hot, the thermal capacity and thermal conduction may delay the temperature rise at the thermocouples.

At the first engine start of the full charge test set, the warm up routine can only be exited once a certain amount of energy is provided by the engine. The purpose is to bring the engine to operating temperature beyond just addressing the exhaust after treatment system temperature. Figure 7-21 also shows the integrated engine crankshaft energy along with the temperature information. Note that the second catalytic convert reaches operating temperatures at 1 MJ of engine energy at 150 seconds. Around 2 to 3 MJ of engine energy, the engine system reaches full operating temperature. Therefore, these numbers are a good starting point for calibrating the engine energy threshold to exit the engine warm up routine after the first engine start.
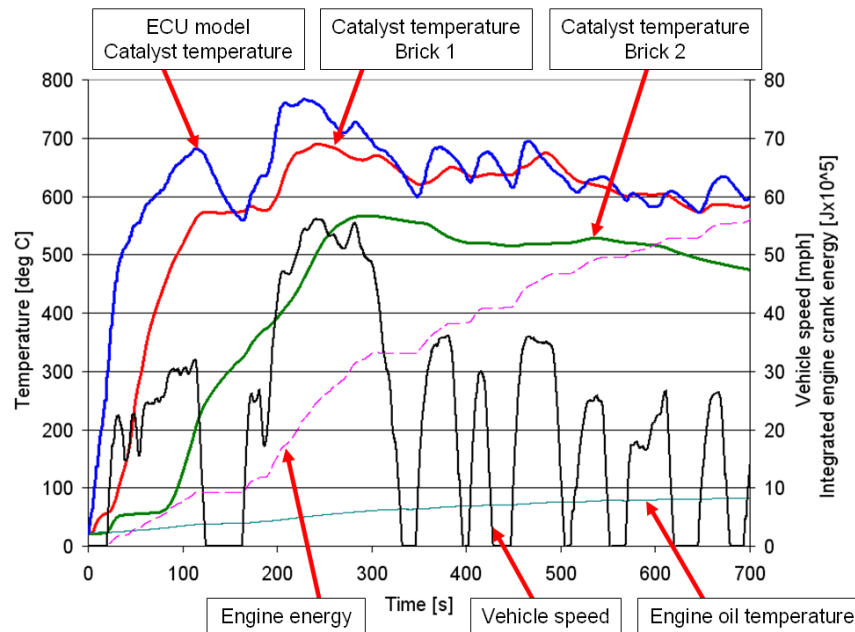
Figure 7-21: Catalyst temperatures on a cold start UDDS in conventional mode

Unfortunately, the testing was not completed due to a transmission failure and a prohibitive testing schedule. The next PHEV project that used MATT was a study on the topic of PHEV emissions mitigation in collaboration with the University of Tennessee. Some of the warm up ideas discussed here were implemented in that project. The energy management strategy for that project is presented in section 7.8. The results of the emissions mitigation study are presented in section 8.4

161

7.8. *Fully integrated hybrid control strategy*

7.8.1. The energy management and torque split strategy

This energy management and torque split strategy is used in a collaborative project with the University of Tennessee. MATT was the only platform available to test the strategy with hardware. The project's purpose was to investigate PHEV tailpipe emissions and to develop mitigating strategies to minimize these emissions. This project and the accompanying control strategy are the basis for David Smith's doctorial dissertation work. The control strategy was developed in Knoxville, TN using the PSAT software. The project turned into an intellectual collaboration during the implementation phase, including the debugging of the control code on the MATT hardware.

The energy management strategy has a modular control process approach. There are four major processes: The vehicle mode control process (VMCP), the regenerative control process (RBCP), the battery mode control process (BMCP) and the energy management control process (EMCP). Each process has some particular function and information circulates between the different processes constantly. The input and output to the control strategy are still the same, as shown in Figure 7-1. The lower level control of the components is also unchanged. This again proves the flexibility MATT's hardware and software.

This control strategy is based on power request and levels instead of torque, as was the case in the previous strategies presented. The VMCP manages the operating modes that should be used, such as conventional mode, electric mode, performance mode and hybrid mode. The charge depletion or charge sustaining is also determined by the VMCP. By determining the vehicle operating mode, the VMCP also decides whether the engine should operate. In the engine status management logic, the engine warm up phase algorithms are defined. The VMCP interprets the driver pedal request as a main input, along with additional available vehicle feedback. The RBCP controls the blending between the regenerative braking and the mechanical brakes. The BMCP monitors the battery health and is responsible for the state of charge maintenance. The BMCP sets a battery state of charge maintenance power (P_SOC), which reflects whether the battery requires charging or discharging. The actual torque split strategy is controlled in the EMCP. The EMCP uses the addition of the driver power request and the battery power request as well as the vehicle mode to determine how to satisfy the driver request. In electric mode, the EMCP ensures that the appropriate torque request is sent to the electric motor within the current hardware limits to satisfy the driver power request. In hybrid mode, the total power request (driver and battery combined) is addressed by using the engine and the hybrid system. Two major operating strategies are available in hybrid mode. The engine load following strategy provides the total power requested. The engine optimum strategy loads the engine to its highest efficiency point and excessively charges the batteries with power beyond the driver request. Both hybrid strategies operate with the hardware limitations. This energy management strategy is illustrated in Figure 7-22. For further details, please refer to Mr. David Smith's dissertation (Ref. 133).
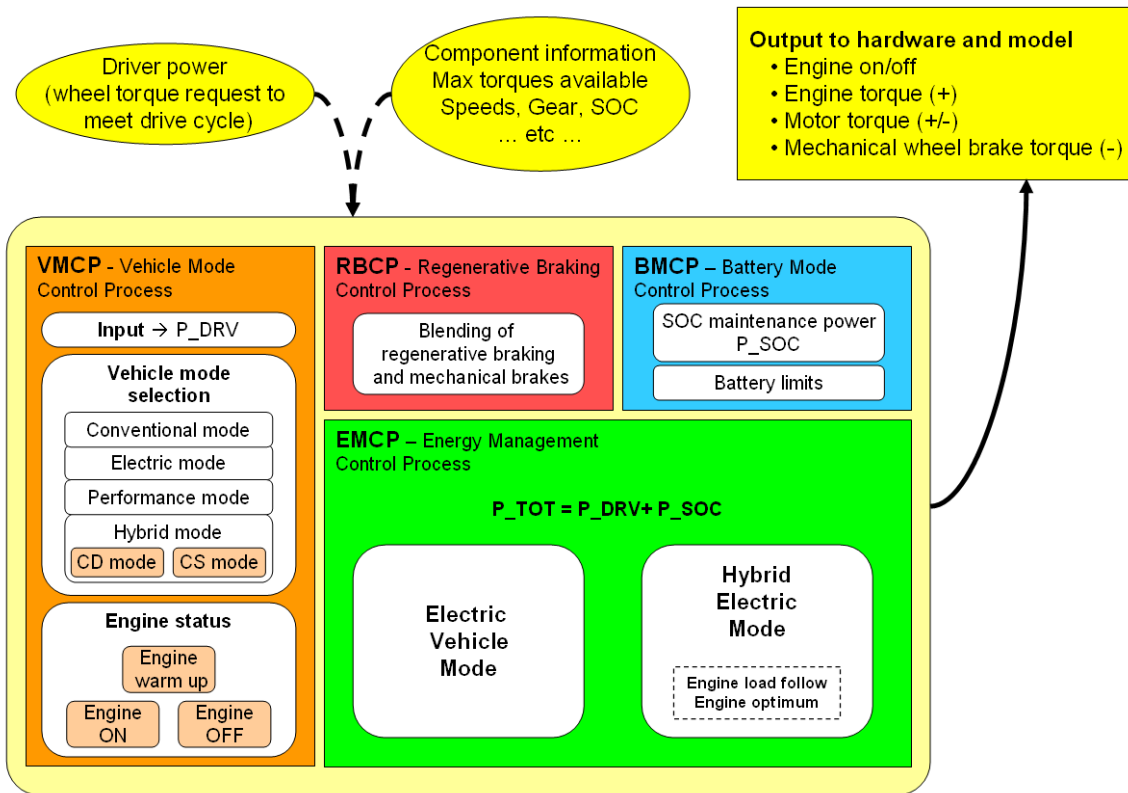
Figure 7-22: Full integrated control strategy

The automatic transmission module was used to complete the testing and provide the following sample results. The conventional vehicle results from section 5.5 were obtained with the same hardware setup (new engine control, automatic transmission and improved coolant system) and can therefore be used for comparison.

The follow sample results show the full charge test results with the charge depleting and the charge sustaining operation. Two vehicle categories are presented. The first operation is an electric vehicle capable plug-in hybrid with an engine optimum control strategy. The second is a blended plug-in hybrid with an engine load following control strategy.

7.8.2.   EV capable 'engine optimum' plug-in hybrid results

Figure 7-23 summarizes this full charge test set for this particular plug-in hybrid type. The first two first urban cycles are covered in electric only mode. On the third urban cycle, during the high load acceleration on hill 2, the engine turns on for the first time as the SOC reaches the target SOC for the charge sustaining operation mode. In charge sustaining mode, the engine oil warms up as the engine is used more frequently. As the charge sustaining mode is reached, the fuel usage increases and the net battery usage is

zeroed. For the first two cycles no fuel was used, thus 100% of the petroleum was displaced in this case, which is the intent of PHEVs.
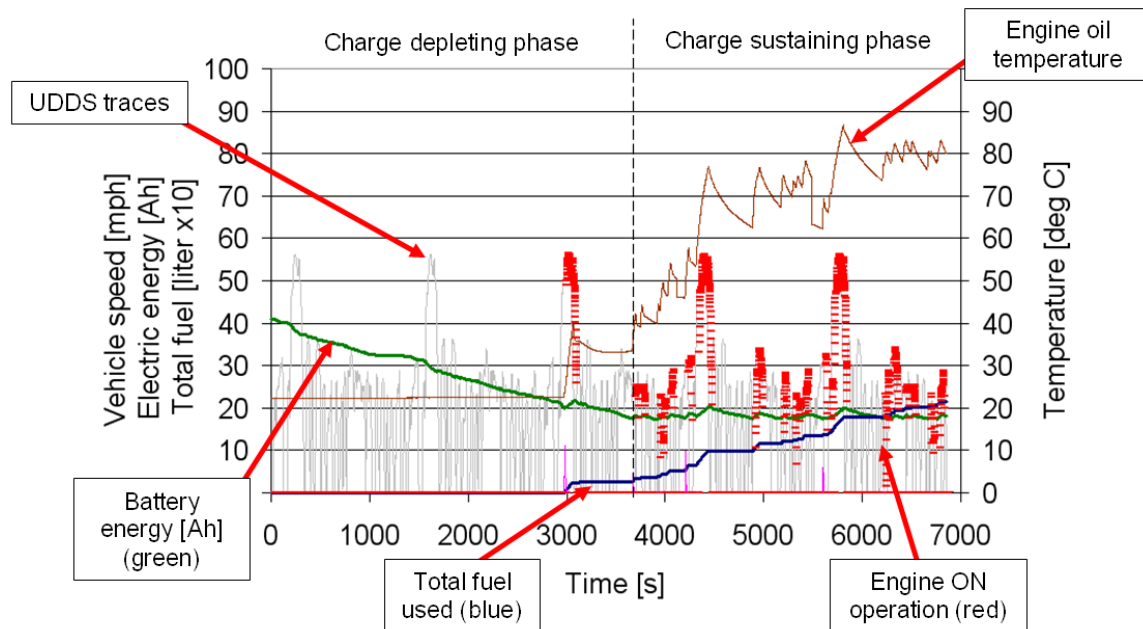
Figure 7-23: Summary of the Plug-in hybrid test set

Note that the start of the charge sustaining phase is apparent from the battery capacity. In charge sustaining mode, the battery energy swings is noticeable, which is due to the engine excess charging the battery in order to maintain an efficient operating point. The engine is operating at high loads or is OFF, which translates into a jagged engine oil temperature signal.

The same test results are summarized in Figure 7-24. This is an energy consumption graph which plots fuel consumption on one axis and electric consumption on the other axis. The electric consumption is based on the voltage and current simulated at the battery terminals. These are the best plots to view plug-in hybrid energy consumption since both energy sources are represented. The graphs first point is the electric vehicle cold start cycle, which falls on the electric consumption axis. The second cycle was also an all electric operation test but the electric consumption was lower since the powertrain was already at operating temperature. The cold and hot losses described in section 6.7.1 appear on this graph. During the 3rd UDDS cycle, the engine came ON for the first time, thus fuel and electricity were consumed. This cycle is called the transition cycle since it is between the charge depleting phase and the charge sustaining phase. The final two points are the charge sustaining cycles. This graph provides a complete energy consumption picture for a full charge test of a plug-in hybrid. The emissions results are the other key information used to characterize the plug-in hybrid vehicle. The highest emissions will occur on the first engine ON event, especially with this 'engine optimum' control strategy, which will load the engine immediately. Table 7-3 includes the emission information. In fact, the third cycle has the highest emissions, due to the engine cold start.
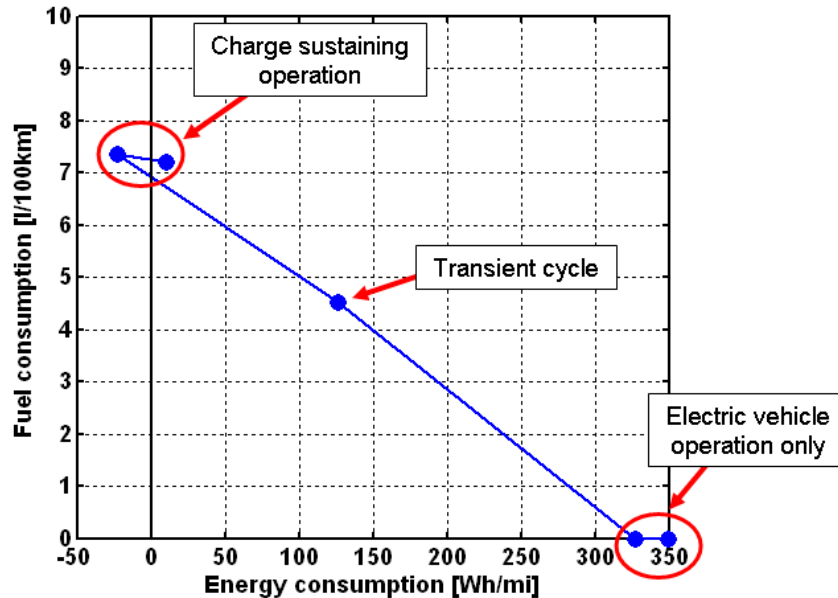
Figure 7-24: Energy and fuel consumption graph for the 'engine optimum' plug-in hybrid test

Table 7-3: Energy consumption and emission summary for the 'engine optimum'

	FE [mpg]	EC [Wh/mi]	THC [g/mi]	NOx [g/mi]
UDDS 1	0	350	N/A	N/A
UDDS 2	0	327	N/A	N/A
UDDS 3	52.6	126	0.022	0.024
UDDS 4	32.3	-23	0.009	0.005
UDDS 5	33.0	10	0.005	0.003

Currently no available PHEV is EV capable on the UDDS. MATT occupies that role to generate data for that part of the design space. That data is important to understand the PHEV capabilities and to help in the development of the SAE J1711 PHEV test procedures.

7.8.3. Charge sustaining 'engine optimum' hybrid results

This section simply zooms in on the charge sustaining UDDS cycle to show the details of the hybrid operation with this energy management strategy. The test data presented Table 7-4 is from a slightly charge-depleting test. The fuel economy over the UDDS is 33 mpg, which is a 10% fuel economy gain over the conventional vehicle with a hot start. The hydrocarbon emissions are increased by an order of magnitude.

Table 7-4: Charge sustaining 'Engine optimum' hybrid vehicle test results on UDDS

	UDDS (warm start)
Fuel economy bag [mpg]	33.0
THC [g/mi]	0.005
NOx [g/mi]	0.0003
SOC init [%]	31.0
SOC end [%]	30.5

During the hybrid operation, the engine came on 11 times, as shown in Figure 7-25. This test was run after another hybrid test with about 15 minutes of time to readjust the emissions bench. Thus, the components did cool down a bit. Even during the test, while the engine is off, the coolant, the catalytic converter and the engine oil cool off, especially during longer off periods. In this particular hybrid operation, the engine never reaches a thermal steady state operating regime as it does in the conventional vehicle. The catalyst temperature is of special concern. If it cools below the light off temperature, the conversion efficiency greatly suffers. At the first engine start, the catalyst is at 200 deg C, which is slightly below the light off temperature. That engine start generates the major part of the emissions, as shown in Figure 7-26.
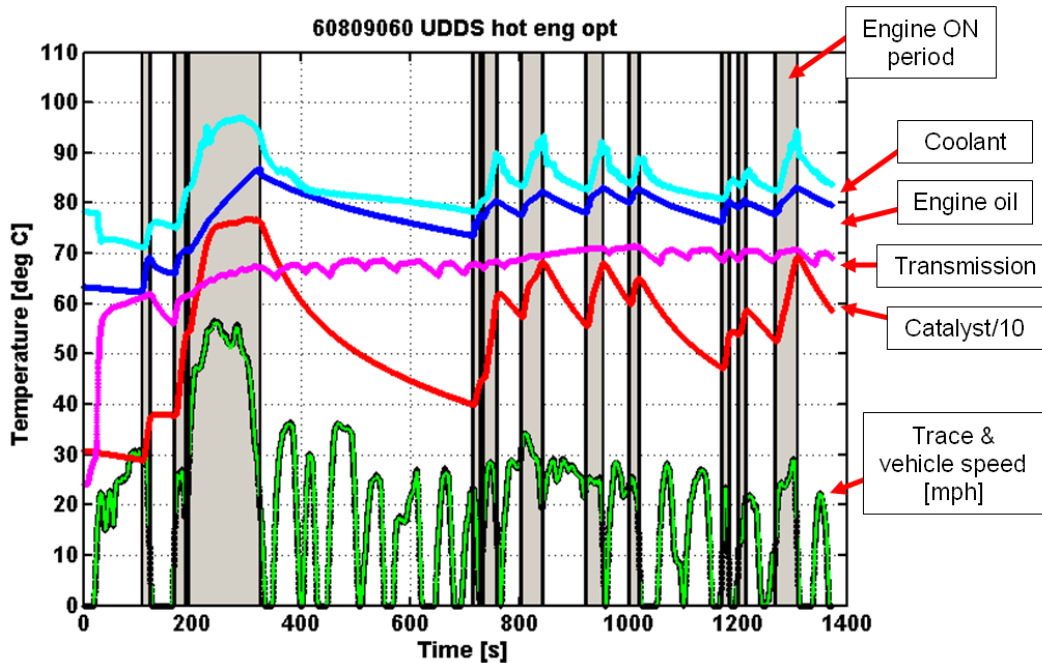
Figure 7-25: Trace, engine operation and temperature information for the 'engine optimum' hybrid (5th cycle of the FCT)
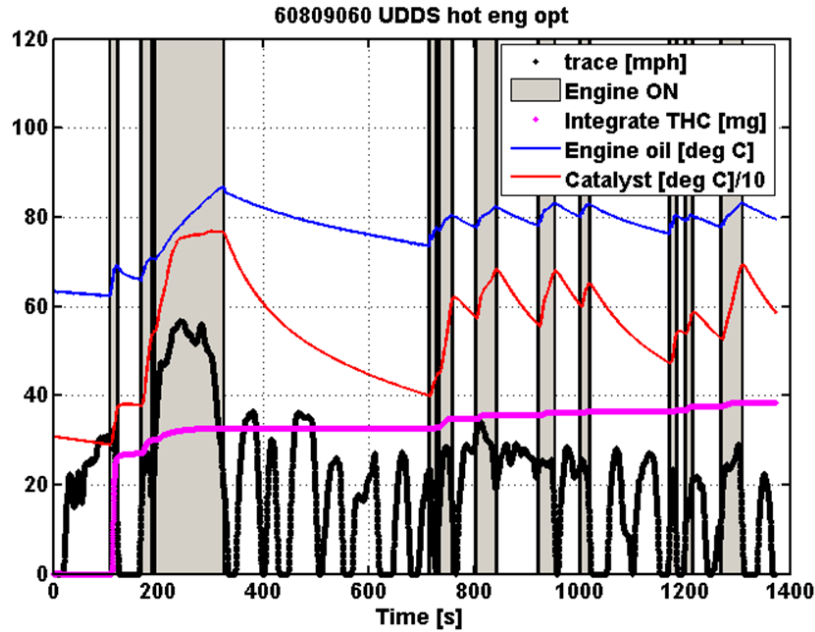
Figure 7-26: Emission details for the 'engine optimum' hybrid operation (5th cycle of the FCT)

The first start generates the highest emissions because the catalyst temperature is too low and the engine is immediately loaded to a high load. This hybrid control strategy is intended to be the first iteration In future versions, the initial load of the engine should be reduced and ramped up until the catalyst temperatures and the engine oil have reached operating temperature.

The first engine start is shown in Figure 7-27. The engine does get loaded between 40 to 50 kW which, at those engine speeds, corresponds to engine torque level of a 140 to 150 N.m.
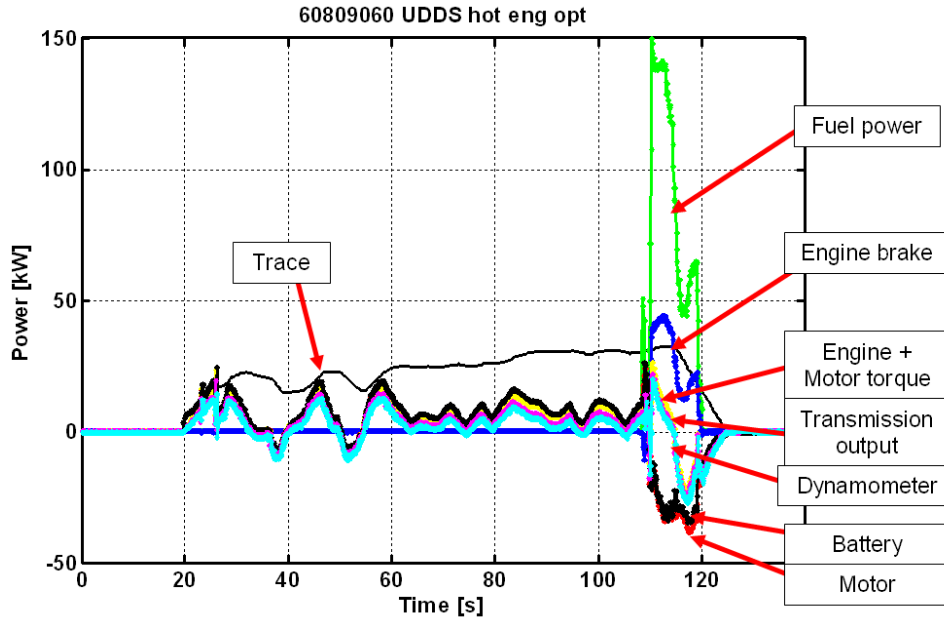
Figure 7-27: Power measurements of components for the first hill of the UDDS operating in the 'engine optimum' strategy

For the first part of the test, the vehicle operates in electric mode without the engine. After a certain amount of battery energy is used, the driver demand threshold to turn the engine is reached by the driver demand. Then, the engine provides power to the wheels and recharges the batteries. During the deceleration, regenerative braking is achieved by using the electric motor, which recharges the batteries. The energy summary is shown in Table 7-5.

Table 7-5: Total positive energy measured for the components during the charge sustaining UDDS in 'engine optimum' hybrid mode

Energy [MJ]	UDDS (warm start)
Fuel	25.77
Engine crankshaft	9.10
Engine + Motor positive	7.95
Engine + Motor negative	1.50
Transmission positive	5.69
Transmission negative	1.86
Dynamometer positive	4.44
Dynamometer negative	2.19

The average cycle engine efficiency is 35.3%, which is much higher than the 25.3% engine efficiency from the conventional hot start. Thus, using the motor and energy storage system to modify the engine operation is beneficial to the engine. The

hybrid system does have its own losses due to charging and discharging the batteries as well as the emulated motor efficiencies. Once the 0.82 MJ in auxiliary loads (600 W continuously) are considered, the overall hybrid system efficiency is 82.5%. The regenerative braking also contributes to the higher overall system efficiency. Table 7-6 summarizes the efficiencies.

Table 7-6: Average component efficiency over test cycles

Average cycle efficiency [%]	UDDS (hot start)
Engine brake	35.3
Overall hybrid system	82.5
Regenerative energy recovery	57.4

The major advantage therefore resides in shifting the engine operation into more efficient areas and eliminating its use in inefficient areas. Figure 7-28 shows the engine operation. The engine optimum is an extreme hybrid case which optimizes the engine operation. In this hybrid mode for this particular vehicle emulation, the fuel used on the UDDS is 0.214 gallons, compared to 0.276 gallons used for the conventional vehicle, which represents 22% of petroleum displacement.
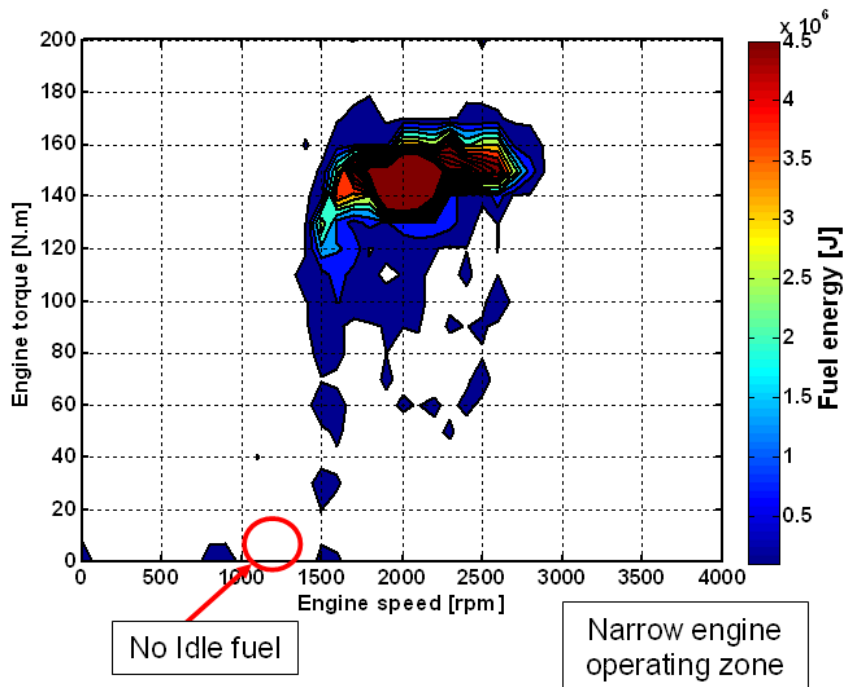
Figure 7-28: Engine operation of the 'engine optimum' mode

This concludes the 'engine optimum' control strategy description.

7.8.4. Blended 'load following' plug-in hybrid results

Figure 7-29 summarizes the full charge test for the following blended 'engine load' plug-in hybrid test. The engine is used on the first test, making it the cold start test for the engine. The engine is used on the faster and more aggressive hills for the first phase (505) for the UDDS. MATT completes over 4 urban cycles in the charge depleting blended mode. The same 41 Ah battery pack was emulated then for the EV capable test, which only yielded two charge depleting test cycles. For this blended hybrid fuel charge test three charge depleting UDDS cycle were completed. The blended plug-in hybrid is still capable to run some of the hills in electric only mode, but it can not complete all the cycle in electric only mode. On the charge sustaining cycle, the engine turns on at almost every mode. This helps the engine to reach a normal operating temperature.
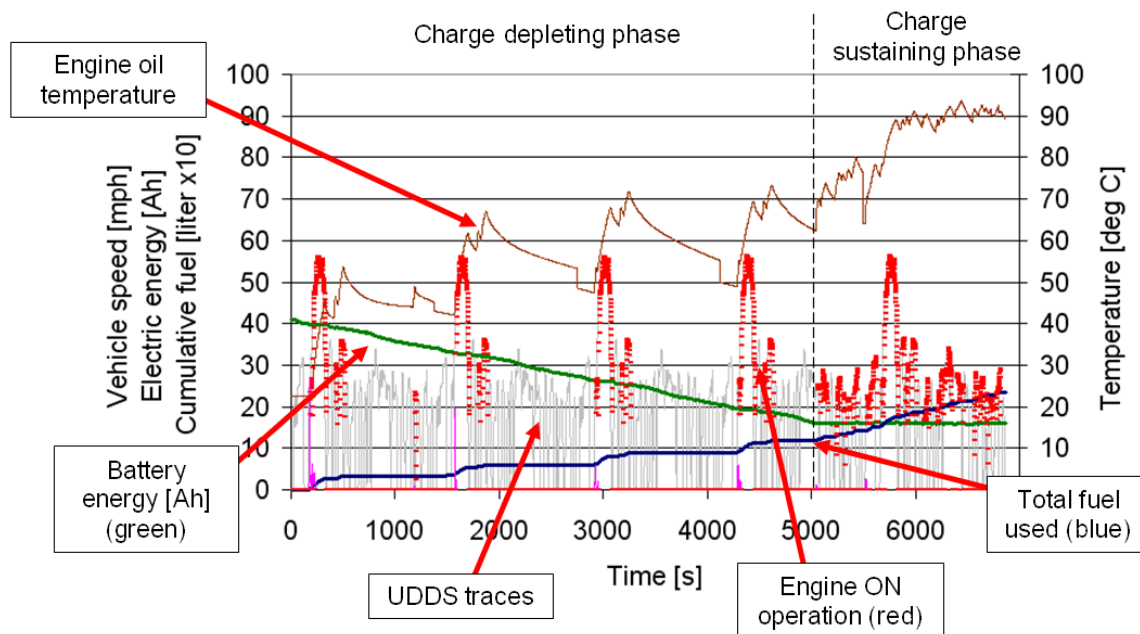
Figure 7-29: Blended PHEV test set as a 'load following' hybrid

Note the start of the charge sustaining phase is even more apparent from the battery capacity since the battery energy does not experience the same swings as it does during the 'engine optimum' strategy. The engine does not excessively charge the battery in 'load following mode.' The engine oil temperature signal is much smoother.

At the end of the five UDDS cycles, a total of 0.649 gallons are used, compared to 0.602 gallons for the EV capable PHEV. The blended hybrid requires a less powerful motor, thus cutting on cost and packaging issues while still displacing a significant amount of petroleum. As a baseline, the conventional vehicle uses 1.393 gallons of fuel to cover the 5 urban cycles.

The full charge 'load following' blended plug-in hybrid test results are summarized in Figure 7-24. The cold start cycle is the first cycle. The cold start losses show a higher electric energy and fuel consumption compared to the subsequent tests. The second and third tests are almost identical, which is due to the automatic driver repeatability. In the fourth cycle, the transition from charge depleting to charge sustaining occurs. The last test is charge sustaining. Note that the following charge sustaining test is not as fuel efficient as the engine optimum charge sustaining test.
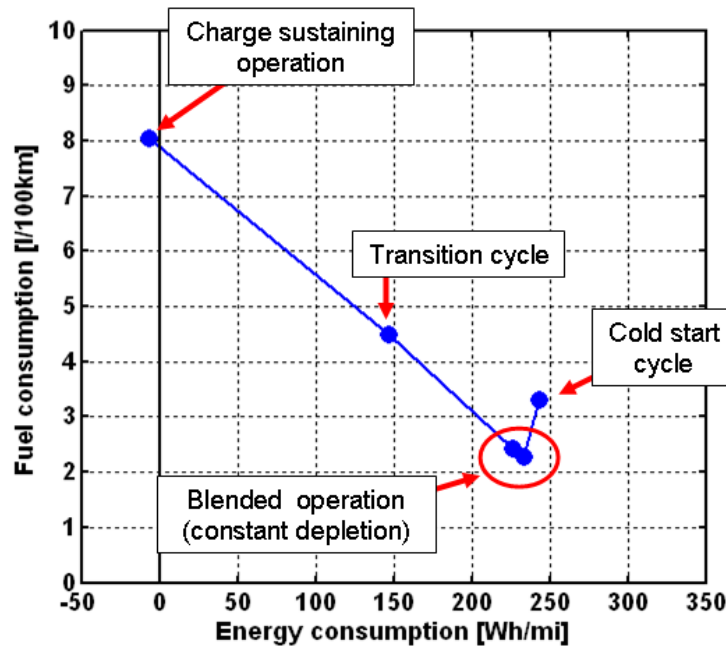
Figure 7-30: Energy and fuel consumption graph for the 'load following' Plug-in hybrid test

Table 7-7 presents the emissions results. The cold start suffers higher emissions than the 'engine optimum' or conventional cold start test. A closer look at the time data shows that the catalytic convert does not reach its light off temperature as fast. The engine optimum control achieves that as a result of higher engine loads and the conventional vehicle benefits from the engine idle time. The measured emissions tend to be lower compared to the 'optimum engine' control in the charge sustaining cycles, which is explained by the lower raw emissions and high conversion efficiencies once the catalytic converter reached its operating temperature.

Table 7-7: Energy consumption and emission summary for the 'load following' PHEV

	FE [mpg]	EC [Wh/mi]	THC [g/mi]	NOx [g/mi]
UDDS 1	71.5	243	0.038	0.006
UDDS 2	104.4	233	0.005	0.014
UDDS 3	98.1	226	0.001	0.002
UDDS 4	52.9	147	0.002	0.002
UDDS 5	30.5	-7	0.003	0.002

Currently, all available plug-in hybrid vehicles are the blended type hybrids, which is the operation demonstrated in this section.

7.8.5.   Charge sustaining 'load following' hybrid results

This section focuses on the charge sustaining UDDS cycle to show the details of the hybrid operation with this energy management strategy. The test data presented in Table 7-8 are from charge balanced test. The fuel economy over the UDDS is 30.5. mpg, which is a 4% fuel economy gain over the conventional vehicle with a hot start.

Table 7-8: Charge sustaining 'Load following' hybrid vehicle test results on UDDS

	UDDS (warm start)
Fuel economy bag [mpg]	33.0
THC [g/mi]	0.003
NOx [g/mi]	0.002
SOC init [%]	29.9
SOC end [%]	29.9

During the hybrid operation, the engine came on 17 times, as shown in Figure 7-31. The engine turned ON more frequently than it did during the 'engine optimum' strategy since it produces a lower average power. The engine does not cool down as much or for as long in the 'load following' strategy. The first engine start generates the major part of the emissions, as shown in Figure 7-32. The following engine starts contribute very little the tailpipe emissions on this 5th UDDS cycle. Once the catalytic convert is hot, the hydrocarbon emissions are extremely low. Also notice that the engine reaches a steady operating temperature that is still lower than in the conventional vehicle operation.
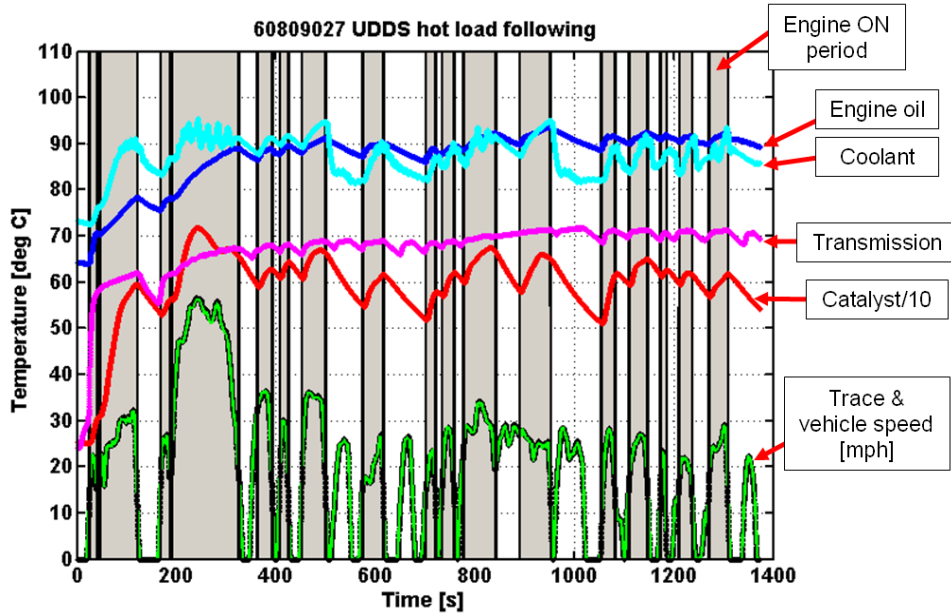
Figure 7-31: Trace, engine operation and temperature information for the 'load following' hybrid
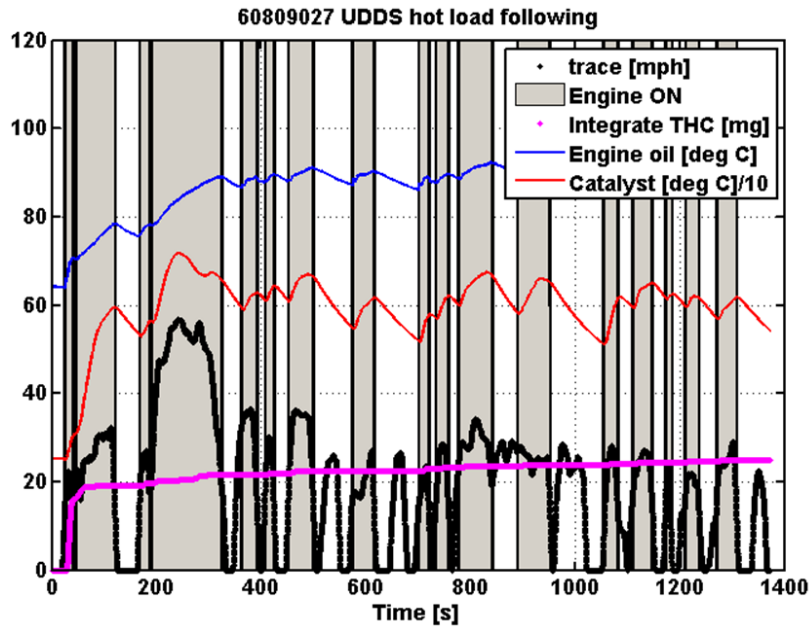
Figure 7-32: Emission details for the 'load following' hybrid operation

Figure 7-33 provides a closer look at the operation of the 'load following' strategy. The launch is performed in electric mode. Once the engine turns ON it provides the power required to meet the trace and charges the battery. At the second engine start, the battery and motor power is at negative 10 kW, which means that 10 kW is the approximate charging rate into the battery. As time progresses, that charging rate slowly

173

decreases, which is due to the BMCP requesting a lower state of charge maintenance power since the battery is close to the target state of charge.
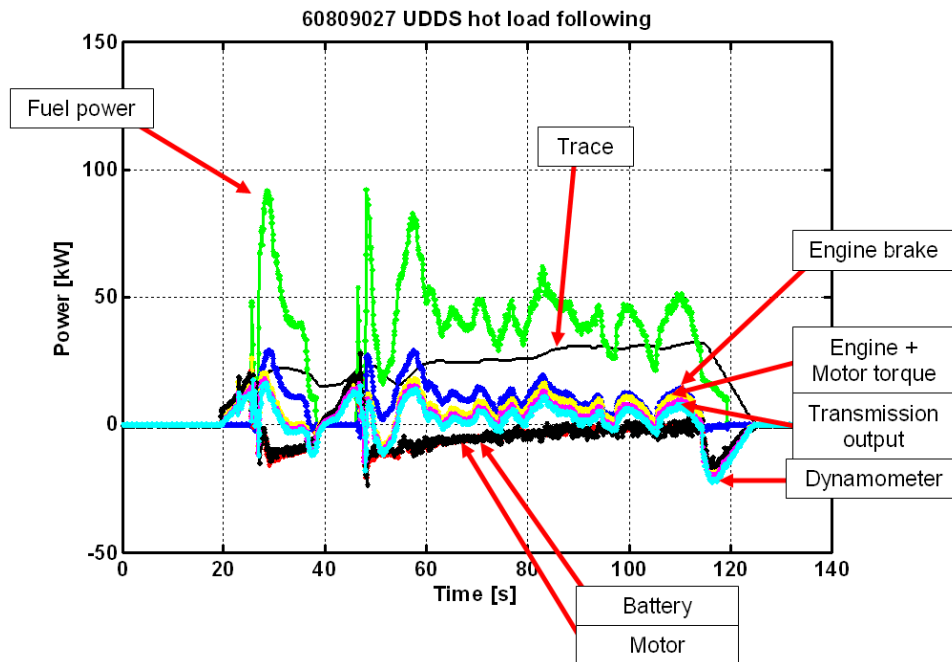
Figure 7-33: Component power flow on the first hill of the UDDS operating in the 'load following' strategy

The full cycle energy summary is shown in Table 7-9.

Table 7-9: Total positive energy measured for the components during the drive cycles in 'engine optimum' hybrid mode

Energy [MJ]	UDDS (warm start)
Fuel	29.21
Engine crankshaft	8.39
Engine + Motor positive	7.66
Engine + Motor negative	1.54
Transmission positive	5.64
Transmission negative	1.54
Dynamometer positive	4.49
Dynamometer negative	2.22

The average cycle engine efficiency is 28.7%, which is much higher than the 25.3 % engine efficiency from the conventional hot start. Thus, using the motor and energy storage system to modify the engine operation is beneficial to the engine. The hybrid

system does still have its own losses due to charging and discharging the batteries as well as the emulated motor efficiencies. Once the 0.82 MJ in auxiliary loads (600 W continuously) are considered, the overall hybrid system efficiency is 84.9%. The regenerative braking also contributes to the higher overall system efficiency. Table 7-6 summarizes the efficiencies.

Table 7-10: Average component efficiency over test cycles

Average cycle efficiency [%]	UDDS (hot start)
Engine brake	28.7
Overall hybrid system	84.9
Regenerative energy recovery	49.6

The engine operation is now more spread across the load range, as shown in Figure 7-34. As opposed to the conventional vehicle shown in Figure 5-39, the lower speed range is not used since that is typically covered by the electric launch mode. Once the engine is in use, the control strategy does not add extra load on the engine to optimize the engine efficiency. The average engine brake efficiency for a charge sustaining hot start load following urban cycle is 29%. It is 25.3% for the conventional. The main improvement is the elimination of idling and the lower speed operating points. A reduction in fuel consumption also occurs, compared to the conventional vehicle. That is explained by the energy recovered by regenerative braking and the electric launch.
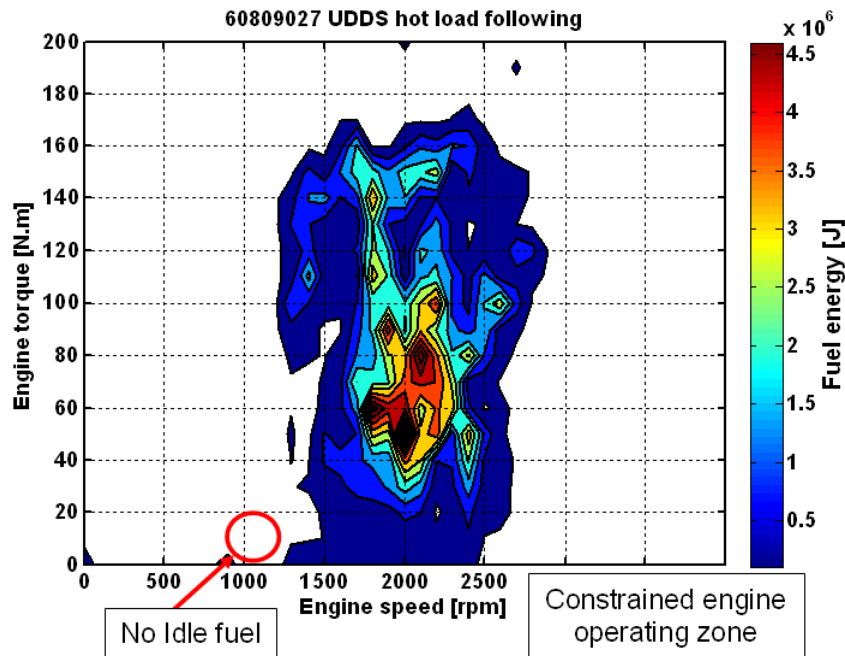
Figure 7-34: Engine operation of the 'load following' mode

These tests are part of the baseline PHEV tests to evaluate the impact of control strategies on emissions and fuel consumption. It appears that the engine needs to operate at reduced loads until the catalyst has reached light off. The major emissions are generated from the first engine start and the first few seconds of the engine operation in a cycle. Further work will be performed in this area, including the development of an improved control strategy that includes emissions control.

Using the same hardware modules and the same lower level control algorithms, MATT was able to execute many different control strategies, ranging from the aggressive 'engine optimum' to the milder 'load following' control.

7.9. Limitations

The slow shifts associated with manual transmission required special routines in the hybrid control strategy so that a driver torque spike did not trigger an engine ON event. But in hybrid mode, 2nd and 3rd gear could still be used to minimize the manual transmission shift problems. Ultimately, one manual transmission failed beyond the point of repair. This failure was likely due to fatigue caused by driveline torque ripple and vibrations as well as a torque impulse caused by an aggressive driver and regenerative braking calibration.

The automatic transmission still suffers from higher than normal losses, but that handicap is the same for all of the different hybrid strategies and thus remains consistent from test to test.

Generally, the hardware performed well in the hybrid environment.

7.10. Synopsis of hybrid and plug-in hybrid vehicle operation

First, some simple hybrid operating algorithms were presented along with test results. These simple hybrid modes progressed into a fully functional hybrid energy management and torque split strategy. This slow and progressive development enabled the debugging of the lower level component control so that the energy management strategy shell could accommodate different control strategies.

A simple plug-in hybrid energy management strategy algorithm was used to test two different types of plug-in hybrids by changing the calibration parameters. The first plug-in test was a blended vehicle with a continuously variable charge depleting rate. The second full charge test was an electric vehicle capable plug-in hybrid with a charge sustaining mode.

Finally, a fully integrated energy management strategy was implemented in collaboration with the University of Tennessee. The control strategy was developed in simulation and then transferred to the hardware controller. Two different types of plug-in hybrid operations were demonstrated with this control. The first was an electric vehicle capable plug-in hybrid using an 'engine optimum' control strategy. This strategy has the best fuel economy results but the highest emissions. The second strategy was a blended plug-in hybrid using a 'load following strategy'. The strategy still improved the fuel

economy over the conventional vehicle, but with emissions results that were better than with the 'engine optimum' strategy. For both strategies, the full charge test data was presented and analyzed rigorously.

In conclusion, the hardware and software on MATT enables it to be an extremely flexible tool that provides in-depth data on the vehicle system level as well as component performance within the vehicle system environment. The open controller approach makes MATT unique, since it gives the researcher the ability to program numerous different hybrid behaviors. The remainder of the chapters in this dissertation is dedicated to a sample set of particular studies and investigations that were enabled by using MATT as a vehicle system research tool.

8. Special PHEV studies

This chapter is dedicated to the most important research studies that would not have been possible without a tool like MATT.

8.1. Cold start correction factor for highway cycles for maximum depletion plug-in hybrids for the PHEV test procedures development

This study used the manual transmission module.

8.1.1. Background and approach

Plug-in hybrids are tested by completing consecutive drive cycles. The first cycle is started with a full battery state of charge. Then, the same cycle is repeated until a charge balanced drive cycle is completed. The fuel economies from these charge depleting and charge sustaining drive cycles are then weighted using U.S. driving statistics and averaged together to obtain a weighted average fuel economy which is representative of what consumers can expect. The SAE J1711 hybrid test procedure proposes to use a utility factor derived from U.S. driving statistics to weigh the individual cycle results, thus the computed fuel economy is referred to as the utility factor weight fuel economy.

For a plug-in hybrid vehicle in a full charge test, all of the energy usage needs to be accounted for and thus, the first highway needs to be considered. The cold start induces extra losses from the engine and the rest of the driveline, as shown in Figure 7-30. For the UDDS, these extra losses are consistent with the conventional vehicle test procedure where cold and hot starts are weighted together. But for the highway cycle, there is not a cold start comparison from the conventional vehicle. Typically, for certification purposes, the highway test cycle for conventional or charge sustaining hybrid vehicles requires completing 2 consecutive highway cycles. The first cycle serves as a warm up and, for hybrid vehicles, to pre-condition the initial state-of-charge of the battery to ensure a second highway is charge sustaining, as described in section 5.6.

CARB (California Air Resource Board) proposed utilizing a correction method using the fuel consumption of a cold start highway test cycle in charge sustaining (low SOC) to correct the first full charge highway cycle. This method does work for a blended PHEV where the engine runs most of the time, but in the case of a maximum depletion PHEV, it may not work. MATT was used to generate data for that case.

8.1.2. Test procedure and results

For this investigation, the hybrid strategy is designed in such a way that the engine operation is limited during the charge depletion portion. The engine only supplies the extra power that the motor cannot provide to make the trace. The engine is even less loaded than it is on the load following hybrid. In charge sustaining mode, the engine optimum strategy is applied. This provides a maximum depletion for a blended almost EV capable PHEV. The energy management and torque split strategy used for this study is detailed in section 7.6.

Full charge cold start test set

The first test is the full charge cold start test set. Figure 8-1 shows some data from the four highway cycles. The first and second highway cycles are the charge depletion tests. The third highway cycle is the transition cycle to charge sustaining, followed by the charge sustaining test. The engine temperature barely rises during the charge depleting cycle. In order to eliminate any soak time impact on cooling between tests, all the cycles are completed in one test. The software robotic driver saves a human driver the exhausting task of driving a trace for 50 minutes.
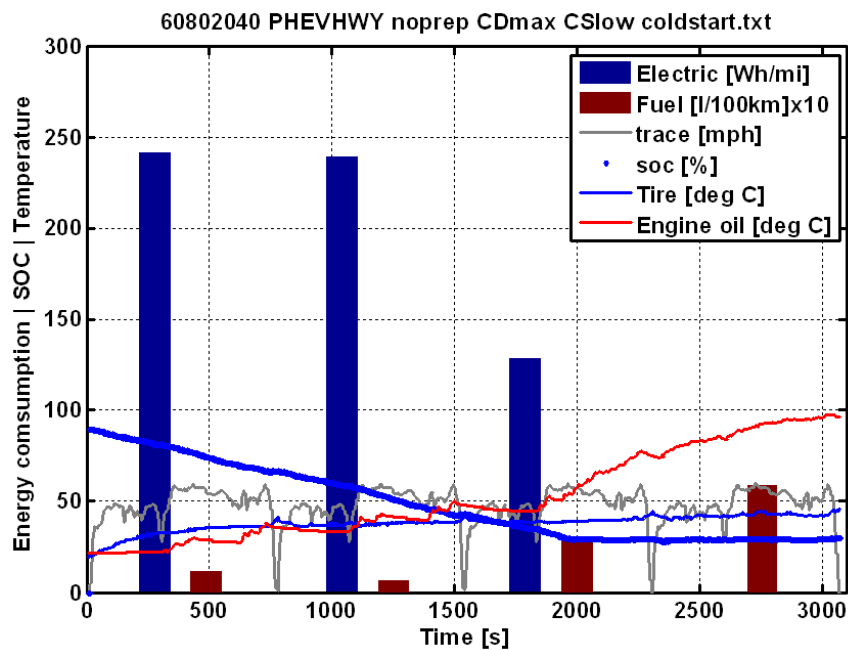
Figure 8-1: Full charge cold start test for maximum charge depletion test

Figure 8-2 summarizes the test set in the energy and fuel consumption plot. The first test, which is the cold start test, does not align with the rest of the tests because of component and engine inefficiencies. Also shown on the graph are the two proposed calculated fuel consumption based utility factor calculations. These calculated fuel

consumptions are slightly off of the average efficiency line. The cold start correction attempts to fix that problem.
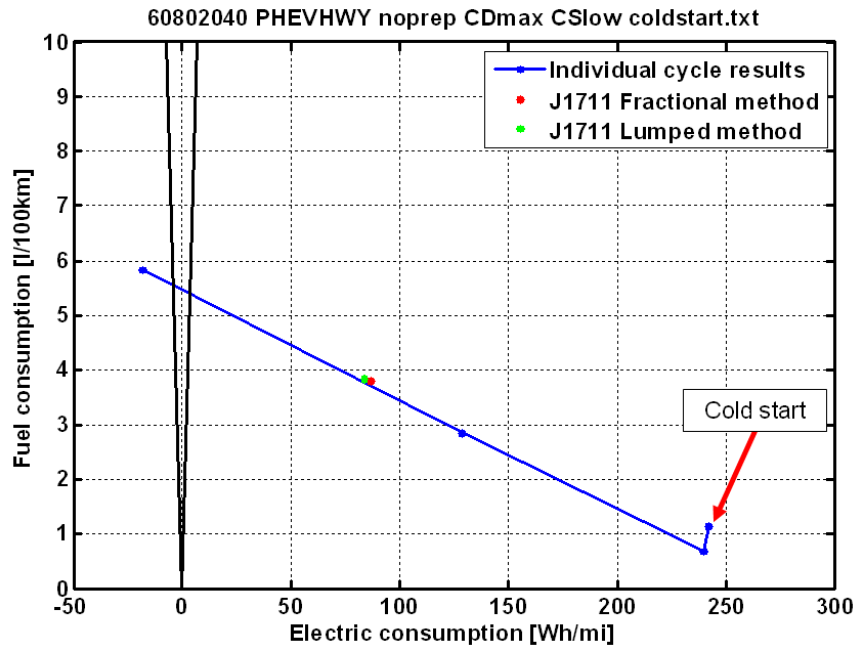
Figure 8-2: Energy and fuel consumption summary for the full charge cold start test

In order to correct the cold start fuel consumption, less than 0.5 l/100 km correction needs to be applied. Additional information on the baseline test is given in Table 8-1. Note that during the charge depletion, the engine is used very little and the average efficiency is low. This is due to the lower loads applied to achieve maximum charge depletion.

Table 8-1: Full charge cold start test for maximum charge depletion PHEV

Cycle #	Fuel consumption [l/100km]	Electric consumption [Wh/mi]	Engine ON time [%]	Engine efficiency [%]
Highway 1 (cold start)	1.14	242	12.0	20.3
Highway 2	0.68	239	9.1	24.1
Highway 3	2.8	128	23.4	30.7
Highway 4 (hot test)	5.3	-18	47.1	31.7

Charge sustaining cold start test (Low SOC)

The second test set is the charge sustaining cold start test. In this case, the initial state of charge of the batteries is 30%, which is the charge sustaining target SOC. Figure

8-3 and Figure 8-4 summarize the cold start test results. Note that the operating temperature of the engine is only reached after the third test.
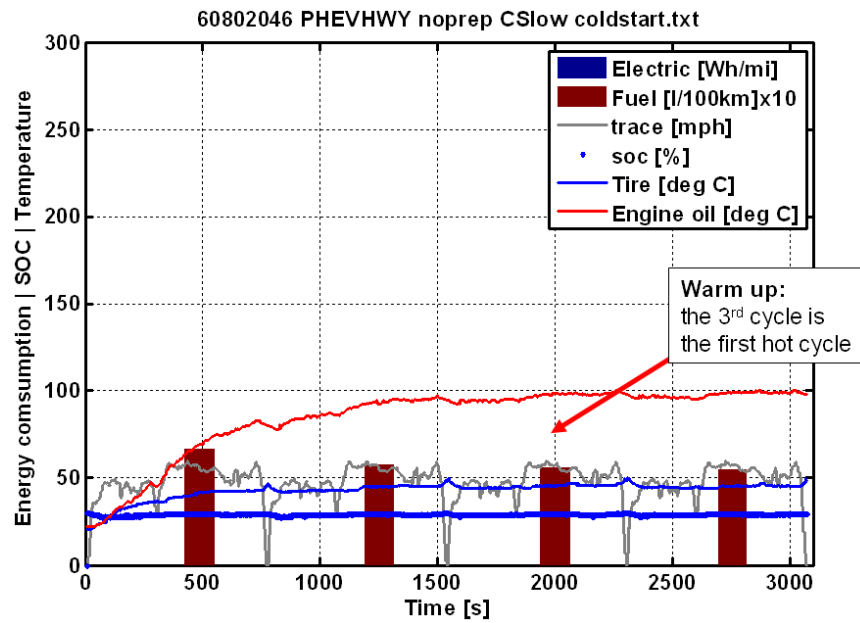
Figure 8-3: Charge sustaining cold start test summary
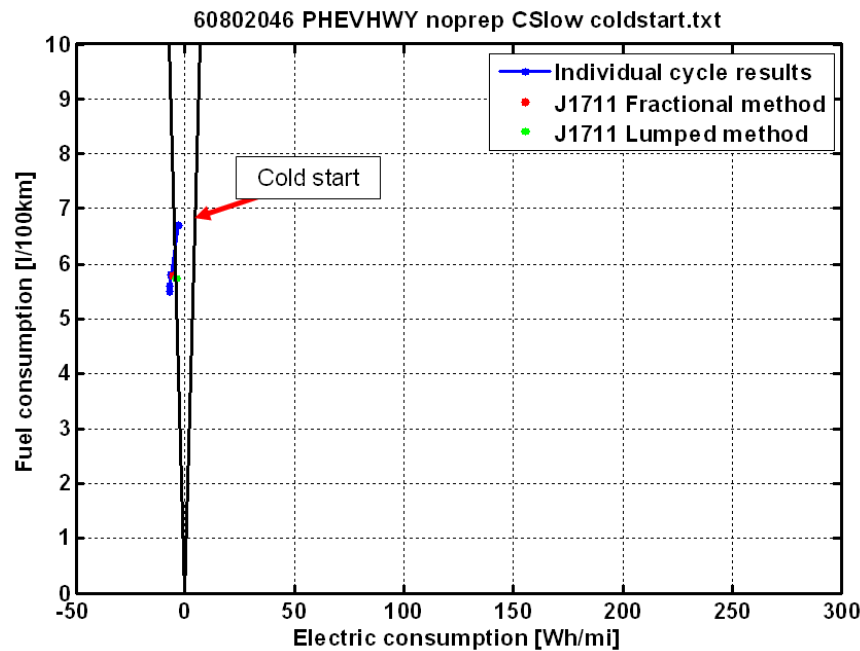
Figure 8-4: Energy and fuel consumption summary for charge sustaining cold start test

In this case, operating as a charge sustaining hybrid, the second highway cycle is still a transient cycle. As expected, the first cycle consumes more fuel (6.71 l/100lm) than the second cycle (5.81 l/1000km), as shown in Table 8-2.

Table 8-2: Charge sustaining cold start test for maximum charge depletion PHEV

Cycle #	Fuel consumption [l/100lm]	Engine ON time [%]	Engine efficiency [%]
Highway 1 (cold start)	6.71	53.3	29.2
Highway 2	5.81	48.6	32.2
Highway 3	5.59	47.6	32.7
Highway 4 (hot test)	5.51	44.1	31.9

8.1.3. Outcome: Proposed method over corrects

From the data in Table 8-2, the correction factor applied to the first cold start cycle on the full charge test is 0.9 l/100km. That correction factor overestimates the fuel compensation, which was estimated at less than 0.5 l/100km.

This is explained by the different "engine on" times for the charge depletion cycles and the charge sustaining cycles. On the cold start charge depletion, the engine was on for 53% of the time at an average efficiency of 29.2% in the engine optimum hybrid strategy. During the charge sustaining cold start cycle, which is providing the correction factor, the engine is used 4 times more at much higher loads. That explains the overestimates in this particular extreme charge depletion blended plug-in hybrid case. The test procedures need to apply to all cases and thus this correction method is not appropriate.

The overestimation is shown in Figure 8-5.

60802040 PHEVHWY noprep CDmax CSlow coldstart.txt

The correction over estimates the cold start fuel compensational
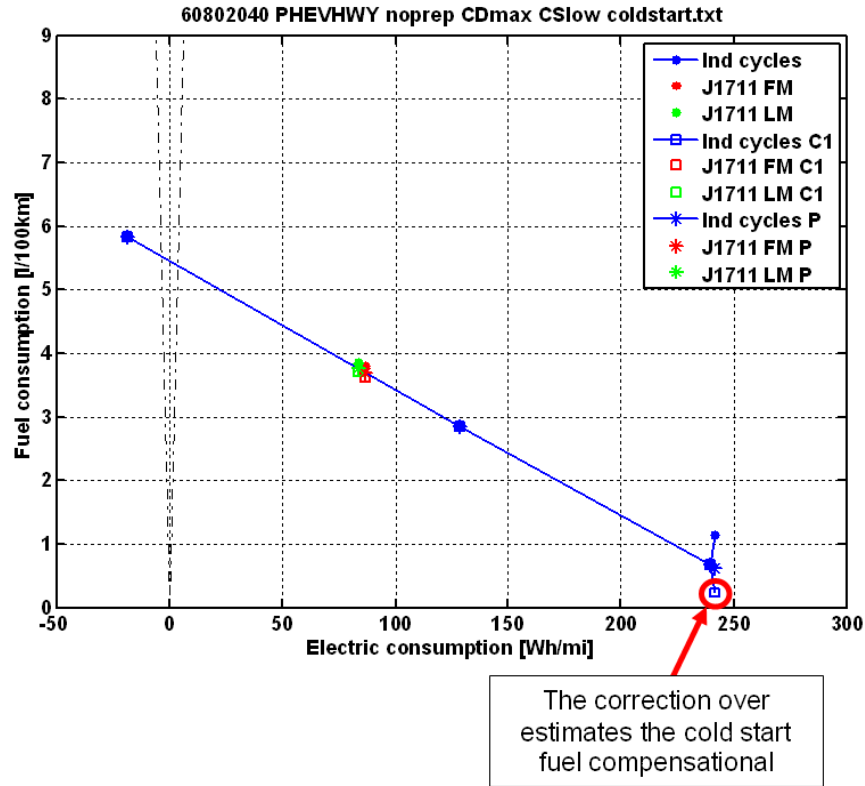
Figure 8-5: Energy and fuel consumption graph showing the proposed cold start correction

8.1.4. An alternate correction method (charge sustaining switch)

If all plug-in hybrids had a charge sustaining switch, then a preparation cycle could be done in a charge sustaining mode to bring the powertrain to operating temperature before starting the full charge test. Since MATT has an open controller, a charge sustaining switch was implemented to test this alternative method. The results for this full charge test set are shown in Figure 8-6.
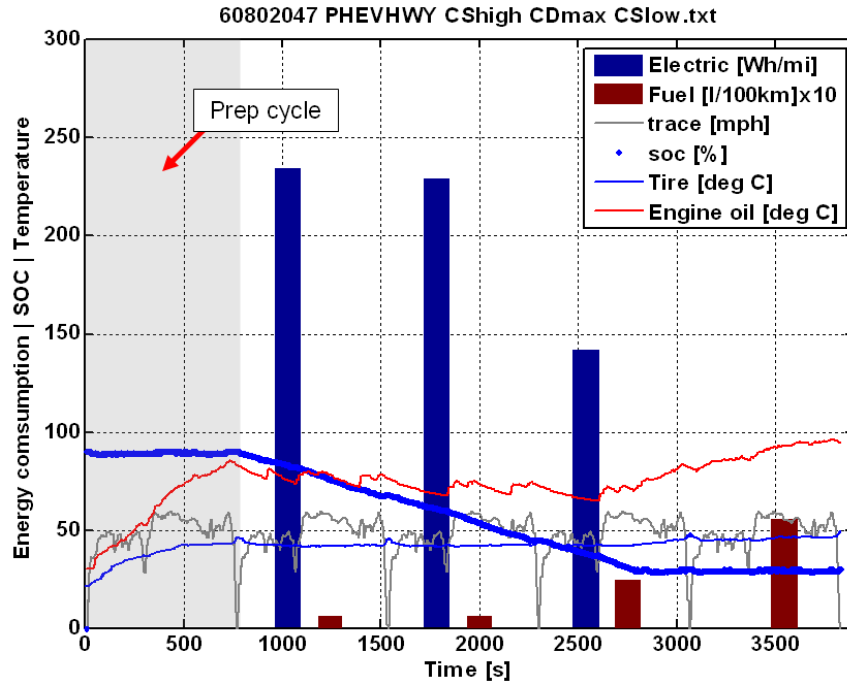
Figure 8-6: Full charge test summary with a prep cycle

The warm up cycle in charge sustaining mode does prevent the cold start offset of the first cycle, as shown in Figure 8-7.
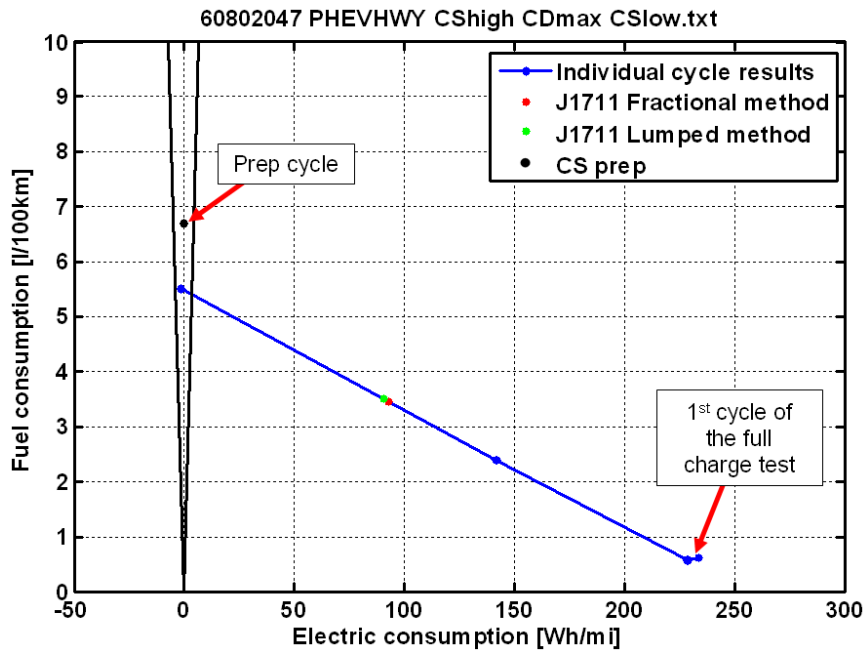
Figure 8-7: Energy and fuel consumption summary for the full charge test with prep cycle

184

8.1.5. Conclusion

When deciding on the highway cycle cold start correction \issue, this study was the first highway data set available to the CARB and the J1711 committee for a maximum depletion blended type hybrid. The test results helped in changing proposed cold start correction methods. MATT's open controller feature was used for this test to obtain information about an unusual hybrid behavior to help investigate the specific issue. As a direct result of the study, the proposed and much discussed correction method was abandoned. Note that simulation could not complete this study since the cold start fuel consumption requires very complex models. Also the emissions are measured.

A senior test engineer working on the test procedures had the following comment regarding the data and analysis provided:

> "Argonne's test data and experience has been instrumental in helping ARB staff make key decisions in our PHEV test procedures for California's ZEV Regulation. In many cases, they had the only data in existence that supported the development"

> Jeffrey Wong, Senior Test Engineer, California Air Resources Board, El Monte, CA

8.2. Soak time sensitivity study for PHEV's

8.2.1. Background and approach

As seen in some earlier PHEV tests, the temperature of the powertrain components have an impact on energy consumption, especially on the engine and exhaust after treatment system. The engine operating temperature in charge depleting operation is always low compared to that of a conventional vehicle. The first engine start seems to dictate the emission for the cycle.

The test procedure to characterize plug-in hybrids is a consecutive set of drive cycles. The first drive cycle is started with a full state of charge and the tests are repeated until the first cycle is achieved. The time between the individual tests is used to reset the equipment, including the emissions bench, the bags and the data acquisition system. At the ARPF, it takes about 10 minutes to recycle the equipment between tests. Other test cells require 20 or 30 minute test frames to reset their equipment. During that time, the vehicle is soaking or cooling down in the temperature conditioned test cell.

This study attempts to determine the impact of the soak time (which is the time from the end of one test to the actual start of the next test) on fuel consumption, energy consumption and emissions.

8.2.2.   Test procedure and results

The test plan is to perform a continuous set of charge depleting urban cycles with varying soak times between the tests. The virtual battery and motor module present a convenient advantage in that they can immediately recharge the battery pack to the same initial SOC. Thus, each test is started with the exact same conditions. The software robotic driver provides the other key component to this study, repeatability. Figure 8-8 illustrates the continuous and uninterrupted test plan and test conditions.
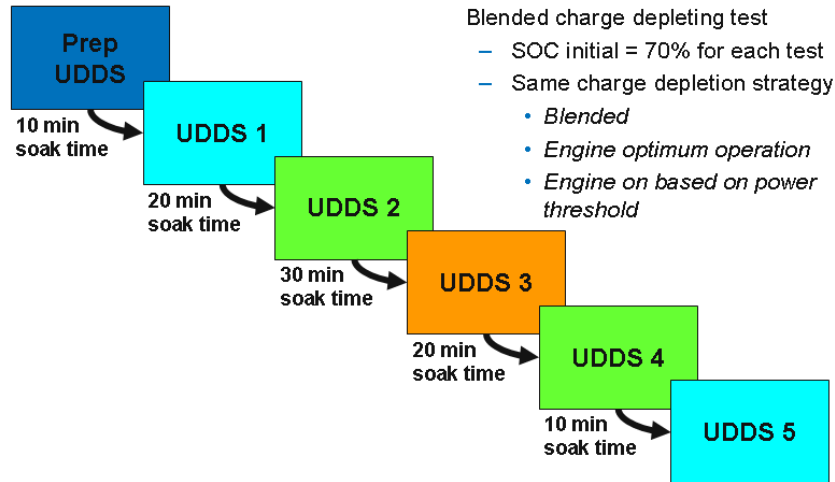
Figure 8-8: Soak time test matrix

Since it is a charge depleting test, the engine usage is low, as shown in Figure 8-9. The major hydrocarbon spike occurs at the first engine start. For the next engine start, the hydrocarbon spikes are low except for the last engine start after 800 seconds of cool down.
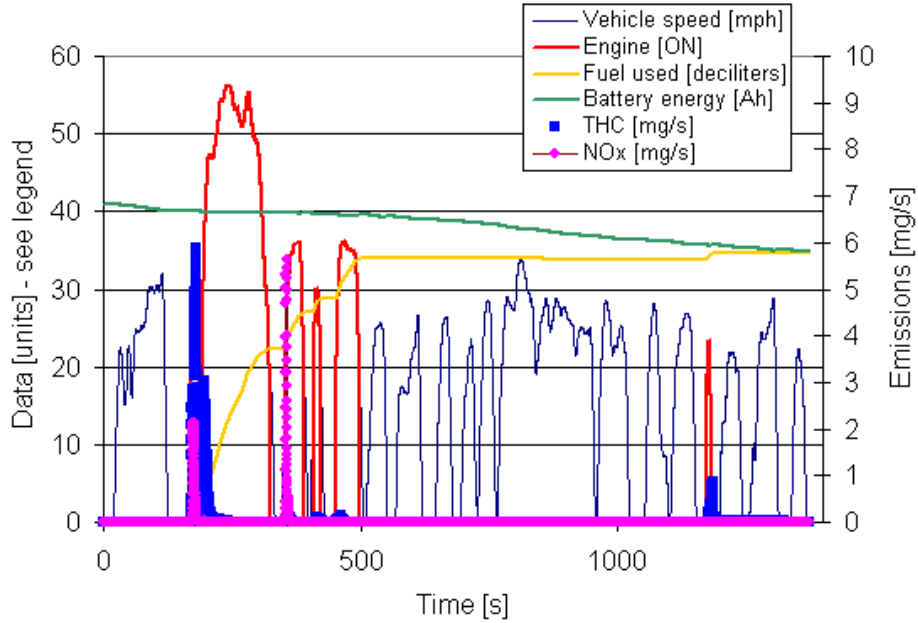
Figure 8-9: Test results for the 1st cycle after 10 min soak

All of the important temperatures for the UDDS 1 are shown in Figure 8-10. The thermostat never opens on these tests, thus the engine coolant heats fast and stays warm in the block. The engine oil never reaches steady operating temperatures either. The most interesting temperature to watch is the catalytic converter's temperature. Light off temperature is between 200 and 300 deg C, thus explaining the first engine start hydrocarbon emissions. At the last engine start, the catalyst temperature drops below 300 degrees again, which may explain the more pronounced hydrocarbon slip.
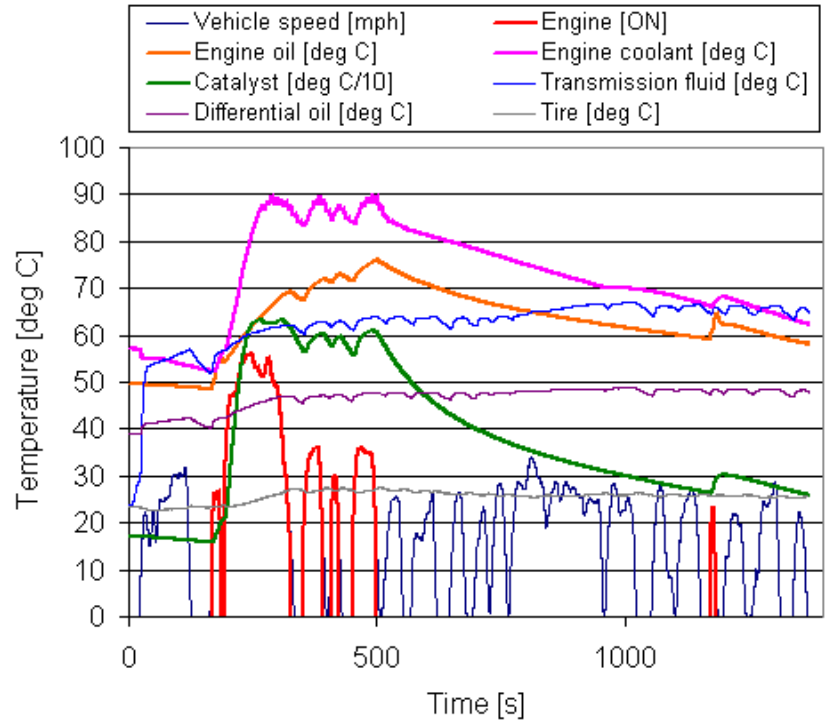
Figure 8-10: Temperature information from the first test after 10 min soak

Some additional interesting information is found in the collection of thermal images taken at different points during soak periods, as shown in Figure 8-11. There is an obvious difference in temperature at the end of the 20 min soak time compared to the temperature at the end of the 10 min soak time. The catalytic converter insulation is very good, since the temperature of the outside of the can is similar immediately after a test and after 10 and 20 minutes.
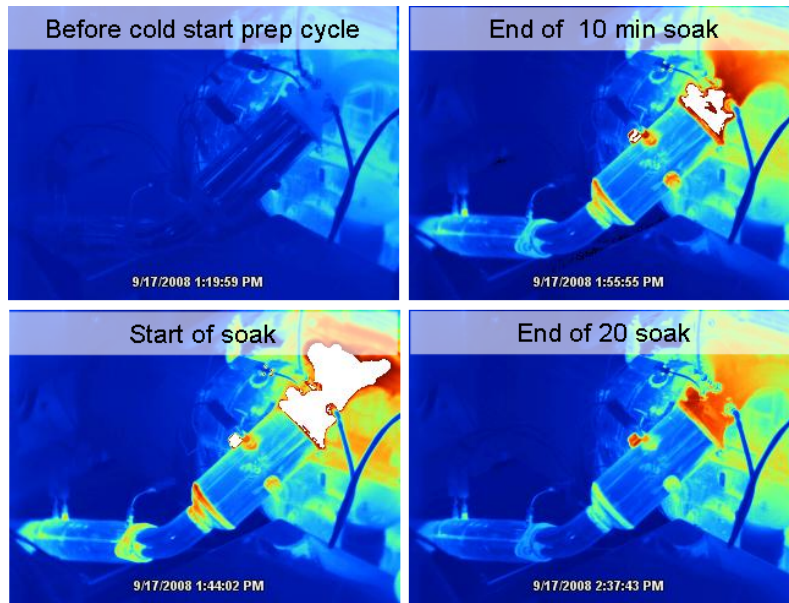
Figure 8-11: Thermal images of the exhaust system on MATT

Of the 6 tests preformed, five of the tests are completely identical in terms of engine operation. The test after the first 20 minute soak period had an extra engine start. Despite the difference, 5 out of 6 is good in terms of repeatability. Figure 8-12 illustrates the repeatability of the test results.
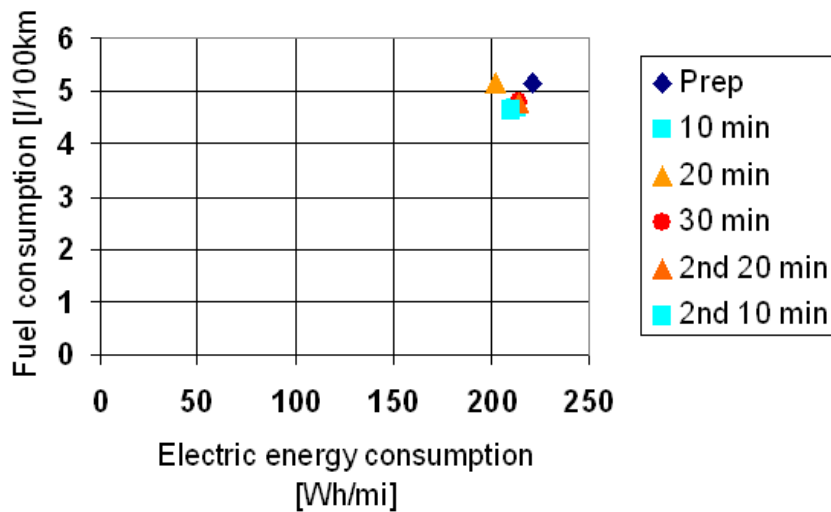
Figure 8-12: Fuel and electric energy summary for the soak time tests

The prep cycle, which was not a cold start, used the most fuel and electric energy, as expected. The 10, 20 and 30 minute soak test results are very close. Setting aside the one 20 minute soak time test with the extra engine start, a pattern is visible. The 10 min soak tests used less energy than the other cycles. The 30 minutes soak time used the most

energy, which is explained by the higher losses in the components due to cooler starting temperatures. It could be concluded that the longer the soak time, the more fuel and electric energy is used, but the difference in the results is not significant or pronounced.

The emissions results are shown in Figure 8-13. The prep cycle has the highest emissions, again, as expected, due to the cooler catalytic converter at the start of the test. After that, all of the tests, with the exception of the one test with the extra engine start, have similar emissions. Thus, it appears that the soak time has no significant impact on the emissions behavior. The number of engine starts seems to correlate with the hydrocarbon emissions level.
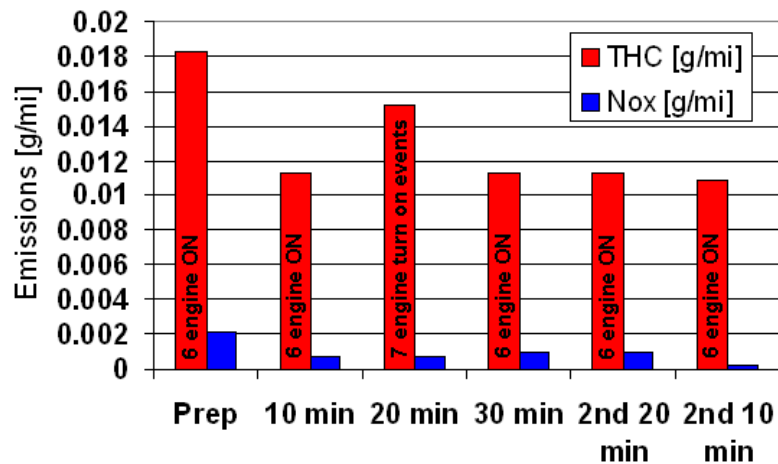
Figure 8-13: Emissions summary for the soak time tests

8.2.3.   Conclusion

The soak time between tests does have an impact on the energy consumption, but the effect is so small that it can be overlooked. Furthermore, different recycle times between tests at vehicle test facilities are an unavoidable fact, and it would be prohibitively expensive to upgrade each test cell. This study provided data to support the test procedure development committee in their decision to allow a wide range of soak times between tests.

This study used MATT's repeatability from test to test as well as the virtual battery pack to guarantee the same initial conditions for each test. Without MATT, this test would have taken several days to complete, since each soak time would have required a full charge test, which would take a full day.

8.3.   Energy consumption sensitivity to drive cycle intensity for a hybrid and an electric capable plug-in hybrid

8.3.1.   Background and approach

The topic of drive cycle intensity is already discussed in section xx for the conventional vehicle. One of the conclusions of the original study on fuel economy sensitivity was that hybrids are more sensitive to drive cycle intensity than conventional vehicles. The topic is further investigated using MATT as a plug-in hybrid in charge depleting mode and charge sustaining mode. Driving intensity is the energy at the wheel required to drive the vehicle at the desired speed and acceleration.

A previous study shows results for a blended plug-in hybrid. All of the conversion plug-in hybrids available for testing today are blended plug-in hybrids based on power split hybrids such as the Toyota Prius. As the drive cycle intensity increases, the fuel consumption increases and at the same time the electric consumption decreases. Therefore, the charge depleting range increases as shown in Figure 8-14. The decreases in electric consumption may appear counter-intuitive at first. As the drive cycle intensity increases, the accelerations become intense, thus the engine will turn on more frequently since the control strategy maintains the same engine ON power threshold. In blended plug hybrids, especially power split hybrids, the engine will also turn ON above a certain speed, but as the drive cycle intensity increases, so does the average speed of the cycle. Therefore, the engine will be ON more often regardless of the increased accelerations. For these reasons, the blended type plug-in hybrid will consume less electricity as the driving intensity increases. For the consumer, this translates into less petroleum displacement (or savings at the pump) as the vehicle is driven more aggressively. Remember that the UDDS is too mild to represent today's driving pattern in the US.
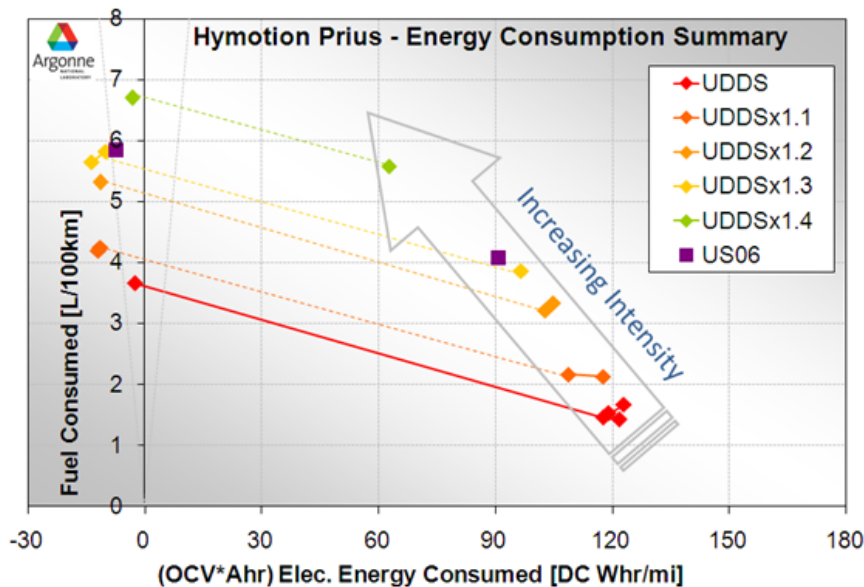
Figure 8-14: Response of a blended type plug-in hybrid to drive cycle intensity (time and speed scaled)

This study is the logical progression of the drive cycle intensity investigation, which is meant to evaluate the response of an electric vehicle capable plug-in hybrid. At this point, MATT is the means to research this part of the design space.

8.3.2.　　　　Test procedure and results

The test plan is to evaluate MATT as an electric capable plug-in hybrid on time and speed scaled UDDS cycles in charge depleting mode as well as in charge sustaining mode. The scaling factors for this drive cycle intensity test are 1.1, 1.2, 1.3 and 1.4. At each drive cycle intensity level, a charge depleting test is performed with 70% as the initial state of charge. Two charge sustaining cycles are completed with the first test using the target SOC of 30% as a starting point. The test set is performed with the automatic transmission module. The shift schedules used for these tests were derived from simulation. The torque split strategy is an 'engine optimum' control when the engine is ON during the charge depleting test and the charge sustaining test. All of the tests are preformed as hot starts.

The results are presented in Figure 8-15. The trend for the electric capable plug-in hybrid for drive cycle intensity is different than for the blended plug-in hybrid. As drive cycle intensity increases, the electric consumption and the fuel consumption increase. The largest energy consumption increase is attributed to the electric consumption. This is explained by the fact that the engine turn ON point is independent of speed in an electric capable plug-in hybrid. The improved fuel economy is explained by the engine ON trigger through the increased power demand from the driver, but the same engine ON power threshold in the control strategy remains constant.
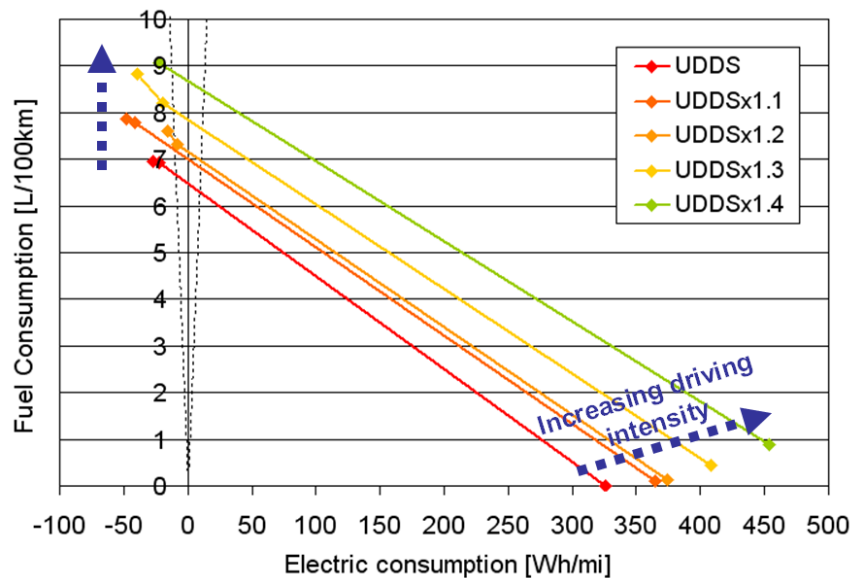
Figure 8-15: Response of an electric capable plug-in hybrid to drive cycle intensity (time and speed scaled)

To bring this back to the consumer, an electric capable plug-in hybrid such as the GM Volt uses more electricity as the driving increases in speed or aggressiveness. Thus, the petroleum displacement and the financial savings at the fuel pump are maintained with an electric capable plug-in hybrid.

8.3.3. Conventional, hybrid and plug-in hybrid drive cycle intensity summary

Now all of the drive cycle intensity tests can be summarized, as shown in Figure 8-16. The plug-in hybrid results are utility factor weighted results using the SAE J1711 recommended procedures. The hybrid electric vehicle fuel economy numbers are charge balanced. The conventional vehicle fuel economy results are based on hot start test cycles as are all of the other test results.
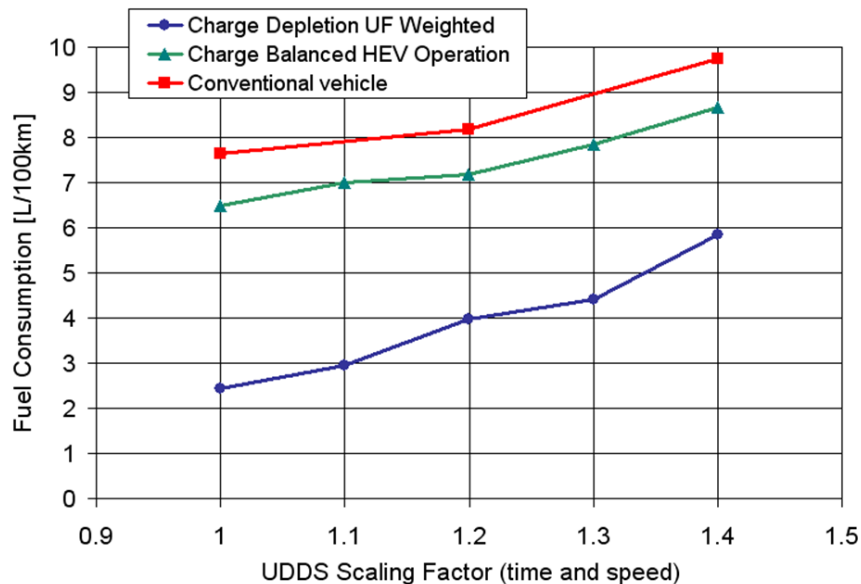
Figure 8-16: Summary of the drive cycle intensity results for the convention vehicle, charge sustaining hybrid and charge depleting plug-in hybrid vehicle

First note that the slope of the charge depleting plug-in hybrid is steepest, which means this vehicle operating mode is the most sensitive to driving intensity. The vertical difference between lines on the graph represents the petroleum displacement between the conventional vehicle, the hybrid and the plug-in hybrid. The petroleum savings between the conventional vehicle and the charge sustaining hybrid is fairly constant at about 10% as drive cycle intensity increases. The petroleum displacement between the charge balanced and the plug-in hybrid is between 30% and 60% as driving intensity increases. This shows why plug-in hybrid vehicles are so attractive to solve the oil addiction in the US and globally.

193

8.3.4. Conclusion

This investigation completed the existing plug-in hybrid energy consumption sensitivity to drive cycle intensity research by testing an emulated electric capable plug-in hybrid on these drives cycles. This study showed that the impact of driving intensity on energy consumption differs with the vehicle's degree of hybridization. The results showed that as drive cycle intensity increases, so does the electric consumption. The opposite is true for the blended type plug-in hybrids. Therefore, with electric capable plug-in hybrids, the petroleum displacement benefits are maintained or increased as driving aggressiveness increases. This is not the case for blended plug-in hybrid vehicles.

The study would have not been possible without MATT's ability to emulate an electric capable plug-in hybrid. Within this study, MATT completed all of the drive cycle intensity work, including the conventional vehicle, the hybrid and the plug-in hybrid emulations. Only a tool like MATT could provide test data on this type of topic for all of the different vehicle types using the same hardware and software basis.

8.4. PHEV emissions mitigation investigation

8.4.1. Background and approach

Plug-in hybrids present a new challenge for the engine and emissions control, as shown in Figure 2-5. Since a plug-in hybrid can operate for an extended period of time without using the engine, the exhaust after-treatment system will take much longer to reach normal operating temperature or the catalytic converter may even cool down enough between engine usages to cause a second 'cold start'. The emissions problem may be compounded by the aggressive use of the engine in some plug-in hybrid strategies.

This investigation intends to quantify the impact of aggressive engine usage in plug-in hybrid modes on emissions and energy consumption. In a second stage, hybrid control will be used to reduce the emissions. The conventional vehicle results will be presented briefly as a baseline. The actual study is centered on two different types of plug-in hybrid vehicles:

- Electric vehicle capable plug-in hybrid with an 'engine optimum' torque split strategy

- Blended plug-in hybrid with a 'load following' torque split strategy

The automatic transmission module is used for this application. The energy management strategy used is described in section 7.8. This work was completed in collaboration with the University of Tennessee.

The project was divided into two phases. The first phase involved developing the energy management and torque split control strategy in simulation and implementing it on MATT. The initial transfer and debugging of the control strategy took a couple of days. The version conflicts between Matlab© used for simulation and hardware control used half of the time. The second half was used in debugging the control strategy. Most

of the issues were related to signal noise and offsets. In simulation, all of the signals are 'ideal'. For example, a zero vehicle speed is a true zero speed in simulation. In hardware, the measured signal suffers from typical signal level noise and offsets. Even with signal processing in hardware and software, a zero vehicle speed will never be a computer zero. Once these issues were debugged, the transfer from simulation to hardware was reduced to several minutes only. All of the control changes were implemented in simulation first and then implemented on the hardware controller. Once the initial code was ready, the baseline tests were completed in the ARPF. A cold start full charge test was completed and recorded for each hybrid vehicle type. These tests were then used as plug-in hybrid emissions baselines to understand the source of the emissions from a control perspective.

The second phase started with developing emissions mitigation routines, such as engine warm up strategies and ramping the engine load. Then, a new set of cold start full charge tests were completed and recorded. The emissions and energy consumption of Phase 1 and Phase 2 were then compared. Figure 8-17 illustrates the investigation's approach.
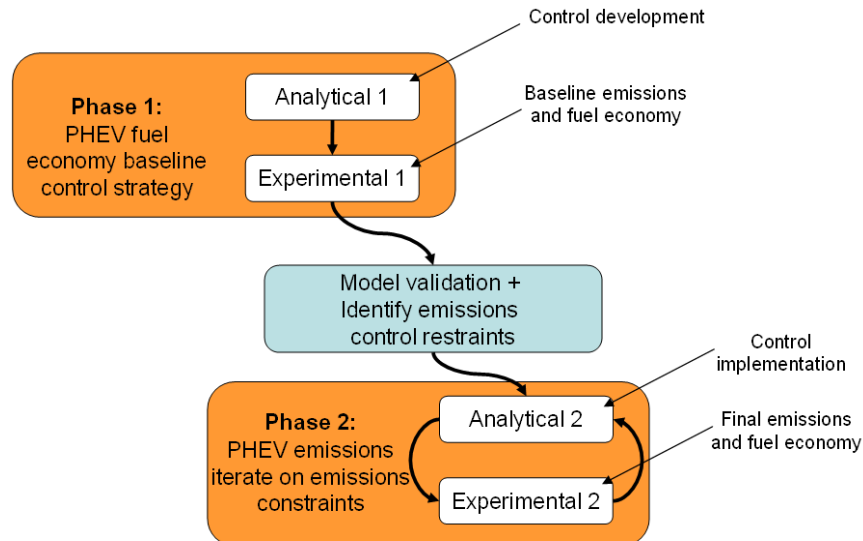
Figure 8-17: PHEV emissions study work flow

8.4.2. Results for phase 1

Conventional vehicle baseline

Phase 1 was performed in September of 2008. First, a conventional vehicle baseline test was completed. Figure 8-18 shows the cold start UDDS in conventional vehicle mode followed by a hot start UDDS, which was then repeated for plug-in testing. The engine is always on in the conventional mode. The engine temperature reaches operating temperature and the battery energy is never used. The engine temperature drop is due to the 10 minute soak time required to reset the emissions equipment.
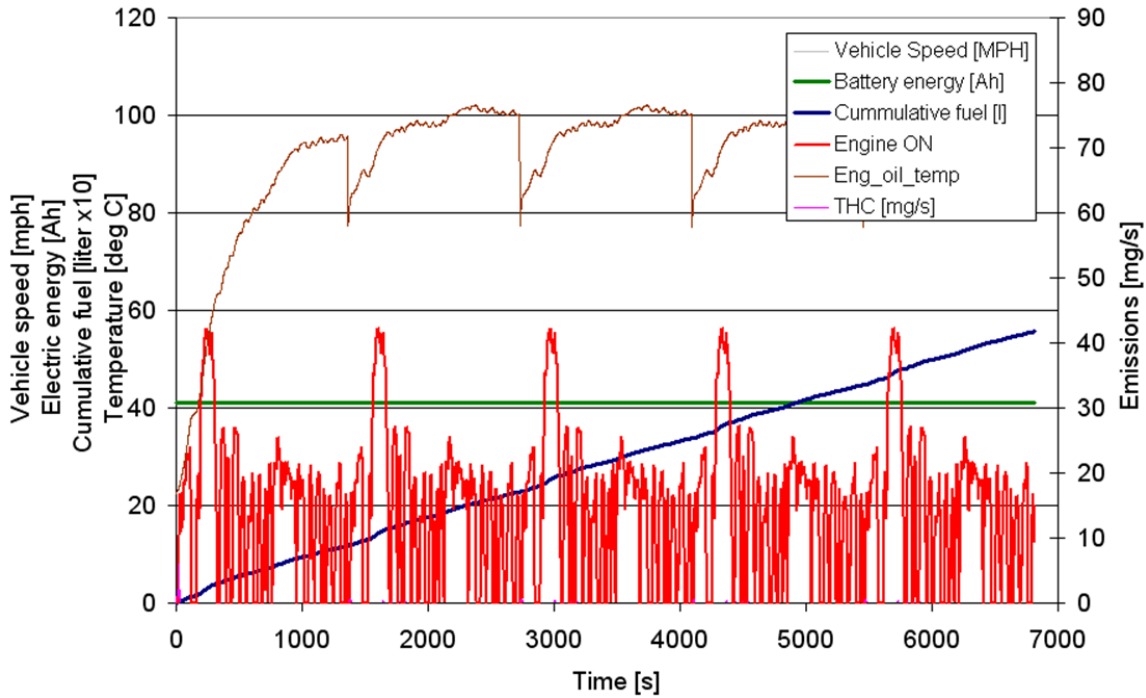
Figure 8-18: Conventional vehicle test results in consecutive UDDS cycles

Figure 8-19 shows the emissions and engine operating range data for the conventional vehicle mode for the cold start test. On the cold start test, the majority of the emissions are generated in the first 30 seconds of the test during the first acceleration. Once the catalytic converter reaches light off temperature, the emissions production is close to zero. The catalytic converter temperature stays constant and high throughout the test. The fuel energy plot shows a wide range of operation for the engine as well as the fuel used on engine idle.
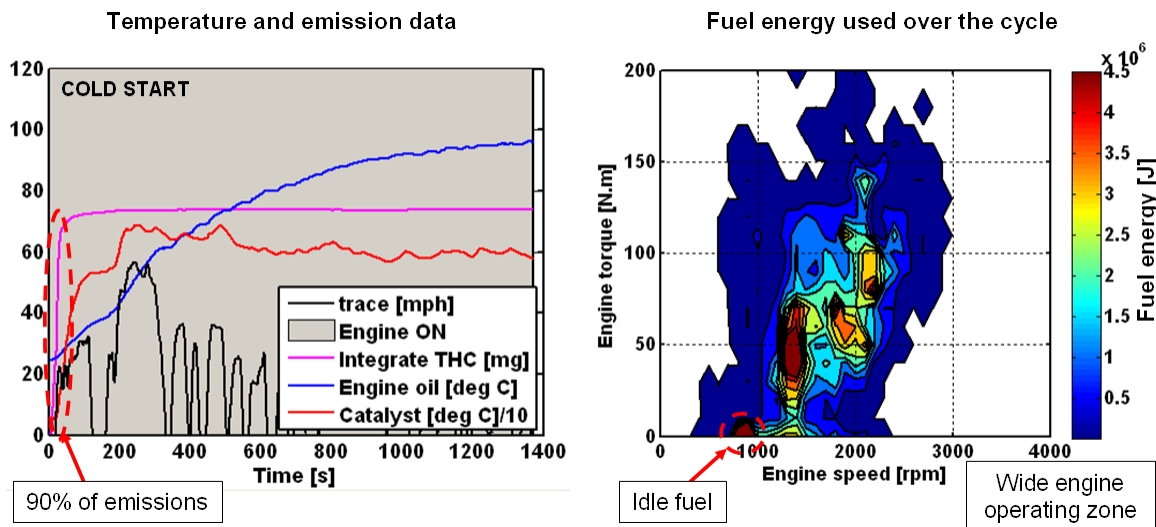
Figure 8-19: Conventional vehicle cold start test summary

Figure 8-20 shows the second cycle, which is the hot start cycle. The emission level is cut by a factor of five. The catalytic converter temperature starts almost at light off temperature. The engine is also almost at operating temperature at the start of the test. The engine operating range is the same on the hot start test as it is on the cold start test.
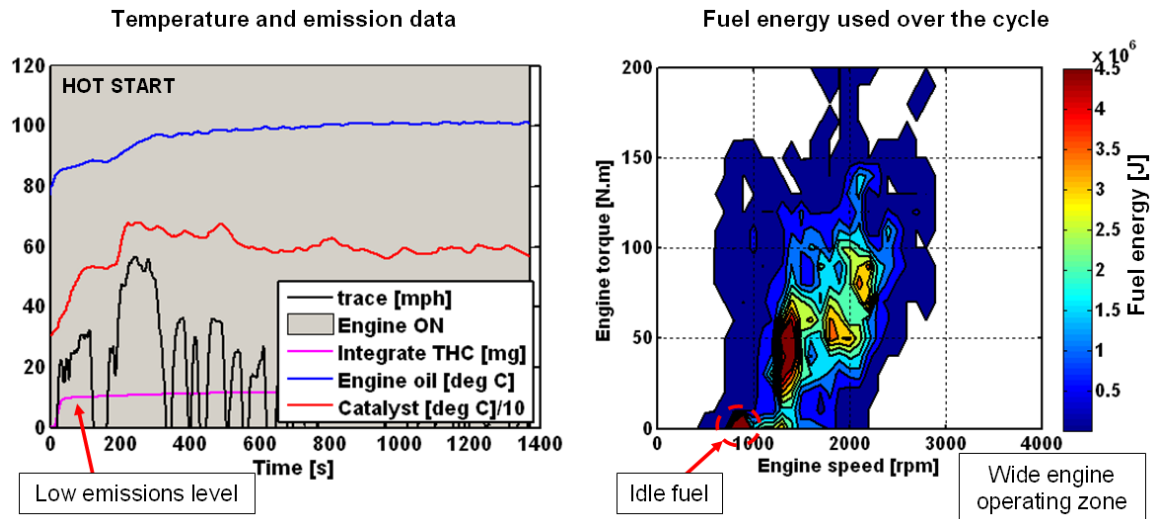
Figure 8-20: Conventional vehicle hot start test summary

Electric vehicle capable plug-in hybrid

The first plug-in hybrid test is the electric vehicle capable test. Figure 8-21 shows the full charge test results. The first two UDDS cycle are the charge depleting cycles completed in the electric vehicle mode. The third cycle is the transition cycle. The engine turns ON for the first time on Hill 2 at higher speeds. Toward the end of the third cycle, the charge sustaining phase starts, based on the battery energy usage. The engine temperature warm up starts on the fourth cycle. The engine does cool off during the longer OFF phases. The engine OFF phases are long, even during the charge balanced cycles. The engine never reaches the operating temperature for the conventional vehicle. It is always 20 degree C below the conventional in the 'engine optimum' control mode.

197
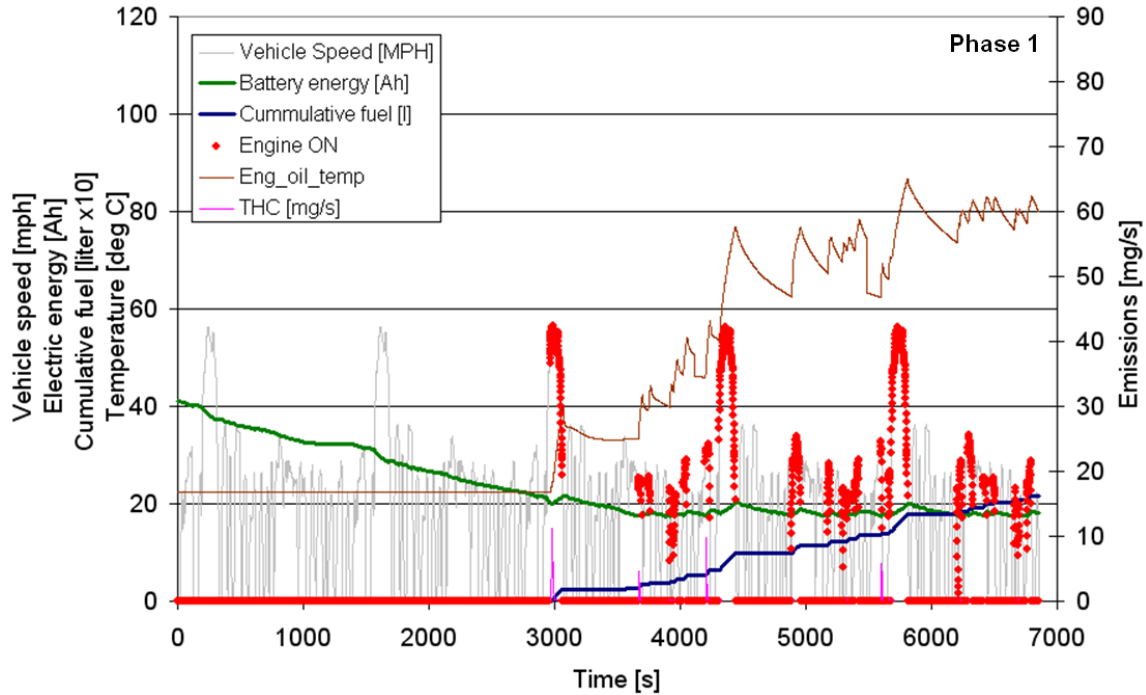
Figure 8-21: Phase 1 full charge test results for the electric vehicle capable plug-in hybrid with 'engine optimum' control

Figure 8-22 shows the emissions and engine operating range of the first engine cold start test, which is the third UDDS cycle in the full charge test. Note that the emissions scale changed from 120 in the conventional vehicle graph to 200 in this graph. The majority of the emissions are still generated on the first engine start. This is a cold start and the engine is immediately loaded to 150 N.m. The second start still produces a large emissions spike. The engine operation is now only in the high load area. Figure 8-23 shows the emissions and engine operating range for the hot start charge sustaining test, which is the 5th UDDS cycle in the full charge test. Even though the engine is still warm from the previous test, the first engine start produces a large emissions spike, which is due to the high load that is directly applied to the engine. The catalytic converter cools off significantly during some of the engine OFF phases, even on this charge sustaining test cycle. The engine operation is the same as it is on the cold start test, except that more engine fuel energy was used compared to the cold start charge depleting test.
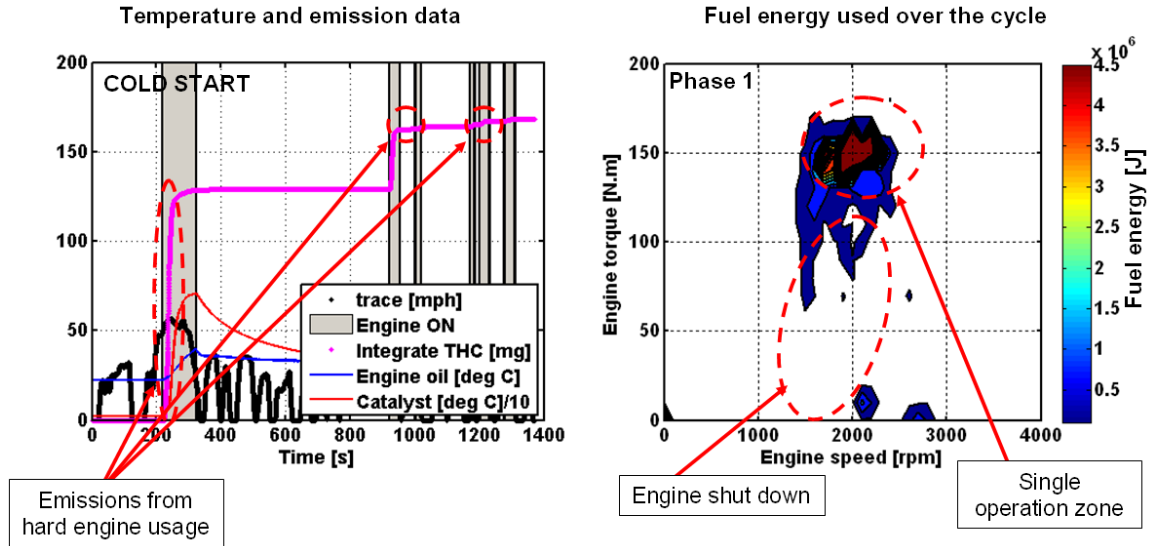
Figure 8-22: Phase 1 cold start cycle summary for the electric vehicle capable plug-in hybrid with 'engine optimum' control
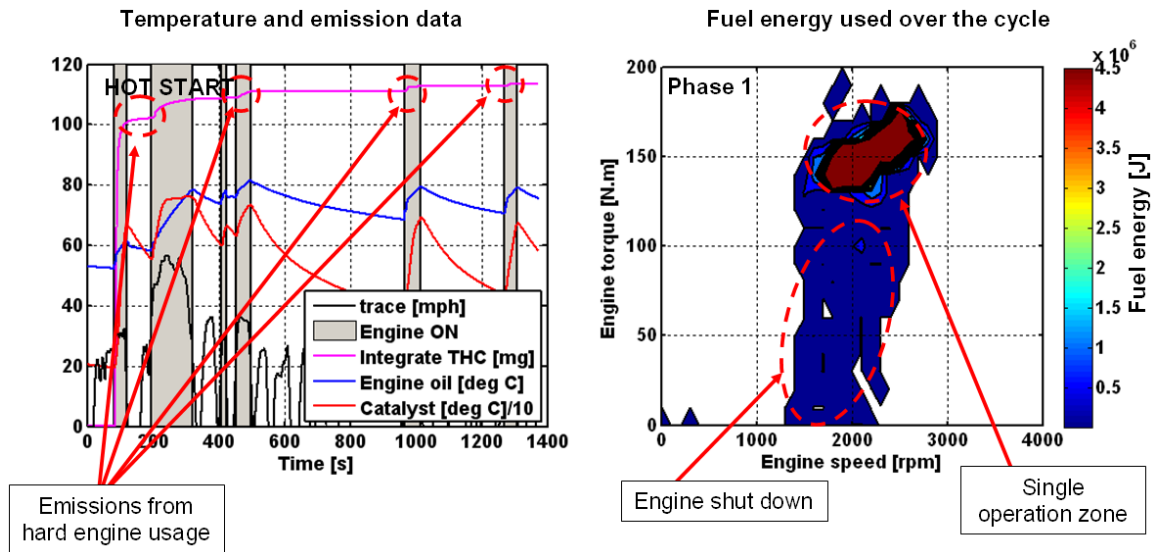
Figure 8-23: Phase 1 charge sustaining hot start cycle summary for the electric vehicle capable plug-in hybrid with 'engine optimum' control

Blended plug-in hybrid

The second plug-in hybrid test is the blended plug-in hybrid vehicle test. The blended plug-in hybrid's full charge test results are shown in Figure 8-24. In this case, the engine is used on the first UDDS cycle. During the charge depleting phase, the engine only turns ON five times during the cycle, which means extended engine OFF periods. Nevertheless, over the three first charge depleting cycles, the engine temperature does rise slowly. On the charge sustaining phase, the engine reaches an operating temperature close to that of the conventional vehicle operation. The engine OFF time on the charge

sustaining cycle is fairly short compare to the prolonged engine OFF period for the 'engine optimum' charge sustaining cycle. The first three cycles are charge depleting, compared to only the first two cycles for the electric vehicle capable plug-in hybrid. Once the charge sustaining phase is reached in the blended plug-in hybrid test, the battery energy usage of the 'load following' strategy is much 'flatter' compared to the 'engine optimum' control. The 'load following' strategy does not work the battery as hard as the 'engine optimum' strategy.
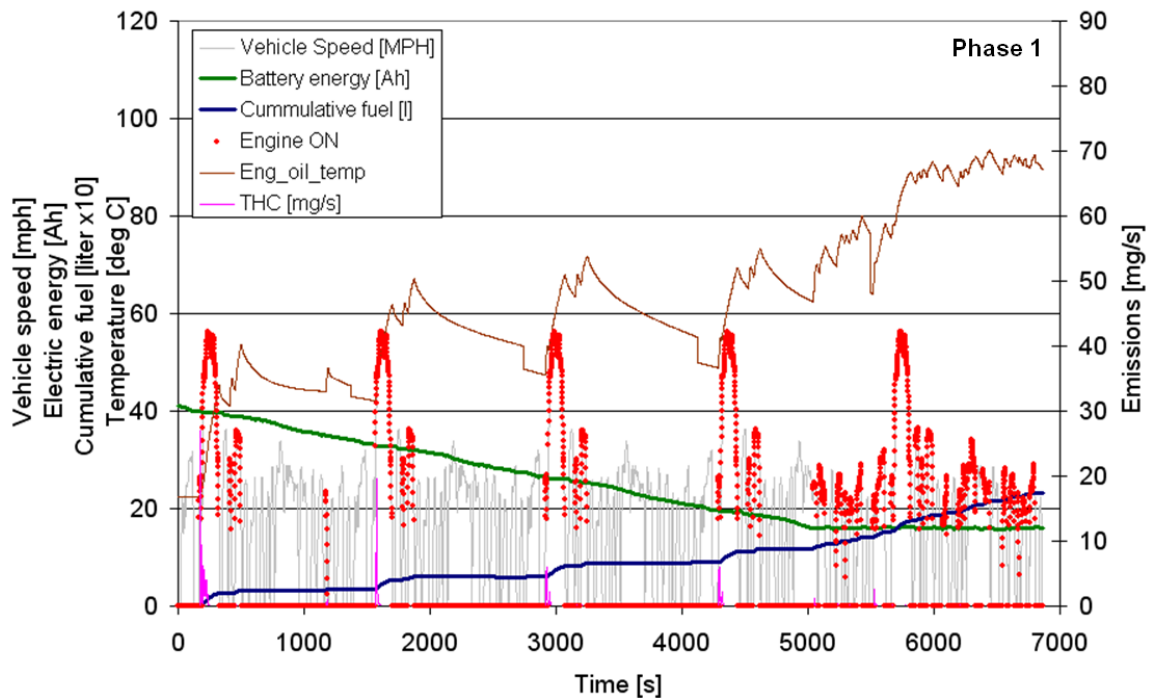
Figure 8-24: Phase 1 full charge test results for the blended plug-in hybrid with 'load following' control
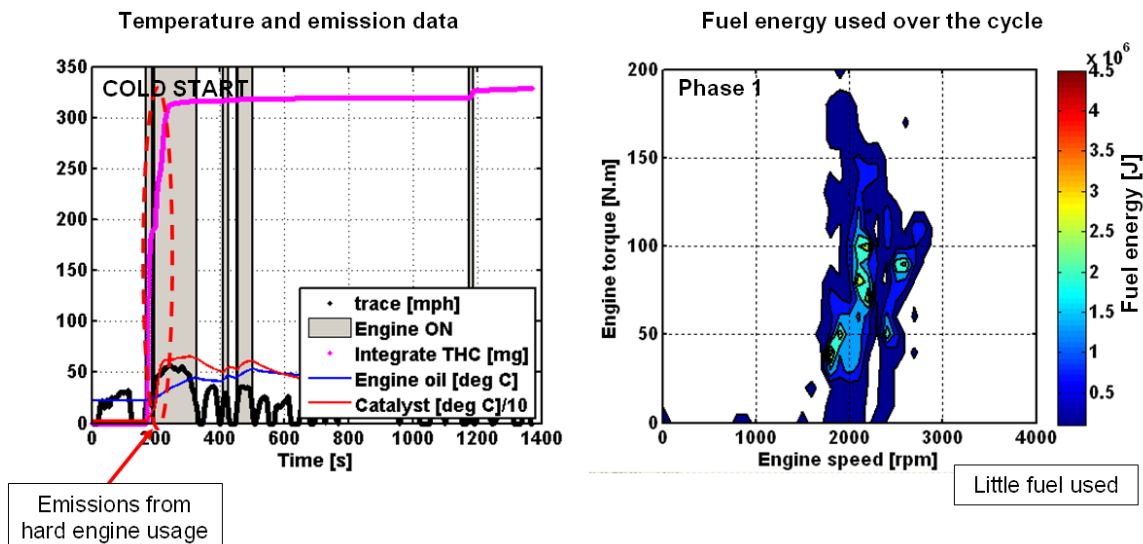
Figure 8-25 summarizes the emissions and engine operating range of the first cold start test of the blended plug hybrid. This is also the first UDDS cycle of the full charge test. Note the emissions scale changed from 120 in the conventional vehicle graph to 350 in this graph. The engine only turned ON 5 times in the charge depleting test. The first engine start caused the majority of the emissions of the test. The engine actually did not start immediately, which caused the large emissions spike. The following engine starts produce only small emissions spikes, which is explained by low engine loads in this 'load following' control strategy. The engine operating range is wide in the load range, but overall, only a small amount of fuel energy is used compared to what is used in the conventional vehicle operation, which is normal in this charge depleting test. Figure 8-26 summarizes the emissions and engine operating range of the charge sustaining cycle, which is the 5th and last UDDS in the full charge test. The engine turns on frequently throughout the cycle, but the total emissions produced are very low. The engine and catalytic converter temperature are close to operating temperature and fairly constant. The engine operating range is quite wide but the average engine load is higher than the conventional vehicle's. The engine idle fuel island of the conventional vehicle has also been eliminated by the hybrid operation. To total fuel energy consumed is higher than in the charge depleting test, which is expected for this charge sustaining test.
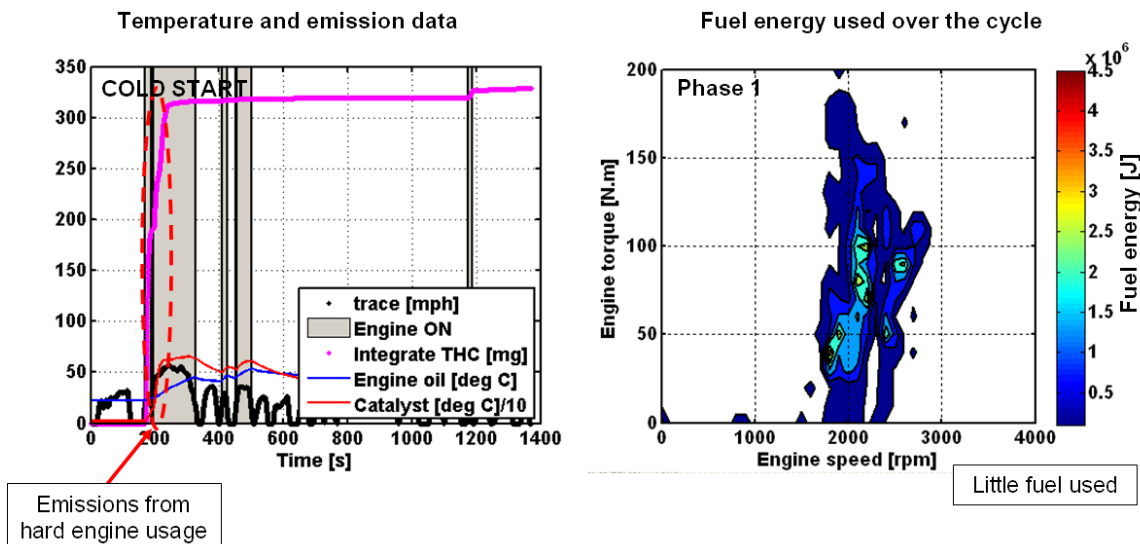
Figure 8-25: Phase 1 cold start cycle summary for the blended plug-in hybrid with 'load following' control
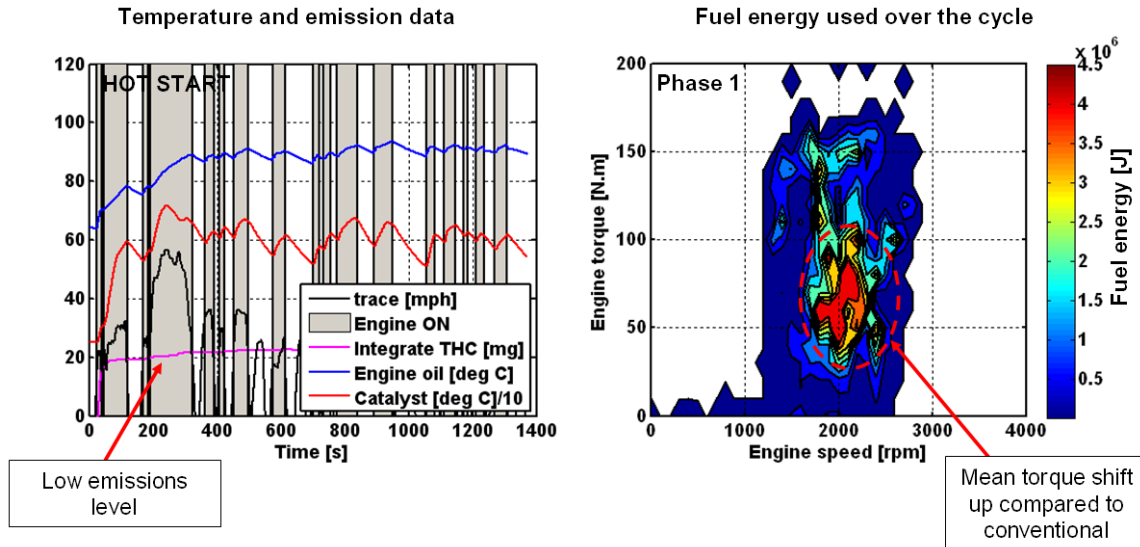
Figure 8-26: Phase 1 charge sustaining hot start cycle summary for the blended plug-in hybrid with 'load following' control

Phase 1: energy consumption and emissions summary

The conventional vehicle, the electric vehicle capable plug-in hybrid vehicle and the blended plug-in hybrid vehicle energy consumption and emissions test results are summarized in Figure 8-27. The energy consumption graph shows the conventional fuel economy data in black. The cold starts for all test sets are marked in green. The electric vehicle capable plug-in hybrid is shown in red. The first test only used electric energy. The cold start test used slightly more electricity energy compared to the second UDDS cycle. The third cycle is the transition cycle, which is charge depleting. The last cycle is charge sustaining. The fuel economy gain, when compared to the conventional vehicle operation, is 25%. The blended plug-in hybrid vehicle is shown in blue. The first cycle is marked in green and slightly offset from the general blended plug energy consumption line. The engine cold start losses cause this offset. With the cold start cycle, the first three tests are the charge depleting cycle. The fourth cycle is the transition cycle. The fifth cycle is the charge sustaining cycle. The 'engine load' following cycles do have a slightly higher fuel economy, which can be explained by the less extreme engine operation compared to that of the 'engine optimum' strategy.
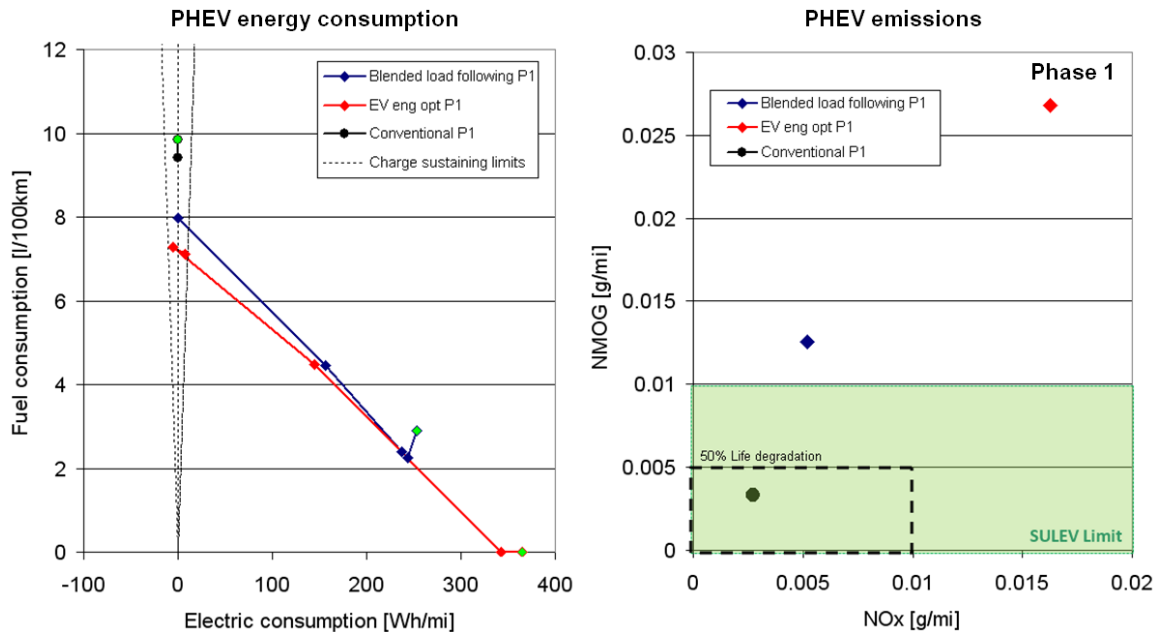
Figure 8-27: Phase 1 energy consumption and emissions summary for all tests

The emissions data is quite revealing. The conventional vehicle achieves SULEV. The blended hybrid is just outside of the SULEV limits. The electric vehicle capable plug-in has the highest emissions. The emissions results in the graph are the average of the five individual full charge cycles for each vehicle type. In the conventional vehicle, the catalytic converter temperature is always high and the engine loads are fairly light with mild tip-ins. In comparison, the electric vehicle capable plug-in with the 'engine optimum' strategy is extremely aggressive on the engine loads. The engine loads are high and the tip-ins immediate. The catalytic converter temperature took several cycles to reach its operating temperature, but still cooled down significantly during some prolonged engine OFF periods. All of these reasons explain why the electric vehicle capable plug-in hybrid with the 'engine optimum' control strategy generated the highest emissions. For similar reasons, the blended plug-in hybrid with the 'load following' strategy is in-between the conventional vehicle and the electric capable plug-in in terms of emissions and energy consumption.

8.4.3. Emission mitigation routines

From the phase 1 results, it is clear that the engine load needs to be reduced while the engine catalytic converter has not reach its light off temperature. Even once the light off temperature is reached, the engine maximum torque should be limited until the engine and the exhaust after treatment systems reach operating temperatures. The original idea was to ramp up the maximum engine torque as a function of time, but after further brainstorming and discussion, it was decided that the engine torque maximum limit will be ramped up as a function of engine energy output. If a certain amount of energy is produced by the engine, it will guarantee that a certain amount of energy goes to warm up the engine and the exhaust after-treatment system. Ramping the maximum available

engine torque based on time could result in a situation where the engine only idled during that period and at the end, the desired operating temperature are not reached. The engine warm up routine, based on engine output energy, was discussed in Section 7.7. Figure 7-27 illustrates that in conventional mode, the engine cranked out about 2 to 3 MJ of energy by the end of Hill 2 on the UDDS, at which point the engine and exhaust after-treatment system have reached their operating temperatures.

Based on the Phase 1 data set, it seems that when the engine is turned ON the engine load should be ramps in with mild tip-ins compared to the immediate load request commanded in Phase 1. Figure 8-28 shows the three routines that are implemented in Phase 2 for the first engine start to reduce the engine emissions for these full charge plug-in hybrid tests.
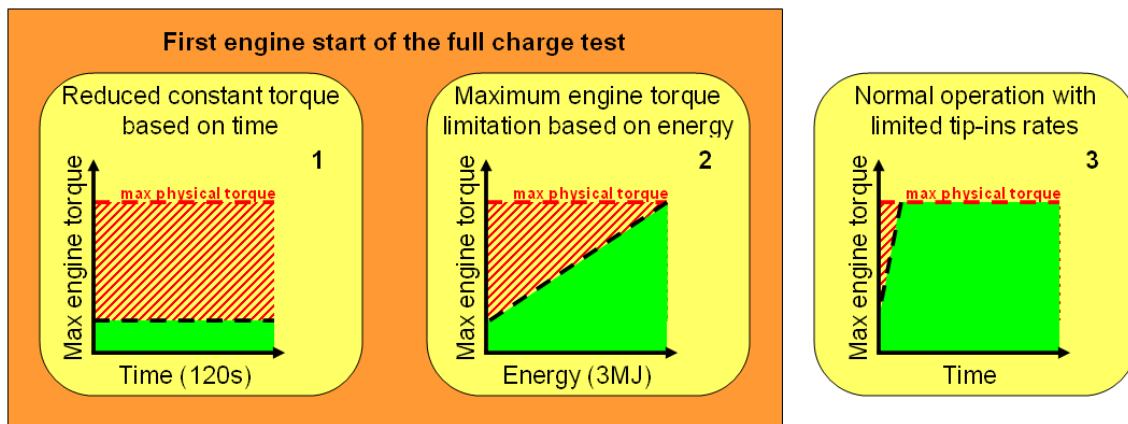
Figure 8-28: First engine cold start warm up routines

The long engine OFF times in Phase 1 allowed the engine and catalytic converter to cool off significantly. Thus, after the first engine start occurred, the catalytic converter temperature was monitored and when the converters temperature dropped below a target temperature, an engine warm up routine was initiated. The engine torque is limited and ramped up based on engine output energy. The target energy during this warm up was much lower. Figure 8-29 show the warm up algorithms for the engine start up triggered if the catalytic converter temperature drops below its target temperature.
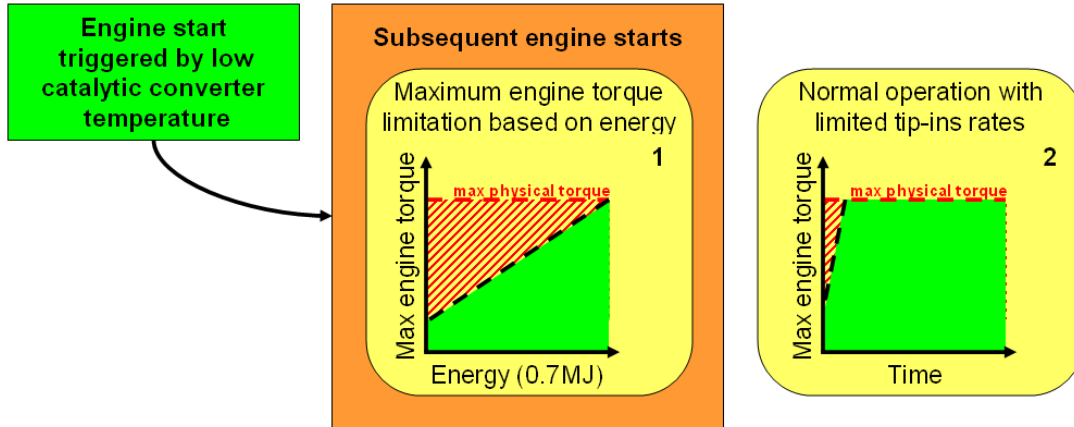
Figure 8-29: Subsequent engine warm start warm up routines triggered by low catalytic converter temperature

In all cases, the engine starts are always followed by a ramp in of the maximum torque to prevent the aggressive engine usage from Phase 1. These are all routines that are not necessary in simulation, but are required with real hardware to obtain reasonable emissions data. These warm up algorithms were easily implemented in the open controller on MATT.

8.4.4.   Results for Phase 2

Phase 2 was tested in February of 2009 with the same hardware used during Phase 1. The cold start FTP testes were performed in the conventional vehicle mode. The fuel economy and emission results were very close to the results of Phase 1, which shows MATT's repeatability, even with a gap of several months.

Electric vehicle capable plug-in hybrid

The Phase 2 results for the electric capable plug-in hybrid are presented in Figure 8-30. The first 2 UDDS cycles are still completed in electric vehicle mode. The first engine start occurs at the start of the 3rd UDDS cycle. Note that the engine oil temperature is (and will be, from this point forward) compared to the Phase 1 test, which shows that the engine warm up strategy is successful. This full charge test looks similar to the Phase 1 test. In the charge sustaining mode, the engine ON time is similar to Phase 1.
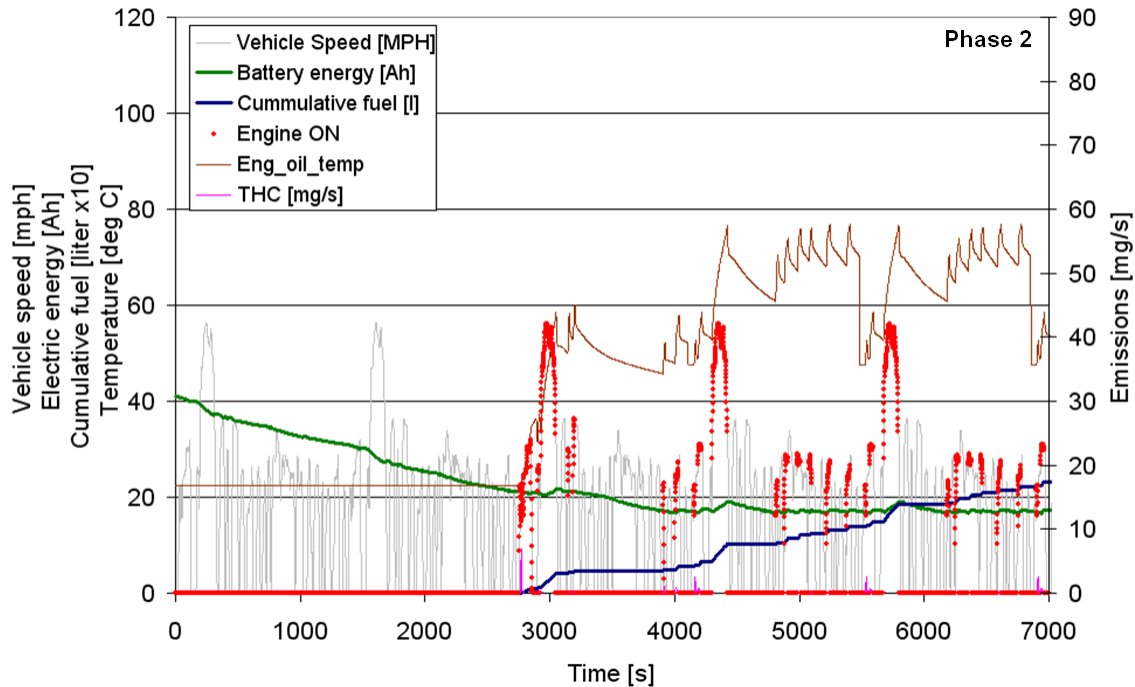
Figure 8-30: Phase 1 full charge test results for the electric vehicle capable plug-in hybrid with 'engine optimum' control with engine warm up

In this case, only the cold start test emissions and engine operating range summary are shown in Figure 8-31. After the first engine start, the engine is ON for an extra 200 seconds. The integrate emissions are three times lower compared to the first engine start cycle on Phase 1, shown in Figure 8-22. The catalytic converter reaches 800 degrees C in Phase 2, compared to 600 degrees C in Phase 1. More importantly, no large loads are applied to the catalytic converter for the first 120 seconds during which the catalytic converter reached 600 degrees C. On the engine operating range graph, a few of the warm up routines are visible. During the initial engine ON phase, the maximum engine load is limited to a constant torque of 25 N.m, which is shown in the graph. Also, a small engine idle fuel island reappears due to the fact the engine is forced to idle during these 120 seconds when the vehicle is stopped. The engine should not be started and stopped until the exhaust after-treatment system reaches light off temperature. Finally, the engine load is not contained to 150 N.m as it was in Phase 1 (Figure 8-22). The graph does show an operating range from 50 N.m to 150 N.m. This is the result of the slow ramp up of the maximum engine torque limit based on the engine energy output.
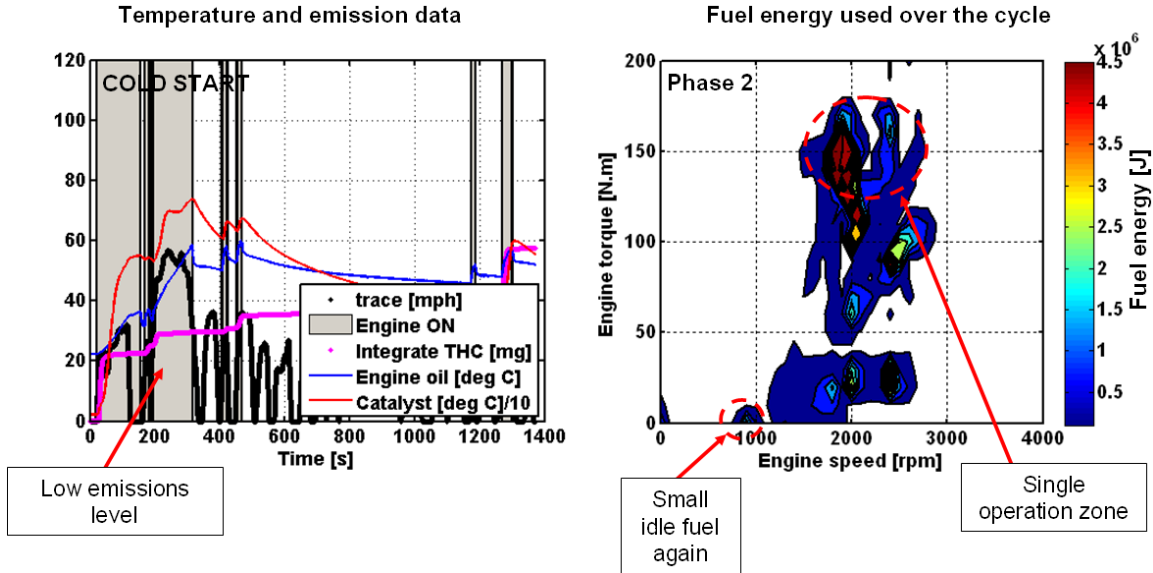
Figure 8-31: Phase 2 cold start cycle summary for the electric vehicle capable plug-in hybrid with 'engine optimum' control with engine warm up

The power flow graphs for Phase 1 and Phase 2, shown in Figure 8-32, provide more detail about the impact of the engine warm up strategies. In Phase 2, the engine turns ON for Hill 1 of the UDDS cycle. During the first hill the engine power is lower than 8 kW due to the 25 N.m limit and the motor provides the dynamic tractive power to meet the trace. At the end of Hill 2, the engine idles for about 30 seconds, which represents the end of the 120 second phase during which is the engine is required to turn ON and limited to a maximum torque of 25 N.m. The engine is used two more times during Hill 2. During Hill 2, the engine torque ramp is shown in the graph. At about 250 seconds, the engine torque is not limited anymore. In Phase 1, the engine turned ON during Hill 2 and is immediately loaded to 150 N.m.
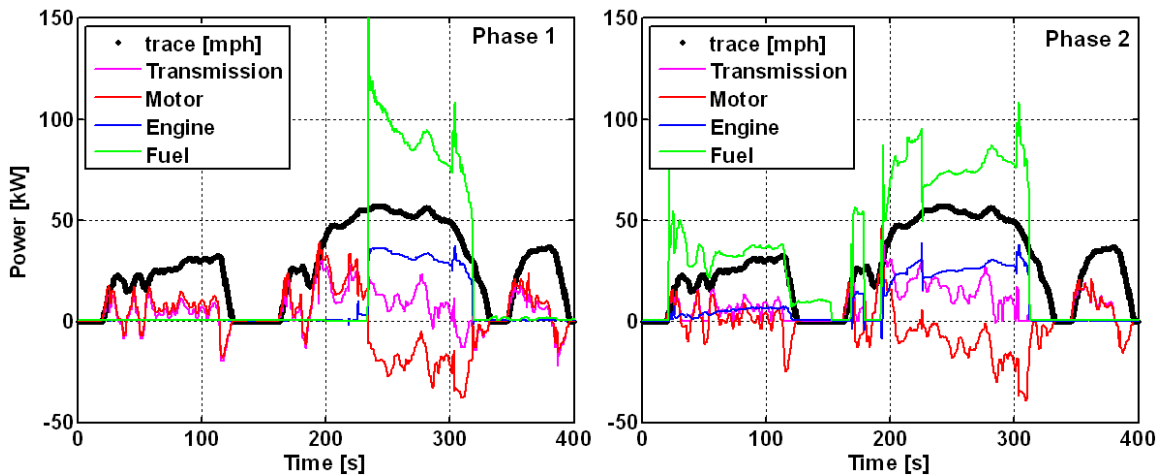
Figure 8-32: Power flow comparison between Phase 1 and 2 of the cold start cycle of the electric vehicle capable plug-in hybrid with 'engine optimum' control

Blended plug-in hybrid

The Phase 2 full charge test results for the blended plug-in hybrid are presented in Figure 8-33. The engine is ON more often at the start of the first UDDS cycle than it is in Phase 1. The engine temperature is about 20 degrees C hotter during the charge depleting phase. In Phase 2, the 6th UDDS cycle is charge sustaining, while that occurs during the 5th UDDS cycle in Phase 1. This is due to the higher engine usage with the engine warm up strategy, thus, less electric energy is on the UDDS cycle in charge depleting mode.
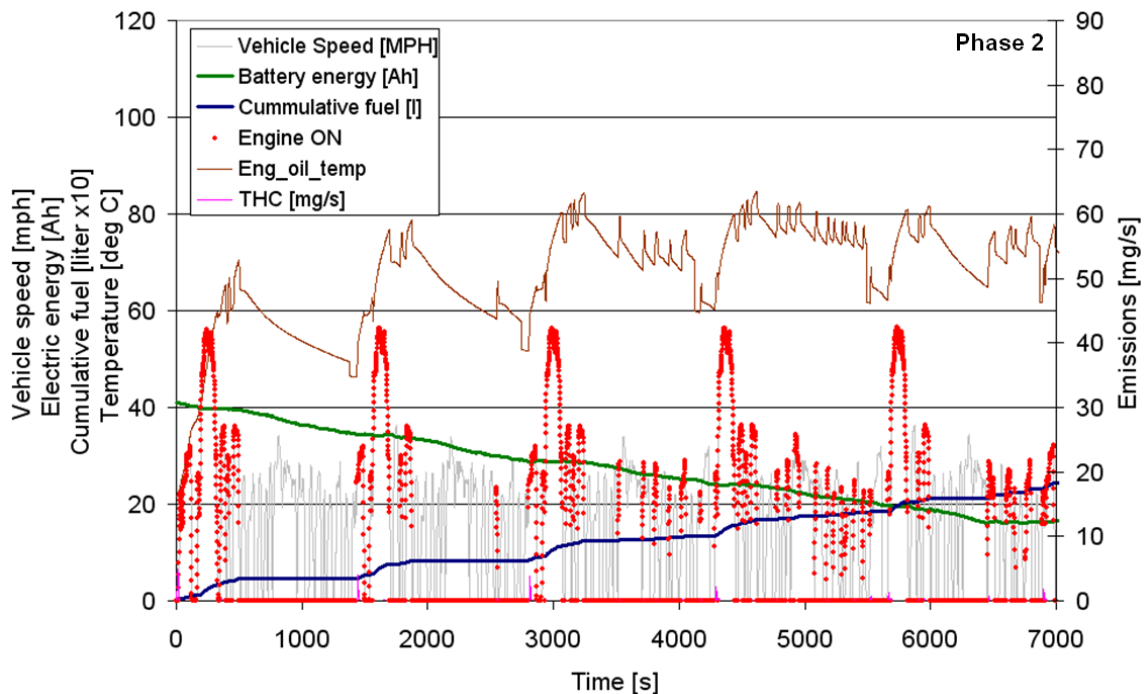
Figure 8-33: Phase 2 full charge test results for the blended plug-in hybrid with 'load following' control with engine warm up

Figure 8-34 shows the emissions and engine operating range UDDS cycle summary for the first engine start test on the full charge test. The engine starts immediately. In the blended plug-in hybrid, the engine needs to be warmed up based on the key start. The engine is ON for the first 3 hills. In the 'load following' strategy, the engine loads are not as high as in the 'engine optimum' control strategy, which causes the load following case to take longer to finish the warm up phase since it is energy based. The integrated emissions level is ten times lower than it is in the Phase 1 results. The engine temperature is higher by 10 degrees C on this charge depleting test than it is in Phase 1. In the engine operating range graph, the idle fuel island reappears, since the engine is forced to idle in the initial warm up phase. The low engine torque operation is also new compared to the Phase 1 test, which is caused by the fact that if the engine is ON, it is used with the maximum engine torque available.
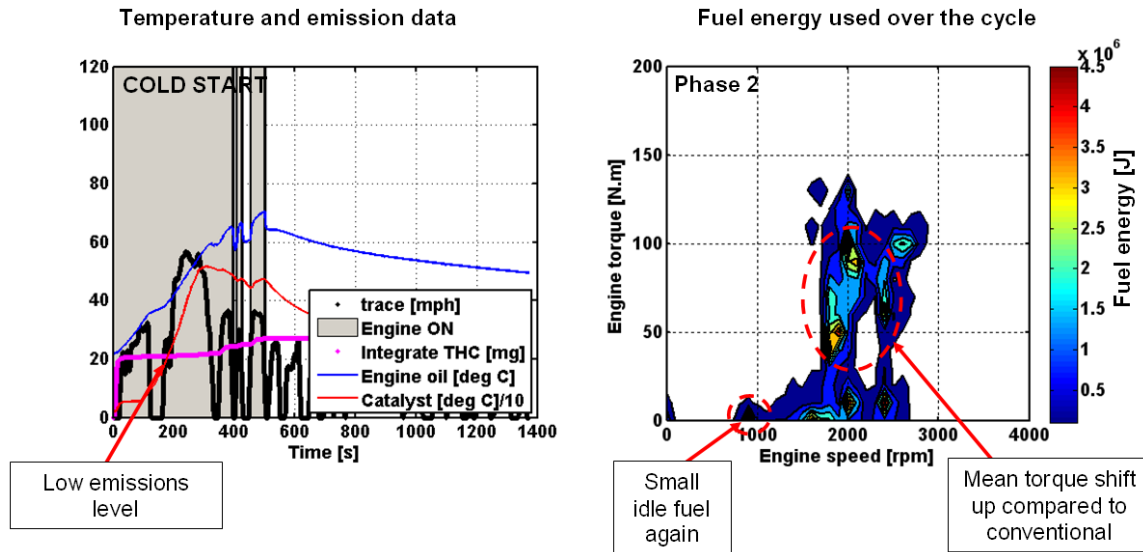
Figure 8-34: Phase 2 cold start cycle summary for the blended plug-in hybrid with 'load following' control with engine warm up

The power flow graphs for Phase 1 and Phase 2 shown in Figure 8-35 provide more details on the impact of the engine warm up strategies for the blended plug-in hybrid. Similar to the 'engine optimum' test, the initial warm up phase, where the engine torque is limited to 25 N.m, is seen on Hill 2. On Hill 2, during the hard acceleration, the motor torque spikes up, which shows that the engine is still limited during the maximum engine torque limit ramp up phase.
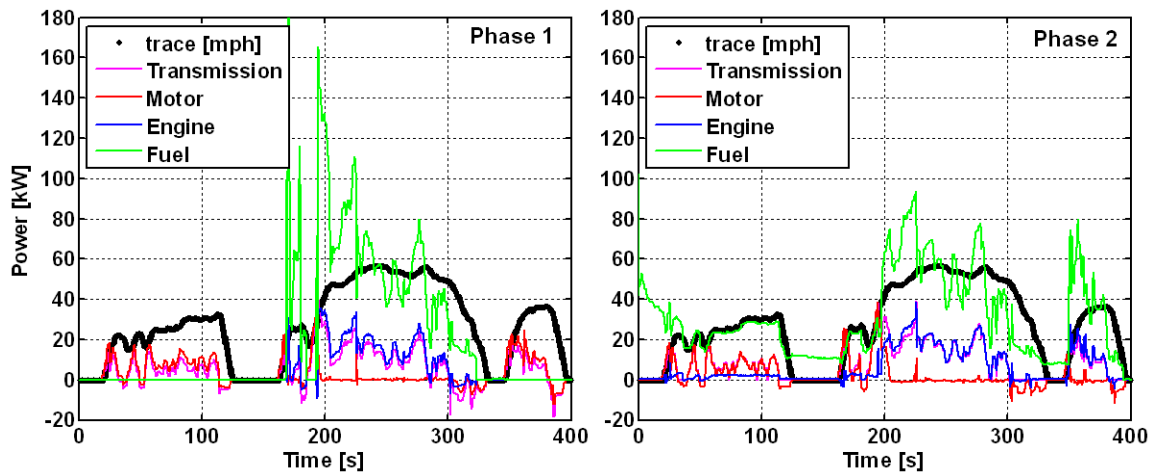
Figure 8-35: Power flow comparison between Phase 1 and 2 of the cold start cycle of the blended plug-in hybrid with 'load following' control

Phase 2: energy consumption and emissions summary.

The conventional vehicle, the electric vehicle capable plug-in hybrid vehicle and the blended plug-in hybrid vehicle energy consumption and emissions test results are summarized in Figure 8-36. The color code and the axes on the graphs are all the same as they are in Phase 1 to make the comparison easier. The conventional vehicle and all charge sustaining fuel consumption for both plug-in hybrids vehicle are the same as in Phase 1 and are shown respectively. This is as expected. For the electric vehicle capable plug-in hybrid with the 'engine optimum' control, the energy consumption on the charge depleting is the same as it is in Phase 1. The transmission cycle used more fuel but less energy, which is a consequence of the engine operating more through the engine warm up routine. For the blended plug-in hybrid with the 'load following' control strategy, an extra cycle had to be tested to obtain a charge sustaining cycle. The charge depleting cycles all used more fuel and thus less electricity as a consequence of the engine warm up routines.
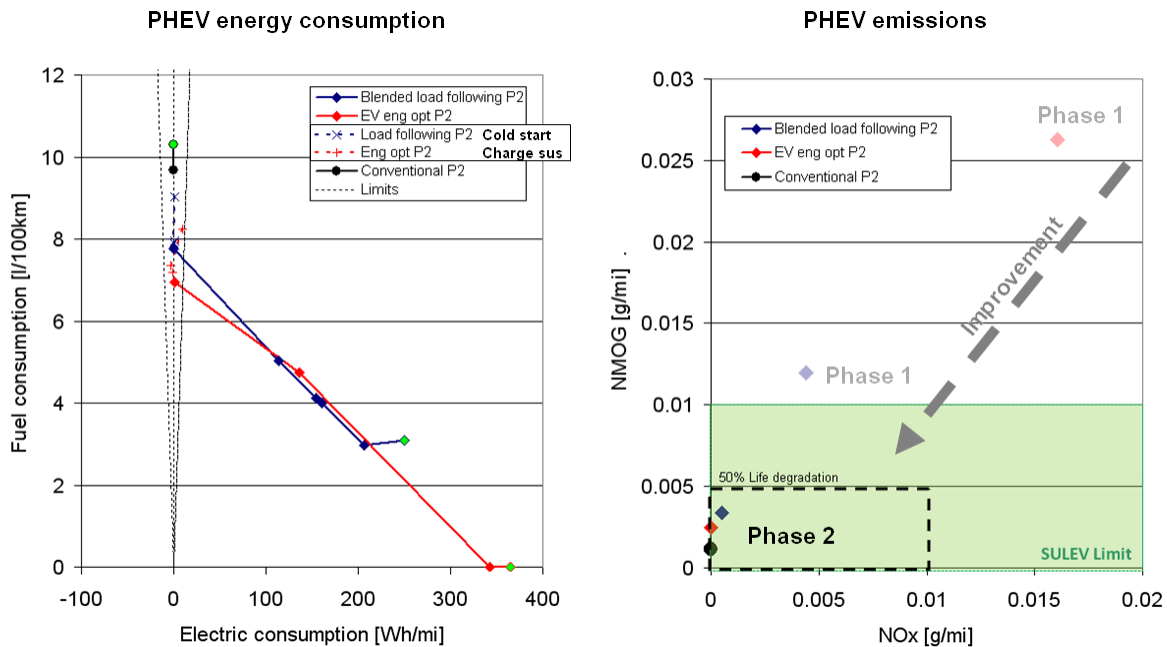
Figure 8-36: Phase 2 energy consumption and emissions summary for all tests

The real success is shown in the emissions summary. Both plug-in hybrid vehicles achieved SULEV limits. The engine warm-up routines, coupled with the slow engine loading after an engine start, do reduce the emissions level dramatically. The emissions results of Phase 1 are shown in faded grey.

8.4.5.   Repeatability tests for consistency.

After the phase 2 was completed, the phase 1 tests were repeated with the exact same control saved in Fall 2009. This is an A-B-A test method, to ensure that the original

baseline data can still be reproduced with the same results, which confirms that the test hardware and instrumentation have not changed. In MATT's the recheck of the baseline test was done to insure that the hardware setup did not change and impact the fuel economy and emissions results. As mentioned earlier a limitation in the flexibility and constantly evolving and improving hardware. Figure 8-37 shows the original test results of phase 1 of Fall 2008 for the electric capable plug-in hybrid test with the 'engine optimum control strategy' along side of the results of Spring 2009 from after the completion of Phase 2 testing. Both fuel economy and emissions match well.
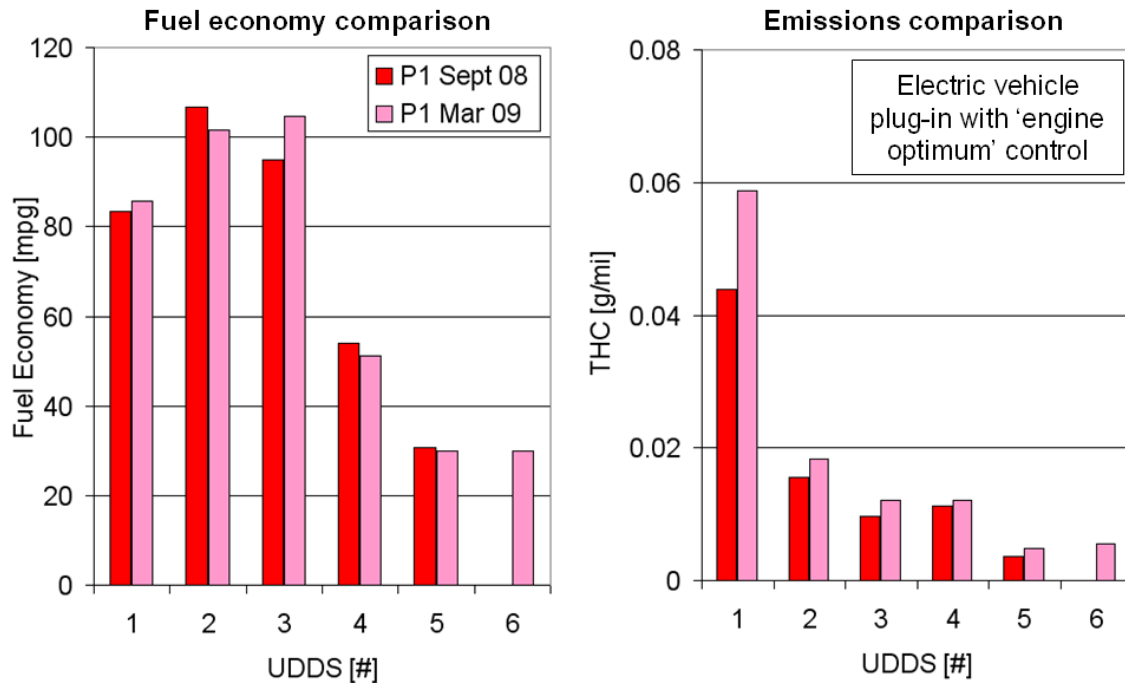
Figure 8-37: Comparison of phase 1 data of Fall 2008 compared Spring 2009 retest at the end of the project

8.4.6.   Conclusion

This study investigated the impact of aggressive engine usage on emissions for PHEVs. The conclusion of the first phase showed that the engine needs to be warm and the exhaust after-treatment system needs to be higher than the light off temperature of the catalytic converter before significant loads are applied. Otherwise, large emissions spikes result. Further, the immediate high engine load request after the engine start also causes larger emission spikes, even while the engine and exhaust system are at operating temperatures. Thus, some warm up routines are designed. On the first engine start, the engine is limited to a maximum torque of 25 N.m. Then the maximum available engine torque is ramped up as a function of the engine energy output. The energy output target is calibrated to ensure that the engine and exhaust system reach their operating temperatures. If the catalytic converter temperature drops below a target temperature, the maximum available engine torque is ramped up as a function of a smaller engine energy

output again. Finally, the engine loads are ramped in using mild tip-ins to further reduce the emissions spikes.

The engine warm up strategies reduced the emissions of all of the plug-in hybrid vehicles to SULEV limits without changing the energy consumption significantly.

This study could not have been performed without MATT's open controller approach and in-depth instrumentation.

8.5.   Synopsis of PHEV studies and relevance of work

Four different, very specific and important studies were performed using MATT with different energy management strategies and several hardware setups.

The first study had the most impact since it directly influenced a much-discussed issue between CARB and the SAE J1711 committee for the new proposed plug-in hybrid test procedures. The study provided data that showed that a proposed correction method for the cold start on the full charge highway test set did not work for all plug-in cases. The case of an extreme charge depleting blended plug-in hybrid had to be simulated. As a direct result of the study, the proposed and much discussed correction method was abandoned. An alternative method, using a charge sustaining switch, was proposed and tested but the manufacturers did not agree on implementing a charge sustaining switch. A senior test engineer at CARB working on the test procedures was impressed by the quality of the data and the in-depth analysis provided on this timely research study.

The second study investigated the soak time between tests for a full charge plug-in hybrid evaluation. It was found that the soak time does have an impact on the energy consumption, but the effect is so small that it is insignificant. There was no impact on emissions. This study provided data to support the test procedure development committee in their decision to allow a wide range of soak times between tests.

The third study provided insights about the impact of drive cycle intensity on energy consumption for electric vehicle capable plug-in hybrids. No electric plug-in hybrid is available for testing today and thus, could only provide data to show that the electric consumption increases with the drive cycle intensity. The opposite is true for blended plug-in hybrids. Therefore, with electric capable plug-in hybrids, the petroleum displacement benefits are maintained or increased as driving aggressiveness increases. This is not the case for blended plug-in hybrid vehicles. This work also completed the wide range of drive cycle intensity research for MATT as a conventional vehicle, a charge sustaining hybrid and a plug-in hybrid. The data set shows the potential of plug-in hybrids to displace up to 60% of petroleum at driving intensity levels on the UDDS cycle.

The final study was the most in-depth and comprehensive work on plug-in research using MATT. This research focused on engine control of blended and electric vehicle capable plug-in hybrids and the impact on emissions. The importance of warm up for the engine and the exhaust after-treatment system was shown in a first phase. Based on the first data set, some engine warm up routines and an engine loading strategies were developed to mitigate the emissions spikes causes by the engine usage of plug-in hybrids. The emissions for both plug-in hybrid types were well within the SULEV limits. The

results showed the success of the warm up routines in mitigating emissions for plug-in hybrids.

All of these studies were very focused and specific, but used MATT as the primary tool to generate data. Several key components enabled MATT to be such a flexible tool:

- The open controller approach, which enables MATT to behave exactly as the studies required. Each study uses a different control.

- The in-depth instrumentation, which provides comprehensive data for analysis of each investigation.

- The virtual scalable energy storage system and virtual scalable motor module, which enable MATT to behave like an electric capable plug-in hybrid. These also allow the setting of identical initial conditions for test repeatability.

- The repeatability of the software robotic driver, which provides consistent and repeatable drive cycle results, even months apart.

- Versatility of operating as a conventional vehicle, an electric vehicle, and many types of hybrid and plug-in hybrid vehicles using the exact same hardware set.

9.   Hydrogen engine calibration and development

9.1.   Background and approach

The U.S. Department of Energy deemed the hydrogen internal combustion engine as the bridging technology to the hydrogen economy. As acknowledged in hydrogen portion of the literature review, the infrastructure and on-board storage still need to be resolved, but hydrogen is an excellent candidate as a renewable, sustainable and clean transportation option for the long term future. Today, the internal combustion engine provides a lower cost than the fuel cell system and can burn several fuels other than hydrogen. The multi-fuel aspect provides the key to a gradual development of the hydrogen infrastructure, as consumers can drive on hydrogen when available, but can also fill up on gasoline when a hydrogen station is not within reach. For further details and background information on the hydrogen engine, please refer to section 2.5.

This hydrogen engine project started in 2005 as a collaboration with the Ford Motor Company. Ford provided the supercharged hydrogen engine. The engine was supplied without an engine control unit. The candidate was hired by Argonne National Laboratory to evaluate the hydrogen engine from the vehicle system perspective.

This investigation was performed in two stages. First, the hydrogen engine was evaluated on an engine dynamometer and combustion strategies were developed for transient operation. The second phase was to evaluate the engine and the calibrations in the vehicle environment, using MATT.

MATT operated in conventional vehicle control only mode for this study, and the automatic transmission module was used.

9.2.   Engine and calibration

9.2.1.   The engine

The specifications are provided in section 3.5.2 and table Table 3-4. The engine is in the same displacement family as the gasoline 2.3 liter DURATEC used in the other MATT applications. This engine has been modified to Ford's specifications (Ref. 128). The engine is port injected with gaseous hydrogen injectors pointed into the intake runners, post intercooler. The induction system uses a belted Lystrom type supercharger with an electronic throttle body pre-supercharger. An air-to-liquid intercooler is integrated in the aluminum air intake. Each cylinder is taped for piezo-electric pressure transducers to record the indicated in-cylinder pressure. Figure 9-1 shows a picture of the engine as it arrived at Argonne.
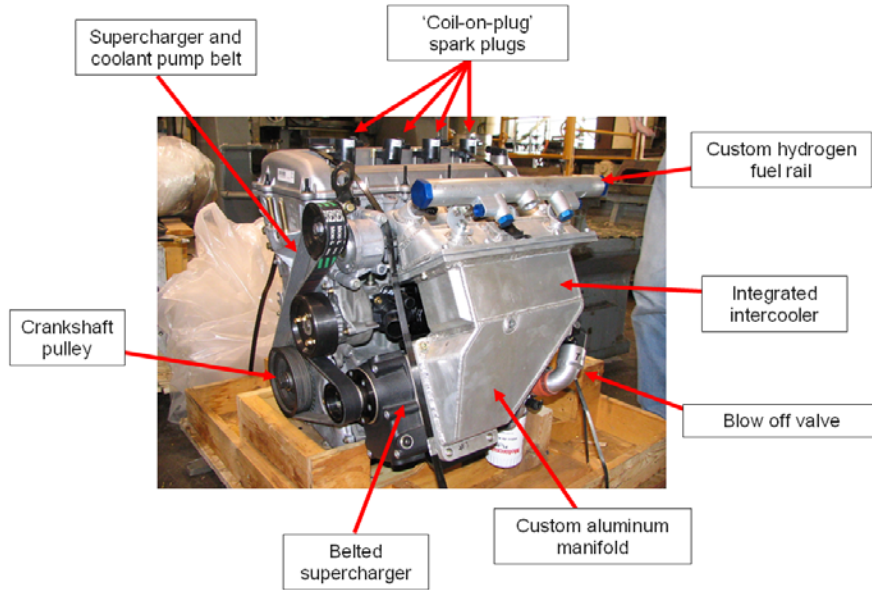
Figure 9-1: Hydrogen engine calibrated for and evaluated on MATT

9.2.2. Test cell setup

General layout

Argonne has a hydrogen engine test cell. A double sided DC engine dynamometer is at the center of the test cell. On the south side of the dyno is a single cylinder hydrogen research engine. This engine is used for basic hydrogen combustion research, from port-injection to direction injection. All of the intake conditions, including air flow, pressure and temperature can be controlled, as well as the exhaust pressure. The engine is also instrumented to in-cylinder combustion visualization equipment to visualize the combustions processes.

The 2.3 liter engine is located on the opposite side of the dynamometer. That side of the dynamometer was a bare side at the start. Thus all of the support systems including the engine support cradle, the liquid to liquid cooling temperature control system, the exhaust system, safety guarding and the safety hood, needed to be designed and implemented. The aftermarket ECU with the wiring and the instrumentation required months to debug before it could be implemented. The electric throttle and a fast hydrogen three way valve are computer controlled from the operator console. Figure 9-2 illustrates the general layout of the test cell.
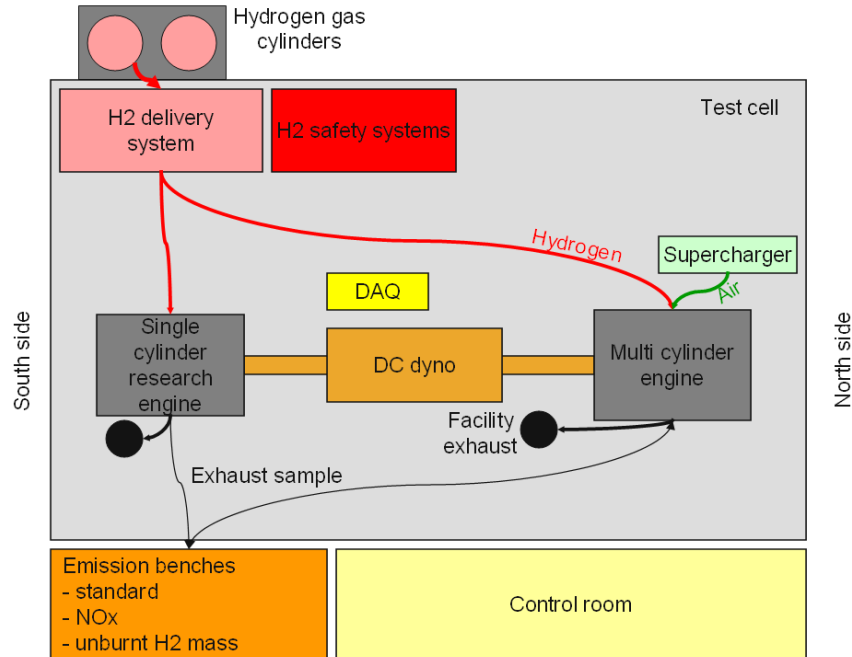
Figure 9-2: Argonne's hydrogen engine test cell layout

Hydrogen safety system

A hydrogen delivery and safety system is located on the north side of the cell. The hydrogen is stored in cylinders. The delivery system precisely meters the hydrogen mass flow, then a pressure regulator steps the pressure down to deliver the hydrogen to the engine's final regulator. A motorized safety valve in the delivery system stops the hydrogen flow when the emergency stop system is triggered by an operator or one of the multiple safety sensors. A hydrogen sensor is located at the top of the deliverer system's enclosure.

An actively vented hood is located above both engines with a hydrogen sensor in each hood along with a sprinkler system Each engine also has infra-red cameras monitoring the engine for external combustion events. Each of these critical safety sensors will trigger the emergency stop which will stop the hydrogen flow, alert the Argonne Fire department and sound the building evacuation alert system. The hydrogen flow will also be stopped if the engine oil pressure is low, the exhaust vent is not operating or the dynamometer encounters a problem, but these critical safety systems will not trigger an alert at the fire department. Some of the safety systems are detailed in Figure 9-3.

216
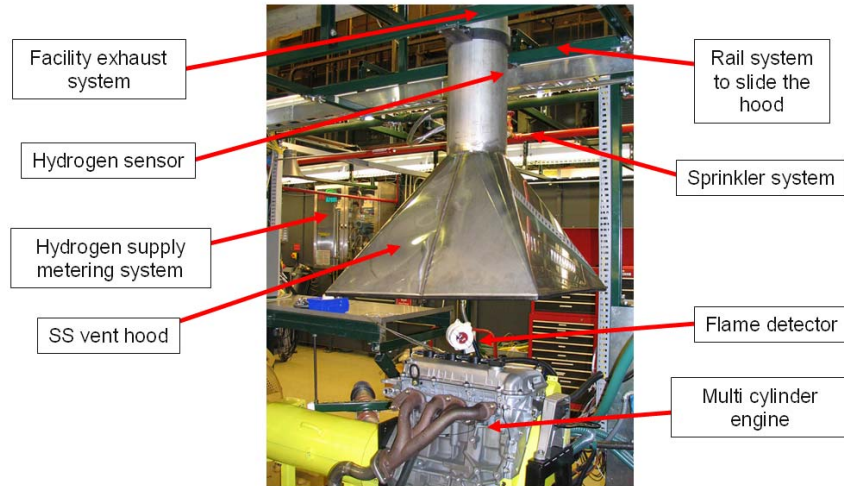
Figure 9-3: Hydrogen engine test cell safety systems

Furthermore, the operator has direct control of a three way hydrogen vent solenoid. During the rest position where there is no power, the solenoid stops the hydrogen supply side and the fuel rail is connected to a vent line. When powered, the valve connects the supply side to the fuel rail. This enables the operator (or the emergency system) to immediately stop and vent the hydrogen away from the engine.

2.3 liter hydrogen engine test cell setup

The hydrogen engine is mounted on a custom-made cradle, which enables the use of the stock vehicle isolation mounts. The engine is coupled to the dynamometer with a guarded dynamometer shaft. All rotating part, such as belts and the flywheel, are guarded as well. The coolant system uses the engines integrated mechanical water pump as well as an external electric pump. This coolant system integrates an electric heater to warm up the engine to its operating temperature through the cooling system before testing is started. Once the engine generates power and rejects heat, a liquid to liquid heat exchanger cools the coolant to maintain operation temperature. The heating and cooling of the system is computer controlled using some back pressure valves to regulate the coolant flow. The coolant flow and the intake and outlet coolant temperatures are measured to determine the total heat rejection at the different test points.

The calibrated venturi with a differential pressure sensor is inline with the combustion air intake. This is used to measure the mass flow of air fed to the engine. The intake air temperature is measure in the test cell, pre and post supercharger, as well as post intercooler, in the intake runners. The intercooler inlet and outlet temperatures are also measured. The intercooler flow is also computer controlled to achieve a target air flow temperature using a PID loop. The aftermarket engine controller, the sensor power supplies and a number of sensors are located in a large enclosure at the side of the engine. The engine and its support system setup are shown in Figure 9-4.
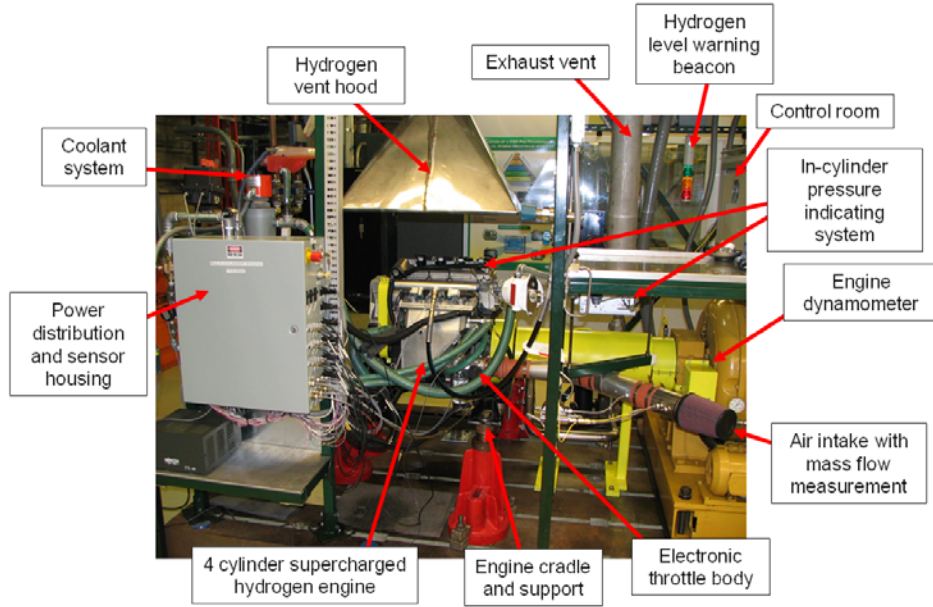
Figure 9-4: Intake side of the hydrogen engine setup in the test cell

The exhaust from the hydrogen engine is simply dumped into the actively vented facility exhaust vent system and after-treatment devices are used. The exhaust temperature of each cylinder is measured, as well as the collector temperature. A wide band oxygen sensor is located in the raw exhaust stream. It can be used by the engine controller as a closed loop air/fuel ratio combustion control. A hydrogen content sensor samples a stream of the exhaust. Finally, the raw emissions bench sample line also taps into the exhaust line. Figure 9-5 show the exhaust system of the engine in the test cell.
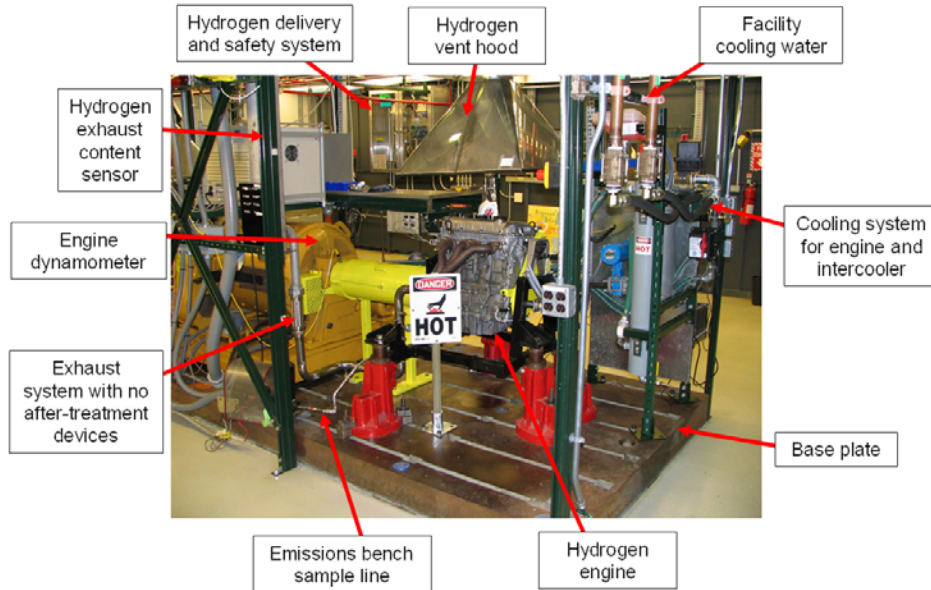
Figure 9-5: Exhaust side of the hydrogen engine setup in the test cell

Engine control

The primary engine control is done through the after market engine controller, which is a MOTEC M800. The fuel injector timing map and the ignition timing map are the primary calibration parameters that dictated the combustion strategy for port injected hydrogen engines. The fuel and ignition maps are a function of engine speed and load command. The load command is an analog voltage control signal sent on the ECU. In the hydrogen engine dynamometer test cell, the signal is generated by the data acquisition system and in the vehicle application this signal is generated by the accelerator pedal. The ECU also uses the load command to modulate the throttle, based on a user defined lookup table.

The throttle is an electronic throttle body that is driven by an h-bridge in the M800. A PID loop controls the Pulse Wide Modulated (PWM) signal to the throttle, which moves the throttle plate by closing the loop on the throttle position signal. The PID requires some tuning and calibration for satisfactory operation. The vacuum between the throttle and the supercharger is such that the throttle cannot seal enough air flow at idle. Thus, the idle is not possible below air/fuel ratios of 3.

Further special functions are used for calibration purposes. The closed loop air/fuel ratio controller, which is also referred to as the lambda controller, is used for a fair bit of calibration. This feature uses the reading from the wide band oxygen sensor. The lambda controller is simple to activate through the MOTEC's user interface during the steady state speed calibration on the engine dynamometer. In the transient vehicle operation, this controller operation does become quite challenging. Another function that was calibrated is the injection time, which was adjustment based on the fuel rail pressure. Most other features, such as fuel enrichment on warm up or acceleration enrichment, were purposely disabled to make sure that the main fuel and ignition map determined the combustion process. For the transient operation of the engine on MATT, some of these features were revisited. For the steady state combustion investigation and engine calibration, the simplest control approach is the most effective.

Instrumentation and emissions equipment

The engine instrumentation can be divided into several categories. The first system is a NI SCXI data acquisition system which records analog and temperature signals. The second system is calibration parameters and command values directly from the engine controller. The next data set is from the high speed data acquisition, which provides the indicated mean effective pressure as well as its derived information. The emissions equipment data is recorded continuously on a 1 Hz basis throughout the test period. For each load and speed point, the data acquisition system records for a 30 second period, which is then averaged to create a single data line in the saved data set.

The NI SCXI records some of the crucial energy flow information, such as the dynamometer speed and the load cell data, as well as the hydrogen fuel flow data. The cell test conditions, including temperature, pressure and relative humidity, are saved as well. On the intake side, the mass air flow, throttle position, intake, pre and post

supercharger, post intercooler air temperature and post supercharger pressure are all measured. The exhaust system and the coolant system instrumentation (described earlier) are all recorded using the NI SCXI. The MOTEC is set to broadcast some of the engine control parameters, such as injector pulse width and ignition timing.

The high speed data uses the engine crankshaft position encoder and pressure transducers. This information is recorded separately from the low speed data. Along with the pressure traces, the injector pulse width and ignition timing are measured as a function of the crank angle with the high speed data.

The final component recorded in the data file is the measured exhaust gas data. An AMA 2000, which is a raw emission composed of six gases (THC, CH4, CO, NOx, CO2 and O2) is used to analyzed the product of the combustion process in real time. Combustion completeness is measured by the hydrogen exhaust content sensor, which samples the exhaust in parallel to the emissions bench.

The instrumentation and data acquisition system is quite extensive and was time consuming to implement and debug. About six months after the start of the engine test setup build phase, the first power was produced using the engine. A screen shot of the data acquisition interface on the 4 cylinder hydrogen engine is shown in Figure 9-6 producing power for the very first time.

Figure 9-6: Screen shot of the data acquisition shows the first power produced by the engine

9.2.3. Engine dynamometer calibration and results

Calibration approach

The plan was to establish calibrations for four different air/fuel ratio points. Using the existing literature and prior experience from the single cylinder research hydrogen engine, air fuel ratios between 2 and 3 were selected. At lambda, which is the air/fuel ratio, of 2.2~2.3 the hydrogen combustion produces significant amounts of NOx. As lambda is decreased, the NOx production increases exponentially. This is due to higher temperatures and pressure in the combustion chamber, which favor the production of NOx from the nitrogen and oxygen in the combustion air. The final air/fuel ratios selected were 2, 2.25 2.5 and 3.

For each air fuel ratio, the engine was calibrated at 800, 1500 and 3000 rpm. The torque level targets for the calibration started at zero torque and increased in 25 N.m increments until Wide Open Throttle (WOT) operation was achieved at the set air fuel ratio. The zero torque is actually a fired operation. The zero crank shaft torque occurs when the engine produces just enough power to offset all of the losses (valve train, supercharger, friction, …etc…) experienced by the engine at that particular speed. When the engine is spun at a particular speed and no combustion occurs, the engine is said to be motored. The motor operation was recorded as well to provide the engine compressor brake torque for the vehicle operation and the motored in-cylinder pressure traces.

For each calibration point, the engine speed was locked in place using the engine dynamometer. The fuel injection timing and the throttle opening was modified until the target torque was reached. Once the fuel and air flows at the target air fuel ratio produced the desired torque, a spark sweep was performed. The ignition timing was adjusted until the maximum brake torque (MBT) was achieved. All of the data presented from the hydrogen engine is at the MBT spark. Once MBT spark is determined, the air and fuel are readjusted to the desired torque level. This procedure is repeated for each load and speed point for each air fuel ratio. The integrated air fuel ratio controller (Lambda controller) in the MOTEC was used to help maintain the target air fuel ratio. In this mode, the engine controller adjusts the fuel trim based on the wide band oxygen sensor to achieve the target air fuel ratio.

Efficiency test results

Figure 9-7, Figure 9-8, Figure 9-9 and Figure 9-10 show the brake thermal efficiency and torque envelope for each air fuel ratio calibration.
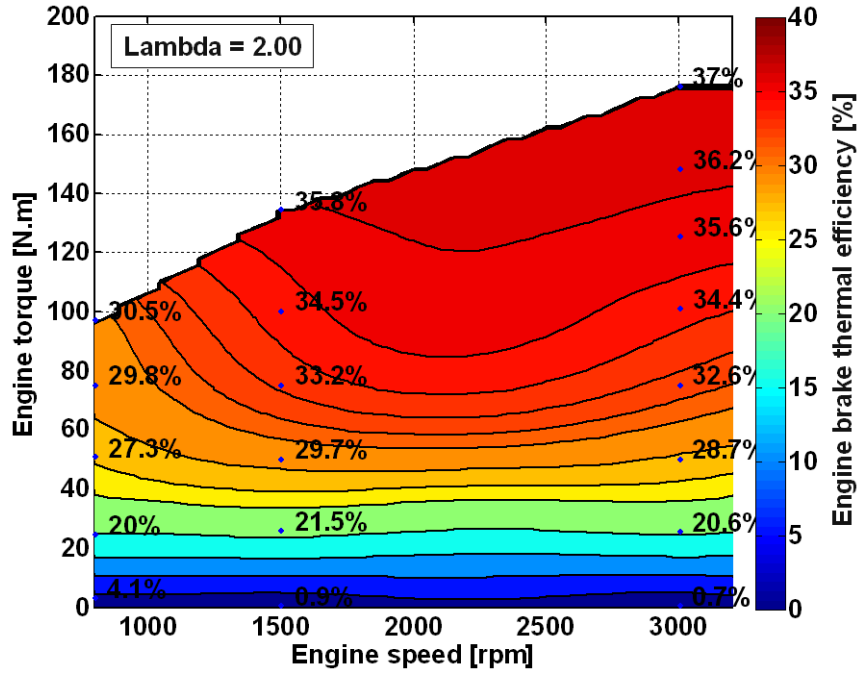
Figure 9-7: Engine brake thermal efficiency at lambda 2
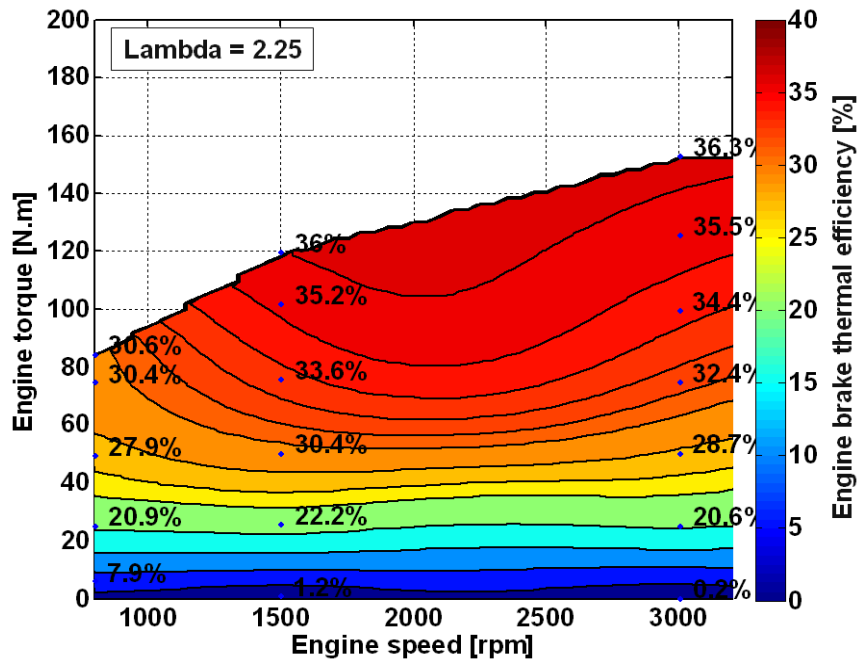
Figure 9-8L Engine brake thermal efficiency at lambda 2.25
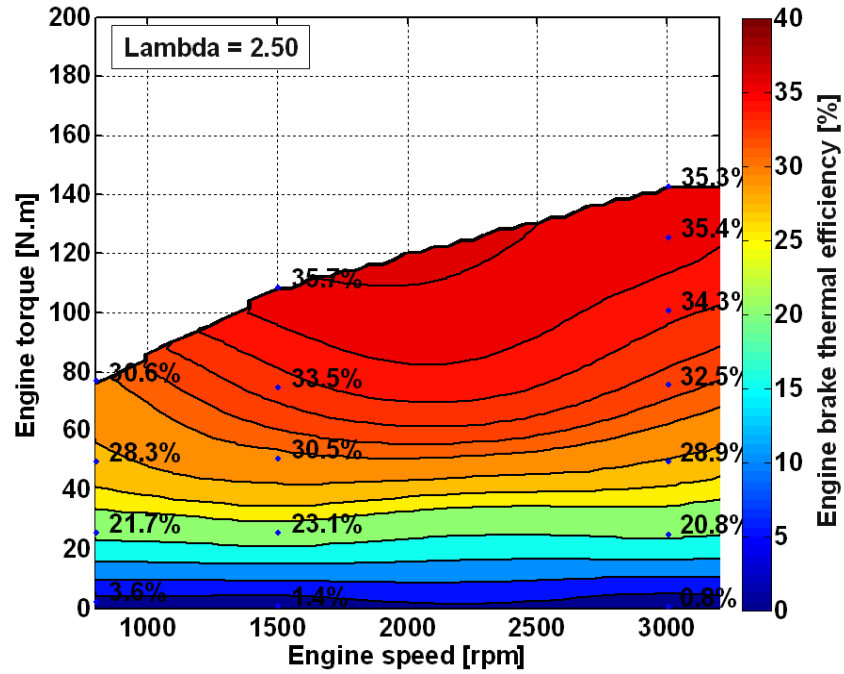
Figure 9-9: Engine brake thermal efficiency at lambda 2.5
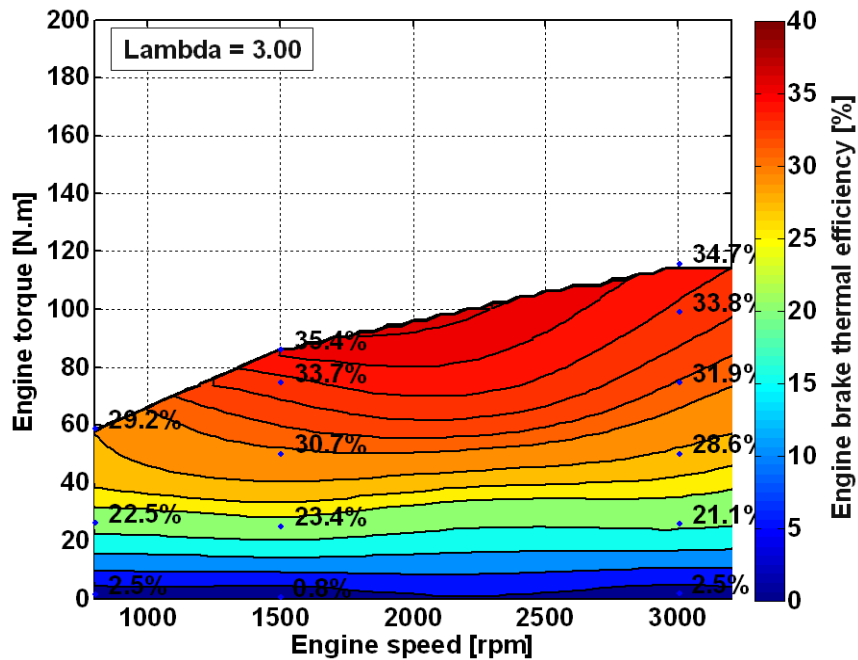
Figure 9-10: Engine brake thermal efficiency at lambda 3

As the air fuel ratio gets leaner, the maximum torque of the engine is significantly reduced. The maximum torque available at lambda 2 is about 180 N.m, compared to less than 120 N.m for lambda 3. At WOT, which causes the maximum air mass flow to the

engine, the only control to adjust is the fuel flow. Thus, to achieve higher air fuel ratios, the fuel flow has to be scaled back, resulting in a reduced maximum torque.

The peak brake thermal efficiency of this supercharge port injected hydrogen engine is 37% at 3000 rpm and WOT for lambda 3. The hydrogen engine has a higher efficiency than the gasoline engine, which has a measured peak efficiency of 35% with no accessories on the crankshaft. In the case of the hydrogen engine, the mechanical water pump and the supercharger rob the engine of some efficiency. The peak brake thermal efficiency for lambda 3 is 34.7% at 3000 rpm and WOT as well. The lower efficiency is explained by the lower load and the proportionally higher engine losses.

Emissions test results

Figure 9-11, Figure 9-12, Figure 9-13, Figure 9-14 show the raw NOX emissions concentrations for each air fuel ratio calibration.
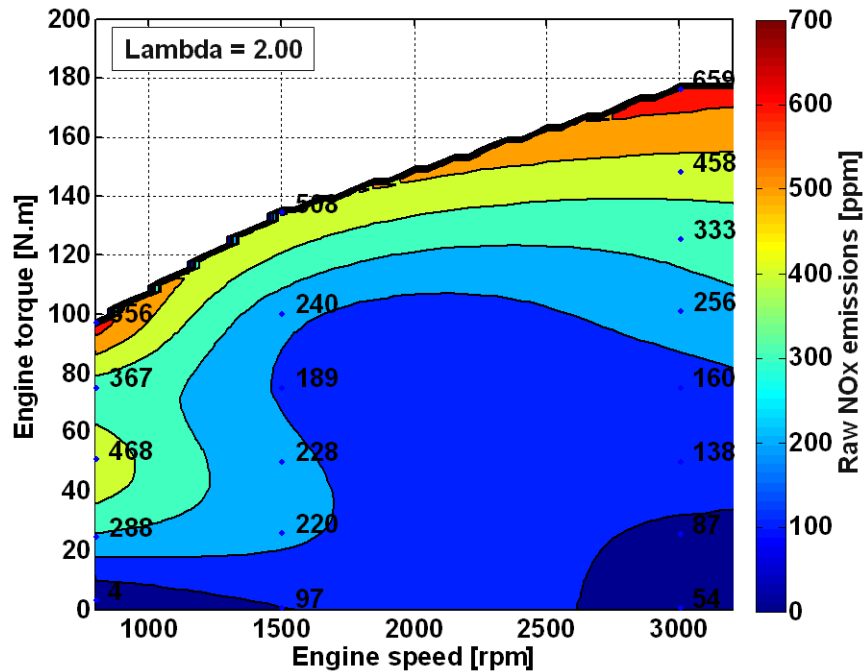
Figure 9-11: NOX emissions at lambda 2

224
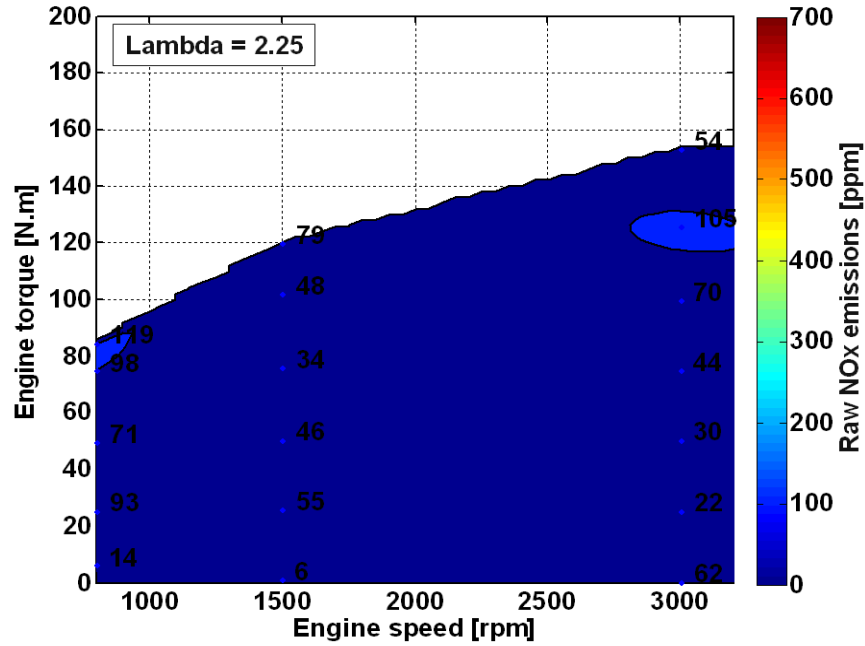
Figure 9-12: NOX emissions at lambda 2.25
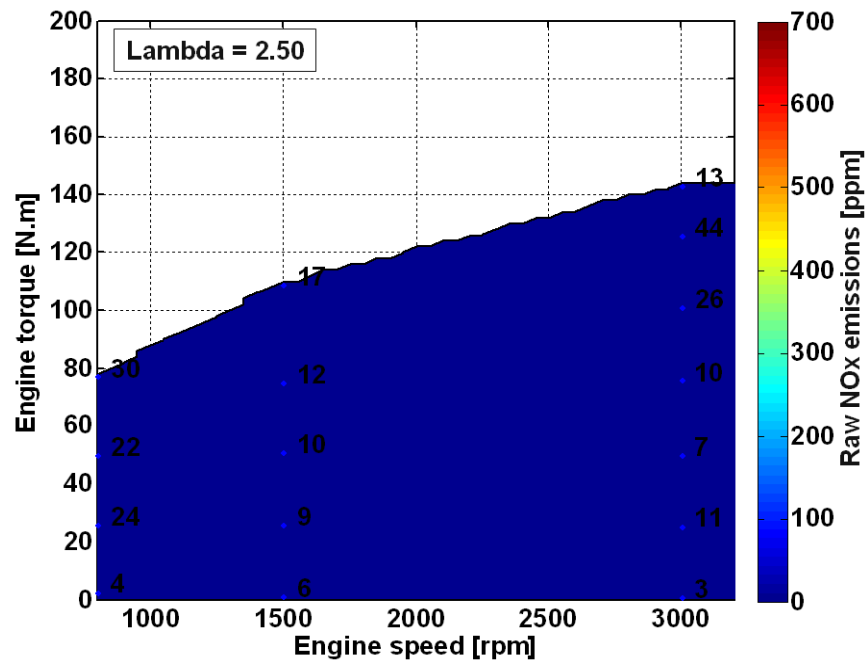
Figure 9-13: NOX emissions at lambda 2.5
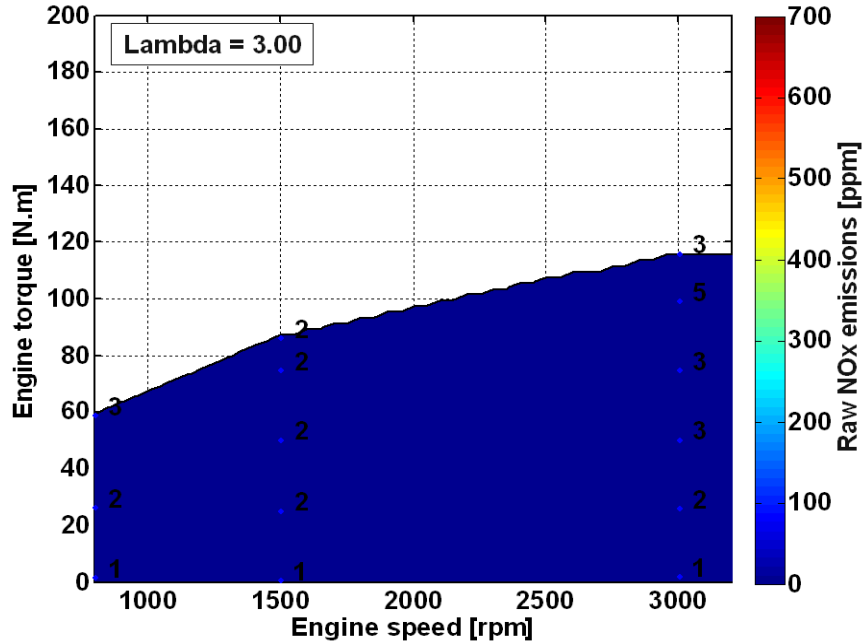
Figure 9-14: NOX emissions at lambda 3

The NOx production is clearly a function of lambda. At lambda 2, the NOx reaches levels that are two orders of magnitude higher than at the lambda 3 calibration. At a lambda of 2.5, the NOx concentrations are already in the single digits. At lambda 2, the peak combustion temperature and pressure in the cylinder are high enough that they favor the NOx production.

Efficiency and emissions test results as a function of the air fuel ratio

Figure 9-15 shows the efficiency data as a function of the air fuel ratio for an engine speed of 1500 rpm. 1500 rpm is a commonly used speed in engine research and analysis since that is a typical average speed for an engine on the UDDS and highway cycle. Some interesting trends become apparent. First, maximum torque is proportional to the air fuel ratio. Second, at the same speed and load point, the leaner combustion is more efficient. This efficiency improvement for leaner combustion is more pronounced at lower loads. That can be seen in the example of the 25 N.m case. The brake thermal efficiency at lambda 2 is 21.5% but at the same load, the efficiency is 23.4% at lambda 3. This efficiency improvement is mainly due to the reduction in pump losses at the leaner operation. At the same load, the same amount of fuel is needed and thus, the air fuel ratio adjustment is the air flow. For the leaner operation, the throttle is open more and therefore the pressure drop across the throttle is reduced. At the same load, the leanest combustion strategy is the most efficiency combustion strategy. This low load efficiency improvement is ideal for a conventional vehicle, since most of the engine operation on the UDDS and the highway cycles occurs at lower loads, as shown in Chapter 5.
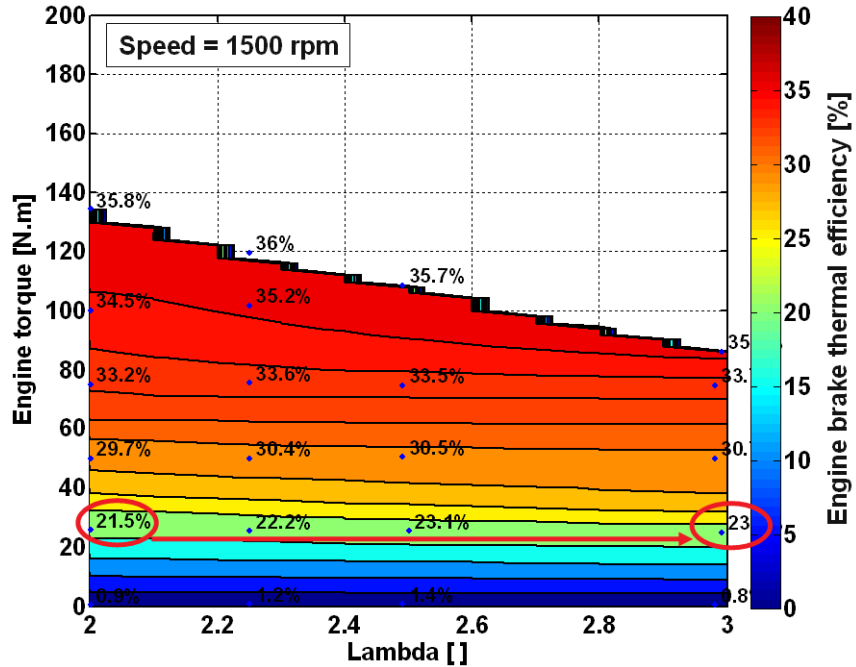
Figure 9-15: Brake thermal efficiency as a function of the air fuel ratio at 1500 rpm

Figure 9-16 shows the emissions data as a function of the air fuel ratio for an engine speed of 1500 rpm.
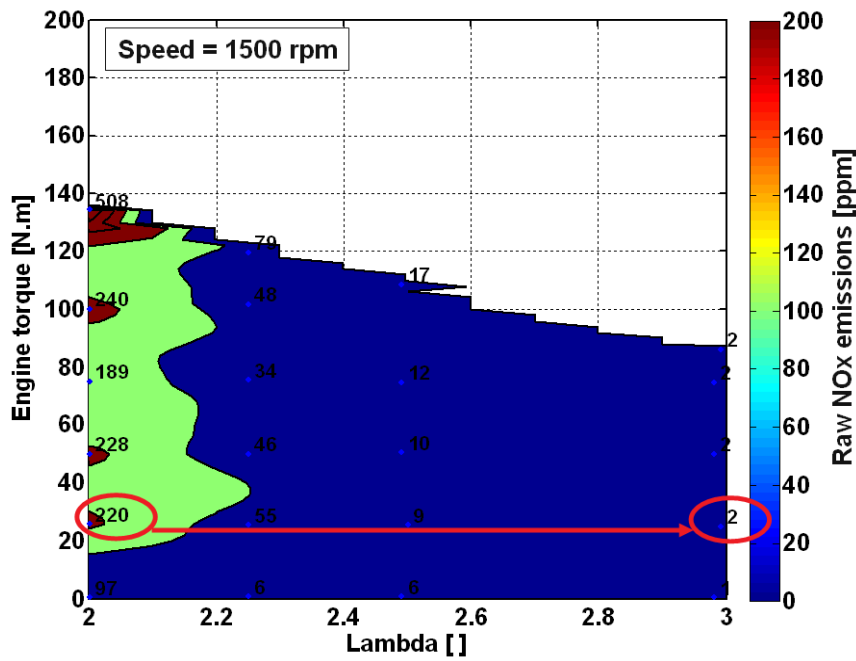
Figure 9-16: NOx production as a function of the air fuel ratio at 1500 rpm

The clear trend for the emissions graph is that the NOx production increases exponentially as the air fuel ratio changes from lean to the richer lambda of 2. Thus, from an emissions standpoint, the leaner the combustion strategy, the lower the tailpipe emissions.

In general, both from the efficiency and the emissions standpoints, the leanest combustion strategy is the most beneficial. The leaner combustion strategies are torque limited, which is detrimental to the vehicle performance.

9.2.4. Variable air fuel ratio strategy

Variable air fuel ratio combustion strategy concept

Based on the efficiency and emissions results from the calibration phase, a new variable air fuel ratio combustion strategy is proposed. This combustion strategy operates the engine at lambda 3 at the low loads until the maximum torque at lambda 3 is reached. After that point is reached, the air fuel ratio increases with load demand until lambda 2 is reached. This combustion strategy benefits from higher efficiencies and lower emissions at lower loads but still provides the high torque levels required to maintain acceptable vehicle performance. Figure 9-17 illustrates the combustion strategy approach.
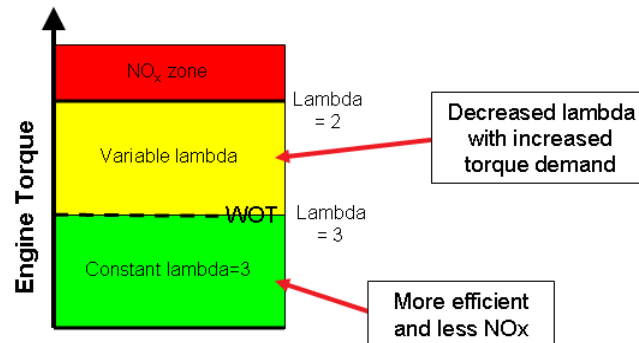
Figure 9-17: Illustration of the variable air fuel ratio combustion strategy

This combustion strategy requires the throttle command be decoupled from the load command in the engine controller. All of the constant air fuel ratio calibrations used a linear relationship between the load command signal sent to the ECU and the throttle command the ECU sent to the throttle body. With this calibration, WOT is required before the maximum load request is reached. The load command is the input that the fuel and ignition calibration map. A look up table is used in the software to establish a correlation between the throttle position command and the load command signal.

Variable air fuel ratio combustion strategy engine dynamometer data

Figure 9-18 shows the achieved air fuel ratio map for this combustion strategy.
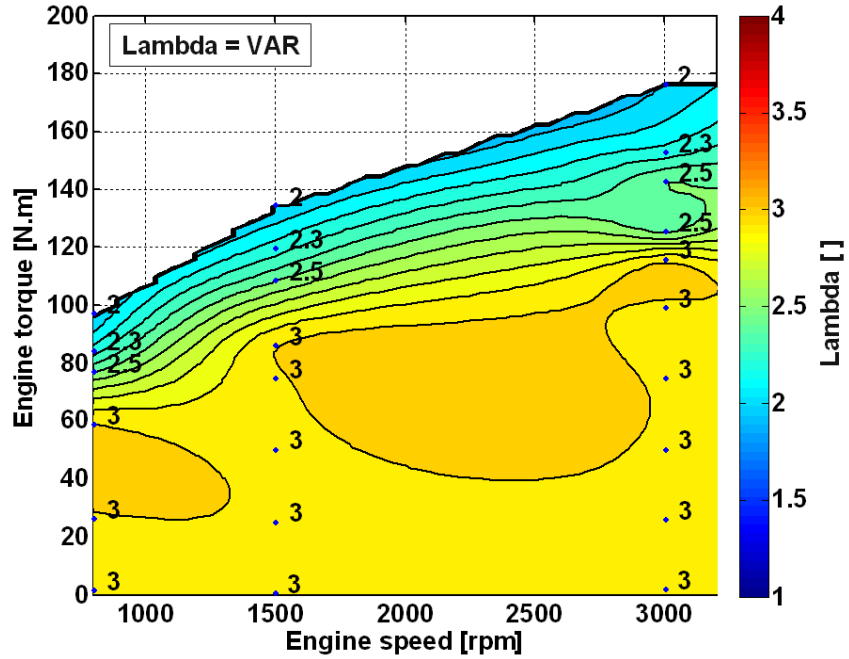
Figure 9-18: Air fuel ratio map of the variable lambda combustion strategy

Figure 9-19 and Figure 9-20 show the measured efficiency and emissions results for the variable air fuel ratio combustion strategy.
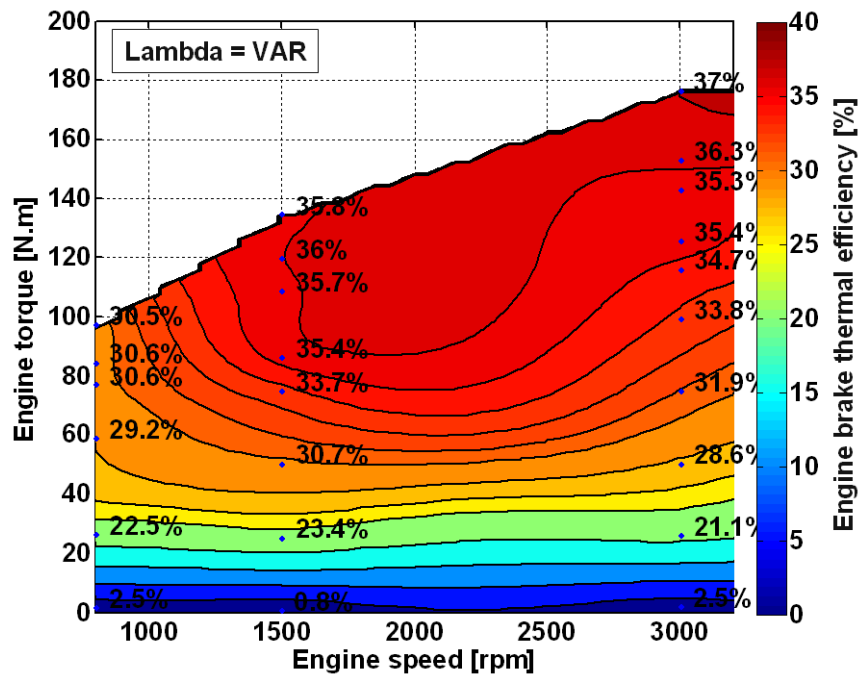
Figure 9-19: Engine brake thermal efficiency for the variable lambda combustion strategy
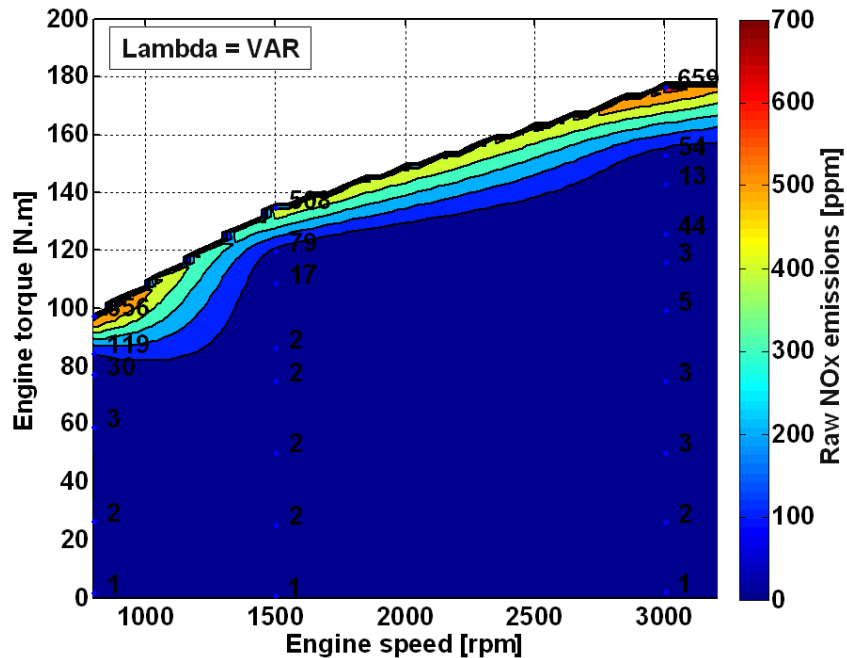
Figure 9-20: NOX emissions for the variable lambda combustion strategy

The air fuel ratio distribution data is the variable air fuel ratio concept that is intended to be described. The efficiency map has the highest overall efficiency in low and high loads. The emissions map also has the low lambda 3 emissions at low loads, but the high loads are penalized by the NOx production. Overall, this combustion strategy appears quite promising for high fuel economy and low emissions on a transient drive cycle.

9.2.5. Engine control for transient operation

The engine dynamometer calibrations are performed at steady state speeds. The calibration is a lengthy process where the engine reaches a perfect steady state and minor control adjustments are performed to tweak the calibration at a steady state operating point. The basic fuel and ignition maps are expected to be good enough to run in a transient manner in a vehicle environment. Fuel enrichment and cold start compensation are functions that may improve the engine operation or drivability, but they are not required.

For the final calibrations, including the four constant air fuel ratios and the variable air fuel ratio combustion strategy, the engine was recalibrated in the summer of 2008 at engine speeds ranging from 1000 to 3000 rpm at 500 rpm intervals.

The final element required for vehicle operation is the engine idle. This is rarely tested on an engine dynamometer setup. The dynamometer shaft was removed and a standard 12V automotive starter was used to crank the engine. The engine controller

provides fuel enrichment for the engine start-up, which is calibratable for fuel added and time of enrichment. With the electronic throttle, the engine controller uses a PID to modulate the air flow to maintain a target engine idle speed. At lean operation, such as lambda 3, the engine starts and fires without hesitation and then maintains the target idle speed. At a lambda of 2, the engine idles at a higher speed than the target idle speed. This is caused by an air leak around the throttle plate and the supercharger pulling air around this closed throttle.

9.3.   In vehicle evaluation

9.3.1.   Vehicle and test cell basics

Vehicle and hardware

As shown in the conventional gasoline vehicle results, the transient operation uses a wide range of the engine torque speed operating range. The vehicle characteristics, the drive cycle and the shift schedule defined the required engine operation. MATT is still emulating a Ford Focus sized vehicle, which enables a comparison between the gasoline conventional vehicle and the hydrogen conventional vehicle. All of the hydrogen engine vehicle tests are performed with the automatic transmission module.

The hydrogen engine uses the same block as the gasoline engine. Thus, the hydrogen engine is a direct replacement of the gasoline engine. The mounting and the coolant system use the same structure. The hydrogen engine also uses the same clutch assembly, but uses a different exhaust system. The exhaust system for the hydrogen engine does not use any catalytic converters. In addition, several support systems on the engine module had to be upgraded, including the fuel supply system and the safety detection systems. In general, MATT's modular approach makes the implementation of the new engine easy. The hydrogen engine was implemented on MATT within 2 weeks.

Hydrogen features for the APRF

The APRF is fully designed and approved for hydrogen vehicle testing. A hydrogen supply system similar to the one from the hydrogen engine test cell provides the hydrogen to the vehicle. This system also measures the hydrogen mass flow and integrates the hydrogen safety systems.

The hydrogen is stored outside of the building in a secured area in 12 packs of gaseous high pressure cylinders plumbed together. One twelve pack stores about 6 kg of hydrogen. The hydrogen is regulate to 300 psi outside and then supplied to the hydrogen delivery system in the test cell. The delivery system is pictured in Figure 9-21.
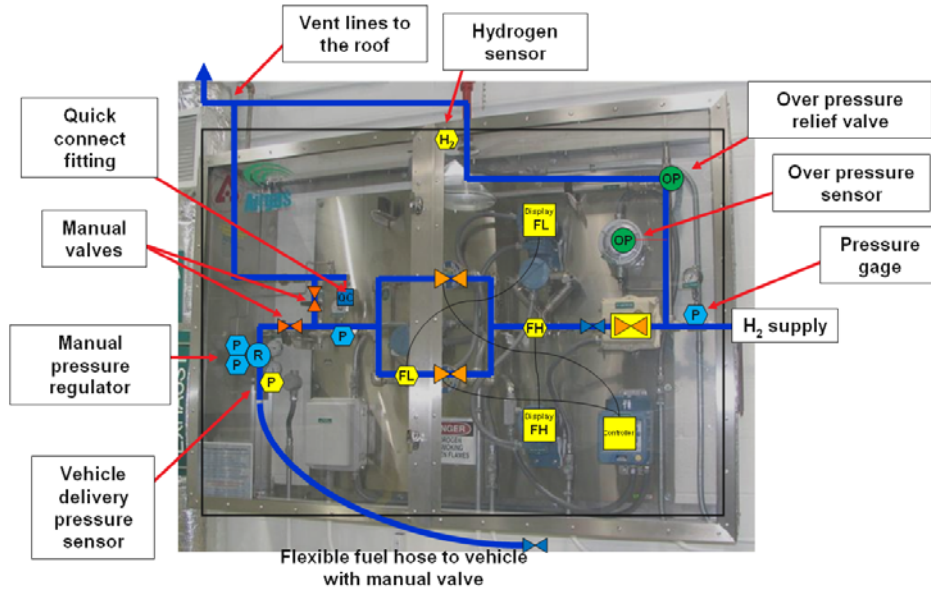
Figure 9-21: Hydrogen delivery and safety system in the chassis dynamometer test cell

The system has a mechanical overpressure relief valve, which will release the system pressure in the vent line that is open to the atmosphere at the rooftop of the facility. A hydrogen sensor is located at the top of the enclosure. If the sensor reads hydrogen levels of 50% of the Lower Explosion Limit (LEL) or higher, the hydrogen flow is stopped, the build emergency evacuation system is triggered, the test cell ventilation system is ramped up to maximum air exchange in the test cell and the Argonne fire department is called. In a second stage, the hydrogen delivery system meters the hydrogen flow. A low range as well as a high range mass flow meter measures the hydrogen flow. At high fuel flow rates, the low range flow meter is isolated from the system and a bypass is opened to ensure that the pressure drop across the delivery system is minimal. The final function if the delivery system is to enable precise regulation of the hydrogen pressure delivered to the vehicle.

9.3.2. Hardware integration and its challenges

Hydrogen engine module

The engine module integrates the supercharged hydrogen engine. Along with the engine, the after-market engine controller and the wiring moved from the test cell to MATT. The cooling system is identical to the gasoline's coolant system. The electronic water was removed, as the hydrogen engine uses a belted mechanical coolant pump. A hydrogen sensor is mounted above the fuel rail in the hydrogen engine module. Figure 9-22 shows a picture of MATT's hydrogen engine module with the hydrogen delivery system in the background.
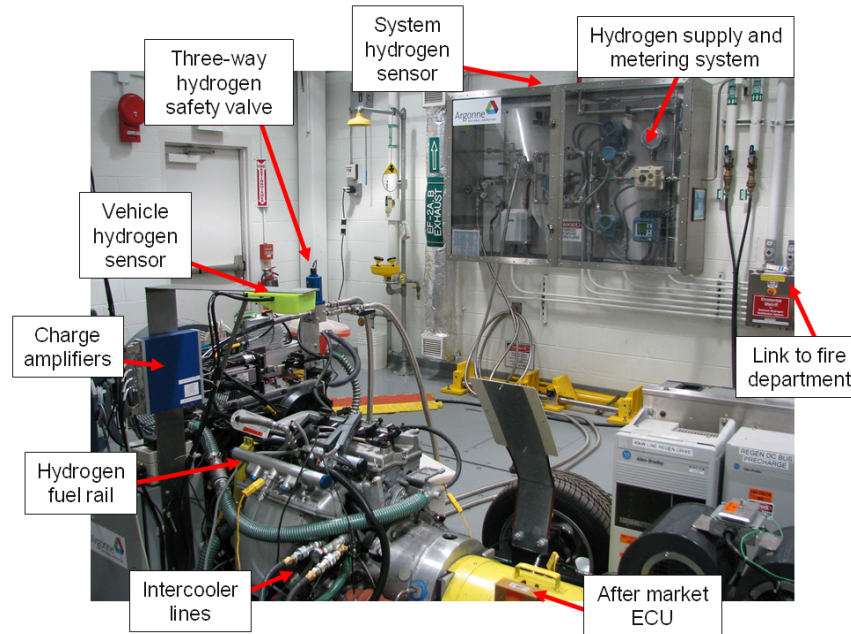
Figure 9-22: Hydrogen engine module on MATT in the ARPF test cell

The flexible hydrogen fuel hose that connects the hydrogen fuel rail to the hydrogen delivery system is visible in Figure 9-22. The vehicle delivery pressure to MATT is set to 80~85 psi static, which is the same pressure used to calibrate the engine in the hydrogen engine test cell.

Figure 9-23 shows the exhaust side of the hydrogen engine module. MATT's hydrogen safety systems are the hydrogen engine sensor located right above the fuel rail and the three-way hydrogen safety valve. The operation is the same as it is in the hydrogen engine test cell. When activated, the solenoid pressurizes the fuel rail with the hydrogen from the hydrogen delivery system. When the solenoid is not powered, the fuel rail is connected to the vent line and thus no hydrogen is delivered to the engine. The hydrogen three-way safety solenoid is powered by the emergency stop system, which ensures that the fuel supply is immediately cut from the engine. In addition, the supply system cuts the fuel supply at the storage source and the delivery system.
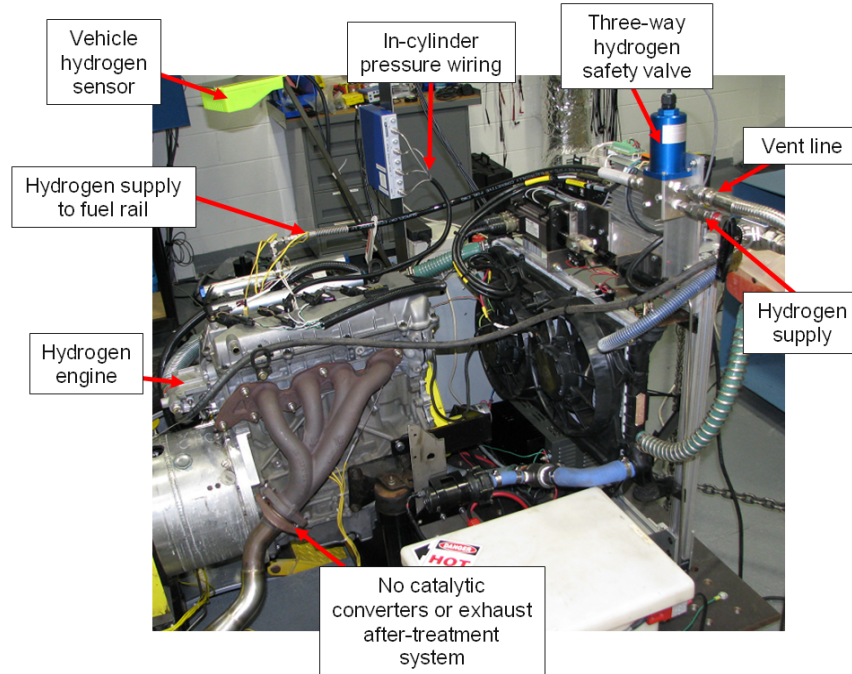
Figure 9-23: Exhaust side of the hydrogen engine module on MATT

Figure 9-23 shows the exhaust system at the engine. Note that no catalytic converter is used for the hydrogen engine.

Transient hydrogen engine calibration challenges

The first challenge encountered was the closed loop lambda control used to maintain the target air fuel ratio. The lambda controller was very useful during the steady state engine calibration phase where it slowly adjusted the fuel trim to match the target air fuel ratio. In transient operation, the lambda controller can only be used during cruise phases because the acceleration transients are too fast for the controller to effectively compensate for any air fuel ratio variations. These findings were determined experimentally. The lambda controller adds too much fuel, which causes rich excursions. For example, on a throttle tip in after a deceleration, the engine would make a knocking sound, accompanied by the characteristic pinging sound and the pressure traces showed the evidence of the ringing. In a second phase, the control logic of the lambda controller engagement was investigated. The best method was to engage the lambda controller based on the rate of change in engine speed. Even in this configuration, the engine would occasionally knock. Therefore, in order to protect the hardware, the lambda controller was not used on MATT. In fact, the open loop fuel maps produced combustion that was very close to the target air fuel ratios. Even with the lambda controller permanently disabled, some rich excursion occurred on vehicle deceleration. This was due to the engine dynamometer calibration. The engine was calibrated to produce zero torque at zero load command, which means the engine controller provided just enough fuel to overcome the engine losses. During vehicle deceleration, when zero load is commanded,

234

the engine does not need any fuel. Therefore, on accelerations that followed a deceleration, some extra fuel was present in the intake runner. The solution was to implement a full fuel cut off during engine deceleration, which would also help to reduced fuel consumption. Figure 9-24 shows all of the air fuel ratios achieved for constant air fuel ratio combustion strategies as well as the variable air fuel ration strategy with the final engine controller calibrations.
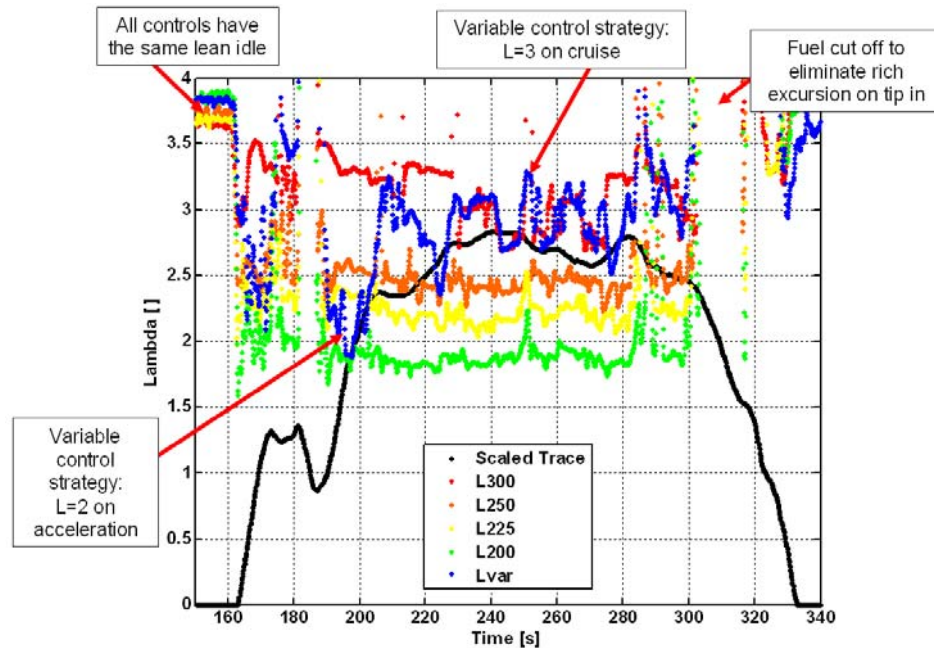
Figure 9-24: Air fuel ratios achieved on the second hill of the UDDS in transient operation

A couple of points on the graph are noteworthy. The idle air fuel ratio is very lean for all of the combustion strategies since the throttle did not seal against the supercharger vacuum. These very lean idle operations contribute to reducing NOx. During the cruise phase of hill, the air fuel ratios are very close to their intended targets. The lambda 3 calibration did exhibit some erratic behavior, which was matched by the variable lambda combustion strategy. This also operated as a lambda 3 combustion during these light load cruise conditions. Note that during the accelerations, which represent the higher loads the engine has to provide during a drive cycle, the variable air fuel ratio combustion strategy behaves like the lambda 2.5 except for the high load acceleration of hill 2 where the variable lambda strategy clearly reaches lambda 2 operation. Thus, from the air fuel ratio perspective, the variable lambda combustion strategy behaves as expected. The final interesting feature shown in the graph is the behavior of the air fuel ratios for all of the combustion strategies during deceleration. The air fuel ratio disappears since the fuel is cut off. This strategy works as well.

The final technical challenge to overcome before starting the full testing was linked to the software robotic driver. The torque request changes of the robotic driver

were very jerky, which translated in the load command signal to the engine controller, causing the engine controller to hunt in the engine fuel map. This resulted in an unstable air fuel ratio control. The solution was simple because of MATT's flexible software driver logic. The software driver was disabled and a pedal that was set for a human driver was used to drive MATT on the drive cycles. The driver had to soften the tip-ins and tip outs, but by anticipating the trace, it was never a problem for the engine to meet the drive cycles.
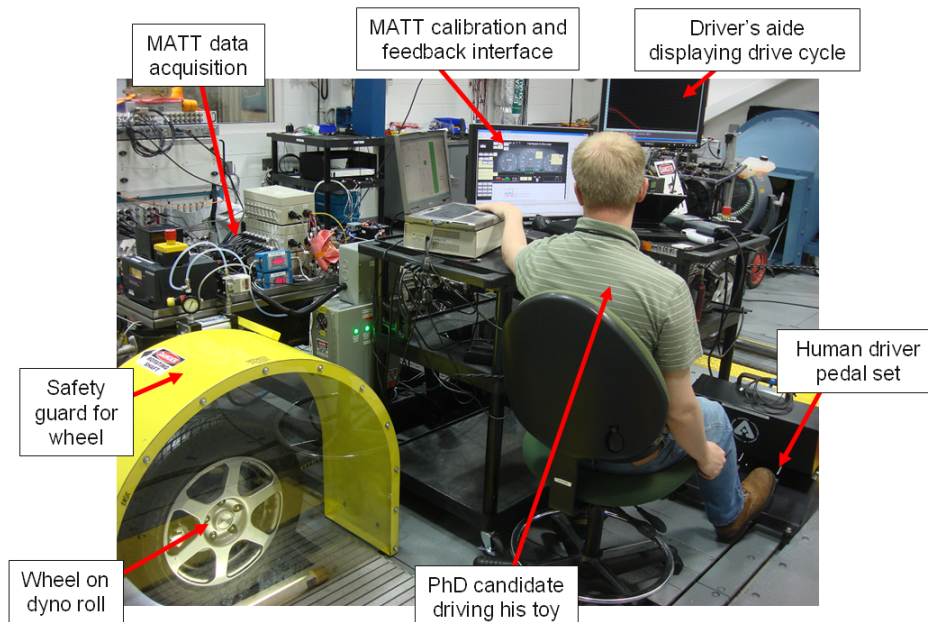
Figure 9-25: MATT with the hydrogen driven using pedal set interface

Finally the conventional vehicle launch had to be recalibrated in the MATT interface for each specific engine combustion strategy. The shifting was also adjusted to each combustion strategy. The procedure for these tasks was well established from the conventional vehicle and required little time.

9.3.3. UDDS tests results

Test results on the UDDS for the different air fuel ratios

Once the engine controller operated to a satisfactory level, the different combustion strategies were tested on the UDDS cycle. For each calibration, the cycle was repeated two to three times. All of these tests were performed back to back and are thus all considered hot starts. A definite trend in the fuel economy results as well as the emissions results emerged. Figure 9-26 summarizes the fuel economy and emissions results for the different combustion strategies on the UDDS. The air fuel ratio does have a direct impact on both fuel economy and emissions on a hydrogen internal combustion engine, even during transient cycles.

236
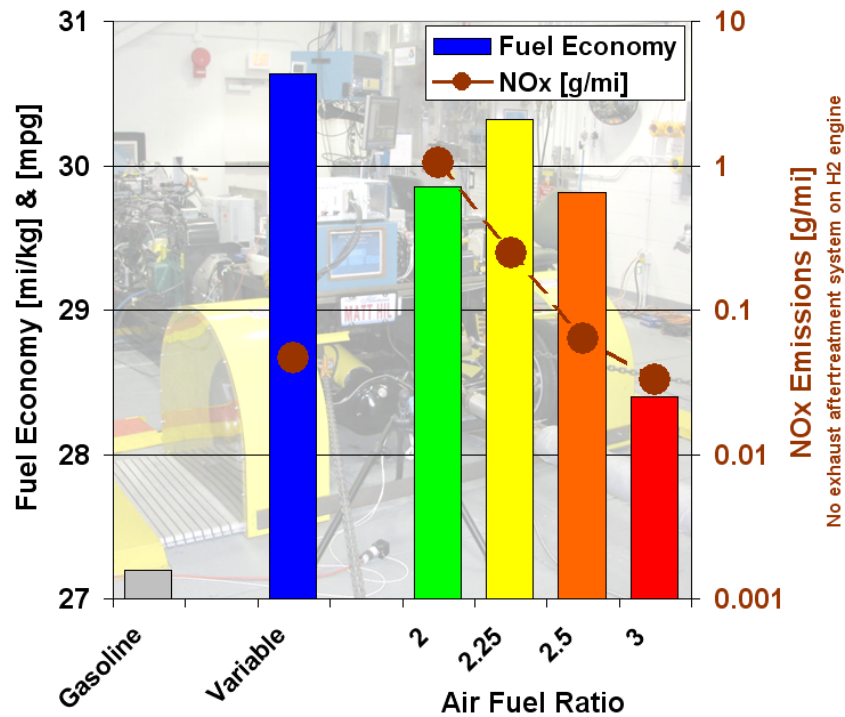
Figure 9-26: Original fuel economy and emissions results measured on the UDDS for each combustion strategy

The fuel economy results show that the variable air fuel combustion ratio strategy did achieve the highest fuel economy in this comparison, as expected. On the constant air fuel ratio strategies, the lambda 2.25 achieved the best fuel economy. The emissions results are very clear and show that the NOx emissions increase exponentially as the air fuel ratio approaches lambda 2, even in the transient operation of the engine. The variable air fuel ratio combustion strategy did produce among the lowest NOx numbers, but the NOx production was still twice as high as it was for lambda 3 combustion.

The cycle average results need to be investigated to explain these fuel trends. Table 9-1 summarizes the test results, such as efficiencies and average component operating values for each combustion strategy. It should also be noted that the engine efficiency trend is fairly close to the fuel economy trend observed.

Table 9-1: Detailed results for the different combustion strategies on the UDDS

	Lambda value		VAR	2	2.25	2.5	3
	Test # (60811XXX)		081	072	078	080	065
	Fuel economy	**[mi/kg]**	**31.22**	**30.63**	**31.08**	**30.76**	**28.88**
Cycle average (excludes idle)	Idle cut off speed	[rpm]	1200	1200	1200	1200	1200
	Average engine speed	[rpm]	1545	1589	1599	1624	1675
	Average engine torque	[N.m]	48.1	42.8	44.8	44.4	43.7
	Average engine power	[kW]	8.2	7.5	8.0	8.0	8.4
	Average engine efficiency	[%]	30.3	28.0	29.3	29.7	29.4
Energy	Fuel energy	[MJ]	28.64	29.19	28.77	29.06	30.96
	Engine crank energy	[MJ]	7.757	7.504	7.659	7.811	8.31
	Motor energy	[MJ]	7.095	7.012	7.147	7.191	7.47
	Drive shaft energy (pos)	[MJ]	5.79	5.88	5.91	5.89	5.94
	Dyno energy (pos)	[MJ]	4.57	4.76	4.73	4.72	4.81
Efficiency	Average Engine efficiency (includes idle time)	[%]	27.1	25.7	26.6	26.9	26.8
	Transmission efficiency	[%]	81.6	83.8	82.7	81.9	79.6
	Rear end	[%]	78.9	81.0	80.0	80.0	80.9

Details on the signal recorded for each test are available in Appendix 9. Further details on the hydrogen engine test results are shown in Appendix 10.

Cycle average engine efficiencies for the different combustion strategies

The average cycle engine efficiency is certainly the main driver for the fuel economy improvements. The engine efficiency across its torque speed domain combined with the actual engine operating areas defines the engine average cycle efficiency for each combustion strategy. The engine efficiency for each combustion strategy was determined by the engine dynamometer data presented earlier. The engine operating areas are determined by the shift schedule used for each calibration. The shift was modified for each combustion strategy. The intent for the shifting was to maintain the highest possible load on the engine while meeting the drive cycle trace. This means that with combustion strategies that enable high torque, the engine was shifted aggressively since the available torque was still high enough to meet the trace. Conversely, in the leanest strategy, the maximum engine torque was so low that the engine speed had to be increases to provide the power required to meet the trace. In lambda 3, the engine ran at WOT conditions during the UDDS to meet the trace.

To understand the average engine cycle efficiency for each combustion strategy, a graph that super-imposes the engine efficiency map with the engine operating range on the drive cycle is helpful. Figure 9-27, Figure 9-28, Figure 9-29, Figure 9-30 and Figure 9-31 show this combined graph for each combustion strategy.

Figure 9-27: Fuel energy consumed over the engine operating range for lambda 2

Figure 9-28: Fuel energy consumed over the engine operating range for lambda 2.25
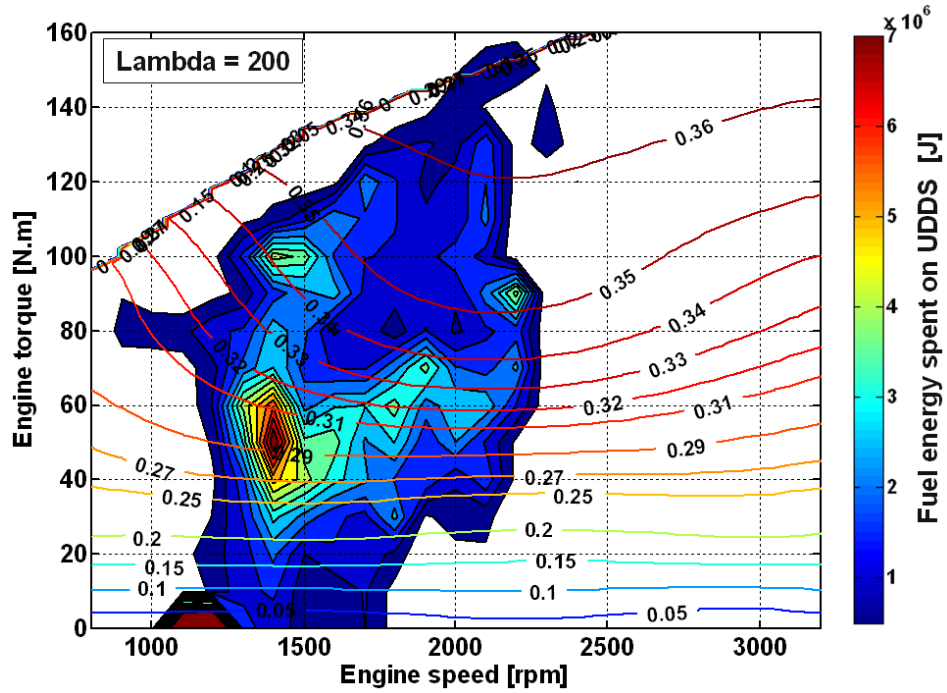
Figure 9-29: Fuel energy consumed over the engine operating range for lambda 2.5
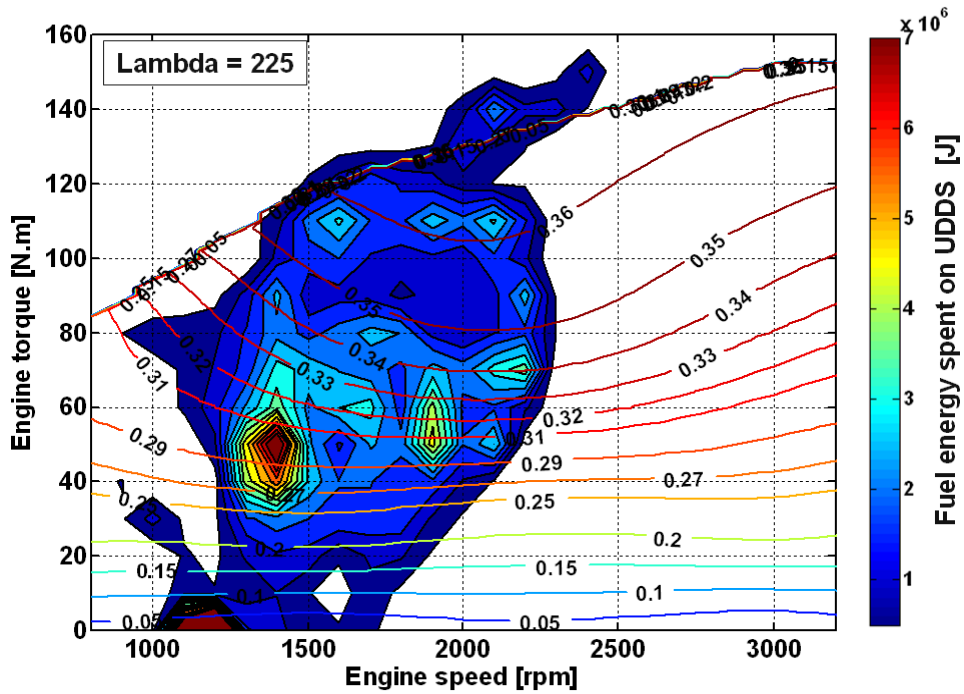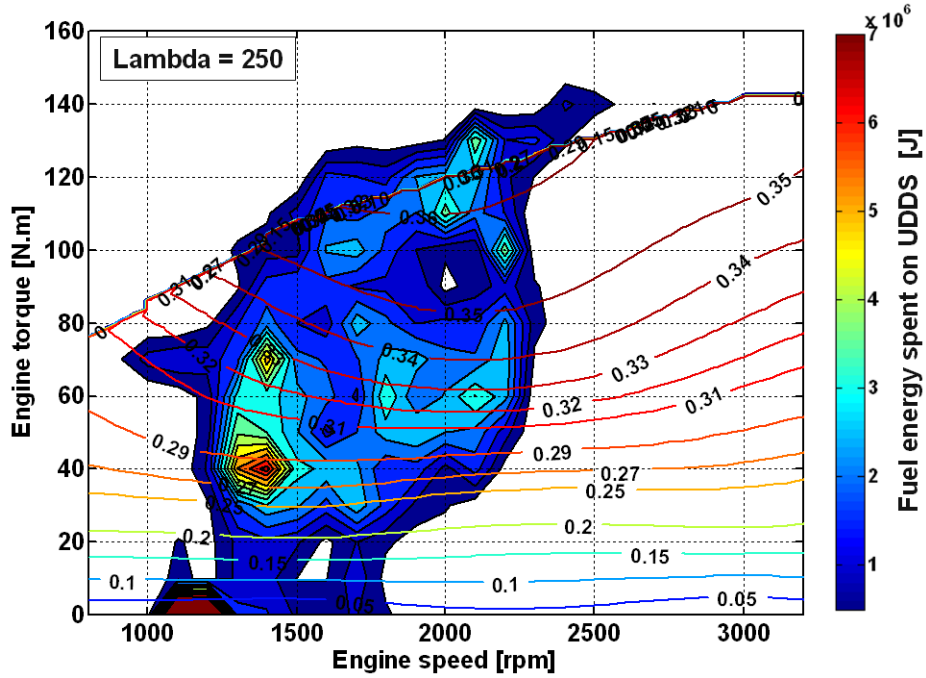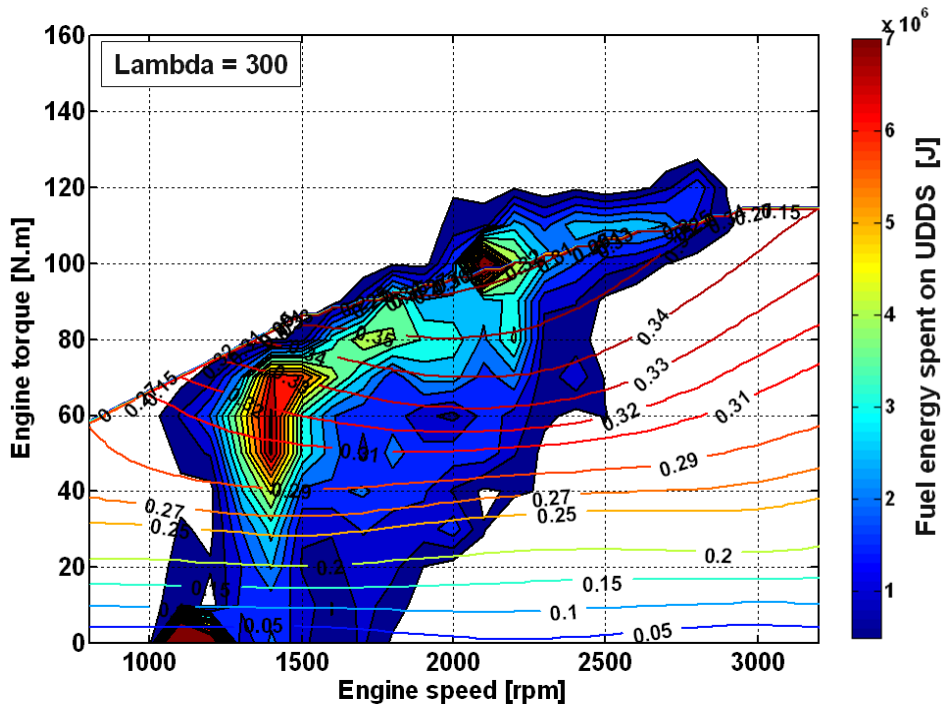

Figure 9-30: Fuel energy consumed over the engine operating range for lambda 3
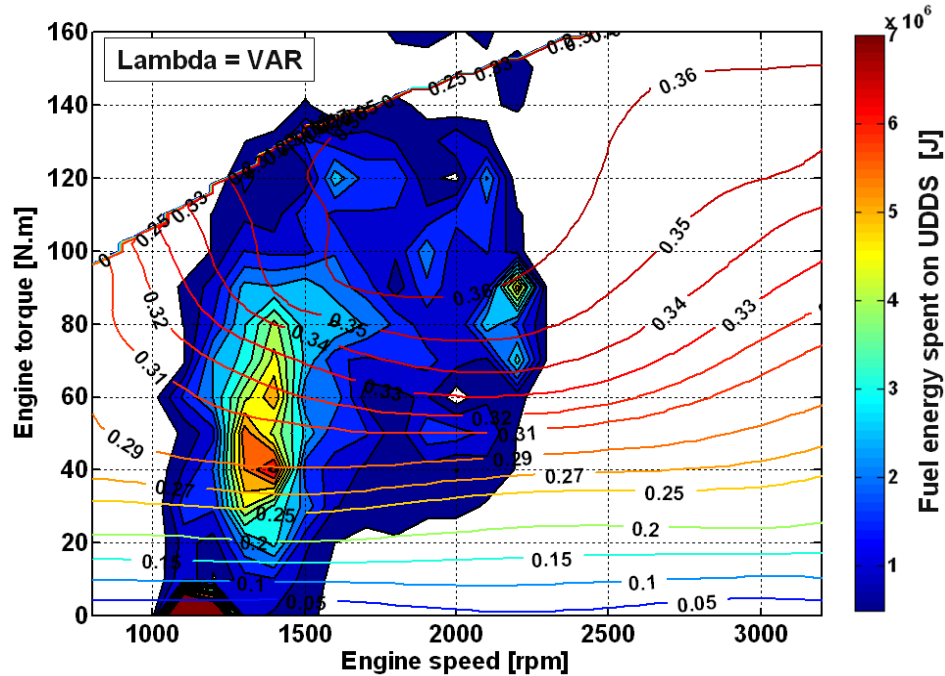
Figure 9-31: Fuel energy consumed over the engine operating range for the variable lambda strategy

On the lambda 2 combustion strategy, the majority of the time the engine operates at just below 1500 rpm at loads varying from 40 to 60 N.m. A smaller amount of energy is used close to the maximum torque, and the maximum speed is 2300 rpm. In contrast, the lambda 3 combustion strategy also spends a lot of energy below 1500 rpm in a medium load range, but a much more significant amount of energy is spent at the maximum available torque at speeds close to 3000 rpm. This provide data to support the theory that in order to compensate for the lack of torque, the leaner combustion strategies have to increase the engine speed to maintain the power output required to meet the drive trace. The variable air fuel combustion strategy engine operation range looks extremely similar to the lambda 2 combustion strategy since enough torque was available to maintain a lower average engine speed and higher engine load. The major difference between the variable air fuel ratio strategy and the lambda 2 combustion strategy is the engine efficiency at the low loads, where the variable combustion strategy runs the more efficient combustion of lambda 3.

Figure 9-32 shows the engine average cycle efficiencies for each combustion strategy. Two efficiencies are shown. The first bar shows the engine efficiency excluding the engine idle time and the second efficiency include the engine idle time. The variable air fuel combustion strategy has the highest engine cycle efficiency. The lambda 2.5 has the next highest engine efficiency. For the constant air fuel ratio combustion strategies, the trade-off appears to be between the maximum engine torque available and the low speed at low to medium load engine efficiency. The maximum engine torque enables higher average engine efficiencies during accelerations and low speed at low to medium load engine efficiency corresponds to cruising where the engine also spends a significant amount of energy on the UDDS in a conventional vehicle.

241
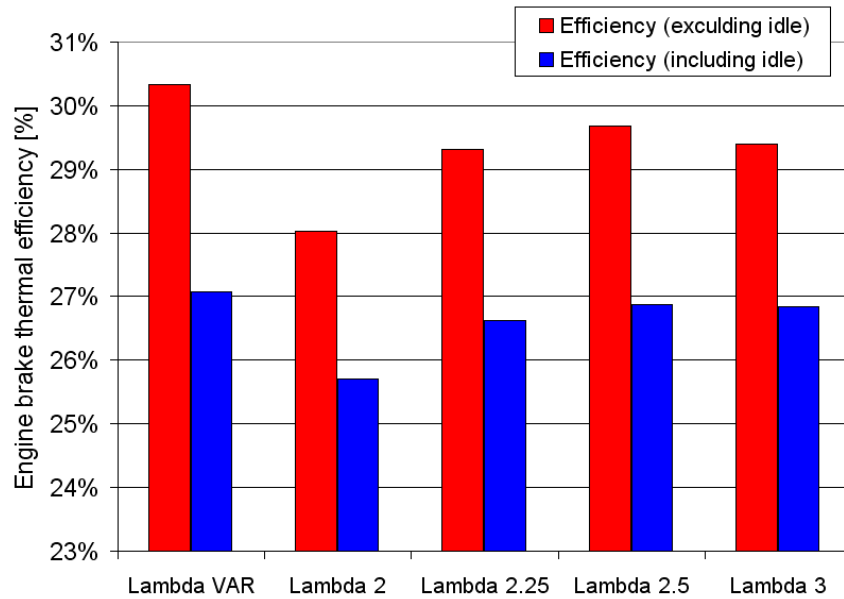
Figure 9-32: Average cycle engine efficiency for the different combustion strategies

It is possible to decompose the test data by acceleration, cruise, deceleration and stopped phases. The acceleration and cruise phases are probably the most interesting phases to consider when analyzing the cycle engine efficiencies. For the purpose of calculating the phase from the data, 1 mph/s was used as the acceleration rate at which the vehicle is considered in acceleration. Table 9-2 shows the results for the variable lambda combustion strategy and the lambda 2 and 3 combustion strategies. For the constant lambda combustion strategies, the highest engine acceleration cycle efficiency is the lambda 2 but the highest engine cruise cycle efficiency is the lambda 3. This supports the data from engine efficiency graphs and the engine operating ranges. Finally, the variable air fuel ratio combustion strategy truly encompasses the best aspects of all of the constant air fuel ratio combustion strategies in the cruise as well as in the acceleration engine efficiency.

Table 9-2: Engine cycle efficiency decomposed into acceleration phases and cruise phases

Lambda strategy	Acceleration	Cruise (|accel|<1 mph/s)	Acceleration and cruise combined
Variable	36.0 %	32.2 %	34,3 %
2	35.3 %	29.8 %	33.3 %
3	35.0 %	31.7 %	33.3 %

Transmission efficiency mistake

The transmission efficiencies are plotted in Figure 9-33. First, the variable air fuel ratio combustion strategy and the lambda 2 combustion strategy should have very similar transmission efficiencies, since their shift pattern were extremely close due to the similar maximum torque curve. Second, the impact of the transmission efficiencies for the constant air fuel ratio combustion strategies is much larger than expected.
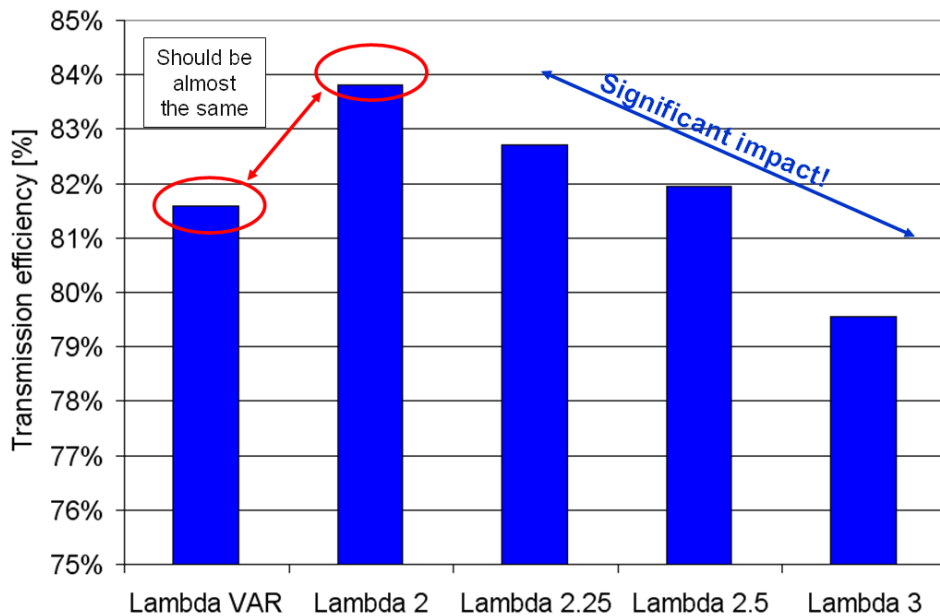
Figure 9-33: Transmission efficiencies for the different combustion strategies

The two problems are due to an oversight in the hardware setup. The automatic transmission controller receives a synthesized transmission torque input signal from the high level controller, as explained in section 5.3.3. The synthesized signal is based on the sum of engine torque and motor torque. The engine torque signal is based on the engine torque command. The torque command for the gasoline engine is based on an open loop look-up table that generates the engine load command. This table was calibrated for the gasoline engine, but should have been recalibrated for each combustion strategy. At lean operating strategies, the high level controller operates as though the torque command is very large compared to the torque command for the lambda 2. This causes an erroneous signal to be sent to the transmission controller, which raises the clamping pressures to transfer the higher torque that the transmission controller expects. This explains the dramatic and linear decreased transmission efficiency trend, and was discovered during the data analysis phase after the hydrogen engine module was removed from MATT.

In order to investigate the issue further, the gasoline engine module was used with the automatic transmission module to repeat the hydrogen engine shift schedules to re-measure transmission efficiencies with the correct calibration setup. A shift schedule for each combustion strategy was stripped from the data sets using a purpose built code. Then, MATT was tested as a conventional vehicle using the exact shift schedules from

the hydrogen engine testing. Figure 9-34 shows the transmission efficiencies measured with the gasoline repeat testing. The efficiencies are in fact much closer to each other, but they are also much lower compared to the hydrogen engine testing. This shows the sensitivity of the transmission losses on the internal operating pressures of the transmission fluid. As mentioned in section 5.3.3, the operating pressure of the transmission fluid was increased in the transmission controller to ensure that the internal clutches would not slip during torque transfer. The higher pressures imply the internal transmission pump requires more power from the shaft, thus lowering the transmission efficiency. This was done after the operating pressure was too low, causing some damage in the transmission.
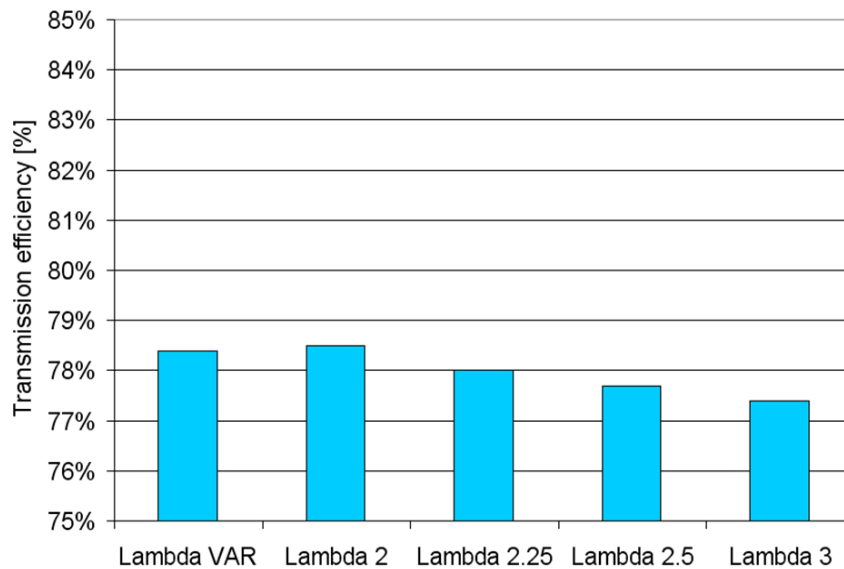
Figure 9-34: The transmission efficiencies based on the hydrogen shift schedules using the gasoline engine module

The repeat engine torque speed profiles performed with gasoline engines using the hydrogen shift schedules were recorded. These engine torque speed profiles would have been the engine torque speed profiles if the appropriate calibrations would have been used with the hydrogen engine. Using the engine efficiency maps produced on the engine dynamometer along with this 10 Hz engine torque speed profile and some interpolation, the hydrogen consumption and fuel economy can be calculated. In order to verify the validity of the process, the engine efficiency maps were used with the engine torque speed profiles from the actual hydrogen testing to calculate the hydrogen fuel economy. Therefore, the calculated fuel economy can be compared to the actual measured fuel economy. The results are shown in Table 9-3. The calculated and the measured fuel economies are within 2% percent of one another, which is extremely good.

Table 9-3: Corrected fuel economy results for the UDDS for the different combustion strategies

Lambda value	VAR	2	2.25	2.5	3
Test # (60811XXX)	081	072	078	080	065
Measured fuel economy [mi/kg]	31.2	30.6	31.0	30.7	28.8
Calculated fuel economy [mi/kg]	31.0	30.4	29.2	29.1	28.3
Corrected fuel economy [mi/kg]	30.0	28.7	29.2	29.1	28.3

Thus the corrected fuel economy can be calculated using the same interpolation technique with the gasoline repeat torque speed profile. The results are also shown in Table 9-3. The variable air fuel ratio combustion strategy provides a 3% fuel economy improvement over the next best combustion strategy.

Emissions results for the different combustion strategies

The emissions results are summarized in Table 9-4. As mentioned earlier, the NOx production increases proportionally as the air fuel ratio gets closer to 2. The transmission calibration mistake has very little impact on the emissions results since the air fuel ratio has the biggest influence on the NOx production as discussed and shown later.

Table 9-4: Measured emissions on the UDDS for the different combustion strategies

Lambda value	VAR	2	2.25	2.5	3
Test # (60811XXX)	081	072	078	080	065
NOx [g/mi]	0.045	1.002	0.242	0.067	0.042
THC [g/mi]	~0	~0	~0	~0	~0

The time plot of the NOx production along with the air fuel ratio provides some interesting insights, as shown in Figure 9-35. Individual excursion where the air fuel ratio drops below 2.5 produces significant NOx, as can be seen in the integrated NOx curve. In fact, the first excursion (highlighted in purple) is a random excursion that is likely due to a fast tip-out and then tip-in. The larger excursion (highlighted in red) as the vehicle comes to stop is a consequence of a crude lower level control code, which works for the gasoline engine without side effects. In the conventional mode, the clutch is opened based on engine speed as the vehicle comes to a stop. The clutch opens when the engine speed is 10% below the set target idle speed. The lower level control code was kept the same for the hydrogen engine. For the hydrogen engine with idle speed, the engine controller enters the idle mode, which modulates the throttle and adjusts the fuel to maintain the target idle speed. When the engine is pulled to 10% below its idle speed, the engine controller adds some extra fuel to maintain the idle speed. This can create a rich excursion (and thus NOx) as the vehicle comes to a stop. These excursions only happen on a minority of all vehicle stops, but when they do they can represent a significant

amount of the NOx production on the cycle, especially on the lean combustion strategies such as lambda 3 or the variable air fuel ratio combustion strategy.
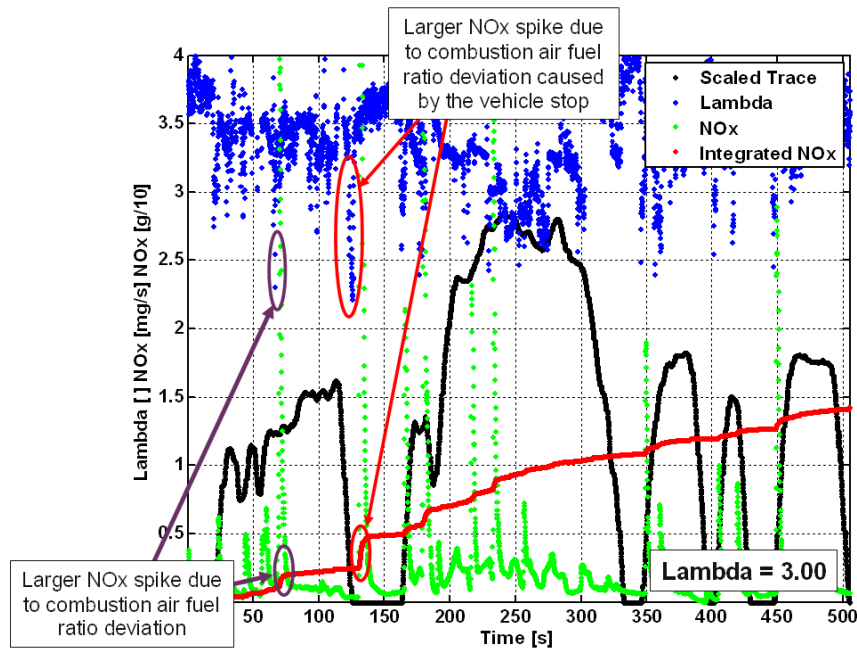
Figure 9-35: NOx production details for the lambda 3 strategy

The variable air fuel ratio combustion strategy case is shown in Figure 9-36. For this data set, the major NOx producing air fuel ratio deviations are the enrichment during high load demands for the accelerations. This shows the variable lambda control working. Comparing the integrated NOx between the lambda 3 case and the variable lambda control case at 150 seconds after hill 1, it appears that the total NOx produced is higher for the lambda 3 case. This is unexpected but explained by NOx production from the rare engine declutching issue.
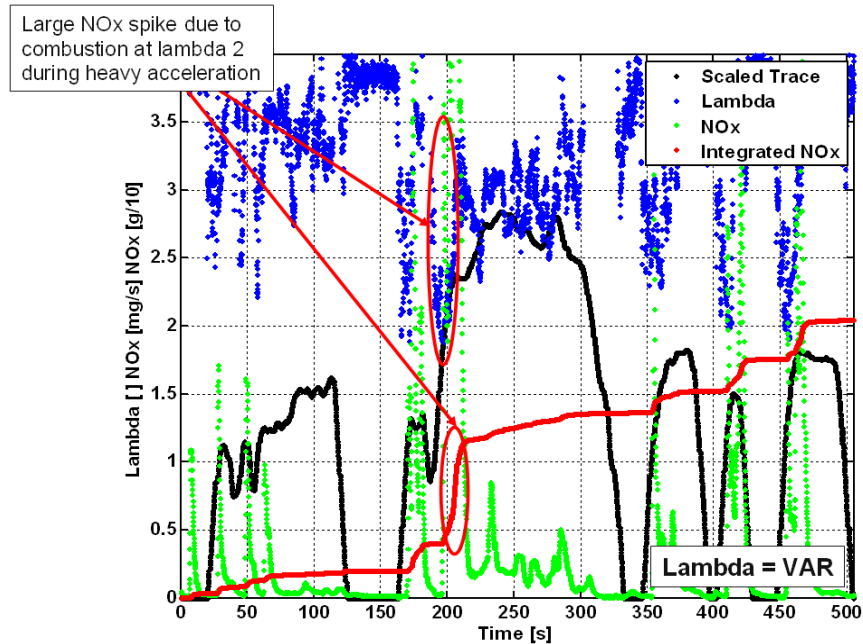
Figure 9-36: NOx production details for the variable air fuel ratio combustion strategy

Performance and drivability

These different lambda strategy provide very different drivability feel and performance levels. Since all of the hydrogen tests were driven by the same driver, a direct comparison can be drawn, although it is still subjective. The lambda 3 strategy requires constant wide open throttle events to meet the trace of the UDDS cycle, which represents only mild driving. Gradually, as the air fuel ratio get closer to 2, the drivability improves with great torque reserve and a certain ease of meeting the trace. The best combustion strategy, from the driver perspective, is the variable lambda control strategy. This strategy is the most controllable on the torque delivery at low loads. Once the maximum torque for the lambda 3 combustion is reached, the high torque is available with the fuel enrichment, which provides much reserved torque for the driver to meet the trace. Figure 9-37 shows the engine torque profiles for the different combustion strategies overlaid on hill 1 of the UDDS. This data provides information that is similar to the driver feedback data. First note that the variable lambda strategy is the smoothest, especially during the cruise conditions between 60 and 70 seconds. The WOTs are also quite recognizable for the lambda 3 strategy.

Figure 9-37: Torque profile of the different combustion strategies to demonstrate drivability

The final metric for comparison is the absolute performance, including the acceleration time from zero speed to 60 mph. Figure 9-38 illustrates individual acceleration performance for the different air fuel ratios.
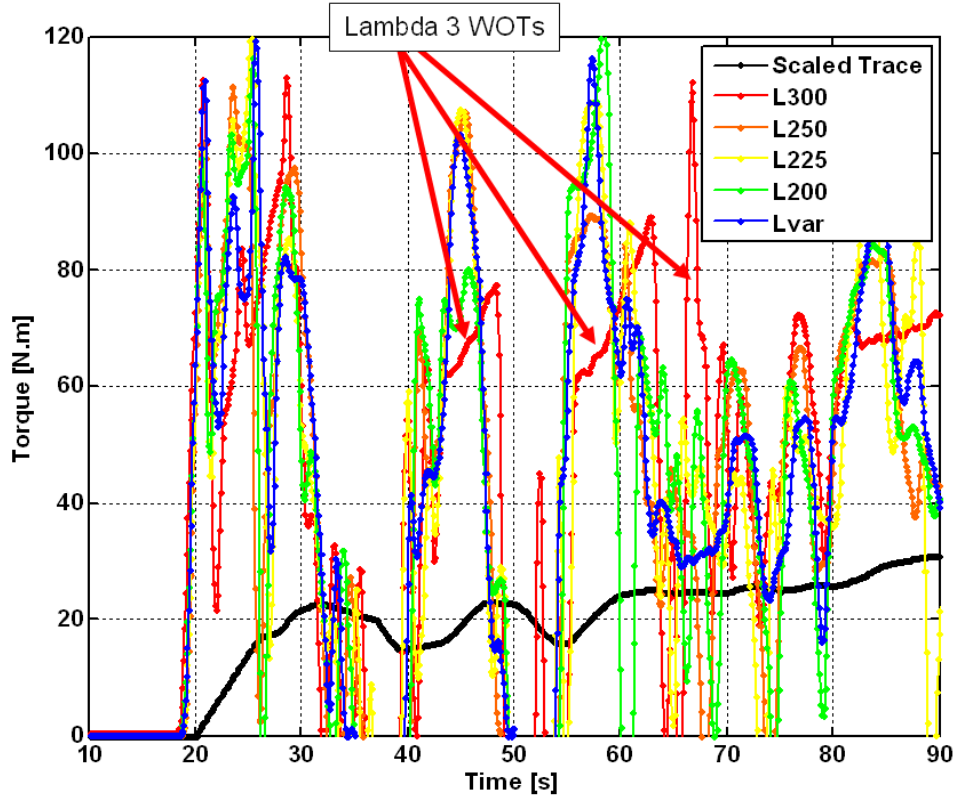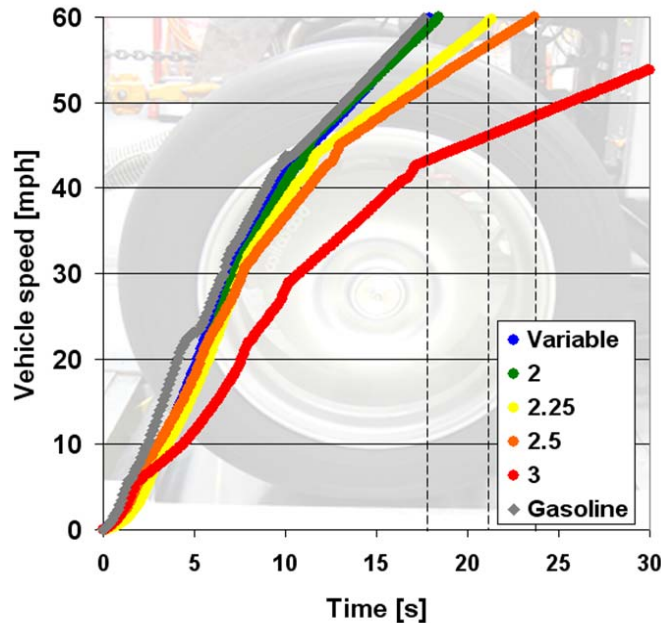
Figure 9-38: WOT performed test results for the different hydrogen combustion strategies

The leanest air fuel ratio has simply unacceptable performance because it requires more than twice as much time as the gasoline engine. The variable combustion strategy provides the same performance as the gasoline engine. The variable air fuel ratio combustion strategy provides the best fuel economy, one of the lowest tailpipe emissions, the best drivability and the best performance of all of the proposed hydrogen combustion strategies.

9.4. Conclusion of hydrogen engine evaluation

In this research application, a supercharged port injected hydrogen engine was first calibrated on a steady state engine dynamometer and then evaluated in a vehicle environment on MATT. The hydrogen engine dynamometer test cell setup had to build up its subsystems, instrumentation and combustion strategies with the 2.3 liter hydrogen engine.

First, the engine was calibrated on four constant air fuel ratios in the hydrogen engine test cell. For each calibration, the engine efficiency map and NOx emissions were established. From those four constant lambda strategies, a variable air fuel ratio combustion strategy was developed to improve efficiency and maintain the low emissions level. At low loads, the engine combustion runs at lambda 3 and the air fuel ratio increases with the load from lambda to lambda 2 as the load request becomes larger than the maximum lambda 3 torque.

The hydrogen engine and the different combustion strategies were tested on MATT in a conventional vehicle environment. The variable air fuel ratio combustion strategy achieved the best fuel economy and one of the lowest emissions. The lambda 3

combustion strategy had the lowest emissions results of ULEV without any catalytic converters. After in-depth analysis, the fuel economy improvements for the variable air fuel ratio combustion strategy are attributed to a combination of the high efficiency at high engine torque for acceleration and the higher efficiency at the extremely lean combustion during the vehicle cruise operation.

MATT was an ideal tool to evaluate the different combustion strategies. The modular integration made the engine implementation easy. The pedal set enabled a human driver to drive for smoother pedal tip-ins and tip-outs. The full instrumentation enabled the comprehensive analysis of the variable air fuel ratio combustion. The instrumentation also provided the immediate feedback required to adapt the steady state dynamometer calibration for transient operation.

The automatic transmission and the calibration complexity were the limiting factors in this application. The transmission calibration was not updated for the hydrogen engine strategies and thus causes some penalty in the transmission efficiencies for some of the hydrogen calibrations. Thanks to the in-depth data collected on MATT as well as on the engine dynamometer, the fuel economy results could be corrected with little effort.

This study was also unique in that a component was developed, researched and calibrated first on a steady state dynamometer and then evaluated in a transient vehicle environment on the standard drive cycles. The full control and flexibility available with MATT enabled a good evaluation of the technology.

10. Limitations

MATT's major limitation is that the component evaluation is only as good as the understanding and control available for the component.

The transmission modules are the weakest link on MATT. The manual transmission is lacking an integrated clutch, which translates into extremely long shift times. These long shift times cause MATT to get behind on meeting the trace, which consequently causes the software driver to command a close to wide open throttle to catch the trace. The automatic transmission shifts fast without torque interruption, but overall efficiency of the transmissions is low and the regenerative braking is limited due to the restriction the transmission. The major limitations of the automatic transmission are caused by the transmission calibration which lacks the refinement of a professional calibration.

But these hardware limitations do not prevent MATT from being a versatile and powerful research tool. The low automatic transmission efficiency is the same limitation present in all of the emulated vehicle types in a study. The manual transmission is launched in 2nd or 3rd gear in the hybrid mode with the traction motor, therefore eliminating the longest shifts (such as the 1st to 2nd gear and 2nd to 3rd gear). The manual transmission is being upgraded by integrating a clutch assembly on the module, as shown in Figure 10-1. The clutch will enable faster shift times.
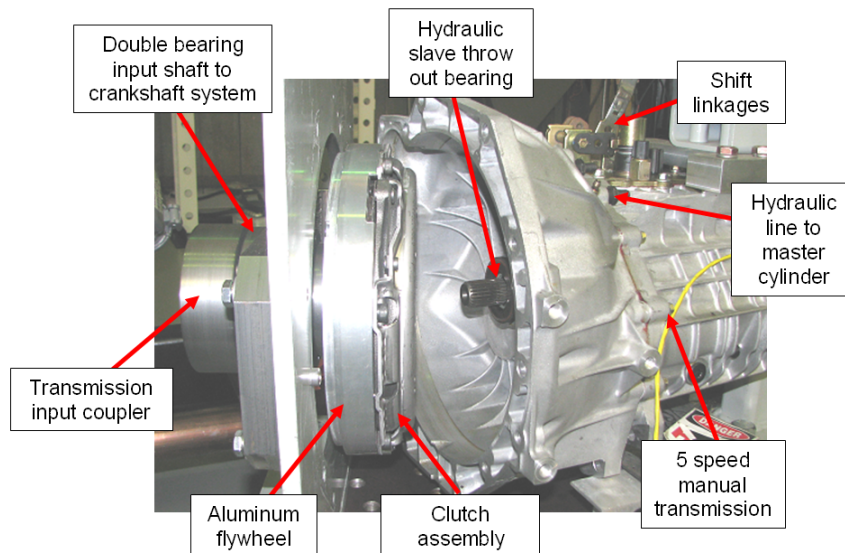

Figure 10-1: Manual transmission with integrated clutch

Another limitation is also linked to the transmission modules. The shifting is performed with a shift schedule that is developed by hand, based on component performance or developed in simulation. For more consistency, a shift algorithm should

251

be developed that could work for different sized vehicles and operation types, including conventional vehicle and hybrid operation.

Another weakness of MATT is the hardware's reliability. Especially during early development, MATT fell victim to several hardware failures. Typically, the input or output shafts of the transmission would break. This was due to a combination of torque spikes caused by the manual transmission speed match shifting logic and the initial aggressive regenerative braking. A number of smaller failures linked to connectors or melted wires also occurred. These issues were resolved and the hardware or software was improved to prevent the failures from happening again. After three years of operation, the reliability is much improved, as proven by the last round of intensive test phases during which over a thousand miles were covered in UDDS and highway cycles without any failures. The development of a new energy management strategy does require a new debugging phase which may wear on the hardware.

In addition to its advantages, MATT's flexibility can also be a disadvantage. The flexibility implies complexity, which impacts MATT's calibration parameters. Component control is continuously improved through tuning and calibration and sometimes even slight algorithm changes. It is therefore possible to omit required recalibration of other components, as shown the hydrogen engine study where the transmission controller command signal had not been remapped for the hydrogen engine. For special comparative studies, it is a common practice to repeat a baseline test at the start of the study to ensure that the same calibrations are used.

Although the simulation software has been used for the plug-in hybrid emissions mitigation study, the simulation tool still needs to become more integrated. This would allow the use of the simulation to explore a wider design space and MATT could be used to spot check some of the simulation cases to provide measured energy consumption and emissions data.

11. Conclusion and Recommendations for Future Work

Conclusions

The goal of this PhD work is to design, build and demonstrate a modular powertrain test bench that can evaluate technology components in a hybrid vehicle system environment. This test bench is also used to evaluate torque split and energy management control strategies by generating hard data on emissions behavior.

The Modular Automotive Technology Testbed (MATT) is the test bench designed, built and demonstrated within this body of work. MATT is composed of component modules, which are combined and clamped to an automotive frame to make up a hybrid vehicle environment. The modular approach enables the testing of different powertrain components and different hybrid configurations in the vehicle system environment. Note that MATT is tested on a chassis dynamometer with a full emissions bench. MATT's high level controller has an open architecture. Any energy management and torque split strategy can be developed in simulation and then implemented on MATT in order to test and measure fuel economy and emissions. This hardware and software flexibility makes MATT such a novel and unique tool. The purpose of the tool is to test new powertrain technology components or to generate hardware-based data for specific automotive research topics.

Based on a review of the existing literature, the candidate has concluded that MATT is a unique and novel tool. MATT is a large-scale powertrain HIL (Hardware-In-the-Loop) system, or vehicle HIL. The virtual scalable energy storage and virtual scalable motor module uses a physical motor powered by the electric grid, which emulates a desired traction motor and energy storage system in a real time simulation. With this, MATT can emulate different sizes and types of vehicles, ranging from conventional to full plug-in hybrid vehicles, without any hardware change. None of the HIL setups use the same modular component approach to build a comprehensive hybrid vehicle environment. Existing technologies include hybrid prototypes, but their powertrain flexibility is limited and their price is typically high. MATT's modular powertrain component approach enables higher flexibility to test different technologies instead of building a more expensive and dedicated prototype mule or component HIL test cell. The open component modules make instrumentation easy, which is very beneficial in this research application. All of these elements make MATT a unique and novel tool for automotive powertrain research.

The hardware was developed in an iterative process over several years. Currently, several powertrain modules are available: a gasoline engine module, a hydrogen engine module, a virtual scalable energy storage and scalable motor module, a manual transmission module and an automatic transmission module. These physical powertrain modules provide the advantage of being able to test emissions and thermal effects, which are impossible to evaluate in computer simulations. The instrumentation establishes a full energy balance of the powertrain components for drive cycles as well as for steady state performance mapping. In addition, MATT was built with integrated systems, as it is an experimental test bench for new technologies. MATT is only operated by trained

operators with access to software feedback and emergency stop switches. Today, the Modular Automotive Technology Testbed is a fully operational tool, as demonstrated by the research investigations and studies detailed in the second half of the dissertation. MATT is shown in Figure 3-6.
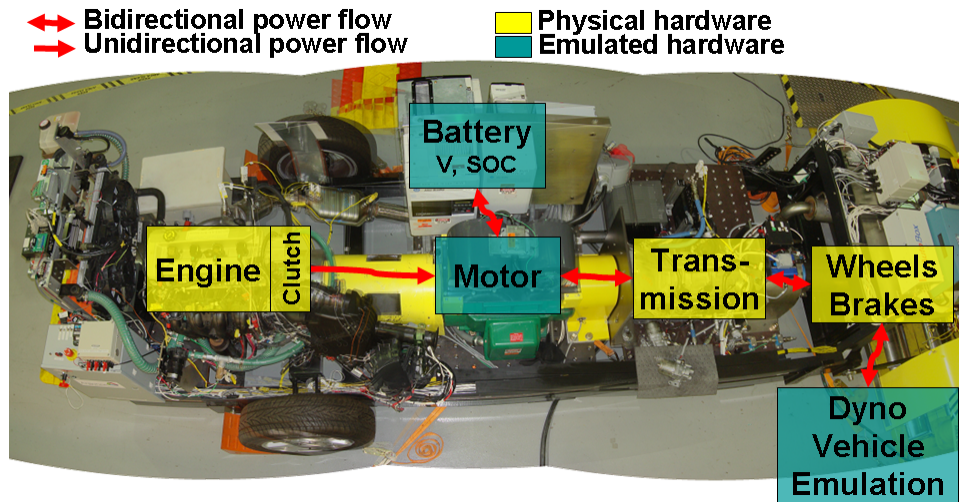

Figure 11-1: MATT with the different component modules

The second objective of this work is to test the conventional vehicle operation. The specific component control for the engine, the clutch, the transmission and the friction brakes are described in detail. The engine and manual transmission efficiency maps are also fully established. The software robotic driver logic is described. Fuel economy and emissions results for a cold start and hot start UDDS cycle are established as the baseline case for future studies. The UDDS cycles are analyzed in detail from the energy and emissions standpoint. Further cycle results are presented for US and international standard cycles, including results for different drive cycle intensities. Several types of vehicle emulations, ranging from a small, efficient vehicle to a larger cross-over SUV, are shown. The conventional vehicle, which is the baseline vehicle operation, has been fully tested and analyzed. For the conventional operation, MATT has proven itself to be a flexible tool that can perform a wide selection of studies while providing comprehensive and in-depth data for the components.

The next objective of the dissertation is to test and analyze the electric vehicle architecture. The battery and motor emulated with the virtual scalable energy storage system and virtual scalable motor module correlate well with a test mule vehicle, using the battery and motor as well as the Battery HIL setup (which tests the physical battery). On the UDDS, the manual transmission module enables an all-electric range of 25.7 miles compared to only 18 miles for the automatic transmission module. The automatic transmission module is handicapped by a lack of refinement in the calibration as well as the hardware limitations involved with transferring reverse torque at low speeds. Two studies are performed with the electric vehicle operation. First, it is determined that a

10% penalty is associated with a cold start in the electric vehicle operation using the manual transmission. Second, the hardware has proven itself capable of emulating both a small and a large vehicle. Again, even in electric vehicle operation, MATT is a flexible tool that can perform a wide variety of studies while providing comprehensive and in-depth data for the components.

The next objective is to operate MATT as a hybrid vehicle. Chapter 5 details the development of the first hybrid operating mode that uses MATT. These simple operating modes evolve into fully integrated energy management and torque split strategies. MATT emulates a simple engine idle stop hybrid, an engine dominant hybrid with electric assist and several different full hybrid operations. All of the hybrid modes are tested and the results are shown and analyzed. The fully integrated hybrid strategy is capable of two modes; the 'engine optimum' hybrid control, where the engine is loaded to operate at high efficiencies and the 'load following,' where the engine provides the tractive effort without excess charging of the battery pack. For both strategies, the full charge test data is presented and analyzed rigorously. In conclusion, by changing the software, MATT's hardware enables it to behave in extremely different hybrid modes. The open controller approach makes MATT unique since it gives the researcher the ability to program numerous hybrid behaviors.

Four different, very specific and important PHEV studies are performed using MATT with different energy management strategies and several hardware setups.

The first PHEV study has the most impact, since it directly influenced a much-discussed issue between CARB and the SAE J1711 committee concerning the newly proposed plug-in hybrid test procedures. The study provides data that shows that a proposed correction method for the cold start on the full charge highway test set does not work for all plug-in cases. In this study, for an extreme charge depleting blended plug-in hybrid, simulation is necessary. As a direct result of the study, the proposed and much discussed correction method was abandoned. An alternative method, using a charge sustaining switch, is proposed and tested, but the manufactures did not agree on implementing a charge sustaining switch. A senior test engineer at CARB working on the test procedures was impressed by the quality of the data and the in-depth analysis provided on this timely research study.

The second PHEV study investigates the soak time between tests for a full charge plug-in hybrid evaluation. It is found that the soak time does have an impact on the energy consumption, but the effect is so small that it is insignificant. There is no impact on emissions. This study provides data to support the test procedure development committee in their decision to allow a wide range of soak times between tests.

The third PHEV study provides insights about the impact of drive cycle intensity on energy consumption for electric vehicle capable plug-in hybrids. No electric plug-in hybrid is available for testing today and thus, only MATT can provide data to show that the electric consumption increases with the drive cycle intensity. The opposite is true for blended plug-in hybrids. Therefore, with electric capable plug-in hybrids, the petroleum displacement benefits are maintained or increased as driving aggressiveness increases. This is not the case for blended plug-in hybrid vehicles. This work also completes the

255

wide range of drive cycle intensity research for MATT as a conventional vehicle, a charge sustaining hybrid and a plug-in hybrid. The data set shows the potential of plug-in hybrids to displace up to 60% of petroleum at driving intensity levels on the UDDS cycle.

The final PHEV study is the most in-depth and comprehensive piece of plug-in research using MATT. This research focuses on engine control of blended and electric vehicle capable plug-in hybrids and the impact on emissions. The importance of warm up for the engine and the exhaust after-treatment system is shown in a first phase. Based on the first data set, some engine warm up routines and an engine loading strategy are developed to mitigate the emissions spikes causes by the engine usage of plug-in hybrids. The emissions for both plug-in hybrid types are well within the SULEV limits. The results show the success of the warm up routines in mitigating emissions for plug-in hybrids. The major results are summarized in Figure 8-36.
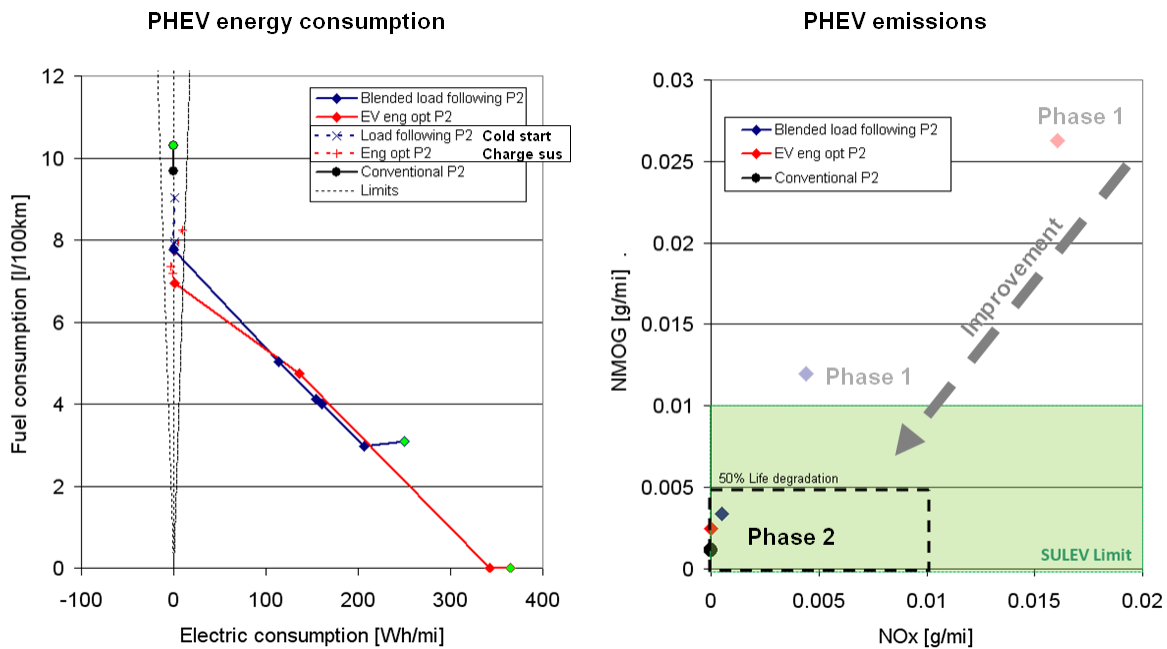

Figure 11-2: PHEV emissions improvement achieved with the energy management strategies

The final objective of the dissertation is to demonstrate the evaluation of a new technology component such as a hydrogen internal combustion engine. In this research application, a supercharged port injected hydrogen engine is first calibrated on a steady state engine dynamometer and then evaluated in a vehicle environment on MATT. First, the engine is calibrated on four constant air fuel ratios in the hydrogen engine test cell. From those four constant lambda strategies, a variable air fuel ratio combustion strategy is developed to improve efficiency and maintain a low emissions level. At low loads, the engine combustion runs at lambda 3 and the air fuel ratio increases with the load from lambda to lambda 2 as the load request becomes larger than the maximum lambda 3 torque.

256

The hydrogen engine and the different combustion strategies are tested on MATT in conventional vehicle operation. The variable air fuel ratio combustion strategy achieves the best fuel economy and one of the lowest emissions, as shown in Figure 11-3. The lambda 3 combustion strategy has the lowest emissions results of ULEV without any catalytic converters. After an in-depth analysis, the fuel economy improvement of the variable air fuel ratio combustion strategy is attributed to a combination of the high efficiency at high engine torque for acceleration and the higher efficiency at the extremely lean combustion during the vehicle cruise operation. This study is also unique in that a component is developed, researched and calibrated first on a steady state dynamometer and then in a transient vehicle environment on the standard drive cycles. The ability to have full control of MATT's components enables a good evaluation of the technology.
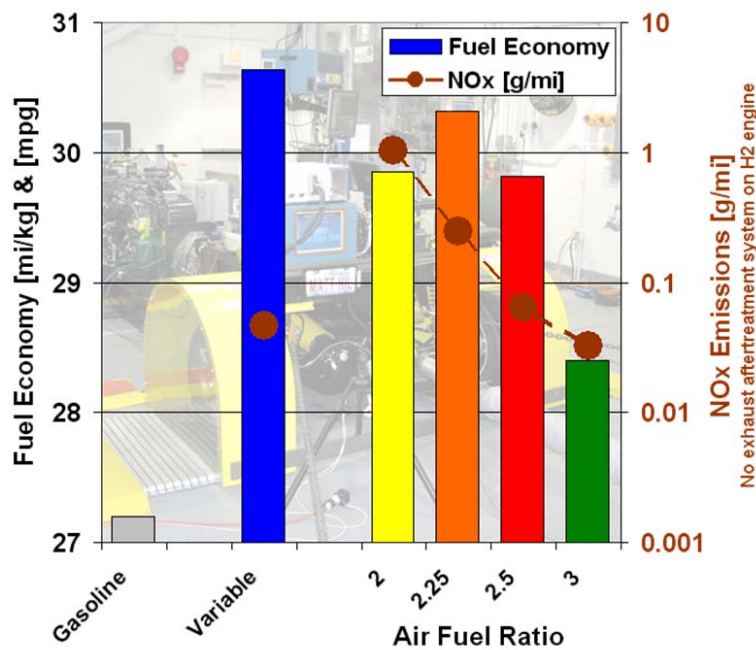

Figure 11-3: Fuel economy and emissions results achieved with the hydrogen engine on the UDDS

All of these studies are very focused and specific, but used MATT as the primary tool to generate data. Several key components enable MATT to be such a flexible tool:

- The open controller approach, which enables MATT to behave exactly as the studies require. Each study uses a different control.

- The in-depth instrumentation, which provides comprehensive data for analysis of each investigation.

- The virtual scalable energy storage system and virtual scalable motor module, which enables MATT to behave like an electric capable plug-in

hybrid. It also allows the setting of identical initial conditions for test repeatability.

- The repeatability of the software robotic driver, which provides consistent and repeatable drive cycle results, even months apart.

- Versatility of operating as a conventional vehicle, an electric vehicle, and many types of hybrid and plug-in hybrid vehicles using the exact same hardware set.

- The possibility of driving the MATT with a manual pedal set provides extra flexibility.

- MATT has a physical engine that produces real emissions and is submitted to real thermal effects. These conditions are extremely difficult to achieve in simulation.

Recommendations for future work

By integrating a clutch into the manual transmission module, this issues raised by the transmission modules will be solved. Another suggested improvement is a better integration of the simulation software so that studies can be approached in a more comprehensive manner.

On the PHEV research, further investigation into the plug-in hybrid operation and tailpipe emissions would be beneficial. Further research into the impact of different hybrid strategies on emissions would broaden the understanding of emissions production in hybrid vehicles.

On the hydrogen engine module, hybridization would be the natural extension of the current work. The hybrid system could be used to overcome the lack of power of the lambda 3 combustion. Thus, a hybrid hydrogen vehicle could provide very low emissions while still performing at an acceptable level.

In the long term, it would be interesting to investigate a post transmission architecture by simply swapping the hybrid module with the transmission module. Another possible additional feature for MATT would be a belted or integrated starter-alternator on the engine module. This would provide a series path on MATT and therefore enable another major hybrid operation mode.

Reference list

INTRODUCTION

Ref. 1 Bureau of transportation statistic, National Transportation Statistics , http://www.bts.gov/publications/national_transportation_statistics/html/table_01_11.html

Ref. 2 Greene, Leiby, Patterson, Plotkin and Singh , 'Oil Independence: Achievable National Goal or Empty Slogan?' TRB 2007 Annual Meeting, http://www1.eere.energy.gov/ba/pba/pdfs/oil_independence_report.pdf

Ref. 3 Robert L. Hirsch, Atlantic Council Workshop on Transatlantic Energy Issues , 'Peaking of World Oil Production: An Overview ' October 26th 2006 Energy bulletin

Ref. 4 ASPO (Association for the Study of Peak Oil and Gas), Newsletter No. 85 – January 2009

Ref. 5 Deffeyes, Kenneth S (2007-01-19). "Current Events - Join us as we watch the crisis unfolding". Princeton University: Beyond Oil. http://www.princeton.edu/hubbert/current-events.html. Retrieved on 2008-07-27.

Ref. 6 Cohen, Dave (2007-10-31). "The Perfect Storm". ASPO-USA. http://www.aspo-usa.com/index.php?option=com_content&task=view&id=243&Itemid=91. Retrieved on 2008-07-27.

Ref. 7 Boone Pickens Warns of Petroleum Production Peak". Association for the Study of Peak Oil and Gas. 2005-05-03

Ref. 8 Medium-Term Oil Market Report". IEA. 2007-07. http://omrpublic.iea.org/

Ref. 9 Peter Glover (2008-01-17). "Aramco Chief Debunks Peak Oil". Energy Tribune. http://www.energytribune.com/articles.cfm?aid=764. Retrieved on 2008-07-10.

Ref. 10 Lynch Michael C (2004). "The New Pessimism about Petroleum Resources: Debunking the Hubbert Model (and Hubbert Modelers)" (PDF). American Geophysical Union, Fall Meeting 2004. http://www.energyseer.com/NewPessimism.pdf.

Ref. 11 Mouawad, Jad (2007-03-05). "Oil Innovations Pump New Life Into Old Wells". New York Times. http://www.nytimes.com/2007/03/05/business/05oil1.html.

Ref. 12 Leonardo Maugeri (2004-05-21). "Oil: Never Cry Wolf—Why the Petroleum Age Is Far From Over". Science (Science) 304. no. 5674, pp. 1114 - 1115: 1114. doi:10.1126/science.1096427. PMID 15155935. http://www.sciencemag.org/cgi/content/summary/304/5674/1114.

Ref. 13 "Clearing the Air". The Surface Transportation Policy Project. 2003-08-19. http://www.transact.org/report.asp?id=227. Retrieved on 2007-04-26.

Ref. 14 "Emission Facts". United States Environmental Protection Agency. http://www.epa.gov/otaq/consumer/f00013.htm.

Ref. 15 EPA http://www.epa.gov/air/caa/peg/carstrucks.html

Ref. 16 Michael Schesinger, "Summary Material: The relationship between Human Activity and Climate Change', Climate Change Group, University of Illinois at Urbana-Champaign and The Intergovernmental Panel on Climate Change, May 2008

Ref. 17 Fred Singer, "Nature, Not Human Activity, Rules the Climate, Summary for Policymakers", Nongovernmental International Panel on Climate Change, April 2008

Ref. 18 Wang M., 'GREET Is A Standard Tool for Well-to-Wheel Analyses of Vehicle/Fuel Systems',
http://www.transportation.anl.gov/modeling_simulation/GREET/greet_gold_standard.html

Ref. 19 Barry Winfield "2003 Dodge Stratus vs. Honda Accord, Hyundai Sonata, Kia Optima, and Six More Mid-Size Sedans", Test results, Car and Driver, February 2003

Ref. 20 Patrick Bedard, "Honda Accord Hybrid - Road Test", Test results, Car and Driver, December 2004

Ref. 21 Passier G., "Status Overview of Hybrid and Electric Vehicle Technology (2007)", Final report Phase III, Annex VII Hybrid vehicles, International Energy Agency, December 2007

Ref. 22 Duoba M. H. Lohse-Busch, and T. Bohn, 2005. 'Investigating Vehicle Fuel Economy Robustness of Conventional and Hybrid Electric Vehicles.', Electric Vehicle Symposium 21, Monaco. April 2–6.

Ref. 23 Light-Duty Automotive Technology and Fuel Economy Trends:1975 Through 2008, Executive Summary Office of Transportation and Air Quality U.S. Environmental Protection Agency, EPA420-S-08-003, September 2008

Ref. 24 H. Hanselmann, 'Hardware-In-The-Loop Simulation as a Standard Approach for the Development, Customization, and Production Test of EcuS', SAE 931953, International Pacific Conference On Automotive Engineering, November 1993, Phoenix, AZ

Ref. 25 N. O. Tiffany, G. A. Cornell, R. L. Code, 'Hybrid Simulation of Vehicle Dynamics and Subsystems', SAE-700155, February 1970

Ref. 26 R. A. Grimm, R. J. Bremer, F. J. Jain, W. A. Levijoki, General Motors Corp, 'Evaluation of Vehicle Installed Wheel Lock Control Hardware With a Hybrid Computer Simulation', SAE 770098, February 1977

Ref. 27 Deborah J. Kempf, Loren S. Bonderson, Loren I. Slafer, 'Real Time Simulation for Application to ABS Development', SAE-870336, February 1987

Ref. 28 H. Hanselmann, 'Hardware-In-The-Loop Simulation as a Standard Approach for Development, Customization, and Production Test', SAE-930207, SAE International Congress, March 1993, Detroit, MI, USA

Ref. 29 Hans-Jurgen von Thun, 'A New Dynamic Combustion Engine Test Stand With Real-Time Simulation of the Vehicle Drive Line', SAE-870085, June 1987

Ref. 30 Ford Motor Company, Midwest Research Institute, 'Final Technical Report, Systems Integration / Vehicle Test Phase Report (Phase IV), US Hybrid Propulsion Systems Development Program, December 1999 – US DOE contract # DE-AC36-83CH10093, section 8Hardware-in-the-Loop (HITL), p8-1 to 8-11

Ref. 31 Judy Che, Poyu Tsou, Mark Jennings, Lawrence Rose,'Dual Drive Hybrid System Vehicle Model Development', SAE-2009-01-0147, SAE World Congress, April 2009, Detroit, MI

Ref. 32 Quan-Zhong Yan, Fasal Queslati, Jim Bielenda and John Hirshey, Chrysler Corp., 'Hardware in the Loop for a Dynamic Driving System Controller Testing and Validation', SAE-2005-01-1667, SAE world congress, April 2005, Detroit, MI

Ref. 33 Nabi, Syed; Balike, Mahesh; Allen, Jace; Rzenien, Kevin. "An Overview of Hardware-In-the-Loop Testing Systems at Visteon." SAE 2004-01-1240. Detroit, MI, March 8-11, 2004.

Ref. 34 Kalyana Chakravarthy, C. S. Daw and J. C. Conklin, 'Intra-Channel Mass and Heat-Transfer Modeling in Diesel Oxidation Catalysts', SAE-2002-01-1879, Future Car Congress, June 2002, Crystal City VA.

Ref. 35 Zoran Filipi, Hosam Fathy, Jonathan Hagena, Alexander Knafl, Rahul Ahlawat, Jinming Liu, Dohoy Jung, Dennis Assanis, Huei Peng and Jeffrey Stein, Engine-in-the-Loop Testing for Evaluating Hybrid Propulsion Concepts and Transient Emissions – HMMWV Case Study, SAE paper 2006-01-0443, SAE congress 2006, Detroit Michigan. Automotive Research Center, University of Michigan.

Ref. 36 Zoran Filipi, Engine-in-the-Loop Testing for Evaluating Hybrid Emissions in Truck Applications, SAE presentation, 2006 Hybrid Vehicle Symposium

Ref. 37 Filipi, Z., Hagena, J., Fathy, H., Assanis, D., Stein, J., "Investigating Effects of Transients on Diesel Emissions using Engine-in-the-Loop Testing", THIESEL 2006, Conference on Thermo- and Fluid Dynamic Processes in Diesel Engines, Valencia, Spain, Sept. 2006

Ref. 38 Liu, J., Peng, H., Hagena, J., Filipi, Z.,"Engine-in-the-loop study of the stochastic dynamic programming optimal control design for a hybrid electric HMMWV", International Journal of Heavy Vehicle Systems, Volume 15, Number 2-4/2008, Pages: 309-326

Ref. 39 Joe Steiber, Bapiraju Surampudi, Ben Trichel and Mike Kluger, Vehicle HIL, The Near Term Solution for Optimizing Engine and Transmission Development, SAE paper 2005-01-1050, 2005

Ref. 40 Cameron Massey, Arthur Bekaryan, Ping Lu - HRL Laboratories LLC, Antony Parulian - Arbin Instruments, Damon Frisch, Trudy Weber, Mark Verbrugge - General Motors Corp, Hardware-in-the-Loop Testing for Electrochemical Cells in Hybrid Electric Vehicles', SAE 2005-01-3500 , 2005 Commercial Vehicle Engineering Conference, Rosemont, IL

Ref. 41 Martin Ganchev, Arno Ebner, Claus-Juergen Fenz, Ulf Riesenbiecher, Arsenal Research, 'Hardware and software platform for rapid prototyping of electric vehicles', EVS-22 Yokohama, Japan, Oct. 23-28, 2006, The 22nd International Battery, Hybrid and Fuel Cell Electric Vehicle Symposium & Exposition

Ref. 42 Neeraj Shidore, T Bohn, M Duoba, H Lohse-Busch, P Sharer, 'PHEV 'All electric range' and fuel economy in charge sustaining mode for low SOC operation of the JCS VL41M Li-ion battery using Battery HIL', EVS-23, December 2-5, 2007 in Anaheim, California

Ref. 43 Neeraj S. Shidore, Theodore Bohn, 'Evaluation of cold temperature performance of the JCS-VL41M PHEV battery using Battery HIL', SAE 2008-01-1333, World congress, April 2008, Detroit, MI

Ref. 44 Argonne National Laboratory's PSAT (Powertrain System Analysis Toolkit) http://www.transportation.anl.gov/ modeling_simulation/PSAT/index.html

Ref. 45 Hybrid Committee, 'Recommended Practice for Measuring the Exhaust Emissions and Fuel Economy of Hybrid-Electric Vehicles', SAE J1771 Standards, In-progress, renewal not yet published

Ref. 46 Maxime Pasquier, Mike Duoba, Keith Hardy, Aymeric Rousseau, and Dave Shimcoski, 'Evaluation of a CIDI Pre-Transmission Parallel Hybrid Drivetrain with CVT', Electric vehicle symposium 19, October 2002, Busan, Switzerland

Ref. 47 Sung Chul Oh, Justin Kern, Ted Bohn, Aymeric Rousseau, and Maxime Pasquier, 'Axial Flux Variable Gap Motor: Application in Vehicle Systems, SAE 2002-01-1088, World Congress, Detroit MI

Ref. 48 Pasquier Maxime, Monnet Gilles, 'Diesel Hybridization and Emissions' Summary report to U.S. Department of Energy, ANL/ES/RP-113184 / DOI 10.2172/834705. April 2004

Ref. 49 M. Pasquier, 'Continuously Variable Transmission Modifications and Control for a Diesel Hybrid Electric Powertrain', SAE Paper 2004-34-2896, SAE 2004 International Continuously Variable and Hybrid Transmission Congress, September 2004, San Francisco CA USA.

Ref. 50 Rousseau, A., and Larsen, R., 'Simulation and Validation of Hybrid Electric Vehicles Using PSAT', Global powertrain conference, June 2000, Detroit, MI

Ref. 51 M. Pasquier and A. Rousseau, 'PSAT and PSAT-PRO, an Integrated and Validated Toolkit from Modeling to Prototyping,' SAE- 2001-01P-178, SAE World Congress, March 2001, Detroit, MI

Ref. 52 Rousseau, Aymeric; Sharer, Phil; Pasquier, Maxime, 'Validation Process of a HEV System Analysis Model: PSAT', SAE-2001-01-0953, SAE World Congress, March 2001, Detroit, MI

Ref. 53 EV world, 'Quebec Advanced Transportation Institute Opens New Lab', Press Release, May 2009.

Ref. 54 L'Institut du transport avancé du Québec (ITAQ), 'UNIQUE ADVANCED TRANSPORTATION INFRASTRUCTURES IN CANADA', http://www.itaq.qc.ca/en/profile-equipment-advanced-transport.php?id=5, printed on May 2009,

Ref. 55 Salem Mourad, Edwin van de Eijnden, Darren Foster, Rinie van Helden, Marcel Rondel, Peter Schmal, 'How to simultaneously achieve low emissions and high efficiency in a parallel hybrid powertrain', EVS 18, 2001, Berlin, Germany

Ref. 56 Graham, R., et al. 2001. Comparing the Benefits and Impacts of Hybrid Electric Vehicle Options, Final Report. Electric Power Research Institute Report EPRI 1000349, Palo Alto, CA.

Ref. 57 Plotkin, S., et al. 2001. Hybrid Electric Vehicle Technology Assessment: Methodology, Analytical Issues, and Interim Results. Argonne National Laboratory Report ANL/ESD/02-2, Argonne, IL.

Ref. 58 http://en.wikipedia.org/wiki/Hybrid_vehicle

Ref. 59 D.J. Santini, A.D. Vyas, J.L. Anderson, 'Fuel Economy Improvement via Hybridization vs. Vehicle Performance Level', SAE 02-FCC-27, Future Car Congress, June 2002, Washington, DC.

Ref. 60. http://www.autoblog.com/2009/01/20/ironic-legislation-carb-ruling-to-kill-aftermarket-plug-in-hybr/

Ref. 61 Duoba M., 'Hybrid NOx Excursions', Argonne Internal presentation, May 2005, Argonne IL

Ref. 62 Won, Jong-Seob; Langari, Reza; Ehsani, Mehrdad. "An Energy Management and Charge Sustaining Strategy for a Parallel Hybrid Vehicle With CVT." IEEE Transactions on Control Systems Technology. Volume 13, No. 2, March 2005.

Ref. 63 Niasar, Abolfazl Halvaei; Moghbelli, Hassan; Vahedi, Abolfazl. "Drive Train Sizing and Power Flow Control of a Series-Parallel Hybrid Electric Vehicle."

Ref. 64 Jaura, Arun K.; Buschhaus, Wolfram; Tamor, Michael A. "Systems Approach in Achieving Higher Fuel Economy in Hybrid Vehicles." SAE 2000-01-1585 Future Car Congress, April 2000, Crystal City, VA, USA

Ref. 65 Boyd, Steven, and Douglas J. Nelson. "Hybrid Electric Vehicle Control Strategy Based on Power Loss Calculations." SAE 2008-01-0084, SAE World congress, April 2008, Detroit, MI

Ref. 66 Tamai, Goro. "Development of the Hybrid System for the Saturn VUE Hybrid." SAE 2006-01-1502, 2006.

Ref. 67 Hanyu, Tomoyuki. "A Study of the Power Transfer Systems for HEVs." SAE 2006-01-0668, SAE World Congress, April 2006, Detroit MI

Ref. 68 Koichiro Muta, Makoto Yamazaki, Junji Tokieda, 'Development of New-Generation Hybrid System Ths Ii-Drastic Improvement of Power Performance and Fuel Economy', SAE-2004-01-0064, World congress, March 2004, Detroit, MI

Ref. 69 Boyd, Steven, "Hybrid Electric Vehicle Control Strategy Based on Power Loss Calculations.", Master thesis, Mechanical Engineering, Virginia Tech, August 2006

Ref. 70 Chu, Liang; Wang, Qingnian; Li, Minghui Lui Jun. "Control Algorithm Development for Parallel Hybrid Transit Bus." IEEE 0-7803-9280-9/05, 2005.

Ref. 71 Huang, Miaohua; Yu, Houyu. "Optimal Energy Management Strategy for Parallel Hybrid Electric Vehicles." EVS-22 Yokohama, Japan, Oct. 23-28, 2006.

Ref. 72 Oh, Kyoungcheol; Kim, Youngchul; Min, Junhong; Choi, Donghoon; Kim, Hyunsoo. "Optimization of Control Strategy for a Hard Type Parallel Hybrid Electric Vehicle." EVS-22 Yokohama, Japan, October 23-28, 2006.

Ref. 73. Gao, Haiou; Xu, Shunyu; Gao, Xuefeng. "Vehicle Control System Design for a Parallel Hybrid Electric Vehicle.", Electric Vehicle Symposium 21, Monaco, France

Ref. 74 Duoba M. H. Lohse-Busch, and T. Bohn, 2005. Investigating Vehicle Fuel Economy Robustness of Conventional and Hybrid Electric Vehicles. Proc. of the EVS-21, the 21st Worldwide Battery, Hybrid and Fuel Cell Electric Vehicle Symposium and Exposition, Monaco. April 2–6.

Ref. 75 Stiegeler, Markus; Rohr, Stephan; Kabza, Herbert. "Basic Gear Shifting Method for Automatic Gear Box in Mild-Hybrid Vehicles Using Cost Functions', Electric Vehicle Symposium 21, Monaco, France

Ref. 76 Amano, Masahiko; Gopal, Ram V.; Matsuo, Takeshi; Hayashi, Masaaki. "Practical Optimization of Energy Management for Parallel Hybrid Electric Vehicles.", Electric Vehicle Symposium 20, September 2003, Long Beach, CA

Ref. 77 Koot, Michiel; Kessels, J.T.B.A.; de Jager, Bram. "Fuel Reduction of Parallel Hybrid Electric Vehicles." IEEE 0-7803-9280-9/05, 2005.

Ref. 78 Johnson, Valerie H.; Wipke, Keith B.; Rausen, David J. "HEV Control Strategy for Real-Time Optimization of Fuel Economy and Emissions." SAE 2000-01-1543. Future Car Congress, April 2000, Crystal City, VA

Ref. 79 Brahma, A.; Guezennec, Y.; Rizzoni, G. "Dynamic Optimization of Mechanical/Electrical Power Flow in Parallel Hybrid Electric Vehicles." IEEE Transactions on Control Systems Technology, Vol 15, No 3, p506-518, May 2007

Ref. 80 He, Xiaolai; Parten, Michael; Maxwell, Tim. "Energy Management Strategies for a Hybrid Electric Vehicle." IEEE 0-7803-9280-9/05, 2005.

Ref. 81 Rajagopalan, G. Washington, G. Rizzoni, and Y. Guezennec. Development of Fuzzy Logic and Neural Network Control and Advanced Emissions Modeling for Parallel Hybrid Vehicles. NREL/SR-540-32919, Ohio State University, December 2003.

Ref. 82 Glenn, Bradley, Gregory Washington, and Giorgio Rizzoni. "Operation and Control Strategies for Hybrid Electric Automobiles." SAE 2000-01-1537, Future Car Congress, April 2000, Crystal City, VA

Ref. 83 S. Delprat, T.M. Guerra, J. Rimaux, 'Optimal control of a parallel powertrain: From global optimization to real time control strategy', EVS 18,

Ref. 84 Dominik Karbowski, Sylvain Pagerit, Jason Kwon, Aymeric Rousseau, Karl-Felix Freiherr von Pechmann, "Fair" Comparison of Powertrain Configurations for Plug-In Hybrid Operation Using Global Optimization', SAE 2009-01-1334, World congress, APril 2009, Detroit. MI

Ref. 85 Gao, Wenzhong; Porandla, Sachin Kumar. "Design Optimization of a Parallel Hybrid Electric Powertrain.", Vehicle Power and Propulsion Conference, setember 2005, Chicago IL

Ref. 86 GM-volt, 'Frank Weber Says Chevy Volt is Necessary and Relevant For Energy Independence', http://gm-volt.com/2009/05/29/frank-weber-says-chevy-volt-is-necessary-and-relevant-for-energy-independence/, accessed July 2009

Ref. 87 Wikipedia, 'GM EV1', http://en.wikipedia.org/wiki/General_Motors_EV1, accessed July 2009

Ref. 88 Nelson P., Amine K., Rousseau A., Yomoto H., 'Advanced Lithium-Ion batteries for plig-in hybrid electric vehicles', Electric vehicle symposium 23, December 2007, Anaheim, CA

Ref. 89 http://www.teslamotors.com/ accessed June July 2009

Ref. 90 Bush G. W., 'State of the Union Address', 2007, http://www.washingtonpost.com/wp-dyn/content/article/2007/01/23/AR2007012301075.html

Ref. 91.Department of National Transportation Survey, Driving statistics of drivers across the US,' 2001

Ref. 92 Duoba, M., and R. Carlson. 2007a. Test Procedures and Benchmarking: Blended-Type and EV-Capable Plug-in Hybrid Electric Vehicles. Proceedings of the Advanced Lithium-Ion Batteries for Plug-in Hybrid-Electric Vehicles, Electric Vehicle Symposium 23, Anaheim, CA, December 2-5, 2007.

Ref. 93 Plug-In Hybrid Electric Vehicle R&D Plan. Washington D.C.: US Department of Energy Office of Energy Efficiency and Renewable Energy Vehicle Technologies Program, February 2007.

Ref. 94 Badin F., Jeanneret B., Trigui R., Harel F., 'Hybrid vehicles, should we plug then to the grid or not?', Electric vehicle symposium 18, October 2001, Berlin, Germany

Ref. 95 Duvall, M., and E. Knipping. 2007. Environmental Assessment of Plug-in Hybrid Electric Vehicles, Vol. 1, Nationwide Greenhouse Gas Emissions. Electric Power Research Institute Final Report 1015325, Palo Alto, CA.

Ref. 96 Society of Automotive Engineers, SAE J1711 'Recommended Practice for Measuring the Exhaust Emissions and Fuel Economy of Hybrid-Electric Vehicles'

Ref. 97 Carlson, Richard, et al. 2007. Testing and Analysis of Three Plug-in Hybrid Electric Vehicles. SAE 2007-01-0283, SAE World Congress & Exhibition, April 16-19, Detroit, MI.

Ref. 98 Rousseau A., Shidore N., Carlson R., Freyermuth V, 'Research on PHEV battery requirements and evaluation of early prototypes', Advanced Automotive Battery Conference, May 2007, Long Beach CA

Ref. 99 Greencar Congress. 2007. Toyota Delivers Plug-in Prius to UC Irvine and UC Berkeley as Part of Clean Mobility Partnership. www.greencarcongress.com. Nov. 10.

Ref. 100 Vyas, A., et al. 2007. Plug-In Hybrid Electric Vehicles: How Does One Determine Their Potential for Reducing U.S. Oil Dependence? Presented at Electric Vehicle Symposium No. 23, Anaheim, CA, Dec. 2-5.

Ref. 101 Gonder, Jeffrey, and Andrew Simpson. "Measuring and Reporting Fuel Economy of Plug-In Hybrid Electric Vehicles.", Electric vehicle symposium -22. Yokohama, Japan, 2006.

Ref. 102 Michael Duoba, Richard W. Carlson, Ji Wu , 'Test Procedure Development for "Blended Type" Plug-In Hybrid Vehicles', SAE 2008-01-0457, SAE world congress, April 2008, Detroit, MI

Ref. 103 Alexander, M., M. Duvall, and S. Chhaya. 2007. An Assessment of Plug-in Hybrid Electric Vehicle Powertrain Architectures. Electric Vehicle Symposium 23, Anaheim CA, Dec.2-5.

Ref. 104 Michael Duoba, 'Calculating Results and Performance Parameters from Plug-In Hybrid Electric Vehicles', SAE 2009-01-1328, SAE world congress, April 2009, Detroit, MI

Ref. 105 O'Keefe, M.P., and Tony Markel. Dynamic Programming Applied to Investigate Energy Management Strategies for a Plug-In HEV. NREL/CP-540-40376, National Renewable Energy Laboratory, November 2006.

Ref. 106 Frank A., Francisco A., 'Drive system analysis and optimization for plug-in hybrid electric vehilces', Electric vehicle symposium 18, October 2001, Berlin, Germany

Ref. 107 Rousseau, Aymeric, and David Gao. Plug-In Hybrid Electric Vehicle Control Strategy Parameter Optimization. Argonne National Laboratory, 2008.

Ref. 108 Gonder, Jeffrey, and Tony Markel. "Energy Management Strategies for Plug-In Hybrid Electric Vehicles." SAE 2007-01-0290, April 2007.

Ref. 109 Gonder, J. D. Route-Based Control of Hybrid Electric Vehicles. NREL/CP-540-42557, National Renewable Energy Laboratory, January 2008.

Ref. 110 Stephen D. Gurski, et al, 'Design of a Zero-Emission Sport Utility Vehicle for Futuretruck 2002', SAE 2003-01-1264, SAE world congress, March 2003, Detroit MI

Ref. 111 Lohse-Busch H., Boyd S., 'Magellan: A hydrogen powered hybrid', Presentation only, SAE Advanced vehicle competition special session, SAE world congress, March 2004, Detroit MI

Ref. 112 Lohse-Busch H. et al,' Design and Implementation of a hydrogen powered hybrid electric SUV', FutureTruck 2004 Final report for HEVT, April 2004, Blacksburg, VA

Ref. 113 Lohse-Busch H., 'Annual report of hydrogen vehicle testing', Annual report to DOE for FY2008, ANL/DOE Internal report, September 2008, Argonne IL

Ref. 114 Larminie J., Dicks A., 'Fuel Cell Systems Explained' ,2nd edition, Wiley, ISBN 978-0470848579 , April 2003

Ref. 115 U.S. Department of Energy, FreedomCAR and Vehicles Technologies Program, "Advanced Vehicle Technology Analysis and Evaluation Activities," Annual Progress Report, 2004.

Ref. 116 Wallner T., Lohse-Busch H., Gurski S., Duoba M., and Thiel W., 'Fuel economy and emissions evaluation of BMW Hydrogen 7 mono-fuel demonstration vehicles.', International Journal of Hydrogen Energy, 2008, vol. 33, no24, pp. 7607-7618

Ref. 117 U.S. Department of Energy, 'Multi-year program plan – Freedom car and vehicle technologies program', 2006. Washington, DC

Ref. 118 Wikipedia, 'Hydrogen Economy', http://en.wikipedia.org/wiki/Hydrogen_economy, accessed July 2009

Ref. 119 Thomas Wallner, Steve Gurski, Henning Lohse-Busch, Mike Duoba, Wolfgang Thiel, 'Challenges in Fuel Efficiency and Emissions Measurements for Hydrogen Vehicles', 2008 National Hydrogen Association Annual Conference, April 2008, Sacramento CA

Ref. 120 Michael Wang and Marianne Mintz, 'Benefits and Costs of Hydrogen Fuels', Presentation, 2003 Annual TRB Meeting, January 2003, Washington, DC

Ref. 121 Frankfort J.; Karner D.; 'Hydrogen ICE Vehicle Testing Activities'; SAE 2006-01-0433, SAE world congress, April 2006, Detroit MI

Ref. 122 Gerrit Kiesgen, Manfred Klueting, Christian Bock, Hubert Fischer, 'The New 12-Cylinder Hydrogen Engine in the 7 Series: The H2 ICE Age has Begun', SAE 2006-01-0431, SAE world congress, April 2006, Detroit MI

Ref. 123 Rosa C. Young, Ben Chao, Yang Li, Vitaliy Myasnikov, Baoquan Huang, Stanford Ovshinsky, 'A Hydrogen Ice Vehicle Powered By Ovonic Metal Hydride Storage', SAE 2004-01-0699, SAE World congress, March 2004, Detroit, MI

Ref. 124 Carl A. Kukkonen Mordecai Shelef, 'Hydrogen as An Alternative Automotive Fuel: 1993 Update', SAE 940766, International Congress, March 1994, Detroit MI

Ref. 125 Eichlseder, H., T. Wallner, R. Freymann, and J. Ringler, "The Potential of Hydrogen Internal Combustion Engines in a Future Mobility Scenario," SAE Paper No. 2003-01-2267.

Ref. 126 White CM, Steeper RR, Lutz AE. The hydrogen-fueled internal combustion engine: a technical review. International Journal of Hydrogen Energy 2006;31:1292–305.

Ref. 127 Robert J. Natkin, Xiaoguo Tang, Kathy M. Whipple, Daniel M. Kabat, William Francis Stockhausen, 'Ford Hydrogen Engine Laboratory Testing Facility', SAE 2002-01-0241, SAE world congress, March 2002, Detroit MI

Ref. 128 William F. Stockhausen, Robert J. Natkin, Daniel M. Kabat, Lowell Reams, Xiaoguo Tang, Siamak Hashemi, Steven J. Szwabowski, Vance Zanardelli, 'Ford P2000 Hydrogen Engine Design and Vehicle Development Program', SAE 2002-01-0240, SAE world congress, March 2002, Detroit MI

Ref. 129 Tang, X., D. Kabat, R. Natkin, and W. Stockhausen, 'Ford P2000 Hydrogen Engine Dynamometer Development', SAE 2002-01-0242, SAE world congress, March 2002, Detroit MI

Ref. 130 Steven J. Szwabowski, Siamak Hashemi, William F. Stockhausen, Robert J. Natkin, Lowell Reams, Daniel M. Kabat, Curtis Potts, 'Ford Hydrogen-Engine-Powered P2000 Vehicle', SAE 2002-01-0243, SAE world congress, March 2002, Detroit MI

Ref. 131 Xiaoguo Tang, Robert J. Natkin, Brad A. Boyer, Bret A. Oltmans, Curtis Potts, 'Hydrogen Ic Engine Boosting Performance and Nox Study', SAE 2003-01-0631, SAE world congress, March 2003, Detroit MI

Ref. 132 Henning Lohse-Busch, Thomas Wallner, John Fleming, 'Transient Efficiency, Performance, and Emissions Analysis of a Hydrogen Internal Combustion Engine Pick-up Truck', SAE 2006-01-3430, Powertrain & Fluid Systems Conference and Exhibition, October 2006, Toronto Canada

Ref. 133 David Smith, 'Plug-in Hybrid Electric Vehicle emissions impacts on control strategy and fuel economy', PhD Dissertation, University of Tennesse, April 2009, Knoxville TN

Ref. 134: Jeongwoo Lee (2009), "Vehicle Inertia Impact on Fuel Consumption of Conventional and Hybrid Electric Vehicles Using Acceleration and Coast Driving Strategy", Ph.D. dissertation, Virginia Polytechnic Institute and State University, Sept. 2009.

List of appendices

Appendix 1: The Advanced Powertrain Research Facility (APRF)

Appendix 2: Clutch torque transfer characterizations

Appendix 3: Manual transmission efficiency maps

Appendix 4: Automatic transmission calibration

Appendix 5: Information and statics of all standard drive cycles

Appendix 6: Typical signal list collected on MATT during a test

Appendix 7: Conventional vehicle results for all standard drive cycles

Appendix 8: Conventional vehicle results for drive cycle intensity study

Appendix 9: Signal list collected during the hydrogen engine calibration

Appendix 10: Hydrogen engine detailed test results

Appendix 11: Vita and Publication list of Henning Lohse-Busch

Appendix 1: The Advanced Powertrain Research Facility (APRF)

The APRF is the chassis dynamometer where MATT is tested. Additionally, MATT is a tool that is part of the APRF to enable component testing in a vehicle system environment and investigate very specific research problem for which control or behavior changes are needed.

The Advanced Powertrain Research Facility is the advanced technology vehicle and component test center created by the US Department of Energy. The primary goal of this facility is to benchmark and analyze advanced technology vehicles as such hybrids, plug-in hybrids and alternative fuel vehicles. The powertrain components of the test vehicles are heavily instrumented to characterize the component's performance and operation in the vehicle system environment. The vehicles are evaluated for energy consumption, tailpipe emissions and performance. The APRF is illustrated in Figure A2-1.

Figure A1-1: Illustration of the Advanced Powertrain Research Facility infrastructure

At the core of the APRF is a four-wheel drive chassis dynamometer. Two 48 inch dynamometer rolls are capable of 250 hp each. The variable wheel base can accommodate small light duty vehicles and larger medium duty vehicles. The chassis dynamometer simulates road and inertia loads with high fidelity. It is also a motored dynamometer. The emissions equipment in the facility is capable of resolving SULEV (Super Ultra Low Emissions Vehicle) levels. The emissions bench is a Pierburg AMA 4000, which is a 5 gas analyzer (THC, CH4, CO, NOX and CO2) coupled to a CVS

(Constant Volume Sampling) system. The air handling unit maintains the temperature and humidity of the combustion air in the test cell. The data acquisition is a purpose built system to provide flexibility and ease of use. The test cell has state of the art integrated safety systems such as a hazardous gas detection system, direct link to the fire department, integrated emergency stop loop and full automated test cell air scavenging.

Figure A1-2 shows the test cell interior. Two rolls with variable wheel base can accommodate different sized vehicles. The four-wheel drive dynamometer is needed to test through the road hybrids such as the Argonne TTR mentioned in Section 6 of this dissertation, which transfers power from one driven axle to the other driven axle. The vehicle is restrained in the test cell by chains and posts at the extremities of the test cell. For the two-wheel drive vehicle, the axle not driven is typically clamped to the ground. Other standard features are the air flow simulator fan which provides air flow for the vehicle cooling system. The driver display show the drive cycle and the vehicle speed, which is used by the driver to meet the trace. An infra red temperature sensor typically records the tire temperature. Finally several safety features are shown, such as the hazardous gas detectors displays, the hydrogen supply and safety system and the yellow operations warning beacon.
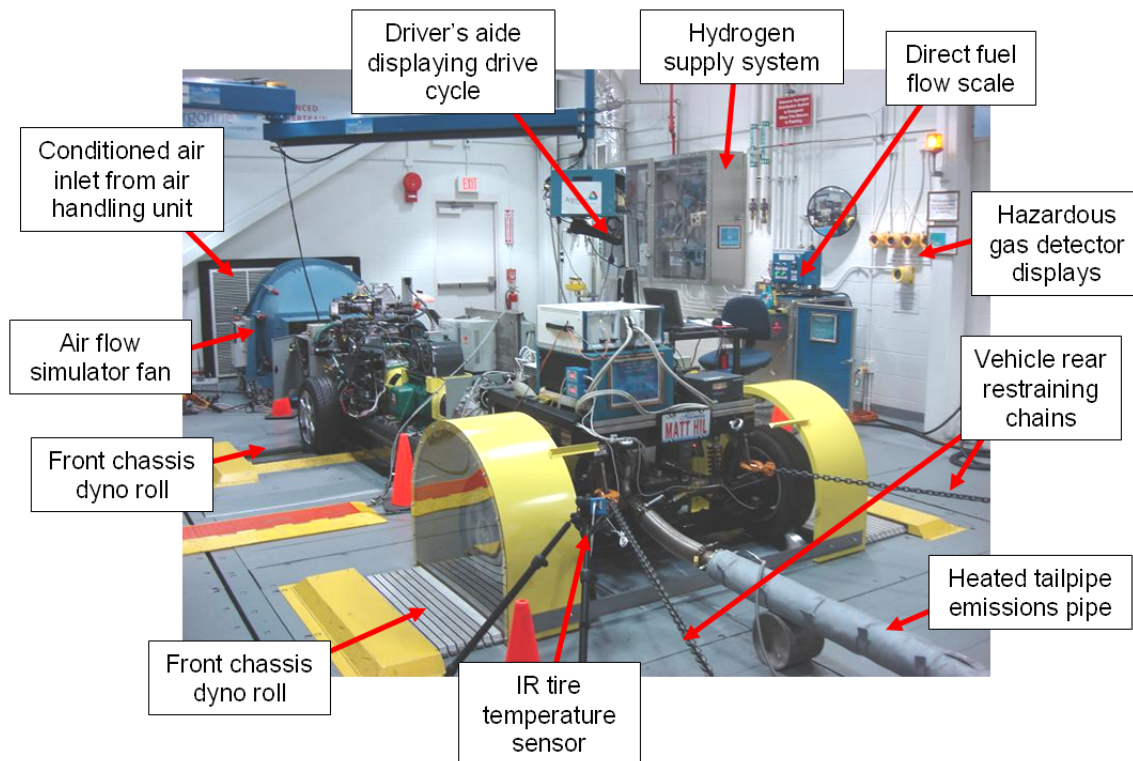
Figure A1-2: Picture of the APRF 4 wheel drive chassis dynamometer test cell

Figure A1-3 provides a view from the control room. Several computer interfaces are available to the operator. The dynamometer user interface is used to set road load,

inertia loads, and grade as well as performed special tests such as coast downs or steady state speeds tests. The host computer communicates with all of the vital systems to orchestrate the actual test by triggering the emissions bench modes, the data acquisition systems and performing the final calculations before saving the data. A vehicle data acquisition system computer and facilities computer are also available. The driver aide display is duplicated for the test operator.
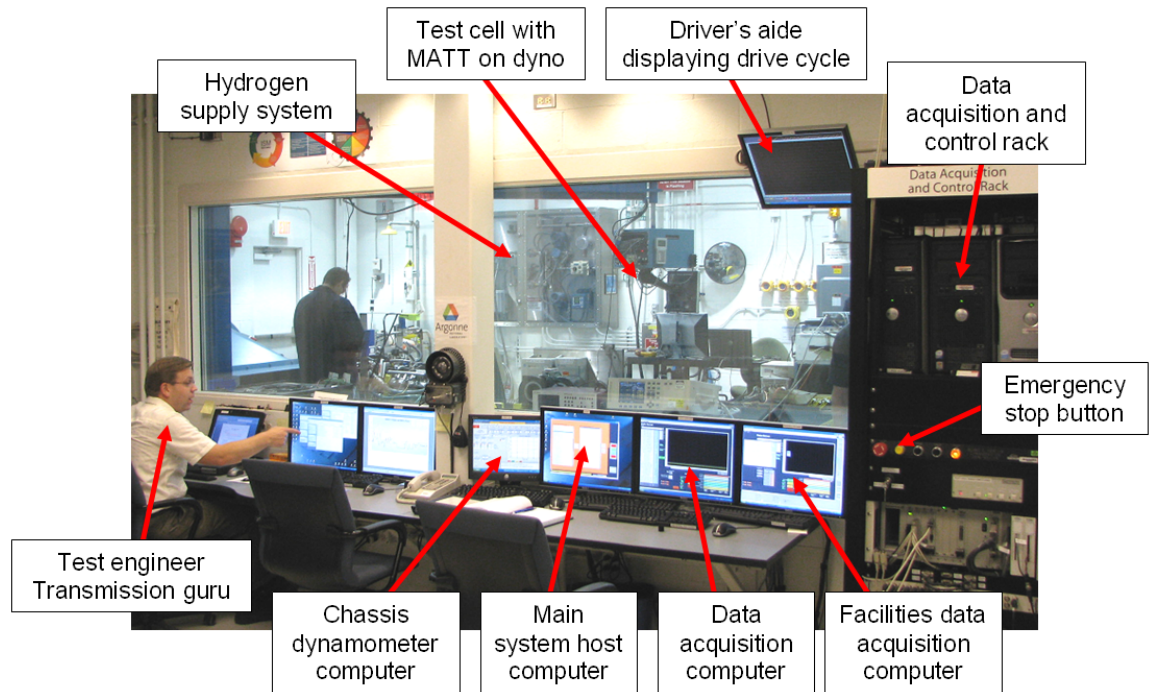
Figure A1-3: Picture of the APRF control room

The tailpipe emissions collect and pipe into the exhaust dilution air mixing tee, which mixes the full exhaust sample with dry dilution air. This diluted exhaust gets funneled into the emissions bench were the CVS diverts a know flow into the 'bags' as well as past the analyzer, which provides real time emissions measurements. The 'bags' are literally bags which get filled with emissions gas so that at the total emissions can be measure at the end of the test. Each phase in a drive cycle has a corresponding bag set. One back is the emissions sample at know flow rate and the other sample is the background air sample. The difference between the two bags and some calculations to convert the concentrations and flows into mass provides the total emissions for the bag. One of the species measured is CO2. The carbon balance to calculate the fuel economy uses CO2. The full exhaust system is illustrated in Figure A1-4.
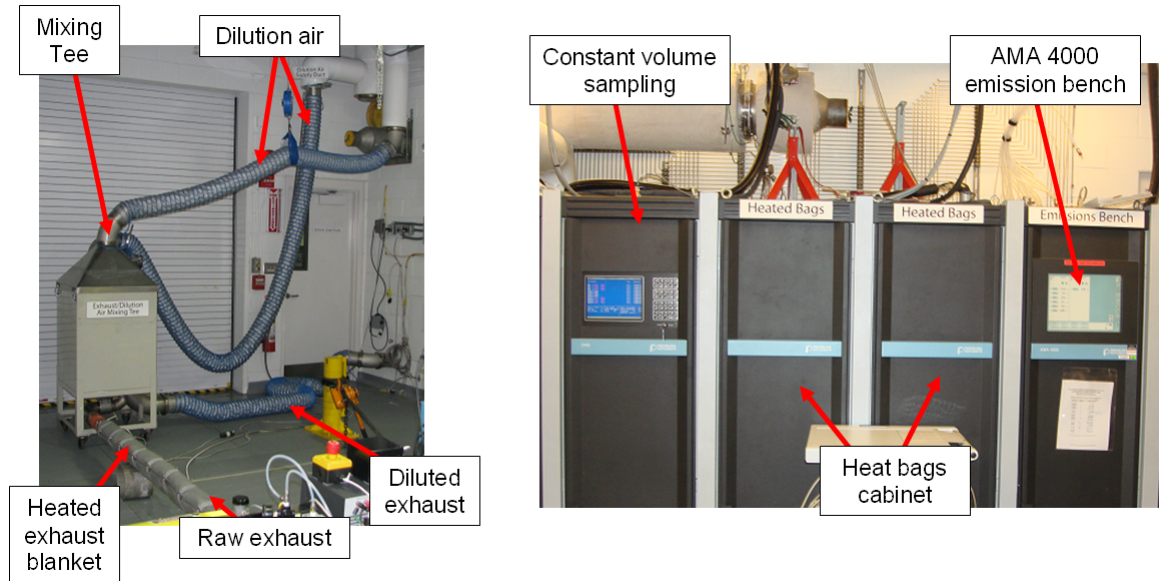
Figure A1-4: Exhaust sampling and measuring system details

Some of the APRF's additional features which make this facility unique are listed below:

- Flexible in-house data acquisition systems
- Measurement of criteria emissions and particulate of super-ultra low-emission vehicles (SULEVs)
- Ability to test a wide range of fuels including gasoline, diesel, renewable fuels, hydrogen, and natural gas. The test cell is fully hydrogen rate.
- Hydrogen exhaust content measurement (H-sense) and water analyzer (VnF) for water balance fuel economy determination for hydrogen vehicles
- Fast hydrocarbon and NOx Combustion analyzers
- High precision power analyzer to measure electricity utilization in electrified vehicles (PHEVs and EV)
- High voltage and high power drop for ABC 170 power supply to emulate battery packs
- Dedicated indicated in-cylinder pressure system (AVL)
- High precision thermal IR camera

Appendix 2: Clutch torque transfer characterizations

In order to improve the clutch engagement to launch MATT in the conventional vehicle mode, several special tests were performed to characterize the clutch torque transfer. The tests were performed with MATT in manual control mode on the APRF 2 wheel drive Clayton chassis dynamometer.

The tests:

- A series of clutch engagement tests were performed at different engagement rates, engine idle speeds.
- In all the tests the first gear was engaged on the manual transmission. The manual transmission module was used for these tests.
- Some tests include engaged mechanical vehicle brakes to increase torque transfer across the clutch.
- MATT specific DAQ used. Signal recorded: engine speed, clutch output speed, engine torque output and several others.
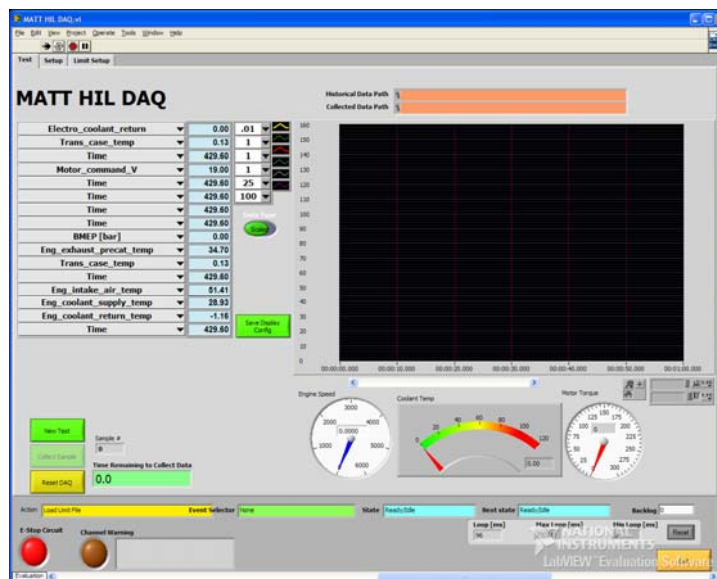
The goal:

- To determine the correlation between clutch position and torque transfer while quantifying the influence of engine speed and engagement speed

The following test series was performed

Test data shown in detail in the next slides

Test #	1	2	3	4	5	6	7	8	9	10	11	12	13	14	15
Throttle	4.1	4.1	4.1	4.1	4.1	4.1	4.1	4.1	4.1	3.8	3.8	3.8	3.8	3.8	3.8
Brakes	Off	Off	Off	Off	Off	Off	On	On	On	Off	Off	Off	Off	On	On

A throttle of 4.1 indicates the idle throttle position and the throttle of 3.8 indicates an elevated engine speed. Brakes on indicate that the mechanical wheel brakes were engaged.

Individual test results are shown in the following pages.

**MATT Manual clutch engagement launch
Engine idle - 03-16-07_Run3 Test 2**

**MATT Manual clutch engagement launch
Engine idle - 03-16-07_Run3 Test 2**

**MATT Manual clutch engagement launch
Engine idle / Brakes ON - 03-16-07_Run3 Test 9**

**MATT Manual clutch engagement launch
Engine idle / Brakes ON - 03-16-07_Run3 Test 9**

MATT Manual clutch engagement launch
Constant throttle - 03-16-07_Run3 Test 13

MATT Manual clutch engagement launch
Constant throttle - 03-16-07_Run3 Test 13

**MATT Manual clutch engagement launch
Constant throttle / Brakes ON - 03-16-07_Run3 Test 15**

**MATT Manual clutch engagement launch
Constant throttle / Brakes ON - 03-16-07_Run3 Test 15**

Following graphs show all the test results combined in a single graph.

**MATT Manual clutch engagement launch
at different clutch closing rates - 03-16-07_Run3**
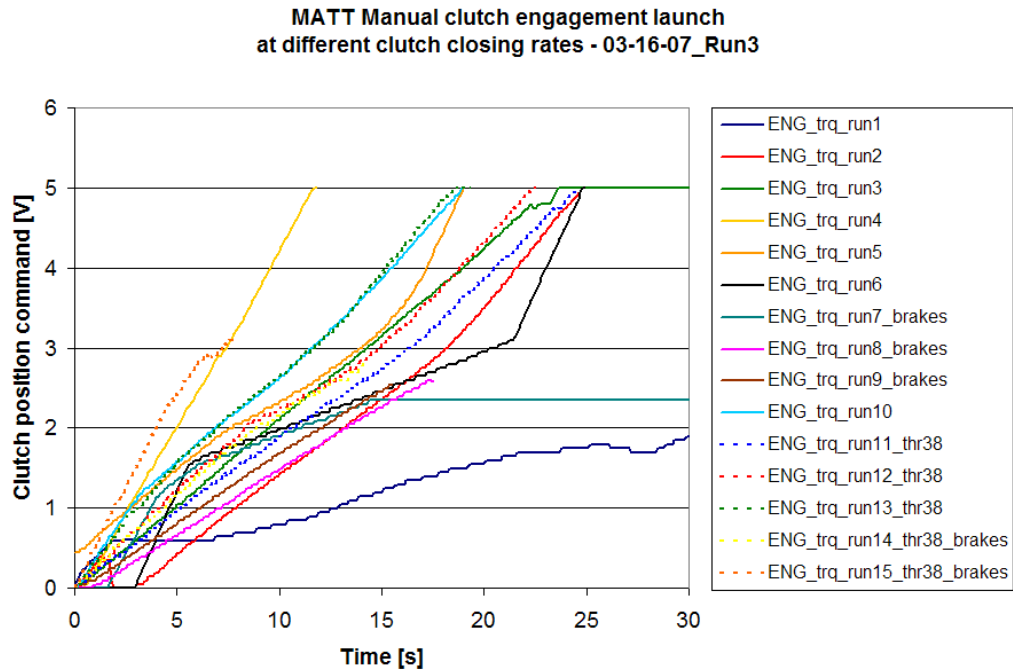
There is no good correlation between the different engagement speeds or engine speeds.

**MATT Manual clutch engagement launch
in different conditions - 03-16-07_Run3**
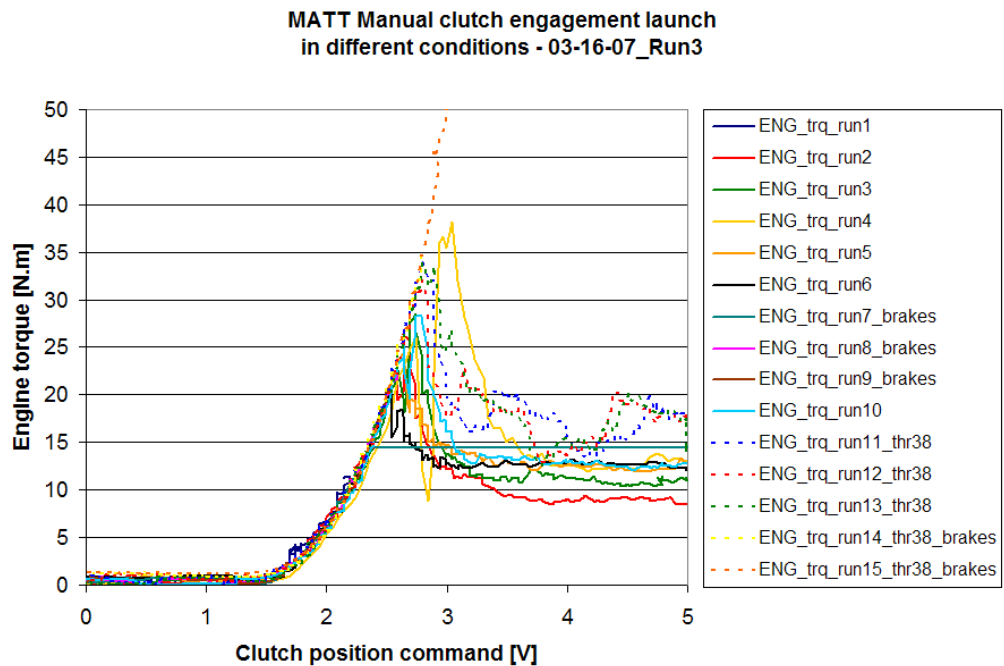
There is an excellent correlation between clutch engagement position and torque transfer independent of engine speed or engagement rate as long as the wheel are not turning. Once the wheels are spinning the torque is dependent on inertial loads at the wheel and the engine torque output.

Appendix 3: Manual transmission efficiency maps

This appendix provides the efficiency mapping in all gears for the manual transmission.

1st gear hot

MATT MTX efficiency / Gear #2
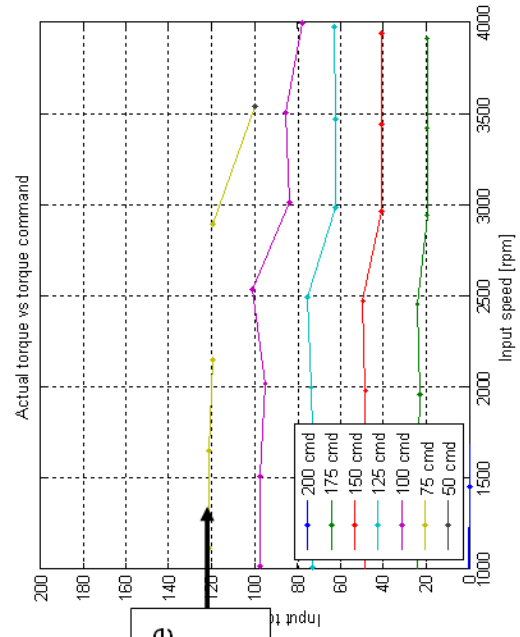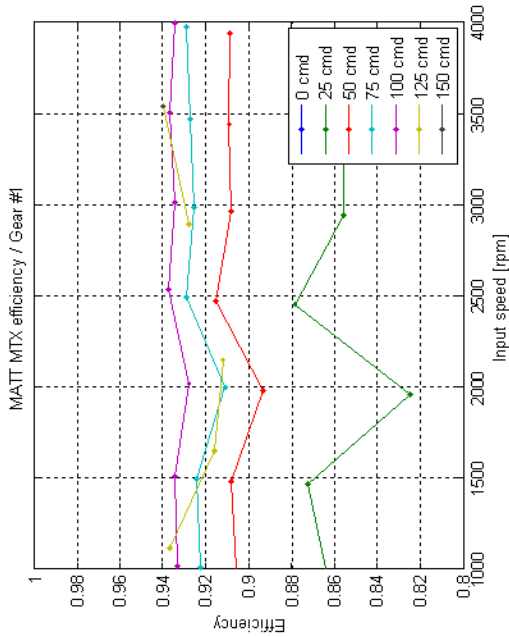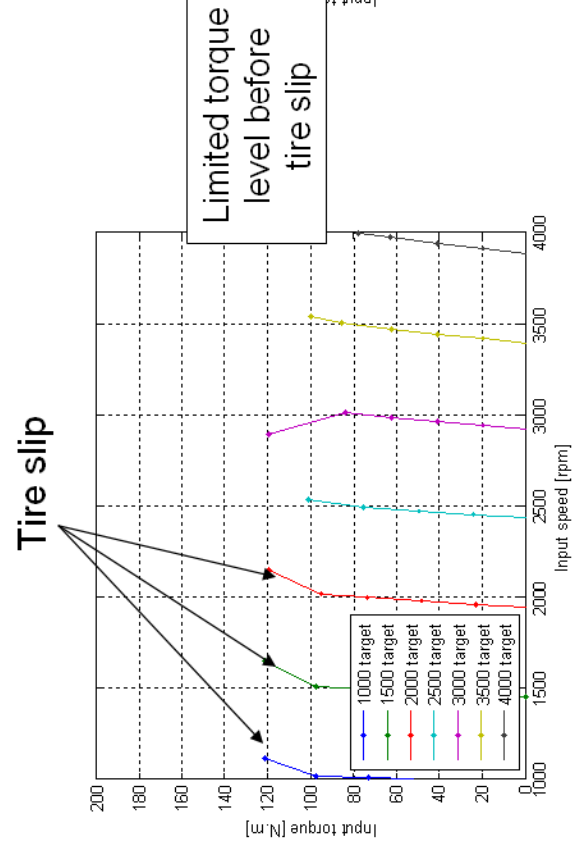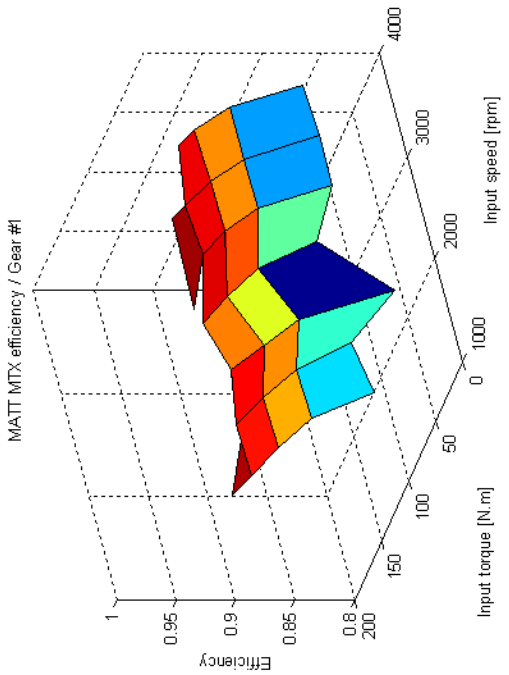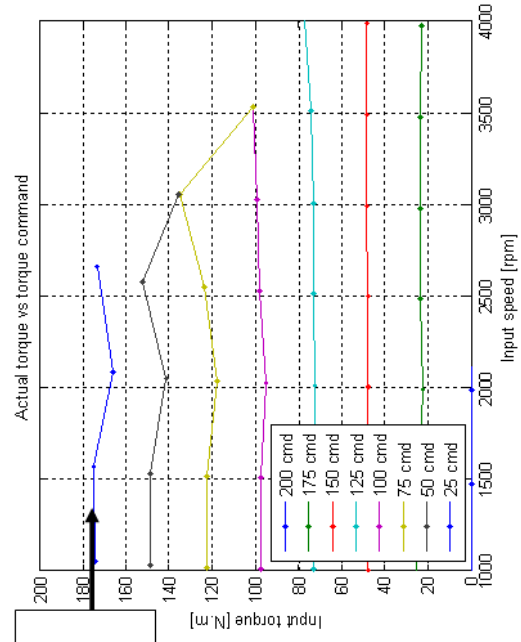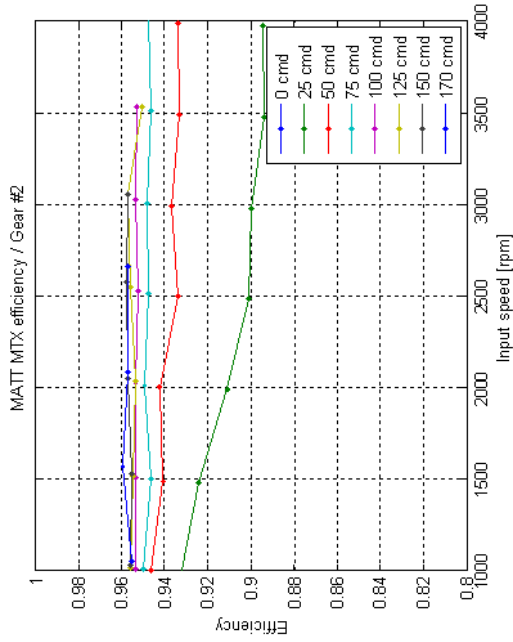
2nd gear
Hot

Tavg=53.8C
Tmin=52.9C
Tmax=54.7C

Higher input
torque level
until tire slip

Tire slip

MATT MTX efficiency / Gear #3

Efficiency

Input speed [rpm]

Legend: 0 cmd, 25 cmd, 50 cmd, 75 cmd, 100 cmd, 125 cmd, 150 cmd, 170 cmd, 200 cmd
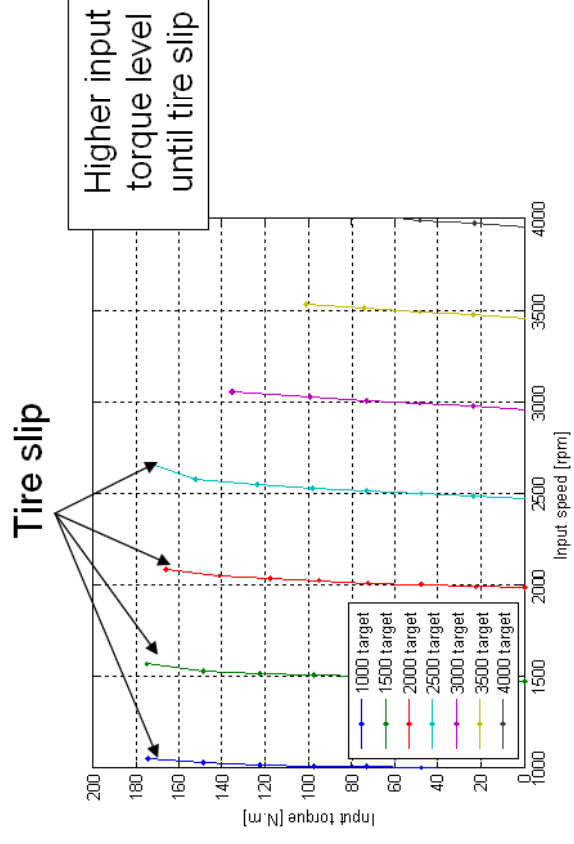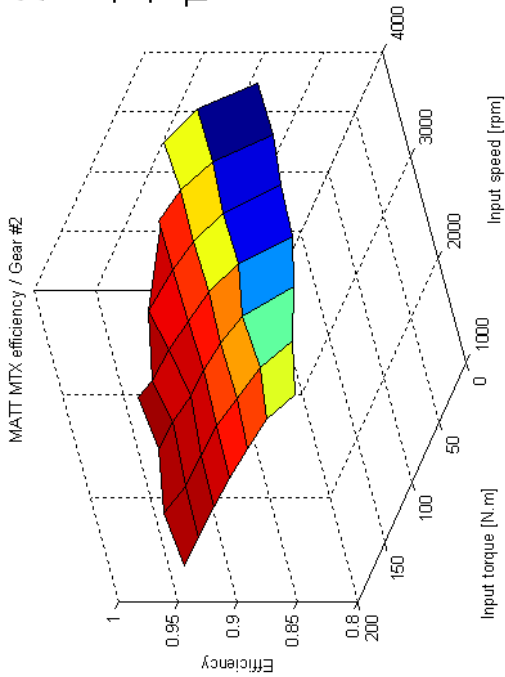
3rd gear
Hot

Tavg=50.0C
Tmin=52.8C
Tmax=52.4C

Actual torque vs torque comm

Input torque [N.m]

Input speed [rpm]

Legend: 200 cmd, 175 cmd, 150 cmd, 125 cmd, 100 cmd, 75 cmd, 50 cmd, 25 cmd, 0 cmd

Max constant power region of motor
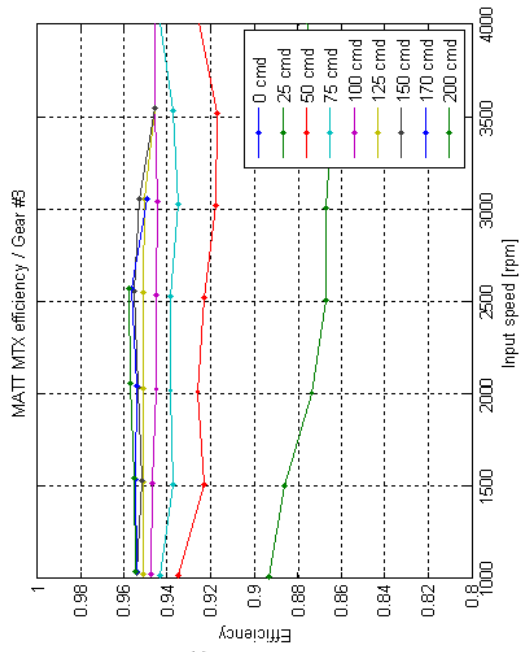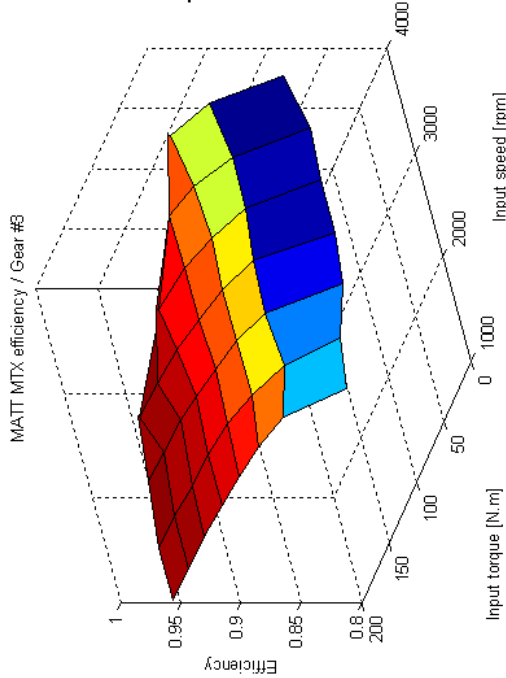
Max input torque level with notire slip

MATT MTX efficiency / Gear #3

Efficiency

Input torque [N.m]

Input speed [rpm]

Input torque [N.m]

Input speed [rpm]

Legend: 1000 target, 1500 target, 2000 target, 2500 target, 3000 target, 3500 target, 4000 target
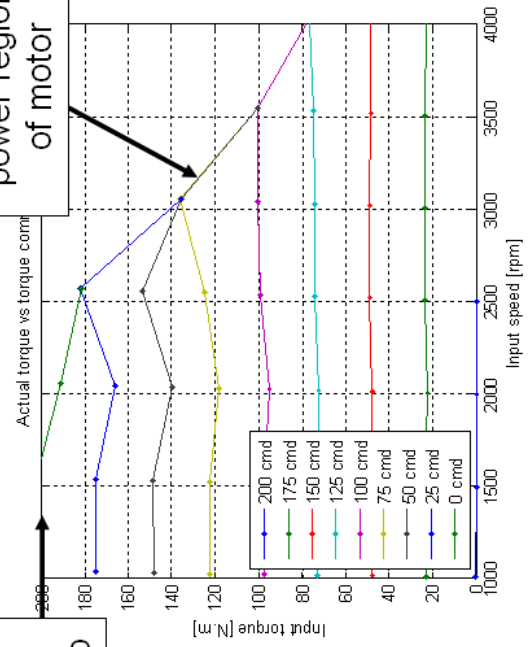
Appendix 3 - 3

4th gear
Hot
Tavg=56.5C
Tmin=54.8C
Tmax=58.1C
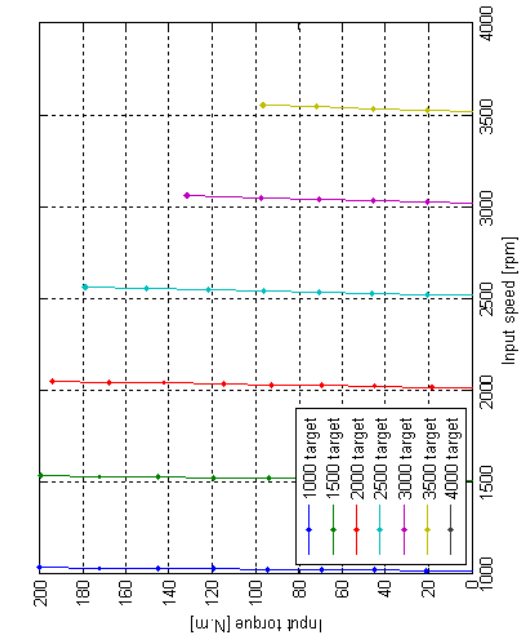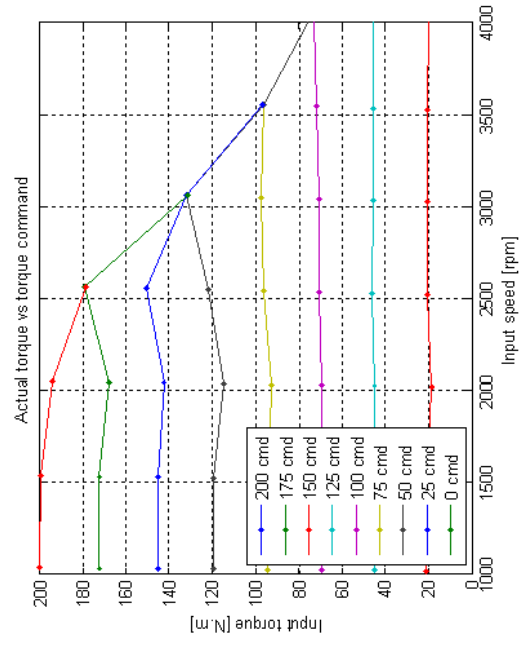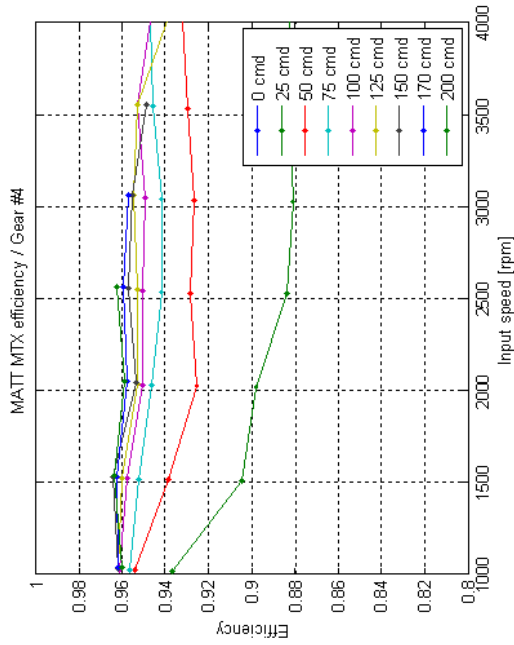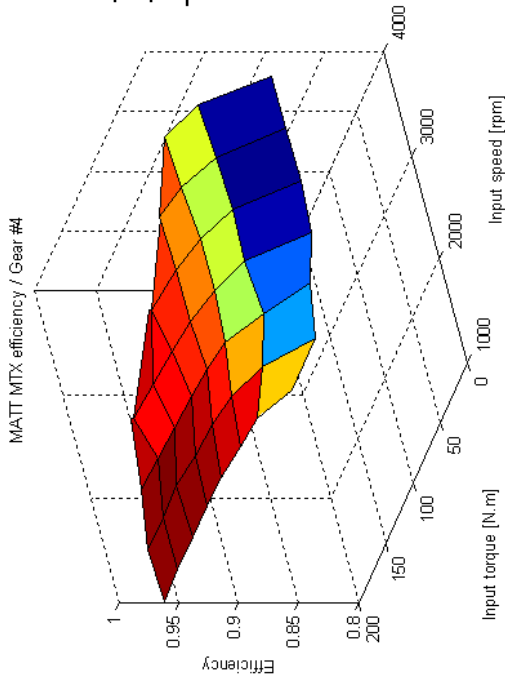
5th gear
Hot
Tavg=58.7C
Tmin=57.9C
Tmax=59.6C

High input speed limited by max dyno speed
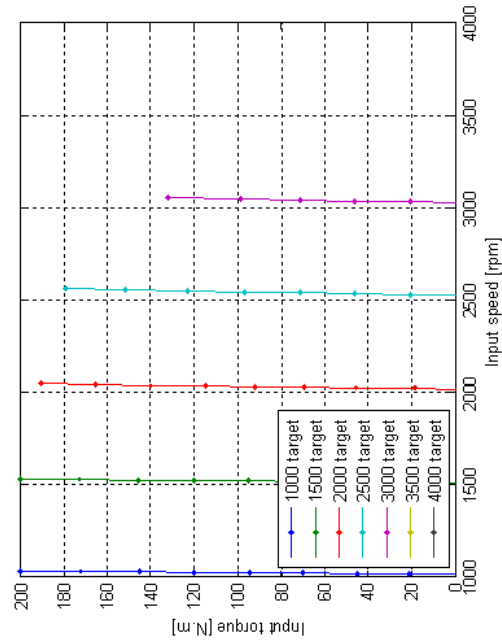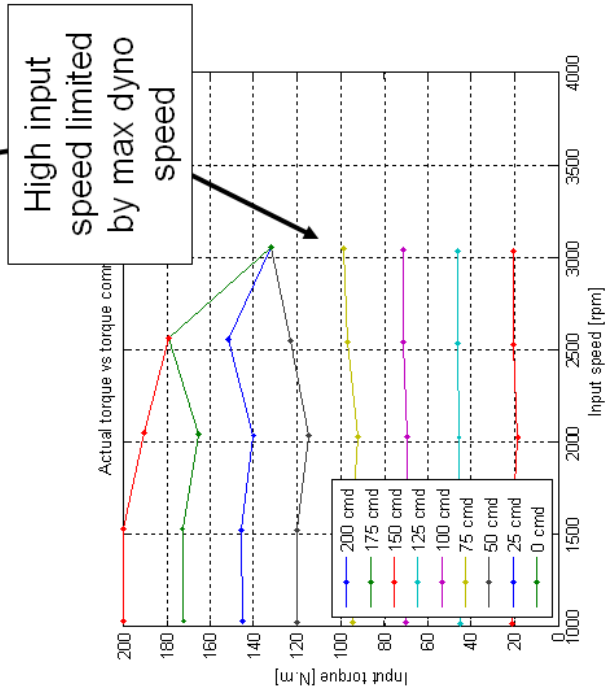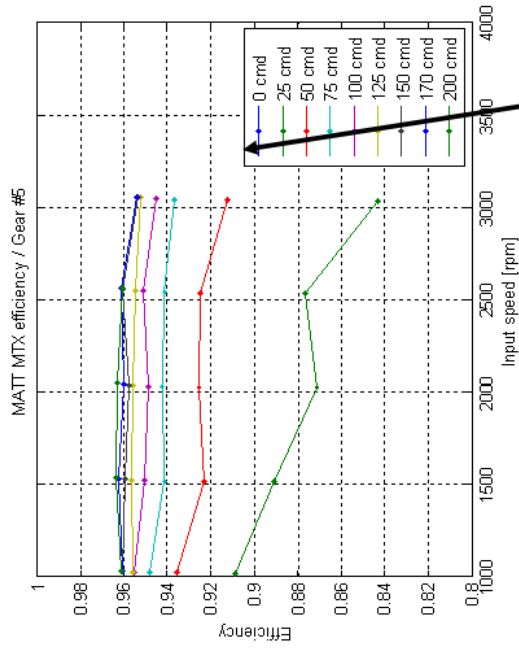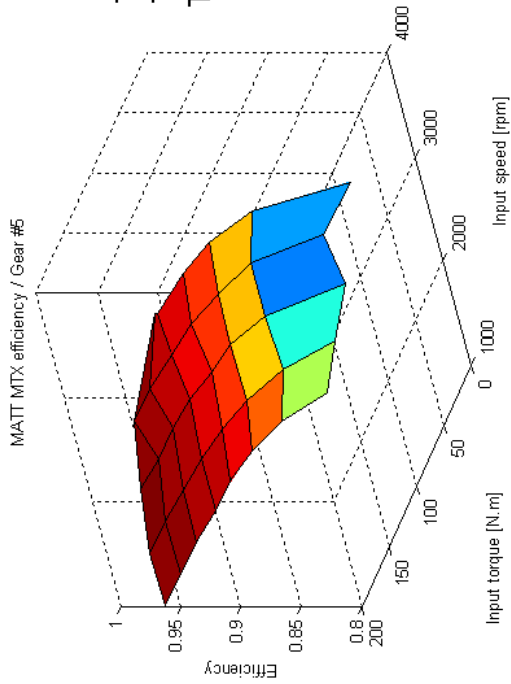
Appendix 4: Automatic transmission details

This appendix provides the lever diagrams for the 5R55 automatic transmission along with a screen shot of the transmission calibration interface.
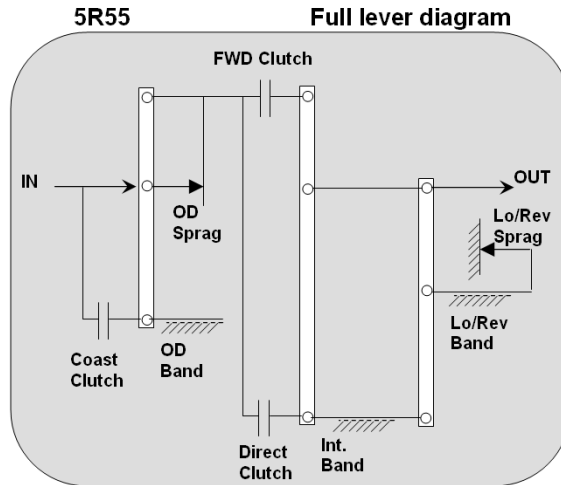

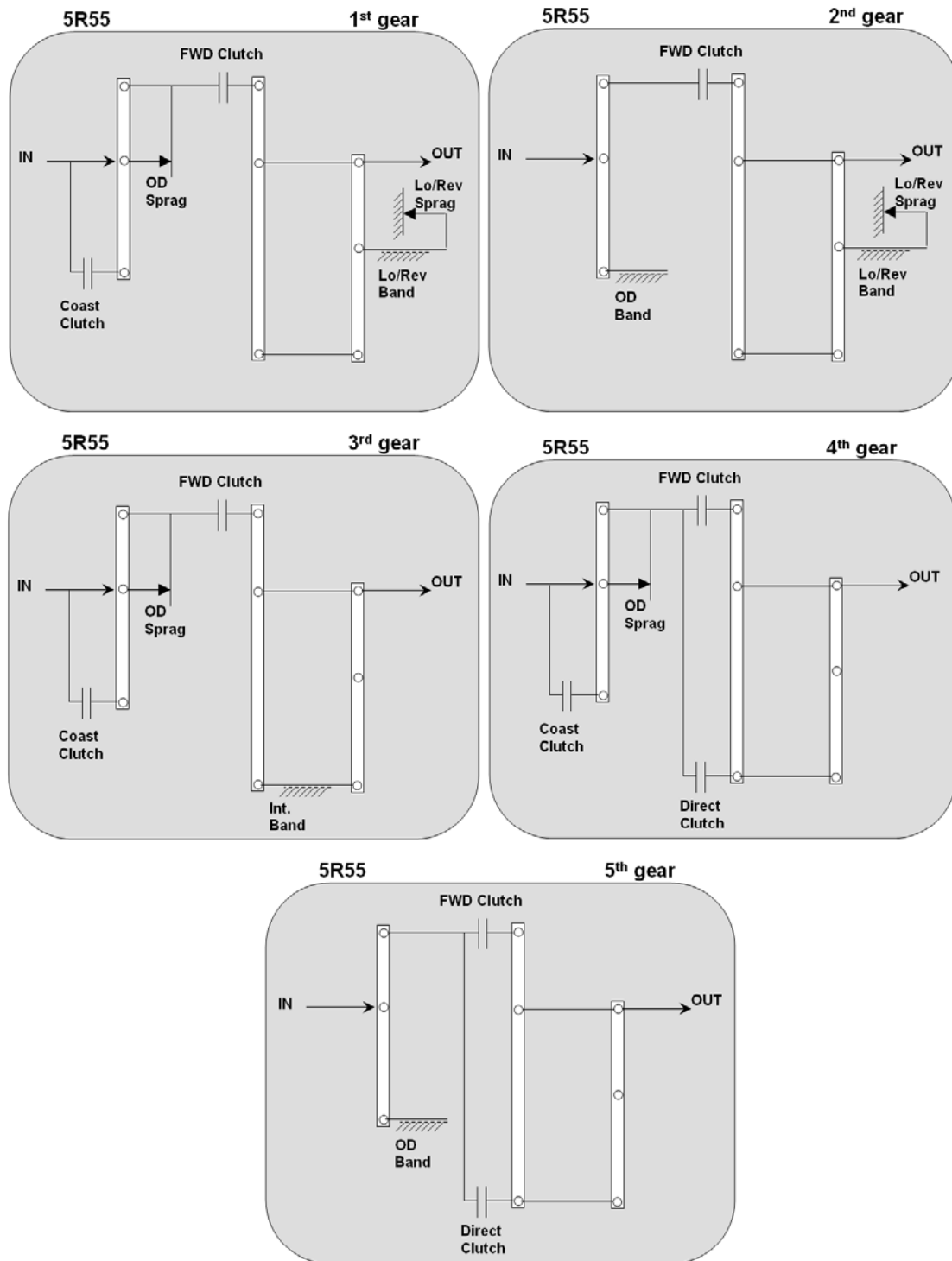**Figure A4-1: Full lever diagram of the 5R55 automatic transmission**
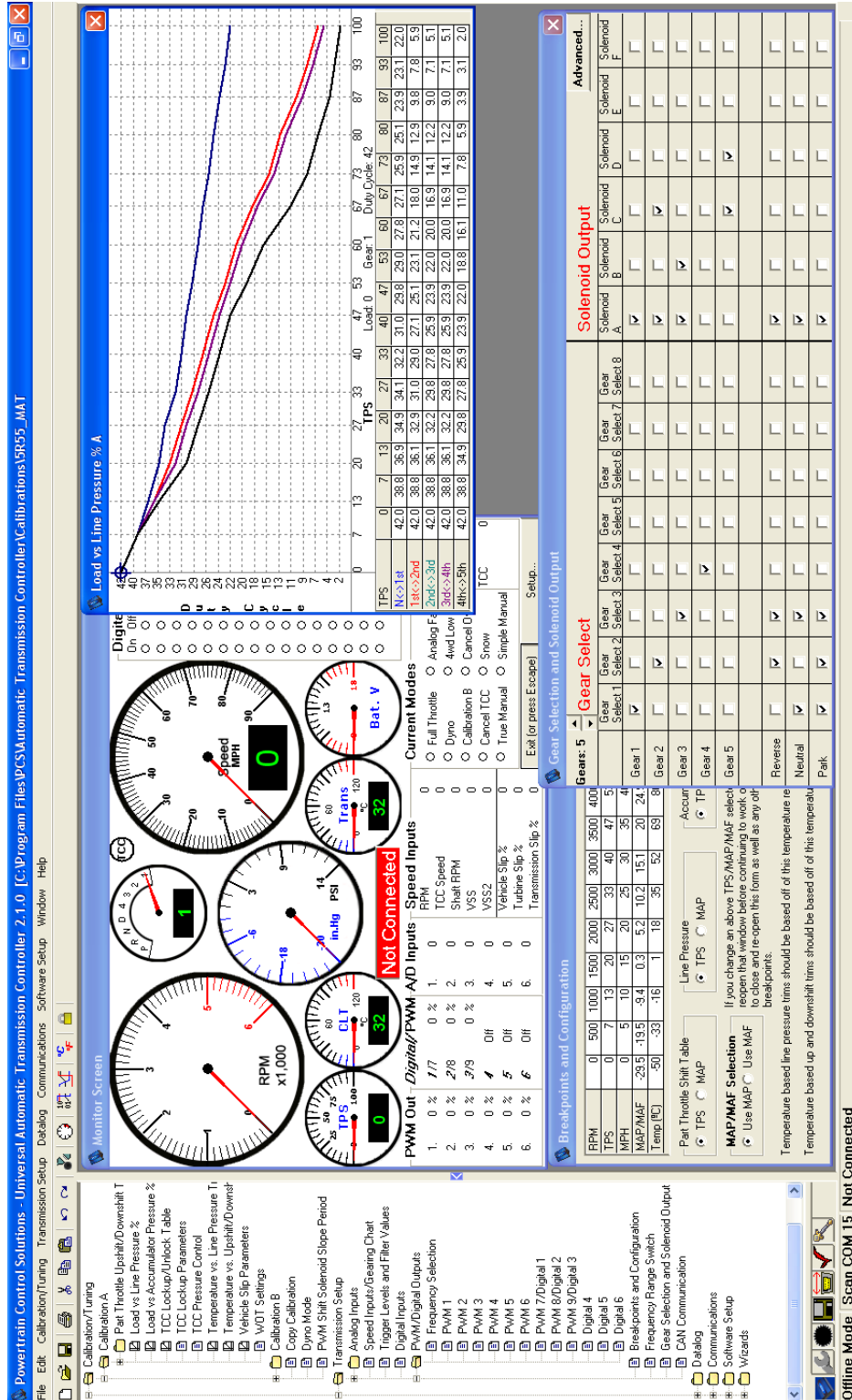
Figure A4-2: Lever diagrams for all gears for the 5R55 automatic transmission

Figure A4-3: Calibration interface to the PCS transmission controller

Appendix 5: Information and statics of all standard drive cycles

This appendix shows a vehicle speed as a function of time graph as well as an acceleration and power as function of vehicle speed graph for all the cycles.

Some generic drive cycle statistics are shown for the drive cycle. All the vehicle related statistics are calculated based on a Ford Focus which is the vehicle is emulated with MATT in most of this work.

```
VEHICLE SPECS USED
% Correlation Focus
A = 30.85;      %lb
B = 0.508;      %lb/mph
C = 0.0165;     %lb/mph^2m
m_stand = 3125; %lb
```

The cycles presented here are:

- UDDS
- Highway
- US06
- NEDC
- Japan 1015
- LA92
- ATDS
- JC08
- Scale speed UDDS
    - 0.8 x UDDS
    - 1.2 x UDDS
    - 1.4 x UDDS
- Scale speed and time UDDS
    - 0.8 x UDDS
    - 1.2 x UDDS
    - 1.4 x UDDS

Drive cycle	UDDS 2bags 5spd 1373.txt	HWY 1bag 5spd 1373.txt	US06 1bag 5spd 773.txt	NEDC 2bags 5spd 1179.txt	Jap1015 1Bag 659.txt	LA92 2Bags 1435.txt	ATDS 2bag 1799.txt	JC08 1bag 1376.txt	0.8xUDDS 2 bag 1376.txt	1.2xUDDS 2 bag 1373.txt	1.4xUDDS 2 bag 1373.txt	0.8xUDDS 2 bag 1716.txt	1.2xUDDS 2 bag 1144.txt	1.4xUDDS 2 bag 991.txt	
accel_max	1.48	1.43	3.76	1.07	0.81	3.08	3.29	1.69	1.18	1.77	2.07	0.94	2.12	2.89	m/s^2
accel_min	-1.48	-1.48	-3.08	-1.43	-0.83	-3.93	-3.29	-1.22	-1.18	-1.77	-2.07	-0.94	-2.12	-2.89	m/s^2
accel_pos_avg	0.5	0.19	0.67	0.6	0.57	0.67	0.61	0.42	0.4	0.6	0.71	0.32	0.73	0.99	m/s^2
accel_neg_avg	-0.58	-0.22	-0.73	-0.79	-0.65	-0.75	-0.6	-0.47	-0.46	-0.69	-0.81	-0.37	-0.83	-1.13	m/s^2
trace_speed_avg	19.5	47.6	48	21	14.1	24.6	31.5	16.8	15.6	23.4	27.3	15.6	23.4	27.3	mph
trace_speed_max	56.7	59.9	80.3	75	43.5	67.2	79.4	50.7	45.4	68	79.4	45.4	68	79.4	mph
distance	7.45	10.25	8.01	6.88	2.59	9.82	15.75	6.41	5.96	8.94	10.43	7.45	7.45	7.45	mi
stoppercent	17.8	1.8	6.5	23.6	31.2	15.1	20.1	26.1	17.8	17.8	17.8	17.8	17.8	17.8	%
accelpercent	39.7	43.6	45.8	20.9	25.2	38.2	36.6	38.2	39.7	39.7	39.7	39.7	39.7	39.7	%
decelpercent	34.6	38.3	42.1	15.8	22.1	34.1	36.9	34.1	34.6	34.6	34.6	34.6	34.6	34.6	%
cruisepercent	7.9	16.2	5.5	39.6	21.4	12.5	6.3	1.5	7.9	7.9	7.9	7.9	7.9	7.9	%
drivepercent	82.2	98.2	93.5	76.4	68.8	84.9	79.9	73.9	82.2	82.2	82.2	82.2	82.2	82.2	%
Vehicle	Focus.	Focus.	Focus.	Focus.	Focus.	Focus.	Focus.	Focus.	Focus.	Focus.	Focus.	Focus.	Focus.	Focus.	
vehicle_power_kW_max	37.7	31.1	95.3	42.8	22	52.8	84.4	23.7	24.3	54.2	73.8	20.2	63.6	99.5	kW
vehicle_power_kW_min	-25.2	-35.6	-49.5	-26.6	-11	-87.1	-82.3	-20.9	-15.9	-36.5	-49.8	-12.2	-44.8	-72.5	kW
vehicle_power_kW_pos_avg	8	12.6	24.8	8.4	6.8	12.8	18.3	8.1	5.2	11.5	15.7	4.5	13	19.8	kW
vehicle_power_kW_neg_avg	-6.7	-9.2	-18	-7.7	-5.6	-10.1	-9.9	-5.2	-4.3	-9.6	-13.1	-3.5	-11.6	-18.3	kW
vehicle_energy_kJ_pos	6377	8789	10717	5968	2086	10847	18021	5347	4193	9106	12425	4735	8379	10738	kJ
vehicle_energy_kJ_neg	-2092	-595	-2215	-1326	-772	-3595	-4381	-1806	-1294	-3066	-4210	-1182	-3241	-4625	kJ
vehicle_energy_kJ_total	4285	8194	8502	4642	1313	7252	13641	3542	2899	6040	8215	3553	5138	6113	kJ
vehicle_energy_Whpm_net	160	222	295	187	141	205	241	153	135	188	219	132	192	228	Wh/mi

Appendix 5 - 2

UDDS - Urban Dynamometer Drive Schedule (1373 seconds)
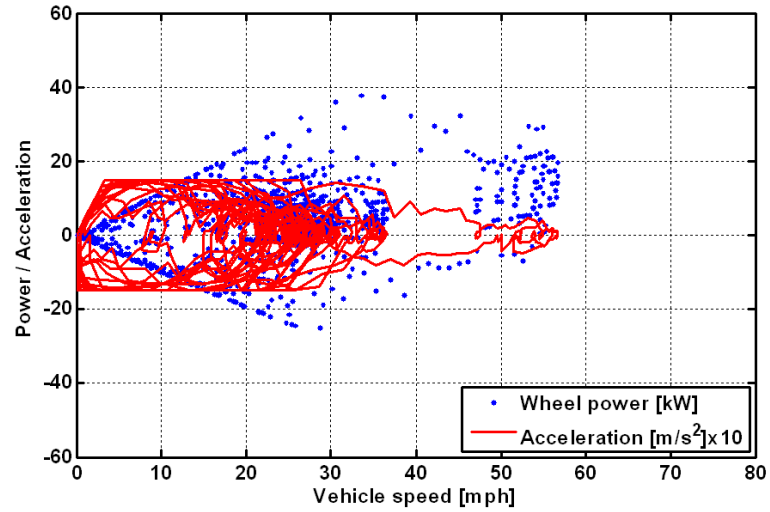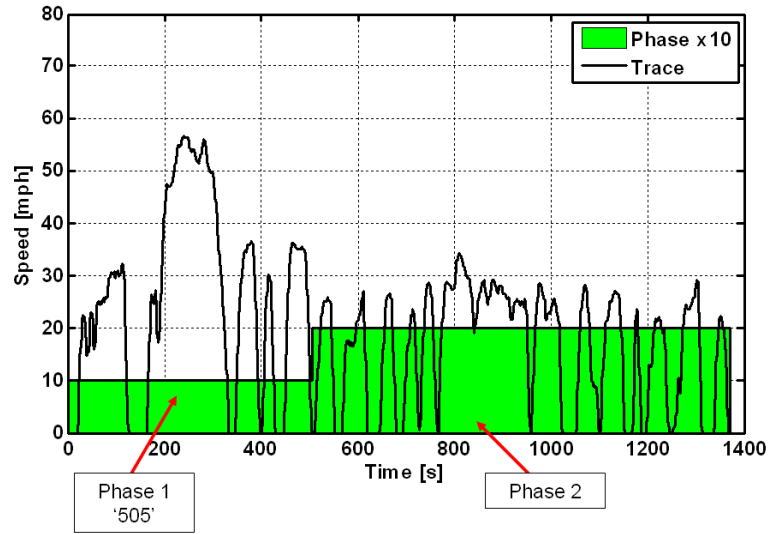
UDDS 2Bags 5spd 1373.txt.

accel_max	1.48	m/s^2
accel_min	-1.48	m/s^2
accel_pos_avg	0.5	m/s^2
accel_neg_avg	-0.58	m/s^2
trace_speed_avg	19.5	mph
trace_speed_max	56.7	mph
distance	7.45	mi
stoppercent	17.8	%
accelpercent	39.7	%
decelpercent	34.6	%
cruisepercent	7.9	%
drivepercent	82.2	%

Vehicle	Focus.	
vehicle_power_kW_max	37.7	kW
vehicle_power_kW_min	-25.2	kW
vehicle_power_kW_pos_avg	8	kW
vehicle_power_kW_neg_avg	-6.7	kW
vehicle_energy_kJ_pos	6377	kJ
vehicle_energy_kJ_neg	-2092	kJ
vehicle_energy_kJ_total	4285	kJ
vehicle_energy_Whpm_net	160	Wh/mi

Appendix 5 - 3

Highway Cycle (773 seconds)
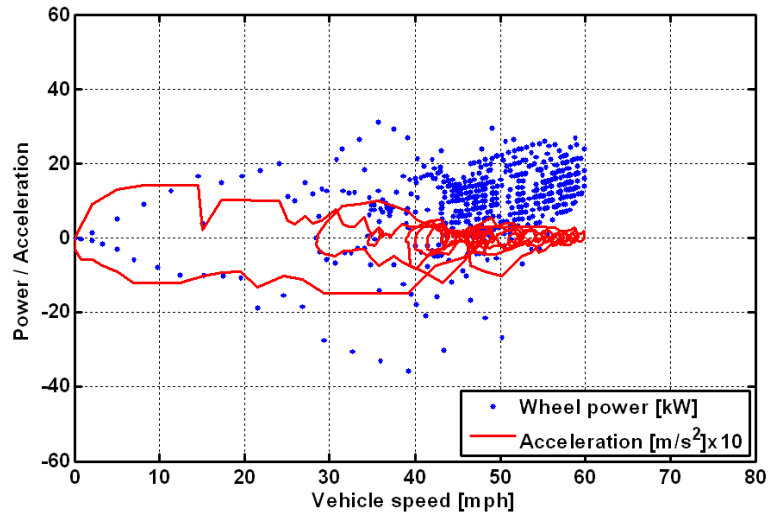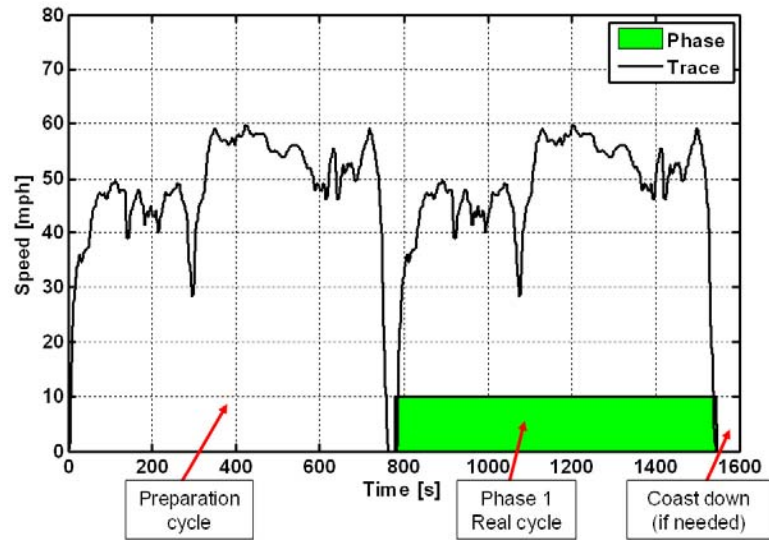
HWY 1Bag 5spd 773.txt.

accel_max	1.43	m/s^2
accel_min	-1.48	m/s^2
accel_pos_avg	0.19	m/s^2
accel_neg_avg	-0.22	m/s^2
trace_speed_avg	47.6	mph
trace_speed_max	59.9	mph
distance	10.25	mi
stoppercent	1.8	%
accelpercent	43.6	%
decelpercent	38.3	%
cruisepercent	16.2	%
drivepercent	98.2	%

Vehicle	Focus.	
vehicle_power_kW_max	31.1	kW
vehicle_power_kW_min	-35.6	kW
vehicle_power_kW_pos_avg	12.6	kW
vehicle_power_kW_neg_avg	-9.2	kW
vehicle_energy_kJ_pos	8789	kJ
vehicle_energy_kJ_neg	-595	kJ
vehicle_energy_kJ_total	8194	kJ
vehicle_energy_Whpm_net	222	Wh/mi

Appendix 5 - 4

US06 cycle (600 seconds)
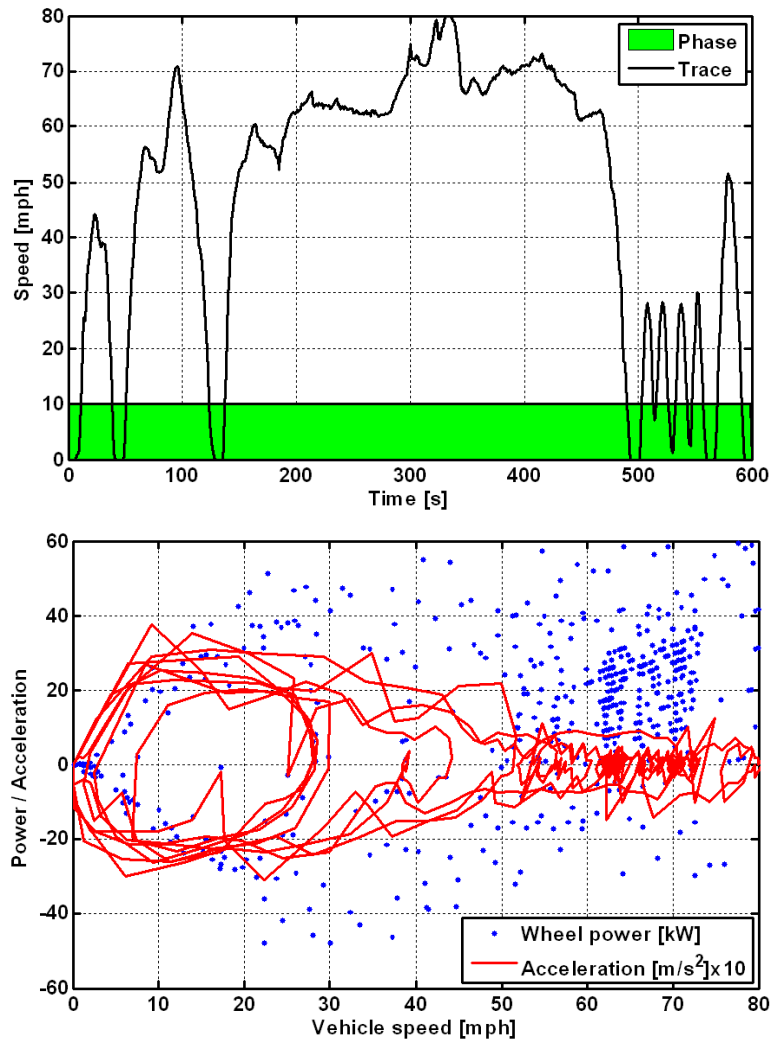
USO6 1Bag 600.txt.

accel_max	3.76	m/s^2
accel_min	-3.08	m/s^2
accel_pos_avg	0.67	m/s^2
accel_neg_avg	-0.73	m/s^2
trace_speed_avg	48	mph
trace_speed_max	80.3	mph
distance	8.01	mi
stoppercent	6.5	%
accelpercent	45.8	%
decelpercent	42.1	%
cruisepercent	5.5	%
drivepercent	93.5	%

Vehicle	Focus.	
vehicle_power_kW_max	95.3	kW
vehicle_power_kW_min	-49.5	kW
vehicle_power_kW_pos_avg	24.8	kW
vehicle_power_kW_neg_avg	-18	kW
vehicle_energy_kJ_pos	10717	kJ
vehicle_energy_kJ_neg	-2215	kJ
vehicle_energy_kJ_total	8502	kJ
vehicle_energy_Whpm_net	295	Wh/mi

NEDC cycle (1179 seconds)
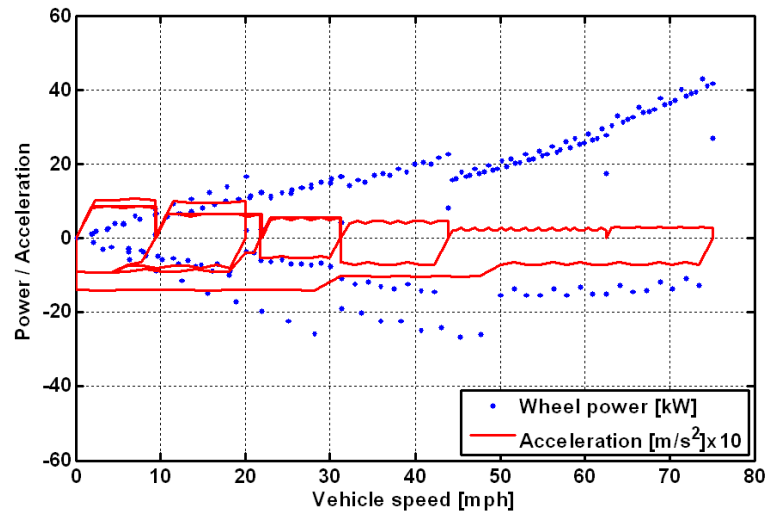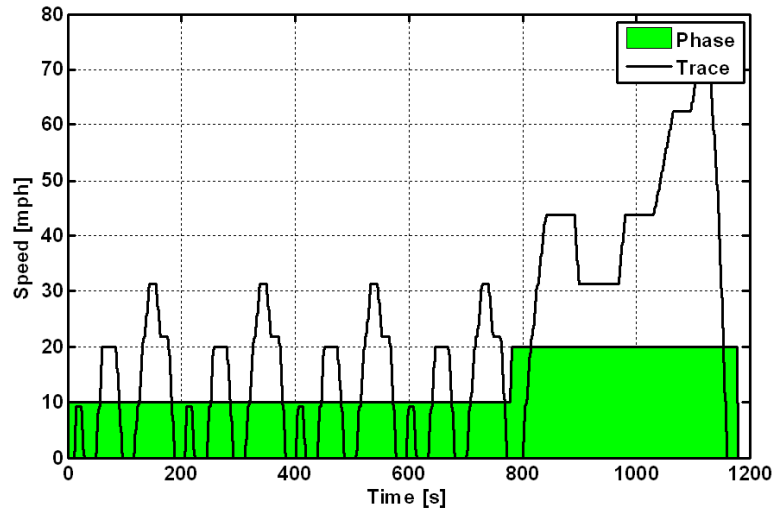
NEDC 2Bags 5Spd 1179.txt

accel_max	1.07	m/s^2
accel_min	-1.43	m/s^2
accel_pos_avg	0.6	m/s^2
accel_neg_avg	-0.79	m/s^2
trace_speed_avg	21	mph
trace_speed_max	75	mph
distance	6.88	mi
stoppercent	23.6	%
accelpercent	20.9	%
decelpercent	15.8	%
cruisepercent	39.6	%
drivepercent	76.4	%

Vehicle	Focus.	
vehicle_power_kW_max	42.8	kW
vehicle_power_kW_min	-26.6	kW
vehicle_power_kW_pos_avg	8.4	kW
vehicle_power_kW_neg_avg	-7.7	kW
vehicle_energy_kJ_pos	5968	kJ
vehicle_energy_kJ_neg	-1326	kJ
vehicle_energy_kJ_total	4642	kJ
vehicle_energy_Whpm_net	187	Wh/mi

Appendix 5 - 6

Japan 1015 cycle (659 seconds)
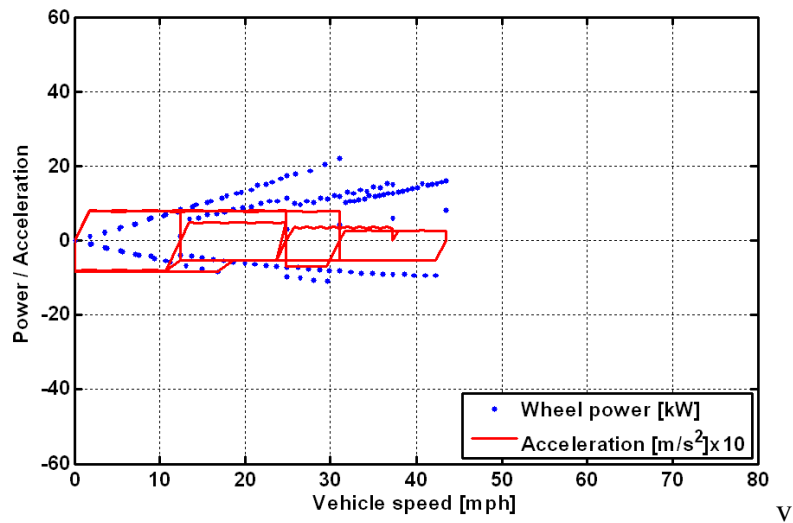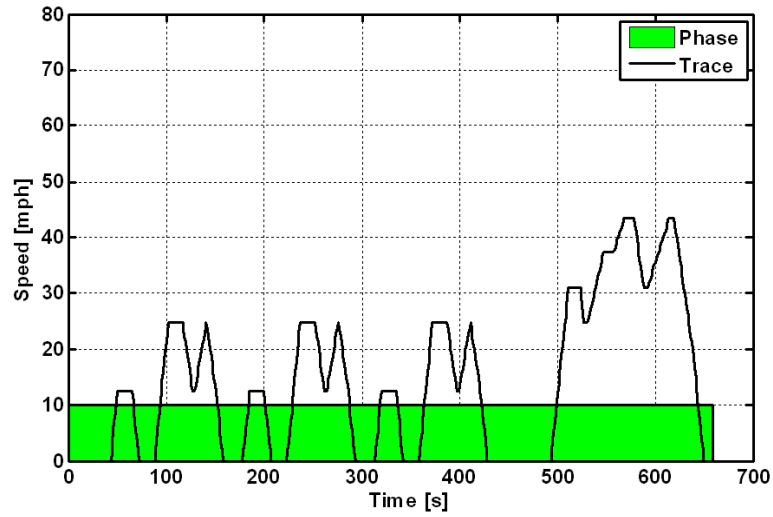
Jap1015 1Bag_659.txt

accel_max	0.81	m/s^2
accel_min	-0.83	m/s^2
accel_pos_avg	0.57	m/s^2
accel_neg_avg	-0.65	m/s^2
trace_speed_avg	14.1	mph
trace_speed_max	43.5	mph
distance	2.59	mi
stoppercent	31.2	%
accelpercent	25.2	%
decelpercent	22.1	%
cruisepercent	21.4	%
drivepercent	68.8	%

Vehicle	Focus.	
vehicle_power_kW_max	22	kW
vehicle_power_kW_min	-11	kW
vehicle_power_kW_pos_avg	6.8	kW
vehicle_power_kW_neg_avg	-5.6	kW
vehicle_energy_kJ_pos	2086	kJ
vehicle_energy_kJ_neg	-772	kJ
vehicle_energy_kJ_total	1313	kJ
vehicle_energy_Whpm_net	141	Wh/mi

Appendix 5 - 7

LA92 cycle (1435 seconds)
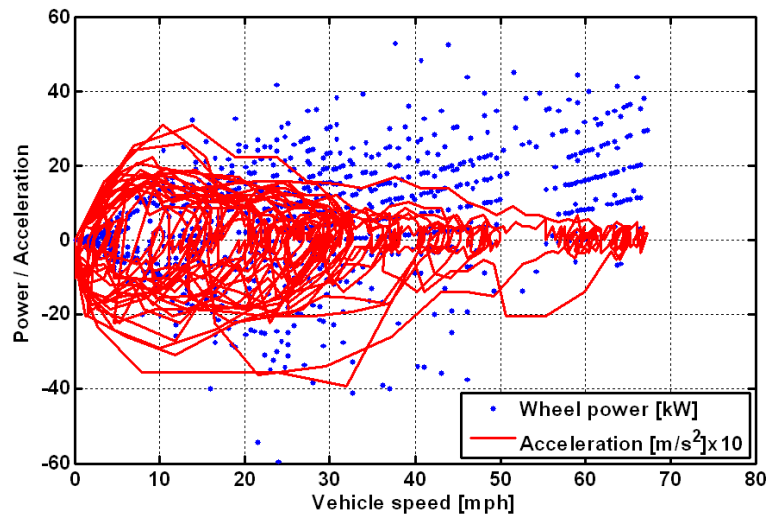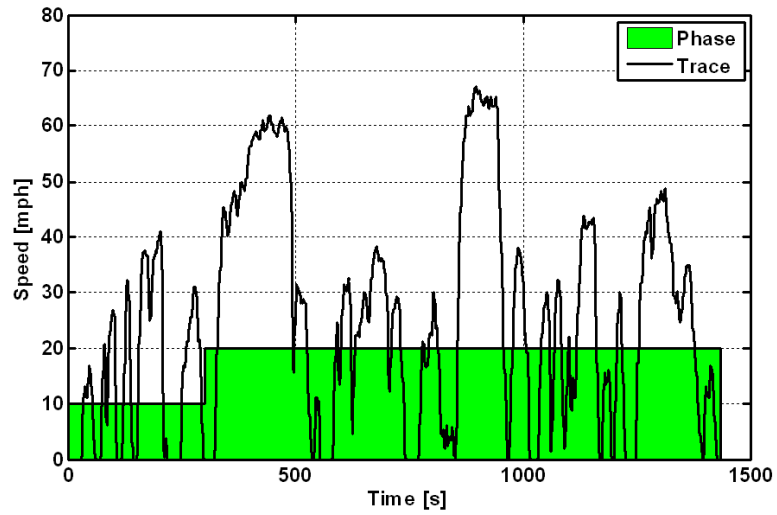
LA92 2Bags 1435.txt

accel_max	3.08	m/s^2
accel_min	-3.93	m/s^2
accel_pos_avg	0.67	m/s^2
accel_neg_avg	-0.75	m/s^2
trace_speed_avg	24.6	mph
trace_speed_max	67.2	mph
distance	9.82	mi
stoppercent	15.1	%
accelpercent	38.2	%
decelpercent	34.1	%
cruisepercent	12.5	%
drivepercent	84.9	%

Vehicle	Focus.	
Vehicle_power_kW_max	52.8	kW
Vehicle_power_kW_min	-87.1	kW
Vehicle_power_kW_pos_avg	12.8	kW
Vehicle_power_kW_neg_avg	-10.1	kW
Vehicle_energy_kJ_pos	10847	kJ
Vehicle_energy_kJ_neg	-3595	kJ
Vehicle_energy_kJ_total	7252	kJ
Vehicle_energy_Whpm_net	205	Wh/mi

ATDS cycle (1799 seconds)
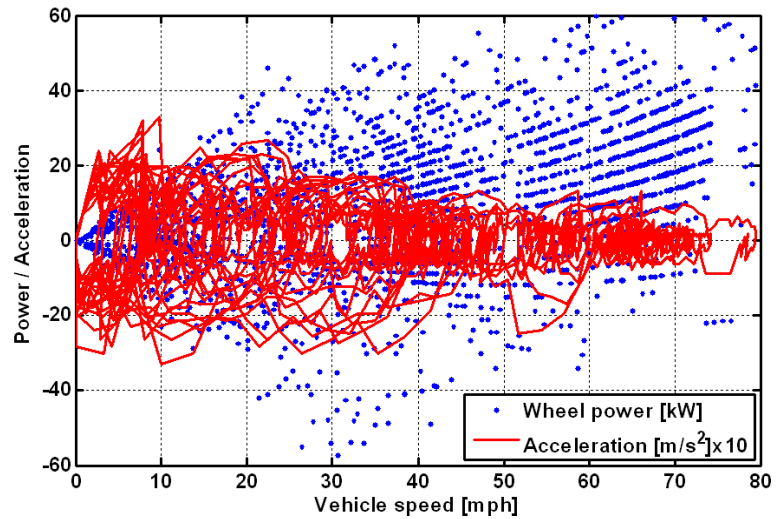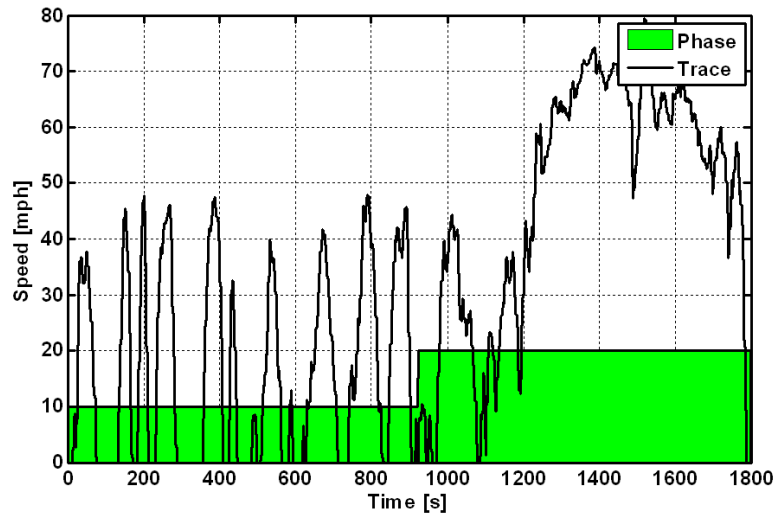
ATDS 2bag 1799.txt

accel_max	3.29	m/s^2
accel_min	-3.29	m/s^2
accel_pos_avg	0.61	m/s^2
accel_neg_avg	-0.6	m/s^2
trace_speed_avg	31.5	mph
trace_speed_max	79.4	mph
distance	15.75	mi
stoppercent	20.1	%
accelpercent	36.6	%
decelpercent	36.9	%
cruisepercent	6.3	%
drivepercent	79.9	%

Vehicle	Focus.	
vehicle_power_kW_max	84.4	kW
vehicle_power_kW_min	-82.3	kW
vehicle_power_kW_pos_avg	18.3	kW
vehicle_power_kW_neg_avg	-9.9	kW
vehicle_energy_kJ_pos	18021	kJ
vehicle_energy_kJ_neg	-4381	kJ
vehicle_energy_kJ_total	13641	kJ
vehicle_energy_Whpm_net	241	Wh/mi

Appendix 5 - 9

JC08 cycle (1376 seconds)
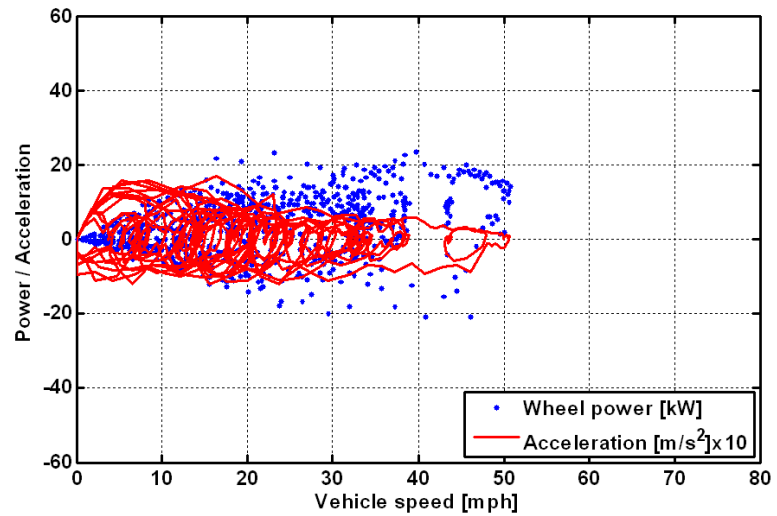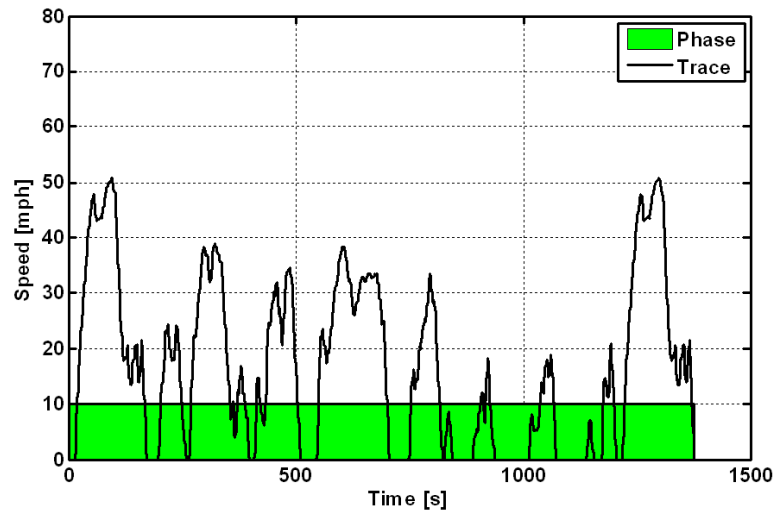
JC08 1bag 1376.txt

accel_max	1.69	m/s^2
accel_min	-1.22	m/s^2
accel_pos_avg	0.42	m/s^2
accel_neg_avg	-0.47	m/s^2
trace_speed_avg	16.8	mph
trace_speed_max	50.7	mph
distance	6.41	mi
stoppercent	26.1	%
accelpercent	38.2	%
decelpercent	34.1	%
cruisepercent	1.5	%
drivepercent	73.9	%

Vehicle	Focus.	
vehicle_power_kW_max	23.7	kW
vehicle_power_kW_min	-20.9	kW
vehicle_power_kW_pos_avg	8.1	kW
vehicle_power_kW_neg_avg	-5.2	kW
vehicle_energy_kJ_pos	5347	kJ
vehicle_energy_kJ_neg	-1806	kJ
vehicle_energy_kJ_total	3542	kJ
vehicle_energy_Whpm_net	153	Wh/mi

Appendix 5 - 10

0.8 X UDDS speed scaled (1373 seconds)
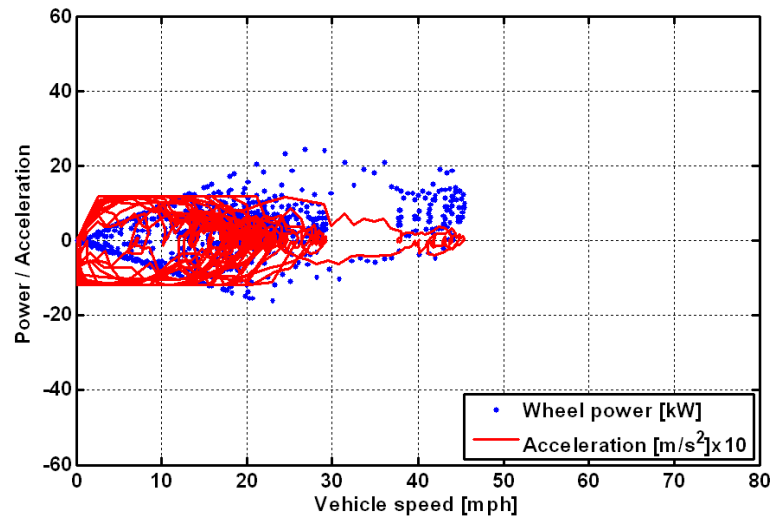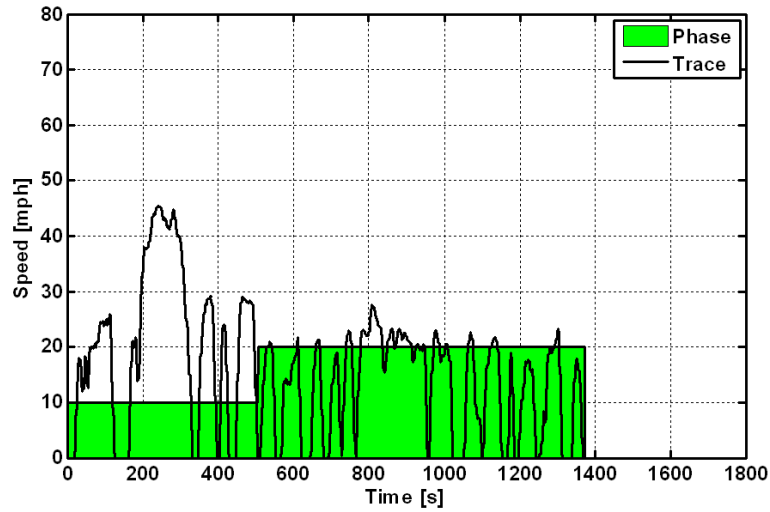
0.8xUDDS 2 bag 1373.txt

accel_max	1.18	m/s^2
accel_min	-1.18	m/s^2
accel_pos_avg	0.4	m/s^2
accel_neg_avg	-0.46	m/s^2
trace_speed_avg	15.6	mph
trace_speed_max	45.4	mph
distance	5.96	mi
stoppercent	17.8	%
accelpercent	39.7	%
decelpercent	34.6	%
cruisepercent	7.9	%
drivepercent	82.2	%

Vehicle	Focus.	
vehicle_power_kW_max	24.3	kW
vehicle_power_kW_min	-15.9	kW
vehicle_power_kW_pos_avg	5.2	kW
vehicle_power_kW_neg_avg	-4.3	kW
vehicle_energy_kJ_pos	4193	kJ
vehicle_energy_kJ_neg	-1294	kJ
vehicle_energy_kJ_total	2899	kJ
vehicle_energy_Whpm_net	135	Wh/mi

Appendix 5 - 11

1.2 X UDDS speed scaled (1373 seconds)
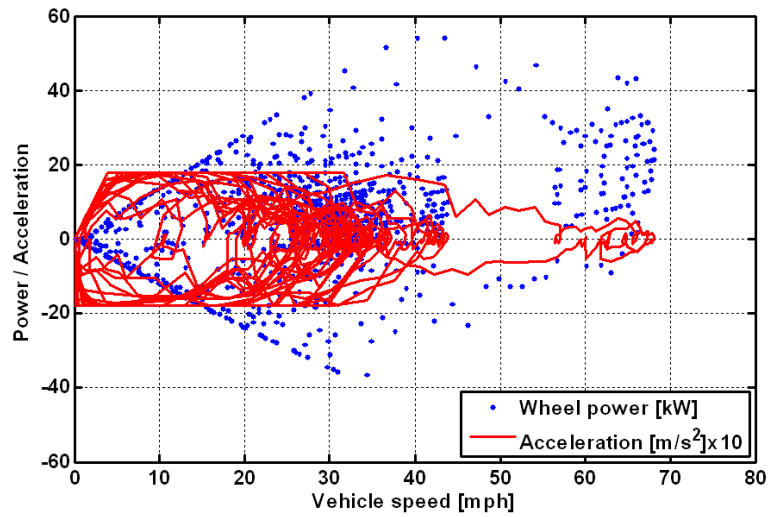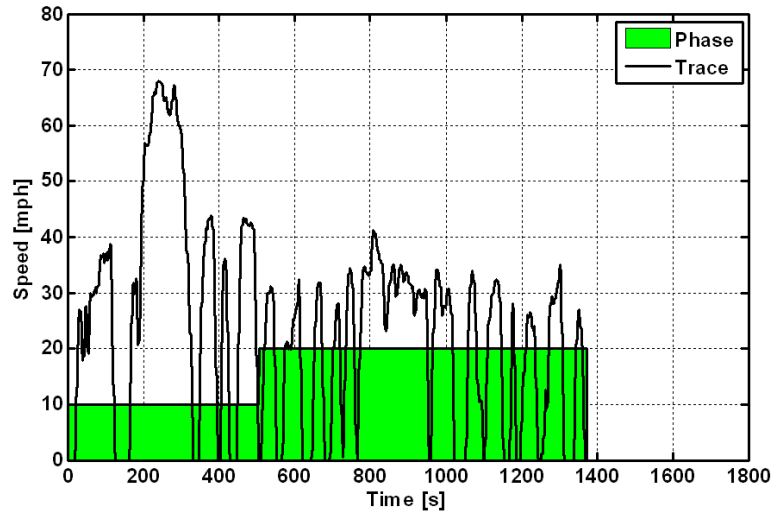
1.2xUDDS 2 bag 1373.txt

accel_max	1.77	m/s^2
accel_min	-1.77	m/s^2
accel_pos_avg	0.6	m/s^2
accel_neg_avg	-0.69	m/s^2
trace_speed_avg	23.4	mph
trace_speed_max	68	mph
distance	8.94	mi
stoppercent	17.8	%
accelpercent	39.7	%
decelpercent	34.6	%
cruisepercent	7.9	%
drivepercent	82.2	%

Vehicle	Focus.	
vehicle_power_kW_max	54.2	kW
vehicle_power_kW_min	-36.5	kW
vehicle_power_kW_pos_avg	11.5	kW
vehicle_power_kW_neg_avg	-9.6	kW
vehicle_energy_kJ_pos	9106	kJ
vehicle_energy_kJ_neg	-3066	kJ
vehicle_energy_kJ_total	6040	kJ
vehicle_energy_Whpm_net	188	Wh/mi

Appendix 5 - 12

1.4 X UDDS speed scaled (1373 seconds)
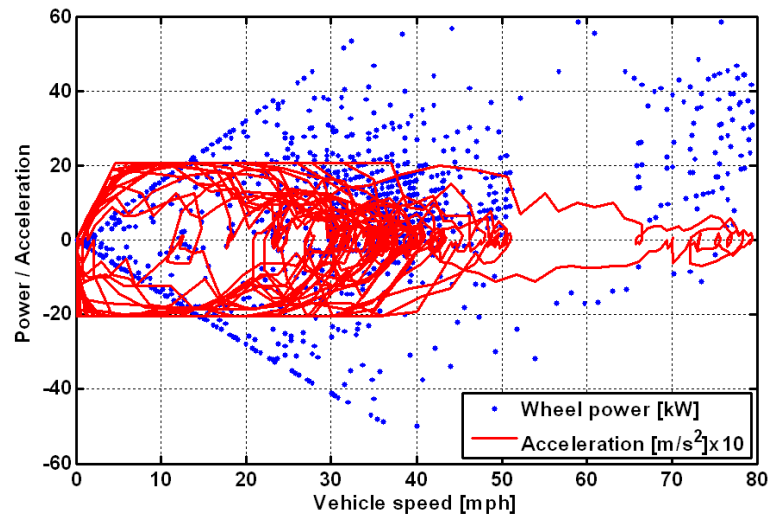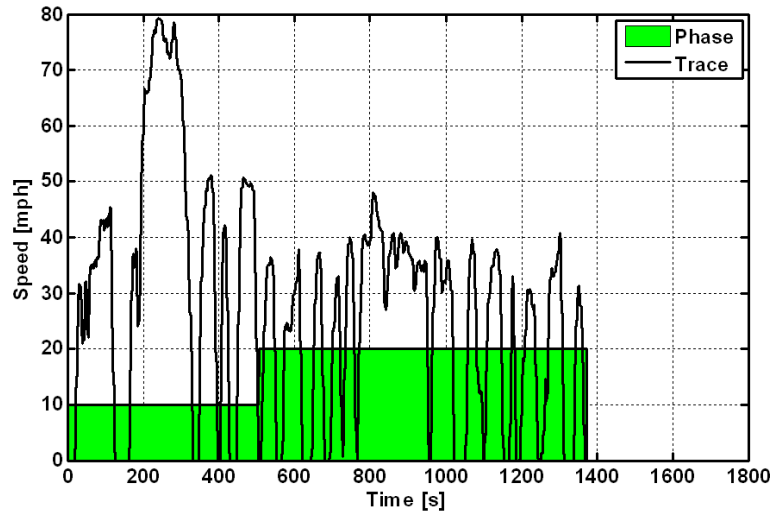
1.4xUDDS 2 bag 1373.txt

accel_max	2.07	m/s^2
accel_min	-2.07	m/s^2
accel_pos_avg	0.71	m/s^2
accel_neg_avg	-0.81	m/s^2
trace_speed_avg	27.3	mph
trace_speed_max	79.4	mph
distance	10.43	mi
stoppercent	17.8	%
accelpercent	39.7	%
decelpercent	34.6	%
cruisepercent	7.9	%
drivepercent	82.2	%

Vehicle	Focus.	
vehicle_power_kW_max	73.8	kW
vehicle_power_kW_min	-49.8	kW
vehicle_power_kW_pos_avg	15.7	kW
vehicle_power_kW_neg_avg	-13.1	kW
vehicle_energy_kJ_pos	12425	kJ
vehicle_energy_kJ_neg	-4210	kJ
vehicle_energy_kJ_total	8215	kJ
vehicle_energy_Whpm_net	219	Wh/mi

0.8 X UDDS time and speed scaled (1716 seconds)
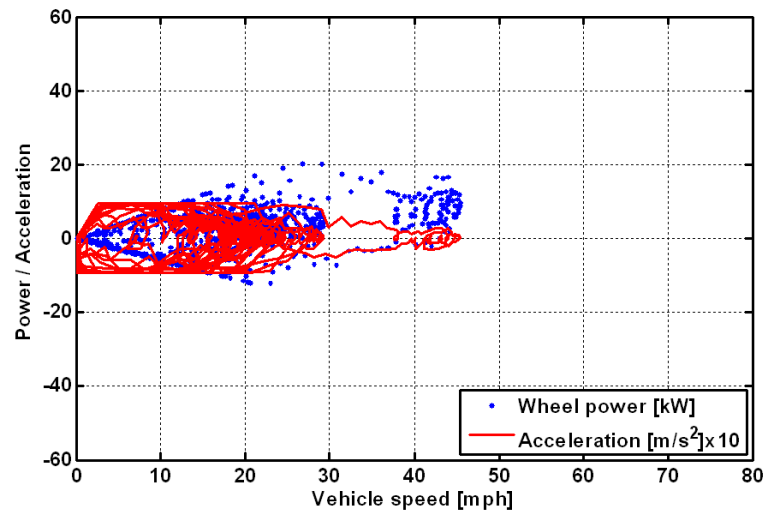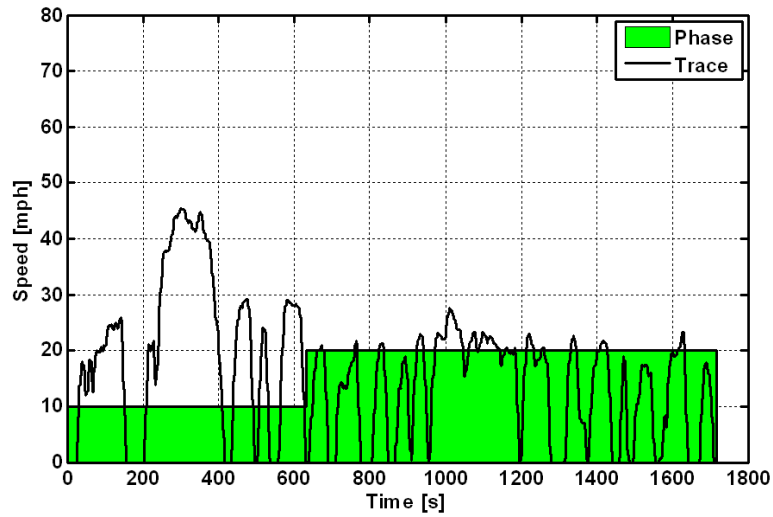
0.8xUDDS 2 bag 1716.txt

accel_max	0.94	m/s^2
accel_min	-0.94	m/s^2
accel_pos_avg	0.32	m/s^2
accel_neg_avg	-0.37	m/s^2
trace_speed_avg	15.6	mph
trace_speed_max	45.4	mph
distance	7.45	mi
stoppercent	17.8	%
accelpercent	39.7	%
decelpercent	34.6	%
cruisepercent	7.9	%
drivepercent	82.2	%

Vehicle	Focus.	
vehicle_power_kW_max	20.2	kW
vehicle_power_kW_min	-12.2	kW
vehicle_power_kW_pos_avg	4.5	kW
vehicle_power_kW_neg_avg	-3.5	kW
vehicle_energy_kJ_pos	4735	kJ
vehicle_energy_kJ_neg	-1182	kJ
vehicle_energy_kJ_total	3553	kJ
vehicle_energy_Whpm_net	132	Wh/mi

Appendix 5 - 14

1.2 X UDDS time and speed scaled (1144 seconds)
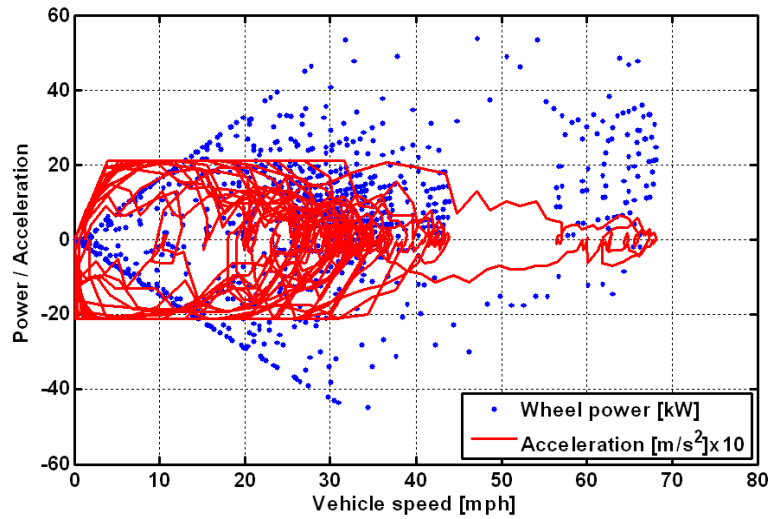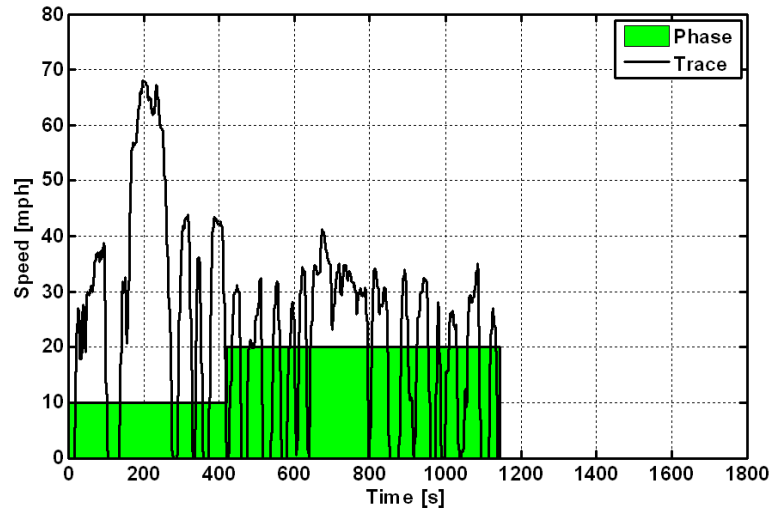
1.2xUDDS 2 bag 1144.txt

accel_max	2.12	m/s^2
accel_min	-2.12	m/s^2
accel_pos_avg	0.73	m/s^2
accel_neg_avg	-0.83	m/s^2
trace_speed_avg	23.4	mph
trace_speed_max	68	mph
distance	7.45	mi
stoppercent	17.8	%
accelpercent	39.7	%
decelpercent	34.6	%
cruisepercent	7.9	%
drivepercent	82.2	%

Vehicle	Focus.	
vehicle_power_kW_max	63.6	kW
vehicle_power_kW_min	-44.8	kW
vehicle_power_kW_pos_avg	13	kW
vehicle_power_kW_neg_avg	-11.6	kW
vehicle_energy_kJ_pos	8379	kJ
vehicle_energy_kJ_neg	-3241	kJ
vehicle_energy_kJ_total	5138	kJ
vehicle_energy_Whpm_net	192	Wh/mi

Appendix 5 - 15

1.4 X UDDS time and speed scaled (981 seconds)
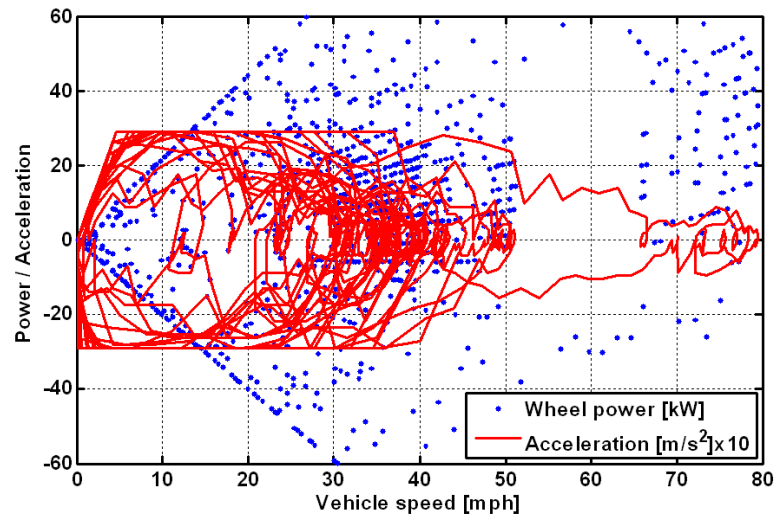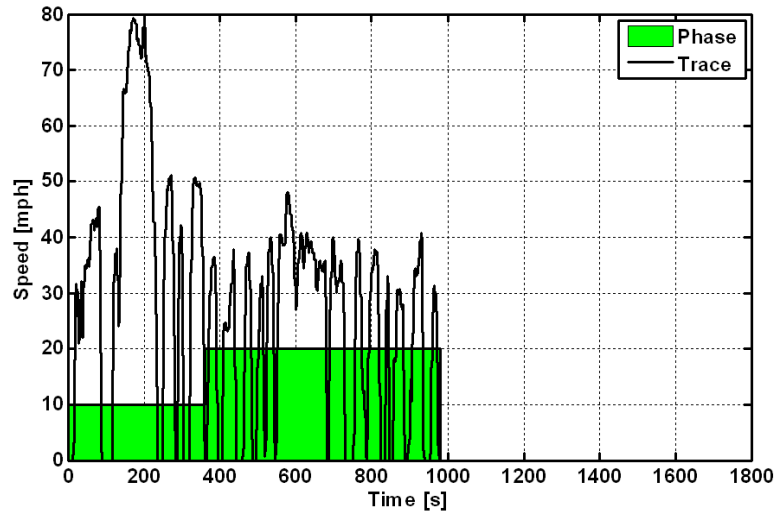
1.4xUDDS 2 bag 981.txt		
accel_max	2.89	m/s^2
accel_min	-2.89	m/s^2
accel_pos_avg	0.99	m/s^2
accel_neg_avg	-1.13	m/s^2
trace_speed_avg	27.3	mph
trace_speed_max	79.4	mph
distance	7.45	mi
stoppercent	17.8	%
accelpercent	39.7	%
decelpercent	34.6	%
cruisepercent	7.9	%
drivepercent	82.2	%

Vehicle	Focus.	
vehicle_power_kW_max	99.5	kW
vehicle_power_kW_min	-72.5	kW
vehicle_power_kW_pos_avg	19.8	kW
vehicle_power_kW_neg_avg	-18.3	kW
vehicle_energy_kJ_pos	10738	kJ
vehicle_energy_kJ_neg	-4625	kJ
vehicle_energy_kJ_total	6113	kJ
vehicle_energy_Whpm_net	228	Wh/mi

Appendix 5 - 16

Appendix 6: Typical signal list collected on MATT during a test

Here is a typical channel list of data collected for MATT tests in the ARPF.

Dynamometer data	Time [s]		**Vehicle DAQ temperatures**	DAQ Time [s]
	Trace Time [s]			Eng_coolant_supply_temp
	Drive Schedule [MPH]			Eng_coolant_return_temp
	Bag Number [n]			Eng_exhaust_precat_temp
	Vehicle Speed [MPH]			Eng_exhaust_brickcat1_temp
	Dyno Spd Front [MPH]			Eng_exhaust_midcat_temp
	Dyno_TractiveForce_Front [N]			Eng_exhaust_brickcat2_temp
	Dyno Front Load Cell			Eng_exhaust_postcat_temp
	Dyno Spd Rear [MPH]			Eng_oil_temp
	Dyno Rear Load Cell			Eng_intake_air_temp
	Dyno_TractiveForce_Rear [N]			Trans_coolant_supply_temp
	DilAir RH [%]			Trans_coolant_return_temp
	Tailpipe Pressure [in H2O]			Eng_coolant_return_WP
	Cell Temp [C]			Radiator_air_outlet_temp
	Cell RH [%]			Rear_diff_temp
	Cell Press [inHg]		**Vehicle DAQ temperatures**	Engine_speed_rpm
	Tire_Temp [F]			Engine_torque_Nm
Emissions information	Dilute THC [ppm]			Motor_speed_rpm
	Dilute CH4 [ppm]			Motor_torque_Nm
	Dilute NOx [ppm]			Driveshaft_speed_rpm
	Dilute COlow [ppm]			Driveshaft_torque_Nm
	Dilute COmid [ppm]			Clutch_feedback_V
	Dilute CO2 [ppm]			Eng_FuelFlow_Direct2 [cc/s]
	Dilute H2O [ppm]			Throttle_command_V
	CVS Volume Flow [Nm^3/min]			Motor_command_V
	CVS Corrected Volume Flow [Nm^3/min]			Clutch_command_V
	CVS Pressure [hPa]			Brake_command_V
	CVS Temperature [K]			Rotor_temp_degC
				Tire_temp_degC
				Fuel_temperature [C]
				New_Direct_FuelFlow [cc/sec]

Indicated in-cylinder pressure data	IFILE1:CY'IMEP1
	IFILE1:CY'IMEP3
	IFILE1:CY'IMEPH1
	IFILE1:CY'IMEPH3
	IFILE1:CY'AI50%_1
	IFILE1:CY'AI50%_3
	IFILE1:CY'PMAX1
	IFILE1:CY'PMAX3
	IFILE1:CY'RMAX1
	IFILE1:CY'RMAX3
	IFILE1:MSC'COVIMEP1
	IFILE1:MSC'COVIMEP3
	IFILE1:CY'SPEED
	Dyno Distance [mi]
Processed modal emissions data	THC [mg/s]
	CH4 [mg/s]
	NOx [mg/s]
	COlow [mg/s]
	COmid [mg/s]
	CO2 [mg/s]
	HFID [mg/s]
	NMHC [mg/s]
	Fuel [g/s]

Control system data (control parameters and real time simulation)	ess_current
	ess_voltage
	emcp_mode
	emcp_p_elec_des_W
	emcp_p_eng_des_W
	emcp_ptot_W
	bmcp_charge_power_limit_W
	bmcp_discharge_power_limit_W
	bmcp_psoc_W
	ecm_max_power_W
	emcp_pdrv_W
	emcp_peng_opt_W
	vmcp_eng_opt_ok
	vmcp_hybrid_ok
	vmcp_operating_mode
	vmcp_target_SOC_out
	ecm_engine_speed_RPM
	scope_engtrqdmd
	scope_mctrqdmd
	scope_whbkrqdmd
	trace
	drv_trq_dmd
	key_on
	gb_gear
	clutch_state
	trs_mc_spd
	eng_spd_rpm
	eng_pedal_position_deg
	ess_soc
	mc_trq_cmd_voltage
	mc_spd
	mc_trq
	mc_trq_bis
	wh_trq
	wh_trq_filtered
	wh_spd_mph

Appendix 7: Conventional vehicle results for all standard drive cycles

This appendix provides further details and analysis on the conventional vehicle operation.

Simple linear drive cycles

	NEDC hot	Jap 1015 hot
Test number	60807056	60807055
Fuel economy	**35.01 [mpg]**	**30.69 [mpg]**
Emissions		
THC	0.0017 [g/mi]	0.0028 [g/mi]
CH4	0.0005 [g/mi]	0.0035 [g/mi]
NMHC	0.0016 [g/mi]	0.0016 [g/mi]
NOx	0.0023 [g/mi]	0.0620 [g/mi]
CO	0.0766 [g/mi]	0.0299 [g/mi]
CO2	253.8 [g/mi]	289.7 [g/mi]
Energy summary		
Fuel	27.8 [MJ]	12.45 [MJ]
Engine indicated	10.23 [MJ]	4.00 [MJ]
Engine crankshaft	6.88 [MJ]	2.53 [MJ]
Transmission	5.35 [MJ]	1.84 [MJ]
Dynamometer	3.96 [MJ]	1.42 [MJ]
Braking (possible regen)	1.39 [MJ]	0.82 [MJ]
Average cycle efficiency		
Engine indicated	36.8 [%]	32.1 [%]
Engine brake	24.8 [%]	20.3 [%]
Transmission	74.1 [%]	77.5 [%]

60807056 NEDC hot

60807056 NEDC hot

60807056 NEDC hot

60807056 NEDC hot

60807055 Jap1015 hot

60807055 Jap1015 hot

60807055 Jap1015 hot

60807055 Jap1015 hot
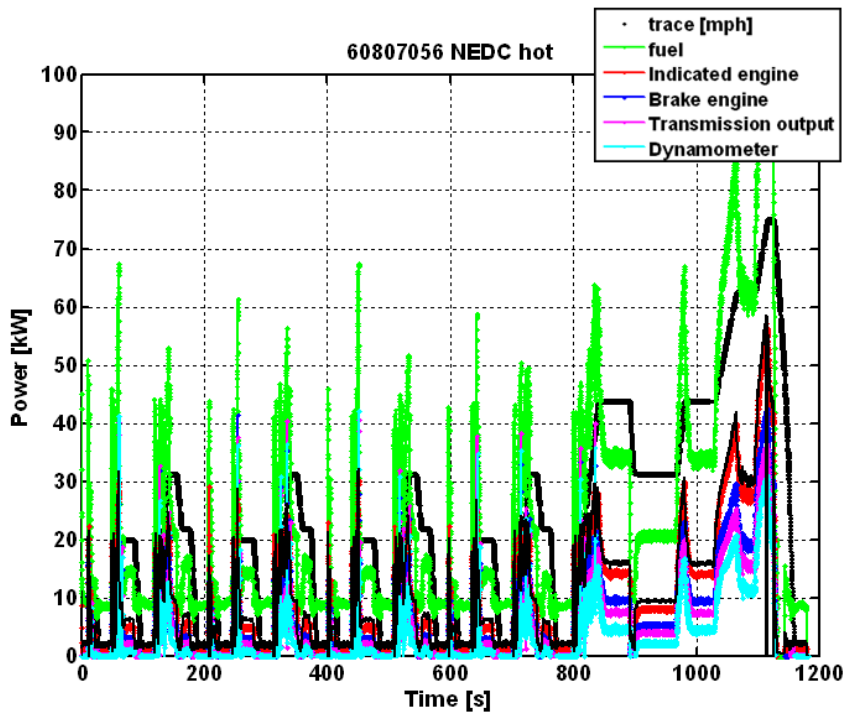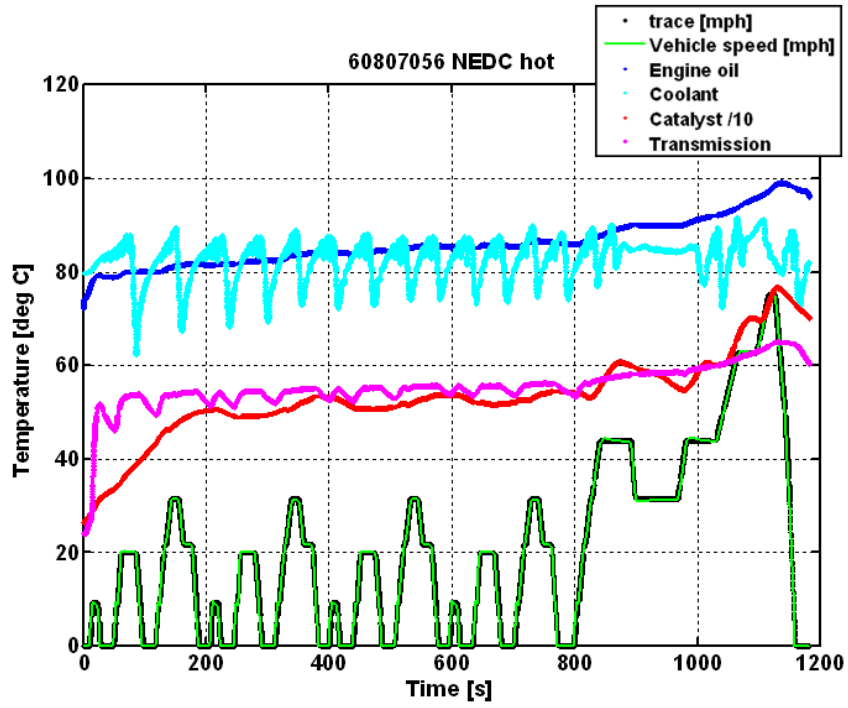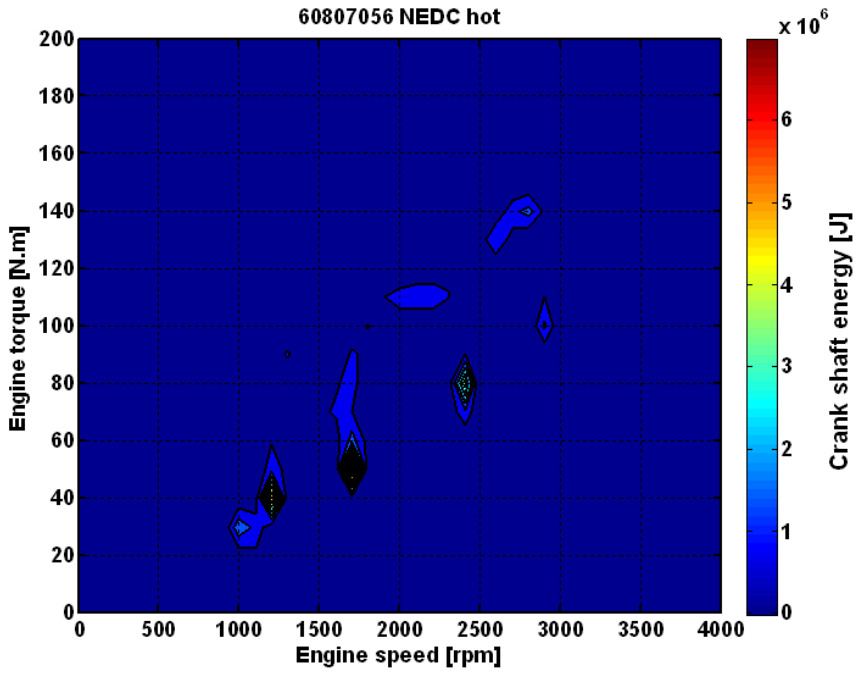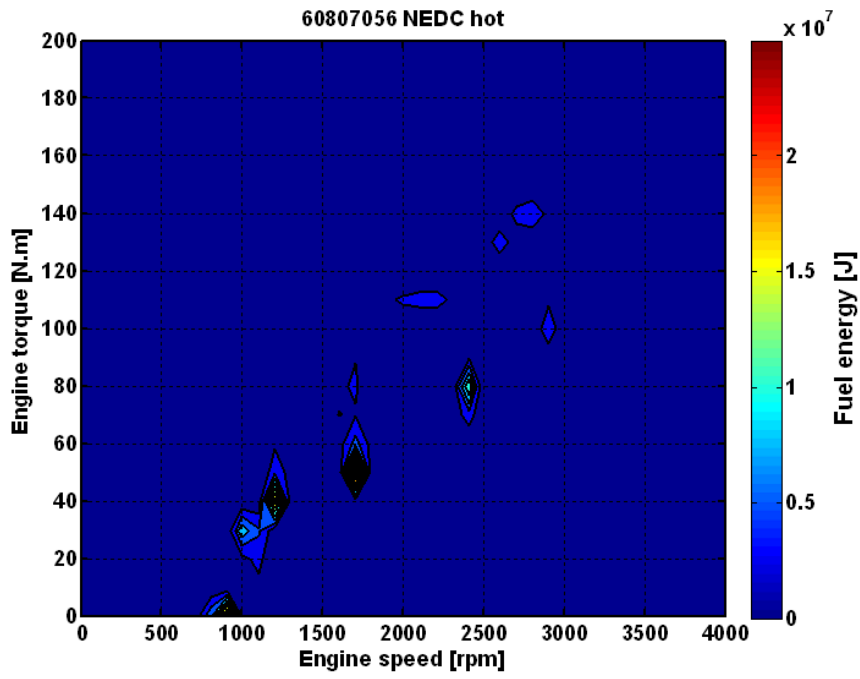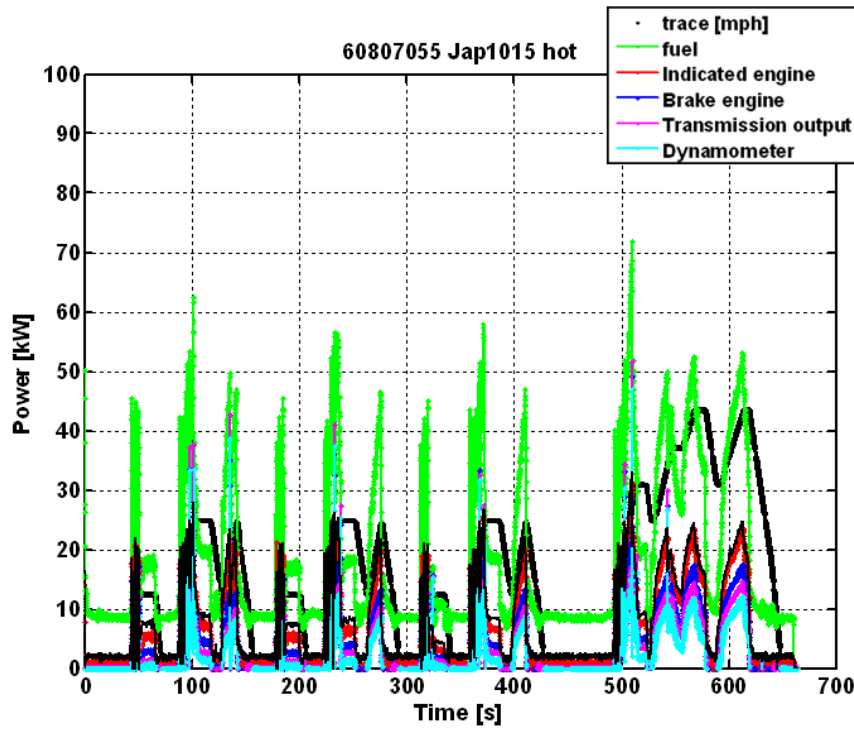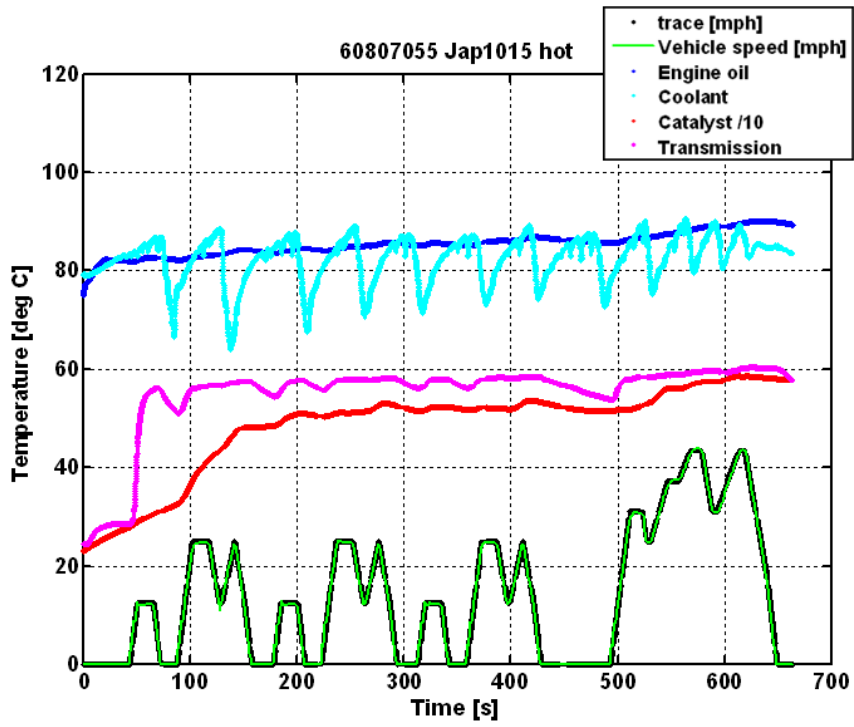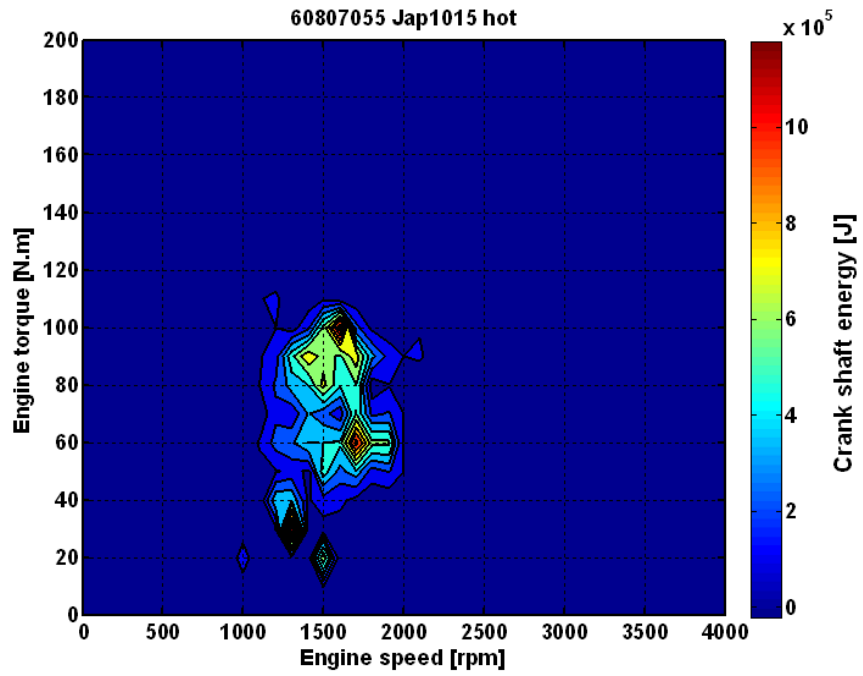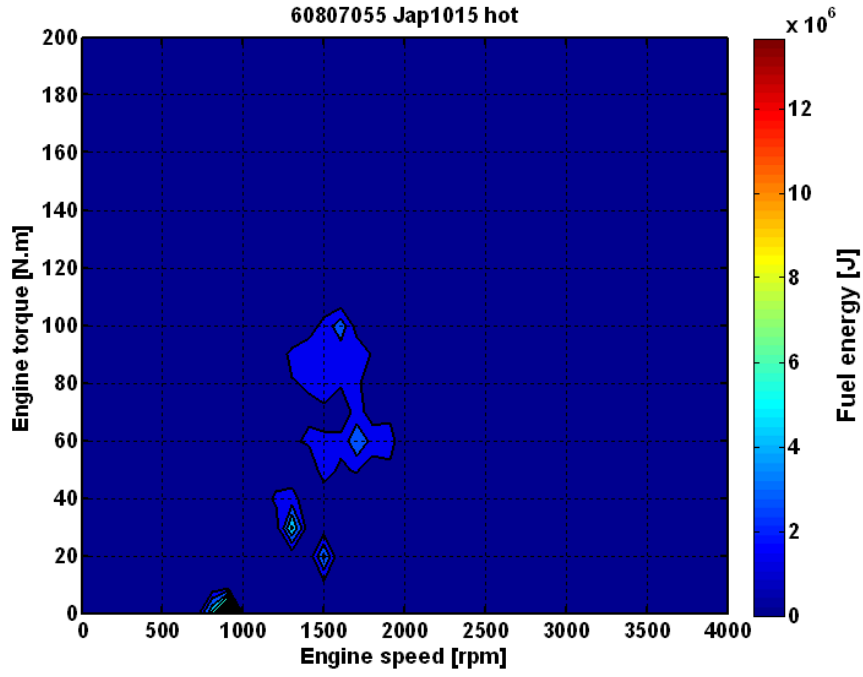
More complex drive cycles

	LA92 hot	**ATDS hot**	**JC08 hot**
Test number	60807061	60807063	60807062
Fuel economy	**28.22 [mpg]**	**30.22 [mpg]**	**30.80 [mpg]**
Emissions			
THC	0.0019 [g/mi]	0.0001 [g/mi]	0.0021 [g/mi]
CH4	0.0010 [g/mi]	0.0009 [g/mi]	0.0017 [g/mi]
NMHC	0.0015 [g/mi]	0.0002 [g/mi]	0.0015 [g/mi]
NOx	0.0064 [g/mi]	0.1091 [g/mi]	0.0564 [g/mi]
CO	0.0408 [g/mi]	0.0211 [g/mi]	0.0749 [g/mi]
CO2	315.08 [g/mi]	294.20 [g/mi]	288.55 [g/mi]
Energy summary			
Fuel	47.06 [MJ]	69.00 [MJ]	29.47 [MJ]
Engine indicated	18.99 [MJ]	30.24 [MJ]	10.74 [MJ]
Engine crankshaft	12.42 [MJ]	19.16 [MJ]	6.28 [MJ]
Transmission	9.67 [MJ]	15.17 [MJ]	4.69 [MJ]
Dynamometer	7.68 [MJ]	12.30 [MJ]	3.66 [MJ]
Braking (possible regen)	3.70 [MJ]	3.80 [MJ]	1.92 [MJ]
Average cycle efficiency			
Engine indicated	40.4 [%]	43.8 [%]	36.4 [%]
Engine brake	26.4 [%]	27.8 [%]	21.3 [%]
Transmission	79.4 [%]	80.1 [%]	78.0 [%]

60807061 LA92 hot

60807061 LA92 hot

60807061 LA92 hot

60807061 LA92 hot

60807063 ATDS hot

60807063 ATDS hot

60807063 ATDS hot

60807063 ATDS hot

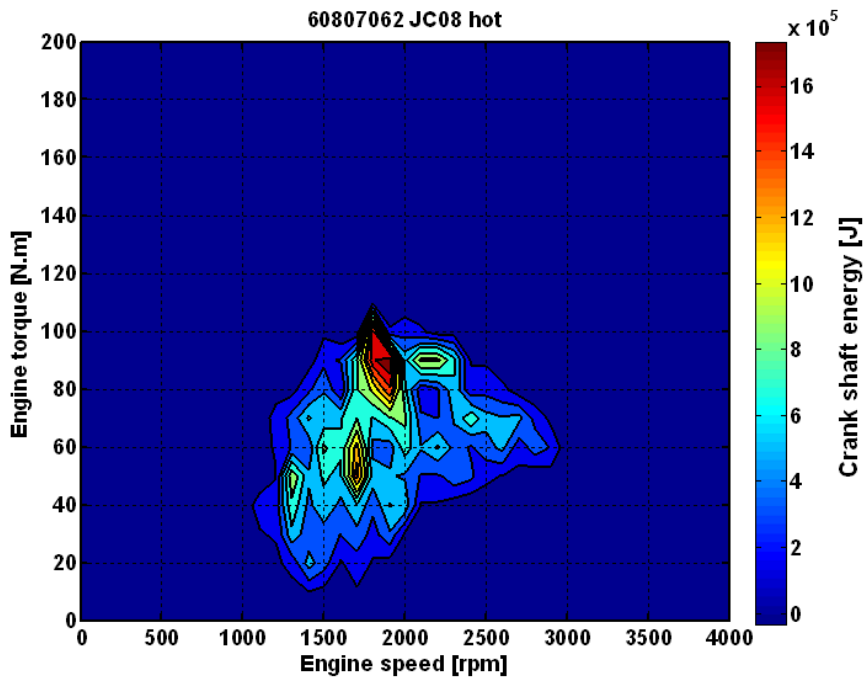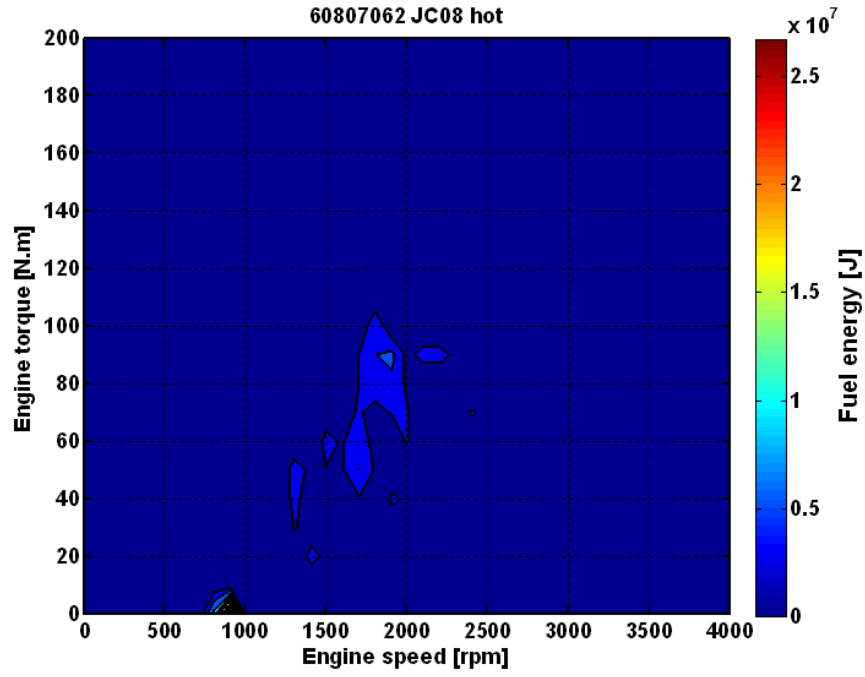60807062 JC08 hot

60807062 JC08 hot
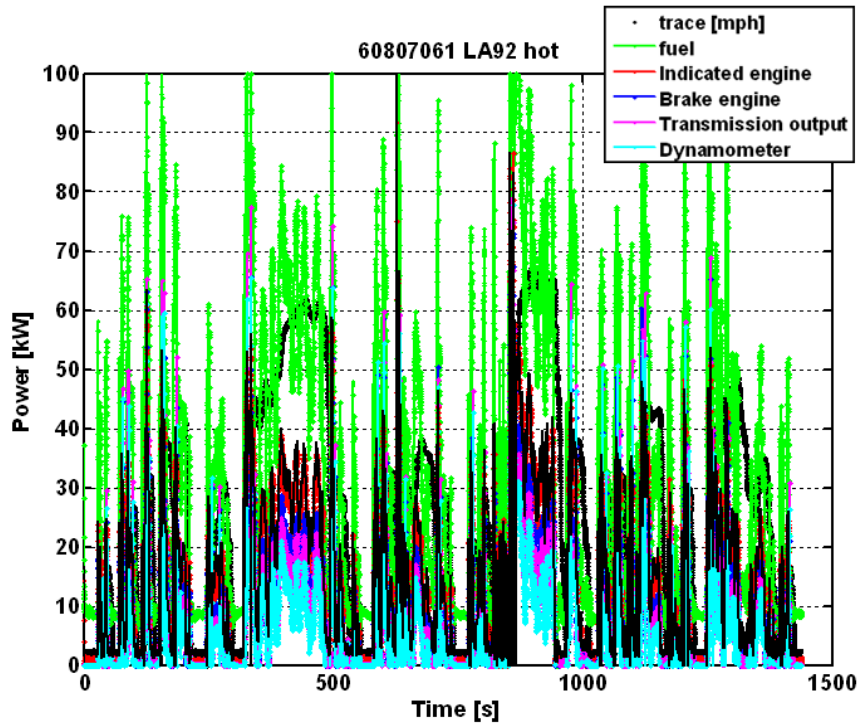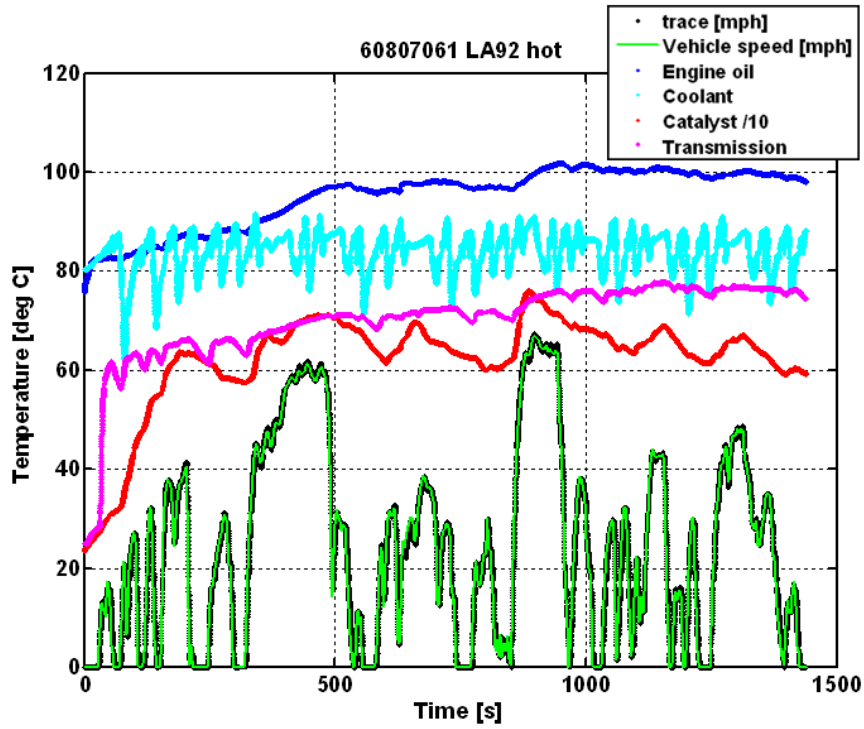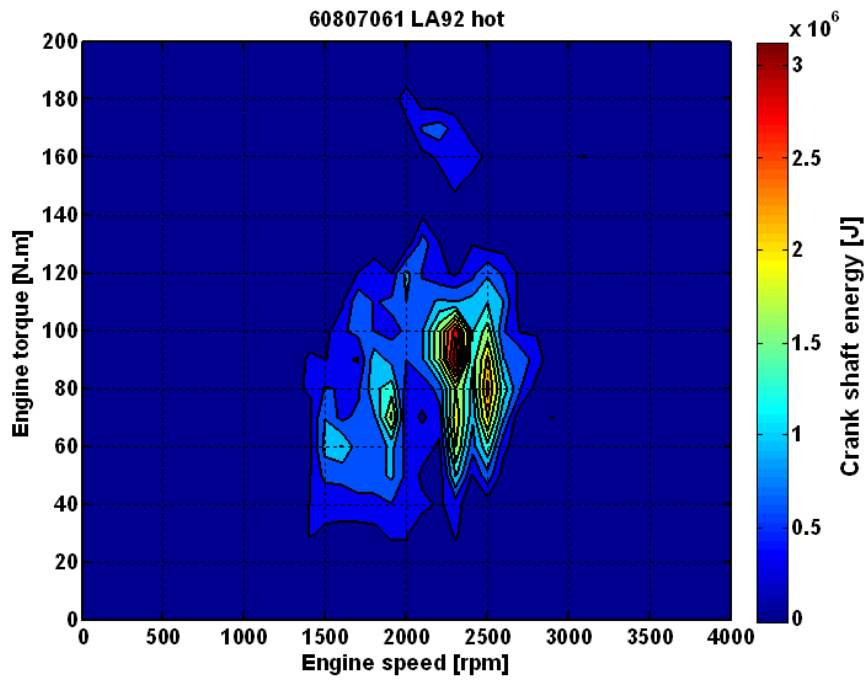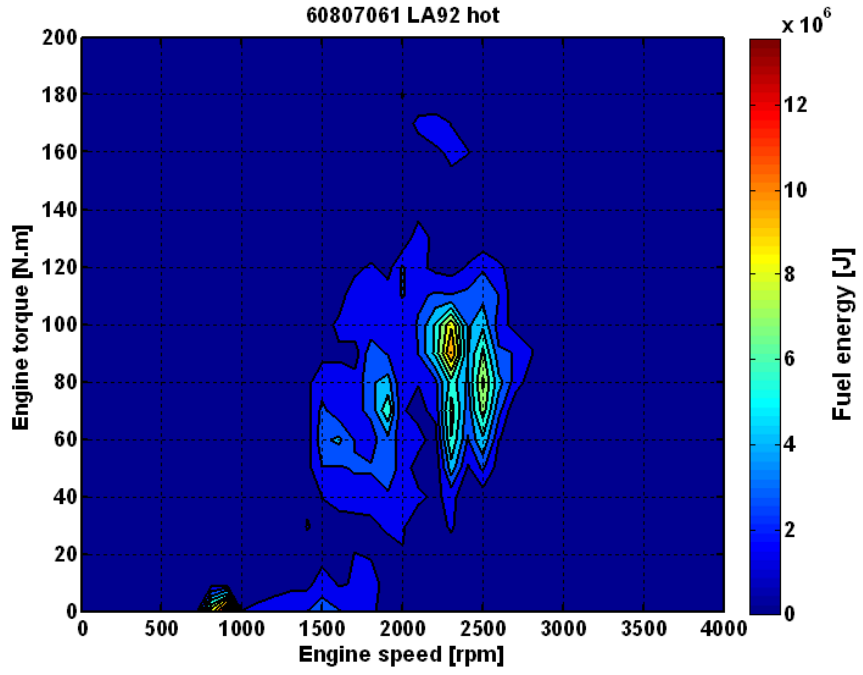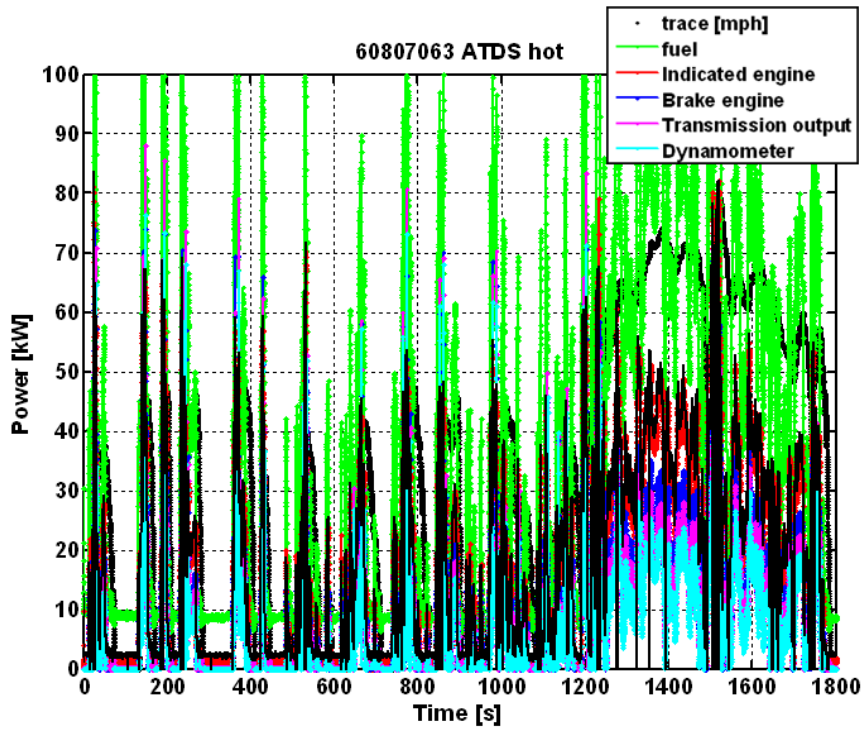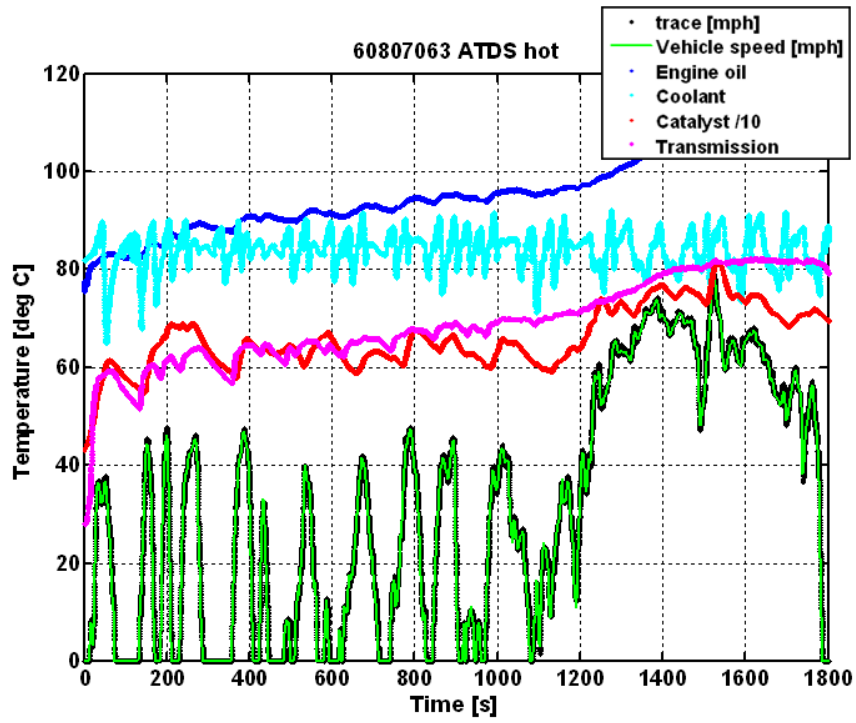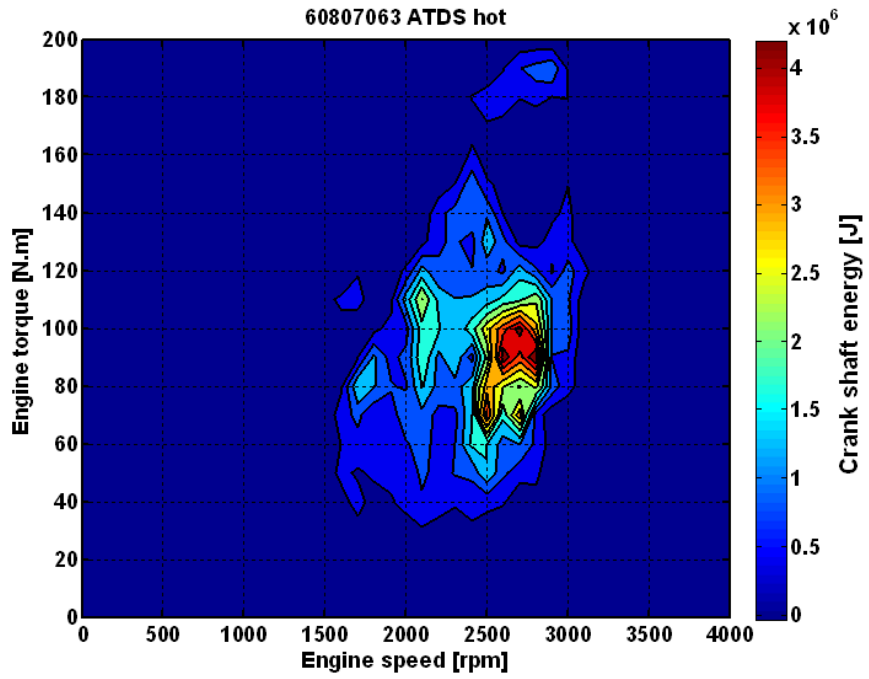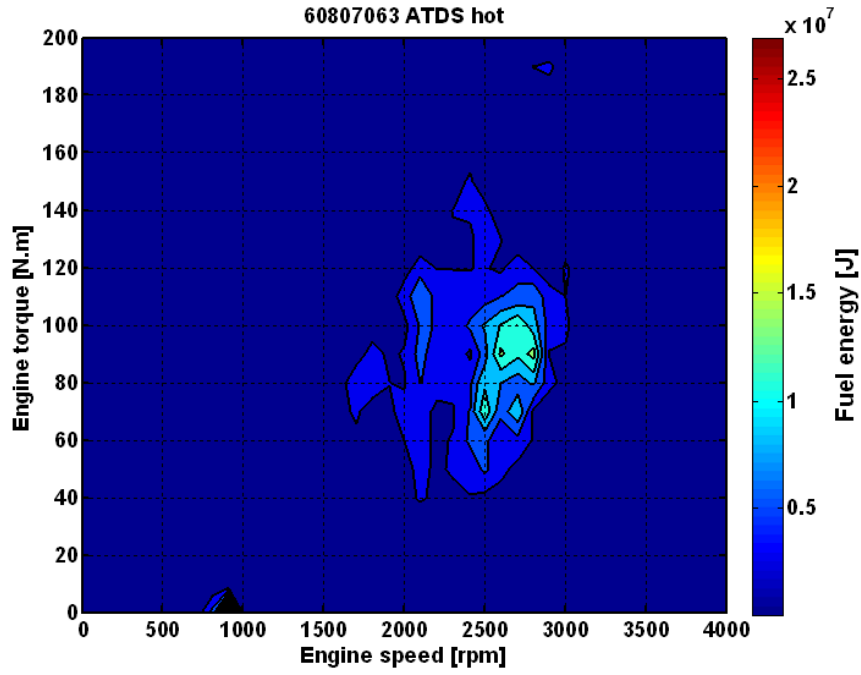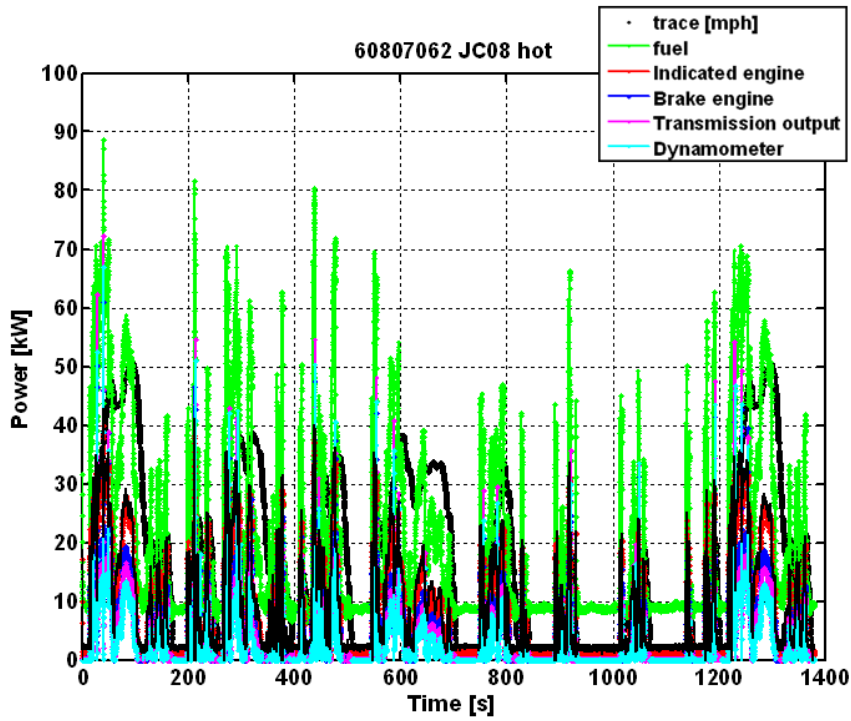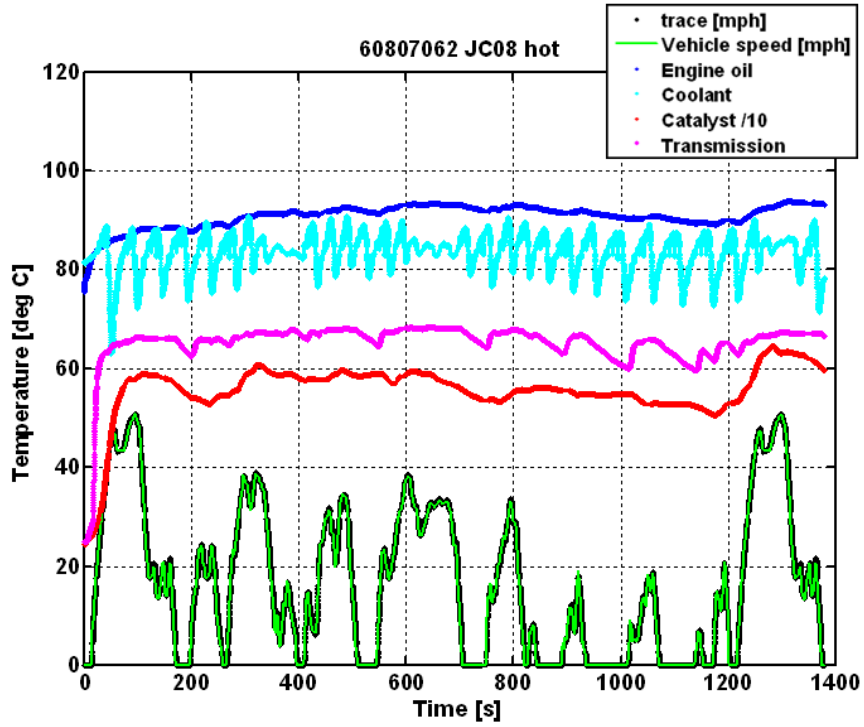
Appendix 8: Conventional vehicle results for drive cycle intensity study

This appendix provides further details and analysis on the conventional vehicle operation.

First the 'standard' UDDS cycle results are presented.

	UDDS
Test number	60807041
Fuel economy	**30.76 [mpg]**
Emissions	
THC	0.0015 [g/mi]
CH4	0.0015 [g/mi]
NMHC	0.0010 [g/mi]
NOx	0.5025 [g/mi]
CO	0.0200 [g/mi]
CO2	289.06 [g/mi]
Energy summary	
Fuel	33.33 [MJ]
Engine indicated	N/A
Engine crankshaft	7.89 [MJ]
Transmission	5.71 [MJ]
Dynamometer	4.27 [MJ]
Braking (possible regen)	2.20 [MJ]
Average cycle efficiency	
Engine indicated	N/A
Engine brake	23.6 [%]
Transmission	74.9 [%]

Then the scaled speed UDDS cycle results are presented.
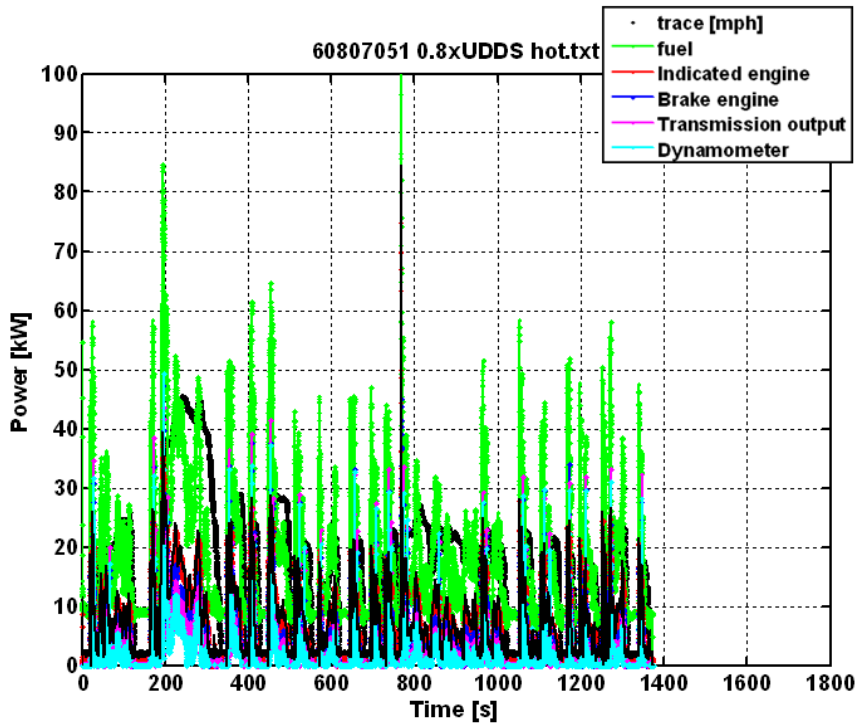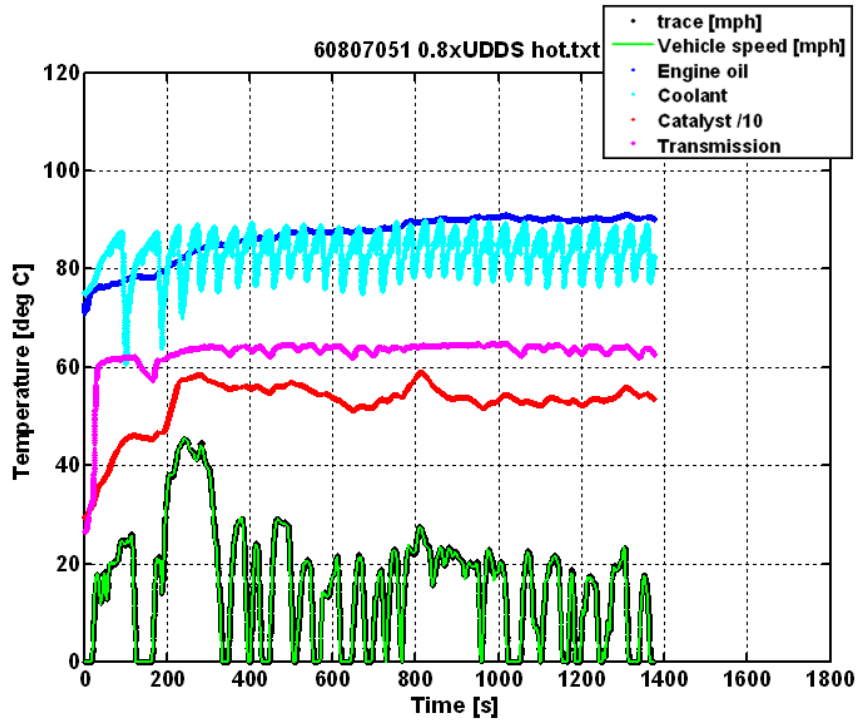
Finally the speed and time scaled UDDS cycles results are presented.
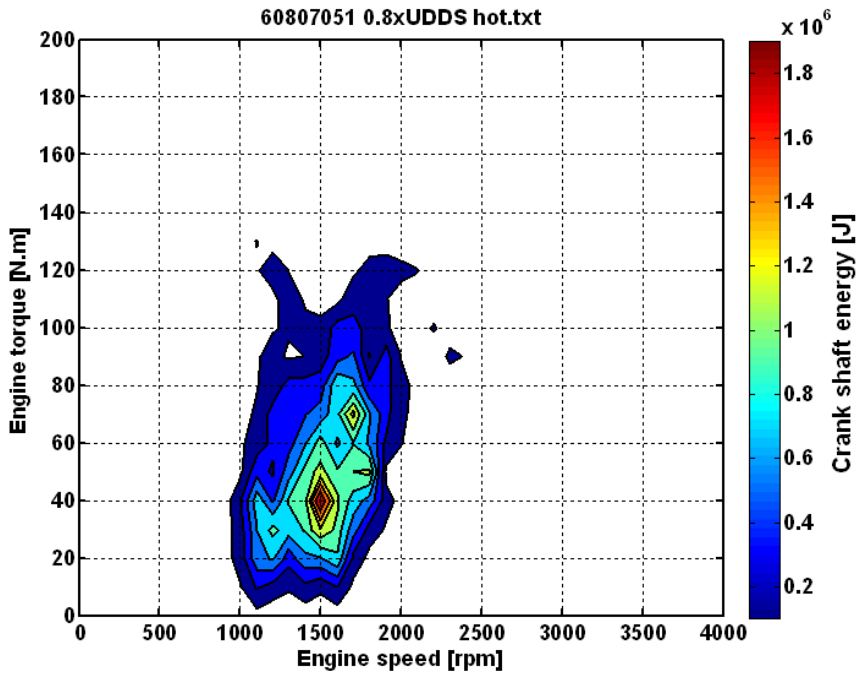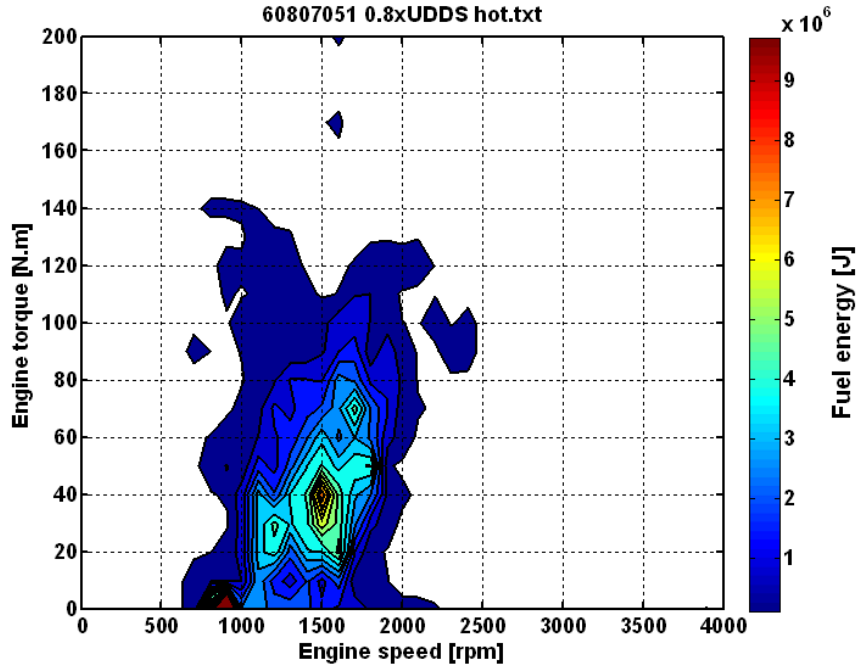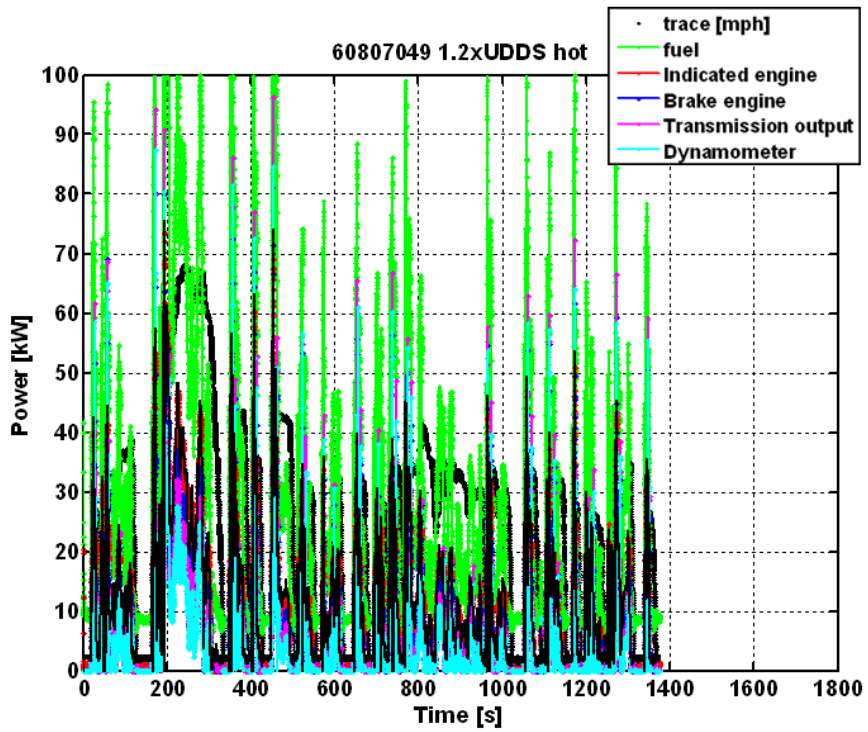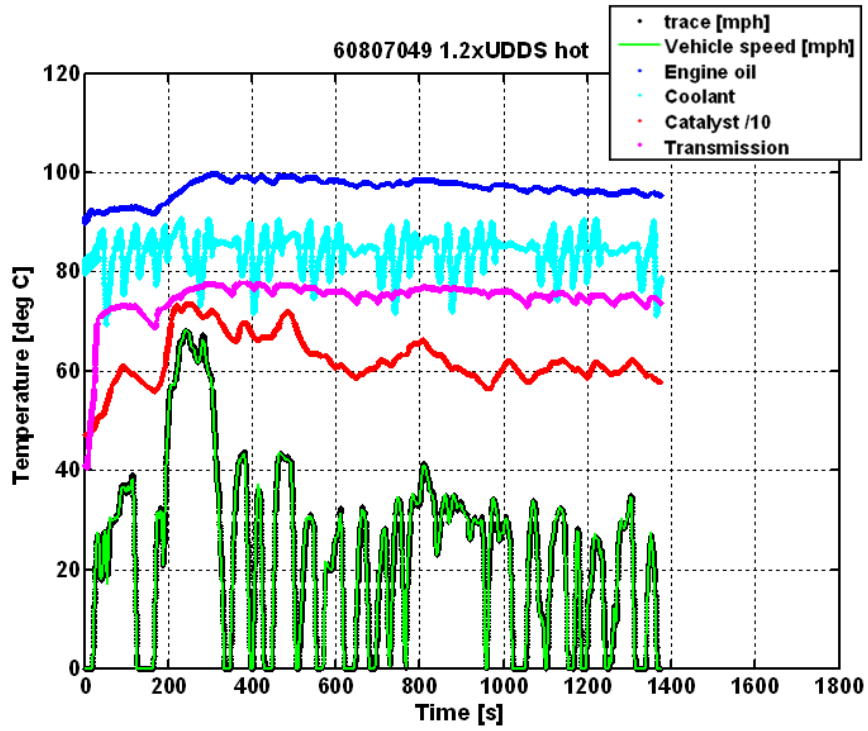
Baseline standard UDDS cycles results

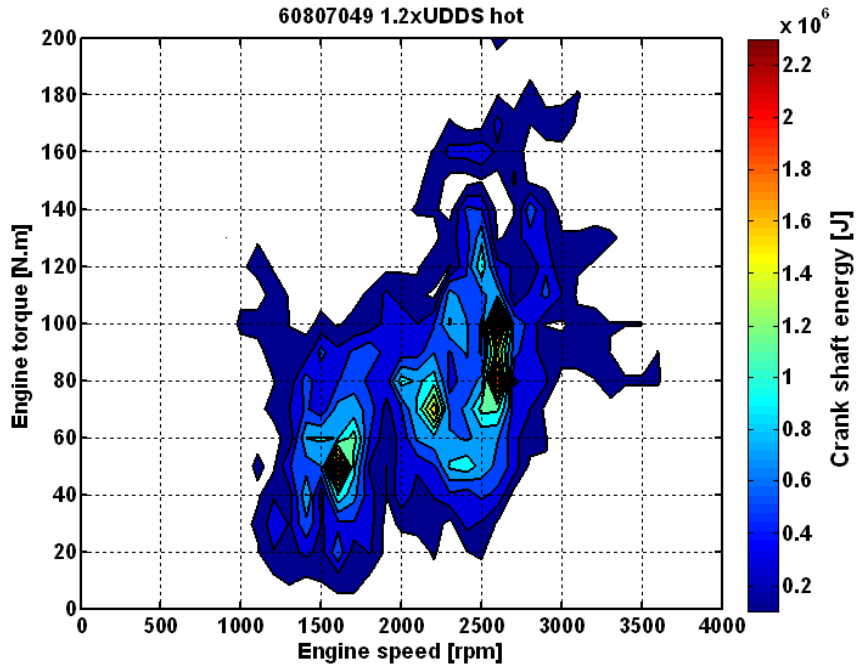60807041 1.0xUDDS hot

60807041 1.0xUDDS hot
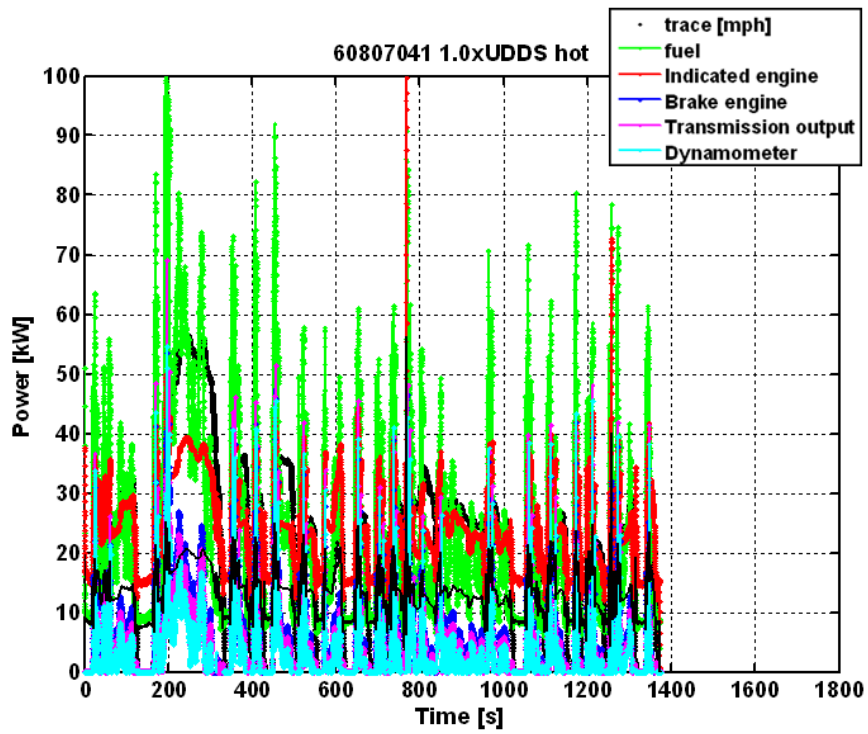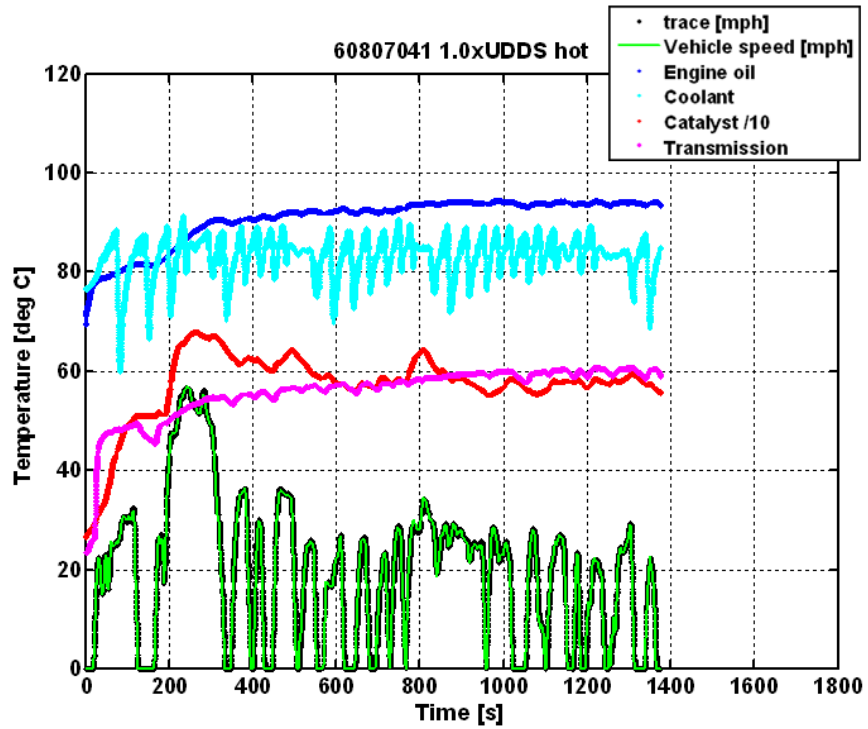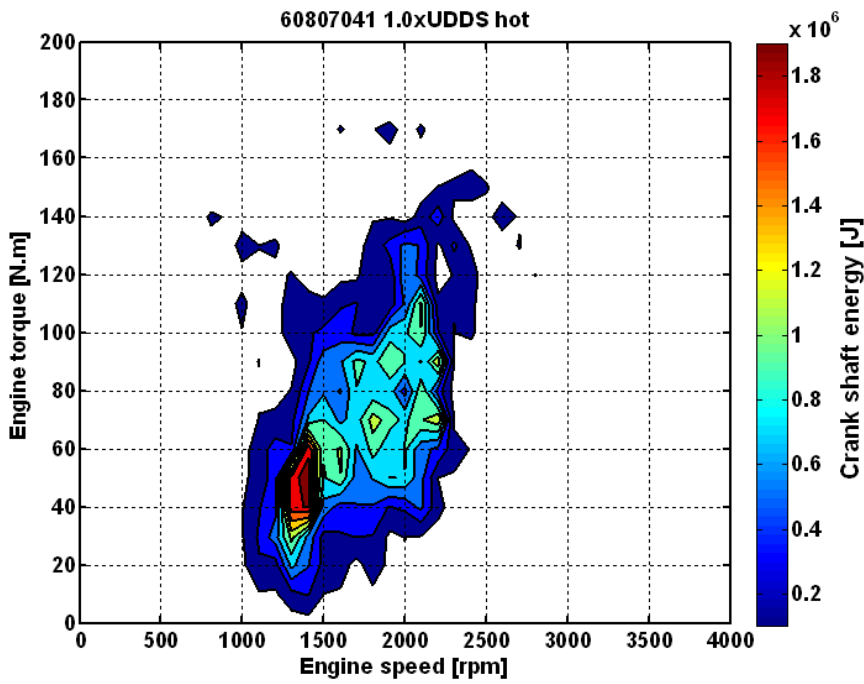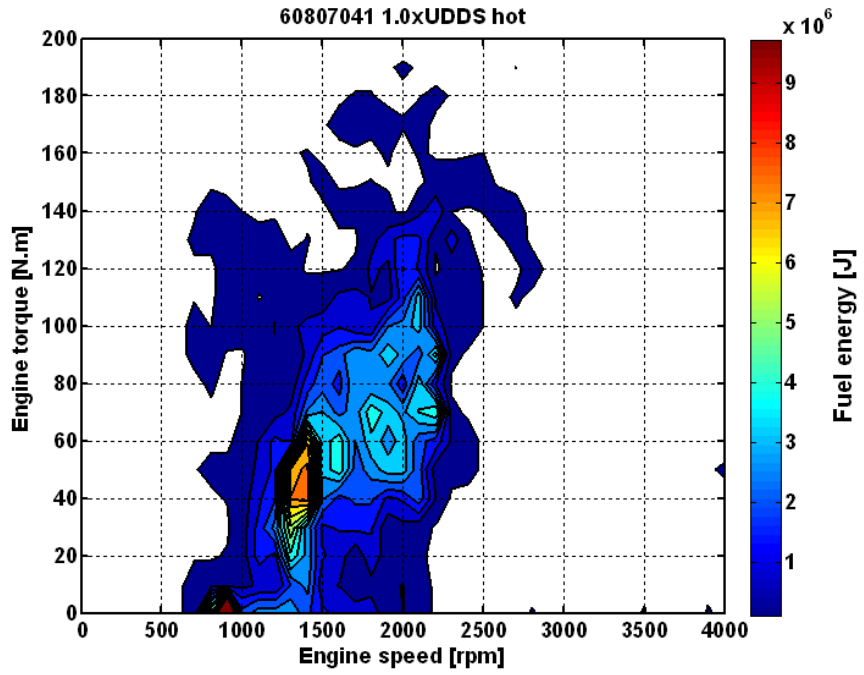
Speed scaled drive cycles same time

	UDDS	0.8 UDDS	1.2 UDDS	1.4 UDDS
Test number	60807041	60807051	60807049	60807050
Fuel economy	**30.76 [mpg]**	**34.06 [mpg]**	**29.57 [mpg]**	**27.93 [mpg]**
Emissions				
THC	0.0015 [g/mi]	0.0010 [g/mi]	0.0007 [g/mi]	0.0013 [g/mi]
CH4	0.0015 [g/mi]	0.0027 [g/mi]	0.0038 [g/mi]	0.0000 [g/mi]
NMHC	0.0010 [g/mi]	0.0001 [g/mi]	0.0006 [g/mi]	0.0013 [g/mi]
NOx	0.5025 [g/mi]	0.0201 [g/mi]	0.0310 [g/mi]	0.0907 [g/mi]
CO	0.0200 [g/mi]	0.0477 [g/mi]	0.0350 [g/mi]	0.0504 [g/mi]
CO2	289.06 [g/mi]	261.03 [g/mi]	300.68 [g/mi]	318.24 [g/mi]
Energy summary				
Fuel	33.33 [MJ]	25.63 [MJ]	40.50 [MJ]	49.96 [MJ]
Engine indicated	N/A	8.36 [MJ]	14.67 [MJ]	18.99 [MJ]
Engine crankshaft	7.89 [MJ]	5.22 [MJ]	10.29 [MJ]	13.78 [MJ]
Transmission	5.71 [MJ]	3.63 [MJ]	7.84 [MJ]	10.80 [MJ]
Dynamometer	4.27 [MJ]	2.69 [MJ]	6.34 [MJ]	8.85 [MJ]
Braking (possible regen)	2.20 [MJ]	1.43 [MJ]	3.16 [MJ]	4.26 [MJ]
Average cycle efficiency				
Engine indicated	N/A	32.6 [%]	36.2 [%]	38.0 [%]
Engine brake	23.6 [%]	20.4 [%]	25.4 [%]	27.6 [%]
Transmission	74.9 [%]	74.2 [%]	80.8 [%]	81.9 [%]

60807051 0.8xUDDS hot.txt

60807051 0.8xUDDS hot.txt

60807050 1.4xUDDS hot

60807050 1.4xUDDS hot

60807050 1.4xUDDS hot

60807050 1.4xUDDS hot

Speed scaled drive cycles and scaled time

	UDDS	0.8 UDDS	1.2 UDDS	1.4 UDDS
Test number	60807041	60807054	60807052	60807053
Fuel economy	**30.76 [mpg]**	**34.45 [mpg]**	28.77 [mpg]	**24.12 [mpg]**
Emissions				
THC	0.0015 [g/mi]	0.0004 [g/mi]	0.0023 [g/mi]	0.0023 [g/mi]
CH4	0.0015 [g/mi]	0.0003 [g/mi]	0.0015 [g/mi]	0.0007 [g/mi]
NMHC	0.0010 [g/mi]	0.0005 [g/mi]	0.0018 [g/mi]	0.0021 [g/mi]
NOx	0.5025 [g/mi]	0.0114 [g/mi]	0.0832 [g/mi]	0.6823 [g/mi]
CO	0.0200 [g/mi]	0.0273 [g/mi]	0.0263 [g/mi]	0.0452 [g/mi]
CO2	289.06 [g/mi]	250.80 [g/mi]	309.08 [g/mi]	368.63 [g/mi]
Energy summary				
Fuel	33.33 [MJ]	30.77 [MJ]	35.17 [MJ]	41.134 [MJ]
Engine indicated	N/A	9.95 [MJ]	13.47 [MJ]	16.13 [MJ]
Engine crankshaft	7.89 [MJ]	6.02 [MJ]	9.42 [MJ]	11.82 [MJ]
Transmission	5.71 [MJ]	4.17 [MJ]	7.27 [MJ]	9.31 [MJ]
Dynamometer	4.27 [MJ]	2.94 [MJ]	5.90 [MJ]	7.73 [MJ]
Braking (possible regen)	2.20 [MJ]	1.40 [MJ]	3.19 [MJ]	4.34 [MJ]
Average cycle efficiency				
Engine indicated	N/A	32.4 [%]	38.3 [%]	39.2 [%]
Engine brake	23.6 [%]	19.6 [%]	26.8 [%]	28.7 [%]
Transmission	74.9 [%]	70.5 [%]	81.2 [%]	83.0 [%]

60807054 0.8xUDDS time scaled hot

60807054 0.8xUDDS time scaled hot

60807052 1.2xUDDS time scaled

60807052 1.2xUDDS time scaled

60807052 1.2xUDDS time scaled hot

60807052 1.2xUDDS time scaled hot

60807053 1.4xUDDS time scaled hot

60807053 1.4xUDDS time scaled hot

Appendix 9: Signal list collected during the hydrogen engine calibration

Here the channel list collected during the combustion research and calibration of the hydrogen engine on the low speed data acquisition system.

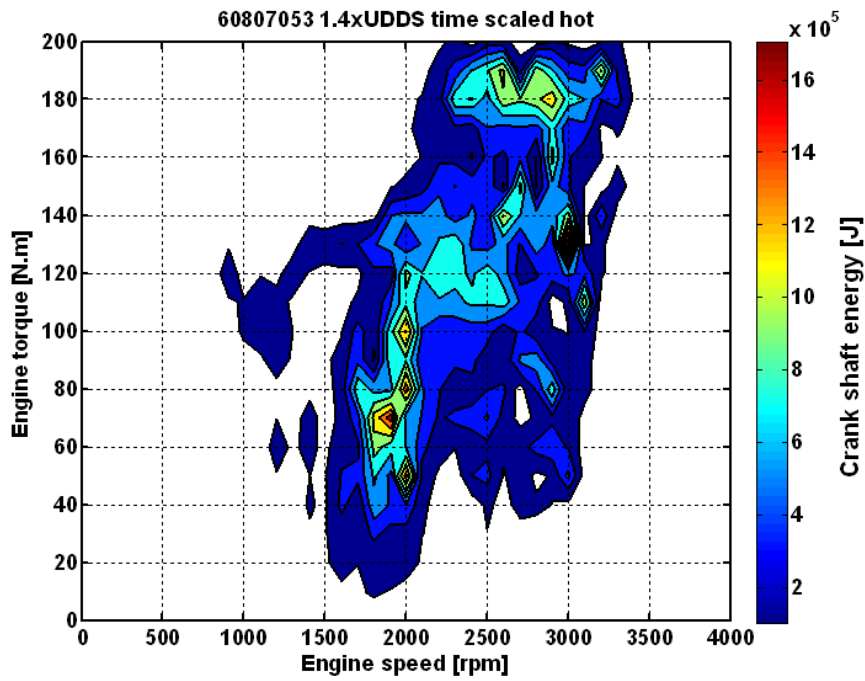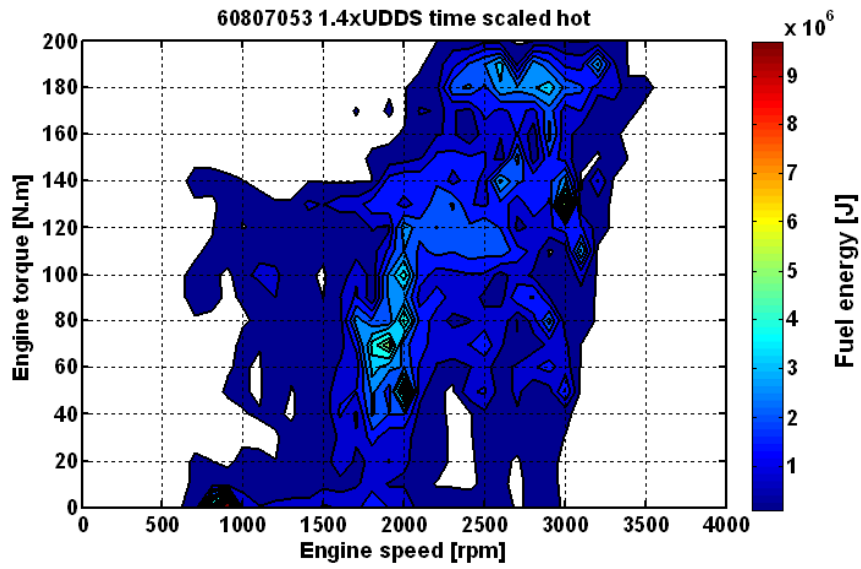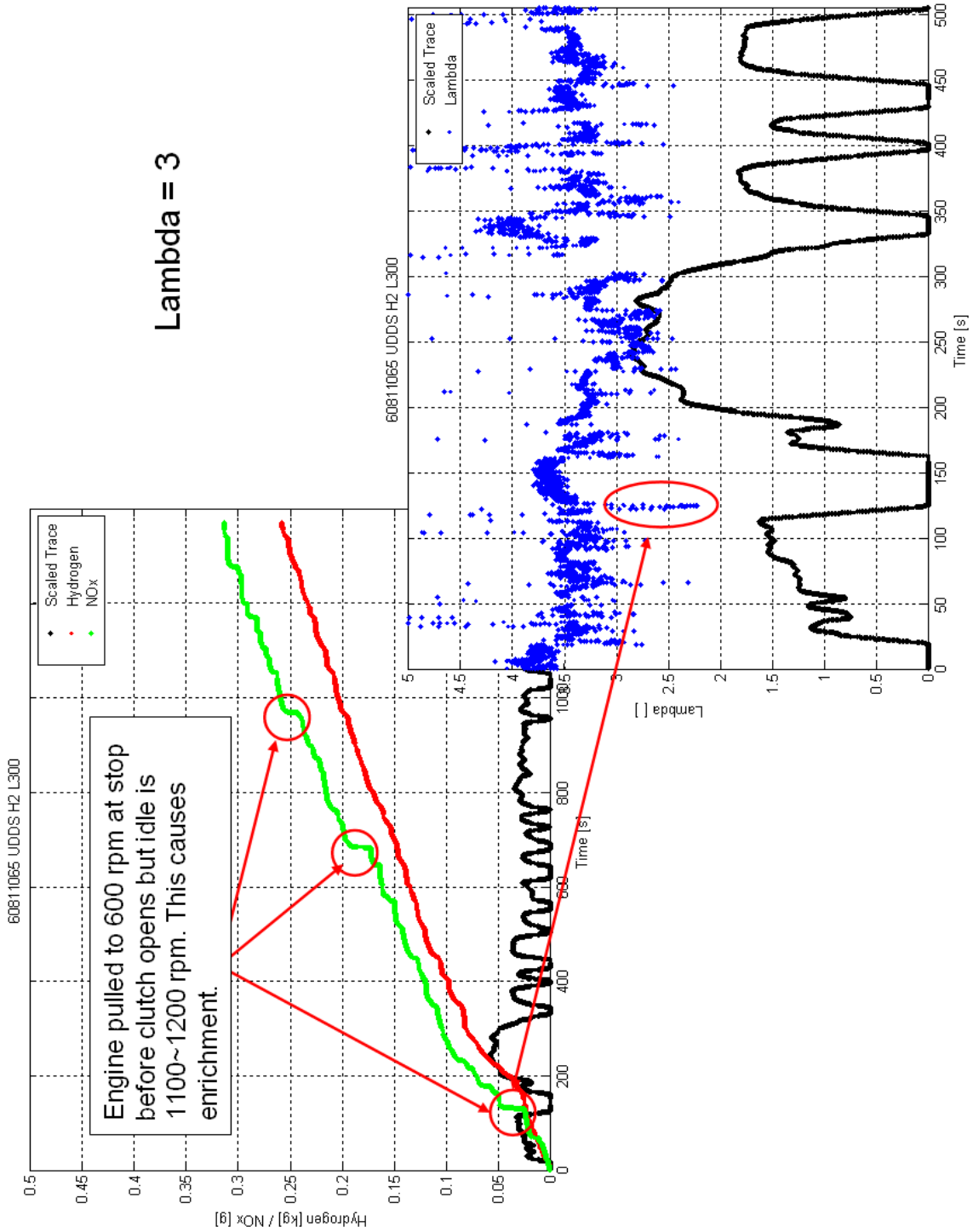|	
Sample Number	Oil Temperature [C]
Start Capture Time	Cyl 1 Exhaust Temp [C]
Stop Capture Time	Cyl 2 Exhaust Temp [C]
Intake Air Pressure [psia]	Cyl 3 Exhaust Temp [C]
Coolant Pressure [psig]	Cyl 4 Exhaust Temp [C]
Oil Pressure [psig]	Exhaust Collector Temp
Exhaust Pressure [psig]	Water Temp Intercooler Out [C]
Coolant Flow [l/min]	Engine Speed [RPM]
Pre-Charger Air Pressure [psia]	Throttle Position [%]
Airflow Meter Absolute Pressure [psia]	Manifold Pressure [kPa]
Airflow Meter Differential Pressure [psid]	Injection Duration 1st Injection
H2-Sensor Fumehood Multi [%LEL]	Ignition Timing
H2-Sensor Enclosure [%LEL]	Wideband O2 Sensor
H2-Sensor Fumehood [%LEL]	Engine Temperature [C]
Status Estop [unitless]	Fuel Rail Pressure [psi]
Dyno Speed [RPM]	Fuel Rail Temperature [C]
Torque [Nm]	Air Flow [kg/h]
Humidity [%]	CH4 [ppm]
H2 Mass [kg/h]	THC [ppm]
H2 Pressure at Supply Panel [psig]	NOx [ppm]
Ambient Pressure [psia]	CO [ppm]
Airflow Meter Temp [C]	CO2 [ppm]
Pre-Charger Air Temp [C]	O2 [ppm]
Intake Air Temp [C]	H2 [ppm]
Coolant Temp Engine In [C]	BMEP [bar]
Coolant Temp Heater In [C]	Lambda
Coolant Temp Engine Out [C]	Phi
Water Temp Intercooler In [C]	Lambda (O2 Content)
	Phi (O2 Content)

In addition in-cylinder pressure for each cylinder was recorded on the high speed data acquisition system. In 2006 a Win600 was used for the high speed data recording. For the final calibration a full AVL indicating system was used to record and process the high speed indicated data. The pressure traces, the measured ignition timing and the injector current were recorded. The indicating system will then infer indicated pressure, heat release, maximum pressure cylinder, maximum rate of pressure rise, 50% mass fraction burn among other parameters using the pressure traces and the engine geometry.

Appendix 10: Hydrogen engine detailed test results

Lambda = 3

60811065 UDDS H2 L300
FE low: 28.8767 mi/kg
FE high: 28.517 mi/kg
Idle speed cut off point: 1200 rpm
Average engine speed: 1674.931 rpm
Average engine torque: 43.6852 N.m
Average engine power: 8.3752 kW
Average engine power: 29.3989 percent
Fuel energy: 30.962 MJ
Engine crank energy: 8.31 MJ
Motor energy: 7.47 MJ
Drive shaft energy (pos): 5.943 MJ
Dyno shaft energy (pos): 4.817 MJ

Lambda = 3

Engine pulled to 600 rpm at stop before clutch opens but idle is 1100~1200 rpm. This causes enrichment.

Lambda = 2.5

60811080 UDDS H2 L2.5
FE low: 30.7638 mi/kg
FE high: 30.6821 mi/kg
Idle speed cut off point: 1200 rpm
Average engine speed: 1624.0734 rpm
Average engine torque: 44.3887 N.m
Average engine power: 8.0323 kW
Average engine power: 29.6884 percent
Fuel energy: 29.063 MJ
Engine crank energy: 7.811 MJ
Motor energy: 7.191 MJ
Drive shaft energy (pos): 5.893 MJ
Dyno shaft energy (pos): 4.716 MJ

Lambda = 2.5

Lambda = 2.25

60811078 UDDS H2 L2.25
FE low: 31.0797 mi/kg
FE high: 30.7769 mi/kg
Idle speed cut off point: 1200 rpm
Average engine speed: 1599.4156 rpm
Average engine torque: 44.8451 N.m
Average engine power: 7.9565 kW
Average engine power: 29.3176 percent
Fuel energy: 28.767 MJ
Engine crank energy: 7.659 MJ
Motor energy: 7.147 MJ
Drive shaft energy (pos): 5.911 MJ
Dyno shaft energy (pos): 4.73 MJ

Lambda = 2.25

Lambda = 2

6081172 UDDS H2 L200
FE low: 30.6317 mi/kg
FE high: 30.6718 mi/kg
Idle speed cut off point: 1200 rpm
Average engine speed: 1589.1813 rpm
Average engine torque: 42.7563 N.m
Average engine power: 7.5396 kW
Average engine power: 28.0353 percent
Fuel energy: 29.188 MJ
Engine crank energy: 7.504 MJ
Motor energy: 7.012 MJ
Drive shaft energy (pos): 5.877 MJ
Dyno shaft energy (pos): 4.758 MJ

Lambda = 2

Lambda = VAR

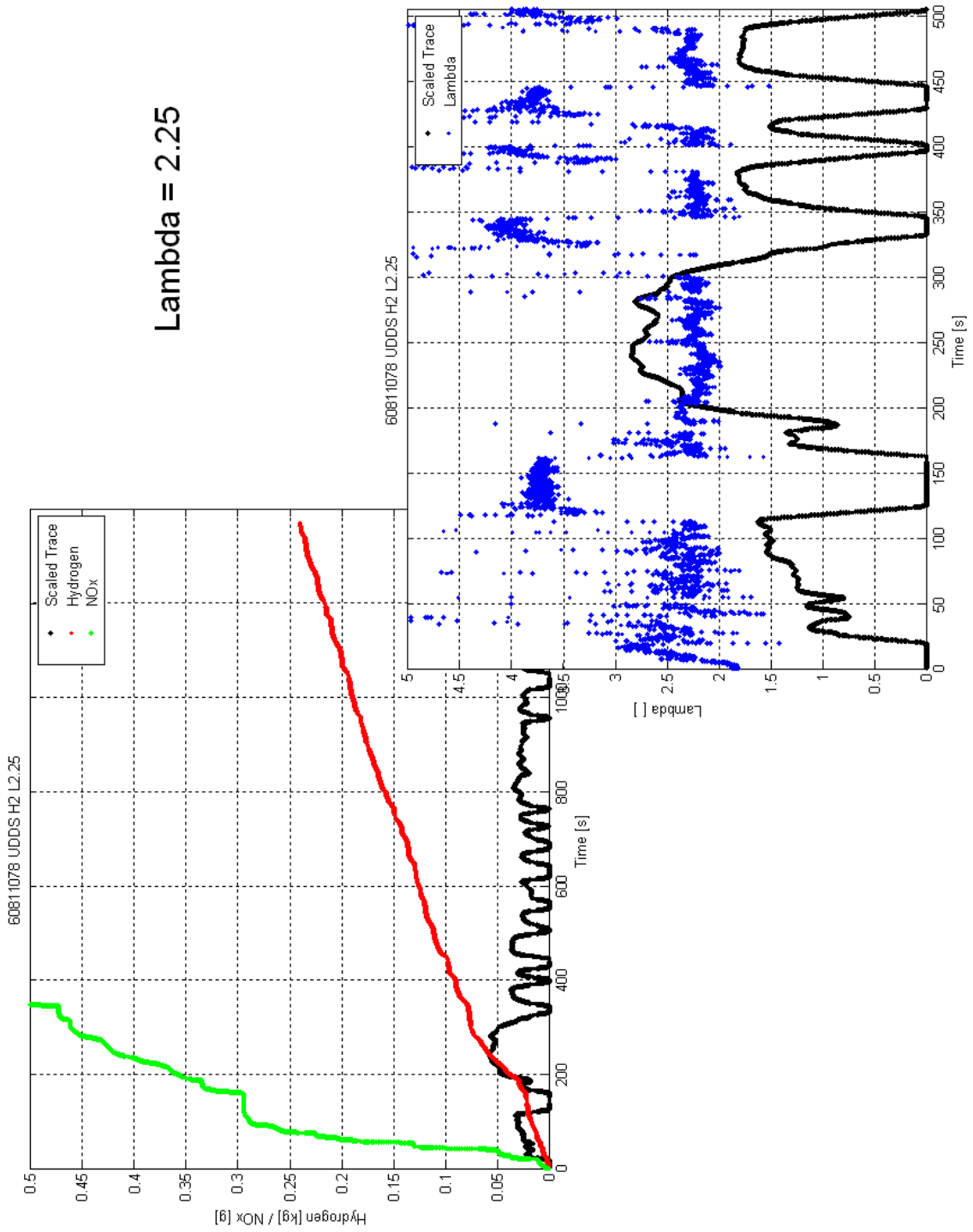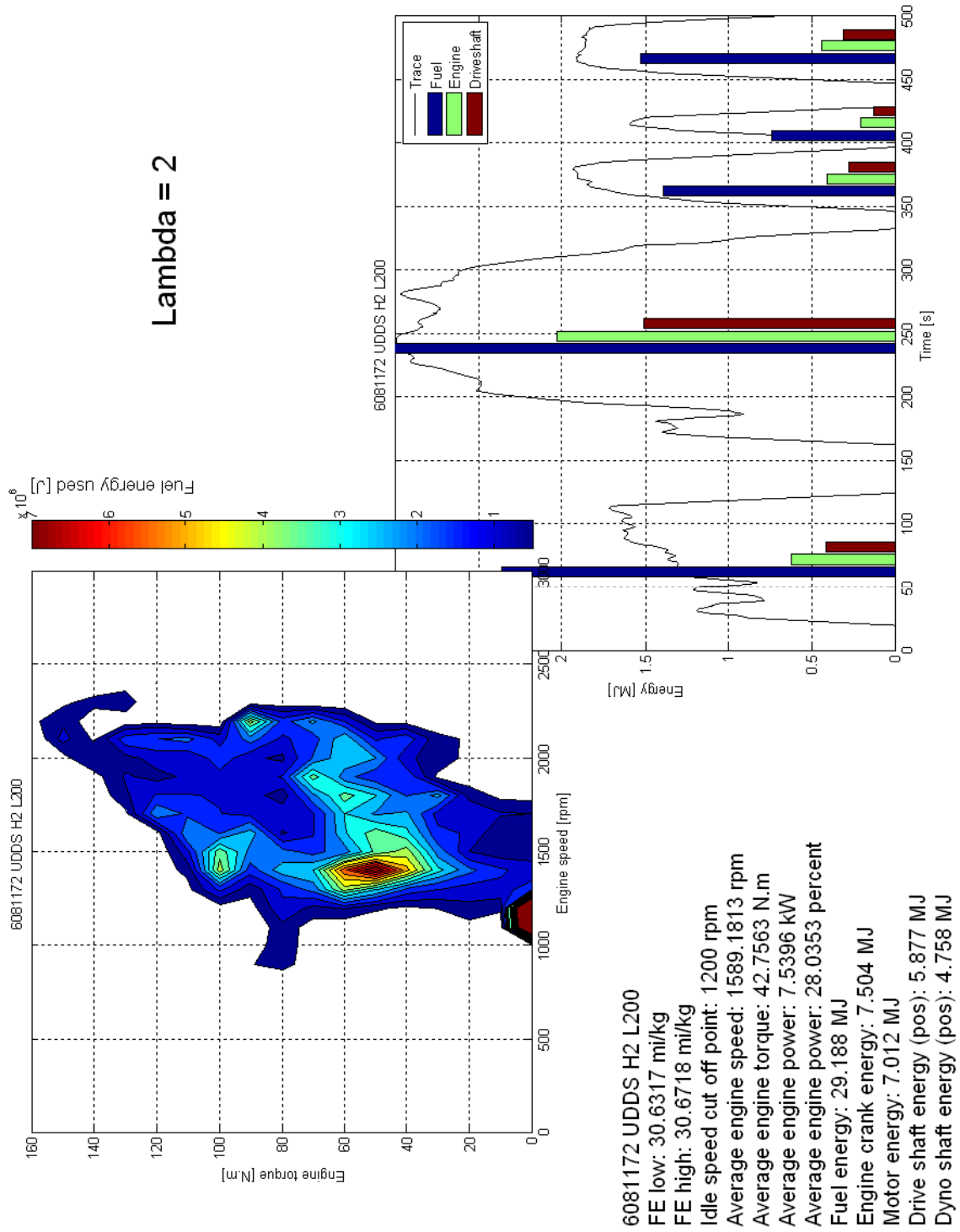60811081 UDDS H2 LVAR
FE low: 31.2155 mi/kg
FE high: 31.167 mi/kg
Idle speed cut off point: 1200 rpm
Average engine speed: 1545.2418 rpm
Average engine torque: 48.0769 N.m
Average engine power: 8.2099 kW
Average engine power: 30.3264 percent
Fuel energy: 28.642 MJ
Engine crank energy: 7.757 MJ
Motor energy: 7.095 MJ
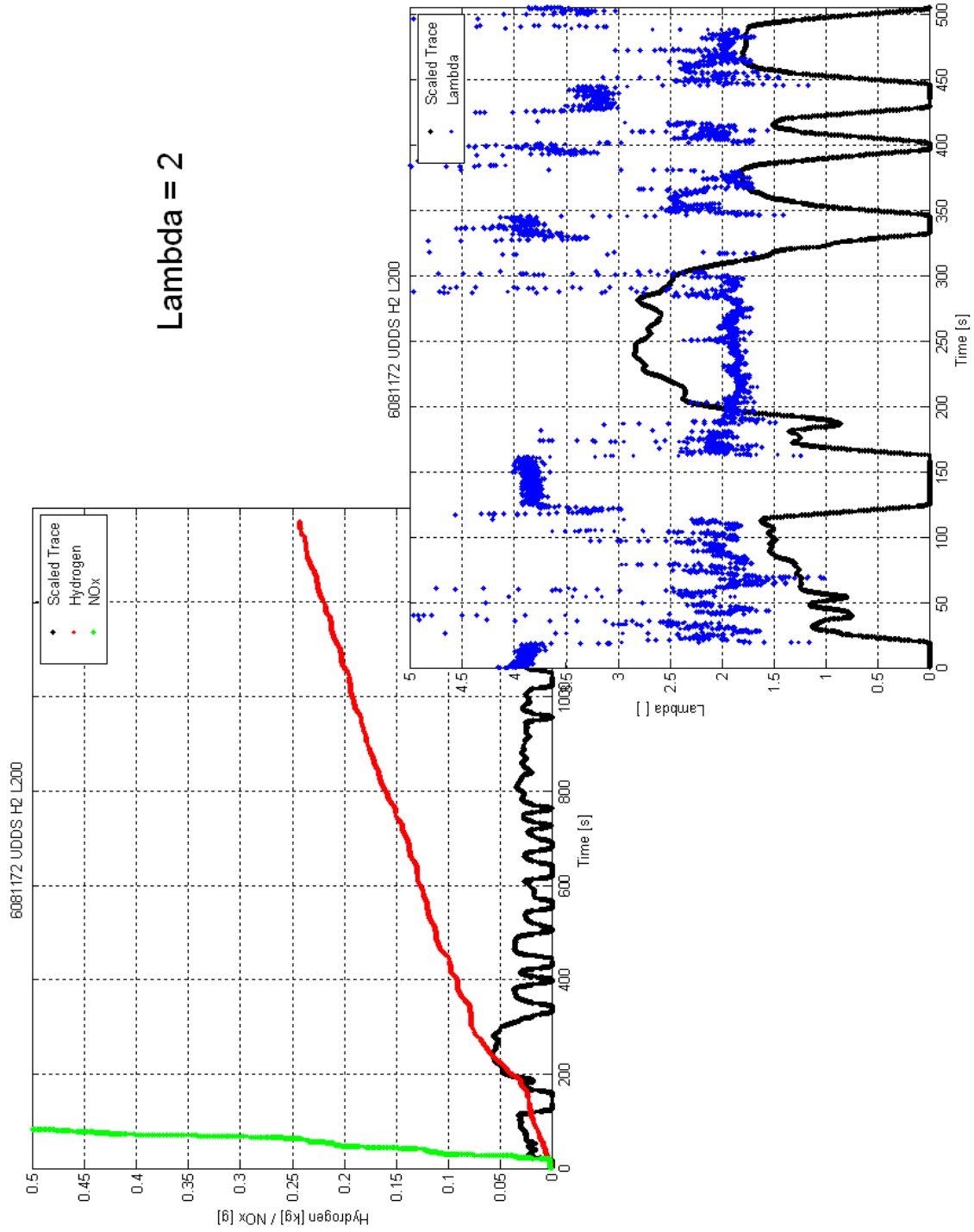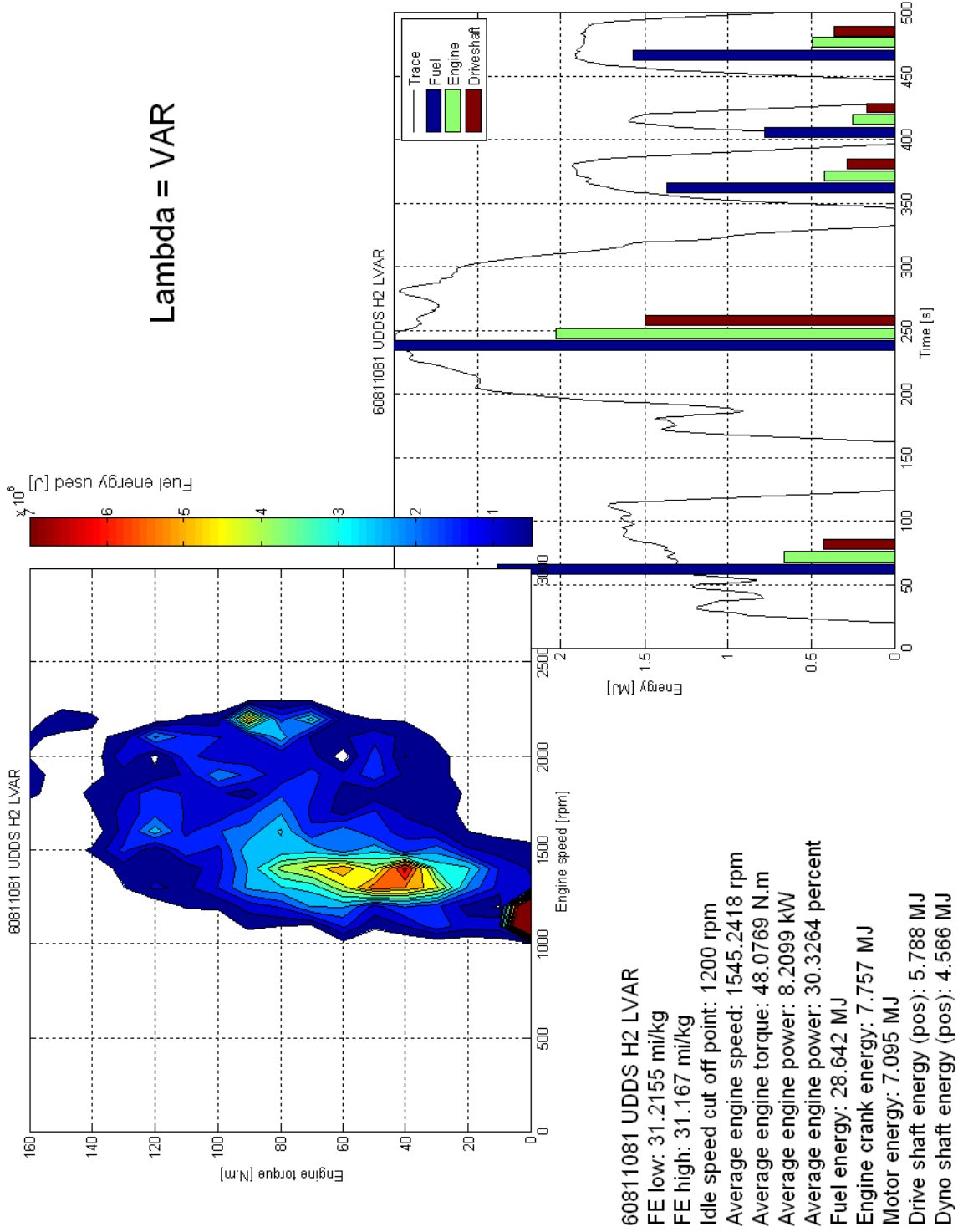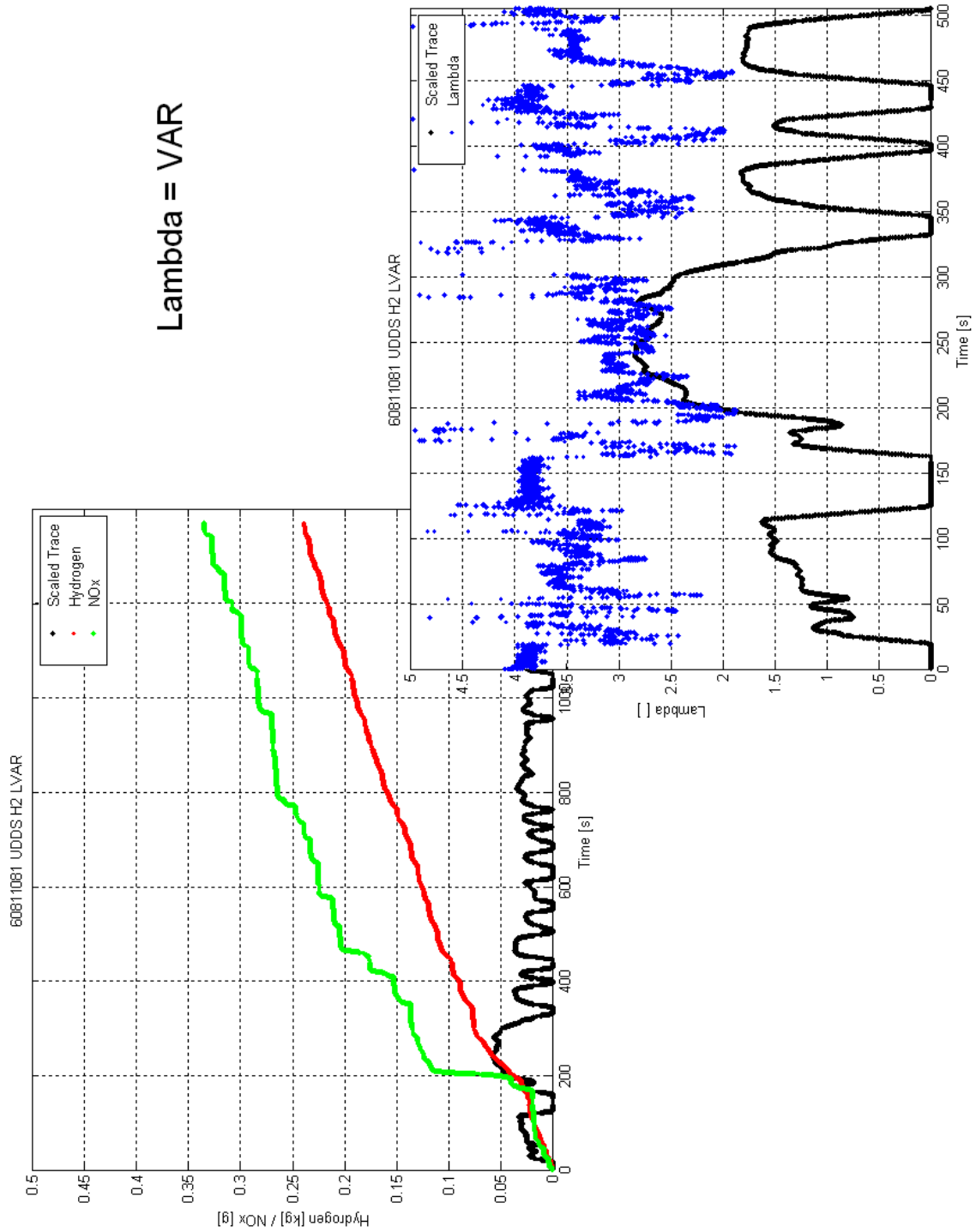Drive shaft energy (pos): 5.788 MJ
Dyno shaft energy (pos): 4.566 MJ

Lambda = VAR

Appendix 11: Vita and Publication list of
Henning Lohse-Busch

Henning was born on May 9th 1979 in Germany. In 1987 his family moved to France where received his high school degree in 1997. He started his studies in Mechanical Engineering at the Euro-American Institute of Technology in France and finished his undergraduate degree at Virginia Tech.

Henning has always had an interest in the automotive world, which translated into hours of reading about and studying engines. The Hybrid Electric Vehicle Team at Virginia Tech sparked Henning's passion for advanced technology vehicles and he quickly took on an active role within the team. For four years, Henning spent countless hours in the HEVT shop working on the fuel cell and hydrogen engine series hybrid to compete in DOE's advanced vehicle student competition. These hours provided valuable opportunities to transfer the theories he'd been taught at VT into practice, as well as developing his hands on skills while building a hybrid vehicle.

Henning's remembers many highlights from his HEVT days, including making power from the fuel cell for the first time to driving a full lap of the on-road fuel economy event using hydrogen power. His most memorable experiences as team leader were when new students demonstrated their own passion for the technology and began to understand the workings of the car. He will always remember when his team drove off with the competition car into DC rush hour traffic and he could see that he had helped to teach a new generation of students who would be the future of hybrids. These HEVT years will never be forgotten. This experience enabled Henning to find himself and made him into the person he is today. Henning credits Professor Nelson for his excellent teaching and mentoring style, which includes the theoretical foundation coupled with a hands-on approach to teaching.

After Henning obtained his Masters, passed the qualifier and completed all of the required course work for the Ph.D. at Virginia Tech, he took a job at Argonne National Laboratory, where he could perform his Ph.D. research while gaining invaluable experience in a laboratory that is on the cutting edge of hybrid vehicle and alternative fuel research. A major portion of his work at Argonne is presented in this dissertation. He is also a test engineer at the Advanced Powertrain Research Facility where he tests and analyzes production hybrid vehicles, prototype hybrid and plug-in hybrid electric vehicles and alternative fuel vehicle including hydrogen powered and bio-fueled vehicles.

While living in Chicago, he met Emily Pratzel. They got married on November 1st of 2008. Without her support, encouragement, and assistance, this dissertation would not have been possible.

Henning Lohse-Busch – Resume (August 2009)

Education	**PhD candidate, Mechanical Engineering,** Virginia Tech, Fall 2009, Professor D. J. Nelson, Virginia Polytechnic Institute and State University, (Virginia Tech), Blacksburg, VA, USA accepted in PhD program summer 2003, PhD qualifier summer 2003, defense date 9/11/2009 "Development and Applications of the Modular Automotive Technology Testbed (MATT) to Evaluate Hybrid Electric Powertrain Components and Energy Management Strategies"
	Master of Science, Mechanical Engineering, Virginia Tech, Spring 2004, GPA: 3.85/4.0, "Thermal Overload Capability of an Electric Motor and Inverter Units through Modeling"
	Bachelor of Science, Mechanical Engineering, Virginia Tech, Spring 2001, GPA 3.83/4.0, "*Summa cum Laude*" • Fall 1999, Virginia Polytechnic Institute and State University, Blacksburg, VA, USA • Spring 1998, Euro-American Institute of Technology, Sophia Antipolis, France • Fall 1997, Clarkson University, Potsdam, NY, USA
	Baccalauréat Scientifique, spécialité Mathématique, option Informatique, Summer 1997, Munster, France
Professional Experience	**Research Engineer**, Argonne National Laboratory, Center for Transportation Research, Energy Systems Division, Vehicle Systems and Fuels group, Chicago, IL, USA • 2006-present, Principal Investigator, Modular Automotive Technology Testbed project • 2004-present, Hardware-In-the-Loop engineer • 2004-present, Test Engineer in the Advanced Powertrain Research Facility, Hybrid vehicle testing with an expertise in hydrogen vehicle testing • 2005-2008, Principal Investigator , Hydrogen test cell expansion and multi cylinder engine calibration
	Graduate Research Assistant for Dr. D.J. Nelson, Virginia Tech • Fall 2001 Fuel Cell Modeling funded by National Renewable Energy Laboratory (NREL) • Fall 2002 Cooling of Power Electronics funded by Virginia Power Technologies (VPT) **Graduate Teaching Assistant** for Dr. D.J. Nelson ,Virginia Tech • Fall 2003 ME 4015: Engineering Design and Projects (Fall 2003)
	Hybrid Electric Vehicle Team of Virginia Tech, HEVT, www.hevt.me.vt.edu, www.futuretruck.org, • FutureTruck 2001, Fuel Cell Hybrid Vehicle Control group leader, Senior Design • FutureTruck 2002, Fuel Cell Hybrid Team leader assistant, Volunteer • FutureTruck 2003, H2ICE Hybrid Team leader, Volunteer • FutureTruck 2004, H2ICE Hybrid Team leader, Graduate Teaching Assistant
	Engineer Assistant, Basic research on shockwave medical machinery, Storz Medical, Kreuzlingen, Switzerland, Summer 1998, 4 weeks
Languages	**German:** first native language **French:** second native language **English:** fluently spoken and written
Activities	Society of Automotive Engineers (SAE), regular volunteer as peer-reviewer and session chair American Society of Mechanical Engineers (ASME) National Mechanical Engineering Honor Society (Pi Tau Sigma) National Engineering Honor Society (Tau Beta Pi)
Awards	• **VT College of Engineering, Deans List,** Fall 1999, Spring 2000 and Fall 2000 • **VT IR Student Award,** Mechanical Engineering, 2001 • **VT Pratt Fellowship,** Mechanical Engineering, 2001-2002 • **ANL Pace Setter award,** 2008 for BMW Hydrogen 7 testing
Trainings	Available on request
Publications	Available on request
References	Available on request

Henning Lohse-Busch – Publication List (August 2009)

Published / Peer-reviewed conference papers:

Henning Lohse-Busch, Michael Duoba, Neeraj Shidore, Douglas Nelson, Theodore Bohn, Richard Carlson, 'A Modular Automotive Hybrid Testbed Designed to Evaluate Various Components from the Vehicle System', SAE 2009-01-1315, SAE World Congress, Detroit 04/20/2009

Jeongwoo Lee, Douglas J. Nelson, Henning Lohse-Busch, 'Vehicle Inertia Impact on Fuel Consumption of Conventional and Hybrid Electric Vehicles Using Acceleration and Coast Driving Strategy', SAE 2009-01-1322, SAE World Congress, Detroit, 04/20/2009

Richard W. Carlson, Michael Duoba, Neeraj Shidore, Henning Lohse-Busch, 'Drive Cycle Fuel Consumption Variability of Plug-In Hybrid Electric Vehicles due to Aggressive Driving', SAE 2009-01-1335, SAE World Congress, Detroit 04/20/2009

Wallner, T, Scarcelli, R, Lohse-Busch, H., Wozny, B. and Miers, S., 'Safety Considerations for Hydrogen Test Cells', International Conference on Hydrogen Safety, Pisa, Italy

Henning Lohse-Busch, Thomas Wallner, John Fleming, "Transient Efficiency, Performance, and Emissions Analysis of a Hydrogen Internal Combustion Engine Pick-up Truck", SAE, 2006-01-3430, Powertrain & Fluid Systems Conference and Exhibition, October 2006, Toronto, ON, CANADA

Thomas Wallner, Henning Lohse-Busch, "Performance, Efficiency, and Emissions Evaluation of a Supercharged, Hydrogen-Powered, 4-Cylinder Engine", SAE, 2007-01-0016, 2007 Fuels and Emissions Conference, January 2007, Cape Town, SOAFR

Thomas Wallner, Henning Lohse-Busch, "Light Duty Hydrogen Engine Application Research at ANL", Bridging the Technology... Hydrogen Internal Combustion Engines, Febuary 1/22/06, San Diego, CA (Presentation and poster)

Thomas Wallner, Henning Lohse-Busch, "Research Update: Hydrogen Projects at Argonne National Laboratory", Hydrogen Internal Combustion Engine symposium, 2/13/07, Los Angeles, CA (Presentation)

Thomas Wallner, Henning Lohse-Busch, Henry Ng, Robert Peters, "Results of Research Engine and Vehicle Drive Cycle Testing during Blended Hydrogen/Methane Operation", NHA Annual - hydrogen Conference 2007, 3/19/07 - 3/22/07, San Antonio, TX (Presentation and Manuscript)

M. Duoba, H. Lohse-Busch, R. Carlson, T. Bohn, S. Gurski, "Production Power-Split HEV Test Data Analysis of Control Strategy Behavior and Its Influence on Vehicle Efficiency", SAE, 2007-01-0291, SAE World Congress & Exhibition, April 2007, Detroit, MI, USA (TRANSACTION JOURNAL PAPER)

Michael Duoba, Henning Lohse-Busch, Theodore Bohn,, "Investigating Vehicle Fuel Economy Robustness of Conventional and Hybrid Electric Vehicles," EVS-21, April 2-6, 2005, Monaco, Monte Carlo

Michael Duoba, Henning Lohse-Busch, Theodore Bohn, "Investigating HEV Vehicle Fuel Economy Sensitivity Under More Aggressive Driving," Presentation at SAE 2005 SAE Future Transportation Technology Conference, September 7-9. 2005, IIT Campus, Chicago, IL.

N. Shidore, T Bohn, M. Duoba, H. Lohse-Busch, M. Pasquier, "Innovative approach to vary degree of hybridization for avdanved powertrain testing using a single motor".EVS-22, October 12-18, 2006, Yokohama, Japan

Michael Duoba, Theodore Bohn, Henning Lohse-Busch, "Investigating Possible Fuel Economy Bias Due to Regenerative Braking in Testing Hevs on 2wd and 4wd Chassis Dynamometers", SAE, 2005-01-0685, SAE 2005 World Congress & Exhibition, April 2005, Detroit, MI, USA

H Lohse-Busch, S Boyd, (2004), "Magellan: Design and Results of a Hydrogen Powered Hybrid Electric Vehicle", SAE World Congress 2004, Technical session: Developing New Technologies Through Student Design Competitions (session code P20)

H Lohse-Busch, T Stinchfield, M Mital, A Hines, DJ Nelson, (2003), "Design and implementation of a hybrid electric vehicle powered by a hydrogen engine," Proceedings of the 2003 FutureTruck Challenge, June 1-12, 2003, Ford Romeo Proving Grounds, MI, SAE paper pending, 18 p

S Gurski, H Lohse-Busch, G Henshaw, DJ Nelson, (2002), "Design of a zero emission sport utility vehicle," Proceedings of the 2002 FutureTruck Challenge, June 11-21, 2002, Ford Arizona Proving Grounds, AZ, SAE paper 2000-01-1264, 17 p

S Gurski, D Evans, D Knox, M Conover, A Harris, H Lohse-Busch, S Kraft, DJ Nelson, (2002), "Design and Development of the 2001 Virginia Tech FutureTruck: A Fuel Cell Hybrid Electric Vehicle," Proceedings of the 2001 FutureTruck Challenge, June 4-13, 2001, Ford Milford Proving Grounds, MI, SAE paper SP-1701, 18 p

Journal Paper:

Wallner T, Lohse-Busch H, Shidore N., 'Operating strategy for a hydrogen engine for improved drive-cycle efficiency and emissions behavior', International Journal of Hydrogen Energy (2008), doi:10.1016/ j.ijhydene.2008.07.099